EMERGING INFECTIOUS DISEASES®

December 2014

Zoonotic Infections

EMERGING INFECTIOUS DISEASES®

Emerging Infectious Diseases is published monthly by the Centers for Disease Control and Prevention, 1600 Clifton Road, Mailstop D61, Atlanta, GA 30333, USA. Telephone 404-639-1960, fax 404-639-1954, email eideditor@cdc.gov.

∞ Emerging Infectious Diseases is printed on acid-free paper that meets the requirements of ANSI/NISO 239.48-1992 (Permanence of Paper)

EMERGING INFECTIOUS DISEASES

December 2014

On the Cover

Fred Tomaselli
Starling (2010)

Photo collage, acrylic, and resin on wood panel
80 x 80 in. (203.2 x 203.2 cm)

About the Cover p. 2187

Research

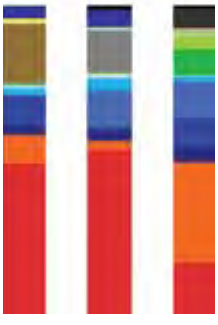

p. 1996

Medscape EDUCATION ACTIVITY

p. 2000

Medscape EDUCATION ACTIVITY

EMERGING INFECTIOUS DISEASES
December 2014

p. 2011

Dispatches

p. 2101

EMERGING INFECTIOUS DISEASES
December 2014

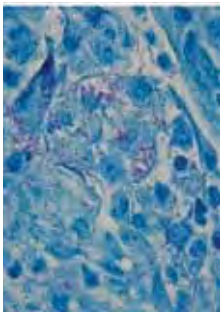

p. 2112

p. 2169

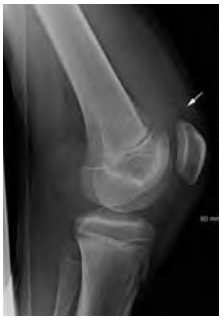

Letters

About the Cover

Etymologia

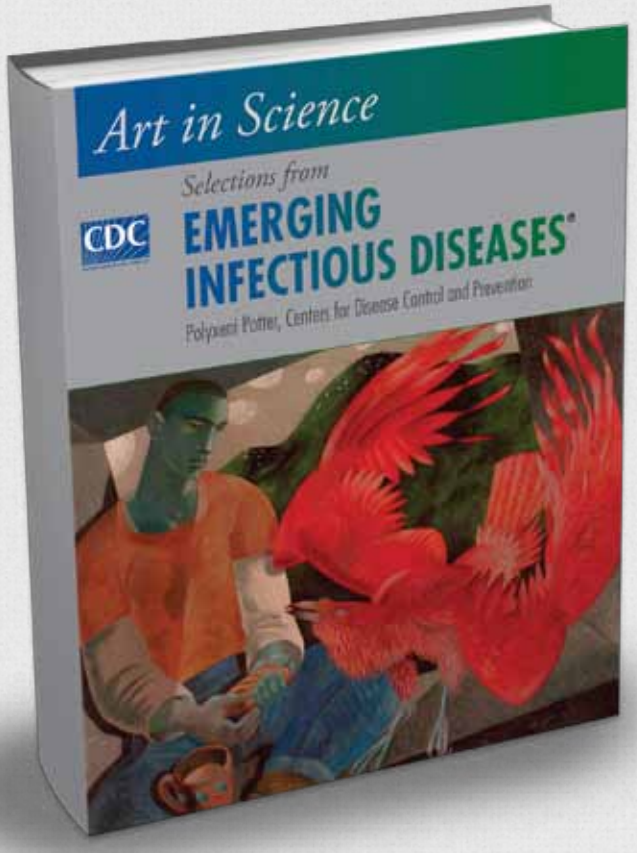

NOW AVAILABLE

Art in Science: **Selections from EMERGING INFECTIOUS DISEASES**
[Hardcover]

The journal's highly popular fine-art covers are contextualized with essays that address how the featured art relates to science, and to us all.

Available at
http://bit.ly/16sJI6R
Use promo code 32327
for an additional
20% off

This collection of 92 excerpts and covers from **Emerging Infectious Diseases** will be of interest to readers of the journal or to anyone who wishes to reach across the aisle between art and science.

Variably Protease-Sensitive Prionopathy, a Unique **Prion Variant with Inefficient** Transmission Properties

Abigail B. Diack,[1] Diane L. Ritchie,[1] Alexander H. Peden, Deborah Brown, Aileen Boyle, Laura Morabito, David Maclennan, Paul Burgoyne, Casper Jansen, Richard S. Knight, Pedro Piccardo, James W. Ironside,[1] and Jean C. Manson[1]

Variably protease-sensitive prionopathy (VPSPr) can occur in persons of all codon 129 genotypes in the human prion protein gene (*PRNP*) and is characterized by a unique biochemical profile when compared with other human prion diseases. We investigated transmission properties of VPSPr by inoculating transgenic mice expressing human *PRNP* with brain tissue from 2 persons with the valine-homozygous (VV) and 1 with the heterozygous methionine/valine codon 129 genotype. No clinical signs or vacuolar pathology were observed in any inoculated mice. Small deposits of prion protein accumulated in the brains of inoculated mice after challenge with brain material from VV VPSPr patients. Some of these deposits resembled microplaques that occur in the brains of VPSPr patients. Comparison of these transmission properties with those of sporadic Creutzfeldt-Jakob disease in the same lines of mice indicated that VPSPr has distinct biological properties. Moreover, we established that VPSPr has limited potential for human-to-human transmission.

Human prion diseases, also called transmissible spongiform encephalopathies, are a group of rare and inevitably fatal neurodegenerative diseases. Prion diseases are unique in that they occur as idiopathic (sporadic), familial, and acquired disorders. The sporadic form of Creutzfeldt-Jakob disease (sCJD) accounts for >80% of all human prion diseases. Six subtypes of sCJD have been classified according to the prion protein (PrP) genotype at codon 129 (methionine [M]/M, M/valine [V], VV) and the biochemical profile of the protease-resistant core of the abnormal disease-specific PrP (PrP^{res}) (PrP^{res} type 1 or PrP^{res} type 2A or 2B) (*1*,*2*). Experimental transmission of brain tissue from patients of these 6 different sCJD subtypes into 3 transgenic mouse lines expressing different human prion protein gene *PRNP* sequences (coding for 129MM, MV, and VV) has identified 4 distinct strains of the CJD agent (*3*).

In 2008, a novel prion disease, initially referred to as protease-sensitive prionopathy, was reported in 11 patients who had been referred to the National Prion Disease Pathology Surveillance Center (Cleveland, OH, USA) during May 2002–January 2006. All 11 patients were of the *PRNP* codon 129VV genotype, and postmortem examination of brain tissues showed that the patients had a spongiform encephalopathy (*4*). As with patients with sCJD, these patients had no mutations in the *PRNP* coding region, and no risk factors for the development of iatrogenic CJD were identified among the patients. The defining feature of this group of patients was the unusual biochemical properties of the abnormal PrP in the brain. Compared with the biochemical properties of PrP^{res} in sCJD, the PrP^{res} in VPSPr was found to be much less resistant to protease digestion. VPSPr PrP^{res} shows a faint ladder-like appearance of protease-resistant fragments on Western blot and a prominent low–molecular weight fragment of ≈8 kDa. The neuropathologic features in this group were also unusual, in particular, the accumulation of microplaques within the cerebellum and thalamus, which stained intensely for PrP.

Since the original description of those 11 cases, 19 additional cases have been reported, including some in patients of the *PRNP* codon 129MM and 129MV genotypes (*5*–*7*). Although case numbers remain low, the prevalence

Author affiliations: The Roslin Institute, University of Edinburgh, Easter Bush, Scotland, UK (A.B. Diack, D. Brown, A, Boyle, L. Morabito, D. Maclennan, P. Burgoyne, J.C. Manson); School of Clinical Sciences, University of Edinburgh, Edinburgh, Scotland, UK (D.L. Ritchie, A.H. Peden, R.S. Knight, J.W. Ironside); Food and Drug Administration, Rockville, Maryland, USA (P. Piccardo); and University Medical Centre Utrecht, Utrecht, the Netherlands (C. Jansen)

DOI: http://dx.doi.org/10.3201/eid2012.140214

[1]These authors contributed equally to this article.

of this novel prion disease appears to vary according to the codon 129 genotype of affected persons: 62% of reported cases have been detected in persons of the *PRNP* codon 129VV genotype. In comparison, 17% of sCJD cases and only 12% of the general white population are of the *PRNP* codon 129VV genotype (*8*,*9*). Subsequent studies showed differences between the 3 codon 129 genotypes in protease digestion sensitivity of the abnormal PrP in the brain. This difference in protease sensitivity has resulted in the condition being renamed variably protease-sensitive prionopathy (VPSPr) (*10*).

The presence of PrP^{res} in VPSPr suggests that PrP plays a central role in the disease process. However, the relationship between different forms of PrP and prion disease has not been established. It is possible that the protease-sensitive and the truncated forms of the abnormal PrP may contribute to the unique neuropathology of VPSPr and may also influence the potential for transmission of disease to other persons.

Human-to-human transmission of prion diseases is of great concern for public health reasons (*11*–*13*). The use of gene-targeted transgenic mice expressing human PrP enables the direct comparison of transmission properties by using well-defined strains of sCJD and variant CJD (vCJD). Moreover, this system enables the prediction of disease transmission between persons and has been used extensively to predict the potential for human-to-human spread of sCJD and vCJD (*3*,*14*–*16*). In this study, we challenged human PrP–expressing transgenic mice with brain tissue from 3 persons with VPSPr and directly compared the data with those from previous sCJD transmission experiments in these mouse lines. Thus, we determined whether any biological similarities exist between these apparently different prion diseases. Furthermore, these transmissions enabled an assessment of the potential for human-to-human transmission of VPSPr.

Methods

Human Tissues

Frozen brain tissues from 3 patients with VPSPr were investigated in this transmission series. Tissues analyzed were obtained from 2 patients who originated from the United Kingdom: 1 patient had the *PRNP* codon 129VV genotype (patient UK-VV), and the other had the 129MV genotype (patient UK-MV). The third patient originated from the Netherlands and had the *PRNP* codon 129VV genotype (patient NL-VV). The clinical, neuropathologic and PrP biochemical features of these cases have been described in detail elsewhere (*5*,*6*,*17*). Patient details for the 3 cases, including age, sex, neuropathologic features, and PrP^{res} type, are summarized in Table 1. As reference standards in Western blot experiments, we used frozen brain tissues in which the 8-kDa and the 2A PrP^{res} types were readily detectable; the tissues were from patients with typical UK cases of sCJD (subtypes MM1, MM2, VV1, and VV2) and from another UK patient (codon 129VV) with VPSPr.

Consent and ethical approval for the retention and use of these materials for research was obtained by the Lothian NHS Board Research Ethics Committee (Reference: LREC/2000/4/157). Material was sourced through The Edinburgh Brain Bank (Scotland, UK).

Gray matter–enriched frontal cortex tissue samples (≈250 mg) had been obtained at autopsy from each of the 3 persons in our study. The samples were homogenized at a 10% (wt/vol) concentration in sterile physiologic saline and stored at –20°C until use. Before being inoculated into mice, the homogenates were further diluted to a 1% (wt/vol) concentration in sterile physiologic saline.

Experimental Animals

Mice from 3 lines of transgenic mice expressing human PrP (designated HuMM, HuMV, and HuVV, according to the *PRNP* codon 129 genotype) were challenged in this transmission series (*15*). Mice were anesthetized and inoculated intracerebrally with 20 μL of a 1% brain homogenate. Beginning on postinoculation day 100, the mice were scored on a weekly basis for clinical signs of neurologic disease, as described by Fraser and Dickinson (*18*). Mice were humanely killed at the clinical endpoint for prion disease or at the end of the animal's full life span. Incubation periods were calculated as the number of days between brain-tissue inoculation and the clinical endpoint, when mice showed unequivocal neurologic disease. In the absence of an incubation period, the survival time (in days) was calculated. Brains were removed from the mice postmortem and sagittally sectioned; half of the brain was snap-frozen for biochemical analysis, and the other half was fixed in 10% formal saline for histologic analysis. These animal experiments were approved by The Roslin Institute's (University of Edinburgh) Animal Welfare and Ethical Review Committee and conducted according to the regulations of the UK Home Office Animals (Scientific Procedures) Act 1986.

Scoring of Vacuolation

Mouse brains for histologic analysis were fixed in formal saline for a minimum of 48 h before being immersed in 96% formic acid for 1.5 h to reduce the titer of the infectious agent. Brains were trimmed coronally into 5 standard rostrocaudal levels, resulting in 5 brain slices. Tissues were then embedded in paraffin wax and cut into serial 5-μm sections. A single section from all inoculated mice was stained with hematoxylin and eosin to determine the presence and severity of disease-specific vacuolation in 9 standard gray

Table 1. Characteristics of patients with variably protease-sensitive prionopathy whose brain samples were selected for transmission studies*

Patient, sex	Age at death, y	Disease duration, mo	Clinical signs and symptoms	Neuropathologic features	PrP^{res} type
NL-VV, M†	57	20	Progressive dementia, spastic paraplegia, sensorimotor polyneuropathy	Mild to moderate spongiform change in basal ganglia, and cerebral and cerebellar cortices. Coarse granular deposits of PrP in cerebral cortex, basal ganglia, and thalamus. PrP microplaques present within molecular layer of cerebellar cortex	Faint ladder-like appearance of protease-resistant fragments with a prominent low–molecular weight fragment
UK-VV, F‡	59	42	Progressive dementia, emotional and obsessive behavior (early), very occasional myoclonus (late)	Mild to moderate spongiform change in basal ganglia, thalamus, and cerebral and cerebellar cortices. Widespread granular accumulations of PrP in all brain regions. PrP microplaques present within molecular layer of cerebellar cortex	Faint, ladder-like appearance of protease-resistant fragments with a prominent low–molecular weight fragment
UK-MV, M§	76	12	Forgetfulness, visuospatial perceptual problems, difficulties walking, action tremor, akinetic mutism	Spongiform change most prominent in the frontal cortex. PrP microplaques, synaptic and granular accumulations of PrP restricted to cerebral cortex, basal ganglia, and thalamus. Diffuse Lewy body and tau pathology observed, with amyloid-β plaques and a widespread amyloid angiopathy	Faint ladder-like appearance of protease-resistant fragments including a low–molecular weight fragment

*PrP, prion protein; PrP^{res}, protease-resistant isoform of the disease-specific PrP.
†NL-VV, patient from the Netherlands who was homozygous for valine at codon 129 of the PrP gene (*PRNP*). Case report, Jansen et al. (*6*).
‡UK-VV, patient from the United Kingdom who was homozygous for valine at *PRNP* codon 129. Case report, Head et al. (*5*).
§UK-MV, patient from the United Kingdom who was heterozygous for methionine/valine at *PRNP* codon 129. Case report, Head et al. (*17*).

matter regions and 3 white matter regions, a protocol referred to as lesion profiling (*18*).

Immunohistochemistry

Immunohistochemical analysis for PrP was performed by using 4 PrP monoclonal antibodies that recognize different residues of the PrP: 1) 3F4/epitope: aa 109–112 (Cambridge Bioscience, Cambridge, UK); 2) 12F10/epitope: aa 142–160 (Bioquote Ltd, York, UK); 3) 6H4/epitope: aa 144–152 (Prionics AG, Schlieren, Switzerland); and 4) monoclonal antibody KG9/aa140–180 (TSE Resource Centre, The Roslin Institute). In brief, 5-μm paraffin-embedded tissue sections were autoclaved at 121°C in distilled water for 10 min and then immersed in 96% formic acid for 10 min. Sections were immersed in proteinase K solution (5 μg/mL) for 10 min and then blocked for 20 min in normal rabbit serum, after which they were incubated overnight at room temperature with the primary antibodies (3F4, 5 μg/mL; 6H4, 500 ng/mL; 12F10, 30 ng/mL; and KG9, 40 ng/mL). After overnight incubation, sections were incubated for 1 h in an anti-mouse biotinylated antibody (Jackson ImmunoResearch Laboratories, Inc., West Grove, PA, USA), and then immunolabeling was completed by using a VECTASTAIN Elite ABC Kit (Vector Laboratories, Burlingame, CA, USA). Staining was then visualized by using 3,3′-diaminobenzidine chromogen.

The presence of gliosis was assessed by incubating tissue sections with Polyclonal Rabbit Anti-Cow Glial Fibrillary Acidic Protein (Dako, Ely, UK) for 1 h at room temperature. Sections were then incubated for 1 h at room temperature with an anti-rabbit biotinylated antibody (Jackson ImmunoResearch Laboratories, Inc.) before the immunolabeling was completed by using a VECTASTAIN Elite ABC Kit. Staining was then visualized by using 3,3′-diaminobenzidine chromogen.

Thioflavin-S Visualization

Paraffin-embedded tissue sections were immersed in hematoxylin solution for 1 min and rinsed in running water before being immersed in Scott's tap water for 30 s. Sections were then immersed in 1% Thioflavin-S (Sigma, Gillingham, UK) for 5 min, followed by 3 dips in 70% alcohol. Tissue sections were then rinsed well in water and mounted.

Biochemical Studies of Brain Samples

The method we used for studying brain tissues was based on our previous Western blotting technique (*19*). For analysis, 10% (wt/vol) brain tissue homogenates were prepared by homogenization of brain material in 9 volumes (wt/vol) of Tris-buffered saline, pH 7.6, containing 0.5% Nonidet P40 and 0.5% sodium deoxycholate. Aliquots of the cleared 10% brain homogenates were subjected to limited proteolysis by digestion with proteinase K (50 μg/mL) for 1 h at 37°C. The reaction was terminated by the addition of Pefabloc SC (Roche, Burgess Hill, UK) to a final concentration of 1 mM/L. Proteinase K–treated and non–proteinase K–treated samples (5 μL) were analyzed by Western blot. Polyacrylamide gel electrophoresis and Western blotting were performed by using NuPAGE Novex 10% Bis-Tris Protein Gels, 1.0 mm, (Life Technologies, Paisley, UK) as previously described (*19*). The gel

electrophoresis time was abbreviated to retain low–molecular mass proteins (*5*,*6*). The proteins were transferred onto Hybond-P PVDF membrane (GE Healthcare Life Sciences, Amersham, UK). Immunodetection of PrP was carried out by using monoclonal antibody 3F4 (Millipore, Watford, UK) at a final concentration of 75 ng/mL for 1 h. For comparison, immunodetection of PrP on proteinase K–treated extracts was carried out by using monoclonal antibody 1E4 (provided by J. Langeveld) at a final concentration of 1 μg/mL (*6*). The secondary antibody was ECL Anti-mouse IgG, peroxidase-linked species-specific F(ab′)2 fragment (from sheep) (GE Healthcare Life Sciences), used at a concentration of 1/25,000 for 1 h. Amersham ECL Prime Western Blotting Detection Reagent (GE Healthcare Life Sciences) was used for detection of proteins. The blots were exposed to ECL Hyperfilm (GE Healthcare Life Sciences) for various amounts of time or were analyzed by using the ChemiDoc XRS+ System with Image Lab Software (Bio-Rad, Hemel Hempstead, UK).

Results

Biochemical Analysis of Brain Tissue from VPSPr Patients

We performed Western blot analysis on extracts of homogenates prepared from brain samples from all 3 VPSPr patients. For comparison, we ran these extracts alongside extracts of homogenates prepared from brain samples from 4 sCJD patients (sCJD subtypes MM1, MM2, VV1, and VV2) representing each of the 4 distinct strains of sCJD agent, as identified by transmission to transgenic mice (*3*). Western blotting was performed with and without proteinase K digestion by using the PrP antibody 3F4 (Figure 1). In the absence of proteinase K digestion, extracts from the 3 VPSPr patients showed a similar relative load of PrP when compared with extracts from sCJD patients (Figure 1, panel B). After the sCJD and VPSPr extracts were digested with proteinase K, their biochemical profiles and PrP^{res} loads differed (Figure 1, panel A). The biochemical profile of the extracts prepared from brain tissue from patients UK-VV and NL-VV VPSPr showed a single low–molecular weight fragment (<10 kDa), characteristic of VPSPr. In the extract from the UK-MV case, this low–molecular weight fragment was detected in addition to a faint ladder-like pattern of PrP^{res} fragment.

Increased sensitivity in the detection of PrP fragments by Western blotting using the monoclonal antibody 1E4 has been reported in cases of VPSPr (*4*,*10*). In this study, a direct comparison of the detection sensitivity of 2 PrP antibodies (monoclonal antibodies 1E4 and 3F4) was carried out by Western blot by using brain homogenate from all 3 VPSPr patients in the transmission series. Consistent with our previous findings (*5*,*6*), we found no increase in the PrP detection sensitivity by using 1 antibody or the other (Figure 2).

Absence of Clinical Disease and Vacuolar Pathology

No evidence of clinical disease with vacuolar pathology was observed in any of the 133 mice inoculated in this transmission series (Table 2). Furthermore, no vacuolar

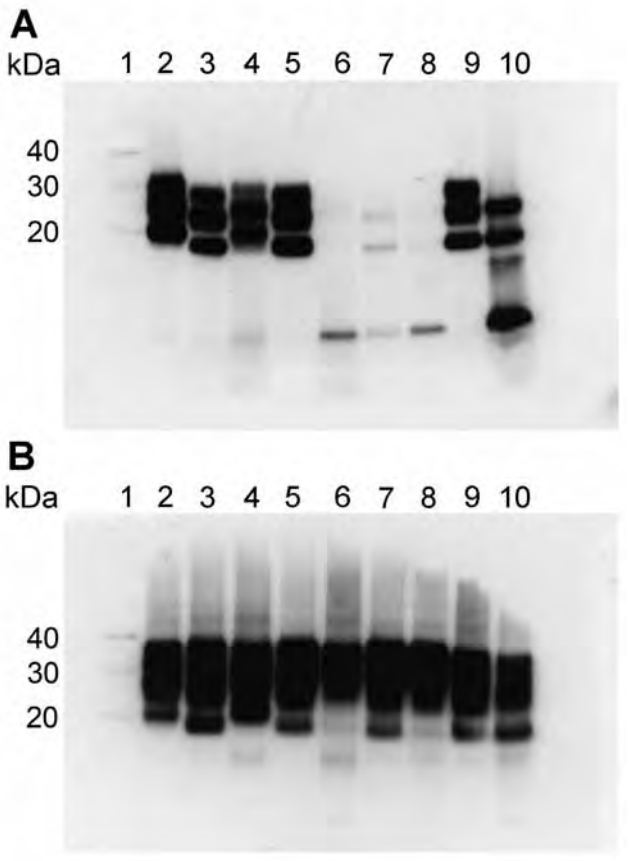

Figure 1. Western blot analysis of protease-resistant isoforms of PrP (PrP^{res}) in extracts of frontal cortex tissue prepared from postmortem samples from 4 persons with sCJD and from 3 persons with VPSPr whose brain samples were used for experimental transmission studies in transgenic mice. Results are shown for extracts treated (A) and not treated (B) with proteinase K. All lanes were loaded with 5.0 μL of 10% (wt/vol) brain homogenate, except lanes 9 and 10 in (A), which were loaded with 1.5 μL and 20.0 μL, respectively. Blots were probed with Anti-Prion Protein Antibody monoclonal antibody 3F4 (Millipore, Watford, UK). Lane 1, molecular weight marker (sizes indicated at left in kDa); lane 2, sCJD subtype MM1; lane 3, sCJD subtype MM2; lane 4, sCJD subtype VV1; lane 5, sCJD subtype VV2; lane 6, VPSPr UK-VV; lane 7, VPSPr UK-MV; lane 8, VPSPr NL-VV; lane 9, diagnostic reference sample (sCJD subtype VV2); lane 10, diagnostic reference sample (VPSPr VV). MM, homozygous for methionine; MV, heterozygous for methionine/valine; NL-VV, patient from the Netherlands who had VPSPr and the codon 129VV genotype; sCJD, sporadic Creutzfeldt-Jakob disease; UK-VV and UK-MV, patients from the United Kingdom who had VPSPr and the codon 129VV and 129MV genotypes, respectively; VPSPr, variably protease-sensitive prionopathy; VV, homozygous for valine.

pathology was observed in any of the asymptomatic mice in the study. Clinical neurologic signs were observed on a few occasions without pathologic confirmation of prion disease, suggesting a nontransmissible spongiform encephalopathy condition related to the age of the mice in the study.

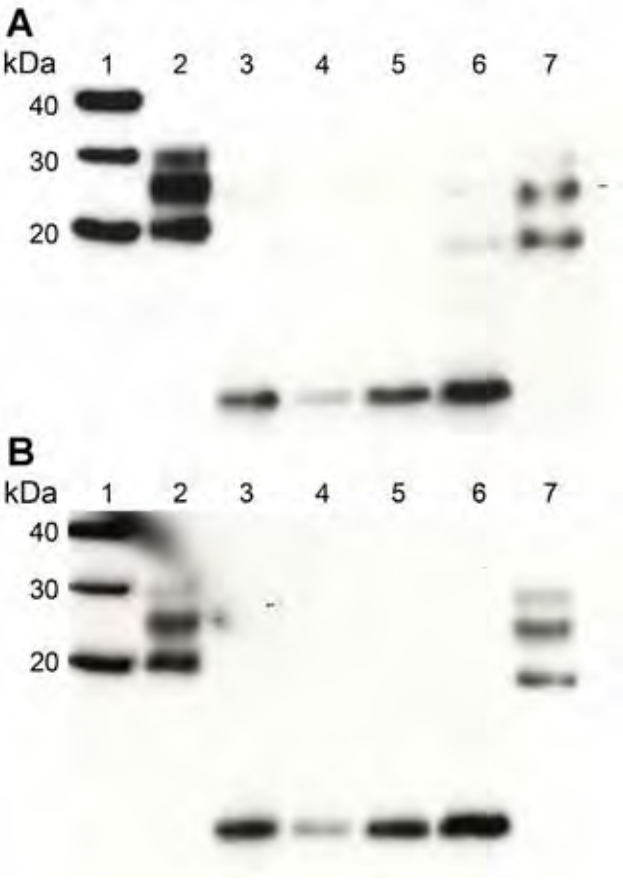

Figure 2. Western blot analysis of PrP^{res} in extracts of frontal cortex tissue prepared from postmortem samples from 2 persons with sCJD (subtypes MM1 and VV2) and the 3 persons with VPSPr whose brain samples were used for experimental transmission studies in transgenic mice (patients NL-VV, UK-VV, and UK-MV). Extracts from another patient who had VPSPr of UK origin (codon 129VV genotype) was also included on the blot (lane 6). Duplicate blots were probed with the following monoclonal antibodies: Anti-Prion Protein Antibody monoclonal antibody 3F4 (Millipore, Watford, UK) (A) and 1E4 (provided by J. Langeveld) (B). The 2 antibodies detected PrP^{res} equally well in extracts from persons with sCJD or with VPSPr. All lanes were loaded with 5 μL of a 10% (wt/vol) brain homogenate. Brain homogenates were analyzed after digestion with Proteinase K. Lane 1, molecular weight marker (sizes indicated at left in kDa); lane 2, sCJD MM1; lane 3, VPSPr UK-VV; lane 4, VPSPr UK-MV; lane 5, VPSPr NL-VV; lane 6, additional VPSPr of UK origin; lane 7, sCJD VV2. MM, homozygous for methionine; PrP^{res}, protease-resistant isoform of the disease-specific prion protein; NL-VV, patient from the Netherlands who had VPSPr and the codon 129VV genotype; sCJD, sporadic Creutzfeldt-Jakob disease; UK-VV and UK-MV, patients from the United Kingdom who had VPSPr and the codon 129VV and 129MV genotypes, respectively; VPSPr, variably protease-sensitive prionopathy; VV, homozygous for valine.

Minimal PrP Deposition in Restricted Brain Regions

Immunohistochemical analysis for PrP in mice challenged with brain homogenate prepared from VPSPr patient UK-MV showed no evidence of PrP accumulation within the brain of inoculated mice. Immunohistochemical analysis for PrP in mice challenged with homogenate prepared from the brain of patient NL-VV showed PrP accumulation in 7 of 14 HuVV and 3 of 15 HuMV transgenic mice, but no PrP deposition was found in the HuMM mice (Table 2). PrP deposits were detected most frequently with the PrP antibodies 6H4 and 3F4 and less frequently with antibodies KG9 and 12F10. This differential labeling is similar to that reported in human cases of VPSPr and may be related to the conformation of VPSPr-associated PrP and the availability of the epitopes that the antibodies detect (*5*,*17*,*20*). The pattern of PrP accumulation was limited to small, often numerous, focal plaque-like deposits located within the corpus callosum and the stratum oriens and stratum lacunosum moleculare of the hippocampus and parallel to the lateral ventricle (Figure 3, panels A–C). Sections treated with Thioflavin-S confirmed that these plaque-like deposits in the corpus callosum and its vicinity were composed of amyloid (Figure 3, panel D).

In mice challenged with a homogenate prepared from the brain of patient UK-VV, 5 of 14 HuVV, 2 of 14 HuMV, and 1 of 15 HuMM mice showed evidence of PrP deposits (Table 2). HuVV and HuMV mice showed PrP deposits similar to those found in the mice challenged with extract prepared from the brain of patient NL-VV, with 1 exception: a single HuVV mouse showed plaque-like accumulations and a pattern of intensely stained, small, round granules surrounded by fine target-like punctate staining within the CA3 region of the hippocampus and hippocampal fissure (Figure 4, panels A–C). The larger granular deposits resembled the microplaque accumulations found within the molecular layer of the cerebellum (Figure 4, panel D), hippocampal formation, basal ganglia, and thalamus in humans with VPSPr (*5*). The PrP-positive granules within the hippocampus stained most intensely with antibodies 3F4 and 12F10 and less intensely with antibodies KG9 and 6H4; this finding was similar to that observed in brains of patients with VPSPr (*5*,*6*,*17*) (Figure 4).

No PrP^{res} Detected by Biochemical Analysis

Western blot analysis was performed on frozen brain tissue from 6 HuVV mice challenged with brain homogenate from VPSPr patient UK-VV. Immunohistochemistry results showed that 4 of the 6 mice had small, plaque-like deposits within the corpus callosum, and 1 of the 4 mice also had microplaque-like deposits in the hippocampus.

Table 2. Results of intracerebral inoculation of brain tissue homogenates from 3 patients with variably protease-sensitive prionopathy into 3 lines of human transgenic mice*

Brain inoculum source, mouse line†	No. mice positive/no. total			Mean no. PrP plaque–like deposits (range)¶
	Clinical signs of prion disease‡	Vacuolar degeneration‡	PrP deposition§	
UK-VV				
HuMM	0/15	0/15	1/15	0#
HuMV	4/15	0/15	2/14	5 (2–8)
HuVV	0/14	0/14	5/14	10 (1–17)
UK-MV				
HuMM	1/15	0/15	0/15	0
HuMV	1/15	0/15	0/15	0
HuVV	0/15	0/15	0/15	0
NL-VV				
HuMM	0/15	0/15	0/15	0
HuMV	0/15	0/15	3/15	8 (1–15)
HuVV	0/14	0/14	7/14	3 (2–4)

*HuMM, HuMV, and HuVV, transgenic mice expressing the different forms of the human PrP gene (i.e., those homozygous for methionine [MM] or valine [VV] or heterozygous for methionine and valine [MV]); PrP, prion protein.
†Brain inoculum was prepared from postmortem samples from persons with variably protease-sensitive prionopathy. NL-VV, patient from the Netherlands who had the PrP codon 129VV genotype; UK-MV, patient from the United Kingdom who had the PrP codon 129MV genotype; UK-VV, patient from the United Kingdom who had the PrP codon 129VV genotype.
‡In mice with a positive score for clinical signs of a prion disease and a negative score for vacuolar pathology, the neuropathologic assessment was considered definitive.
§A positive score for PrP pathology was given to mice showing PrP deposition in the brain with at least 1 of the 4 PrP antibodies used in the immunohistochemical analysis.
¶The number of plaque-like deposits was counted per mouse, and results are given as mean (range) for each genotype.
#Mouse showed evidence of PrP deposition in a tumor.

Neuropathologic examination of the remaining 2 mice showed no evidence of transmission. Four noninoculated HuVV mice were included as negative controls. No disease-specific banding was observed in any of the mice (data not shown); this finding is consistent with the extremely low levels of PrP deposition detected by immunohistochemistry.

Astrocytic Reactivity Associated with a Single Transmission

HuVV mice were examined for evidence of astrocytic gliosis. In mice showing only plaque-like deposits of PrP, there was no association between astrocytosis and PrP deposition and no evidence of reactive astrocytosis (Figure 5). In contrast, in the HuVV mice inoculated with brain homogenate from patient UK-VV, a single mouse showed reactive astrocytosis in the vicinity of the microplaque-like deposits (Figure 5). This HuVV mouse is the same mouse that showed evidence of plaque-like and microplaque-like deposits similar to those found in humans with VPSPr.

Discussion

The inoculation of homogenates prepared from the brains of 3 patients with VPSPr (UK-MV, UK-VV and NL-VV) into transgenic mice expressing the different forms of the human PrP gene has resulted in very

Table 3. Results of intracerebral inoculation of brain tissue homogenates from 4 patients with different subtypes of the sporadic form of Creutzfeldt-Jakob disease into 3 lines of human transgenic mice*

Brain inoculum source, mouse line†	No. mice positive/no. total		
	Clinical signs of prion disease	Vacuolar degeneration	PrP deposition
MM1			
HuMM	10/13	13/13	13/13
HuMV	9/14	14/14	14/14
HuVV	8/16	13/16	14/16
MM2			
HuMM	0/16	0/16	0/15
HuMV	0/18	0/18	2/18
HuVV	0/17	0/17	3/17
VV1			
HuMM	0/16	0/16	2/16
HuMV	2/14	9/14	1/14
HuVV	2/14	7/14	7/14
VV2			
HuMM	4/18	6/18	15/17
HuMV	1/15	5/15	12/14
HuVV	13/16	16/16	15/15

*Data adapted from Bishop et al. (*3*). HuMM, HuMV, and HuVV, transgenic mice expressing the different forms of the human PrP gene (i.e., those homozygous for methionine [MM] or valine [VV] or heterozygous for methionine and valine [MV]). PrP, prion protein.
†Brain inoculum was prepared from postmortem samples from persons who had the MM1, MM2, VV1, or VV2 subtype of sporadic Creutzfeldt-Jakob disease.

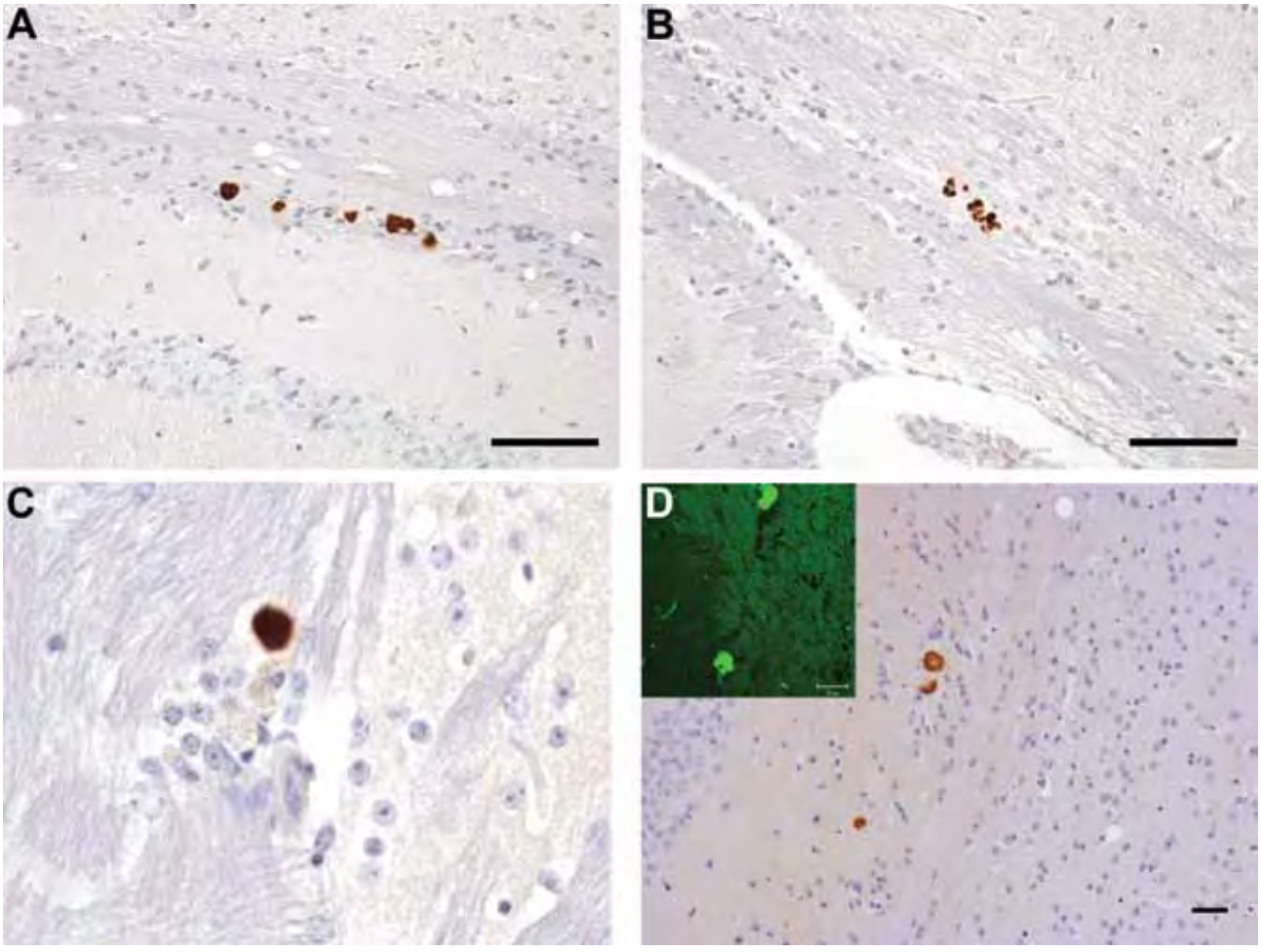

Figure 3. Neuropathology in transgenic mice following inoculation with brain homogenate prepared from a postmortem sample from a person with VPSPr. Numerous PrP-labeled plaque-like deposits within the corpus callosum of HuVV (A) and HuMV (B) mice inoculated with brain homogenate from patient UK-VV. C) A single small PrP-labeled plaque in the stratum oriens of the hippocampus following experimental challenge with brain homogenate from patient NL-VV. D) PrP-labeled plaque-like-deposits in the corpus callosum of a HuVV mouse inoculated with brain homogenate from patient UK-VV; inset: Thioflavin-S (Sigma, Gillingham, UK) staining of amyloid, viewed under ultraviolet light in a HuVV mouse challenged with brain homogenate from patient UK-VV. HuVV and HuMV, transgenic mice expressing human PrP gene sequence coding for the valine-homozygous and methionine/valine-heterozygous codon 129 genotypes, respectively; NL-VV and UK-VV, patients from the Netherlands and United Kingdom, respectively, who had VPSPr and the valine-homozygous codon 129 genotype; PrP, prion protein; VPSPr, variably protease-sensitive prionopathy. Scale bars indicate 25 μm.

different transmission properties when compared with those of previously characterized sCJD strains (*3*). No clinical disease or vacuolar pathology was observed in any of the mice. The only evidence for transmission of disease was the neuropathologic finding of abnormal PrP accumulation in the form of microplaque-like and granular deposits in the hippocampus and subventricular areas of the brain. These results contrast considerably with those observed with sCJD in the same HuMM/HuMV/HuVV mouse lines (*3*). Sporadic CJD transmits to all these mouse lines, as indicated by evidence of clinical signs and vacuolar pathology and/or PrP deposition, and the combination of these transmission properties has resulted in the identification of 4 strains of sCJD (*3*). Of the 4 sCJD strains, subtype VV2 showed the greatest frequency of clinical (13/16), vacuolar (16/16), and pathologic (15/15) signs of prion disease following inoculation into HuVV mice (Table 3) (*3*). In contrast, the MM2 subtype of sCJD showed the least transmission to the mice: no mice had clinical signs or vacuolar pathology, and only 3 of 17 HuVV and 2 of 18 HuMV mice had evidence of PrP deposition in the form of small punctate deposits in the thalamus (Table 3) (*3*). Although this transmission of the MM2 subtype might be considered similar to that of VPSPr, the PrP deposition differed in form and brain area compared with the deposition observed in the VPSPr studies. Unlike sCJD, which shows transmission from patients with all 3 codon 129 genotypes, only VPSPr from

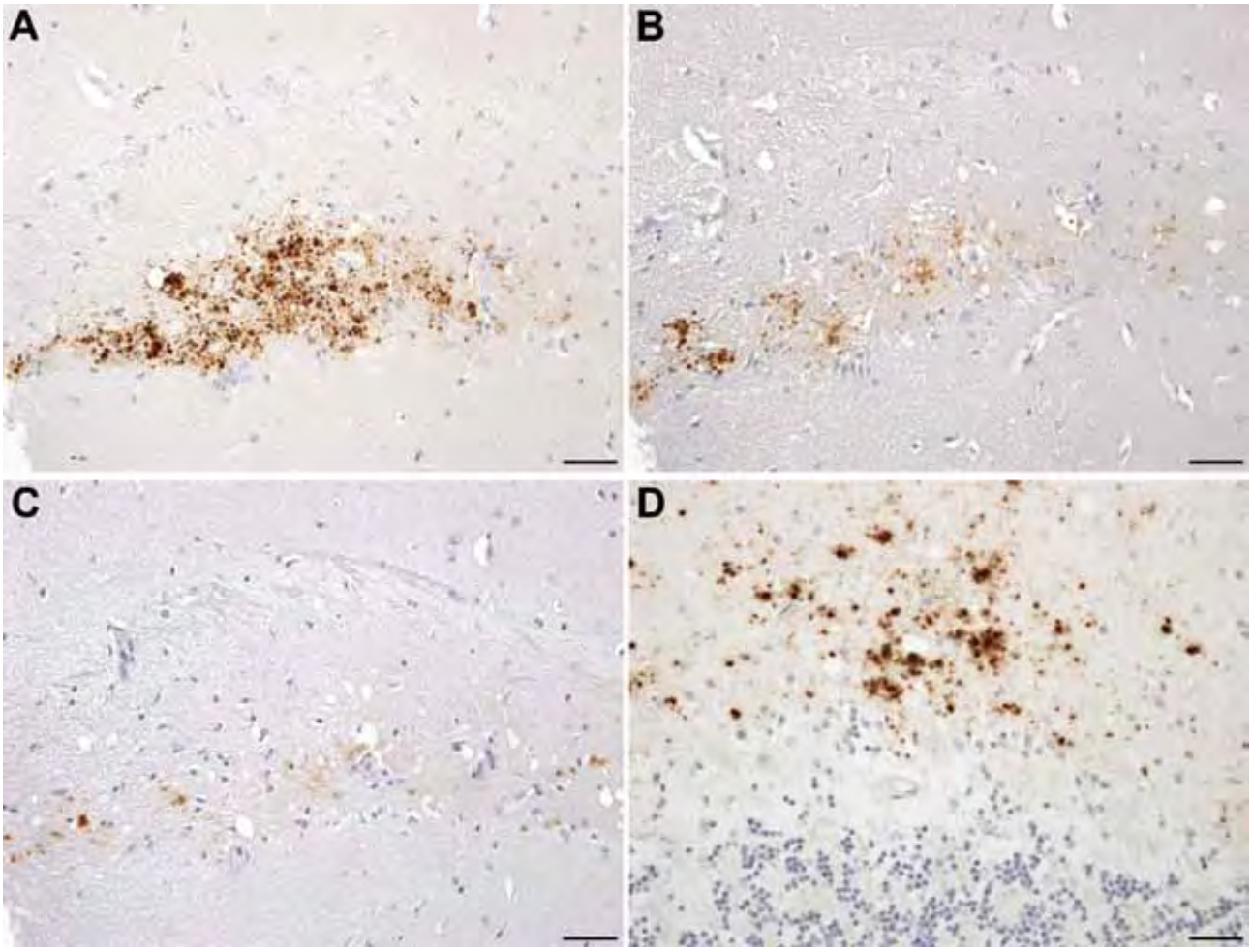

Figure 4. Neuropathology in transgenic mice following inoculation with brain homogenate prepared from a postmortem sample from a person with VPSPr. A–C) Immunohistochemistry for the PrP, showing small granular and microplaque-like deposits within the CA3 region of the hippocampus of a HuVV mouse challenged with VPSPr inoculum prepared from patient UK-VV. Differential staining was observed in this mouse by using the following PrP antibodies: Purified (3F4) (Cambridge Bioscience, Cambridge, UK) (A); Prion Protein Monoclonal Antibody (12F10) (Bioquote Ltd, York, UK) (B); and mAb 6H4 (Prionics AG, Schlieren, Switzerland) (C). D) Molecular layer of the cerebellum of a person with VPSPr, showing microplaque deposits stained with monoclonal antibody 3F4. HuVV, transgenic mouse expressing human PrP gene sequence coding for the valine-homozygous codon 129 genotype; PrP, prion protein; UK-VV, patient from the United Kingdom who had VPSPr and the valine-homozygous codon 129 genotype; VPSPr, variably protease-sensitive prionopathy. Scale bars indicate 25 μm.

the 2 patients with codon 129VV provided evidence of transmission. This low rate of transmission may be due to low levels of PrP^{res} in the brain homogenates that were inoculated, or it could be that the PrP genotype plays a role in transmission of disease.

Prion disease propagation involves the aggregation of abnormal PrP that acts as a template for further aggregation within the brain, a process termed seeding (*21*,*22*). The spread of PrP within the brain appears to occur in cell-to-cell fashion in well-defined neuroanatomic pathways (*23*), the mechanisms of which are yet to be elucidated despite extensive studies. Prion diseases have the potential to be transmissible between persons, a fact that raises public health concerns, particularly regarding vCJD. Assessing the risk for transmission is a challenge because of the varied nature of prion diseases and conflicting evidence over the mechanisms of transmission. Risk assessment is made even more complicated by the existence of prion disease models in which negligible amounts of PrP^{res} are associated with high infectivity titers in vivo (*24*) and also of models in which PrP^{res} in the form of amyloid plaques develops in the absence of clinical disease or spongiform changes (*25*).

It could be argued that the observation of small plaque-like amyloid deposits in the brains of mice with no neurologic signs of disease after the inoculation of brain homogenates prepared from patients with VPSPr does not indicate disease transmission. Instead, the deposits could

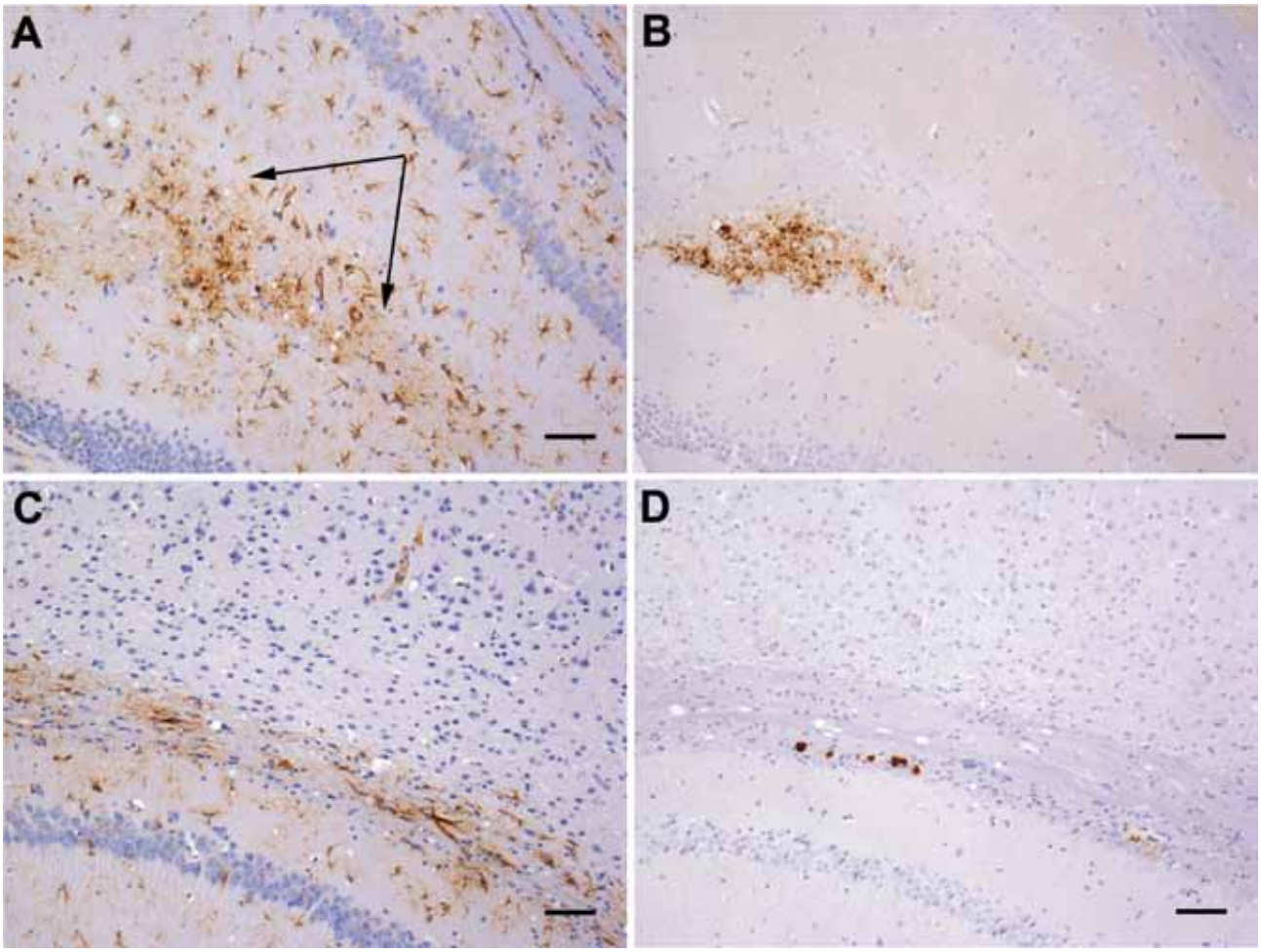

Figure 5. Gliosis in transgenic mice following inoculation with brain homogenate prepared from a postmortem sample from a person with variably protease-sensitive prionopathy. A) Immunohistochemical staining for GFAP in the hippocampus of a HuVV mouse showing microplaque-like deposits. Arrows indicate areas of reactive astrocytosis. B) A serial section from the same HuVV mouse immunolabeled for PrP by using monoclonal antibody (Purified [3F4], Cambridge Bioscience, Cambridge, UK). C) Immunohistochemical staining for GFAP in the hippocampus of a HuVV mouse showing plaque-like deposits. No reactive astrocytosis is seen in the vicinity of plaques. D) A serial section from the same HuVV mouse immunolabeled for PrP by using monoclonal antibody 3F4. GFAP, glial fibrillary acid protein; HuVV, transgenic mouse expressing human PrP gene sequence coding for the valine-homozygous codon 129 genotype; PrP, prion protein. Scale bars indicate 50 μm.

indicate an amyloid seeding phenomenon akin to that observed following the experimental inoculation of primates with brain tissue from patients with Alzheimer disease (*26*). In those experiments, amyloid β seeding occurred in the primate brain in the absence of any clinical signs. Precedence of this phenomenon in prion disease has been set by Piccardo et al. (*27*), who showed similar results in a mouse model system of prion disease transmission. However, in our study, the brain of 1 mouse exhibited intensely stained, small, round granules within the hippocampus in addition to the plaque-like deposits (Figure 4). These small granules are reminiscent of the microplaques found in brain tissue of humans with VPSPr (*4*,*5*). Furthermore, with 4 PrP antibodies, the microplaque deposits in the mouse brain showed the same pattern of differential immunoreactivity as that in the brain of patients with VPSPr (*5*,*6*,*17*). Moreover astrocytosis in the vicinity of the microplaques was also observed in this mouse (Figure 5). This type of astrocytic response is observed in all our model systems of transmissible prion disease, but is absent from the nontransmissible forms of PrP (i.e., amyloid plaques in absence of clinical disease), suggesting that this single mouse may represent a transmission of infection rather than a consequence of seeding of inoculum (*25*,*28*). Second passage in the same mouse line will be required to prove this interpretation, but such a study will take an additional 3 years to complete.

Although understanding the mechanisms of transmission is an interesting facet of this study, our primary finding is that VPSPr is capable of transmission to transgenic mice

expressing PrP, albeit at extremely low levels compared with those of other transmissible prion diseases (e.g., sCJD and vCJD). We demonstrate that VPSPr is a disease with biological properties distinct from those of sCJD and with a limited, but not negligible, potential for infectivity. These results demonstrate the importance of continuing surveillance to fully uncover the growing spectrum of human prion diseases.

Acknowledgments

We thank the animal facility staff of the Neurobiology Division, The Roslin Institute for animal care and clinical scoring; the pathology staff of The Roslin Institute for sectioning the mouse brains and assessing levels of transmissible spongiform encephalopathy vacuolation; Dorothy Kisielewski for technical support; Mark Head for advice on the biochemistry of VPSPr; Annemieke Rozemuller for collaboration and neuropathologic expertise; and Jan Langeveld for providing the 1E4 antibody.

The Edinburgh Brain Bank, a source of material for this study, is supported by the Medical Research Council (MR/L016400/1). This report is independent research commissioned and funded by the Department of Health Policy Research Programme (Strain typing and investigation of transmission potential of unusual cases of CJD).

Dr Diack is a research fellow at The Roslin Institute, University of Edinburgh. Her research interests focus on prion diseases, in particular, strain characterization and modeling of human diseases.

References

1. Parchi P, Saverioni D. Molecular pathology, classification, and diagnosis of sporadic human prion disease variants. Folia Neuropathol. 2012;50:20–45.
2. Jansen C, Parchi P, Capellari S, Ibrahim-Verbaas CA, Schuur M, Strammiello R, et al. Human prion diseases in the Netherlands (1998–2009): clinical, genetic and molecular aspects. PLoS ONE. 2012;7:e36333. http://dx.doi.org/10.1371/journal.pone.0036333
3. Bishop MT, Will RG, Manson JC. Defining sporadic Creutzfeldt-Jakob disease strains and their transmission properties. Proc Natl Acad Sci U S A. 2010;107:12005–10. http://dx.doi.org/10.1073/pnas.1004688107
4. Gambetti P, Dong Z, Yuan J, Xiao X, Zheng M, Alshekhlee A, et al. A novel human disease with abnormal prion protein sensitive to protease. Ann Neurol. 2008;63:697–708. http://dx.doi.org/10.1002/ana.21420
5. Head MW, Knight R, Zeidler M, Yull H, Barlow A, Ironside JW. A case of protease sensitive prionopathy in a patient in the UK. Neuropathol Appl Neurobiol. 2009;35:628–32. http://dx.doi.org/10.1111/j.1365-2990.2009.01040.x
6. Jansen C, Head MW, van Gool WA, Baas F, Yull H, Ironside JW, et al. The first case of protease-sensitive prionopathy (PSPr) in the Netherlands: a patient with an unusual GSS-like clinical phenotype. J Neurol Neurosurg Psychiatry. 2010;81:1052–5. http://dx.doi.org/10.1136/jnnp.2009.175646
7. Rodríguez-Martínez AB, Garrido JM, Zarranz JJ, Arteagoitia JM, de Pancorbo MM, Atares B, et al. A novel form of human disease with a protease-sensitive prion protein and heterozygosity methionine/valine at codon 129: case report. BMC Neurol. 2010;10:99. http://dx.doi.org/10.1186/1471-2377-10-99
8. Parchi P, Giese A, Capellari S, Brown P, Schulz-Schaeffer W, Windl O, et al. Classification of sporadic Creutzfeldt-Jakob disease based on molecular and phenotypic analysis of 300 subjects. Ann Neurol. 1999;46:224–33. http://dx.doi.org/10.1002/1531-8249(199908)46:2<224::AID-ANA12>3.0.CO;2-W
9. Nurmi MH, Bishop M, Strain L, Brett F, McGuigan C, Hutchison M, et al. The normal population distribution of *PRNP* codon 129 polymorphism. Acta Neurol Scand. 2003;108:374–8. http://dx.doi.org/10.1034/j.1600-0404.2003.00199.x
10. Zou WQ, Puoti G, Xiao X, Yuan J, Qing L, Cali I, et al. Variably protease-sensitive prionopathy: a new sporadic disease of the prion protein. Ann Neurol. 2010;68:162–72. http://dx.doi.org/10.1002/ana.22094
11. Wroe SJ, Pal S, Siddique D, Hyare H, Macfarlane R, Joiner S, et al. Clinical presentation and pre-mortem diagnosis of variant Creutzfeldt-Jakob disease associated with blood transfusion: a case report. Lancet. 2006;368:2061–7. http://dx.doi.org/10.1016/S0140-6736(06)69835-8
12. Peden AH, Head MW, Ritchie DL, Bell JE, Ironside JW. Preclinical vCJD after blood transfusion in a *PRNP* codon 129 heterozygous patient. Lancet. 2004;364:527–9. http://dx.doi.org/10.1016/S0140-6736(04)16811-6
13. Llewelyn CA, Hewitt PE, Knight RSG, Amar K, Cousens S, Mackenzie J, et al. Possible transmission of variant Creutzfeldt-Jakob disease by blood transfusion. Lancet. 2004;363:417–21. http://dx.doi.org/10.1016/S0140-6736(04)15486-X
14. Bishop MT, Diack AB, Ritchie DL, Ironside JW, Will RG, Manson JC. Prion infectivity in the spleen of a *PRNP* heterozygous individual with subclinical variant Creutzfeldt-Jakob disease. Brain. 2013;136:1139–45. http://dx.doi.org/10.1093/brain/awt032
15. Bishop MT, Hart P, Aitchison L, Baybutt HN, Plinston C, Thomson V, et al. Predicting susceptibility and incubation time of human-to-human transmission of vCJD. Lancet Neurol. 2006;5:393–8. http://dx.doi.org/10.1016/S1474-4422(06)70413-6
16. Bishop MT, Ritchie DL, Will RG, Ironside JW, Head MW, Thomson V, et al. No major change in vCJD agent strain after secondary transmission via blood transfusion. PLoS ONE. 2008;3:e2878. http://dx.doi.org/10.1371/journal.pone.0002878
17. Head MW, Lowrie S, Chohan G, Knight R, Scoones DJ, Ironside JW. Variably protease-sensitive prionopathy in a *PRNP* codon 129 heterozygous UK patient with co-existing tau, α synuclein and Aβ pathology. Acta Neuropathol. 2010;120:821–3. http://dx.doi.org/10.1007/s00401-010-0766-y
18. Fraser H, Dickinson AG. The sequential development of the brain lesion of scrapie in three strains of mice. J Comp Pathol. 1968;78:301–11. http://dx.doi.org/10.1016/0021-9975(68)90006-6
19. Yull HM, Ritchie DL, Langeveld JP, van Zijderveld FG, Bruce ME, Ironside JW, et al. Detection of type 1 prion protein in variant Creutzfeldt-Jakob disease. Am J Pathol. 2006;168:151–7. http://dx.doi.org/10.2353/ajpath.2006.050766
20. Kovács GG, Head MW, Hegyi I, Bunn TJ, Flicker H, Hainfellner JA, et al. Immunohistochemistry for the prion protein: comparison of different monoclonal antibodies in human prion disease subtypes. Brain Pathol. 2002;12:1–11. http://dx.doi.org/ 10.1111/j.1750-3639.2002.tb00417.x
21. Prusiner SB. Novel proteinaceous infectious particles cause scrapie. Science. 1982;216:136–44. http://dx.doi.org/10.1126/science.6801762
22. Jucker M, Walker LC. Pathogenic protein seeding in Alzheimer disease and other neurodegenerative disorders. Ann Neurol. 2011;70:532–40. http://dx.doi.org/10.1002/ana.22 615
23. Scott JR, Davies D, Fraser H. Scrapie in the central nervous system: neuroanatomical spread of infection and *Sinc* control of pathogenesis. J Gen Virol. 1992;73:1637–44. http://dx.doi.org/10.1099/0022-1317-73-7-1637
24. Barron RM, Campbell SL, King D, Bellon A, Chapman KE, Williamson RA, et al. High titers of transmissible spongiform

encephalopathy infectivity associated with extremely low levels of PrP^{Sc} in vivo. J Biol Chem. 2007;282:35878–86. http://dx.doi.org/10.1074/jbc.M704329200
25. Piccardo P, King D, Telling G, Manson JC, Barron RM. Dissociation of prion protein amyloid seeding from transmission of a spongiform encephalopathy. J Virol. 2013;87:12349–56. http://dx.doi.org/10.1128/JVI.00673-13
26. Baker HF, Ridley RM, Duchen LW, Crow TJ, Bruton CJ. Experimental induction of β-amyloid plaques and cerebral angiopathy in primates. Ann N Y Acad Sci. 1993;695:228–31. http://dx.doi.org/10.1111/j.1749-6632.1993.tb23057.x
27. Piccardo P, Manson JC, King D, Ghetti B, Barron RM. Accumulation of prion protein in the brain that is not associated with transmissible disease. Proc Natl Acad Sci U S A. 2007;104:4712–7. http://dx.doi.org/10.1073/pnas.0609241104
28. Plinston C, Hart P, Chong A, Hunter N, Foster J, Piccardo P, et al. Increased susceptibility of human-PrP transgenic mice to bovine spongiform encephalopathy infection following passage in sheep. J Virol. 2011;85:1174–81. http://dx.doi.org/10.1128/JVI.01578-10

Address for correspondence: Jean C. Manson, The Roslin Institute and Royal (Dick) School of Veterinary Studies, University of Edinburgh, Easter Bush, Midlothian, Scotland. EH25 9RG; email: jean.manson@roslin.ed.ac.uk

Geographic Divergence of Bovine and Human Shiga Toxin–Producing *Escherichia coli* O157:H7 Genotypes, New Zealand[1]

Patricia Jaros, Adrian L. Cookson, Donald M. Campbell, Gail E. Duncan, Deborah Prattley, Philip Carter, Thomas E. Besser, Smriti Shringi, Steve Hathaway, Jonathan C. Marshall, and Nigel P. French

Shiga toxin-producing *Escherichia coli* (STEC) O157:H7 is a zoonotic pathogen of public health concern worldwide. To compare the local and large-scale geographic distributions of genotypes of STEC O157:H7 isolates obtained from various bovine and human sources during 2008–2011, we used pulsed-field gel electrophoresis and Shiga toxin–encoding bacteriophage insertion (SBI) typing. Using multivariate methods, we compared isolates from the North and South Islands of New Zealand with isolates from Australia and the United States. The STEC O157:H7 population structure differed substantially between the 2 islands and showed evidence of finer scale spatial structuring, which is consistent with highly localized transmission rather than disseminated foodborne outbreaks. The distribution of SBI types differed markedly among isolates from New Zealand, Australia, and the United States. Our findings also provide evidence for the historic introduction into New Zealand of a subset of globally circulating STEC O157:H7 strains that have continued to evolve and be transmitted locally between cattle and humans.

Shiga toxin–producing *Escherichia coli* (STEC) O157:H7 and related non-O157 STEC strains are zoonotic pathogens that can cause severe gastrointestinal illness in humans; clinical signs and symptoms of disease range from diarrhea and hemorrhagic colitis to life-threatening hemolytic uremic syndrome (*1*,*2*). Ruminants, asymptomatic carriers of STEC, shed the pathogen in their feces, and are considered a primary source of foodborne and environmental outbreaks of STEC infection in humans (*3*).

The incidence of STEC infections in New Zealand has been among the highest in the world. In 2012, a total of 147 clinical STEC cases (3.3 cases/100,000 population) were notified, of which 142 were confirmed (*4*). Consistent with observations in previous years, the predominant serotype among the confirmed cases was O157:H7 (83.8%; 119/142). STEC became a notifiable disease in New Zealand in 1997, and since then, the annual number of notifications has increased steadily (*4*). Although the spatial distribution of STEC cases in New Zealand suggests an association with farming and other rural activities, limited epidemiologic data are available on the transmission pathways of STEC from cattle to humans.

The objectives of this research were to 1) compare the population structure and geographic distribution of different genotypes of STEC O157:H7 isolates from bovine and human sources in New Zealand; 2) assess evidence for localized transmission of STEC from cattle to humans in New Zealand; and 3) compare the genotype distribution of isolates from New Zealand with those from Australia, the predominant historic source of imported New Zealand cattle (*5*), and the United States. To investigate the molecular divergence of isolates, we used 2 molecular typing methods: Shiga toxin–encoding bacteriophage insertion (SBI) typing and pulsed-field gel electrophoresis (PFGE) profiling. Although PFGE can provide an indication of genomic similarities, it cannot provide a reliable measure of

Author affiliations: Massey University, Palmerston North, New Zealand (P. Jaros, D. Prattley, J.C. Marshall, N.P. French); AgResearch Ltd, Palmerston North (A.L. Cookson); Ministry for Primary Industries, Wellington, New Zealand (D.M. Campbell, G.E. Duncan, S. Hathaway); Institute of Environmental Science and Research Ltd, Porirua, New Zealand (P. Carter); and Washington State University, Pullman, Washington, USA (T.E. Besser, S. Shringi)

DOI: http://dx.doi.org/10.3201/eid2012.140281

[1]Preliminary results from this study were presented at the New Zealand Veterinary Association Conference; June 16–20, 2014, Hamilton, New Zealand.

genetic relatedness of isolates, and the visual assessment of bands on an agarose gel to create PFGE profiles can result in misclassification bias (*6*). By using 2 methods and by examining the concordance between them, we could use the combined genotyping datasets to assess structuring and patterns of diversity among STEC O157:H7 isolates of bovine and human origin in New Zealand.

Methods

Human Isolates and Data

For the study, we obtained a total of 363 human-derived STEC O157:H7 isolates from the national Enteric Reference Laboratory (Institute of Environmental Science and Research Ltd, Upper Hutt, New Zealand) along with the associated PFGE profiles (restriction enzyme *Xba*I) and geographic data (North or South Island, New Zealand, and region on each island). Of the 363 isolates, 278 (76.6%) originated from the North Island. The isolates were from patients with clinical STEC infections that occurred in New Zealand during 2008–2011 and represent 71.3% (363/509) of the STEC O157 cases notified and confirmed during 2008–2011 (*7*). The cases were reported as sporadic cases or household clusters (i.e., 2 STEC infections in the same home) and were not associated with confirmed foodborne outbreaks.

Bovine Fecal Isolates and Data

Fecal STEC O157:H7 isolates (n = 40) used in the study had been collected from cattle in previous studies conducted at beef slaughter plants in New Zealand during 2008 (*8*) and 2009–2011 (*9*). Data regarding the origin (North or South Island, region, farm location) of the cattle and the virulence profiles of the isolates (virulence genes *ehx*A, *eae*, *stx*1, *stx*2, and subtype *stx*2c) were available. The isolates were retrieved from feces samples collected from 26 calves and 14 adult cattle, most (80.0%, 32/40) of which were from the North Island; the animals originated from 35 farms.

Bovine Meat Isolates and Data

Bovine meat isolates (n = 235) used in the study were from test samples used in routine mandatory testing at beef-processing plants across New Zealand during 2008–2011. Only PFGE profiles (*Xba*I) of STEC O157:H7 isolates were available for this study; the profiles were obtained from the national Enteric Reference Laboratory. Geographic data associated with meat-sample location (regions in North and South Islands) were obtained from the Ministry for Primary Industries (Wellington, New Zealand). Most isolates (85.5%, 201/235) originated from beef-slaughtering plants in the North Island. Virulence profiles of the isolates were not available.

PCRs for Detection of Virulence Genes

All human isolates were regrown on Columbia Horse Blood Agar (Fort Richard Laboratories, Auckland, New Zealand). Bacterial DNA was extracted from 5 colonies by using 2% Chelex beads solution (Chelex 100 Resin; Bio-Rad, Richmond, CA, USA) and analyzed in 2 PCR assays by using an automated real-time thermocycler (Rotor Gene 6200HRM; Corbett Research, Mortlake, NSW, Australia).

A multiplex PCR assay was performed using previously published primer sequences to detect the presence of virulence genes encoding for enterohemolysin (*ehx*A) (*10*), intimin (*eae*) (*10*), and Shiga toxins (*stx*1 and *stx*2) (*11*). Primers for detection of genes *stx*1 and *stx*2 did not differentiate between subtypes of toxins. The final 25-mL PCR reaction volume contained 2× PCR buffer (Express qPCR SuperMix; Invitrogen, Carlsbad, CA, USA), 2 μmol/L of each primer, 2.0 μL of DNA, and 2.5 μL of sterile water. The amplification program included an initial enzyme-activation step of 5 min at 94°C, which was followed by 40 cycles of, 20 s at 94°C, 20 s at 64°C, and 20 s at 72°C, followed in turn by a final extension of 5 min at 72°C. The PCR products were detected by electrophoresis using a 2% (wt/vol) agarose gel (Agarose low EEO; AppliChem, Darmstadt, Germany) and then stained with ethidium bromide and visualized under ultraviolet illumination.

*stx*2-positive isolates were further tested to determine whether the *stx*2 gene that was present was the genetic subtype *stx*2c. The *stx*2c gene was detected by using previously published primer sequences (*12*,*13*). The final 20-μL PCR reaction volume contained 2× PCR buffer (Express qPCR SuperMix; Invitrogen), 2 μmol/L of each primer, 2.0 μL of DNA, and 6.0 mL of sterile water. The PCR included an initial enzyme-activation step of 5 min at 94°C, followed by 35 cycles of 20 s at 94°C and 20 s at 55°C; no extensions were used. The amplified PCR product was detected as described above.

Molecular Typing Methods

All human and bovine fecal isolates were genotyped by using SBI typing (*12*,*13*); SBI typing is a multiplex PCR method for screening specific *stx*-associated bacteriophage insertion sites and *stx* genes (*stx*1 and genetic subtypes *stx*2a and *stx*2c of *stx*2). The characters A, W, Y, S and 1, 2a, 2c represent bacteriophage insertion sites *argW*, *wrbA*, *yehV*, *sbcB*, and Shiga toxin genes *stx*1, *stx*2a, *stx*2c (2 subtypes of *stx*2), respectively (*12*,*14*). All bovine fecal isolates were subtyped by using PFGE (*Xba*I) according to the standardized laboratory protocol published by PulseNet International (*15*). The SBI typing was completed at Washington State University, Pullman, Washington, USA.

Location of Work and Ethical Approval

This work was completed at the Molecular Epidemiology and Public Health Laboratory, Infectious Disease

Research Centre, Hopkirk Research Institute, Massey University, Palmerston North, New Zealand. The use of STEC isolates from clinical case-patients in New Zealand was approved by the Multi-region Ethics Committee, Wellington, New Zealand, on March 19, 2012; reference number MEC/11/04/043.

Data Management and Statistical Analysis

For initial analysis, SBI types were grouped into 4 categories of 3 predominant SBI types (AY2a, WY12a, and ASY2c/SY2c) and other, less common, SBI types (AS12c, AS2c, ASWY2c, ASY12c, ASY2a2c, AWY12a, AWY2a, SWY2c, and Y2c). SBI types SY2c and ASY2c were grouped together because both were relatively common and shared the same virulence gene profile.

Although bovine meat isolates were not SBI-typed, a close correlation between PFGE profile and SBI type was observed for the human samples (online Technical Appendix Figure 1, http://wwwnc.cdc.gov/EID/article/20/14/14-0281-Techapp1.pdf) and the bovine fecal samples (online Technical Appendix Figure 2). On the basis of the PFGE/SBI clusters, the most likely SBI type was inferred from the PFGE profiles for the meat isolates by taking the following approach. First, BioNumerics software version 6.6 (Applied Maths, Sint-Martens-Latem, Belgium) was used to compare PFGE profiles of human and bovine fecal isolates by conducting an UPGMA (unweighted pair group method with arithmetic mean) cluster analysis using the Dice similarity coefficient, with a band matching tolerance of 1%. Second, the UPGMA cluster analysis was applied on PFGE profiles of bovine meat isolates. The dominant SBI types in human and bovine fecal isolates were used to assign SBI-like types (AY2a, WY12a, and ASY2c/SY2c) to clusters with similar PFGE band patterns in bovine meat isolates.

χ^2 and Fisher exact test for count data were used to evaluate associations between island and SBI type (AY2a, WY12a, ASY2c/SY2c, and other SBI types) for bovine fecal, bovine meat, and human isolates; R software (http://www.r-project.org/) was used for statistical computing. p values for associations between SBI types and region and between SBI types and year for human and bovine meat isolates were computed by simulating 10^8 tables from the null hypothesis (independence) and comparing the results with the test statistic from the observed data.

Population differentiation among human and bovine meat isolates was assessed by using analysis of molecular variance (AMOVA) applied to haplotypes of isolates' PFGE profiles (generated in BioNumerics) using Arlequin software version 3.5.1.2 (http://cmpg.unibe.ch/software/arlequin3/). A multilevel hierarchy was used for the AMOVA model to assess population differentiation between island, between regions within island, and within regions. Regions with <5 isolates were excluded from the analysis. A matrix of pairwise F_{ST} values was computed by comparing the PFGE haplotype frequency distributions for each pair of regions (using Arlequin, version 3.5.1.2). F_{ST} is an index of population differentiation, measuring the variance between subpopulations relative to the total variance, and ranges from 0 (no divergence) to 1 (complete divergence). The computed pairwise F_{ST} matrix, representing genetic distances between the regional populations of STEC O157:H7, was illustrated graphically as a NeighborNet tree by using SplitsTree software version 4.12.6 (*16*).

To illustrate the molecular relatedness and genotypic clustering of isolates, we used Primer 6 software (http://www.primer-e.com/primer.htm) to link distance matrices of PFGE profiles of human and bovine meat isolates (generated in BioNumerics) with explanatory variables (SBI type and region) to create multidimensional scaling plots. Regions with <5 isolates were excluded from the analysis.

To assess the population structure of New Zealand isolates, we compared published frequency distributions of SBI types in 205 cattle and 79 human STEC O157:H7 isolates sourced from Australia and in 143 cattle and 179 human STEC O157:H7 isolates sourced from the United States (*17*) with frequency distributions of SBI types among bovine and human STEC O157:H7 isolates from New Zealand. To evaluate genetic similarities of human and bovine fecal isolates, we computed proportional similarity indices (PSI) based on the frequency distributions of SBI types in humans and cattle from all 3 countries. PSI is a similarity measure that estimates the area of congruence between 2 frequency distributions (*18*); measurements range from 0 (distributions with no common SBI types) to 1 (highest possible similarity between distributions). Bootstrapped 95% confidence intervals for PSI values were calculated according to the percentile method described by Efron and Tibshirani (*19*), using 2,000 iterations. No grouping of SBI types was applied for PSI calculations. To illustrate the international geographic divergence of isolates, we used differences in PSI values (1 – PSI) to construct a NeighborNet tree with SplitsTree software version 4.12.6.

Results

Genotype Diversity

All 403 human and bovine fecal isolates were positive for *ehx*A, *eae*, and *stx*2 (except 1 *ehx*A-negative human isolate); of these, 61 (15.1%) were also positive for *stx*1. The different virulence profiles of isolates, each represented by a dominant SBI type, are shown in Table 1. The predominant SBI types AY2a, WY12a, and ASY2c/SY2c accounted for 55.0% (22/40), 15.0% (6/40), and 22.5% (9/40) of the studied bovine fecal isolates, respectively. Similarly, in human isolates, SBI types AY2a, WY12a, and ASY2c/SY2c were detected in

Table 1. Virulence profiles and SBI types of Shiga toxin–producing *Escherichia coli* O157:H7 isolates obtained from humans and fecal samples from slaughterhouse cattle, New Zealand, 2008–2011*

Species,			Virulence genes†					SBI type	
no. isolates	NI	SI	*ehx*A	*eae*	*stx*2	*stx*2c	*stx*1	Dominant (no., %)	Other (no., %)
Bovine									
6	6	0	+	+	+	–	+	WY12a (6, 100.0)	–
10	2	8	+	+	+	+	–	ASY2c (7, 70.0), SY2c (2, 20.0)	AS2c (1, 10.0)
24	24	0	+	+	+	–	–	AY2a (22, 91.7)	AWY2a (2, 8.3)
Human									
51	43	9	+	+	+	–	+	WY12a (49, 96.2)	AWY12a (2, 3.8)
1	0	1	+	+	+	–	+	WY12a (1, 100.0)	–
94	54	40	+	+	+	+	–	ASY2c (69, 73.4), SY2c (15, 16.0)	SWY2c (3, 3.2), ASWY2c (2, 2.1), AS2c (2, 2.1), Y2c (2, 2.1), ASY2a2c (1, 1.1)
214	179	35	+	+	+	–	–	AY2a (210, 98.1)	AWY2a (4, 1.9)
3	2	1	+	+	+	+	+	ASY12c (2, 66.7)	AS12c (1, 33.3)

*NI, North Island of New Zealand; SBI, Shiga toxin–encoding bacteriophage insertion; SI, South Island of New Zealand; +, gene present; –, gene absent.
†*ehx*A gene encodes for enterohemolysin; *eae* gene encodes for intimin; *stx*2, primers for detection of this gene did not differentiate between subtypes of Shiga toxin type 2; *stx*2c gene encodes for Shiga toxin subtype 2c; *stx*1, primers for detection of this gene did not differentiate between subtypes of Shiga toxin type 1.

57.9% (210/363), 13.8% (50/363), and 23.1% (84/363) of the isolates, respectively. The distributions of AY2a, WY12a, ASY2c/SY2c, and other SBI types varied by year (p = 0.037) (Figure 1). On the basis of the genotype calibration of PFGE profiles of bovine meat isolates, SBI-like types AY2a, WY12a, and ASY2c/SY2c were prevalent in 64.7% (152/235), 23.4% (55/235), and 11.9% (28/235) of the isolates, respectively. Association between SBI-like type and year was marginally nonsignificant (p = 0.052).

Between-Island Comparisons

The distribution of SBI types observed differed between North and South Islands in bovine fecal and human isolates; SBI types AY2a and WY12a were more common in the North Island, and ASY2c/SY2c was more common in the South Island (Table 2). Similarly, a significant difference in the prevalence of SBI-like types between islands was observed in bovine meat isolates (Table 2).

Within-Island Comparisons

By using a 3-level hierarchy of island, region within island, and within region for the AMOVA model, we found that most of the molecular variation (>98%) resided between isolates within regions (on the basis of PFGE haplotypes). However, for the human isolates, a small but highly significant proportion of the molecular variation was estimated to be between regions within islands (1.03% variation, p<0.001); this finding provided evidence for highly localized geographic structuring. After we allowed for between region variation in the model, island was no longer

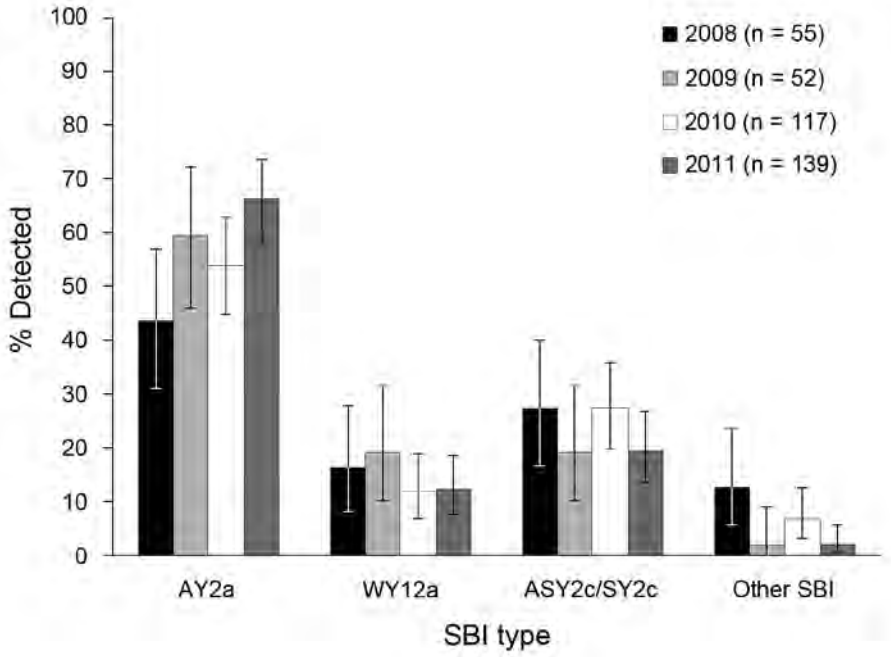

Figure 1. Proportional distributions, stratified by year, of Shiga toxin–encoding bacteriophage insertion (SBI) types AY2a, WY12a, and ASY2c/SY2c of 363 human Shiga toxin–producing *Escherichia coli* O157:H7 isolates from clinical case-patients in New Zealand, 2008–2011. Error bars indicate 95% CIs.

Table 2. Frequency distribution of predominant SBI genotypes of Shiga toxin–producing *Escherichia coli* O157:H7 isolates obtained from humans, bovine fecal samples, and bovine meat samples, New Zealand, 2008–2011*

Isolate type, SBI type	No. with SBI type/no. total (%) North Island	No. with SBI type/no. total (%) South Island	p value†
Human			
AY2a	175/278 (62.9)	35/85 (41.2)	<0.001
WY12a	41/278 (14.7)	9/85 (10.6)	
ASY2c/SY2c	49/278 (17.6)	35/85 (41.2)	
Other	13/278 (4.7)	6/85 (7.1)	
Bovine fecal			
AY2a	22/32 (68.8)	0/8	<0.001
WY12a	6/32 (18.8)	0/8	
ASY2c/SY2c	1/32 (3.1)	8/8 (100.0)	
Bovine meat			
AY2a-like	137/201 (68.2)	15/34 (44.1)	<0.001
WY12a-like	49/201 (24.4)	6/34 (17.6)	
ASY2c/SY2c-like	15/201 (7.5)	13/34 (38.2)	

*SBI, Shiga toxin–encoding bacteriophage insertion.
†Values refer to differences between frequency distributions of SBI types and North and South Islands (χ^2 and Fisher exact test).

a significant source of variation for the human isolates (p = 0.212). In contrast, a very small but significant amount of molecular variation was apparent between islands among the bovine meat isolates (0.38% variation, p = 0.017), but the proportion of variation between regions within islands was nonsignificant (0.34% variation, p = 0.121).

The population differentiation and geographic clustering of genotypes of STEC O157:H7 isolates from human cases and bovine meat samples from regions of both islands of New Zealand are illustrated in Figure 2. Consistent with the AMOVA results, we found evidence of within-island clustering of human isolates. Two main clusters were observed representing North and South Island regions, with the exception of Canterbury, which clustered with North Island regions, and Wellington, Taranaki, and Gisborne, which were North Island outliers. Among human cases, the highest population differentiation of genotypes of STEC O157:H7 isolates was observed between the regions of Wellington (15 isolates) and Gisborne (12 isolates) on the North Island (pairwise F_{ST} value of 0.071), followed by Wellington and Otago (10 isolates) (F_{ST} = 0.060); the isolates from Gisborne included 2 household clusters (2 human cases each). For bovine meat isolates, no obvious structuring was apparent; however, Auckland region (5 isolates) appeared as a strong North Island outlier. Consequently, the most distinct difference in genotypes was observed between the regions of Auckland and Otago (9 isolates) (F_{ST} = 0.060), followed by Auckland and Northland (26 isolates) (F_{ST} = 0.057).

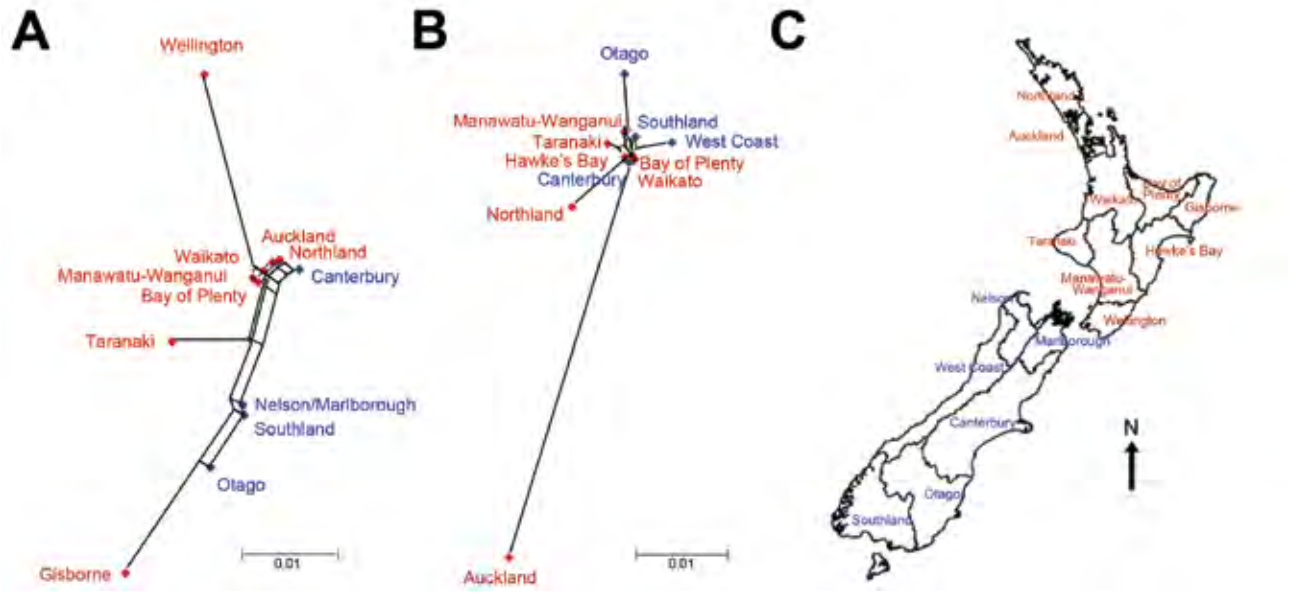

Figure 2. NeighborNet (*16*) trees showing population differentiation of Shiga toxin–producing *Escherichia coli* O157:H7 isolates from humans and cattle from different regions in the North Island (red) and the South Island (blue), New Zealand. A) Isolates from human case-patients (n = 355, 8 isolates excluded). B) Isolates from bovine meat samples (n = 233, 2 isolates excluded). C) Map of New Zealand showing different regions from which samples were collected. The distances indicate population differentiation measured as pairwise F_{ST} values.

The molecular relatedness between PFGE profiles of human isolates, considering SBI type and region of origin as explanatory variables, is shown in Figure 3. PFGE profiles showed genotypic clustering that was strongly associated with SBI types AY2a, WY12a, and ASY2c/SY2c, even after stratifying by island of origin (Figure 3, panels A, B). Clusters containing SBI type AY2a and ASY2c/SY2c were the predominant genotypes in the Taranaki and Gisborne regions, respectively, on the North Island (Figure 3, panel C); the association between SBI type and region of origin was statistically significant ($p<0.001$). A similar genotypic clustering of regions was observed in bovine meat isolates from the North and South Islands (online Technical Appendix Figure 3).

International Comparison

Within each country, similar frequencies of SBI types were observed in cattle and human cases, but there were distinct differences in the population structure of SBI types between countries (Figure 4). Bovine and human genotypes in New Zealand shared the highest similarity (PSI value 0.92, 95% CI 0.74–0.93), followed by those in Australia (PSI 0.69, 95% CI 0.57–0.79) and the United States (PSI 0.61, 95% CI 0.51–0.69) (online Technical Appendix Figure 4). The observed differences in proportional similarities of SBI types among isolates from cattle and humans in all 3 countries are shown in Figure 5.

Discussion

We assessed the molecular epidemiologic evidence for transmission of STEC from cattle to humans in New Zealand and the relationship between population structure and geography at multiple spatial scales. The molecular analysis of bovine and human STEC O157:H7 isolates showed a concordant geographic variation of genotypes (SBI types)

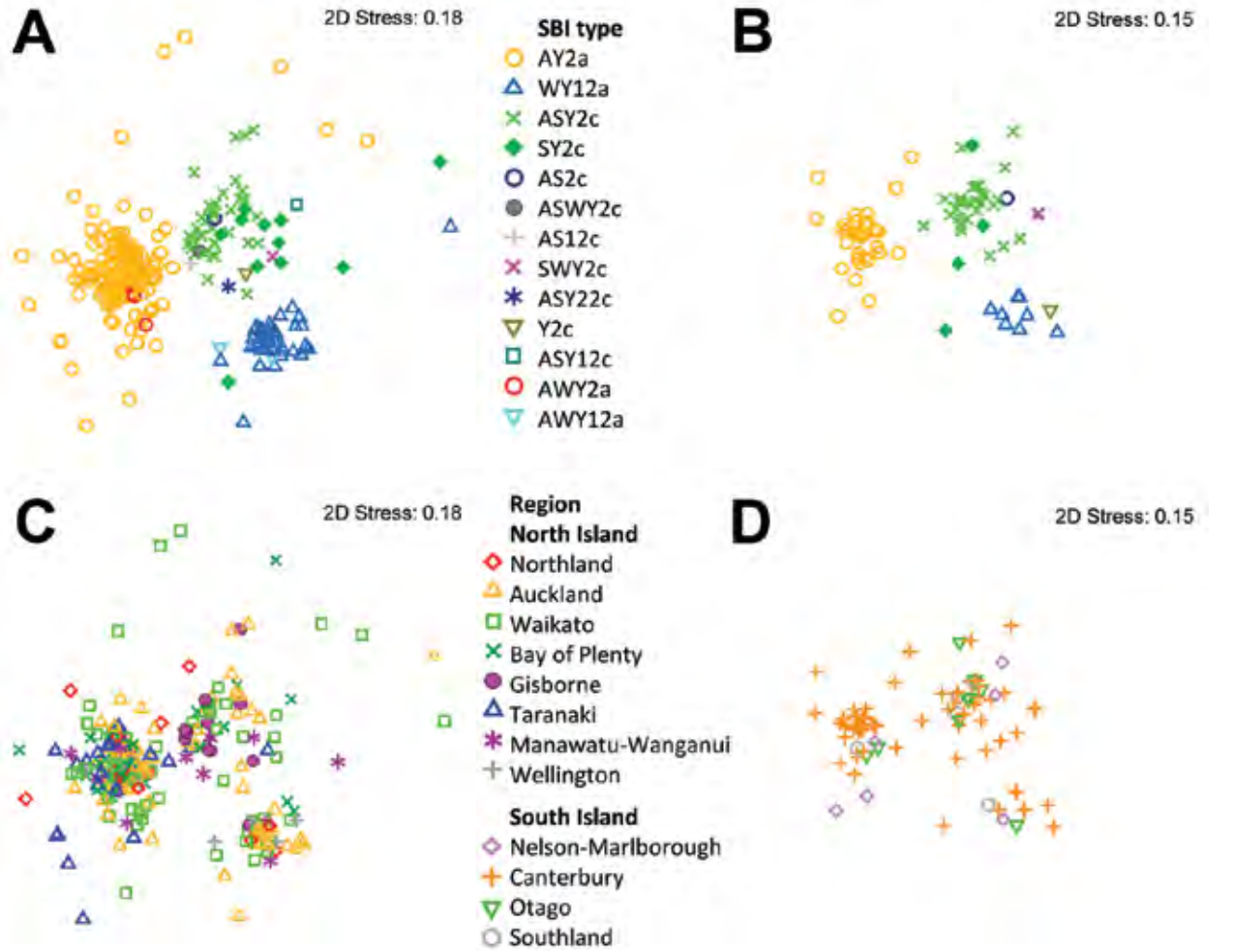

Figure 3. Multidimensional scaling plots showing the genotypic clustering of human Shiga toxin–producing *Escherichia coli* O157:H7 isolates originating from the North Island (n = 274, 4 isolates excluded) and the South Island (n = 81, 4 isolates excluded), New Zealand. The plots were determined on the basis of the isolates' pulsed-field gel electrophoresis profiles. Clusters associated with Shiga toxin–encoding bacteriophage insertion (SBI) types (A) and regions (C) for isolates from the North Island. Clusters associated with SBI types (B) and regions (D) for isolates from the South Island. 2D, 2 dimensional.

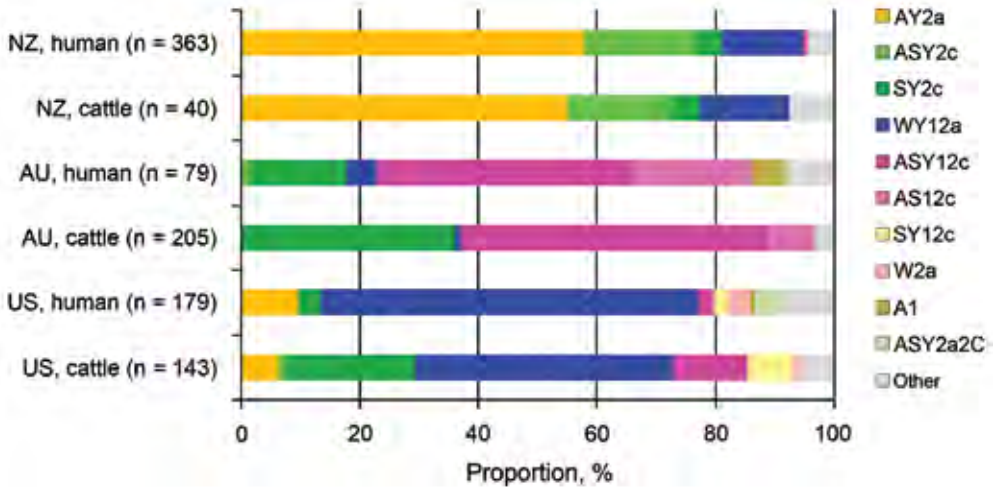

Figure 4. Proportional distributions of Shiga toxin–encoding bacteriophage insertion types of Shiga toxin–producing *Escherichia coli* O157:H7 isolates sourced from cattle and humans in New Zealand (NZ), Australia (AU), and the United States (US).

in both populations. In addition, there were marked differences between isolates from New Zealand's North and South Islands, a finding that is consistent with localized transmission of STEC between cattle and humans.

The evidence of localized transmission of STEC between cattle and humans in New Zealand has advanced our understanding of the epidemiology of sporadic STEC infections in the country and is consistent with environmental- or animal-associated sources of infection rather than more disseminated foodborne outbreaks (*20*). Measures to prevent direct contact with animal fecal material in the environment include the wearing of protective clothing, increased hand washing, and targeted education of the population at risk regarding possible sources of STEC infection.

The North and South Islands of New Zealand are separated by the Cook Strait, a geographic barrier of >20 km. This barrier might contribute to the island-associated differences in distribution of genotypes observed in this study, by restricting the movement of carrier animals between islands. Cattle populations on each island are large: ≈6.6 million on the North Island and ≈3.5 million on the South Island (*21*). Despite the islands' large cattle populations, the number of livestock moved between the islands (i.e., from farm to farm or farm to slaughter) is relatively low: ≈42,400 cattle from North to South Island, and ≈64,600 cattle from South to North Island per year (*22*). Thus, the movement of cattle probably has a limited influence on the distinct distribution of genotypes across both islands.

Although none of the bovine meat isolates were SBI typed, the PFGE data showed a strong island-associated distribution of bovine STEC O157:H7 genotypes, which was equivalent to the patterns observed in fecal isolates from cattle and humans. Bovine meat isolates were retrieved from carcass swab samples and bulk meat samples collected at beef-processing plants, so it could be hypothesized that fresh beef meat might be an exposure pathway for humans. However, although various food sources (including beef) were considered as potential risk factors during a nationwide prospective case-control study on sporadic STEC infections in humans, food was not identified as a major exposure pathway of infections in New Zealand (*20*).

Significant genetic variation was observed among human isolates at the regional level, indicating a more localized spatial clustering of STEC O157:H7 genotypes. Strong regional variation in the prevalence of zoonotic diseases has been observed previously in New Zealand. For example, there is marked regional variation in the distribution of serotypes in human cases of salmonellosis: *Salmonella enterica* ser. Brandenburg was associated with sheep and human infections in the southern regions of the South Island (*23*), whereas the wild bird–associated *S. enterica* ser. Typhimurium DT160 was distributed more evenly across the whole country (*24*). *S. enterica* ser. Brandenburg has not been found to be endemic in any other regions in New Zealand, and it is likely that the spatial pattern of disease is influenced by environmental factors, such as the presence and density of local maintenance hosts.

Cattle are considered the most likely maintenance host of STEC O157:H7, and the association between human cases and cattle density suggests that spillover from cattle to humans is the main pathway (*20*); however, overseas, the pathogen has frequently been isolated from sheep (*25–27*) and deer (*28*,*29*). Cookson et al. (*30*,*31*) identified STEC serotypes of public health concern in sheep from the lower North Island of New Zealand but did not isolate STEC O157:H7. No nationwide studies of sheep or deer have been undertaken in New Zealand, hence sheep cannot be ruled out as potential maintenance hosts for region-specific populations of STEC O157:H7.

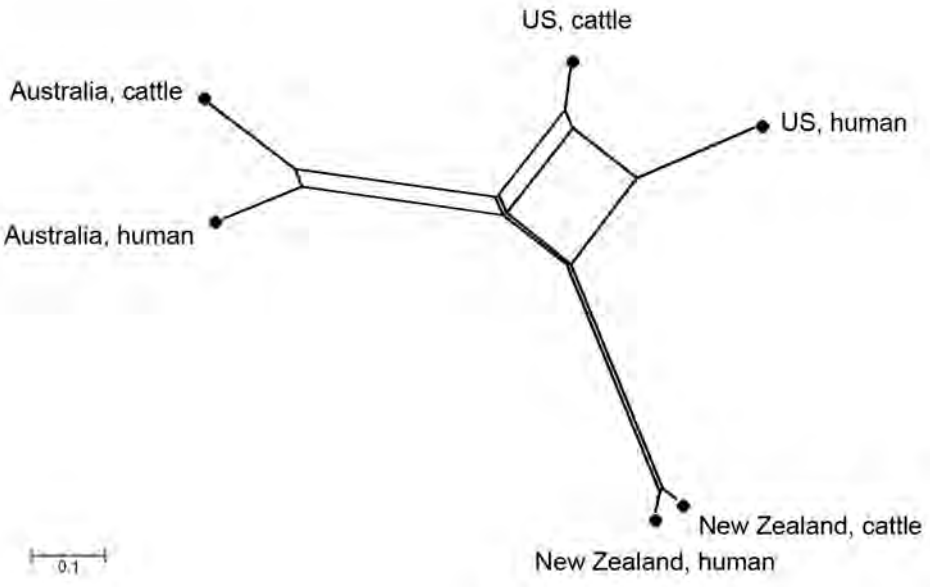

Figure 5. NeighborNet (*16*) tree showing geographic divergence of bovine and human Shiga toxin–producing *Escherichia coli* O157:H7 isolates sourced from New Zealand (40 cattle, 363 human), Australia (205 cattle, 79 human), and the United States (US) (143 cattle, 179 human). The distance indicates the difference in proportional similarity of Shiga toxin–encoding bacteriophage insertion types among the isolates.

The observed regional clustering of genotypes among human STEC O157:H7 isolates leads to another hypothesis: other, yet unidentified, hosts could be reservoir/maintenance hosts in the epidemiology of STEC, and cattle are possibly only serving as "bridging hosts" at the human–animal interface (*32*), transmitting STEC to humans. For example, starlings have been implicated as biologic vectors in the dissemination of STEC among dairy farms in Ohio, United States (*33*,*34*), indicating that wildlife might play a key role in the epidemiology and ecology of STEC.

A relatively high prevalence of SBI types AY2a and ASY2c was observed in human and bovine fecal isolates from New Zealand. These findings are in contrast to those from the Australian study by Mellor et al. (*17*), in which SBI type AY2a was not identified (0/284 isolates; $p<0.001$) and accounted for only 8.1% (26/322) of the isolates from the United States (human and cattle combined); SBI type ASY2c was prevalent in <1.0% of combined isolates in both countries. These differences in frequency distributions of SBI types indicate marked differences in the population structure of SBI types between countries. Australia and New Zealand are neighboring countries but separated by the Tasman Sea, a distance of ≈1,250 km. On the basis of historic data, Australia has been the predominant source of imported New Zealand cattle, mainly in the 19th century (*5*). Hence, the distinct geographic divergence of STEC O157:H7 genotypes between the 2 countries is somewhat puzzling and would suggest a limited historic introduction of STEC O157:H7 from Australia or elsewhere into New Zealand and a subsequent evolution in the New Zealand host population. Alternatively, the observed divergence of genotypes between Australia and New Zealand could be the result of genetic drift and/or selection driven by different environmental factors, such as climate, types of feed, husbandry systems, or animal genetics.

In this study, the highest PSI was observed between cattle and human isolates from New Zealand, followed by that between isolates from Australia and the United States. These findings provide evidence for a close association between populations of isolates from cattle and humans, which is consistent with the transmission of STEC from cattle to humans. This finding is in agreement with the national case–control study on clinical STEC cases in New Zealand, which identified variables related to beef and dairy cattle as major risk factors (*20*).

The molecular analysis of STEC O157:H7 isolates from cattle and persons with STEC infection revealed that prevalences of bovine and human isolates in the North Island were distinctly different from those of the South Island, suggesting localized transmission of STEC between cattle and humans. Furthermore, a distribution of STEC O157:H7 genotypes different from that observed overseas suggests a historic introduction of a subset of the globally circulating STEC O157:H7 strains into New Zealand.

Acknowledgments

We thank Muriel Dufour, Brent Gilpin, Kari Gobius, and Glen Mellor for their contributions and Charlotte Bolwell for very helpful comments on this manuscript.

This work was supported by the Meat Industry Association of New Zealand and the Ministry for Primary Industries.

Dr Jaros is a postdoctoral research fellow at the Molecular Epidemiology and Public Health Laboratory, Hopkirk Research Institute at Massey University. Her research interests include the molecular epidemiology of infectious diseases.

References

1. Karmali M, Petric M, Steele BT, Lim C. Sporadic cases of haemolytic-uraemic syndrome associated with faecal cytotoxin and cytotoxin-producing *Escherichia coli* in stools. Lancet. 1983;321:619–20. http://dx.doi.org/10.1016/S0140-6736(83)91795-6
2. Riley LW, Remis RS, Helgerson SD, McGee HB, Wells JG, Davis BR, et al. Hemorrhagic colitis associated with a rare *Escherichia coli* serotype. N Engl J Med. 1983;308:681–5. http://dx.doi.org/10.1056/NEJM198303243081203
3. Griffin PM, Tauxe RV. The epidemiology of infections caused by *Escherichia coli* O157:H7, other enterohemorrhagic *E. coli* and the associated hemolytic uremic syndrome. Epidemiol Rev. 1991;13:60–98.
4. Institute of Environmental Science and Research Ltd. Surveillance report. Notifiable and other diseases in New Zealand: annual report 2012 [cited 2013 Sep 10]. https://surv.esr.cri.nz/surveillance/annual_surveillance.php?we_objectID=3565.
5. Binney B, Biggs PJ, Carter PE, Holland BR, French NP. Quantification of historical livestock importation into New Zealand [cited 2014 Jun 15]. N Z Vet J. 2014. Epub 2014 May 28 http://dx.doi.org/10.1080/00480169.2014.914861
6. Davis MA, Hancock DD, Besser TE, Call DR. Evaluation of pulsed-field gel electrophoresis as a tool for determining the degree of genetic relatedness between strains of *Escherichia coli* O157:H7. J Clin Microbiol. 2003;41:1843–9. http://dx.doi.org/10.1128/JCM.41.5.1843-1849.2003
7. Institute of Environmental Science and Research Ltd. Public Health Surveillance. VTEC isolates [cited 2013 Dec 28]. https://surv.esr.cri.nz/enteric_reference/vtec_isolates.php
8. Irshad H, Cookson AL, Hotter G, Besser TE, On SLW, French NP. Epidemiology of Shiga toxin-producing *Escherichia coli* O157 in very young calves in the North Island of New Zealand. N Z Vet J. 2012;60:21–6. http://dx.doi.org/10.1080/00480169.2011.627063
9. Jaros P, Cookson AL, Prattley DJ, Campbell DM, Hathaway S, French NP. Shedding of *Escherichia coli* O157:H7 and O26 STEC by slaughter cattle in New Zealand. In: Abstracts of the annual meeting of the New Zealand Microbiological Society; Palmerston North, New Zealand; 2011 Nov 23–25. New Zealand Microbiological Society; 2011. p. 86.
10. Paton AW, Paton JC. Detection and characterization of Shiga toxigenic *Escherichia coli* by using multiplex PCR assays for stx_1, stx_2, *eaeA*, enterohemorrhagic *E. coli hlyA*, rfb_{O111}, and rfb_{O157}. J Clin Microbiol. 1998;36:598–602.
11. Sharma VK, Dean-Nystrom EA. Detection of enterohemorrhagic *Escherichia coli* O157:H7 by using a multiplex real-time PCR assay for genes encoding intimin and Shiga toxins. Vet Microbiol. 2003;93:247–60. http://dx.doi.org/10.1016/S0378-1135(03)00039-7
12. Shringi S, Schmidt C, Katherine K, Brayton KA, Hancock DD, Besser TE. Carriage of *stx2a* differentiates clinical and bovine-biased strains of *Escherichia coli* O157. PLoS ONE. 2012;7:e51572. http://dx.doi.org/10.1371/journal.pone.0051572
13. Besser TE, Shaikh N, Holt NJ, Tarr PI, Konkel ME, Malik-Kale P, et al. Greater diversity of Shiga toxin–encoding bacteriophage insertion sites among *Escherichia coli* O157:H7 isolates from cattle than in those from humans. Appl Environ Microbiol. 2007;73:671–9. http://dx.doi.org/10.1128/AEM.01035-06
14. Jung WK, Bono JL, Clawson ML, Leopold SR, Shringi S, Besser TE. Lineage and genogroup-defining single nucleotide polymorphisms of *Escherichia coli* O157:H7. Appl Environ Microbiol. 2013;79:7036–41. http://dx.doi.org/10.1128/AEM.02173-13
15. PulseNet International. Molecular typing, PFGE protocols [cited 2013 Dec 28]. http://www.pulsenetinternational.org/protocols/
16. Huson DH, Bryant D. Application of phylogenetic networks in evolutionary studies. Mol Biol Evol. 2006;23:254–67. http://dx.doi.org/10.1093/molbev/msj030
17. Mellor GE, Besser TE, Davis MA, Beavis B, Jung W, Smith HV, et al. Multilocus genotype analysis of *Escherichia coli* O157 isolates from Australia and the United States provides evidence of geographic divergence. Appl Environ Microbiol. 2013;79:5050–8. http://dx.doi.org/10.1128/AEM.01525-13
18. Feinsinger P, Spears EE, Poole RW. A simple measure of niche breadth. Ecology. 1981;62:27–32. http://dx.doi.org/10.2307/1936664
19. Efron B, Tibshirani R. Bootstrap methods for standard errors, confidence intervals, and other measures of statistical accuracy. Stat Sci. 1986;1:54–75. http://dx.doi.org/10.1214/ss/1177013815
20. Jaros P, Cookson A, Campbell D, Besser T, Shringi S, Mackereth G, et al. A prospective case-control and molecular epidemiological study of human cases of Shiga toxin–producing *Escherichia coli* in New Zealand. BMC Infect Dis. 2013;13:450. http://dx.doi.org/10.1186/1471-2334-13-450
21. Statistics New Zealand. Infoshare [cited 2013 Dec 20]. http://www.stats.govt.nz/infoshare/
22. NAIT—national animal identification and tracing [cited 2013 Sep 6]. http://www.nait.co.nz/
23. Clark RG, Fenwick SG, Nicol CM, Marchant RM, Swanney S, Gill JM, et al. *Salmonella* Brandenburg–emergence of a new strain affecting stock and humans in the South Island of New Zealand. N Z Vet J. 2004;52:26–36. http://dx.doi.org/10.1080/00480169.2004.36387
24. Alley MR, Connolly JH, Fenwick SG, Mackereth GF, Leyland MJ, Rogers LE, et al. An epidemic of salmonellosis caused by *Salmonella* Typhimurium DT160 in wild birds and humans in New Zealand. N Z Vet J. 2002;50:170–6. http://dx.doi.org/10.1080/00480169.2002.36306
25. Kudva IT, Hatfield PG, Hovde CJ. *Escherichia coli* O157:H7 in microbial flora of sheep. J Clin Microbiol. 1996;34:431–3.
26. Paiba GA, Pascoe SJS, Wilesmith JW, Kidd SA, Byrne C, Ryan JBM, et al. Faecal carriage of verocytotoxin-producing *Escherichia coli* O157 in cattle and sheep at slaughter in Great Britain. Vet Rec. 2002;150:593–8. http://dx.doi.org/10.1136/vr.150.19.593
27. Oporto B, Esteban JI, Aduriz G, Juste RA, Hurtado A. *Escherichia coli* O157:H7 and non-O157 Shiga toxin–producing *E. coli* in healthy cattle, sheep and swine herds in northern Spain. Zoonoses Public Health. 2008;55:73–81. http://dx.doi.org/10.1111/j.1863-2378.2007.01080.x
28. Renter DG, Sargeant JM, Hygnstorm SE, Hoffman JD, Gillespie JR. *Escherichia coli* O157:H7 in free-ranging deer in Nebraska. J Wildl Dis. 2001;37:755–60. http://dx.doi.org/10.7589/0090-3558-37.4.755
29. Mora A, López C, Dhabi G, López-Beceiro AM, Fidalgo L, Díaz EA, et al. Seropathotypes, phylogroups, Stx subtypes and intimin types of wildlife-carried, Shiga toxin–producing *Escherichia coli* strains with the same characteristics as human-pathogenic isolates. Appl Environ Microbiol. 2012;78:2578–85. http://dx.doi.org/10.1128/AEM.07520-11
30. Cookson AL, Taylor SCS, Bennett J, Thomson-Carter F, Attwood GT. Serotypes and analysis of distribution of Shiga toxin–producing *Escherichia coli* from cattle and sheep in the lower North Island, New Zealand. N Z Vet J. 2006;54:78–84. http://dx.doi.org/10.1080/00480169.2006.36616
31. Cookson AL, Taylor SCS, Attwood GT. The prevalence of Shiga toxin–producing *Escherichia coli* in cattle and sheep in the lower North Island, New Zealand. N Z Vet J. 2006;54:28–33. http://dx.doi.org/10.1080/00480169.2006.36600
32. Lloyd-Smith JO, George D, Pepin KM, Pitzer VE, Pulliam JR, Dobson AP, et al. Epidemic dynamics at the human–animal interface. Science. 2009;326:1362–7. http://dx.doi.org/10.1126/science.1177345
33. Swirski AL, Pearl DL, Williams ML, Homan HJ, Linz GM, Cernicchiaro N, et al. Spatial epidemiology of *Escherichia coli* O157:H7 in dairy cattle in relation to night roosts of *Sturnus vulgaris* (European starling) in Ohio, USA (2007–2009). Zoonoses Public Health. 2014;61:427–35. http://dx.doi.org/10.1111/zph.12092

34. Williams ML, Pearl DL, LeJeune JT. Multiple-locus variable-nucleotide tandem repeat subtype analysis implicates European starlings as biological vectors for *Escherichia coli* O157:H7 in Ohio, USA. J Appl Microbiol. 2011;111:982–8. http://dx.doi.org/10.1111/j.1365-2672.2011.05102.x

Address for correspondence: Patricia Jaros, mEpiLab, Hopkirk Research Institute, IVABS, Massey University, Private Bag 11 222, Palmerston North 4442, New Zealand; email: p.jaros@massey.ac.nz

Bacterial Pathogens Associated with Hidradenitis Suppurativa, France

Hélène Guet-Revillet, Hélène Coignard-Biehler, Jean-Philippe Jais, Gilles Quesne, Eric Frapy, Sylvain Poirée, Anne-Sophie Le Guern, Anne Le Flèche-Matéos, Alain Hovnanian, Paul-Henry Consigny, Olivier Lortholary, Xavier Nassif, Aude Nassif, and Olivier Join-Lambert

Medscape EDUCATION ACTIVITY

Medscape, LLC is pleased to provide online continuing medical education (CME) for this journal article, allowing clinicians the opportunity to earn CME credit.

This activity has been planned and implemented in accordance with the Essential Areas and policies of the Accreditation Council for Continuing Medical Education through the joint providership of Medscape, LLC and Emerging Infectious Diseases. Medscape, LLC is accredited by the ACCME to provide continuing medical education for physicians.

Medscape, LLC designates this Journal-based CME activity for a maximum of 1.0 ***AMA PRA Category 1 Credit(s)™***. Physicians should claim only the credit commensurate with the extent of their participation in the activity.

All other clinicians completing this activity will be issued a certificate of participation. To participate in this journal CME activity: (1) review the learning objectives and author disclosures; (2) study the education content; (3) take the post-test with a 75% minimum passing score and complete the evaluation at http://www.medscape.org/journal/eid; (4) view/print certificate.

Release date: November 12, 2014; Expiration date: November 12, 2015

Learning Objectives

Upon completion of this activity, participants will be able to:

- Analyze the epidemiology and pathophysiology of hidradenitis suppurativa
- Distinguish specific bacteria associated with milder forms of hidradenitis suppurativa
- Identify bacteria associated with more severe forms of hidradenitis suppurativa
- Assess characteristics of hidradenitis suppurativa associated with colonization with different pathogens.

CME Editor

Jean Michaels Jones, Technical Writer/Editor, *Emerging Infectious Diseases. Disclosure: Jean Michaels Jones has disclosed no relevant financial relationships.*

CME Author

Charles P. Vega, MD, Clinical Professor of Family Medicine, University of California, Irvine. *Disclosure: Charles P. Vega, MD, has disclosed the following financial relationships: served as an advisor or consultant for McNeil Pharmaceuticals.*

Authors

Disclosures: ***Hélène Guet-Revillet, MD; Hélène Coignard-Biehler, PhD,; Jean-Philippe Jais, MD, PhD; Gilles Quesne, BA; Eric Frapy; Anne-Sophie Le Guern, PharmD; Anne Le Flèche-Matéos, MS; Alain Hovnanian, MD, PhD; Xavier Nassif, MD, PhD; Aude Nassif, MD;*** *and* ***Olivier Join-Lambert, MD, PhD,*** *have disclosed no relevant financial relationships.* ***Sylvain Poirée, MD,*** *has disclosed the following relevant financial relationships: owns stock, stock options, or bonds from Gilead Sciences, Inc.; Roche GS.* ***Paul-Henry Consigny, MD,*** *has disclosed the following relevant financial relationships: served as a speaker or member of a speakers bureau for Pfizer Inc.; received a travel grant from Novartis Vaccines.* ***Olivier Lortholary, MD, PhD,*** *has disclosed the following relevant financial relationships: served as an advisor or consultant for Gilead Sciences, Inc.; served as a speaker or member of a speakers bureau for Gilead Sciences, Inc.; Pfizer Inc.; MSD; Astellas Pharma, Inc.; received grants for clinical research from Gilead Sciences, Inc.; Pfizer Inc.*

Hidradenitis suppurativa (HS) is a frequent skin disease characterized by recurrent nodules or abscesses and chronic suppurating lesions. In the absence of clear pathophysiology, HS is considered to be an inflammatory disease and has no satisfactory medical treatment. Recently, prolonged antimicrobial treatments were shown to improve or resolve HS lesions. We prospectively studied the microbiology of 102 HS lesions sampled from 82 patients by using prolonged bacterial cultures and bacterial metagenomics on 6 samples. *Staphylococcus lugdunensis* was cultured as a unique or predominant isolate from 58% of HS nodules and abscesses, and a polymicrobial anaerobic microflora comprising strict anaerobes, milleri group streptococci, and actinomycetes was found in 24% of abscesses or nodules and in 87% of chronic suppurating lesions. These data show that bacteria known to cause soft tissue and skin infections are associated with HS lesions. Whether these pathogens are the cause of the lesions or are secondary infectious agents, these findings support targeted antimicrobial treatment of HS.

Hidradenitis suppurativa (HS), also known as acne inversa and Verneuil disease, is a chronic disease of the apocrine gland–bearing areas of the skin (*1*). The prevalence of HS is estimated to be as high as 1% to 2% in the general population, and the disease has a serious effect on quality of life, placing it among the most distressing conditions observed in dermatology (*2*). It is therefore of major public health concern.

HS usually begins after puberty; the clinical severity of the disease varies among patients. Most patients have a mild form of the disease, manifested as painful large and deep-seated nodules. These lesions can resolve spontaneously, persist as "silent" nodules, or lead to abscess formation. In contrast, patients with severe HS have chronic, painful, suppurating lesions that persist for years. Chronic lesions usually involve multiple areas connected by inflamed and suppurating sinus tracts surrounded by hypertrophic scars.

The pathophysiology of HS is mostly unknown and probably multifactorial, including genetic, infectious, hormonal, and immunologic factors (*3*). Approximately one third of HS patients have a familial history of HS. Familial HS is transmitted with a dominant autosomal inheritance pattern, and mutations in the gamma secretase genes have been associated with a subset of familial cases (*4*,*5*). The current hypothesis is that the HS primary event is a hyperkeratinization of the follicular infundibulum, followed by follicular occlusion, dilatation and rupture; the spread of bacterial and cellular remnants would trigger the local inflammatory response (*3*). Previous microbiological studies found a wide range of bacteria sporadically associated with HS lesions: *Staphylococcus aureus*, *Streptococcus agalactiae*, coagulase-negative staphylococci, milleri group streptococci, anaerobes, and corynebacteria (*6*–*8*). Because of these confusing microbiological observations and the rapid relapse of HS lesions after standard antimicrobial drug treatments, bacteria were considered to be contaminants of primarily inflammatory lesions.

Recently, the rifampin-clindamycin drug combination was reported to substantively improve HS lesions (*9*,*10*), and our research team showed that complete healing of HS lesions can be obtained by using the rifampin-moxifloxacin-metronidazole drug combination (*11*). These findings suggest that suppurative lesions associated with HS may be of infectious origin. In this study, we performed an extensive microbiological study of HS lesions and identified 2 main profiles of opportunistic bacterial pathogens associated with HS lesions. These pathogens are commonly isolated from skin and soft tissue infections and are known to be sensitive to antimicrobial drug treatments used to obtain improvement or remission of HS lesions.

Materials and Methods

Patients and Lesions

In the Centre Médical de l'Institut Pasteur, a referral center for HS patients in France, microbiological samples are routinely obtained before initiation of antimicrobial treatment of HS patients. In this study, we performed a microbiological analysis of all HS lesions sampled from patients who consulted for the first time in our center for active HS during June 2007–February 2011 (Table 1). We excluded patients who received systemic or topical antibiotic drugs during the month before sampling. The clinical severity of lesions was assessed and designated by the same physician using the clinical severity staging of Hurley (*12*). Briefly, according to Hurley, stage 1 lesions correspond to nodules or abscesses, single or multiple, without sinus tracts or hypertrophic scars. Stage 2 lesions are single or multiple but nonconfluent lesions with sinus tracts and formation of scarring. Stage 3 lesions correspond to diffuse or nearly diffuse involvement of multiple interconnected sinus tracts or abscesses across an entire area.

Author affiliations: Université Paris Descartes, Sorbonne Paris Cité, Paris, France (H. Guet-Revillet, J-P. Jais, E. Fr py, A. Hovnanian, O. Lortholary, X. Nassif, O. Join-Lambert); Assistance-Publique Hôpitaux de Paris, Paris (H. Guet-Revillet, H. Coignard-Biehler, J-P. Jais, G. Quesne, S. Poirée, O. Lortholary, X. Nassif, O. Join-Lambert); Institut National de la Santé et de la Recherche U1151 eq11, Paris (H. Guet-Revillet, E. Frapy, X. Nassif, O. Join-Lambert); Institut National de la Santé et de la Recherche U872 eq22 (J-P. Jais); Institut National de la Santé et de la Recherche U 781, Paris (A. Hovnanian); and Institut Pasteur, Paris (A. Le Flèche-Matéos, A-S. Le Guern, P.-H. Consigny, A. Nassif)

DOI: http://dx.doi.org/10.3201/eid2012.140064

Table 1. Characteristics of patients with hidradenitis suppurativa, France, June 2007–February 2011

Characteristics	Value
No. patients	82
Sex ratio (no. M/F)	0.33 (27/55)
Age, median y, ± SD	34 ± 9.5
Age, median y, ± SD at onset of disease	29 ± 9.9
Duration of Hurley stage,* y (range)	5.8 (0.5–21)
No. lesions	102
Clinical severity of lesions*	
Hurley stage 1	38
Hurley stage 2	45
Hurley stage 3	19
Location of lesions, no. (%)	
Inguinal fold and perineal area	32 (31)
Buttocks and thigh	19 (19)
Gluteal fold	13 (13)
Axilla	28 (27)
Breast	6 (6)
Trunk and neck	4 (4)
Microbiological samples, no.	183
Lesional samples†	125
Aspirates	11
Biopsy material	49
Lesional swabs	65
Perilesional control swabs	58

*Hurley staging: Hurley, stage 1 lesions correspond to nodules or abscesses, single or multiple, without sinus tracts or hypertrophic scars. Stage 2 lesions are single or multiple but nonconfluent lesions with sinus tracts and formation of scarring. Stage 3 lesions correspond to diffuse or nearly diffuse involvement of multiple interconnected sinus tracts or abscesses across the entire area.
†Each lesion was sampled 1 or 2 times. Open lesions with purulent drainage were sampled by swabbing of the purulent drainage. On consent of the patient, closed, nonsuppurative lesions were sampled only by biopsy or needle aspiration.

Lesion Samples

We collected 2 types of lesion samples: 1) transcutaneous samples (from punch biopsies, ultrasonography guided biopsies, and needle aspirations) performed under strict asepsis using 5% povidone-iodine solution, and 2) swab specimens of superficial purulent drainage collected by using the Portagerm system (bioMérieux, Marcy l'Etoile, France) without aseptic preparation. Transcutaneous samples were collected only from patients who gave informed consent. Such samples were obtained from all closed abscesses or nodules and were also recommended for suppurative lesions. For suppurative lesions, we also suggested collecting purulent drainage by swab and collecting an additional control specimen at a 5-cm distance from the lesion, considering that biopsy may fail to reach the infectious site. No transport medium was used for punch biopsy specimens and purulent drainage collected by puncture. Samples were sent to the laboratory within 1 hour after sampling.

Bacterial Cultures and Identification Methods

To grow anaerobic bacteria, we homogenized biopsy samples using a sterile porcelain mortar in 0.5 mL of Schaedler broth (bioMérieux, Marcy l'Etoile, France). Purulent drainage and swab specimens were directly discharged in 0.5 mL of Schaedler broth; 50 μL of the suspension was seeded on agar plates, including an Uriselect4 agar plate (Bio-Rad, Marnes-la-Coquette, France), a colistin-nalidixic acid (CNA) blood agar plate, and a Columbia blood agar plate (bioMérieux). Uriselect4 and CNA agar plates were incubated at 37°C under 5% CO_2 for the isolation of aerobic and microaerophilic bacteria. Columbia agar plates were incubated anaerobically for 2 weeks. Cultures were analyzed at days 2, 7, and 15 by the same physician throughout the study. Anaerobic cultures were considered positive when the abundance or diversity of the bacterial culture was increased under anaerobic conditions. Plates were streaked by using the 4-phase pattern for isolation of predominant colonies. When the number of bacterial colonies was <200, colonies were counted; when >200 colonies, we assigned a colony count of 500 or 1,000 to bacterial colonies that reached the third or fourth quarter of the plate, respectively.

A maximum of 10 colonies per sample was identified by matrix-assisted laser desorption–time-of-flight mass spectrometry by using the Andromas system (*13*). When no identification was obtained, the 16S ribosom al RNA gene was sequenced. Altogether, 417 bacterial isolates were identified from the 162 culture-positive samples. Bacterial species were grouped in 12 categories (online Technical Appendix Figures 1–5, wwwnc.cdc.gov/EID/article/20/12/14-0064-Techapp1.pdf).

Bacterial Metagenomics

To investigate more precisely the anaerobic microflora and to decipher whether nonculturable species could be associated with HS lesions, we performed a metagenomic study on 6 consecutive samples including 1 Hurley stage 1 abscess and 5 chronic suppurating lesions. We used sterile dry swabs to collect samples that were immediately frozen at –80°C. We extracted DNA by using the MagNa Pure technology (Roche Pharma, Boulogne-Billancourt, France). We amplified each sample by using the eubacterial universal 16S primer set 27F/338R described by Fierer et al. that targets the V1 and V2 hypervariable regions of the small subunit of the ribosomal RNA gene (*14*). We used Platinium PCR SuperMix (Invitrogen, Carlsbad, CA, USA) to elicit amplification reactions. PCR products were purified and concentrated by using the UltraClean PCR Clean-up Kit (MoBio, Carlsbad, CA, USA). Samples were sent to GATC Biotech AG (Konstanz, Germany) to be pyrosequenced by using 454 Life Sciences sequencing (454 Life Sciences, a Roche Company, Branford, Connecticut, USA).

An average of 4,407 quality sequences (range 2,564–7,008 sequences) were obtained from each sample. We analyzed data using the QIIME software (*15*). Similar sequences were clustered into operational taxonomic units by using Uclust (*16*), with a minimum identity of 0.97. We assigned taxonomy using the RDP Classifier (*17*).

Table 2. Microbiological profiles of 102 hidradenitis suppurativa lesions according to patient sex, clinical severity, and topography, France

Characteristics	Profile A	Profile B	No profile	Negative culture	p value*
Sex					0.2
M, n = 35	5	24	3	3	
F, n = 67	19	41	1	6	
Clinical severity of lesions†					2×10^{-11}
Hurley stage 1, n = 38	22	9	2	5	
Hurley stage 2, n = 45	2	40	0	3	
Hurley stage 3, n = 19	0	16	2	1	
Topography of lesions					0.01
Inguinal fold, n = 32	5	24	1	2	
Buttock and thigh, n = 19	8	6	1	4	
Gluteal fold, n = 13	2	10	0	1	
Trunk, n = 4	1	2	1	0	
Breast, n = 6	4	2	0	0	
Axilla, n = 28	4	21	1	2	

*By Fisher exact test comparing the repartitions of profiles A and B.
†Hurley staging: Hurley, stage 1 lesions correspond to nodules or abscesses, single or multiple, without sinus tracts or hypertrophic scars. Stage 2 lesions are single or multiple but nonconfluent lesions with sinus tracts and formation of scarring. Stage 3 lesions correspond to diffuse or nearly diffuse involvement of multiple interconnected sinus tracts or abscesses across the entire area.

Biostatistics

Statistical analyses were performed with R software version 3.01 (http://www.r-project.org). Hierarchical ascending classifications were performed to characterize sample profiles according to their bacterial composition. We computed the Euclidean distances between samples or species according to the bacterial abundance and then built dendrograms using the Ward aggregation criterion (*18*). Clustering results were figured in a heatmap chart (pheatmap R package, http://cran.r-project.org/web/packages/pheatmap/index.html) where samples and species are reordered according to the dendrograms.

We used the Fisher exact test to compare =categorical variables. All tests were 2-sided; p values <5% were considered to be significant. We performed statistical analyses in R software.

Results

We analyzed the microbiological test results of 102 typical HS lesions excised from 82 patients, comprising 38 nodules and abscesses (Hurley stage 1 lesions) and 64 chronic suppurating lesions (45 Hurley stage 2 and 19 Hurley stage 3 lesions) (Table 1). Altogether, we collected 125 lesional samples, including 11 needle aspirations, 49 biopsies performed under strict asepsis, and 65 swab samples of open suppurating lesions (Table 1). Twenty-three open suppurating lesions were sampled both by biopsy and swabbing. We obtained 58 perilesional control samples by swabbing normal perilesional skin 5 cm away from the lesion, bringing the total number of samples to 183.

Identification of Microbiological Profiles Associated with HS Lesions

Culture results of the 183 samples are presented in online Technical Appendix Figure 1. Of the 125 lesional samples, 106 yielded a positive culture. To identify single or multiple bacterial species specifically associated with HS lesions, hierarchical clustering was performed on these samples (online Technical Appendix Figure 2). This strategy identified 2 microbiological profiles (online Technical Appendix Figures 3–5).

The profile A group identified *Staphylococcus lugdunensis* as a unique or predominant isolate (online Technical Appendix Figure 3). This group of samples comprised 24 lesion samples: 22/38 lesions were at Hurley stage 1 and 2/45 were at Hurley stage 2.

The profile B group was characterized by a mixed anaerobic flora composed of strict anaerobes and/or anaerobic actinomycetes and/or streptococci of the milleri group (online Technical Appendix Figure 4). Various other bacteria, such as *S. aureus*, coagulase-negative staphylococci, corynebacteria, *Enterobacteriaceae*, *Propionibacterium* spp., and *Enterococcus* spp., were inconstantly and in smaller amounts associated with the mixed anaerobic flora, especially when lesions were sampled by swabbing. Profile B organisms were found in 77 samples corresponding to 65 lesions.

Five samples from lesions did not correspond to the 2 identified microbiological profiles (online Technical Appendix Figure 5). These samples were 2 Hurley stage 1 samples yielding pure culture of *Propionibacterium acnes* and 2 samples yielding corynebacteria, *Enterobacteriaceae*, and coagulase negative staphylococci. A pure culture of *Streptococcus pyogenes* was recovered from the fifth sample. A review of the medical file of the patient revealed that he was admitted for an acute infectious syndrome that is unusual in HS patients and probably corresponded to an acute superinfection.

Considering the polymicrobial nature of profile B, including bacterial species known to be nonpathogenic skin

commensals, we aimed at determining the relevance of these bacteria in the pathogenic process. To achieve this goal, we first analyzed the culture results of 45 purulent drainage on swabs for which a perilesional control sample was obtained (online Technical Appendix Figure 6). *S. aureus*, coagulase-negative staphylococci, micrococcaceae, corynebacteria, *Propionibacterium* spp., *Enterobacteriaceae*, and *Enterococcus* spp. were isolated from both purulent drainage and perilesional controls. However, these organisms were isolated less frequently and in lower quantity from purulent drainage than from controls. Conversely, strict anaerobes, actinomycetes, and streptococci of the milleri group were recovered from almost all purulent drainage samples (42/45) and rarely from controls (6/45).

We next compared the culture results of 23 open suppurating lesions that were sampled by biopsy, needle aspiration under strict asepsis, or swabbing, for each of which a control perilesional swab was obtained (online Technical Appendix Figure 7). Anaerobes, actinomycetes, and streptococci of the milleri group were isolated from purulent drainage, biopsies, and aspirations, but not from perilesional swabs. By contrast, *S. aureus*, non-*lugdunensis* coagulase-negative staphylococci, corynebacteria, *Enterobacteriaceae*, and *Propionibacterium* spp. were commonly isolated from purulent drainage and swabs but very rarely from biopsies.

These data demonstrate that anaerobes, actinomycetes, and streptococci of the milleri group are specifically associated with HS lesions. Other species isolated from purulent drainage samples were part of the normal skin flora and were likely to be present as contaminants.

Correlation of Culture Results with Disease Severity and Lesion Topography

Our next task was to analyze the association of microbiological profiles with clinical severity, topography of the lesions, and gender (Table 2). Profile A was almost exclusively associated with Hurley stage 1 lesions, whereas profile B was predominantly associated with Hurley stage 2 and stage 3 lesions. Additionally, profile A tended to be associated with lesions of the breasts and buttocks.

Twelve patients had 2 or more lesions that had positive culture results (Table 3). Microbiological profiles were the same in 2 lesions of the same patient in 8 cases and different in 4 cases, indicating that microbiological profiles are not specific to a given individual.

Composition of Polymicrobial Anaerobic Flora as Assessed by Culture

The predominant anaerobic flora (1–7 different bacterial colonies per lesion) was studied in 36/62 profile B lesions

Table 3. Microbiological profiles of 12 patients who had multiple hidradenitis suppurativa lesions, France*

Case-patient no.	Sample no.	Sampling method	Lesion site	Hurley stage†	Profile‡
30	172	Biopsy	L axilla	1	B
30	173	Swabbing	R axilla	2	B
36	180	Swabbing	Abdomen	2	B
36	181	Swabbing	Axilla	2	B
37	46	Swabbing	Breast	1	A
37	71	Biopsy	Buttock	1	A
39	7	Swabbing	Thigh	1	A
39	8	Swabbing	Inguinal fold	1	A
41	2	Biopsy	Thigh	1	A
41	110	Biopsy, swabbing	Inguinal fold	2	B
58	155	Swabbing	Axilla	3	B
58	156	Swabbing	Inguinal fold	3	B
60	85	Biopsy	Buttock	2	B
60	87	Swabbing	Inguinal fold	2	B
61	134	Needle aspiration	Buttock	1	A
61	137	Biopsy, swabbing	Inguinal fold	1	B
65	14	Swabbing	Pubis	1	B
65	16	Biopsy	Scrotum	1	B
76	177	Swabbing	L axilla	1	B
76	178	Swabbing	R axilla	2	B
76	179	Needle aspiration	Breast	1	A
78	89	Swabbing	L axilla	2	B
78	90	Biopsy	R axilla	2	B
82	96	Needle aspiration	Axilla	1	A
82	97	Swabbing	Inguinal fold	2	B

*For 12 case-patients, >1 lesion was analyzed. For 8 case-patients, samples yielded microbiological characteristics within the same profile, but in samples from lesions in case-patients 41, 61, 76, and 82, differing microbiological profiles were found; R, right; L, left.
†Hurley staging: Hurley, stage 1 lesions correspond to nodules or abscesses, single or multiple, without sinus tracts or hypertrophic scars. Stage 2 lesions are single or multiple but nonconfluent lesions with sinus tracts and formation of scarring. Stage 3 lesions correspond to diffuse or nearly diffuse involvement of multiple interconnected sinus tracts or abscesses across the entire area.
‡Profile A: *S. lugdunensis* as unique or predominant pathogen; profile B: anaerobic microflora.

Table 4. Identification of strictly anaerobic bacteria cultured from 36 hidradenitis suppurativa lesions that had predominant anaerobic microflora, France

Gram type, genus, species	No. isolates
Gram-positive cocci	51
Anaerococcus	17
A. vaginalis	11
A. prevotii	4
A. octavius	1
A. lactolyticus	1
Peptoniphilus	15
P. asaccharolyticus	8
P. harei	3
P. gorbachii	1
P. ivorii	1
P. lacrymalis	1
Unidentified *Peptoniphilus* sp.	1
Other genera	19
Finegoldia magna	11
Peptostreptococcus anaerobius	4
Parvimonas micra	2
Pediococcus acidilactici	1
Facklamia hominis	1
Gram-negative rods	44
Prevotella	13
P. bivia	6
P. disiens	1
P. intermedia	1
P. melaninogenica	1
P. salivae	1
Unidentified *Prevotella* sp.	3
Porphyromonas	10
P. asaccharolytica	7
P. somerae	3
Bacteroides	9
B. coagulans	3
B. ureolyticus	3
B. thetaiotaomicron	2
B. fragilis	1
Other genera	19
Fusobacterium	8
F. nucleatum	7
F. gonidiaformans	1
Dialister	3
D. pneumosintes	2
D. micraerophilus	1
Jonquetella	1
J. anthropi	1

(Table 4). A total of 95 anaerobic isolates were identified, including gram-positive cocci (predominantly *Anaerococcus* spp., *Peptoniphilus* spp., and *Finegoldia* spp.) and gram-negative rods (predominantly *Prevotella* spp., *Porphyromonas* spp., *Bacteroides* spp., and *Fusobacterium* spp.).

Predominant *Actinomyces* species were *A. turicensis* (30% of isolates), *A. radingae* (23% of isolates), *A. neuii* (14% of isolates), and *Actinobaculum schaali* (21% of isolates). Less frequently recovered species were *A. massiliae* (3 isolates), *A. europaeus* (2 isolates), *A. funkei* (1 isolate), and *A. urogenitalis* (1 isolate). In 14 lesions, >1 *Actinomyces* species (2 to 4) was identified.

Among streptococci of the milleri group, *Streptococcus anginosus* and *Streptococcus constellatus*, were recovered from 18 and 12 lesions, respectively. Both species were identified in the same samples in 2 cases.

Composition of the Anaerobic Flora as Assessed by Metagenomics

We investigated the microbial diversity of 6 HS lesions by high-throughput sequencing. These lesions comprised 5 chronic suppurating lesions sampled by swabbing and 1 *S. lugdunensis* abscess sampled by needle aspiration (Figure). High-throughput sequencing confirmed that *Staphylococcus* was the far predominant taxon (99%) within the Hurley stage 1 abscess. In chronic suppurating lesions, anaerobic species (*Prevotella*, *Porphyromonas*, *Anaerococcus*, and *Mobiluncus* spp.) were the predominant taxa. Three bacterial orders were present in all samples: Bacteroidales (mainly *Prevotella* and *Porphyromonas*); Clostridiales (mainly *Peptoniphilus*, *Anaerococcus*, *Parvimonas*, *Dialister*, and *Finegoldia*); and Actinomycetales (*Actinomyces*, *Actinobaculum*, and *Mobiluncus*).

Thus, metagenomic data were consistent with culture results, facilitating a more exhaustive description of the anaerobic flora. It should be pointed out that metagenomics did not identify noncultivable bacteria associated with HS lesions.

Altogether, we identified 2 microbiological profiles specifically associated with HS lesions. Profile A was characterized by pure or predominant culture of *S. lugdunensis* that was mostly associated with Hurley stage 1 lesions. Profile B was represented by a mixed flora composed of gram-negative and Gram-positive strict anaerobes, anaerobic actinomycetes, and streptococci of the milleri group. This profile was mainly associated with open suppurating lesions observed in Hurley stages 2 and 3, but also with 24% of Hurley stage 1 lesions. No microbiological differences could be identified between Hurley stage 2 and 3 lesions by culture methods.

Discussion

Identification of organisms and appropriate treatment are urgently needed to improve the quality of life of HS patients. An infectious process related to HS has been suspected for a long time (*19*). However, considering the polymicrobial nature of the cultures obtained from HS lesions and bacteria usually isolated from the skin microflora, it remained unclear whether bacterial factors were involved in the pathophysiology of HS.

We conducted a large prospective study of the microbiology of HS lesions among a cohort of 82 patients. Altogether, we studied 102 HS lesions using optimized sampling and culture methods. We used matrix-assisted laser desorption–time-of-flight mass spectrometry to identify the predominant microflora of lesions and of normal skin samples. The main advantage of this technique is that identification can be obtained to the species level within a few

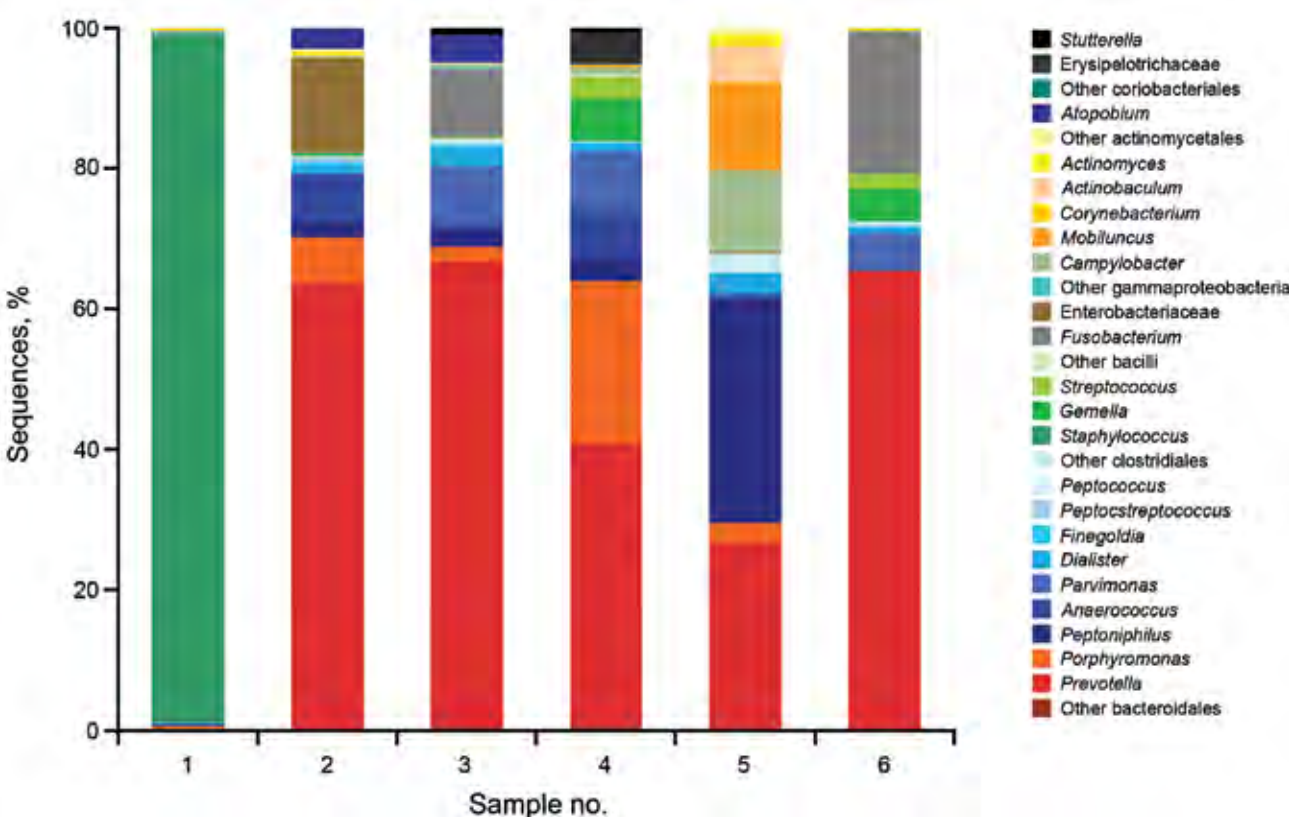

Figure. Microbial diversity of hidradenitis supportava (HS) lesions as assessed by high-throughput 454 sequencing. The bacterial diversity of 6 consecutive and representative HS lesions was assessed by high-throughput sequencing. Sample 1 corresponded to an acute *Staphylococcus lugdunensis* abscess sampled by needle aspiration. Samples 2–3 (swabs) corresponded to Hurley stage 2 lesions of the axilla and inguinal folds, respectively. Samples 4–6 (swabs) corresponded to Hurley stage 3 lesions of the inguinal, axilla and gluteal fold, respectively. *Staphylococcus* spp. represented >99% of sequences of sample 1, whereas *Prevotella* spp. represented the most abundant taxon in 4/5 of these chronic suppurative lesions.

minutes for a very wide range of bacteria, including species of the normal microflora, anaerobes, and bacteria that are usually identified by molecular techniques.

This study demonstrates that 2 specific microbiological profiles, neither corresponding to the normal skin microflora, nor to usual skin pathogens (*S. aureus* and *S. pyogenes*) are associated with HS lesions. Two new bacterial pathogens species associated with HS lesions were identified: *S. lugdunensis* and anaerobic actinomycetes.

S. lugdunensis was mostly cultured from HS nodules and abscesses. *S. lugdunensis* is a skin commensal that primarily colonizes the lower extremities and inguino-perineal area, the latter including typical sites for HS lesions (*20*). *S. lugdunensis* seems to be an infrequent pathogen (*21*), but skin abscesses caused by this organism are similar to those caused by *S. aureus*, demonstrating a particular virulence compared with other coagulase negative staphylococci. This organism was initially described as a cause of post-surgical wound infections (*22*), suggesting that local predisposing factors are required for its pathogenicity.

Conversely, the majority of chronic suppurating lesions and a restricted number of mild HS lesions were associated with a predominant polymicrobial anaerobic microflora, including strict anaerobes, milleri group streptococci, and anaerobic actinomycetes. These bacteria are common inhabitants of the mouth and gastrointestinal tract (*23–25*). Strict anaerobes are usual colonizers but can cause secondary infections in patients who have local or systemic predispositions. They have been previously associated with HS lesions, and in various secondary skin infections including epidermal cysts (*26–28*). Strict anaerobes have been shown to grow synergistically and to cause severe infections especially when associated with other bacterial species, including milleri group streptococci, which were identified as a potential treatment target in HS in the 1980s (*19*,*29–31*), although they appeared to be unusual pathogens in other studies (*32*). Milleri group streptococci can be aggressive pathogens, leading to abscess formation at various sites of the body including the skin, thorax, and brain (*30*). They have been recently associated with chronic infectious conditions such as digestive

fistula in patients who had vascular grafts or cystic fibrosis pulmonary infections (*33*,*34*).

Cultures of the vast majority of severe suppurating lesions produced anaerobic actinomycetes. Anaerobic actinomycetes are fastidious and aerotolerant species that grow slowly on rich media and provide pinpoint colonies after a 1-week culture period; they are also difficult to identify by using phenotypic methods. These factors probably show why they have not been cultured from HS lesions previously. Anaerobic actinomycetes have been associated with difficult-to-treat and relapsing skin and soft tissue infections. They can also cause severe infections such as endophthalmitis, bacteremia, and endocarditis (*35*–*38*). The closely related species *A. schaalii* is considered to be a uropathogen among persons ≥65 years of age and in patients with predisposing neurologic or local factors. *A. schaalii* has been recently associated with cellulitis and bacteremia (*39*).

Altogether, our study demonstrates that HS lesions are associated with bacterial species that can cause abscesses and severe infections. Compared with *S. aureus* or *S. pyogenes*, the low pathogenicity of these bacteria could account for the chronicity of suppuration of HS lesions that can last for years. In addition, the particular propensity of HS patients to develop recurrent or chronic skin infections highly suggests that HS is not primarily an infectious disease but a predisposing condition that allows these low pathogenic species to cause soft tissue and skin infections.

Histopathologic studies of noninflammatory areas of the skin of HS patients have shown the presence of dilated and distorted hair follicles. These anatomic abnormalities are thought to be caused by the hyperkeratinization of the follicular infundibulum, which can lead to dilatation and rupture and release of bacteria within the dermis (*40*). This event may predispose *S. lugdunensis* and anaerobic bacteria to cause nodules and abscesses in HS. Conversely, chronic suppurating HS lesions are deep abscesses drained by interconnected epithelialized sinus tracts. Colonization of these deep-seated lesions by anaerobic bacteria, streptococci of the Milleri group, and actinomycetes may account for chronic inflammation.

A limitation of our study is that HS patients who come to our center usually seek treatment for severe forms of the disease. Thus, the study population may not be representative of the HS patient population.

In summary, this study demonstrates that bacterial pathogens known to cause soft tissue and skin infections are found in HS lesions. The unexpected efficacy of wide-spectrum antimicrobial treatments for HS (*9*,*11*,*41*) highly suggests that these bacteria are partly causative agents for suppurative hidradenitis and should be considered to be treatment targets. These data open an avenue for future research on the pathophysiology of this disease, and provide a rational basis for clinical trials of treatment of HS.

This work was supported by a grant from the Fondation pour la Recherche Médicale en France (ROXANNE project, LMV20100519581) and by the Projet Hospitalier de Recherche Clinique Régional Ile de France AOR11-071.

Dr Guet-Revillet is a physician in the Department of Microbiology of the Necker Enfants Malades hospital. Her main research interest is the role of bacterial pathogens in the pathophysiology of hidradenitis suppurativa.

References

1. Alikhan A, Lynch PJ, Eisen DB. Hidradenitis suppurativa: a comprehensive review. J Am Acad Dermatol. 2009;60:539–61, quiz 62–3. http://dx.doi.org/10.1016/j.jaad.2008.11.911
2. Wolkenstein P, Loundou A, Barrau K, Auquier P, Revuz J. Quality of life impairment in hidradenitis suppurativa: a study of 61 cases. J Am Acad Dermatol. 2007;56:621–3. http://dx.doi.org/10.1016/j.jaad.2006.08.061
3. Paus R, Kurzen H, Kurokawa I, Jemec GB, Emtestam L, Sellheyer K, Giamarellos-Bourboulis EJ, et al. What causes hidradenitis suppurativa? Exp Dermatol. 2008;17:455–6, discussion 7–72. http://dx.doi.org/10.1111/j.1600-0625.2008.00712_1.x
4. Pink AE, Simpson MA, Brice GW, Smith CH, Desai N, Mortimer PS, et al. PSENEN and NCSTN mutations in familial hidradenitis suppurativa (acne inversa). J Invest Dermatol. 2011;131:1568–70. http://dx.doi.org/10.1038/jid.2011.42
5. Miskinyte S, Nassif A, Merabtene F, Ungeheuer MN, Join-Lambert O, Jais JP, et al. Nicastrin mutations in French families with hidradenitis suppurativa. J Invest Dermatol. 2012;132:1728–30. http://dx.doi.org/10.1038/jid.2012.23
6. Highet AS, Warren RE, Weekes AJ. Bacteriology and antibiotic treatment of perineal suppurative hidradenitis. Arch Dermatol. 1988;124:1047–51. http://dx.doi.org/10.1001/archderm.1988.01670070035015
7. Lapins J, Jarstrand C, Emtestam L. Coagulase-negative staphylococci are the most common bacteria found in cultures from the deep portions of hidradenitis suppurativa lesions, as obtained by carbon dioxide laser surgery. Br J Dermatol. 1999;140:90–5. http://dx.doi.org/10.1046/j.1365-2133.1999.02613.x
8. Sartorius K, Killasli H, Oprica C, Sullivan A, Lapins J. Bacteriology of hidradenitis suppurativa exacerbations and deep tissue cultures obtained during carbon dioxide laser treatment. Br J Dermatol. 2012;166:879–83. http://dx.doi.org/10.1111/j.1365-2133.2011.10747.x
9. Gener G, Canoui-Poitrine F, Revuz JE, Faye O, Poli F, Gabison G, et al. Combination therapy with clindamycin and rifampicin for hidradenitis suppurativa: a series of 116 consecutive patients. Dermatology. 2009;219:148–54. http://dx.doi.org/10.1159/000228334
10. van der Zee HH, van der Woude CJ, Florencia EF, Prens EP. Hidradenitis suppurativa and inflammatory bowel disease: are they associated? Results of a pilot study. Br J Dermatol. 2010;162:195–7. http://dx.doi.org/10.1111/j.1365-2133.2009.09430.x
11. Join-Lambert O, Coignard H, Jais JP, Guet-Revillet H, Poiree S, Fraitag S, et al. Efficacy of rifampin-moxifloxacin-metronidazole combination therapy in hidradenitis suppurativa. Dermatology. 2011;222:49–58. http://dx.doi.org/10.1159/000321716
12. Hurley HJ. Axillary hyperhidrosis, apocrine bromhidrosis, hidradenitis suppurativa, and familial benign pemphigus: surgical approach. In: Roegnigk Randall K and Roegnigk Henry H, editors. Roegnigk & Roegnigk's dermatologic surgery: principles and practice, second edition. Boca Raton, FL: CRC Press; 1996. p. 623–45.

13. Bille E, Dauphin B, Leto J, Bougnoux ME, Beretti JL, Lotz A, et al. MALDI-TOF MS Andromas strategy for the routine identification of bacteria, mycobacteria, yeasts, *Aspergillus* spp. and positive blood cultures. Clin Microbiol Infect. 2012;18:1117–25. http://dx.doi.org/10.1111/j.1469-0691.2011.03688.x
14. Fierer N, Hamady M, Lauber CL, Knight R. The influence of sex, handedness, and washing on the diversity of hand surface bacteria. Proc Natl Acad Sci U S A. 2008;105:17994–9. http://dx.doi.org/10.1073/pnas.0807920105
15. Caporaso JG, Kuczynski J, Stombaugh J, Bittinger K, Bushman FD, Costello EK, et al. QIIME allows analysis of high-throughput community sequencing data. Nat Methods. 2010;7:335–6. http://dx.doi.org/10.1038/nmeth.f.303
16. Edgar RC. Search and clustering orders of magnitude faster than BLAST. Bioinformatics. 2010;26:2460–1. http://dx.doi.org/ 10.1093/bioinformatics/btq461
17. Wang Q, Garrity GM, Tiedje JM, Cole JR. Naive Bayesian classifier for rapid assignment of rRNA sequences into the new bacterial taxonomy. Appl Environ Microbiol. 2007;73:5261–7. http://dx.doi.org/10.1128/AEM.00062-07
18. Ward, J.H. Hierarchical grouping to optimize an objective function. Journal of the American Statistical Association, 1963;58:236–44. http://www.jstor.org/stable/2282967
19. Highet AS, Warren RE, Staughton RC, Roberts SO. *Streptococcus milleri* causing treatable infection in perineal hidradenitis suppurativa. Br J Dermatol. 1980;103:375–82. http://dx.doi.org/10.1111/j.1365-2133.1980.tb07259.x
20. Bieber L, Kahlmeter G. *Staphylococcus lugdunensis* in several niches of the normal skin flora. Clin Microbiol Infect. 2010;16:385–8. http://dx.doi.org/10.1111/j.1469-0691.2009.02813.x
21. Frank KL, Del Pozo JL, Patel R. From clinical microbiology to infection pathogenesis: how daring to be different works for *Staphylococcus lugdunensis*. Clin Microbiol Rev. 2008;21:111–33. http://dx.doi.org/10.1128/CMR.00036-07
22. Vandenesch F, Eykyn SJ, Etienne J, Lemozy J. Skin and post-surgical wound infections due to *Staphylococcus lugdunensis*. Clin Microbiol Infect. 1995;1:73–4. http://dx.doi.org/10.1111/j.1469-0691.1995.tb00449.x
23. Murdoch DA. Gram-positive anaerobic cocci. Clin Microbiol Rev. 1998;11:81–120.
24. Mejàre B, Edwardsson S. *Streptococcus milleri* (Guthof); an indigenous organism of the human oral cavity. Arch Oral Biol. 1975;20:757–62. http://dx.doi.org/10.1016/0003-9969(75)90048-5
25. Clarridge JE III, Zhang Q. Genotypic diversity of clinical *Actinomyces* species: phenotype, source, and disease correlation among genospecies. J Clin Microbiol. 2002;40:3442–8. http://dx.doi.org/10.1128/JCM.40.9.3442-3448.2002
26. Brook I. The role of anaerobic bacteria in cutaneous and soft tissue abscesses and infected cysts. Anaerobe. 2007;13:171–7. http://dx.doi.org/10.1016/j.anaerobe.2007.08.004
27. Brook I, Frazier EH. Aerobic and anaerobic microbiology of axillary hidradenitis suppurativa. J Med Microbiol. 1999;48:103–5. http://dx.doi.org/10.1099/00222615-48-1-103
28. Brook I. Secondary bacterial infections complicating skin lesions. J Med Microbiol. 2002;51:808–12.
29. Nagashima H, Takao A, Maeda N. Abscess forming ability of *Streptococcus milleri* group: synergistic effect with *Fusobacterium nucleatum*. Microbiol Immunol. 1999;43:207–16. http://dx.doi.org/10.1111/j.1348-0421.1999.tb02395.x
30. Belko J, Goldmann DA, Macone A, Zaidi AK. Clinically significant infections with organisms of the *Streptococcus milleri* group. Pediatr Infect Dis J. 2002;21:715–23. http://dx.doi.org/10.1097/00006454-200208000-00002
31. Hirai T, Kimura S, Mori N. Head and neck infections caused by *Streptococcus milleri* group: an analysis of 17 cases. Auris Nasus Larynx. 2005;32:55–8. http://dx.doi.org/10.1016/j.anl.2004.09.003
32. Jemec GB, Faber M, Gutschik E, Wendelboe P. The bacteriology of hidradenitis suppurativa. Dermatology. 1996;193:203–6. http://dx.doi.org/10.1159/000246246
33. Bonnet EP, Arista S, Archambaud M, Boot B, Clave D, Massip P, et al. *Streptococcus milleri* group infection associated with digestive fistula in patients with vascular graft: report of seven cases and review. Infection. 2007;35:182–5. http://dx.doi.org/10.1007/s15010-007-6040-0
34. Sibley CD, Sibley KA, Leong TA, Grinwis ME, Parkins MD, Rabin HR, et al. The *Streptococcus milleri* population of a cystic fibrosis clinic reveals patient specificity and intraspecies diversity. J Clin Microbiol. 2010;48:2592–4. http://dx.doi.org/10.1128/JCM.00414-10
35. Hall V. Actinomyces–gathering evidence of human colonization and infection. Anaerobe. 2008;14:1–7. http://dx.doi.org/10.1016/j.anaerobe.2007.12.001
36. Sabbe LJ, Van De Merwe D, Schouls L, Bergmans A, Vaneechoutte M, Vandamme P. Clinical spectrum of infections due to the newly described *Actinomyces* species *A. turicensis*, *A. radingae*, and *A. europaeus*. J Clin Microbiol. 1999;37:8–13.
37. Zautner AE, Schmitz S, Aepinus C, Schmialek A, Podbielski A. Subcutaneous fistulae in a patient with femoral hypoplasia due to *Actinomyces europaeus* and *Actinomyces turicensis*. Infection. 2009;37:289–91. http://dx.doi.org/10.1007/s15010-008-7392-9
38. von Graevenitz A. *Actinomyces neuii*: review of an unusual infectious agent. Infection. 2011;39:97–100. http://dx.doi.org/10.1007/s15010-011-0088-6
39. Beguelin C, Genne D, Varca A, Tritten ML, Siegrist HH, Jaton K, et al. *Actinobaculum schaalii*: clinical observation of 20 cases. Clin Microbiol Infect. 2011;17:1027–31. http://dx.doi.org/10.1111/j.1469-0691.2010.03370.x
40. van der Zee HH, Laman JD, Boer J, Prens EP. Hidradenitis suppurativa: viewpoint on clinical phenotyping, pathogenesis and novel treatments. Exp Dermatol. 2012;21:735–9. http://dx.doi.org/10.1111/j.1600-0625.2012.01552.x
41. van der Zee HH, Boer J, Prens EP, Jemec GB. The effect of combined treatment with oral clindamycin and oral rifampicin in patients with hidradenitis suppurativa. Dermatology. 2009;219:143–7. http://dx.doi.org/10.1159/000228337

Address for correspondence: Hélène Guet-Revillet, Laboratoire de Microbiologie, Hôpital Necker-Enfants Malades, 149 rue de Sèvres, 75015 Paris, France; email: helene.guet-revillet@nck.aphp.fr

Replication and Shedding of MERS-CoV in Upper Respiratory Tract of Inoculated Dromedary Camels

Danielle R. Adney, Neeltje van Doremalen, Vienna R. Brown, Trenton Bushmaker, Dana Scott, Emmie de Wit, Richard A. Bowen,[1] and Vincent J. Munster[1]

In 2012, a novel coronavirus associated with severe respiratory disease in humans emerged in the Middle East. Epidemiologic investigations identified dromedary camels as the likely source of zoonotic transmission of Middle East respiratory syndrome coronavirus (MERS-CoV). Here we provide experimental support for camels as a reservoir for MERS-CoV. We inoculated 3 adult camels with a human isolate of MERS-CoV and a transient, primarily upper respiratory tract infection developed in each of the 3 animals. Clinical signs of the MERS-CoV infection were benign, but each of the camels shed large quantities of virus from the upper respiratory tract. We detected infectious virus in nasal secretions through 7 days postinoculation, and viral RNA up to 35 days postinoculation. The pattern of shedding and propensity for the upper respiratory tract infection in dromedary camels may help explain the lack of systemic illness among naturally infected camels and the means of efficient camel-to-camel and camel-to-human transmission.

The Middle East respiratory syndrome coronavirus (MERS-CoV) was first recognized in 2012 related to a fatal human case of pneumonia in Saudi Arabia (*1*). Currently, >800 cases of MERS have been identified, and the estimated case-fatality rate is ≈35% (*2*). Most cases have been identified on the Arabian Peninsula, but several travel-associated cases have been reported (*2–4*). Human-to-human transmission has been reported, predominantly among persons in health care facilities and households; the rate of human infection by zoonotic transmission from a reservoir source is currently not known (*4–6*).

The close phylogenetic relationship of human MERS-CoV isolates with those obtained from bats initially suggested a direct link between the emergence of MERS-CoV and a putative natural reservoir (*7–9*). Anecdotal reports mentioned contact of MERS-CoV–infected patients with camels and goats, suggesting that livestock might be the intermediate reservoir host for MERS-CoV (*4*,*10–12*). Serologic studies revealed widespread prevalence of MERS-CoV–specific antibodies in dromedary camels from several countries that reported MERS cases (*4*,*13–19*). Further, MERS-CoV RNA was detected in nasal swab samples obtained from 3 camels on a farm linked to 2 human MERS-CoV cases, and the virus was isolated from nasal swab samples from dromedary camels in Qatar (*14*). MERS-CoV isolation and subsequent full genome sequencing directly linked a dromedary camel and a fatal MERS-CoV case in a person in Saudi Arabia (*20*,*21*). Despite these associations, the role of camels as a primary reservoir for MERS-CoV is still debated (*22*,*23*). Here we report on the experimental inoculation of 3 camels with a human isolate of MERS-CoV.

Materials and Methods

Virus and Cells

MERS-CoV (strain HCoV-EMC/2012) was provided by the Department of Viroscience, Erasmus Medical Center, Rotterdam, The Netherlands. The virus was propagated in Vero E6 cells cultured in Dulbecco modified Eagle medium (Invitrogen, Carlsbad, CA, USA) supplemented with 2% fetal bovine serum, 2 mmol/L glutamine, 50 U/mL penicillin, and 50 μg/mL streptomycin.

Author affiliations: Colorado State University, Fort Collins, Colorado, USA; (D.R. Adney, V.R. Brown, R.A. Bowen); and National Institutes of Health, Hamilton, Montana, USA (N. van Doremalen, T. Bushmaker, D. Scott, E. de Wit, V.J. Munster)

DOI: http://dx.doi.org/10.3201/eid2012.141280

[1]These senior authors contributed equally to this article.

Animal Study

Three native-born adult male dromedary camels (*Camelus dromedarius*) were obtained through private sale; the animals tested negative by neutralization assay for MERS-CoV and for bovine coronavirus by ELISA. Camels 1, 2, and 3 were 2, 3, and 5 years old, respectively. Camels 1 and 2 were intact males, and camel 3 had been castrated. Animals were housed in an Animal Biosafety Level 3 facility for the duration of the experiment and fed ad libitum. Camels were acclimated to the facility for 2 weeks before virus inoculation. We sedated the camels with xylazine, then inoculated them with a total dose of 10^7 50% tissue culture infective dose ($TCID_{50}$) of MERS-CoV (strain HCoV-EMC/2012) in a total volume of 15 mL, by way of intratracheal (8 mL using transcutaneous catheter), intranasal (3.3 mL in each nostril by expulsion from a syringe), and conjunctival (0.2 mL in each conjunctival sac) routes. The routes of inoculation and infectious dose were chosen to reflect a combination of most likely routes of exposure and to increase the potential of infection. The animals were observed at least 1× daily for the duration of the experiment for behavior, food consumption, activity level, and nasal discharge. Rectal temperature was taken daily from 2 to 7 days postinoculation, then 3× weekly until the animals were euthanized. Nasal and oral swab samples and fecal samples were collected into virus transport medium or virus lysis buffer daily from 0 to 7 days postinoculation (dpi), then 3× weekly until the animal was euthanized. Blood was collected into evacuated EDTA and serum-separating tubes daily at 0–7 dpi and 3× weekly thereafter. Urine was collected by convenience and at necropsy. To evaluate whether virus is exhaled from infected camels, a funnel was placed over the muzzle of each camel and connected to a vacuum pump to capture exhaled air in tissue culture media (10 mL Dulbecco modified Eagle medium, 1% fetal bovine serum, 0.013% SE-15 (anti-foam) with an All Glass Impinger (Ace Glass Inc., Vineland, NJ, USA). Exhaled breath was collected for ≈2 minutes and analyzed by quantitative real-time PCR (qPCR) and virus titration. On days 5, 28, and 42, camels 1, 2, and 3, respectively, were euthanized, and samples were collected from nasal turbinates, lungs, trachea, larynx, pharynx, liver, spleen, kidney, bladder, urine, duodenum, jejunum, colon, rectum, abomasum, forestomachs, prescapular lymph node, retropharyngeal lymph node, tracheobronchial lymph node, mediastinal lymph node, mesenteric lymph node, medulla, and olfactory cortex.

RNA Extraction and Quantitative PCR

We extracted RNA from swab samples, fecal samples, and serum samples using the QIAamp Viral RNA kit (QIAGEN, Valencia, CA, USA) according to the manufacturer's instructions. For detection of viral RNA, we used 5 mL of RNA in a one-step real-time reverse transcription PCR upE assay (*24*) using the Rotor-GeneTM probe kit (QIAGEN) according to manufacturer's instructions. Standard dilutions of a titered virus stock were run in parallel, to calculate $TCID_{50}$ equivalents in the samples (*25*).

Virus Titration and Plaque Reduction Neutralization Test

We titrated swab samples in viral transport medium, whole blood, and homogenized tissues (≈10% wt/vol) for MERS-CoV virus by plaque assay. Briefly, 10-fold serial dilutions of samples were prepared in BA-1 medium (MEM, 1% bovine serum albumin, 350 mg/L sodium bicarbonate, 50 mM Tris, pH 7.6, 5 mg/L phenol red) containing 100 mg gentamicin, 200,000 U penicillin G, 100 mg streptomycin, and 5 mg amphotericin/L; plaque assay was conducted as

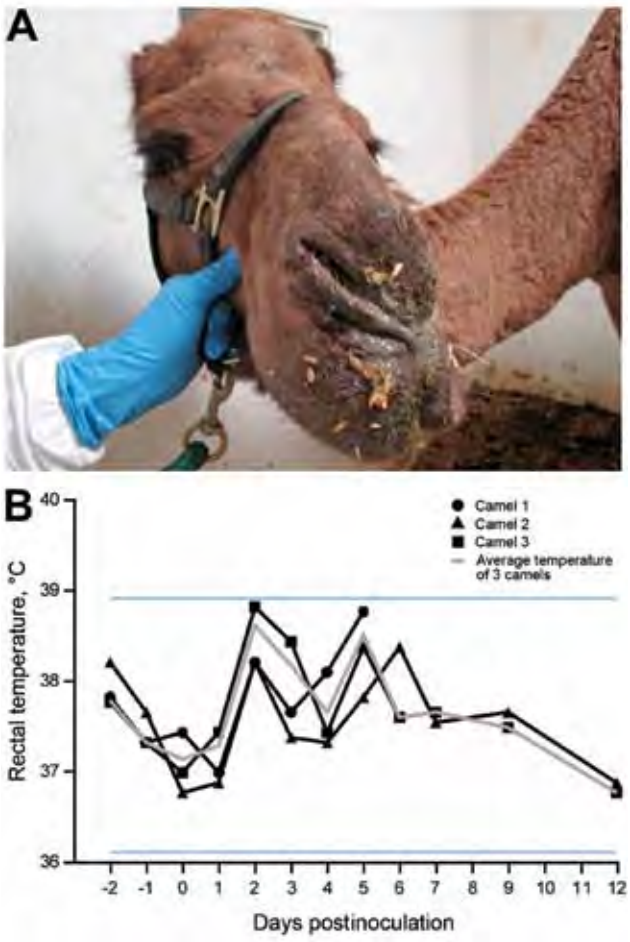

Figure 1. Clinical signs in dromedary camels inoculated with Middle East respiratory syndrome coronavirus (MERS-CoV). A) Nasal discharge observed in camel 3; each of 3 inoculated camels had nasal discharge during the first 2 weeks of the experiment. B) Rectal temperatures are indicated for each camel by lines with geometric shapes. Horizontal lines indicate the normal temperature range observed among these dromedary camels as calculated by mean ± 3×, the SD before inoculation.

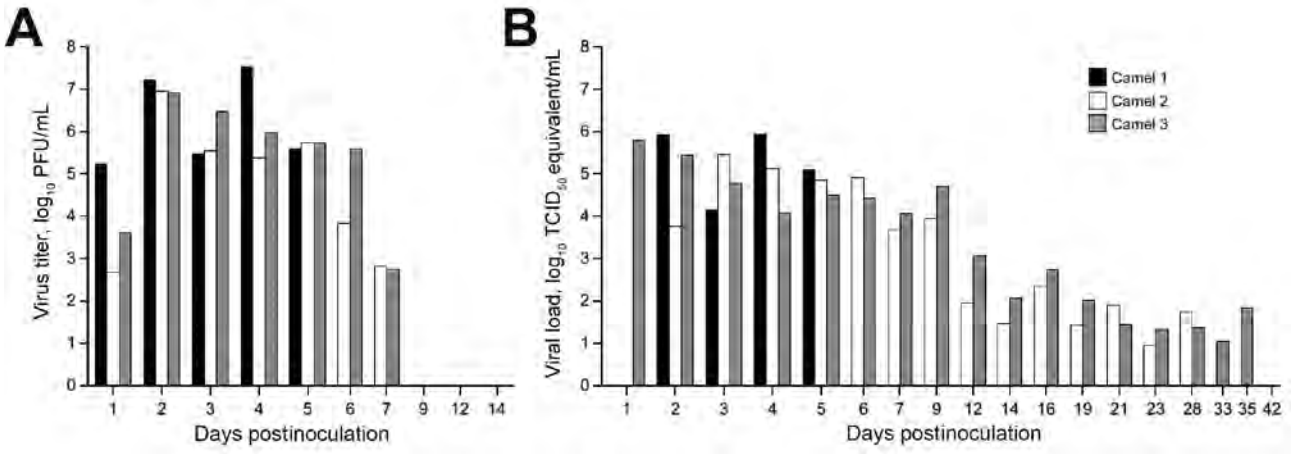

Figure 2. Virus shedding from the upper respiratory tract in dromedary camels inoculated with Middle East respiratory syndrome coronavirus MERS-CoV (MERS-CoV). Shedding was determined by A) infectious titers by plaque assay and B) viral load by quantitative real-time PCR. We extrapolated 50% tissue culture infective dose ($TCID_{50}$) equivalents from standard curves generated by 10-fold dilutions of a MERS-CoV stock (HCoV-EMC/2012) with known virus titer in parallel to each quantitative real-time PCR run.

described for West Nile virus (*26*). Plaques were counted on days 1 and 3 after the second overlay and virus titers were expressed as PFUs per mL or gram. We determined neutralizing antibody titers by plaque reduction neutralization test as described (*26*), using a 90% neutralization cutoff.

Histopathologic Examination and Immunohistochemical Testing

Tissues were fixed for >7 days in 10% neutral-buffered formalin and embedded in paraffin. Tissue sections were stained with hematoxylin and eosin. To detect MERS-CoV antigen, we completed immunohistochemical testing using a rabbit polyclonal antiserum against HCoV-EMC/2012 (1:1,000) as a primary antibody.

Results

Clinical Signs in Dromedary Camels Inoculated with MERS-CoV

Each camel showed minor clinical signs of disease, consisting of rhinorrhea (Figure 1, panel A) and a mild elevation in body temperature at 2 dpi and 5–6 dpi (Figure 1, panel B); no other clinical signs were observed. Rhinorrhea developed in all 3 camels beginning at 2 (camels 1 and 3) and 5 (camel 2) dpi, and persisted ≤2 weeks. The nasal discharge drained from both nares and varied in character from serous to purulent; minor hemorrhage was observed on some occasions, but may have been caused by trauma that occurred during collection of samples.

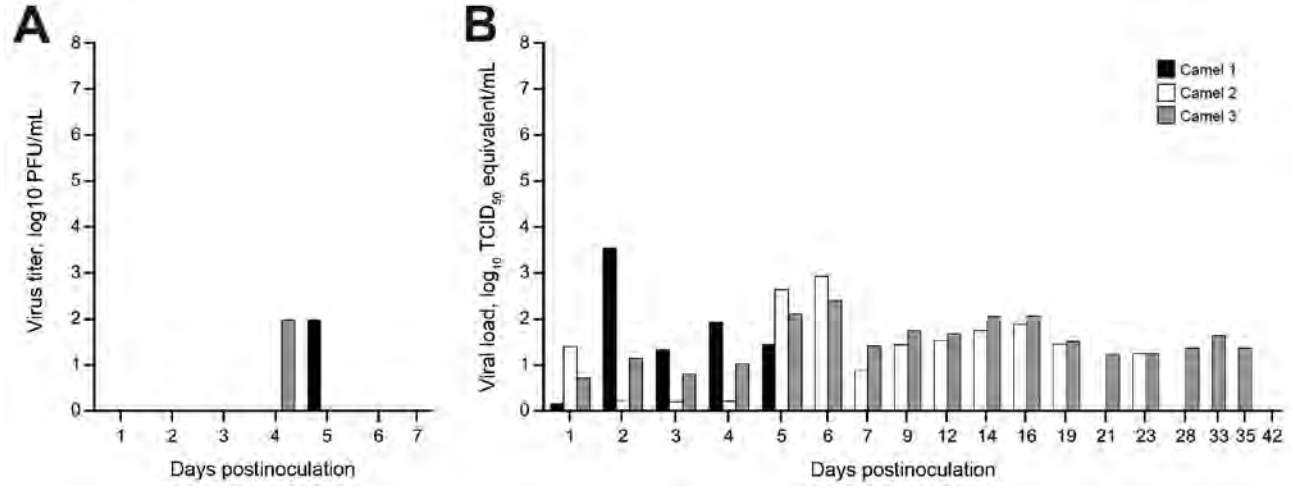

Figure 3. Virus shedding determined by oral swabs obtained from dromedary camels inoculated with Middle East respiratory syndrome coronavirus MERS-CoV (MERS-CoV. Shedding was determined by A) determining infectious titers and B) viral RNA. Virus titers were determined by plaque assay and viral load by qRT-PCR. $TCID_{50}$ equivalents were extrapolated from standard curves generated by 10-fold dilutions of a MERS-CoV stock (HCoV-EMC/2012) with known virus titer in parallel to each run.

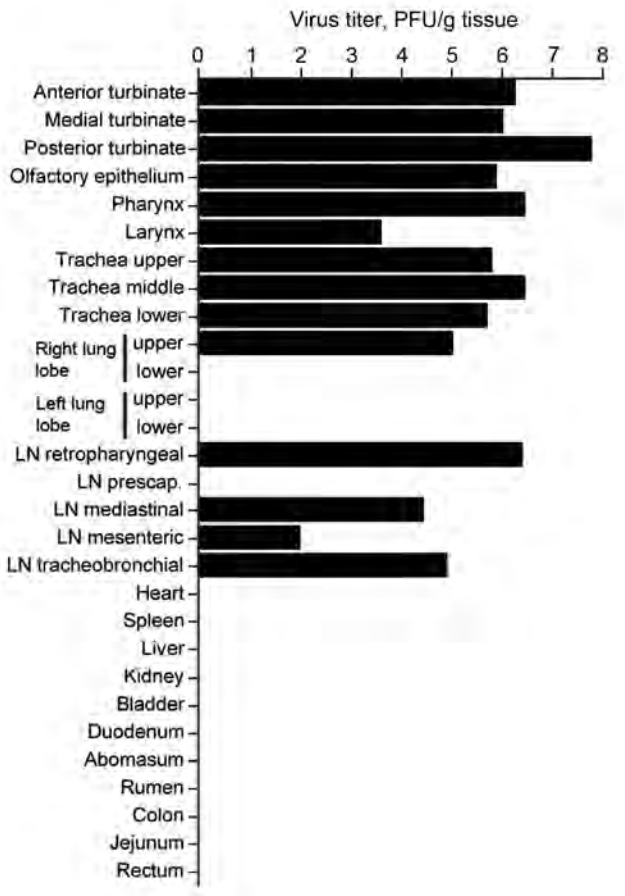

Figure 4. Virus titers in tissues collected from dromedary camel 1 inoculated with Middle East respiratory syndrome coronavirus. Tissues were collected at 5 days postinoculation (dpi) for camel 1, 28 dpi for vamel 2 and 42 dpi for camel 3. Detectable infectious virus in the collected tissues was found only in camel 1. Nasal turbinates were sampled in 3 different sections: anterior, medial, and posterior. Infectious titers were determined by plaque assay. LN, lymph node.

MERS-CoV Shedding

MERS-CoV shedding started during 1–2 dpi, as detected by the presence of infectious virus and viral RNA by qPCR in nasal swab samples. Infectious virus shedding was detected <7 dpi, and shedding of viral RNA was detected <35 dpi in nasal swab samples (Figure 2). Low concentrations of infectious virus and viral RNA were detected in oral samples, likely originating in drainage from the nasal cavity (Figure 3). No viral RNA was detected in fecal samples or in urine samples collected by convenience or at necropsy at 0, 1, 5, 14, 21, 28, and 42 dpi from the 3 camels. No infectious virus or viral RNA was detected in any of the serum or whole blood samples. Small quantities of MERS-CoV RNA were detected in exhaled breath by qPCR ($10^{1.2}$ and $10^{1.4}$ $TCID_{50}$ equivalent/mL) at 3 and 5 dpi, but infectious virus was not detected.

MERS-CoV Tropism and Pathology

Infectious virus was detected in tissues from camel 1, which was euthanized on 5 dpi, but not in tissues obtained from camels 2 and 3, which were euthanized at28 and 42 dpi, respectively. Infectious virus was detected in tissues of the upper respiratory tract (URT), including nasal turbinates, olfactory epithelium, pharynx, and larynx. In the lower respiratory tract, infectious virus was detected in the trachea and in 1 of 4 lung lobes tested. Infectious virus was also detected in the retropharyngeal, mediastinal, mesenteric, and tracheobronchial lymph nodes (Figure 4). On necropsy of camel 1 at 5 dpi, histologic lesions were found in the pseudostratified epithelial cells in the URT and the lower respiratory tract (trachea, bronchi, and bronchioles) but not in the alveoli (Figure 5). The lesions were characterized as mild to moderate acute intraepithelial and submucosal inflammation with multifocal necrosis and loss of pseudostratified epithelial cells, comparable to the common cold among humans. Multifocal loss of epithelial polarity and cilia with squamous metaplasia were observed. The epithelium was infiltrated by small-to-moderate numbers of neutrophils with fewer macrophages; similar inflammatory cells also permeated the submucosa. The submucosal glands of the trachea were multifocally necrotic and infiltrated by small numbers of neutrophils. Viral antigen was detected within the epithelial cells of the nasal turbinates, larynx, trachea, bronchi, and bronchioles, but not the alveoli. In addition, viral antigen was present at the follicular mantle zone of the tonsils and mediastinal and retropharyncheal lymph nodes (Figure 5). The nasal turbinates, larynx, and trachea of camel 2 (necropsied at 28 dpi) had similar but milder lesions when compared with those of camel 1. The nasal turbinate, larynx, and bronchus showed small numbers of infiltrating neutrophils; however, in contrast with the condition of camel 1, the cilia and goblet cells were intact. The remainder of the respiratory tract of camel 2 was unaffected. Immunohistochemical testing revealed the presence of limited viral antigen in the nasal turbinate but not in any of the other tissues at that time. No lesions or viral antigens were detected in camel 3 at 42 dpi.

Humoral Response to MERS-CoV

Serum samples were collected weekly from the camels to monitor the generation of neutralizing antibodies specific to MERS CoV. Each of the 3 camels was seronegative before inoculation. Robust MERS-CoV specific antibody responses developed in camels 2 and 3 (euthanized on 28 and 42 dpi, respectively), detected first on 14 dpi with a plaque-reduction neutralization test titer from 20 to 40 that increased to 640 at 35 dpi (Table). Camel 1 was euthanized at 5 dpi and was not tested for development of antibodies against the virus.

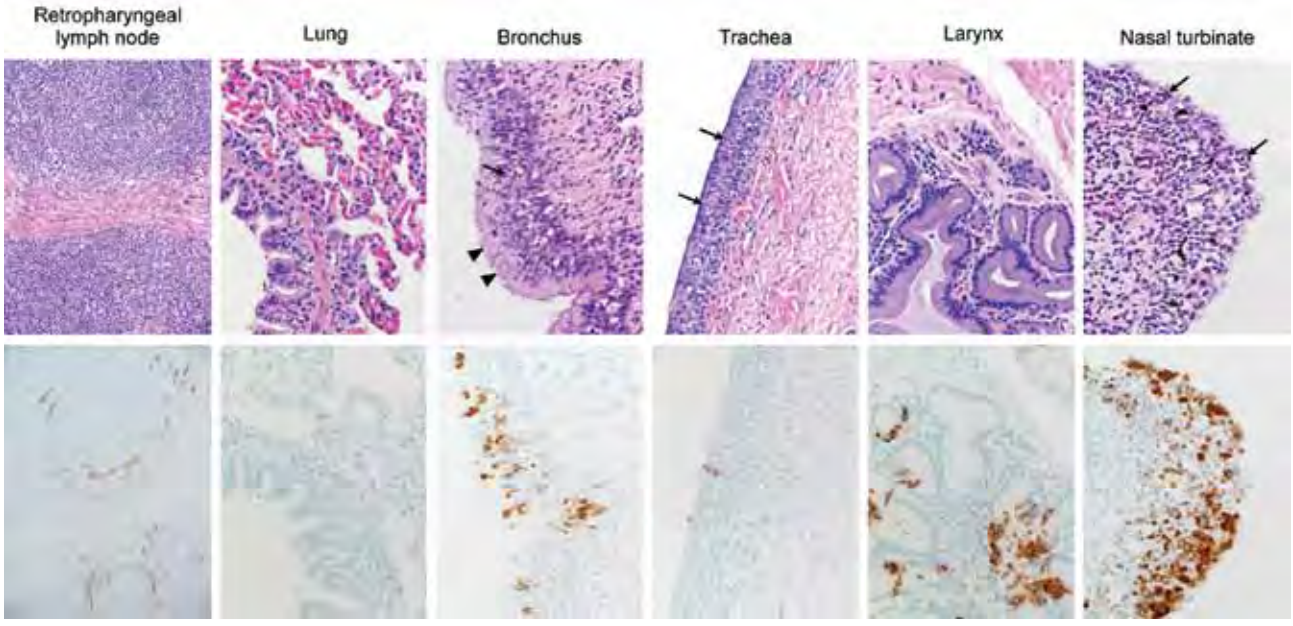

Figure 5. Histopathologic changes at 5 days postinoculation in camel 1 inoculated with Middle East respiratory syndrome coronavirus. Tissues were collected and stained with hematoxylin and eosin (top row). Anti–MERS-CoV immunohistochemical results (bottom row) are visible as a red-brown stain. Degeneration of the pseudostratified epithelium lining the nasal turbinate, trachea, and bronchus is indicated by the absence of goblet cells, cilia and nuclear regimentation with infiltration of neutrophils (arrows). The arrowheads indicate areas where the cilia remained intact. Original magnification ×400.

Discussion

Epidemiologic and surveillance data on the emergence of MERS-CoV strongly point toward a role for dromedary camels as a reservoir for zoonotic transmission (*13–21*,*27*,*28*). To understand the ecology of MERS-CoV in the most likely reservoir host, we experimentally inoculated 3 young adult dromedary camels with MERS CoV. The disease observed was clinically benign, in agreement with the absence of overt illness reported from field surveillance studies (*14*,*17*,*19*,*21*). A large quantity of MERS-CoV and viral RNA was detected in nasal swab specimens from each of the 3 camels. Infectious virus was detected through 7 dpi, and RNA was detected through 35 dpi in camel 3, which was euthanized on day 42. This route of shedding is consistent with data on naturally infected camels (*14*,*18*,*21*,*28*,*29*), and the pattern of shedding suggests that the infectious period of camels may be short. MERS-CoV was not detected in either urine or feces, again consistent with field observations (*21*,*28*).

The large quantities of MERS-CoV shed in nasal secretions by each of the 3 camels suggest that camel-to-camel and camel-to-human transmission may occur readily through direct contact and large droplet, or possibly fomite transmission. Histopathologic examination revealed that the URT, specifically the respiratory epithelium in the nasal turbinates, is the predominant site of MERS-CoV replication in camels.

Neutralizing antibodies were detected from 14 dpi onward, reaching a maximum neutralizing titer of 640 after 35 days. Serologic studies in camels in the field have reported MERS-CoV neutralizing titers as high as 5,120 (*14*,*16*), potentially indicative of repeated exposure and re-infection.

The study reported here was done on the basis of inoculation of 3 male animals with a human isolate of MERS-CoV, and the study design we used imposed several limitations on how these data inform what occurs in natural infections. The camels we inoculated were exposed to a high dose of virus by 3 simultaneous routes of inoculation. In retrospect, the inoculation dose does not seem excessive, based on the large quantity of virus shed nasally in all 3 animals (Figure 2). The total dose inoculated was relatively equivalent to the amount of virus present in a single nasal swab sample taken during the first days postinoculation, and it seems probable that a camel shedding this quantity of virus would readily infect other camels or humans with which it had direct contact. The fact that we inoculated the camels with the virus by 3 routes precludes drawing conclusions regarding efficiency of transmission by a particular route, which is a topic that should be addressed in future studies. The influence of camel age on susceptibility and dynamics of virus shedding is another notable parameter that requires further study. It seems likely that productive infection and shedding of virus in natural settings occurs predominantly in juvenile camels (*28*). This could be the

Table. Antibody titers against MERS-CoV in dromedary camels inoculated with the virus as determined by 90% plaque reduction assay*

Day	Camel 1	Camel 2	Camel 3
0	<10	<10	<10
7	NA†	<10	<10
14	NA	40	20
21	NA	80	20
28	NA	40	160
35	NA	NA	640
42	NA	NA	320

*MERS-CoV, Middle East respiratory syndrome coronavirus.
†NA, serum samples were not available.

result of an intrinsic difference in age-related susceptibility, but is more likely related to the immunologically naïve status of the animals in the context of a high force of infection after decay of passively acquired antibodies. The animals we infected were young adults, but were seronegative and therefore probably as susceptible as juveniles from MERS-CoV–endemic regions. Another aspect of pathogenesis not addressed here is whether virus is present in milk or meat from infected camels and thereby poses another potential route of exposure to humans who consume such products. Despite these limitations, the magnitude and pattern of virus shedding was essentially identical in all 3 animals and supports the available epidemiologic data indicating that camels are likely a major reservoir host for MERS-CoV. Additional experimental and field studies are clearly required to address the duration of shedding of infectious MERS-CoV from infected camels, to determine whether infection results in protective immunity, and to clarify the burden of illness among humans resulting from transmission from camels.

Acknowledgments

We thank Bart Haagmans and Ron Fouchier, for providing MERS-CoV (isolate hCoV-EMC/2012); Tina Thomas, Dan Long, and Rebecca Rosenke for histopathologic examination; and Anita Mora and Ryan Kissinger for figure preparation.

This work was supported by the Intramural Research Program of the National Institute of Allergy and Infectious Diseases, National Institutes of Health, and the Animal Models Core at Colorado State University. D.R.A. was supported through the Infectious Disease: Translational Research Training Program at Colorado State University.

All animal work in this study was approved by the Institutional Animal Care and Use Committee of Colorado State University and was performed in compliance with recommendations in the Guide for the Care and Use of Laboratory Animals of the National Institute of Health.

Ms Adney is a graduate student at Colorado State University in Fort Collins, Colorado. Her research focus is on the pathogenesis of emerging infectious diseases.

References

1. Zaki AM, van Boheemen S, Bestebroer TM, Osterhaus AD, Fouchier RA. Isolation of a novel coronavirus from a man with pneumonia in Saudi Arabia. N Engl J Med. 2012;367:1814–20. http://dx.doi.org/10.1056/NEJMoa1211721
2. World Health Organization. Global Alert and Response. Middle East respiratory syndrome coronavirus (MERS-CoV)—update; 2014 June [cited 30 Jun 2014]. http://www.who.int/csr/don/2014_06_16_mers/en/
3. Puzelli S, Azzi A, Santini MG, Di Martino A, Facchini M, Castrucci MR, et al. Investigation of an imported case of Middle East respiratory syndrome coronavirus (MERS-CoV) infection in Florence, Italy, May to June 2013. Euro Surveill. 2013;18: pii: 20564.
4. Milne-Price S, Miazgowicz KL, Munster VJ. The emergence of the Middle East respiratory syndrome coronavirus. Pathog Dis. 2014;71:121–36. http://dx.doi.org/10.1111/2049-632X.12166
5. Assiri A, McGeer A, Perl TM, Price CS, Al Rabeeah AA, Cummings DA, et al. Hospital outbreak of Middle East respiratory syndrome coronavirus. N Engl J Med. 2013;369:407–16. http://dx.doi.org/10.1056/NEJMoa1306742
6. Memish ZA, Al-Tawfiq JA, Assiri A. Hospital-associated Middle East respiratory syndrome coronavirus infections. N Engl J Med. 2013;369:1761–2. http://dx.doi.org/10.1056/NEJMc1308698
7. van Boheemen S, de Graaf M, Lauber C, Bestebroer TM, Raj VS, Zaki AM, et al. Genomic characterization of a newly discovered coronavirus associated with acute respiratory distress syndrome in humans. MBio. 2012;3:e00473012.
8. Memish ZA, Mishra N, Olival KJ, Fagbo SF, Kapoor V, Epstein JH, et al. Middle East respiratory syndrome coronavirus in bats, Saudi Arabia. Emerg Infect Dis. 2013;19:1819–23. http://dx.doi.org/10.3201/eid1911.131172
9. Graham RL, Donaldson EF, Baric RS. A decade after SARS: strategies for controlling emerging coronaviruses. Nat Rev Microbiol. 2013;11:836–48. http://dx.doi.org/10.1038/nrmicro3143
10. Albarrak AM, Stephens GM, Hewson R, Memish ZA. Recovery from severe novel coronavirus infection. Saudi Med J. 2012;33:1265–9.
11. Buchholz U, Muller MA, Nitsche A, Sanewski A, Wevering N, Bauer-Balci T, et al. Contact investigation of a case of human novel coronavirus infection treated in a German hospital, October-November 2012. Euro Surveill. 2013:18. pii: 20406.
12. Drosten C, Seilmaier M, Corman VM, Hartmann W, Scheible G, Sack S, et al. Clinical features and virological analysis of a case of Middle East respiratory syndrome coronavirus infection. Lancet Infect Dis. 2013;13:745–51. http://dx.doi.org/10.1016/S1473-3099(13)70154-3
13. Reusken CB, Haagmans BL, Muller MA, Gutierrez C, Godeke GJ, Meyer B, et al. Middle East respiratory syndrome coronavirus neutralising serum antibodies in dromedary camels: a comparative serological study. Lancet Infect Dis. 2013;13:859–66. http://dx.doi.org/10.1016/S1473-3099(13)70164-6
14. Haagmans BL, Al Dhahiry SHS, Reusken CBEM, Raj VS, Galiano M, Myers R, et al. Middle East respiratory syndrome coronavirus in dromedary camels: an outbreak investigation. Lancet Infect Dis. 2014;14:140–5. http://dx.doi.org/10.1016/S1473-3099(13)70690-X
15. Reusken CB, Ababneh M, Raj VS, Meyer B, Eljarah A, Abutarbush S, et al. Middle East respiratory syndrome coronavirus (MERS-CoV) serology in major livestock species in an affected region in Jordan, June to September 2013. Euro Surveill. 2013;18:20662.
16. Meyer B, Muller MA, Corman VM, Reusken CB, Ritz D, Godeke GJ, et al. Antibodies against MERS coronavirus in dromedary camels, United Arab Emirates, 2003 and 2013. Emerg Infect Dis. 2014;20:552–9. http://dx.doi.org/10.3201/eid2004.131746
17. Nowotny N, Kolodziejek J. Middle East respiratory syndrome coronavirus (MERS-CoV) in dromedary camels, Oman, 2013. Euro Surveill. 2014;19:20781.

18. Alagaili AN, Briese T, Mishra N, Kapoor V, Sameroff SC, de Wit E, et al. Middle East respiratory syndrome coronavirus infection in dromedary camels in Saudi Arabia. MBiol. 2014; e00884-14. http://dx.doi.org/doi:10.1128/mBio.00884-14
19. Hemida MG, Perera RA, Wang P, Alhammadi MA, Siu LY, Li M, et al. Middle East respiratory syndrome (MERS) coronavirus seroprevalence in domestic livestock in Saudi Arabia, 2010 to 2013. Euro Surveill. 2013;18:20659.
20. Memish ZA, Cotten M, Meyer B, Watson SJ, Alsahafi AJ, Al Rabeeah AA, et al. Human infection with MERS coronavirus after exposure to infected camels, Saudi Arabia, 2013. Emerg Infect Dis. 2014;20:1012–5. http://dx.doi.org/10.3201/eid2006.140402
21. Azhar EI, El-Kafrawy SA, Farraj SA, Hassan AM, Al-Saeed MS, Hashem AM, et al. Evidence for camel-to-human transmission of MERS coronavirus. N Engl J Med. 2014;370:2499–505. http://dx.doi.org/10.1056/NEJMoa1401505
22. Samara EM, Abdoun KA. Concerns about misinterpretation of recent scientific data implicating dromedary camels in epidemiology of Middle East respiratory syndrome (MERS). MBio. 2014;5(4):e01430-14. http://dx.doi.org/10.1128/mBio.01430-14
23. Alagaili AN, Briese T, Karesh WB, Daszak P, Lipkin WI. Reply to "Concerns about misinterpretation of recent scientific data implicating dromedary camels in epidemiology of Middle East respiratory syndrome (MERS)."MBio. 2014;5(4). PubMed http://dx.doi.org/10.1128/mBio.01482-14
24. Corman VM, Muller MA, Costabel U, Timm J, Binger T, Meyer B, et al. Assays for laboratory confirmation of novel human coronavirus (hCoV-EMC) infections. Euro Surveill. 2012;17: pii:20334.
25. de Wit E, Rasmussen AL, Falzarano D, Bushmaker T, Feldmann F, Brining DL, et al. Middle East respiratory syndrome coronavirus (MERS-CoV) causes transient lower respiratory tract infection in rhesus macaques. Proc Natl Acad Sci U S A. 2013;110:16598–603. http://dx.doi.org/10.1073/pnas.1310744110
26. Nemeth NM, Bowen RA. Dynamics of passive immunity to West Nile virus in domestic chickens (*Gallus gallus domesticus*). Am J Trop Med Hyg. 2007;76:310–7.
27. Alexandersen S, Kobinger GP, Soule G, Wernery U. Middle East respiratory syndrome coronavirus antibody reactors among camels in Dubai, United Arab Emirates, in 2005. Transbound Emerg Dis. 2014;61:105–8. http://dx.doi.org/10.1111/tbed.12212
28. Hemida MG, Chu DK, Poon LL, Perera RA, Alhammadi MA, Ng H-Y, et al. MERS coronavirus in dromedary camel herd, Saudi Arabia. Emerg Infect Dis. 2014;20:1231–4. http://dx.doi.org/10.3201/eid2007.140571
29. Briese T, Mishra N, Jain K, Zalmout IS, Jabado OJ, Karesh WB, et al. Middle East respiratory syndrome coronavirus quasispecies that include homologues of human isolates revealed through whole-genome analysis and virus cultured from dromedary camels in Saudi Arabia. MBio. 2014;5:e01146–14. http://dx.doi.org/10.1128/mBio.01146-14

Address for correspondence: Richard A. Bowen, Department of Biomedical Sciences, Colorado State University, W113 ARBL Bldg, Foothills Campus, Fort Collins, CO, 80523-1601, USA; email: Richard.Bowen@colostate.edu

Transmission Characteristics of Variably Protease-Sensitive Prionopathy

Silvio Notari,[1] Xiangzhu Xiao,[1] Juan Carlos Espinosa, Yvonne Cohen, Liuting Qing, Patricia Aguilar-Calvo, Diane Kofskey, Ignazio Cali, Laura Cracco, Qingzhong Kong, Juan Maria Torres, Wenquan Zou, and Pierluigi Gambetti

Variably protease-sensitive prionopathy (VPSPr), a recently identified and seemingly sporadic human prion disease, is distinct from Creutzfeldt-Jakob disease (CJD) but shares features of Gerstmann-Sträussler-Scheinker disease (GSS). However, contrary to exclusively inherited GSS, no prion protein (PrP) gene variations have been detected in VPSPr, suggesting that VPSPr might be the long-sought sporadic form of GSS. The VPSPr atypical features raised the issue of transmissibility, a prototypical property of prion diseases. We inoculated VPSPr brain homogenate into transgenic mice expressing various levels of human PrP (PrP^C). On first passage, 54% of challenged mice showed histopathologic lesions, and 34% harbored abnormal PrP similar to that of VPSPr. Surprisingly, no prion disease was detected on second passage. We concluded that VPSPr is transmissible; thus, it is an authentic prion disease. However, we speculate that normal human PrP^C is not an efficient conversion substrate (or mouse brain not a favorable environment) and therefore cannot sustain replication beyond the first passage.

Prion diseases include a variety of animal and human conditions that might be sporadic, inherited, or acquired by infection. Despite this diversity, most prion diseases are thought to share the same pathogenetic mechanism whereby the cellular prion protein (PrP^C) is templated into an abnormal and pathogenic conformer, commonly identified as scrapie PrP (PrP^{Sc}) (*1*). Therefore, conversion by templating is the basic mechanism that causes disease and sustains disease transmission among humans (*2*). However, data have shown that propagation, disease manifestation, and transmissibility might occur separately in various ways (*3*,*4*).

Author affiliations: Case Western Reserve University, Cleveland, Ohio, USA (S. Notari, X. Xiao, Y. Cohen, L. Qing, D. Kofskey, I. Cali, L. Cracco, Q. Kong, W. Zou, P. Gambetti); and Instituto Nacional de Investigación y Tecnología Agraria y Alimentaria, Madrid, Spain (J.C. Espinosa, P. Aguilar-Calvo, J.M. Torres)

DOI: http://dx.doi.org/10.3201/eid2012.140548

The phenotype of human prion diseases is highly heterogeneous. This characteristic is largely due to the variable genotype at codon 129, the site of a methionine/valine (MV) polymorphism in the human PrP gene, and the molecular characteristics of the associated PrP^{Sc} (*5*). A further major distinction that has been applied to human prion diseases for years is based on the experimental transmissibility of these diseases to hosts thought to be permissive for exogenous human PrP^{Sc} (*6*). Based on this principle, the sporadic form of Creutzfeldt-Jakob disease (sCJD) belongs to the transmissible disease group, whereas most of the Gerstmann-Sträussler-Scheinker diseases (GSS), a group comprising exclusively inherited forms, were considered difficult to transmit or not transmissible (*7*–*10*). However, an increasing number of findings have challenged this distinction. Replication of infectious PrP^{Sc} occurs in the absence of clinical signs in the host, or even in the absence of detectable disease, by histologic and Western blot (WB) examinations. Yet, infectivity can be demonstrated in subsequent passages to more susceptible hosts (*9*,*11*,*12*). Finally, disease transmissibility has recently been demonstrated for a subtype of GSS previously thought to be nontransmissible (*8*,*10*,*13*).

In 2008 and 2010, we introduced a novel human prion disease, presumably sporadic, that we named variably protease-sensitive prionopathy (VPSPr) (*14*–*16*). VPSPr differs from sCJD in several aspects. The clinical presentation and the frequent slow progression evoke the features of atypical dementias, such as frontotemporal dementia, diffuse Lewy body disease, or normal pressure hydrocephalus (*17*). The flocculent PrP immunostaining pattern, which includes the frequent presence of PrP peculiar amyloid plaques, differs from those of other sporadic prion diseases. However, the most distinctive VPSPr feature rests on the characteristics of the associated PrP^{Sc}, especially the electrophoretic profile and resistance to

[1]These authors contributed equally to this article.

the commonly used protease, such as proteinase K (PK) (*14*,*15*,*17*). VPSPr-associated, PK-resistant PrP^{Sc} (resPrP^{Sc}) forms a distinctive 5-band electrophoretic profile, comprising various fragments truncated at the N terminal and at least 1 fragment truncated at both N and C terminals, which consequently lacks the GPI (glycosylphosphatidylinositol) anchor (*14*). Furthermore, the N-truncated fragments do not include the diglycosylated PrP^{Sc} isoforms but only 1 of 2 monoglycosylated and the unglycosylated isoforms (*18*), and upon cleavage of the glycans, these fragments form 3 PK-resistant WB bands in VPSPr preparations. In contrast, the electrophoretic profile of sCJD resPrP^{Sc} is characterized by 3 bands, including diglycosylated, 2 monoglycosylated, and unglycosylated isoform, all of which harbor the GPI anchor and form only 1 band after glycan removal (*19*). However, VPSPr also occasionally displays small amounts of typical 3 electrophoretic band–forming resPrP^{Sc} on WB of basal ganglia and other deep cerebral structures (*14*). On the whole, the VPSPr 5-band ladder profile is more akin to the electrophoretic profile of PrP^{Sc} in most GSS subtypes, although contrary to GSS, no mutation in the PrP gene open reading frame has been observed in VPSPr (*14*–*16*). Given this similarity, Zou et al. hypothesized that VPSPr is the sporadic form of GSS (*15*). Like sCJD, VPSPr affects persons harboring each of 3 PrP^{C} 129 genotypes: methionine and valine homozygosity (MM, VV) and MV heterozygosity. The 3 genotypic subtypes of VPSPr differ slightly in clinical presentation, duration, histopathologic features, and PK resistance of the PrP^{Sc} (*15*).

The similarity in the PrP^{Sc} electrophoretic profiles with GSS, which was regarded as not transmissible, called into question the transmissibility of VPSPr and prompted use of the term prionopathy rather than prion disease. The present study addresses this issue. Transgenic (Tg) mice expressing various levels of human PrP^{C} harboring methionine (M) or valine (V) at position 129 underwent intracranial inoculation with brain homogenates (BH) from several human case-patients with VPSPr associated with each of the three 129 genotypes (*15*). Surprisingly, VPSPr was transmitted as an asymptomatic disease characterized by focal accumulation of VPSPr-like PrP^{Sc} in the first passage, but no prion disease could be demonstrated in the second passage.

Materials and Methods

VPSPr Case-Patients and Controls

We conducted this study during 2007–2013. Twelve case-patients with VPSPr (6 with VPSPr-129VV, 4 with VPSPr-129MV, and 2 with VPSPr-129MM) provided the inocula used in the first passage. The second passage inocula were obtained from Tg mice challenged at first passage with BH from frontal cortex and putamen of 1 case-patient with VPSPr-129VV and 1 with VPSPr-129MM. Two sets of experiments were conducted to generate negative controls by using Tg mice from the same lines: 1) age-matched Tg mice that were not inoculated and 2) age-matched Tg mice challenged with noninfectious BH from mice of the same genetic background. Positive controls were obtained from the same 129M and 129V Tg mice lines inoculated with BH from 5 subtypes of sCJD, sCJDMM1, sCJDMM2, sCJDVV1, sCJDVV2, and sCJDMV2, maintaining the host/donor homology of codon 129. Finally, six 129V Tg mice were euthanized 35 days postinoculation (dpi) with VPSPr-129VV, and the presence of the inoculum was searched by immunohistochemistry and immunoblotting.

Tg Mice

Four mouse lines with different PrP^{C} expression levels were used. The first line was a Tg362 mouse line expressing human PrP^{C}-129V on a mouse PrP^{C} null background at ≈8-fold normal human brain levels, hereafter identified as Tg(HuPrP129V)×8. This line was generated following previously described methods (*20*). For the next 2 lines,Tg40 and Tg21 were generated by replacing the mouse PrP open reading frame in the murine half-genomic PrP clone in plasmid pHGPRP (*21*) with that of human PrP-129M or human PrP-129V as reported (*22*). The generated Tg mice harbored a wild-type FVB background and bred with FVB/PrP null mice (*23*) to obtain Tg mice in mouse PrP null FVB background. For the fourth line, the generated Tg40 mouse line expressing human PrP^{C}-129M at ≈1-fold normal mouse brain level, identified as Tg(HuPrP129M)×1, was then self-bred to obtain the Tg40h mouse line. The generated Tg40h expressing human PrP^{C}-129M at ≈2-fold normal mouse brain levels, was identified as Tg(HuPrP129M)×2. The Tg21 mouse line expressing human PrP^{C}-129V at ≈3-fold normal mouse brain levels was identified as Tg(HuPrP129V)×3.

Intracerebral Inoculations

Ten percent or 1% BH in 5% glucose or phosphate-buffered saline were generated from the frontal cortex, occipital cortex, or putamen. It was inoculated intracerebrally according to procedures previously described (*20*,*22*).

Ethical Considerations

We conducted animal experiments in strict accordance with the recommendations in the guidelines of the Code for Methods and Welfare Considerations in Behavioral Research with Animals (directive 86/609EC). All efforts were made to minimize suffering. Experiments were approved by the Committee on the Ethics of Animal Experiments of the Spanish National Instutute for the Agricultural and Food Research and Technology; permit no. CEEA 2011/046.

Histology and Immunohistochemistry

Standard histologic and immunohistochemical examinations were conducted at 4 brain levels. These were basal ganglia (bregma + ≈0.14 mm), thalamus (bregma – ≈1.46 mm), posterior hippocampus (bregma – ≈2.92 mm), and anterior cerebellum (bregma – ≈6.00 mm), on paraffin sections stained with hematoxylin and eosin or probed with the 3F4 antibody to the prion protein (PrP) (1:1,000–1,400) (*24*).

Immunochemistry

Conventional immunoblotting was conducted on frozen brain tissues homogenized in glucose solution to make 10% BH. To detect PK-resistant PrP^{Sc}, we mixed the 10% BH with an equal volume of 2× lysis buffer. BH was treated with different amounts of PK (Sigma Chemical Co., St. Louis, MO, USA) ranging from 0 μg/mL to 50 μg/mL. The samples untreated or treated with PK, equivalent to 0.5–2 mg of wet tissues, were loaded onto 15% Tris-HCl Criterion precast gels (Bio-Rad Laboratories, Hercules, CA, USA) for SDS-PAGE (sodium dodecyl sulfate polyacrylamide gel electrophoresis) and immunoblotted with the widely used PrP antibody 3F4 against human PrP106–112 (*15*) or 1E4 against human PrP97–105 (*25*) (Cell Sciences, Inc., Canton, MA, USA). When required, PrP was deglycosylated with PNGase F (New England Biolabs, Beverly, MA, USA) before immunoblotting following the manufacturer's instructions.

Results

First Passage

Histologic and Immunohistochemical Analyses

We found that 54% of the Tg mice belonging to 3 lines expressing 129V or 129M human PrP showed histologic abnormalities after inoculation of BH from 6 persons with symptomatic VPSPr (inoculum from 1 presymptomatic but histopathologically and immunochemically confirmed person with VPSPr did not transmit) (Table 1). All 30 positive Tg mice were asymptomatic until they were culled, after incubation periods of up to 800 days. Although the low number of mice inoculated with VPSPr-129MM made the comparison difficult, no major differences in the rate of transmission were detected between Tg(HuPrP129V) mice challenged with VPSPr-129VV and Tg(HuPrP129M) mice challenged with VPSPr-129MM. Similarly, we detected no significant difference in plaque prevalence between Tg mice expressing PrP^{C} at levels ×8 and ×3 normal (Table 1). Affected Tg mice were observed only when the 129 genotype of the VPSPr inoculum matched that of the host (Table 2); that is, neither positive Tg(HuPrP129M) nor Tg(HuPrP129V) mice were observed after inoculation with VPSPr-129MV and VPSPr-129VV or VPSPr-129MV BH, respectively. However, VPSPr-129MM transmission to Tg(HuPrP129V) was not tested, and Tg(HuPrP129M)×1, but not Tg(HuPrP129M)×2, was used for transmission of VPSPr-129VV.

The histologic lesions included 2 types. The most common lesion consisted of individual or aggregates of prion plaques often in a row preferentially located immediately below the corpus callosum at the border with the alveus of the hippocampus, which might represent the subependymal region of the lateral ventricles. We occasionally saw individual plaques in other periventricular regions but rarely in the parenchyma (Figures 1, 2). The lesion of the second type consisted of focal spongiform degeneration involving the layer lacunosum moleculare of the hippocampus (Figure 1). This lesion was seen almost exclusively in Tg(HuPrP129V)×8 and predominantly after inoculation of VPSPr BH from the basal ganglia. PrP immunostaining intensely enhanced the plaques and demonstrated PrP granular deposits in the focal areas of spongiform degeneration. Although plaques appeared very compact in Tg(HuPrP129V) mice inoculated with VPSPr-129VV, plaques in Tg(HuPrP129M) mice after VPSPr-129MM

Table 1. First passage VPSPr inoculations to Tg(HuPrP) harboring the same PrP 129 genotype as the inoculum*

			Histology, immunohistochemistry		PrP^{Sc} Western blot	
Inoculum	Tg(HuPrP)	No. with clinical signs/total	No. positive/total	Dpi positive/total†	No. positive/total	Dpi positive/total
VPSPr-129VV 1st‡	(129V)×8§	0/11	3/9	741 ± 76/741 ± 55	4/11	768 ± 74/733 ± 71
VPSPr-129VV 2nd		0/17	10/12	711 ± 65/722 ± 59	6/17	635 ± 204/682 ± 131
VPSPr-129VV 3rd		0/11	3/8	669 ± 92/651 ± 89	3/10	642 ± 157/604 ± 140
VPSPr-129VV 4th	(129V)×3	0/9	7/9	655 ± 67/642 ± 104	NA	NA
VPSPr-129VV 5th		0/6	3/6	541 ± 96/642 ± 76	NA	NA
VPSPr-129MM 1st	(129M)×2	0/6	4/6	678 ± 90/590 ± 154	NA	NA
VPSPr-129MM 2nd (presymptomatic)		0/6	0/6	0/746 ± 59	NA	NA

Dpi, days postinoculation; M, methionine; V, valine; NA, not available; VPSPr, variably protease-sensitive prionopathy associated with homozygous V or M at codon 129 of the PrP gene (VPSPr-129VV or VPSPr-129MM).
†Dpi of positive mice compared with dpi of all mice (including positive mice). Each value represents the mean ± SD.
‡Identifies the VPSPr case-patients providing the inoculum, i.e., inocula were obtained from 5 case-patients with VPSPr-129VV and 2 with VPSPr-129MM.
§Refers to the presence of V or M at PrP residue 129 and expression level indicated as × normal.

Table 2. First passage VPSPr inoculations to Tg(HuPrP) mice harboring different PrP 129 genotypes from those of the inocula*

			Histology, immunohistochemistry		PrP^{Sc} Western blot	
Inoculum	Tg(HuPrP)	No. with clinical signs/total	No. positive/total	Dpi positive/total†	No. positive/total	Dpi positive/total
VPSPr-129VV 6th‡	(129M)×1§	0/5	0/5	0/643 ± 71	NA	NA
VPSPr-129VV 4th		0/4	0/4	0/659 ± 55	NA	NA
VPSPr-129VV 5th		0/5	0/5	0/757 ± 57	NA	NA
VPSPr-129MV 1st	(129M)×2	0/9	0/9	0/745 ± 70	NA	NA
VPSPr-129MV 2nd		0/6	0/6	0/582 ± 101	NA	NA
VPSPr-129MV 3rd		0/4	0/4	0/694 ± 153	NA	NA
VPSPr-129MV 4st	(129V)×8	0/6	0/6	0/586 ± 68	NA	NA
VPSPr-129MV 3rd		0/7	0/7	0/681 ± 102	NA	NA

Dpi, days postinoculation; M, methionine; V, valine; NA, not available; VPSPr, variably protease-sensitive prionopathy associated with homozygosity V or M at codon 129 of the PrP gene (VPSPr-129VV or VPSPr-129MM).
†Dpi of positive mice compared with dpi of all mice (including positive mice). Each value represents the mean ± SD.
‡Identifies the VPSPr case-patients providing the inoculum, i.e., inocula were obtained from 5 case-patients with VPSPr-129VV and 2 with VPSPr-129MM.
§Refers to the presence of V or M at PrP residue 129 and expression level indicated as × normal.

inoculation were less well formed and were often replaced by loose aggregates of irregular granules (Figure 1). The topographic distribution of the plaque deposits and focal spongiform change are shown in Figure 2.

Neither prion-related lesions nor PrP^{Sc} were observed in 23 age-matched Tg(HuPrP129)V×8 mice that had not been inoculated or had undergone inoculations with noninfectious BH (Table 3). As expected, the 3 Tg(HuPrP) mouse lines used for VPSPr transmission easily transmitted sCJD subtypes that were 129 genotypically compatible with the host PrP, indicating that the Tg mice used for VPSPr transmission are competent to propagate classical human prion diseases (Table 3). No PrP immunostaining was detected in the 6 Tg(HuPrP129V)×8 35 dpi with VPSPr-129VV BH.

WB Analysis

Thirteen (34%) of the 38 VPSPr-inoculated Tg (HuPrP129V)×8 mice examined showed a definitively positive WB, despite the mouse BH treatment with a wide range of PK to maximize the recovery of PrP^{Sc}, including PrP^{Sc} species with low resistance to PK. The 34% prevalence of positive cases harboring detectable PrP^{Sc} was nearly half that of PrP^{Sc}-positive Tg mice detected at histopathologic examination (Table 1). Tg mouse $resPrP^{Sc}$ immunoreacted much more readily with the monoclonal antibody 1E4 than with 3F4, as previously reported for VPSPr PrP^{Sc} (*14*). Probed with 1E4, Tg mouse $resPrP^{Sc}$ exhibited a 5-band electrophoretic profile, similar to that of VPSPr (Figure 3). Deglycosylation by PNGase resulted in 3 $resPrP^{Sc}$ bands that co-migrated with the analogous VPSPr bands at ≈20 kDa, ≈17 kDa, and ≈7 kDa (Figure 3) (*15*). No definitely positive WB conducted with standard methods was observed in VPSPr-inoculated Tg(HuPrP129V)×3 and Tg(HuPrP129M)×2 mice (Table 1).

All negative controls, including noninoculated Tg mice and Tg mice inoculated with noninfectious BH, had negative WB. In contrast, WB were positive, with the classical 3-band profile, in all mice from the 3 Tg(HuPrP) lines challenged with BH from different sCJD subtypes used as positive controls (Table 3). WB examination of brains from 3 Tg(HuPrP129V)×8 mice challenged with VPSPr-129VV BH showed no evidence of PrP^{Sc} 35 dpi, indicating that the inoculum was too diluted to be detected or no longer present.

Second Passage

The second passage yielded a surprising finding. None of the 13 mice belonging to the Tg(HuPrP129V)×8 and Tg(HuPrP129M)×2 lines showed prion-related histologic lesions or had a definitely positive WB upon secondary transmission, even up to nearly 800 dpi (Table 4).

Discussion

The experiments reported here, which probed transmissibility of VPSPr to Tg mice expressing human PrP^{C}, yielded puzzling results. On first passage, all hosts remained asymptomatic, but 54% showed focal deposition of PrP^{Sc} in the form of prion plaques by immunohistochemical analysis. In 34% of animals, small amounts of $resPrP^{Sc}$ were demonstrated by WB (Figures 1, 3). The PrP^{Sc} recovered from affected mice recapitulated the electrophoretic profile and immunoreactivity features of the VPSPr-129VV PrP^{Sc}, even after removal of the sugar moiety. However, mouse PrP^{Sc} was apparently more PK-resistant than the PrP^{Sc} from VPSPr-129VV case-patients (Figure 3) (*15*). In contrast, on second passage, all Tg mice were negative at clinical and histopathologic examinations and harbored no PrP^{Sc} that could be definitely identified by WB, even up to 800 dpi.

These findings pose several challenging questions. The first question concerns whether the PrP^{Sc} recovered on first passage represents the residual inoculum rather than de novo PrP^{Sc} generated by conversion of the host's PrP^{C}. We believe this possibility is made unlikely by our experiment showing that the PrP^{Sc} in the VPSPr inoculum was no longer detectable by immunohistochemical and WB analyses in Tg(HuPrP-129VV) mice 35 dpi.

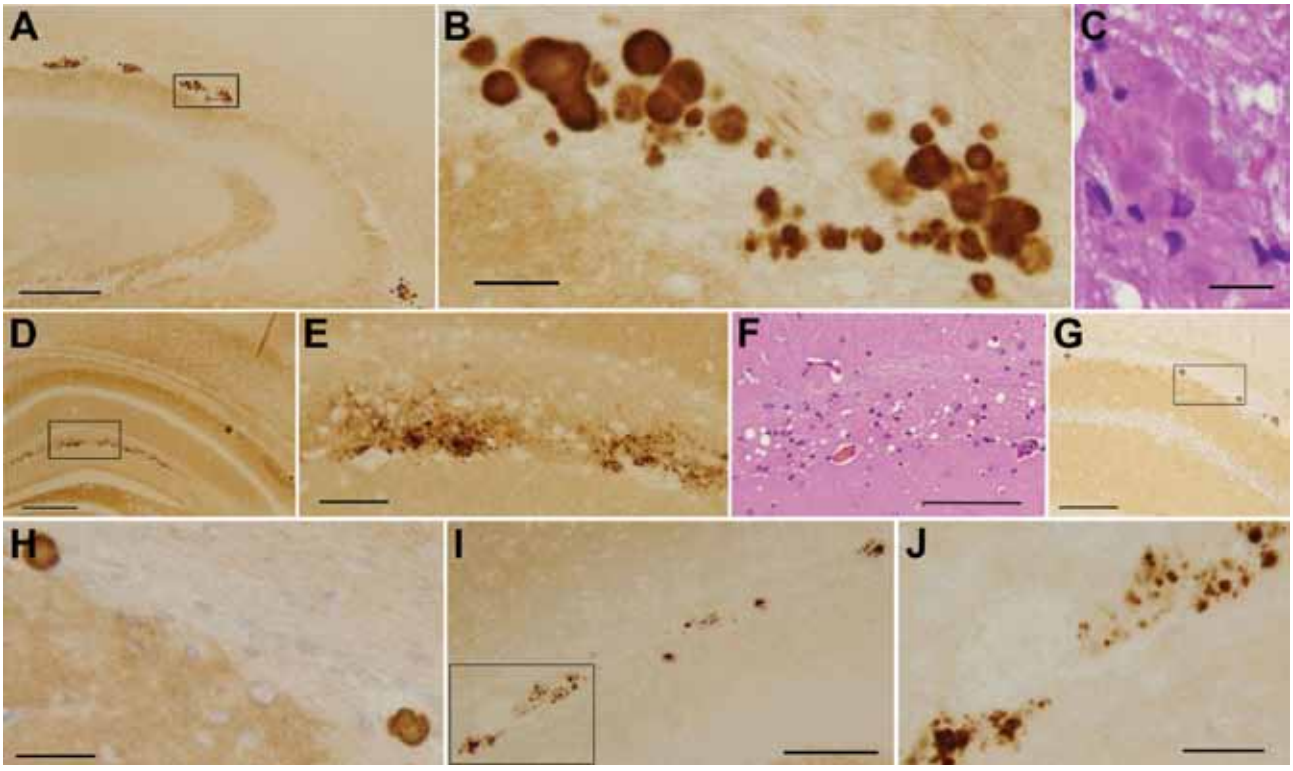

Figure 1. Histologic and immunohistochemical findings from a study of the transmission characteristics of VPSPr. A–E) Two types of lesions typically observed in Tg(HuPrP129V)×8 mice. A–C) Plaques are most often located at the border between the alveus of the hippocampus and the corpus callosum, often forming aggregates distributed in a row. They can be tightly aggregated or partially fused generating multicore plaques. PrP immunostaining (A, B) shows well-formed plaques surrounded by PrP deposits that appear in various stages of aggregation at HE. (C), Where plaque cores appear smooth, lacking the spiny appearance of typical kuru plaques. D–F) The lesion of the second type consists of PrP granular deposits (D and E) co-localized with spongiform degeneration in the layer lacunosum moleculare of the hippocampus (F). G–J) Plaques in Tg(HuPrP129V)×3 mice were fewer but similar in location and appearance to those of Tg(HuPrP129V)×8. In contrast, PrP aggregates generally appeared to be loose and formed fewer real plaques in Tg(HuPrP129M)×2–positive mice (I and J). PrP monoclonal antibody 3F4. . The boxes in panels A, D, G, and I mark the exact areas that are shown at higher magnification in panels B, E, H, and J, respectively. PrP, prion protein; VPSPr, variably protease-sensitive prionopathy; Tg, transgenic. Scale bars in A and E = 250 μm. Scale bars in B, C, H, and J = 25 μm. Scale bar in D = 500 μm. Scale bars in F, G, and I = 100 μm.

Furthermore, histopathologic changes and PrP^{Sc} detection, indicating VPSPr transmission, were observed only when the host and the inoculum were syngenic at PrP codon 129. This genotypic selectivity is not compatible with the notion that the PrP^{Sc} detected in the hosts was from the residual inoculum. Finally, several other studies have shown that PrP^{Sc} associated with the inoculum is rapidly cleared (*12*,*26*–*30*). These observations support the conclusion that histopathologic changes and the PrP^{Sc} recovered in the positive VPSPr-challenged mice result from de novo mouse PrP^{Sc} generated by templated conversion, although at a very low level. The lack of clinical signs in the affected mice can be easily explained by the characteristics and localization of the plaques and of the spongiform degeneration, both of which affected limited regions depopulated of neuronal cells and processes.

Prion plaques similar in type and topography to those we observed have been reported alone or associated with spongiform degeneration in mice challenged with prions of various origins (*9*,*11*,*29*–*32*). In 3 studies, plaque deposits seem to be especially similar to those observed by us. In the first, the plaques were detected on the second passage of vCJD in Tg mice expressing human PrP^{C}-129V (Tg152) (*11*,*29*). The second and third studies used Tg mice expressing mouse PrP harboring the P101L variation (101LL mice), which is the equivalent of the P102L human mutation linked to a GSS subtype (*9*,*30*). In the last 2 experiments, Tg101LL mice were challenged with "atypical" P102L GSS (i.e., GSS associated only with 7-kDa PrP^{Sc} PK-resistant fragment rather than with the "typical" P102L GSS that is also associated with the classical 3-band resPrP^{Sc}) or with BH from TgGSS-22, a Tg mouse model of GSS in which prion disease spontaneously develops (*9*,*30*). All affected mice of these 3 studies remained asymptomatic like

those of our study, further supporting the notion that focal prion plaque deposition in periventricular regions is not sufficient to produce major clinical signs. Despite the common histopathologic features, these mice were associated with electrophoretically distinct PrP^{Sc} species. In the experiment of vCJD transmission, PrP^{Sc} harvested from challenged Tg152 mice showed the classical 3 PK-resistant bands as in vCJD, but they displayed a higher molecular mass than in vCJD (*11*). Minimal quantity of $resPrP^{Sc}$ recovered at ≈30 kDa was detected only in 1 of 5 plaque-harboring 101LL mice challenged with atypical P102L GSS (*9*), whereas 101LL mice inoculated with TgGSS-22 BH showed no detectable PrP^{Sc} by WB (*30*). Although to some extent the variability of the PrP^{Sc} electrophoretic profiles between the experiments with Tg101LL and our experiments might be due to variations in WB methods, the PrP^{Sc} diversity in these 3 studies and in our study suggests that focal plaque formation at the border between the hippocampus and corpus callosum is not strictly PrP^{Sc} strain specific. However, this brief review indicates that peri-hippocampal plaque deposition is preferentially detected in hosts challenged with PrP^{Sc} species that form plaques in the natural disease, such as vCJD, GSS, and VPSPr.

The lack of histologic lesions and PrP^{Sc} on second passage in both Tg(HuPrP129V) and Tg(HuPrP129M) mice challenged with BH from the most severely affected first-passage mice is unusual. However, comparable findings have been reported in at least 2 previous studies. In the first, 101LL mice challenged with affected TgGSS-22 BH (a Tg mouse in which a GSS-like disease spontaneously develops) harbored fewer plaques on second passage than on first, suggesting decreased replication of the seed on second passage (*9*,*30*). In the second study, first passage of BH from cattle affected by bovine spongiform encephalopathy to Tg152 mice (expressing human PrP^{C}-129V) resulted in clinical disease associated with diffuse brain deposition of PrP as demonstrated by immunostaining (*11*), even though no $resPrP^{Sc}$ could be demonstrated by WB. On second passage in the same Tg152 mice, no evidence of prion disease could be demonstrated either by PrP immunostaining or WB, as in our study (*11*). However, BH from these negative Tg152 produced a full prion disease after inoculation into wild-type FVB mice. This remarkable finding indicates that prion transmissibility (or infectivity) can be sustained in hosts with no demonstrable prion diseases (according to commonly used methods), and that it can be rescued through passage to an appropriate host (*11*).

Interpreting our findings also in the light of the above data, we propose that normal human PrP^{C} is not a suitable substrate (or mouse brain is not a favorable environment) to sustain conversion to VPSPr PrP^{Sc}. Thus, long incubations

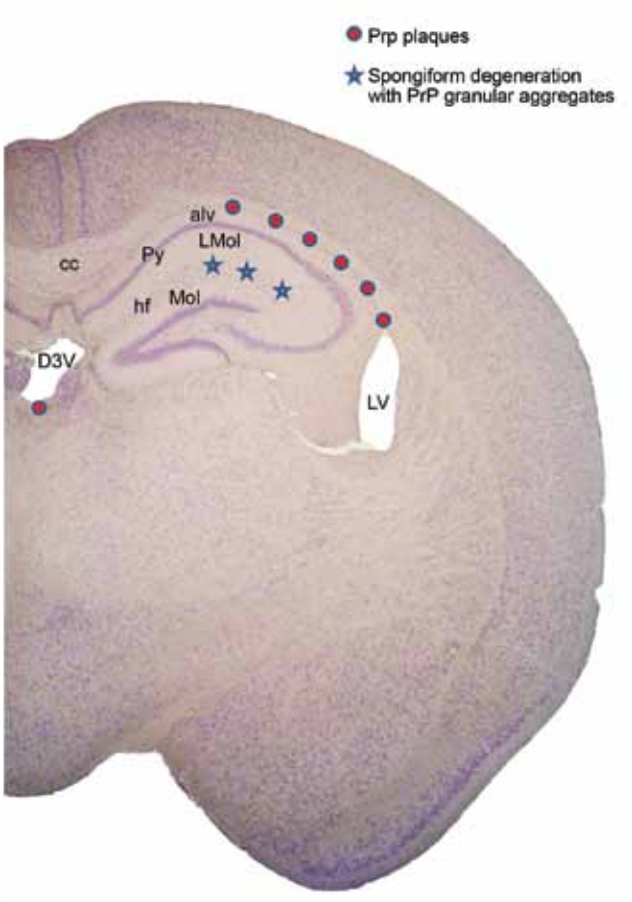

Figure 2. Representation of lesion topography in brain of positive Tg(HuPrP129V)×8 mice inoculated with VPSPr-129VV brain homogenate. alv, alveus of hippocampus; cc, corpus callosum; D3V, dorsal third ventricle; hf, hippocampal fissure; L mol, lacunosum molecular layer; LV, lateral ventricle; Mol, molecular layer dentate gyrus; Py, pyramidal cell layer of hippocampus.

are required to induce modest and asymptomatic PrP^{Sc} deposition. Nevertheless, the PrP^{Sc} generated in the host on first passage seems to match the conformation of the PrP^{Sc} from the inoculum, based on the finding that PK-resistant PrP^{Sc} fragments of similar size are recovered from host and donor preparations. This also indicates that little or no PrP^{Sc} adaptation has occurred during the first passage (*32*). The apparent failure of the second passage to transmit detectable disease might be due to the inadequate amplification of VPSPr PrP^{Sc} during primary transmission, which would result in a second passage PrP^{Sc} inoculum more diluted than the VPSPr brain extract used in the primary transmission. This line of reasoning raises the possibility that if VPSPr PrP^{Sc} were exposed to a favorable PrP substrate (or brain environment), it might replicate efficiently. This conjecture is reinforced by 2 recent findings. First, preliminary findings show that VPSPr can be transmitted to

Table 3. Control studies of VPSPr inoculations to Tg(HuPrP)*

Inoculum	Tg(HuPrP)	No. with clinical signs/total	Histology, immunohistochemistry		PrP^{Sc} Western blot	
			No. positive/total	Dpi positive/total†	No. positive/total	Dpi positive/total
Negative controls						
None	(129V)×8‡	0/15	0/9	0/721 ± 43	0/4	0/704 ± 43
Noninfectious		0/17	0/8	0/744 ± 15	0/5	0/749 ± 112
Positive controls						
sCJDVV2§	(129V)×8	6/6	3/3	223 ± 13/223 ± 13	6/6	223 ± 11/223 ± 11
sCJDVV1		7/7	7/7	353 ± 12/353 ± 12	7/7	353 ± 12/353 ± 12
sCJDMM1	(129M)×2	3/3	3/3	183 ± 22/183 ± 22	3/3	183 ± 22/183 ± 22
sCJDMM2		3/3	3/3	609 ± 139/609 ± 139	3/3	609 ± 139/609 ± 139
sCJDMV2	(129V)×3	6/6	6/6	312 ± 4/312 ± 4	NA	NA

Dpi, days postinoculation; M, methionine; V, valine; NA, not available; VPSPr, variably protease-sensitive prionopathy; sCJD sporadic Creutzfeldt-Jakob disease.
†Dpi of positive mice compared with dpi of all mice (including positive mice). Each value represents the mean ± SD.
‡Refers to the presence of V or M at PrP residue 129 and expression level indicated as × normal.
§Identifies the sCJD case-patients providing the inoculum.

bank voles more easily than to the Tg(HuPrP) used in the present experiments (*33*). Second, transmissibility of GSS linked to the A117V mutation has been recently demonstrated (*10*). GSS-A117V is commonly viewed as a "classic" GSS subtype, given the distinct features of its phenotype that is characterized by prominent prion plaques with limited spongiform degeneration and a PrP^{Sc} WB profile dominated by a highly PK-resistant fragment of 7–8 kDa (*34*). Early failures to transmit GSS-A117V and the evidence that the presence of the A117V mutation altered the topology of PrP led to the conclusions that 1) GSS-A117V was not transmissible and 2) its underlying pathogenetic mechanism was not based on a PrP^{C}-to-PrP^{Sc} conversion process (*8*).

After inoculation with BH from GSS-A117V–affected patients, Tg mice expressing human PrP, harboring the A117V mutation, developed a prion disease associated with a histologic phenotype and PrP^{Sc} that roughly recapitulated those of the human disease. However, only one fourth of the inoculated mice were symptomatic with incubation periods >600 days, whereas more than half harbored plaques, PrP^{Sc}, or both (*10*). No second passage was reported. This study shows that an allegedly nontransmissible prion disease can be transmitted (at least at first passage) if a suitable host is selected.

In conclusion, we propose that VPSPr is transmissible and, therefore, is an authentic prion disease. However, transmissibility cannot be sustained through serial passages presumably because human PrP^{C} (or the mouse brain environment) cannot efficiently convert and propagate the VPSPr PrP^{Sc} species. If this is the case, uncovering the properties of human PrP that are required to replicate more efficiently the prion strains associated with VPSPr may help clarify the PrP^{Sc} mode of formation in this intriguing disease.

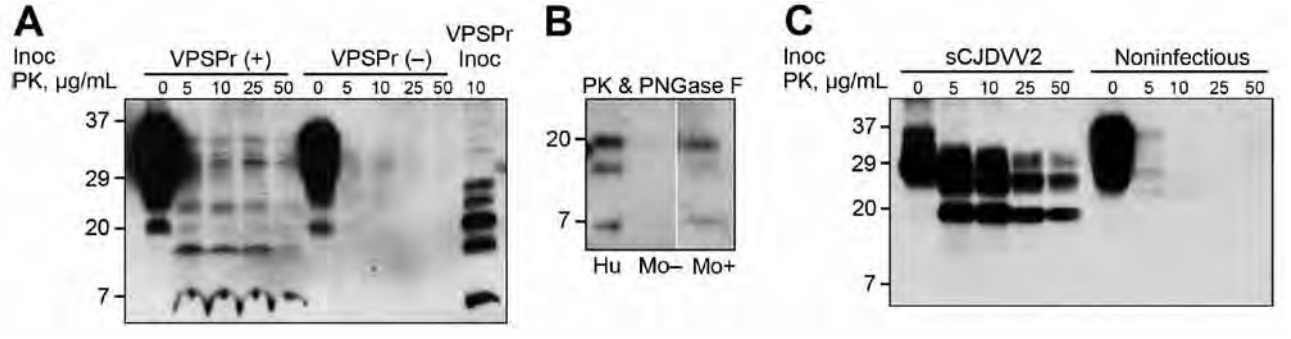

Figure 3. Western blot characteristics of PrP^{Sc} recovered from brain of VPSPr-inoculated Tg mice and controls. A) BH treated with increasing amounts of PK show PK-resistant PrP^{Sc} fragments with a ladder-like electrophoretic profile in positive VPSPr-inoculated mice, VPSPr (+), even at high concentrations of PK (50 µg/mL). In contrast, nonspecific bands are seen in negative VPSPr-inoculated mice, VPSPr (–). The banding pattern in VPSPr (+) roughly recapitulates that of the PK-treated PrP^{Sc} from the VPSPr inoculum (VPSPr Inoc). B) Positive Tg mice BH treated with PK (25 µg/mL) and PNGase F show 3 PrP^{Sc} bands migrating at ≈20 kDa, ≈17 kDa, and ≈7 kDa (Mo +), replicating those of similarly treated VPSPr inoculum (Hu). No bands can be detected in the negative Tg mice (Mo –). (All 3 preparations were run on the same gel, but unnecessary lanes were removed). C) Tg mice inoculated with sCJDVV2 BH (from sCJD homozygous valine harboring PrP^{Sc} type 2) or inoculated with noninfectious BH used as positive and negative controls exhibit typical PK-resistant PrP^{Sc}. Tg(HuPrP129V)×8 BH and monoclonal antibody 1E4 were used in all Western blot tests. Approximate molecular masses are in kDa. BH, brain homogenate; PK, proteinase K; PrP^{Sc}, scrapie prion protein; sCJD, sporadic Creutzfeldt-Jakob disease; VPSPr, variably protease-sensitive prionopathy; Tg, transgenic.

Table 4. VPSPr inoculations to Tg(HuPrP): second passage*

Inoculum	Tg(HuPrP)	No. with clinical signs/total	Histology, immunohistochemistry		PrP^{Sc} Western blot	
			No. positive/total	Dpi positive/total†	No. positive/total	Dpi positive/total
Tg(HuPrP129V) inoculated with VPSPr-129VV 2nd‡	(129V)×8§	0/10	0/10	0/616 ± 135	0/10	0/616 ± 135
Tg(HuPrP129M) inoculated with VPSPr-129MM 1st	(129M)×2	0/3	0/3	0/694 ± 51	NA	NA

Dpi, days postinoculation; M, methionine; V, valine; NA, not available; VPSPr, variably protease-sensitive prionopathy associated with homozygosity V or M at codon 129 of the PrP gene (VPSPr-129VV or VPSPr-129MM);
†Dpi of positive mice compared with dpi of total mice (including the positive mice). Each value represents the mean ± SD.
‡Identifies the Transgenic mice, inoculated with VPSPr in the first passage, providing the inoculum.
§Refers to the presence of V or M at PrP residue 129 and expression level indicated as × normal.

Acknowledgments

We thank Miriam Warren and Katie Glisic for their skillful contributions to the histologic study and manuscript editing, respectively.

This study was supported by National Institutes of Health awards AG14359 and NS062787, Centers for Disease Control and Prevention award UR8/CCU515004, Charles S. Britton Fund, and Spanish Ministerio de Ciencia e Innovación AGL2012-37988-C04-04.

Dr Notari is an instructor at Case Western Reserve University, Cleveland, Ohio, USA. His research interests include prion diseases with particular focus on the characteristics of PrP^{Sc} in different prion strains and their relationships with infectivity.

References

1. Prusiner SB. Biology and genetics of prions causing neurodegeneration. Annu Rev Genet. 2013;47:601–3. http://dx.doi.org/10.1146/annurev-genet-110711-155524
2. Surewicz WK, Apostol MI. Prion protein and its conformational conversion: a structural perspective. Top Curr Chem. 2011;305:135–67. http://dx.doi.org/10.1007/128_2011_165
3. Aguzzi A, Falsig J. Prion propagation, toxicity and degradation. Nat Neurosci. 2012;15:936–9. http://dx.doi.org/10.1038/nn.3120
4. Sandberg MK, Al-Doujaily H, Sharps B, Clarke AR, Collinge J. Prion propagation and toxicity in vivo occur in two distinct mechanistic phases. Nature. 2011;470:540–2. http://dx.doi.org/10.1038/nature09768
5. Gambetti P, Cali I, Notari S, Kong Q, Zou WQ, Surewicz WK. Molecular biology and pathology of prion strains in sporadic human prion diseases. Acta Neuropathol. 2011;121:79–90. http://dx.doi.org/10.1007/s00401-010-0761-3
6. Weissmann C, Flechsig E. PrP knock-out and PrP transgenic mice in prion research. Br Med Bull. 2003;66:43–60. http://dx.doi.org/10.1093/bmb/66.1.43
7. Kong Q, Surewicz WK, Petersen RB, Zou WQ, Chen SG, Gambetti P, et al. Inherited Prion Disease. In: Prusiner SB, editor. Prion biology and diseases. 2nd ed. Cold Spring Harbor (NY): Cold Spring Harbor Laboratory Press; 2004. p. 673–775.
8. Hegde RS, Mastrianni JA, Scott MR, DeFea KA, Tremblay P, Torchia M, et al. A transmembrane form of the prion protein in neurodegenerative disease. Science. 1998;279:827–34. http://dx.doi.org/10.1126/science.279.5352.827
9. Piccardo P, Manson JC, King D, Ghetti B, Barron RM. Accumulation of prion protein in the brain that is not associated with transmissible disease. Proc Natl Acad Sci U S A. 2007;104:4712–7. http://dx.doi.org/10.1073/pnas.0609241104
10. Asante EA, Linehan JM, Smidak M, Tomlinson A, Grimshaw A, Jeelani A, et al. Inherited prion disease A117V is not simply a proteinopathy but produces prions transmissible to transgenic mice expressing homologous prion protein. PLoS Pathog. 2013;9:e1003643. http://dx.doi.org/10.1371/journal.ppat.1003643
11. Wadsworth JD, Asante EA, Desbruslais M, Linehan JM, Joiner S, Gowland I, et al. Human prion protein with valine 129 prevents expression of variant CJD phenotype. Science. 2004;306:1793–6. http://dx.doi.org/10.1126/science.1103932
12. Race R, Meade-White K, Raines A, Raymond GJ, Caughey B, Chesebro B. Subclinical scrapie infection in a resistant species: persistence, replication, and adaptation of infectivity during four passages. J Infect Dis. 2002;186(Suppl 2):S166–70. http://dx.doi.org/10.1086/344267
13. Hegde RS, Tremblay P, Groth D, DeArmond SJ, Prusiner SB, Lingappa VR. Transmissible and genetic prion diseases share a common pathway of neurodegeneration. Nature. 1999;402:822–6. http://dx.doi.org/10.1038/45574
14. Gambetti P, Dong Z, Yuan J, Xiao X, Zheng M, Alshekhlee A, et al. A novel human disease with abnormal prion protein sensitive to protease. Ann Neurol. 2008;63:697–708. http://dx.doi.org/10.1002/ana.21420
15. Zou WQ, Puoti G, Xiao X, Yuan J, Qing L, Cali I, et al. Variably protease-sensitive prionopathy: a new sporadic disease of the prion protein. Ann Neurol. 2010;68:162–72. http://dx.doi.org/10.1002/ana.22094
16. Head MW, Yull HM, Ritchie DL, Langeveld JP, Fletcher NA, Knight RS, et al. Variably protease-sensitive prionopathy in the UK: a retrospective review 1991–2008. Brain. 2013;136:1102–15. http://dx.doi.org/10.1093/brain/aws366
17. Puoti G, Bizzi A, Forloni G, Safar JG, Tagliavini F, Gambetti P. Sporadic human prion diseases: molecular insights and diagnosis. Lancet Neurol. 2012;11:618–28. http://dx.doi.org/10.1016/S1474-4422(12)70063-7
18. Xiao X, Yuan J, Haïk S, Cali I, Zhan Y, Moudjou M, et al. Glycoform-selective prion formation in sporadic and familial forms of prion disease. PLoS ONE. 2013;8:e58786. http://dx.doi.org/10.1371/journal.pone.0058786
19. Gambetti P, Kong Q, Zou W, Parchi P, Chen SG. Sporadic and familial CJD: classification and characterization. Br Med Bull. 2003;66:213–39. http://dx.doi.org/10.1093/bmb/66.1.213
20. Padilla D, Béringue V, Espinosa JC, Andreoletti O, Jaumain E, Reine F, et al. Sheep and goat BSE propagate more efficiently than cattle BSE in human PrP transgenic mice. PLoS Pathog. 2011;7:e1001319. http://dx.doi.org/10.1371/journal.ppat.1001319
21. Fischer M, Rülicke T, Raeber A, Sailer A, Moser M, Oesch B, et al. Prion protein (PrP) with amino-proximal deletions restoring susceptibility of PrP knockout mice to scrapie. EMBO J. 1996;15:1255–64.
22. Kong Q, Huang S, Zou W, Vanegas D, Wang M, Wu D, et al. Chronic wasting disease of elk: transmissibility to humans examined by transgenic mouse models. J Neurosci. 2005;25:7944–9. http://dx.doi.org/10.1523/JNEUROSCI.2467-05.2005

23. Sailer A, Büeler H, Fischer M, Aguzzi A, Weissmann C. No propagation of prions in mice devoid of PrP. Cell. 1994;77:967–8. http://dx.doi.org/10.1016/0092-8674(94)90436-7
24. Paxinos K, Franklin G, editors. The mouse brain in stereotaxic coordinated. 2nd ed. San Diego (CA): Academic Press; 2001.
25. Yuan J, Dong Z, Guo JP, McGeehan J, Xiao X, Wang J, et al. Accessibility of a critical prion protein region involved in strain recognition and its implications for the early detection of prions. Cell Mol Life Sci. 2008;65:631–43. http://dx.doi.org/10.1007/s00018-007-7478-z
26. Büeler H, Aguzzi A, Sailer A, Greiner RA, Autenried P, Aguet M, et al. Mice devoid of PrP are resistant to scrapie. Cell. 1993;73:1339–47. http://dx.doi.org/10.1016/0092-8674(93)90360-3
27. Race R, Raines A, Raymond GJ, Caughey B, Chesebro B. Long-term subclinical carrier state precedes scrapie replication and adaptation in a resistant species: analogies to bovine spongiform encephalopathy and variant Creutzfeldt-Jakob disease in humans. J Virol. 2001;75:10106–12. http://dx.doi.org/10.1128/JVI.75.21.10106-10112.2001
28. Safar JG, DeArmond SJ, Kociuba K, Deering C, Didorenko S, Bouzamondo-Bernstein E, et al. Prion clearance in bigenic mice. J Gen Virol. 2005;86:2913–23. http://dx.doi.org/10.1099/vir.0.80947-0
29. Wadsworth JD, Joiner S, Linehan JM, Desbruslais M, Fox K, Cooper S, et al. Kuru prions and sporadic Creutzfeldt-Jakob disease prions have equivalent transmission properties in transgenic and wild-type mice. Proc Natl Acad Sci U S A. 2008;105:3885–90. http://dx.doi.org/10.1073/pnas.0800190105
30. Piccardo P, King D, Telling G, Manson JC, Barron RM. Dissociation of prion protein amyloid seeding from transmission of a spongiform encephalopathy. J Virol. 2013;87:12349–56. http://dx.doi.org/10.1128/JVI.00673-13
31. Makarava N, Kovacs GG, Savtchenko R, Alexeeva I, Budka H, Rohwer RG, et al. Genesis of mammalian prions: from non-infectious amyloid fibrils to a transmissible prion disease. PLoS Pathog. 2011;7:e1002419. http://dx.doi.org/10.1371/journal.ppat.1002419
32. Tamgüney G, Giles K, Oehler A, Johnson NL, DeArmond SJ, Prusiner SB. Chimeric elk/mouse prion proteins in transgenic mice. J Gen Virol. 2013;94:443–52. http://dx.doi.org/10.1099/vir. 0.045989-0
33. Nonno R, Di Bari M, Pirisinu L, D'Agostino C, Marcon S, Riccardi G, et al. Variably protease-sensitive prionopathy is transmissible in bank voles. Prion. 2012;6(S):6–7.
34. Pirisinu L, Nonno R, Esposito E, Benestad SL, Gambetti P, Agrimi U, et al. Small ruminant nor98 prions share biochemical features with human Gerstmann-Sträussler-Scheinker disease and variably protease-sensitive prionopathy. PLoS ONE. 2013;8:e66405. http://dx.doi.org/10.1371/journal.pone.0066405

Address for correspondence: Pierluigi Gambetti or Wenquan Zou, Institute of Pathology, Case Western Reserve University, 2085 Adelbert Rd, Cleveland, OH 44106-4907, USA; email: pierluigi.gambetti@case.edu or wenquan.zou@case.edu

Seroconversion for Infectious Pathogens among UK Military Personnel Deployed to Afghanistan, 2008–2011

Edmund N.C. Newman, Penelope Johnstone, Hannah Bridge, Deborah Wright, Lisa Jameson, Andrew Bosworth, Rebecca Hatch, Jenny Hayward-Karlsson, Jane Osborne, Mark S. Bailey, Andrew Green, David Ross, Tim Brooks, and Roger Hewson

Medscape EDUCATION ACTIVITY

Medscape, LLC is pleased to provide online continuing medical education (CME) for this journal article, allowing clinicians the opportunity to earn CME credit.

This activity has been planned and implemented in accordance with the Essential Areas and policies of the Accreditation Council for Continuing Medical Education through the joint providership of Medscape, LLC and Emerging Infectious Diseases. Medscape, LLC is accredited by the ACCME to provide continuing medical education for physicians.

Medscape, LLC designates this Journal-based CME activity for a maximum of 1.0 ***AMA PRA Category 1 Credit(s)™***. Physicians should claim only the credit commensurate with the extent of their participation in the activity.

All other clinicians completing this activity will be issued a certificate of participation. To participate in this journal CME activity: (1) review the learning objectives and author disclosures; (2) study the education content; (3) take the post-test with a 75% minimum passing score and complete the evaluation at http://www.medscape.org/journal/eid; (4) view/print certificate.

Release date: November 13, 2014; Expiration date: November 13, 2015

Learning Objectives

Upon completion of this activity, participants will be able to:

- Describe seroconversion of UK military personnel deployed to Afghanistan between 2008 and 2011 to various vector-borne and zoonotic diseases, based on a biosurveillance study
- Distinguish asymptomatic and symptomatic cases associated with seroconversion of UK military personnel deployed to Afghanistan between 2008 and 2011 against various vector-borne and zoonotic diseases
- Assess clinical and public health implications of the findings from this biosurveillance study on seroconversion of UK military personnel deployed to Afghanistan between 2008 and 2011 to various vector-borne and zoonotic diseases.

CME Editor

Shannon O'Connor, ELS, Technical Writer/Editor, *Emerging Infectious Diseases. Disclosure: Shannon O'Connor has disclosed no relevant financial relationships.*

CME Author

Laurie Barclay, MD, freelance writer and reviewer, Medscape, LLC. *Disclosure: Laurie Barclay, MD, has disclosed no relevant financial relationships.*

Authors

Disclosures: ***Edmund N.C. Newman, BSc (Hons), PhD, ACMI; Penelope Johnstone, BSc, MSc(Hons), FIBMS; Hannah Bridge, BSc(Hons); Andrew Bosworth, BSc; Deborah Wright, RGN, PGDip(Child); Lisa Jameson, BSc (Hons); Rebecca Hatch, BSc(Hons), MSc, FIBMS; Jenny Hayward-Karlsson, SRN; Jane Osborne, BSc, PhD; Mark Bailey, MD, FRCP, FFTM, DTM&H; Andrew Green, MBBS, DTM&H, FFTM, RCPS, FFPH, FRCP, FRCPath; Tim Brooks, MA, MB BChir, LMSSA, MSc, FRCPath, FRSPH;*** *and* ***Roger Hewson, BSc(Hons), DPhil,*** *have disclosed no relevant financial relationships.* ***David Ross, QHP, MSc, MBBS, MRCGP, FRCPCH, FFPHH, FFTM RCPS(Glasg.),*** *has disclosed the following relevant financial relationships: served as an advisor or consultant for MASTA.*

Military personnel are at high risk of contracting vector-borne and zoonotic infections, particularly during overseas deployments, when they may be exposed to endemic or emerging infections not prevalent in their native countries. We conducted seroprevalence testing of 467 UK military personnel deployed to Helmand Province, Afghanistan, during 2008–2011 and found that up to 3.1% showed seroconversion for infection with *Rickettsia* spp., *Coxiella burnetii*, sandfly fever virus, or hantavirus; none showed seroconversion for infection with Crimean-Congo hemorrhagic fever virus. Most seroconversions occurred in personnel who did not report illness, except for those with hantavirus (70% symptomatic). These results indicate that many exposures to infectious pathogens, and potentially infections resulting from those exposures, may go unreported. Our findings reinforce the need for continued surveillance of military personnel and for education of health care providers to help recognize and prevent illnesses and transmission of pathogens during and after overseas deployments.

Military personnel represent a population that travel to and work in environments where they are exposed to endemic or emerging infections that are not prevalent in their native country. Groups of military personnel on international deployments thus form a useful naive sentinel group for infectious diseases; these groups may serve as indicators of the infectious disease agents to which the local populations are exposed and of the diseases that may be encountered by other visitors traveling to the area (e.g., tourists, as well as staff of nongovernmental organizations, aid organizations, and other government agencies). Study of infectious disease exposures and illnesses among military personnel may provide insight into the epidemiology of emerging and reemerging infections and highlight what pathogens could be imported back to the home nations of visitors to these areas.

The recognition that military personnel may act as disease sentinels is not a new concept. Infectious diseases have beleaguered international military operations for centuries, with historic campaigns facing substantial loss of life after soldiers succumbed to infections endemic to the areas in which they were operating at the time (*1*). Examples from British military history include many diseases that may be categorized as "undifferentiated febrile illnesses" (*2*). The causative agents for these fevers, often unidentified at the time they occurred, were predominantly infectious pathogens established in the geographic area in which troops were operating. For example, in the late 19th century, the zoonotic disease brucellosis and the vector-borne parasitic diseases leishmaniasis and malaria were common in British colonial troops deployed to the tropics and subtropics. In India, 24% of troops were admitted to the hospital for malaria in 1908 alone (*3*). During World War I, cases of leptospirosis (*4*) and trench nephritis (in retrospect thought to be caused by hantavirus, which resulted in >35,000 illnesses) (*5*) were also documented.

More recently, since World War II, UK military operations in Korea, Malaya, Borneo, Sierra Leone, Liberia, East Timor, and Haiti have resulted in illnesses among military personnel caused by vector-borne pathogens; these illnesses have included Japanese encephalitis, malaria, and dengue (*2*,*6*). This incidence of infectious disease is not limited to the tropics; campaigns in the Balkans and the Arabian Gulf during the past 25 years resulted in reports of cases of a range of vector-borne and zoonotic infections (*7*–*9*).

Although information about endemic infectious disease in Afghanistan is limited, previous historical reports indicate that several endemic vector-borne and zoonotic diseases, including rickettsial diseases, Crimean-Congo hemorrhagic fever (CCHF), and pappataci fever (now known as sandfly fever) (*10*). Given the country's geographic location, other pathogens endemic to the central Asian region could also be expected to be of concern to military personnel; these pathogens include Sindbis, chikungunya, and West Nile fever viruses (*11*). Although infections with many of these pathogens can be prevented by drugs (chemoprophylaxis) or vaccination, and the risk for exposure can often be reduced by physical measures, the ongoing UK military campaign in Afghanistan has still resulted in infectious diseases occurring in deployed personnel. Severe cases have required restrictions of duties or even hospitalization or evacuation to the United Kingdom, and high illness rates can affect the operational capability of the military force (*12*).

In 2011, Bailey et al. documented numerous cases of "undifferentiated febrile illness" in British military personnel serving in Helmand Province, Afghanistan, during the summer of 2008 (*13*). These cases, for which no organ focus could be determined on clinical and radiologic assessment and no positive results were obtained from microbiological investigations (e.g., blood cultures and malaria antigen tests), have been given the colloquial term "Helmand fever."

Author affiliations: Public Health England, Porton Down, UK (E.N.C. Newman, D. Wright, L. Jameson, A. Bosworth, J. Hayward-Karlsson, J. Osborne, T. Brooks, R. Hewson); Queen Alexandra Hospital, Portsmouth, UK (P. Johnstone, H. Bridge); BMS Training Defence School of Healthcare Education, Birmingham, UK (R. Hatch); Royal Centre for Defence Medicine, Birmingham (M.S. Bailey, A. Green); Army Health Unit, Camberley, UK (D. Ross); National Institute for Health Research, Health Protection Research Unit in Emerging and Zoonotic Infections, Liverpool, UK (T. Brooks, R. Hewson); and London School Hygiene and Tropical Medicine, London, UK (R. Hewson)

DOI: http://dx.doi.org/10.3201/eid2012.131830

For this study, we conducted surveillance among UK military personnel to determine the prevalence of several vector-borne or zoonotic infectious agents that were suspected to be the causative agents of some of these cases of undifferentiated fever: *Rickettsia* spp., *Coxiella burnetii*, sandfly fever virus, hantavirus, and CCHF virus (CCHFV). We conducted serosurveillance testing of 467 military service members who were deployed to Helmand Province during March 2008–October 2011. In this article, we describe the pathogens for which study participants showed seroconversion before and after a tour of duty and the incidence of those seroconversions within the military population.

Methods

Recruitment and Sampling

Study volunteers were recruited from either British Army regiments or Royal Marines units before deployment to Helmand Province, Afghanistan. For each deployment, a research nurse visited the unit and gave study information to the troops. Volunteers were required to give informed consent and to have 1 predeployment blood sample taken. After return from the 6-month tour of duty, volunteers were visited and asked to give a second postdeployment blood sample. At the postdeployment visit, volunteers were also asked to complete a short questionnaire detailing any "flu-like" illness or symptoms they experienced while deployed and any contact they had with livestock, wildlife, or insect vectors. The primary location of each company (i.e., group of ≈100 personnel in which the volunteer was posted) while deployed was also noted. Ethical approval for this survey was provided by the UK National Health Service National Research Ethics Service and Ministry of Defence Research Ethics Committee.

Blood samples were taken by venipuncture using BD SSTII Advance 10-mL vacutainers (Becton Dickinson, Oxford, UK). After a minimum 30-min incubation at room temperature, samples were centrifuged at 3,500 rpm for 15 min to separate the serum. This serum fraction was then separated and stored at -80°C for subsequent serologic testing.

During the study period, March 2008–October 2011, a total of 467 volunteers gave paired serum samples (i.e., predeployment and postdeployment samples). In all cases, samples were kept anonymous (by unique identification numbers), and questionnaire data/confidential information were kept in a secure database with restricted access.

Serologic Testing

Postdeployment samples were tested first for antibodies to all pathogens of interest. If results were positive, the corresponding predeployment sample was then tested to ascertain whether the volunteer seroconverted during the tour of duty for which they were recruited to the study or if they were already seropositive (i.e., exposed/seroconverted to that pathogen) before being recruited for the study. A volunteer whose sample was negative before deployment but positive after deployment was deemed to have seroconverted during that particular tour of duty. For each pathogen of interest, diagnostic tests were used in line with Public Health England's diagnostic laboratory procedures. All assays used have been validated locally for diagnostic use, are approved by UK regulatory authorities, and have been awarded Communauté Européenne marking by the European Union.

C. burnetii ELISA

Antibodies against *C. burnetii*, the causative agent of Q fever, were detected by using a commercial ELISA to detect phase 2 IgG and IgM human antibodies (Serion/Virion, Würzburg, Germany). ELISAs were conducted by using the DS2 Automated ELISA workstation (DYNEX Magellan Biosciences, Chantilly, VA, USA) according to the manufacturer's instructions. All serum samples were tested at an initial dilution of 1:100, as recommended by the manufacturer's product insert for diagnostic samples. If results were calculated as positive (above the automated threshold on DS2 software) for either IgG or IgM, the test was repeated in duplicate for confirmation. Because of the nonacute nature of the survey, all samples showing at least Phase 2 IgG positivity were deemed positive.

Hantavirus Immunofluorescence Assay (IFA)

Antibodies against the hantavirus group of pathogens were detected by using a commercial Hantavirus IIFT Mosaic 1 IgG IFA (Euroimmun, Lübeck, Germany). All serum samples were tested at an initial dilution of 1:100, as recommended by the manufacturer's product insert for diagnostic samples. If results were calculated as positive (for any species/subspecies of hantavirus), the test was repeated and confirmed by using the Recomline Bunyavirus IgG/IgM Line Assay (Mikrogen, Neuried, Germany). All IFA slides were set up by using the AP16 IF Plus automated slide processor (Euroimmun) and viewed by using a conventional fluorescent light microscope.

Rickettsia IFA

Antibodies against *Rickettsia* spp. were detected by using a commercial Rickettsia IgG and IgM IFA (Focus Diagnostics, Cypress, CA, USA). This assay is specific for rickettsial infection; that is, antibodies against *Coxiella* spp. do not cross-react in this test (Public Health England, unpub. data). All serum samples were tested at an initial dilution of 1:64, as recommended by the manufacturer's product insert

for diagnostic samples. If results were calculated as positive, the test were repeated and confirmed by titrating down a 2-fold dilution series to 1:512 (data not shown) to ensure that fluorescence diminished with antibody dilution (as recommended in the product insert). Because samples were not obtained during an acute illness phase, any sample that showed a consistent signal at 1:64 dilution was considered to be positive, even if this diminished by the 1:128 dilution. All IFA slides were prepared in accordance with the manufacturer's instructions and viewed by using a conventional fluorescent light microscope

Sandfly Fever Virus IFA

Antibodies against sandfly fever viruses (genus *Phlebovirus*) were detected in serum by using a commercial sandfly fever assay (IIFT Mosaic 1 IgG immunofluorescence assay; Euroimmun). All serum samples were tested at a dilution of 1:100, as recommended by the manufacturer's product insert for diagnostic samples. Given the nonacute nature of the samples, a positive result was defined as any sample that showed a consistent signal (for any of the 4 species/strains of sandfly fever virus) at 1:100 dilution. All IFA slides were set up by using the AP16 IF Plus automated slide processor (Euroimmun) and viewed by using a conventional fluorescent light microscope.

Crimean-Congo Hemorrhagic Fever ELISA

Antibodies against CCHFV nucleoprotein were detected by using an in-house CCHF recombinant ELISA (*14*). ELISAs were carried out by using the DS2 Automated ELISA workstation (DYNEX Magellan Biosciences). All serum samples were tested at an initial dilution of 1:100, and any tests that gave any signal above background were repeated in duplicate.

Results

The Table shows the results of the respective serology assays performed. For each pathogen (with the exception of CCHFV, for which no seroprevalence was reported), 2 categories of a seropositive volunteer were identified: those who showed detectable levels of antibody before and after deployment; and those who only showed positivity on return, with no detectable antibody in predeployment samples. During deployment, the troops showed the highest seroconversion rates for sandfly fever virus (3.1%) and rickettsiae (2.7%). However, seroconversions for hantavirus and *C. burnetii* (1.3% and 1.7%, respectively) also occurred.

The group of volunteers who were positive for each pathogen before deployment showed that there was a background level of seroprevalence for these pathogens within the UK military. The group of initially antibody-negative personnel seroconverted to the pathogens while on deployment, which suggests that military personnel are being exposed to such diseases while on operations in Afghanistan and that these diseases are being transmitted in the region.

Figure 1 shows the prevalence of volunteers who seroconverted during each deployment period. This comparison enabled us to plot prevalence as a function of season: winter deployments (October–March) compared with summer deployments (March–October). This analysis showed a higher prevalence of seroconversion in the Northern Hemisphere summer months, when the deployment area is hotter and drier than over the winter. Sandfly fever virus showed the greatest seasonal variation, with most cases in the summer months, and *C. burnetii* showed the least variations, findings that are consistent with these pathogens' known modes of transmission.

Many seroconversions for the studied pathogens appeared to be asymptomatic. All volunteers took part in a return questionnaire when the postdeployment sample was taken. This questionnaire was used to determine whether those who seroconverted after deployment experienced a "flu-like" illness during deployment. Figure 2 shows that, for all 4 pathogens acquired (*Rickettsia* spp., *C. burnetii*, sandfly fever virus, and hantavirus), a proportion of volunteers showed seroconversion but did not report feeling ill. As expected, sandfly fever virus and rickettsial infections showed the highest proportion of asymptomatic cases; just 6.5% and 7.4%, respectively, of those who seroconverted reporting feeling ill (i.e., 93.5% of sandfly fever virus exposures and 92.6% of *Rickettsia* spp. exposures were asymptomatic). The less common but often more clinically significant pathogens hantavirus and *C. burnetii* resulted in more reports of illness; 64.7% of *C. burnetii* seroconversions and 30.8% of hantavirus seroconversions were asymptomatic.

Table. Results of antibody testing for 5 infectious pathogens among UK service personnel before and after deployment to Helmand Province, Afghanistan, March 2008–October 2011*

Pathogen	No. persons tested	No. (%) with detectable antibody before deployment	No. (%) with seroconversion after deployment	Total no. (%) with positive antibody test
CCHFV	466	0	0	0
Sandfly fever virus	459	8 (1.7)	14 (3.1)	22 (4.8)
Rickettsia spp.	446	10 (2.2)	12 (2.7)	22 (4.9)
Hantavirus	453	5 (1.1)	6 (1.3)	11 (2.4)
Coxiella burnetii	467	7 (1.5)	8 (1.7)	15 (3.2)

*Assays were run sequentially on samples from all persons tested; some sample sizes were insufficient for testing for all agents. CCHFV, Crimean-Congo hemorrhagic fever virus.

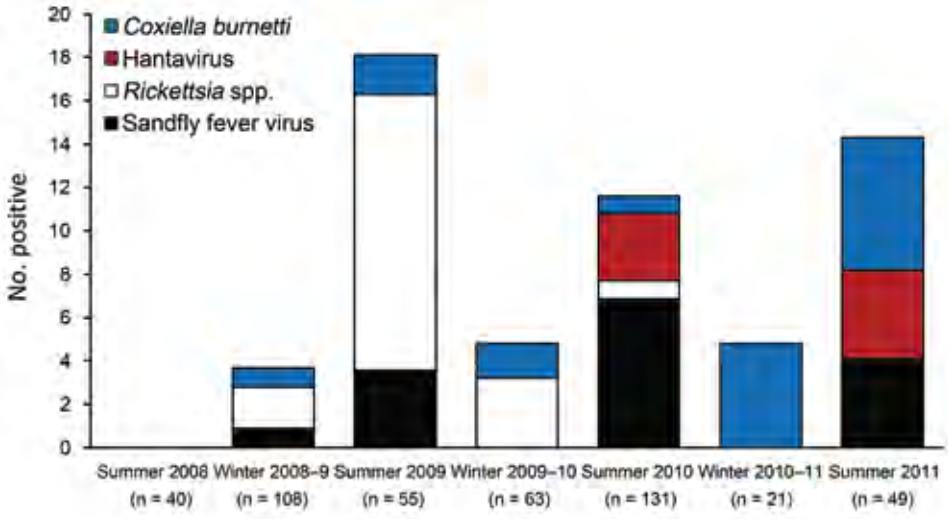

Figure 1. Results of antibody testing for 4 infectious pathogens, by tour of duty, among 467 UK service personnel deployed to Helmand Province, Afghanistan, March 2008–October 2011. n values indicate number of volunteers tested from each tour of duty. Assays were run sequentially on samples from all persons tested; some sample sizes were insufficient for testing for all agents.

Postdeployment questionnaires showed that nearly one fifth (90/467, 19.3%) of all volunteers reported experiencing "flu-like" symptoms while on operations in Helmand Province. A total of 56.7% of those who recorded ≥1 episodes of feeling unwell reported experiencing fever only, whereas 12.2% had no additional/specific symptoms; the remaining 31.2% reported either diarrhea and vomiting (15.6%) or "other" symptoms (Figure 3).

Discussion

UK military personnel consist of ≈237,190 persons (estimate of combined regular and volunteer reserve military personnel in UK, 2010 [UK Ministry of Defence, unpub. data]). Our results show that military personnel are being exposed to, at minimum, *Rickettsia* spp., *C. burnetii*, sandfly fever virus, and hantaviruses while on operations in Afghanistan, a region where these agents and resulting diseases are endemic. These results suggest that human or animal (for the zoonotic pathogens) reservoirs likely exist in the local populations of the Helmand region for these diseases.

Troops often patrol through vegetation and farm land where both reservoir and vector populations are high, which can easily result in exposure to pathogens and further supports the hypothesis that the nature of their work makes armed forces personnel a group with an increased incidence of exposure to such vector-borne or zoonotic pathogens. However, this group may also act as a good sentinel cohort for other populations of nonindigenous workers from governmental and nongovernmental organizations.

UK troops do sometimes stop over at British military bases in Cyprus during their return to the United Kingdom. However, these stopovers are typically very short in duration (2–3 days), and they do not occur in an environment where exposure is likely to occur, with the possible exception of sandfly bites. In addition, for each pathogen studied, a proportion of troops showed antibody positivity before deployment, suggesting that they may have been exposed to these pathogens on previous deployments to Afghanistan (before being recruited to the study) or on other exercises and operations around the world.

Overall, seroprevalence for these pathogens appears to be low, although this is hard to determine without a comprehensive study of nondeploying troops. These results may reflect good discipline or education of UK troops in the use of personal protection measures such as the use of DEET-containing insect repellent and mosquito nets, both of which are actively promoted by the UK military. A higher proportion of those deployed over the summer months showed seroconversion, corresponding with an increase in the numbers of biting vectors such as the *Phlebotomus* sandfly and ticks (rickettsial vectors). Further study of seasonality might show whether these

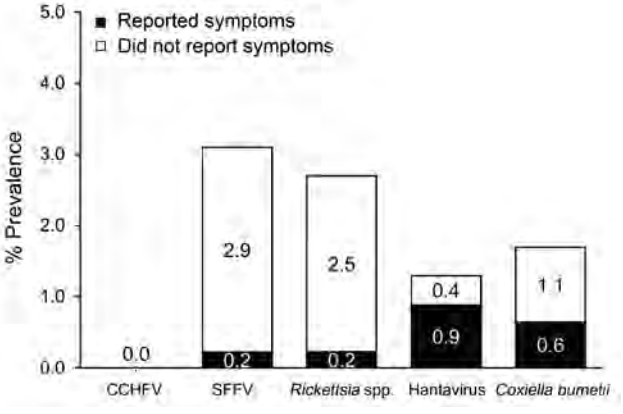

Figure 2. Percentages of UK service personnel who sero-converted to 1 of 5 infectious pathogens who reported feeling unwell or did not report illness during deployment to Helmand Province, Afghanistan, March 2008–October 2011. A total of 90 (19.3%) of 467 deployed service members reported feeling unwell during deployment. CCHFV, Crimean-Congo hemorrhagic fever virus; SFFV, sandfly fever virus.

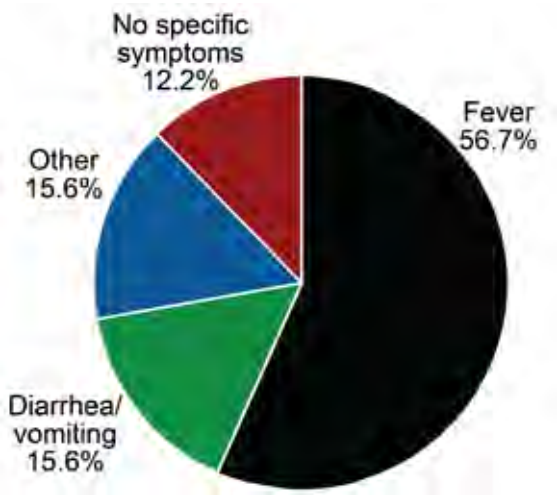

Figure 3. Distribution of signs and symptoms among 90 UK service personnel who seroconverted to 1 of 4 infectious pathogens (sandfly fever virus, hantavirus, *Coxiella burnetii*, *Rickettsia* spp.) and who reported feeling ill during deployment to Helmand Province, Afghanistan, March 2008–October 2011.

increases correlate with increased military activity (e.g., military patrolling and combat operations increase during the summer months), environmental/entomologic changes (e.g., decreases in rain and/or increases in temperature conditions favorable to agent, reservoir, or host density), or possible lapses in discipline regarding personal protective measures.

At first glance, summer seasonality may seem odd for an increase in hantavirus seroconversion, for which incidence would be more likely to correlate with closer proximity of humans with the rodent reservoir. However, UK summer deployments extend to late September and in some cases the first week or two of October; thus, these deployment continue into early autumn, when rodents are actively moving into buildings. In addition, the apparent lack of rickettsial infections after summer 2010 raises questions of whether this might correlate with a change in vector life-cycle, abundance of reservoir species, changes in insect bite prevention regimens, or changes to local livestock management regimens.

The increased incidence of rickettsial and sandfly fever virus infections that we found among deployed troops does not necessarily mean that these vector-borne pathogens are more prevalent in the environment and local population than the zoonotic pathogens *C. burnetii* or hantavirus. Rather, these results may mean that mode of transmission and incidence of encounters with the vectors and reservoirs differ. However, our results do indicate that these pathogens may pose the greatest risk to UK troops.

Although most of the diseases we detected are relatively self-limiting after the initial acute infection, our results suggest ways to improve control measures to reduce the rate of transmission. UK military personnel are already given medical advice and education before deployment, emphasizing the prevention of insect bites while deployed by use of arthropod repellent, insecticide-impregnated clothing, and mosquito nets. The observation that rickettsial infections and Q fever might account for a sizeable proportion of cases of undifferentiated febrile illness seen in military field hospitals has led to the empirical use of doxycycline in such cases because *Rickettsia* and *Coxiella* species are sensitive to this drug. This practice justifies further research on use of doxycycline for chemoprophylaxis in these instances.

More than half (56.7%) of volunteers who reported feeling unwell specifically reported a fever without other specific symptoms, which is consistent with the "undifferentiated febrile illness" that the pathogens we investigated can cause. The 15.6% of volunteers reporting illness who reported diarrhea and vomiting could have had gastrointestinal infections; localized outbreaks of norovirus and similar infections are common in military operating bases) (*15*). Of the many volunteers who experienced fever but did not show seroconversion for the 5 pathogens tested here, exposure to influenza virus or other respiratory infections should be considered. In 2011, Eick et al. reported that deployed US troops experienced 30.1% seroconversion for influenza and 6 other respiratory infections (*16*). However, uptake of influenza vaccination, which is offered to UK military personnel before winter deployments, has increased for each of the past 4 years (*2*). Data from the militaries of other countries, which might have different deployment patterns and protective measures, should be compared only with caution. In addition, although some volunteers who seroconverted for all 4 pathogens reported flu-like symptoms while deployed, we cannot ascertain whether these symptoms were a result of exposure to the pathogen of interest.

Some volunteers who seroconverted for the pathogens tested were asymptomatic for the duration of their deployments. Clinical disease probably did not develop in these patients, despite evidence of an exposure and an antibody response. Our finding that 65% of acute *C. burnetii* infections were asymptomatic is consistent with previous reports (*17*,*18*), but even in asymptomatic persons infected with this pathogen, long-term complications such as chronic Q fever and Q fever fatigue syndrome may develop. Overall, ≈5% of acute cases progress to chronic Q fever, and complications can include endocarditis requiring prolonged antimicrobial drug treatment and possibly heart valve surgery (*19*). In addition, Q fever fatigue syndrome may develop in ≈20% of those infected (*17*), which is generally incompatible with a military career and has substantial effects on patients' quality of life.

Royal et al. (*20*) recently reported *C. burnetii* seroprevalence in US troops deployed to the Al Asad region of Iraq in 2005; a known Q fever outbreak occurred in this region at this time. This smaller study (n = 136) reported a 7.2% prevalence of *C. burnetii* infection among troops located in that area at the time of the outbreak. The report further supports (in addition to original work by Bailey et al. [*13*]) the *C. burnetii* seroprevalence reported here. Although we did not see as high an incidence of seroconversion, we were not specifically looking in an area with a known Q fever outbreak, merely an area in which Q fever is believed to be endemic.

Although this study did not find seroconversion for the viral hemorrhagic fever agent CCHFV, military and public health reports demonstrated that the virus is circulating in the region (*21*). In 2009, a US Army soldier in the neighboring Kandahar Province died of CCHFV infection (*22*), and in 2012, a UK citizen returning from the northwest of the country also died (*23*,*24*).

In conclusion, this study highlights and confirms the potential for vector-borne and zoonotic diseases that are endemic in southern Afghanistan to emerge or reemerge to pose a substantial public health threats as the country rebuilds its public health infrastructure. A study of this type cannot give a specific indication of prevalence for these pathogens in the local population, but this surveillance can provide a valuable way of exploring emerging disease epidemiology, particularly of vector-borne and zoonotic infections, in areas with poor public health reporting and infrastructure. Our findings of seroconversion for 4 of these pathogens among deployed UK troops reinforce the need for continued surveillance and continued education of health care providers so that, should military operations or environmental factors change in such a way that these modest incidence numbers increase, costly outbreaks can be avoided. This study also highlights the need for rapid, field-capable, point-of-care diagnostics in regions or situations for which full laboratory diagnostic facilities are not practical or available.

Acknowledgments

We thank Public Health England Porton's Rare and Imported Pathogens Laboratory diagnostic staff, the Ministry of Defense's Defence Medical Services, and Institute of Naval Medicine for their collaboration and facilitation of this project.

This work was funded by the NIHR, grant/project 104665, and has ethical approval from the UK National Health Service National Research Ethics Service (NRES REC no. 05/Q2008/7) and the UK Ministry of Defense Research Ethics Committee.

Dr Newman is project team leader in the virology and pathogenesis group at Public Health England's Porton Down site. His research interests are global biosurveillance, bioresponse, and associated diagnostic assay development of emerging and reemerging high-consequence human pathogens, focusing on arboviruses and hemorrhagic fever viruses.

References

1. Bailey MS. A brief history of British military experiences with infectious and tropical diseases. J R Army Med Corps. 2013;159:150–7. http://dx.doi.org/10.1136/jramc-2013-000087
2. Burns DS, Bailey MS. Undifferentiated febrile illnesses in military personnel. J R Army Med Corps. 2013;159:200–5. http://dx.doi.org/10.1136/jramc-2013-000118
3. Fowler CE. The prevention of malaria among troops under peace conditions. In: Ross R, editor. The prevention of malaria. New York: Dutton; 1910.
4. Johnston JH, Lloyd J, McDonald J, Waitkins S. Leptospirosis—an occupational disease of soldiers. J R Army Med Corps. 1983;129:111–4.
5. Atenstaedt RL. The medical response to trench nephritis in World War I. Kidney Int. 2006;70:635–40. http://dx.doi.org/10.1038/sj.ki.5001618
6. Pages F, Faulde M, Orlandi-Pradines E, Parola P. The past and present threat of vector-borne diseases in deployed troops. Clin Microbiol Infect. 2010;16:209–24. http://dx.doi.org/10.1111/j.1469-0691.2009.03132.x
7. Stuart LM, Rice PS, Lloyd G, Beale RJ. A soldier in respiratory distress. Lancet. 1996;347:30. http://dx.doi.org/10.1016/S0140-6736(96)91560-3
8. Konstantinou GN, Papa A, Antoniadis A. Sandfly-fever outbreak in Cyprus: are phleboviruses still a health problem? Travel Med Infect Dis. 2007;5:239–42. http://dx.doi.org/10.1016/j.tmaid.2007.02.002
9. Faix DJ, Harrison DJ, Riddle MS, Vaughn AF, Yingst SL, Earhart K, et al. Outbreak of Q fever among US military in western Iraq, June–July 2005. Clin Infect Dis. 2008;46:e65–8. http://dx.doi.org/10.1086/528866
10. Arsen'eva LP. Natural focal zoonoses in Afghanistan (a review of the literature). Med Parazitol (Mosk). 1982;51:54–9.
11. Wallace MR, Hale BR, Utz GC, Olson PE, Earhart KC, Thornton SA, et al. Endemic infectious diseases of Afghanistan. Clin Infect Dis. 2002;34(Suppl 5):S171–207. http://dx.doi.org/10.1086/340704
12. Glennie JS, Bailey MS. UK role 4 military infectious diseases at Birmingham Heartlands Hospital in 2005–9. J R Army Med Corps. 2010;156:162–4. http://dx.doi.org/10.1136/jramc-156-03-07
13. Bailey MS, Trinick TR, Dunbar JA, Hatch R, Osborne JC, Brooks TJ, et al. undifferentiated febrile illnesses amongst British troops in Helmand, Afghanistan. J R Army Med Corps. 2011;157:150–5. http://dx.doi.org/10.1136/jramc-157-02-05
14. Dowall SD, Richards KS, Graham VA, Chamberlain J, Hewson R. Development of an indirect ELISA method for the parallel measurement of IgG and IgM antibodies against Crimean-Congo haemorrhagic fever (CCHF) virus using recombinant nucleoprotein as antigen. J Virol Methods. 2012;179:335–41. http://dx.doi.org/10.1016/j.jviromet.2011.11.020
15. Morgan D, Horstick O, Nicoll A, Brown DW, Gray JJ, Hawker J, et al. Illness in military personnel in Bagram, Afghanistan. Euro Surveill. 2002;6:2140.
16. Eick AA, Faix DJ, Tobler SK, Nevin RL, Lindler LE, Hu Z, et al. Serosurvey of bacterial and viral respiratory pathogens among deployed US service members. Am J Prev Med. 2011;41:573–80. http://dx.doi.org/10.1016/j.amepre.2011.08.006
17. Anderson A, Bijlmer H, Fournier PE, Graves S, Hartzell J, Kersh GJ, et al. Diagnosis and management of Q fever—United States, 2013: recommendations from CDC and the Q Fever Working Group. MMWR Recomm Rep. 2013;62(RR-03):1–30.
18. Million M, Walter G, Thuny F, Habib G, Raoult D. Evolution from acute Q fever to endocarditis is associated with underlying

valvulopathy and age and can be prevented by prolonged antibiotic treatment. Clin Infect Dis. 2013;57:836–44. http://dx.doi.org/10.1093/cid/cit419
19. Khan JN, Tapp LD, Glancy JM, Prasad N, Bailey MS, Graham TR, et al. Successful surgical treatment of Q fever endocarditis with mitral valve repair. J R Army Med Corps. 2012;158:132–4. http://dx.doi.org/10.1136/jramc-158-02-13
20. Royal J, Riddle MS, Mohareb E, Monteville MR, Porter CK, Faix DJ, et al. Seroepidemiologic survey for *Coxiella burnetii* among US military personnel deployed to Southwest and Central Asia in 2005. Am J Trop Med Hyg. 2013;89:991–5. http://dx.doi.org/10.4269/ajtmh.12-0174
21. Mustafa ML, Ayazi E, Mohareb E, Yingst S, Zayed A, Rossi CA, et al. Crimean-Congo hemorrhagic fever, Afghanistan, 2009. Emerg Infect Dis. 2011;17:1940–1. http://dx.doi.org/10.3201/eid1710.110061
22. ProMed Mail. Crimean-Congo hemorrhagic fever, fatal: imported ex Afghanistan [cited 2009 Sep 19]. http://www.promedmail.org, archive no. 20090919.3286.
23. Atkinson B, Latham J, Chamberlain J, Logue C, O'Donoghue L, Osborne J, et al. Sequencing and phylogenetic characterisation of a fatal Crimean–Congo haemorrhagic fever case imported into the United Kingdom, October 2012. Euro Surveill. 2012; 17:20327.
24. Chamberlain J, Atkinson B, Logue CH, Latham J, Newman EN, Hewson R. Genome sequence of ex-Afghanistan Crimean-Congo hemorrhagic fever virus SCT strain, from an imported United Kingdom case in October 2012. Genome Announc. 2013;1:e00161–13. http://dx.doi.org/10.1128/genomeA.00161-13

Address for correspondence: Edmund N.C. Newman, World Health Organization Collaborative Centre for VHF & Arbovirus Reference & Research, Microbiology Services–Research, Public Health England, Porton Down, Salisbury, Wiltshire SP4 0JG, UK; email: edmund.newman@phe.gov.uk

Molecular Evolution of Peste des Petits Ruminants Virus[1]

Murali Muniraju, Muhammad Munir, AravindhBabu R. Parthiban, Ashley C. Banyard, Jingyue Bao, Zhiliang Wang, Chrisostom Ayebazibwe, Gelagay Ayelet, Mehdi El Harrak, Mana Mahapatra, Geneviève Libeau, Carrie Batten, and Satya Parida

Despite safe and efficacious vaccines against peste des petits ruminants virus (PPRV), this virus has emerged as the cause of a highly contagious disease with serious economic consequences for small ruminant agriculture across Asia, the Middle East, and Africa. We used complete and partial genome sequences of all 4 lineages of the virus to investigate evolutionary and epidemiologic dynamics of PPRV. A Bayesian phylogenetic analysis of all PPRV lineages mapped the time to most recent common ancestor and initial divergence of PPRV to a lineage III isolate at the beginning of 20th century. A phylogeographic approach estimated the probability for root location of an ancestral PPRV and individual lineages as being Nigeria for PPRV, Senegal for lineage I, Nigeria/Ghana for lineage II, Sudan for lineage III, and India for lineage IV. Substitution rates are critical parameters for understanding virus evolution because restrictions in genetic variation can lead to lower adaptability and pathogenicity.

Peste des petits ruminants is a highly contagious and devastating viral disease of small ruminants that is endemic to much of Africa, the Middle East, and Asia (*1*,*2*). The causative agent, PPRV virus (PPRV), belongs to the family *Paramyxoviridae*, genus *Morbillivirus* (*3*) and groups with rinderpest virus (RPV), measles virus (MV), and canine distemper virus. Sheep and goats are the major hosts of PPRV, and infection has also been reported in a few wild small ruminant species (*2*). Researchers have speculated that RPV eradication has further enabled the spread of PPRV (*4*,*5*). Transmission of PPRV from infected goats to cattle has been recently reported (*6*), and PPRV antigen has been detected in lions (*7*) and camels (*8*). These reports suggest that PPRV can switch hosts and spread more readily in the absence of RPV (*4*,*6*,*8*). This host range switch had previously been seen after eradication of smallpox virus, which created a niche for monkeypox and cowpox viruses to cross the species barrier into humans (*4*).

PPRV has caused numerous serious epidemics in small ruminant populations across sub-Saharan Africa, the Middle East, and major parts of the Indian subcontinent where PPRV is considered endemic (*1*). In recent years, PPRV has extended its range southward in Africa as far as southern Tanzania (2008) and the Democratic Republic of Congo and Angola (2012). PPR outbreaks have also been reported across North Africa, including within Tunisia (2006), Morocco (2008), and Algeria (2011). In addition, within Europe, Turkey reported ≈20 laboratory-confirmed PPR outbreaks in sheep and goats during 2011 2012. In southwestern Asia, the virus spread to Tibet (2007) and has recently been reported throughout China (2013–2014). It is unclear what factors have favored emergence and spread of the disease, but millions of small ruminants across these regions must now be considered at high risk for infection

Author affiliations: The Pirbright Institute, Pirbright, UK (M. Muniraju, M. Munir, M. Mahapatra, C. Batten, S. Parida); National Institute for Animal Biotechnology, Hyderabad, India (A.R. Parthiban, S Parida); Animal Health and Veterinary Laboratories Agency, Weybridge, UK (A.C. Banyard); China Animal Health and Epidemiology Centre, Qingdao, China (J. Bao, Z. Wang); National Animal Disease Diagnostics and Epidemiology Centre, Entebbe, Uganda (C. Ayebazibwe); National Veterinary Institute, Debre Zeit, Ethiopia (G. Ayelet); Société de Productions Pharmaceutiques et Vétérinaires, Rabat, Morocco (M. El Harrak); and Le Centre de Cooperation Internationale en Recherche Agronomique pour le Développement, Montpellier (G. Libeau)

DOI: http://dx.doi.org/10.3201/eid2012.140684

[1]Preliminary results were presented at the 15th International Negative Strand Virus Meeting, June 16–21, Granada, Spain, 2013.

with PPRV (*9*). The huge effect on small ruminant production has resulted in PPRV emerging as a global animal health concern.

The molecular epidemiology of PPRV, which is based on sequence comparison of a small region of the fusion (F) gene (322 nt) or the nucleoprotein (N) gene (255 nt), has identified 4 distinct lineages (I–IV) of PPRV (*2*). However, this analysis has not generated much information on the evolution and dispersal of PPRV lineages. Lineage I PPRV had gone undetected for 19 years being detected in Senegal in 1994. Lineage IV PPRV, which was believed initially to be confined to India and the Middle East, now has a wider geographic presence and appears to be evolving rapidly. Many aspects of PPRV evolution, such as ancestral virus location, divergence and time of origin, and historical and geographic patterns of spread, are poorly understood (*10*). A better understanding of the evolution of PPRV would enable prediction of how these viruses will lead to further outbreaks and epidemics and provide data for control strategies.

Advanced sequencing technologies have enabled molecular epidemiologic studies of viruses in which whole gene and complete genome data are used to enhance and clarify the evolutionary dynamics of viral infectious disease (*11*). We analyzed genome data for all 4 lineages of PPRV. This analysis will enable a more precise evolutionary and phylogenetic assessment of the relationships between lineages by reducing the associated estimation errors and increased higher confidence in estimates.

Materials and Methods

Complete Genome Sequencing of PPRV

Complete genome sequencing of 7 PPRV isolates (4 from lineage III and 3 from lineage IV) was performed according to the methods described by Muniraju et al. (*12*). Detailed information for each of the isolates is shown in Table 1.

Sequence Datasets

In addition to the 7 complete genomes sequences of PPRV generated in this study, another 7 complete genome sequences were obtained from GenBank (Table 1). However, of these 14 full genome sequences, Nigeria 1975/1 and Sungri 1996 represent vaccine strains generated after extensive serial passage of virus. Therefore, the evolutionary rate and time to most recent common ancestor (TMRCA) were compared with and without inclusion of vaccine strains. The complete genome sequences of 2 clinical isolates each from RPV (GenBank accession nos. AB547189 and X98291) and MV (accession nos. AF266288 and JF791787) and 12 PPRV isolates, excluding vaccine strains, (Table 1) were used for estimation of evolutionary rate and TMRCA. Furthermore, the coding and noncoding sequences of individual structural genes of PPRV (excluding vaccine strains) were used in this study.

Partial N gene sequences of PPRV (nucleotide positions 1253–1507) that have a detailed history of collection date and place were obtained from GenBank (available up to August 2013). These partial sequences were aligned by using the ClustalW algorithm in BioEdit software v7.2.0. (*21*) and edited to remove unreliable sequences/regions. Furthermore, the identical sequences originating from the same geographic location, host, and year were excluded to avoid redundancy in subsequent analysis. The final dataset (partial N gene) contained 159 sequences sampled over a period of 45 years (1968–2012).

Selection Analysis

The nucleotide and amino acid sequence differences between the PPRV lineages for 12 complete genome sequences were estimated by using BioEdit software v7.2.0. Analyses of selection pressure in individual PPRV genes was performed by obtaining mean ratios of nonsynonymous (dN) to synonymous (dS) substitutions per site. The dN/dS was calculated by using codon-based

Table 1. Peste des petits ruminants virus isolates used for complete genome analysis

Virus isolates	GenBank accession no.	Lineage	Source (reference)
Ivory Coast/1989	EU267273	I	Goat (*13*)
Nigeria/1976	EU267274	II	Sheep (*13*)
Nigeria/1975/1	X74443	II	Goat (14), vaccine strain
Uganda/2012*	KJ867543	III	Goat
UAE/1986*†	KJ867545	III	Dorcas gazelle (*15*)
Oman/1983*	KJ867544	III	Goat (*16*)
Ethiopia/1994*	KJ867540	III	Goat (*17*)
Ethiopia/2010*	KJ867541	IV	Goat
India/Sungri/1996*	KJ867542	IV	Goat (provided by Intervet International B.V, Boxmeer, the Netherlands), vaccine strain
Morocco/2008*	KC594074	IV	Goat (*12*)
China/Tibet Bharal/2008	JX217850	IV	Bharal, *Pseudois nayaur* (*18*)
China/Tibet33/2007	JF939201	IV	Goat (*19*)
China/TibetGeg30/2007	FJ905304	IV	Goat (*19*)
Turkey/2000	NC006383	IV	Sheep (*20*)

*Whole genome sequencing was conducted.
†UAE, United Arab Emirates.

maximum likelihood approaches with the single-likelihood ancestor method implemented in hypothesis testing using the phylogenies package (*22*) (http://www.datamonkey.org).

Bayesian Time-Scaled Phylogenetic Analysis

Molecular evolutionary rate and divergence times were co-estimated. A Bayesian maximum clade credibility (MCC) phylogenetic tree was constructed by using Bayesian Markov chain Monte Carlo (MCMC) analysis and Bayesian evolutionary analysis sampling trees (BEAST) software package v1.8.0 (*23*), and BEAST runs were performed by using the CIPRES Science Gateway (*24*). For each sequence dataset, the best-fit nucleotide substitution model was determined on the basis of Akaike information criterion scores using JModel Test software v2.1.4 (*25*). An input file for BEAST analysis was obtained by using Bayesian evolutionary analysis utility software v1.8.0, in which sequences were tip dated according to the year of collection. Four molecular clock models (strict, uncorrelated lognormal distribution, uncorrelated exponential distribution [UCED], and random) were tested alongside different demographic models (nonparametric Bayesian skyline plot and the parametric constant and exponential growth), and the best models were selected by means of a Bayes factor (BF) test (*26*) using marginal likelihoods values (2lnBF>2) obtained from Tracer v1.5 software (http://beast.bio.ed.ac.uk/tracer).

For each analysis, 2 independent MCMC chains were run to get a final output of 10,000 trees (ESS >200 for all the parameters estimated) and were assessed for their proper mixing, convergence, and consistency by Tracer v1.5 with 10% burn in. The 2 individual runs were combined by using LogCombiner v1.8.0 in the BEAST software package. The nucleotide substitution rate (substitutions/site/year) and the TMRCA (year) values were obtained from Tracer v1.5. The posterior tree distributions were summarized by using TreeAnnotator (http://beast.bio.ed.ac.uk/treeannotator) and exclusion of the first 10% of the trees as burn in. Phylogenetic MCC tree with median node heights were visualized in FigTree software v1.4.0 (http://www.molecularevolution.org/software/phylogenetics/figtree). Furthermore, the demographic history of PPRV was studied by using partial N gene dataset and less restrictive Bayesian skyline plot (BSP) models in which the changing profile of genetic diversity is plotted against time.

Phylogeographic Reconstruction

Bayesian phylogeographic analysis was performed by using complete PPRV genome sequence and partial N gene sequence datasets, and isolates were annotated according to their location (longitude and latitude). Partial N gene data were chosen instead of F gene data because of increased divergence reported for the N gene (*2*). For complete genome datasets, sequences from 14 viruses were considered, including 2 vaccine strains (Nigeria 1975/1 and Sungri 1996) to represent all PPRV-endemic areas. Phylogeographic diffusion along the posterior sets of trees and relationships between these locations were identified by using the Bayesian stochastic search variable selection procedure in BEAST v1.8.0 (*27*). Discrete phylogeographic analysis was performed by using the continuous time Markov chain with the flexible Bayesian skyride tree prior.

Results

Sequence Analysis

All 7 PPRV complete genomes are 15,948 nt and conform to the rule of 6 as described for all other morbillivirus genomes (*28*). The genome organization of the isolates was the same as that of other PPRV strains. Phylogenetic analysis of the complete genome sequences of PPRV clustered the sequences into 4 lineages. The complete genomes of PPRV isolates from Ethiopia 1994, Oman 1983, UAE 1986, and Uganda 2012 sequenced in this study belonged to lineage III and the isolates Sungri 1996, Morocco 2008, and Ethiopia 2010 belong to lineage IV. Comparison of the 12 aligned complete genome sequences showed that nucleotide differences ranged from 0.1% to 11.9%, and amino acid differences ranged from 0.1% to 7.2% (Table 2).

The dN/dS for coding regions of the various genes of PPRV (n = 12) for all 4 lineages ranged from 0.06 to 0.45 (Table 3). The dN/dS per site across the coding region of different genes of PPRV genome are shown in Figure 1. The highest dN/dS ratio was observed in the phosphoprotein gene, followed by the hemagglutinin, N, F, large polymerase, and matrix (M) genes. The relative nucleotide substitution rates at all 3 codon positions of the structural genes of PPRV showed that substitutions were more frequent at the third codon position (Table 3) as expected.

Table 2. Nucleotide and amino acid sequence differences in complete genomes of peste des petits ruminants virus lineages*

	Lineage			
Lineage	I	II	III	IV
I		5.1	6.1–7.0	5.7–6.1
II	**9.0**		5.7–6.3	4.0–4.2
III	**10.9–11–9**	**9.9–10.8**	0.2–3.0, **0.2–6.2**	6.1–7.2
IV	**10.3–10.7**	**7.2–7.6**	**10.7–11.8**	0.1–2.0, **0.1–3.2**

*Values are percentage nucleotide (bold) and amino acid sequences differences.

Table 3. Nucleotide substitution rates at codon positions of peste des petits ruminants virus genes by BEAST analysis and dN/dS by SLAC*

Gene†	Total amino acids	Codon position			Mean dN/dS
		CP1.mu	CP2.mu	CP3.mu	
N	526	0.44	0.33	2.23	0.13
P	510	0.81	0.69	1.49	0.45
M	336	0.48	0.15	2.36	0.06
F	547	0.46	0.26	2.29	0.10
H	610	0.57	0.37	2.06	0.19
L	2184	0.42	0.18	2.40	0.08

*BEAST, Bayesian evolutionary analysis sampling trees; dN/dS, nonsynonymous/synonymous substitutions per site; SLAC, single-likelihood ancestor counting; CP, codon position.
†N = nucleoprotein; P, phosphoprotein; M, matrix; F, fusion; H, hemagglutinin; L, large polymerase.

Evolutionary Rate Estimates

Complete genome sequences of 12 PPRV and partial N gene dataset (n = 159) were analyzed by using the coalescent-based Bayesian MCMC approach. The general time-reversible nucleotide substitution model with a gamma distribution for rate variation was selected on the basis of Akaike information criterion scores. Bayes factor test with marginal likelihood comparisons showed that the relaxed UCED clock model best fitted the PPRV complete genome and partial N gene datasets (Table 4). The 2lnBF value was >78 between UCED and strict clocks and 2–6 between UCED/uncorrelated lognormal distribution and UCED/ random clocks, which provided strong evidence for the UCED clock model. There was no difference between different demographic models compared within the UCED clock model (2lnBF <2). However, the exponential demographic model was chosen because it provided a narrow margin of 95% highest posterior density (HPD) estimates.

Accordingly, the UCED and exponential growth model have been directly used for the individual PPRV gene dataset and the PPRV/RPV/MV complete genome dataset to estimate the TMRCA and substitution rate per site per year. When we used the UCED and exponential growth models, we found that the mean evolutionary substitution rate of the PPRV complete genome was estimated to be 9.09×10^{-4} (95% HPD 2.13×10^{-4}–1.64×10^{-3}). When 2 complete genome sequences of vaccine strains were added into this analysis, the same models (general time-reversible nucleotide substitution model with a gamma distribution, UCED, and the exponential growth demographic models) were best fitted, and the mean substitution rate/site/year was reduced to 7.86×10^{-4} (95% HPD 2.17×10^{-4}–1.4×10^{-3}). Furthermore, the evolutionary nucleotide substitution rate for combined PPRV/RPV/MV complete genomes was 1.89×10^{-3} (95% HPD 5.55×10^{-4}–3.31×10^{-3}). Analysis of individual genes of the PPRV coding region dataset, coding and noncoding region datasets, and partial N gene dataset are shown in Table 4.

Temporal Dynamics

A Bayesian time-scaled MCC tree based on complete PPRV genomes was constructed (Figure 2) by using the UCED model with exponential growth demography. The estimated median TMRCA of PPRV for all 4 lineages and divergence of lineage III PPRV were found to be ≈1904 (95% HPD 1730–1966). Lineage I diverged in ≈1939 (95%

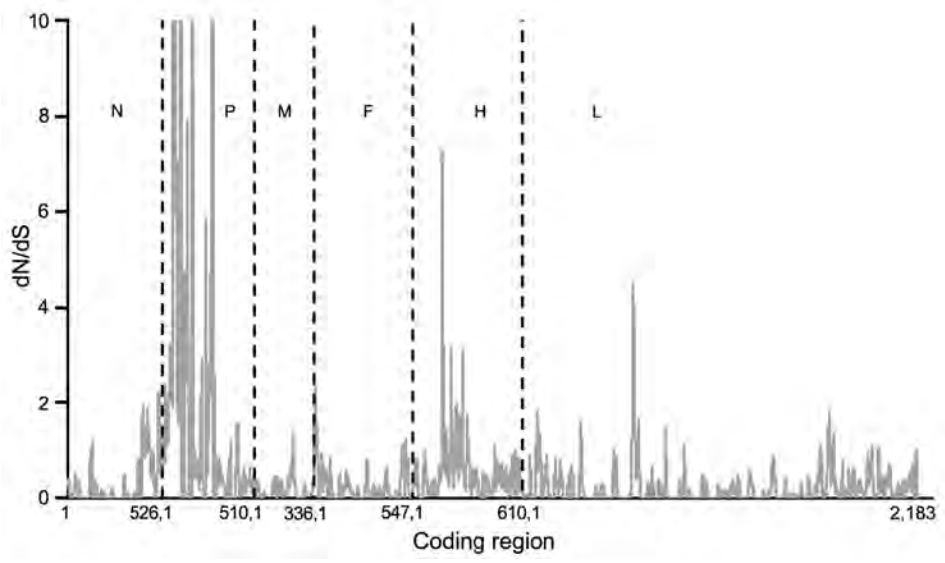

Figure 1. Mean ratios of nonsynonymous (dN) to synon-ymous (dS) substitutions per site of concatenated coding regions of peste des petits ruminants virus genome. Proportion of dS substitutions per potential dS site and proportion of dN substitutions per potential dN site were calculated by using the method of Nei and Gojobori (*29*) and the suite of nucleotide analysis program (www.hiv.lanl.gov). Vertical dashed lines indicate gene junctions with sliding windows of size = 5 codons. dN/dS values ≥ 10 are shown as 10. Numbers along baseline indicate coding regions (basepairs) of individual genes. N, nucleoprotein; P, phosphoprotein; M, matrix; F, fusion; H, hemagglutinin; L, large polymerase.

Table 4. Bayesian Markov chain Monte Carlo analysis for genomes of peste des petits ruminants virus*

Sequence dataset (no.)†	Models, substitution/ clock/demographic	Mean nucleotide substitution rate, substitutions/site/y (95% HPD)	TMRCA, y (95% HPD)	Bayes factor –log likelihood
PPRV complete genome (12)	GTR + G/strict/BSP	3.2×10^{-4} (2.02×10^{-4}–4.31×10^{-4})	1763 (1653–1832)	–46,972.98
	GTR + G/strict/CS	3.21×10^{-4} (2.12×10^{-4}–4.38×10^{-4})	1763 (1659–1834)	–46,973.06
	GTR + G/strict/EG	3.24×10^{-4} (2.12×10^{-4}–4.33×10^{-4})	1765 (1668–1836)	–46,973.06
	GTR + G/UCLD/BSP	2.89×10^{-3} (3.21×10^{-8}–6.92×10^{-4})	1691 (123 BCE–1944 CE)	–46,935.66
	GTR + G/UCLD/CS	3.03×10^{-4} (8.99×10^{-9}–7.07×10^{-4})	1705 (123–1961)	–46,935.86
	GTR + G/UCLD/EG	3.72×10^{-4} (3.01×10^{-5}–7.93×10^{-4})	1767 (1222–1948)	–46,935.89
	GTR + G/UCED/BSP	7.91×10^{-4} (7.46×10^{-5}–1.53×10^{-3})	1889 (1586–1968)	–46,933.82
	GTR + G/UCED/CS	7.98×10^{-4} (8.03×10^{-5}–1.54×10^{-3})	1887 (1569–1968)	–46,933.98
	GTR + G/UCED/EG	**9.09×10^{-4} (2.13×10^{-4}–1.64×10^{-3})**	**1904 (1730–1966)**	**–46,933.96**
	GTR + G/random/BSP	7.01×10^{-4} (5.55×10^{-4}–8.50×10^{-4})	1888 (1862–1908)	–46,934.75
	GTR + G/random/CS	6.97×10^{-4} (5.38×10^{-4}–8.41×10^{-4})	1887 (1860–1908)	–46,934.64
	GTR + G/random/EG	7.04×10^{-4} (5.57×10^{-4}–8.57×10^{-4})	1888 (1861–1908)	–46,934.89
N partial (159)	GTR + G/strict/BSP	1.22×10^{-3} (9.39×10^{-4}–1.51×10^{-3})	1890 (1857–1917)	–2,884.524
	GTR + G/strict/CS	1.23×10^{-3} (9.49×10^{-4}–1.52×10^{-3})	1886 (1853–1913)	–2,887.723
	GTR + G/strict/EG	1.24×10^{-3} (9.71×10^{-4}–1.56×10^{-3})	1893 (1863–1919)	–2,885.44
	GTR + G/UCLD/BSP	1.45×10^{-3} (1.06×10^{-3}–1.87×10^{-3})	1896 (1815–1943)	–2,806.535
	GTR + G/UCLD/CS	1.41×10^{-3} (1.05×10^{-3}–1.80×10^{-3})	1882 (1793–1935)	–2,805.535
	GTR + G/UCLD/EG	1.49×10^{-3} (1.10×10^{-3}–1.89×10^{-3})	1904 (1838–1943)	–2,805.921
	GTR + G/UCED/BSP	1.52×10^{-3} (1.11×10^{-3}–1.98×10^{-3})	1904 (1817–1949)	–2,799.572
	GTR + G/UCED/CS	1.46×10^{-3} (1.05×10^{-3}–1.88×10^{-3})	1886 (1785–1940)	–2,799.512
	GTR + G/UCED/EG	**1.56×10^{-3} (1.16×10^{-3}–1.99×10^{-3})**	**1910 (1846–1947)**	**–2,799.444**
	GTR + G/random/BSP	1.26×10^{-3} (9.44×10^{-4}–1.58×10^{-3})	1881 (1837–1915)	–2,865.846
	GTR + G/random/CS	1.24×10^{-3} (9.38×10^{-4}–1.57×10^{-3})	1875 (1831–1910)	–2,866.111
	GTR + G/random/EG	1.27×10^{-3} (9.62×10^{-4}–1.60×10^{-3})	1880 (1841–1914)	–2,866.929
N CDS (12)	GTR + G/UCED/EG	1.01×10^{-3} (2.79×10^{-4}–1.83×10^{-3})	1924 (1799–1970)	NA
N complete gene (12)	GTR + G/UCED/EG	1.08×10^{-3} (3.19×10^{-4}–1.93×10^{-3})	1923 (1804–1970)	NA
P CDS (12)	GTR + I/UCED/EG	1.11×10^{-3} (3.46×10^{-4}–1.29×10^{-3})	1931 (1833–1972)	NA
P complete gene (12)	GTR + I/UCED/EG	1.19×10^{-3} (3.46×10^{-4}–2.03×10^{-3})	1930 (1828–1971)	NA
M CDS (12)	GTR + G/UCED/EG	6.52×10^{-4} (1.20×10^{-4}–1.20×10^{-3})	1897 (1695–1964)	NA
M complete gene (12)	GTR + I/UCED/EG	2.49×10^{-3} (9.96×10^{-4}–4.14×10^{-3})	1944 (1879–1973)	NA
FCDS (12)	GTR + I/CED/EG	8.95×10^{-4} (2.43×10^{-4}–1.58×10^{-3})	1914 (1766–1968)	NA
F complete gene (12)	GTR + G/UCED/EG	1.33×10^{-3} (3.26×10^{-4}–2.36×10^{-3})	1912 (1754–1967)	NA
H CDS (12)	GTR + G/UCED/EG	1.21×10^{-3} (3.96×10^{-4}–2.04×10^{-3})	1926 (1826–1969)	NA
H complete gene (12)	GTR + G/UCED/EG	1.25×10^{-3} (4.34×10^{-4}–2.14×10^{-3})	1925 (1821–1968)	NA
L CDS (12)	GTR + I/UCED/EG	9.82×10^{-4} (3.76×10^{-4}–1.67×10^{-3})	1929 (1834–1969)	NA
L complete gene (12)	GTR + I/UCED/EG	9.69×10^{-4} (3.36×10^{-4}–1.64×10^{-3})	1927 (1820–1969)	NA
PPRV/RPV/MV (16)	GTR+ G + I/UCED/EG	1.89×10^{-3} (5.55×10^{-4}–3.31×10^{-3})	1616 (1072–1859)	NA

*Bold indicates best-fit models. HPD, highest posterior density; TMRCA, time to most recent common ancestor; GTR + G, general time-reversible with gamma distribution rates; BSP, Bayesian skyline plot; CS, constant size; EG, exponential growth; UCLD, uncorrelated lognormal distribution; UCED, uncorrelated exponential distribution; NA, not applicable; GTR + I, general time-reversible with invariant sites; GTR+ G + I, general time-reversible with gamma distribution rates and invariant sites.
†PPRV, peste des petits ruminants virus; N, nucleoprotein; CDS, coding sequence; P, phosphoprotein; M, matrix; F, fusion; H, hemagglutinin; L, large polymerase; RPV, rinderpest virus; MV, measles virus.

HPD 1843–1970). Lineages II and IV diverged from each other in ≈1956 (95% HPD 1885–1973). The TMRCA for lineage III viruses (n = 4) used in this study was estimated to be ≈1956 (95% HPD 1887–1978). TMRCA for lineages I and II PPRV were not predicted because only 1 virus from each lineage was used. The TMRCA for lineage IV viruses (n = 6) used in this study was estimated to be ≈1987 (95% HPD 1957–1998). When both Nigeria 1975/1 and Sungri 1996 vaccine strains were included in the study, the TMRCA for all lineages of PPRV shifted from 1904 (95% HPD 1730–1966) to 1891 (95% HPD 1705–1960). Analysis of the partial N gene dataset showed the TMRCA as 1910 (95% HPD 1846–1947) for all lineages of PPRV, 1960 (95% HPD 1941–1971) for lineage III, 1958 (95% HPD 1946–1971) for lineage I, 1961 (95% HPD 1941–1967) for lineage II, and 1987 (95% HPD 1969–1988) for lineage IV.

Results of TMRCA analysis using complete coding and coding and noncoding regions of individual PPRV genes are shown in Table 4. If one considers coding and noncoding sequences of individual genes in the analysis, a difference in TMRCA was found only for the M gene (i.e., 1944, 95% HPD 1879–1973). The TMRCA of PPRV/RPV/MV was estimated to be ≈1616 (95% HPD 1072–1859), and the TMRCA for PPRV was estimated to be 1931 (95% HPD 1858–1956) (Figure 3).

Population Demography of PPRV

The demographic history of PPRV was investigated by using the partial N gene sequence dataset according to the BSP method implemented in BEAST. The BSP with an assumed piecewise-constant model has facilitated estimation of effective population size through time. The BSP

Figure 2. Time-scaled Bayesian maximum clade credibility phylogeny tree based on peste des petits ruminants virus complete genome sequences. The tree was constructed by using the uncorrelated exponential distribution model and exponential tree prior. Branch tips correspond to date of collection and branch lengths reflect elapsed time. Tree nodes were annotated with posterior probability values and estimated median dates of time to most recent common ancestor (TMRCA). Corresponding 95% highest posterior density (HPD) interval values of TMRCA are indicated as gray bars. Horizontal axis indicates time in years. UAE, United Arab Emirates.

showed that the population did not show much genetic diversity (effective number of infections) until the mid-1990s when diversity started to increase. Toward the first decade of the 21st century, the population size appeared to reach a peak and then showed a small decrease until the most recent sampling in 2012 (Figure 4). The HPD interval size for the plot is narrow, which indicates strong support for this population trend.

Phylogeographic Analysis

To estimate the geographic origin of PPRV, we summarized the results of Bayesian phylogeographic analyses by visualizing the annotated MCC tree (Figure 5). The complete genome sequence data used in this analysis incorporated all 14 isolates, including the vaccine strains, from 10 discrete locations so as not to leave out any reported virus-endemic area. The root state posterior probabilities for all the locations ranged between 9.02% and 12.69%; Nigeria and the Ivory Coast (now Côte d'Ivoire) receiving marginally higher support, 12.69% and 10.53%, respectively, than the rest of the locations (Figure 5).

Because the geographic origin of PPRV could not be localized to a single country by using 14 complete genome sequences, further phylogeographic analysis was performed by using 159 partial N gene sequences collected from 30 locations during 1968–2012. The root state posterior probabilities of PPRV ranged from 0.11% to 17.20%, and Nigeria (17.20%), Ghana (14.28%), and Sierra Leone (11.68%) showed the highest marginal support (Figure 6). The highest marginal support of root state posterior probabilities indicated that the geographic origin of lineage I PPRV was Senegal (27.44%), that of lineage II PPRV was Nigeria (27.00%), that of lineage III PPRV was Sudan (30.73%), and that of lineage IV PPRV was India (36.00%).

Discussion

We sequenced complete genomes of 4 lineage III and 3 lineage IV isolates of PPRV. We used these genomes and

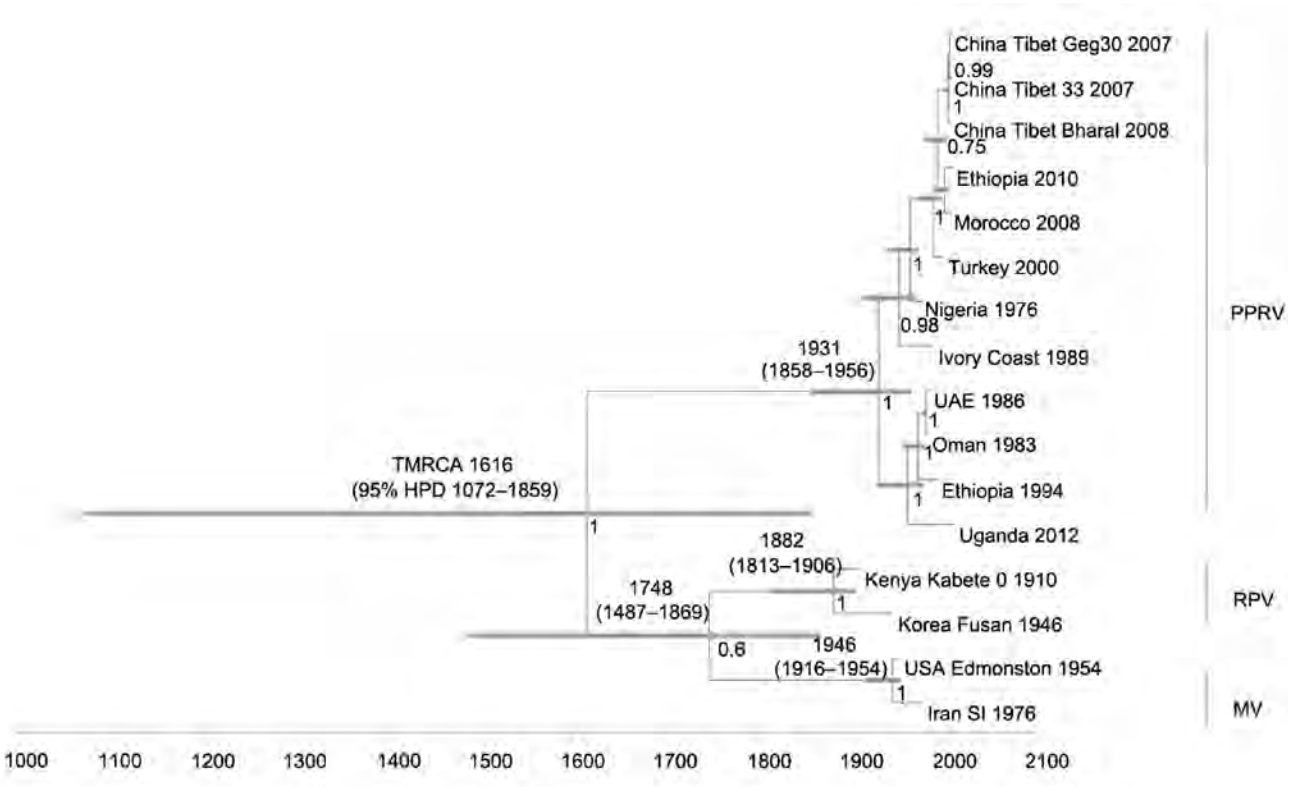

Figure 3. Time-scaled Bayesian MCC phylogeny tree based on peste des petits ruminants virus (PPRV), rinderpest virus (RPV), and measles virus (MV) complete genome sequences. The tree was constructed by using the uncorrelated exponential distribution model and exponential tree prior. Branch tips correspond to date of collection and branch lengths reflect elapsed time. Tree nodes were annotated with posterior probability values, estimated median dates of time to most recent common ancestor (TMRCA). Corresponding 95% highest posterior density (HPD) values of TMRCA are indicated as gray bars. Horizontal axis indicates time in years. UAE, United Arab Emirates.

other available genomes to assess the evolutionary substitution rate, TMRCA, and divergence of PPRV lineages and the geographic origin of PPRV.

The measure of selective pressures acting across the PPRV genome showed only purifying (stabilizing) selection occurring across the genome and no evidence of positive selection. The conservation of amino acid residues was further confirmed by the fact that the relative substitution rates at the third codon position of all the genes were higher than those for the first and second codon positions. The observed upper limit of 11.9% nt divergence (7.2% aa divergence) among PPRVs is consistent with the low level of antigenic divergence observed because despite lineage differentiation, only a single serotype exists for PPRV. Homologous recombination events are generally rare or absent in negative-sense RNA viruses (*30*) and thus could not have been evaluated in this study.

From a genetic perspective, substitution rates are critical parameters for understanding virus evolution, given that restrictions in genetic variation within a population of viruses can lead to lower adaptability and pathogenicity (*31*). Our analyses estimated a range of PPRV nucleotide substitution rates throughout the complete genome of 1.64×10^{-3}–2.13×10^{-4} substitutions/site/year, which is similar to that predicted for other paramyxoviruses (10^{-3}–10^{-4} substitutions/site/year) (*32*–*35*). Despite low levels of antigenic divergence, as shown by existence of a single serotype, genome plasticity of PPRV might explain its ability to emerge and adapt in new geographic regions and hosts, as reported extensively across vast areas in recent years. The TMRCA of PPRV obtained from complete genome sequence was estimated to be during 1904 (95% HPD 1730–1966). Similarly, the estimated TMRCA obtained from individual gene sequence, partial N gene sequence of PPRV, and combined PPRV/RPV/MV complete genome sequences was during 1910–1944.

That the predicted TMRCA for PPRV was during the early 20th century is reasonable because the first recorded description of PPRV was made in 1942 (*36*). The delay of a few decades before identification of PPRV as a distinct viral entity after its initial detection can likely be attributed to confusion in differentiation between PPRV and RPV, a virus for which extensive cross-neutralization is observed after vaccination and natural infection, and lack

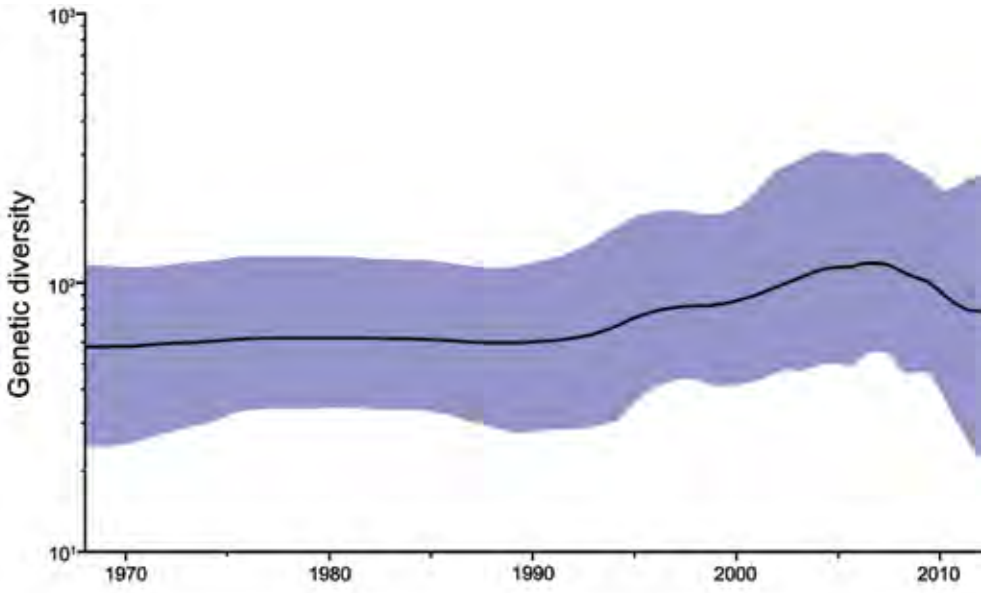

Figure 4. Bayesian skyline plot showing demographic history of global peste des petits ruminants viruses sampled during 1968–2012. Genetic diversity was estimated by using a partial nucleoprotein gene dataset (n = 159). The thick black line represents median genetic diversity and the blue shaded areas show 95% highest posterior density estimate.

of differentiating diagnostic tools. Substitution rates were consistent across each gene for PPRV. However, greater substitution rates were observed in the GC rich regions of the F and M genes. Similarly, the substitution rate was greater, as predicted because of the variability seen at the nucleotide level, in the highly variable region of the N gene sequence (255 nt) for PPRV. The TMRCA estimation was not possible for lineage I and II viruses (vaccine strain was omitted) because only 1 complete genome sequence was available for each lineage. Therefore, more complete genome sequences are required to study evolutionary and phylogenetic relationships for these lineages.

Biased estimates in substitution rate and TMRCA were observed by using datasets that included tissue culture–passaged, attenuated vaccine strain complete genome sequences, in which slower evolutionary substitution rates and earlier TMRCA were predicted. Similar observations were reported for PPRV/RPV/MV N gene sequence analyses, in which a slower and biased nucleotide substitution rate was observed when vaccine strain sequences (*33*) were included in the analysis and faster substitution rates and later TMRCA predictions were suggested when vaccine strain sequence data were excluded (*34*).

Spatial and temporal dynamics of RNA viruses are often reflected by their phylogenetic structure (*37*). Potential divergence events for different PPRV lineages were inferred by using rooted, time-measured phylogenetic trees with higher confidence from the PPRV complete genome sequence dataset. The inferred phylogeny supports the initial divergence of lineage III isolates, followed by lineage I isolates; lineage II and IV isolates were predicted to have diverged from each other at a later time. The inference of divergence events presented facilitated a better understanding of historical divergence of PPRV and offered further opportunities to study viral demographic history and dispersal events.

The demographic analysis of PPRV with the BSP indicated historically constant genetic variability of PPRV over time. This finding could be a reflection of the use of RPV vaccine in small ruminants to protect animals against PPRV through the 1990s, which might have affected the evolution and spread of PPRV. In the early 21st century, genetic diversity of PPRV has gradually increased, which reflects frequent outbreak reports. The increased genetic diversity may be a driver for selection pressures within individual lineages and might result in extinction events, as suggested by an absence of lineage I virus. In recent years, as efforts have increased to actively control and eradicate PPRV, a decrease in genetic diversity has been observed.

Phylogeographic reconstruction with spatial and temporal information of virus isolates has enabled an understanding of the historic emergence and dispersal patterns involved in virus evolution (*38*). Although PPRV existed earlier than its first description in Ivory Coast in 1942 (*39*), PPRV was later reported in Senegal, Chad, Togo, Benin, Ghana, Nigeria, Oman, Sudan, Saudi Arabia, India, Jordan, Israel, Ethiopia, Kenya, Uganda, and Pakistan (*40*). Our phylogeographic analysis indicated that Nigeria was the geographic origin of the most recent common ancestor of PPRV because of the highest root location state probability. Furthermore, geographic origins of the most recent common ancestor of PPRV lineages I, II, and III were predicted to be across Africa; lineage IV likely emerged in India. In

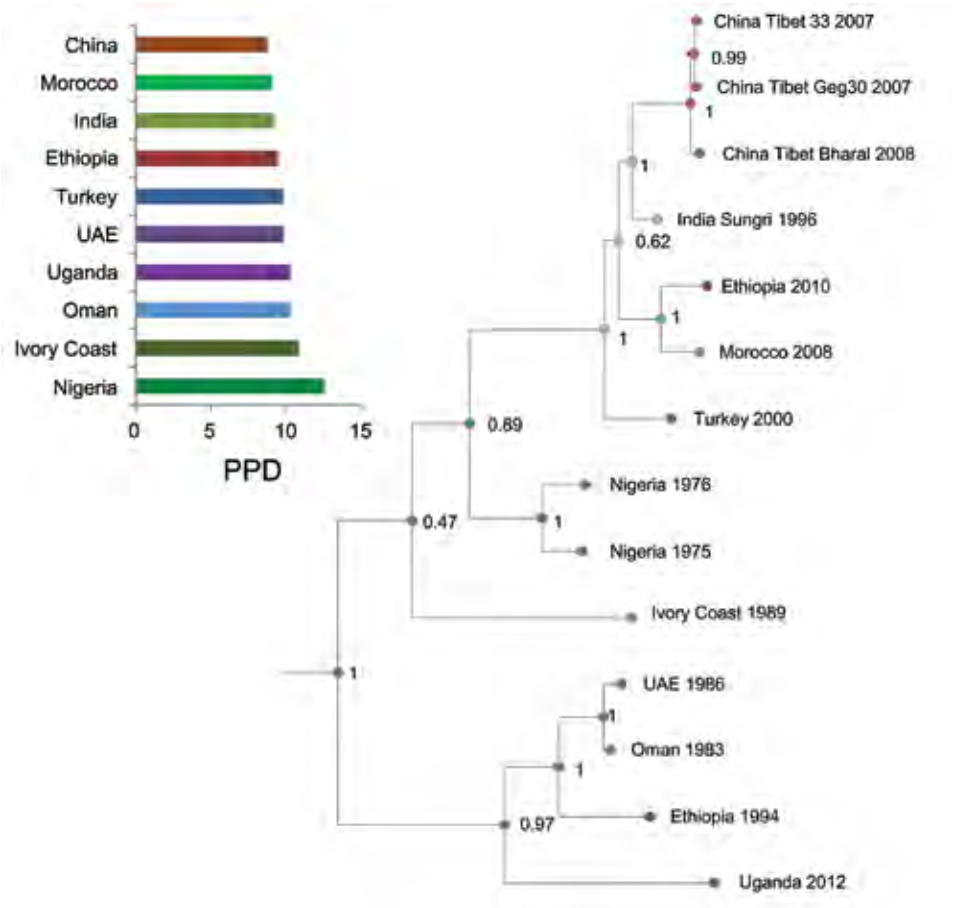

Figure 5. Maximum clade credibility tree constructed for the geospatial analysis of peste des petits ruminants viruses by using complete genome data. Nodes are colored according to the most probable location of their ascendent locations. Posterior probability values are shown along tree nodes. Posterior probability distribution (PPD) values of root location states of the ancestral node are shown along the x-axis at the top left. UAE, United Arab Emirates.

conclusion, these findings suggest that the origin of PPRV was in western Africa, which then spread to eastern Africa, the Middle East, and Asia. However, although these predictions are suggestive of a potential origin for PPRV, caution must be exercised in their interpretation because estimates of geographic origin rely on available datasets, and these datasets need enhancing to provide greater confidence for phylogenetic assessment. As more sequence data become available for PPRV and the other morbilliviruses, ancestral origins of each virus and intraspecies differentiation might become more clear.

Acknowledgment

We thank Vincent Michaud for his critical reading of and comments on the manuscript.

This study was supported by grants EU-BBSRC Anihwa BB/L013657/1, BBSRC-DFID CIDLID BB/H009485/1, and DBT-BBSRC FADH BB/L004801/1.

Mr Muniraju is a final year doctoral student at The Pirbright Institute, Pirbright, UK. His primary research interests are epidemiologic studies of PPRV and developing marker vaccines for peste des petits ruminants by using reverse genetics techniques.

References

1. Dhar P, Sreenivasa BP, Barrett T, Corteyn M, Singh RP, Bandyopadhyay SK. Recent epidemiology of peste des petits ruminants virus (PPRV). Vet Microbiol. 2002;88:153–9. http://dx.doi.org/10.1016/S0378-1135(02)00102-5
2. Banyard AC, Parida S, Batten C, Oura C, Kwiatek O, Libeau G. Global distribution of peste des petits ruminants virus and prospects for improved diagnosis and control. J Gen Virol. 2010;91:2885–97. http://dx.doi.org/10.1099/vir.0.025841-0
3. Gibbs EP, Taylor WP, Lawman MJ, Bryant J. Classification of peste des petits ruminants virus as the fourth member of the genus *Morbillivirus*. Intervirology. 1979;11:268–74. http://dx.doi.org/10.1159/000149044
4. de Swart RL, Duprex WP, Osterhaus AD. Rinderpest eradication: lessons for measles eradication? Curr Opin Virol. 2012;2:330–4. http://dx.doi.org/10.1016/j.coviro.2012.02.010
5. Baron MD, Parida S, Oura CA. Peste des petits ruminants: a suitable candidate for eradication? Vet Rec. 2011;169:16–21. http://dx.doi.org/10.1136/vr.d3947
6. Lembo T, Oura C, Parida S, Hoare R, Frost L, Fyumagwa R, et al. Peste des petits ruminants infection among cattle and wildlife in northern Tanzania. Emerg Infect Dis. 2013;19:2037–40. http://dx.doi.org/10.3201/eid1912.130973
7. Balamurugan V, Sen A, Venkatesan G, Bhanot V, Yadav V, Bhanuprakash V, et al. Peste des petits ruminants virus detected in tissues from an Asiatic lion (*Panthera leo persica*) belongs to Asian lineage IV. J Vet Sci. 2012;13:203–6. http://dx.doi.org/10.4142/jvs.2012.13.2.203

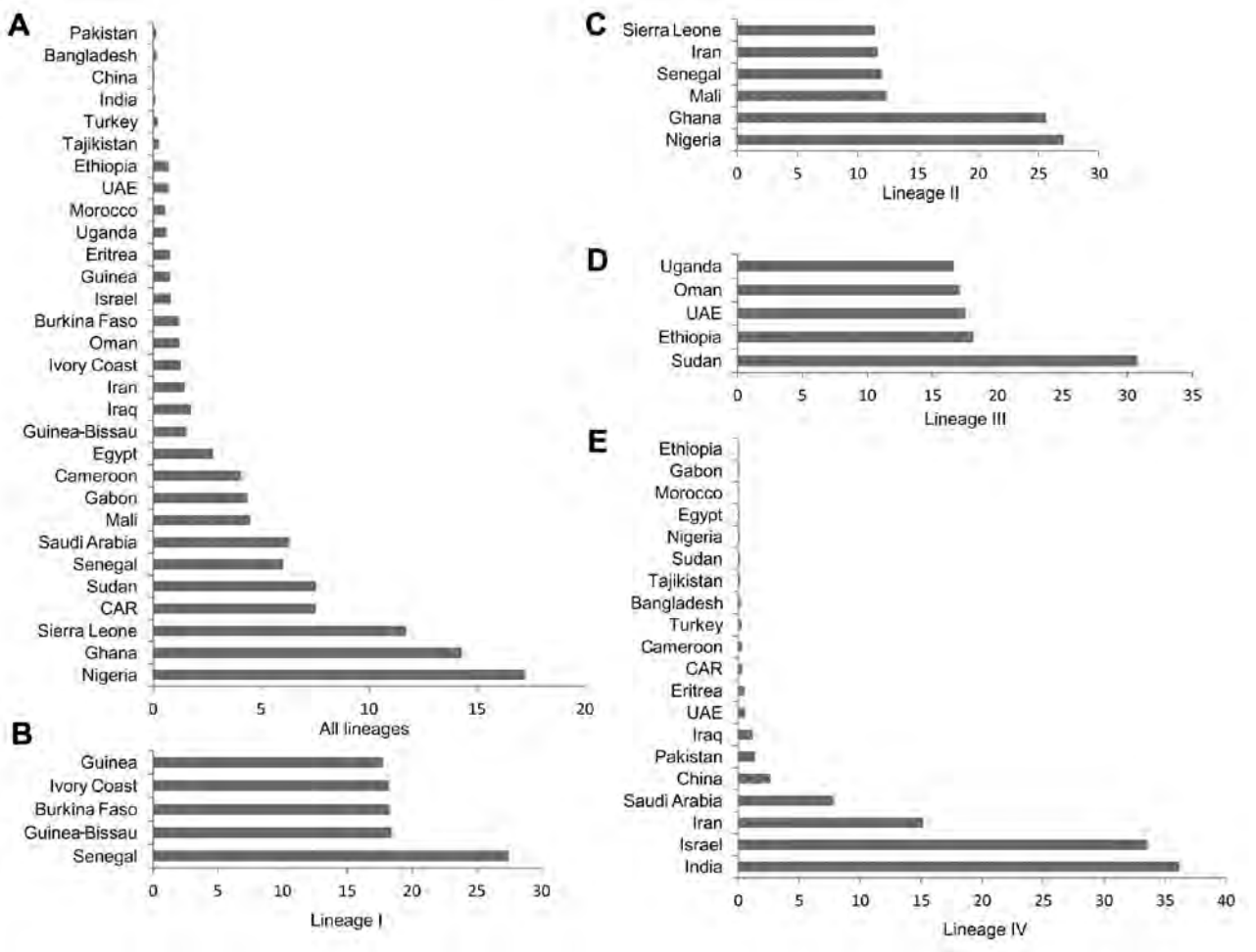

Figure 6. Probability of root locations of the most recent common ancestral peste des petits ruminants (PPRV). MCC trees were obtained by using the continuous time Markov chain and Bayesian stochastic search variable selection procedures. Root location probabilities of the most recent common ancestor using global PPRV isolates (panel A) are shown graphically alongside lineages I–IV (panels B–E) and were estimated by using a complete dataset of PPRV partial nucleoprotein gene data and individual lineages separately. Probabilities of root locations are shown as percentages along the x-axes. UAE, United Arab Emirates; CAR, Central African Republic.

8. Khalafalla AI, Saeed IK, Ali YH, Abdurrahman MB, Kwiatek O, Libeau G, et al. An outbreak of peste des petits ruminants (PPR) in camels in the Sudan. Acta Trop. 2010;116:161–5. http://dx.doi.org/10.1016/j.actatropica.2010.08.002
9. Food and Agriculture Organization of the United Nations. Supporting livelihoods and supporting livelihoods and peste des petits ruminants (ppr) and small ruminant diseases control, 2013 [cited 2014 Sep 2]. http://www.fao.org/docrep/017/aq236e/aq236e00.htm
10. Libeau G, Diallo A, Parida S. Evolutionary genetics underlying the spread of peste des petits ruminants virus. Animal Frontiers. 2014;4:14–20. http://dx.doi.org/10.2527/af.2014-0003
11. Pybus OG, Rambaut A. Evolutionary analysis of the dynamics of viral infectious disease. Nat Rev Genet. 2009;10:540–50. http://dx.doi.org/10.1038/nrg2583
12. Muniraju M, El Harrak M, Bao J, Ramasamy Parthiban AB, Banyard AC, Batten C, et al. Complete genome sequence of a peste des petits ruminants virus recovered from an alpine goat during an outbreak in Morocco in 2008. Genome Announc. 2013;1:e00096–13. http://dx.doi.org/10.1128/genomeA.00096-13
13. Chard LS, Bailey DS, Dash P, Banyard AC, Barrett T. Full genome sequences of two virulent strains of peste-des-petits ruminants virus, the Côte d'Ivoire 1989 and Nigeria 1976 strains. Virus Res. 2008;136:192–7. http://dx.doi.org/10.1016/j.virusres. 2008.04.018
14. Diallo A, Barrett T, Barbron M, Meyer G, Lefevre PC. Cloning of the nucleocapsid protein gene of peste-des-petits-ruminants virus: relationship to other morbilliviruses. J Gen Virol. 1994;75:233–7. http://dx.doi.org/10.1099/0022-1317-75-1-233
15. Furley CW, Taylor WP, Obi TU. An outbreak of peste des petits ruminants in a zoological collection. Vet Rec. 1987;121:443–7. http://dx.doi.org/10.1136/vr.121.19.443
16. Taylor WP, al Busaidy S, Barrett T. The epidemiology of peste des petits ruminants in the Sultanate of Oman. Vet Microbiol. 1990;22:341–52. http://dx.doi.org/10.1016/0378-1135(90)90021-M
17. Roeder PL, Abraham G, Kenfe G, Barrett T. Peste des petits ruminants in Ethiopian goats. Trop Anim Health Prod. 1994;26:69–73. http://dx.doi.org/10.1007/BF02239901
18. Bao J, Wang Q, Parida S, Liu C, Zhang L, Zhao W, et al. Complete genome sequence of a peste des petits ruminants virus

recovered from wild bharal in Tibet, China. J Virol. 2012;86:10885–6. http://dx.doi.org/10.1128/JVI.01503-12
19. Wang Z, Bao J, Wu X, Liu Y, Li L, Liu C, et al. Peste des petits ruminants virus in Tibet, China. Emerg Infect Dis. 2009;15:299–301. http://dx.doi.org/10.3201/eid1502.080817
20. Bailey D, Banyard A, Dash P, Ozkul A, Barrett T. Full genome sequence of peste des petits ruminants virus, a member of the *Morbillivirus* genus. Virus Res. 2005;110:119–24. http://dx.doi.org/10.1016/j.virusres.2005.01.013
21. Hall TA. BioEdit: a user-friendly biological sequence alignment editor and analysis program for Windows 95/98/NT. Nucleic Acids Symposium Series. 1999;41:95–8.
22. Pond SL, Frost SD, Muse SV. HyPhy: hypothesis testing using phylogenies. Bioinformatics. 2005;21:676–9. http://dx.doi.org/10.1093/bioinformatics/bti079
23. Drummond AJ, Suchard MA, Xie D, Rambaut A. Bayesian phylogenetics with BEAUti and the BEAST 1.7. Mol Biol Evol. 2012;29:1969–73. http://dx.doi.org/10.1093/molbev/mss075
24. Miller MA, Pfeiffer W, Schwartz T. Creating the CIPRES science gateway for inference of large phylogenetic trees. Presented at: Proceedings of the Gateway Computing Environments Workshop (GCE); 2010 Nov 14; New Orleans, Louisiana, USA; p. 1– 8.
25. Posada D. jModelTest: phylogenetic model averaging. Mol Biol Evol. 2008;25:1253–6. http://dx.doi.org/10.1093/molbev/msn083
26. Kass RE, Raftery AE. Bayes factors. Journal of the American Statistical Association. 1995;90:773–95. http://dx.doi.org/10.1080/01621459.1995.10476572
27. Lemey P, Rambaut A, Drummond AJ, Suchard MA. Bayesian phylogeography finds its roots. PLOS Comput Biol. 2009;5:e1000520. http://dx.doi.org/10.1371/journal.pcbi.1000520
28. Radecke F, Spielhofer P, Schneider H, Kaelin K, Huber M, Dotsch C, et al. Rescue of measles viruses from cloned DNA. EMBO J. 1995;14:5773–84.
29. Nei M, Gojobori T. Simple methods for estimating the numbers of synonymous and nonsynonymous nucleotide substitutions. Mol Biol Evol. 1986;3:418–26.
30. Han GZ, Worobey M. Homologous recombination in negative sense RNA viruses. Viruses. 2011;3:1358–73. http://dx.doi.org/10.3390/v3081358
31. Denison MR, Graham RL, Donaldson EF, Eckerle LD, Baric RS. Coronaviruses: an RNA proofreading machine regulates replication fidelity and diversity. RNA Biol. 2011;8:270–9. http://dx.doi.org/10.4161/rna.8.2.15013
32. Pomeroy LW, Bjornstad ON, Holmes EC. The evolutionary and epidemiological dynamics of the paramyxoviridae. J Mol Evol. 2008;66:98–106. http://dx.doi.org/10.1007/s00239-007-9040-x
33. Furuse Y, Suzuki A, Oshitani H. Origin of measles virus: divergence from rinderpest virus between the 11th and 12th centuries. Virol J. 2010;7:52. http://dx.doi.org/10.1186/1743-422X-7-52
34. Wertheim JO, Kosakovsky Pond SL. Purifying selection can obscure the ancient age of viral lineages. Mol Biol Evol. 2011;28:3355–65. http://dx.doi.org/10.1093/molbev/msr170
35. Jenkins GM, Rambaut A, Pybus OG, Holmes EC. Rates of molecular evolution in RNA viruses: a quantitative phylogenetic analysis. J Mol Evol. 2002;54:156–65. http://dx.doi.org/10.1007/s00239-001-0064-3
36. Gargadennec L, Lalanne A. Peste des petits ruminants [in French]. Bulletin des Services Zootechniques et des Epizzoties de l'Afrique Occidentale Francaise. 1942;5:16–21.
37. Biek R, Drummond AJ, Poss M. A virus reveals population structure and recent demographic history of its carnivore host. Science. 2006;311:538–41. http://dx.doi.org/10.1126/science.1121360
38. Lemey P, Suchard M, Rambaut A. Reconstructing the initial global spread of a human influenza pandemic: a Bayesian spatial-temporal model for the global spread of H1N1pdm. PLoS Curr. 2009;1:RRN1031. http://dx.doi.org/10.1371/currents.RRN1031
39. Diallo A. Rinderpest and peste des petits ruminants. Constant threats against livestock in many countries [in French]. Impact of Science on Society. 1988;150:191–204.
40. Sen A, Saravanan P, Balamurugan V, Rajak KK, Sudhakar SB, Bhanuprakash V, et al. Vaccines against peste des petits ruminants virus. Expert Rev Vaccines. 2010;9:785–96. http://dx.doi.org/10.1586/erv.10.74

Address for correspondence: Satya Parida, Livestock Viral Diseases, The Pirbright Institute, Ash Rd, Pirbright, Surrey, Woking GU24 0NF, UK; email: satya.parida@pirbright.ac.uk

etymologia

Peste des petits ruminants [pest dā pə-teʹ ru-me-nahʹ]

From the French for "plague of the small, hooved mammals," peste des petits ruminants (PPR) is a severe (mortality rate may be >90%), highly contagious disease of sheep and goats. PPR was first described in Côte d'Ivoire in 1942 and soon discovered in other countries in West Africa. In more recent decades, it has spread to many other parts of the world, including East Africa, the Middle East, and Asia. Also known as ovine rinderpest and goat plague, PPR is caused by a morbillivirus closely related to the rinderpest virus of cattle and buffaloes (which was eradicated in 2011) and the measles virus of humans.

Sources

1. Food and Agriculture Organization of the United Nations (FAO). Recognizing peste des petits ruminants: a field manual. Rome: The Organization; 1999.
2. Dorland's illustrated medical dictionary. 32nd ed. Philadelphia: Elsevier Saunders; 2012.

Address for correspondence: Ronnie Henry, Centers for Disease Control and Prevention, 1600 Clifton Rd NE, Mailstop E03, Atlanta, GA 30333, USA; email: boq3@cdc.gov

DOI: http://dx.doi.org/10.32301/eid2012.ET2012

Circulation of Reassortant Influenza A(H7N9) Viruses in Poultry and Humans, Guangdong Province, China, 2013

Changwen Ke, Jing Lu, Jie Wu, Dawei Guan, Lirong Zou, Tie Song, Lina Yi, Xianqiao Zeng, Lijun Liang, Hanzhong Ni, Min Kang, Xin Zhang, Haojie Zhong, Jianfeng He, Jinyan Lin, Derek Smith, David Burke, Ron A.M. Fouchier, Marion Koopmans, and Yonghui Zhang

Influenza A(H7N9) virus emerged in eastern China in February 2013 and continues to circulate in this region, but its ecology is poorly understood. In April 2013, the Guangdong Provincial Center for Disease Control and Prevention (CDC) implemented environmental and human syndromic surveillance for the virus. Environmental samples from poultry markets in 21 city CDCs (n = 8,942) and respiratory samples from persons with influenza-like illness or pneumonia (n = 32,342) were tested; viruses isolated from 6 environmental samples and 16 patients were sequenced. Sequence analysis showed co-circulation of 4 influenza A(H7N9) virus strains that evolved by reassortment with avian influenza A(H9N2) viruses circulating in this region. In addition, an increase in human cases starting in late 2013 coincided with an increase in influenza A H7 virus isolates detected by environmental surveillance. Co-circulation of multiple avian influenza viruses that can infect humans highlights the need for increased surveillance of poultry and potential environmental sources.

Human infection with a novel avian-origin influenza A(H7N9) virus was first identified in eastern China in February 2013, and a major outbreak occurred from the end of March through the beginning of May (*1*,*2*). Risk factors identified for a severe course of illness were older age (≥65 years) and underlying illnesses, including hypertension and chronic lung diseases, but the full spectrum of illness associated with H7N9 virus remains to be determined (*3*). Molecular characterization has shown that the H7N9 virus emerged by reassortment between H7, N9, and H9N2 avian influenza viruses from the Yangzi River Delta region; this reassortment likely occurred in eastern China in early 2012 (*2*,*4*,*5*). Because infection with H7N9 virus does not cause overt disease in poultry, the spread of infection can be insidious, and the exact modes and extent of geographic spread of the virus remain unknown. Birds commonly used for egg and meat production in China differ in their susceptibility, levels of virus shedding, and ability to transmit the virus; data from experimental infections indicate that quail and chickens are possible candidates for virus transmission (*6*). Detailed analysis of viruses from human patients showed evidence for diversification through reassortment of the originally detected viruses with strains from poultry in the same geographic region (*7*). Infection of humans is linked to exposure to poultry or to environments where poultry are present; closure of live poultry markets (LPMs) has had a measurable effect on controlling the spread of infection (*8*,*9*).

After H7N9 virus was initially detected in eastern China, the Guangdong Provincial Center for Disease Control and Prevention (CDC) implemented environmental surveillance and syndromic surveillance in humans. After H7N9 virus infection in humans was reported, enhanced sentinel hospital surveillance and environmental sampling programs were implemented to identify possible cases and analyze the evolution of the virus. The first case of human infection with H7N9 virus in Guangdong was confirmed in a patient with severe pneumonia on August 10, 2013. This case-patient was a 51-year-old female poultry worker at a local LPM in Huizhou city in Guangdong Province. No other cases were reported until October 2013, when a wave of cases began in several provinces, including Guangdong.

Author affiliations: Guangdong Provincial Center for Disease Control and Prevention, Guangzhou, China (C. Ke, J. Lu, J. Wu, D. Guan, L. Zou, T. Song, L. Yi, X. Zeng, L. Liang, H. Ni, M. Kang, X. Zhang, H. Zhong, J. He, J. Lin, Y. Zhang); University of Cambridge, Cambridge, UK (D. Smith, D. Burke); Erasmus MC, Rotterdam, the Netherlands (R.A.M. Fouchier, M. Koopmans); and National Institute of Public Health and the Environment, Bilthoven, the Netherlands (M. Koopmans)

DOI: http://dx.doi.org/10.3201/eid2012.140765

We present results of ongoing environmental and human syndromic surveillance for H7N9 virus circulation in Guangdong Province, as well as virologic analyses related to the natural history of this outbreak.

Materials and Methods

Syndromic Surveillance in Humans

Since April 16, 2013, enhanced surveillance for influenza A(H7N9) virus has been conducted in 28 sentinel hospitals and 23 collaborating laboratories in 21 cities in Guangdong Province, China. All specimens are first tested for avian influenza A virus; specimens with positive results are then further tested in the laboratories of the 21 city CDCs for subtypes H5, H7, and H9 by using commercial real-time reverse transcription PCR (RT-PCR) (Liferiver, Shanghai ZJ Bio-Tech, Shanghai, China). Results are further verified at the Guangdong Provincial CDC. H7-positive specimens are tested for N9 gene segments by using real-time RT-PCR (*2*). H7N9-positive swab materials and sputum samples are then blindly passaged for 2 or 3 generations in 9- or 10-day-old embryonated chicken eggs for virus isolation. Hemagglutination-positive allantoic fluids are collected, and viruses are subtyped by hemagglutination and neuraminidase inhibition (HI and NI) assays by using a panel of reference antiserum, as described by Huang et al. (*10*). Standard precautions are taken to avoid cross-contamination of specimens. All H7 influenza viruses isolated from patients undergo complete genome sequencing.

Environmental Surveillance

In April 2013, the Guangdong Provincial CDC launched an environmental surveillance program to monitor for avian influenza viruses in LPMs. Environmental samples were collected from LPMs in Guangdong Province during April 15, 2013–February 28, 2014. Each week during April 15–May 31, 2013, twenty environmental samples per market were collected from selected markets in 21 cities at the prefecture level. The environmental sampling was done by collecting wet-swab specimens from poultry feces, chicken epilator surfaces, chopping board surfaces, cage surfaces, and sewage. If a human H7N9 case was confirmed and the case-patient had exposure in an LPM, >20 environmental samples would be collected from that market.

Samples were collected from poultry feces by swabbing the surfaces of the chicken epilator, chopping boards, and cages 4–8 times with separate cotton-tipped swabs (Copan Italia, Brescia, Italy). The swabs were then inserted into a tube containing 3 mL of virus transport medium (Copan Italia) and stored at 4°C before shipping to the CDC laboratory. At arrival in the laboratory, samples were vortexed and swabs were discarded. Total RNA and DNA were extracted simultaneously from 200 mL supernatant of the sample by using the QIAamp minElute Virus Spin Kit (QIAGEN, Crawley, UK), according to the manufacturer's instructions. Then, 5 mL of eluate was tested for influenza A; thereafter, testing for subtypes H5, H7, and H9 was done by commercial real-time reverse transcription PCR (RT-PCR) (Liferiver, Shanghai ZJ Bio-Tech). H7-positive specimens were further subjected to N9 gene-specific RT-PCR. Dual positive samples were blindly passaged for 2–3 generations in 9- to 10-day-old embryonated chicken eggs for virus isolation. Hemagglutinin (HA)–positive isolates were collected and further subtyped by HI and NI assays using a panel of reference antiserum, as described by Huang et al. (*10*). Standard precautions were taken to avoid cross-contamination of specimens. Monoinfluenza virus infection (without mixed infection of other subtypes) was further confirmed by RT-PCR before whole-genome sequencing. All H7N9 isolates from LPMs were subjected to complete genome sequencing, as were 7 H9 influenza viruses that were isolated from different LPMs during May–December 2013.

Whole-Genome Deep Sequencing

For all selected isolates, all 8 gene segments (HA, neuraminidase [NA], nucleoprotein [NP], polymerase basic 1 [PB1] and 2 [PB2], polymerase acidic [PA], matrix [M], and nonstructural [NS]) were sequenced by using a next-generation sequencing strategy for influenza A virus sequencing with the Ion PGM System and PathAmp FluA Reagents (Life Technologies, Carlsbad, CA, USA). Viral RNA extraction was performed by using the QIAamp Viral RNA Mini Kit (QIAGEN, Hilden, Germany). Reverse transcription PCR amplification of all 8 gene segments were performed by using PathAmp Flu A Preamplification Reagents (Life Technologies). Amplicons were purified and quantitated by using the Ampure XP purification kit (Beckman, Brea, CA, USA). The genomic libraries were prepared with the Ion Xpress Plus Fragment Library Kit (Life Technologies). Enzymatic fragmentation was used for the 200-bp read protocol with a 10-min incubation time. Samples were assigned barcodes by using the Ion Xpress Barcode Adapters 1–32 Kit (Life Technologies). Automated template preparation was performed by using the Ion OneTouch 2 System (Ion PGM Template OT2 200 Kit; Life Technologies). Final sequencing was performed with the Ion PGM Sequencing 200 Kit v2 (Life Technologies) using the Ion 316 Chip V2.

Genome Sequence Alignment

Genome sequence assembly was done with the pathogen analysis program of the Ion PGM server (Life Technologies). Multiple sequence alignment against previously published complete genome sequences of H7N9 and H9N2

viruses was performed by using ClustalW (http://www.clustal.org) and BioEdit software version 7.14 (http://www.mbio.ncsu.edu/bioedit/bioedit.html). The whole-genome sequences were submitted to GISAID (http://www.gisaid.org; accession nos. EPI148417 and EPI151429–151437).

Phylogenetic Analysis and Data Visualization

Maximum-likelihood trees were estimated for all 8 gene segments by using MEGA version 5.2 (http://www.megasoftware.net) with the general time reversible + G model (*11*). To assess the robustness of individual nodes on phylogenetic trees, a bootstrap resampling process (1,000 replications) and the neighbor-joining method were used.

The initial trees were constructed in PhyML by using general time reversible + I + Γ4 as the evolutionary model (*12*). GARLI (https://code.google.com/p/garli/) was run on the best tree from PhyML for 1 million generations to optimize tree topology and branch lengths.

Results

Syndromic Surveillance

A total of 34,342 samples from patients with pneumonia or influenza-like illness from 21 cities in Guangdong Province were tested during April 2013–February 2014. Of these, samples from 81 patients from 10 cities tested positive for influenza A(H7N9) virus. With the exception of 1 case confirmed in August 2013, all other cases were found starting in October 2013. In total, 6 cases were confirmed in 2013 and 75 in early 2014.

Patient characteristics are summarized in Table 1. Most patients were male, and the median age of all patients was 52 years. Of the 81 patients, 70 (84%) had severe illness, which likely reflected the design of the surveillance (hospitalized patients). Twenty-two (27%) patients died; 14 remained hospitalized as of May 2014, and 45 had recovered. Overall, 73 patients (90.1%) reported poultry contact (Table 1).

Table 1. Demographic and clinical characteristics of influenza A(H7N9) case-patients detected through enhanced surveillance in Guangdong Province, China, March 2013–February 2014

Characteristic	No. (%) case-patients
Sex*	
M	48 (59.3)
F	33 (40.7)
Age group, y†	
≤20	12 (14.8)
21–40	13 (16.0)
41–60	25 (30.9)
≥61	31 (38.3)
Exposure history	
Live poultry market visit	47 (58.0)
Household poultry breeding	10 (12.3)
Poultry processing	5 (6.2)
Mixed	11 (13.6)
None known	8 (9.9)
Clinical use of oseltamivir‡	
Used	65 (80.2)
Unknown	16 (19.8)
Clinical condition	
Influenza-like illness	11 (13.6)
Pneumonia	14 (17.3)
Mild influenza	2 (2.5)
Severe influenza	54 (66.7)
Outcome	
Death	22 (27.2)
Recovery	45 (55.6)
Hospitalization	14 (17.3)

*M:F sex ratio 1.5:1.
†Median patient age 52.0 y.
‡Mean time from symptom onset to diagnosis 8.5 d; mean time from symptom onset to use of oseltamivir 5.2 d.

Environmental Surveillance

A total of 8,942 swab samples from LPMs were collected and screened in laboratories of city CDCs at the prefecture level and at Guangdong Provincial CDC (*2*). Overall, 425 samples (4.8%) from 13 cities tested positive for H7 viruses, and 1,050 (11.8%) from 19 cities were positive for H9 viruses. The prevalence of viral genes in regions with positive findings ranged from 1%–14% of swab samples for H7 viruses and 1.7%–27.5% for H9. The H9 detection rate remained ≈12% throughout the year, except during June, when only 4% of samples tested positive. H9 viruses were detected throughout Guangdong Province (19 of the 21 cities; Figure 1, panel A). In contrast, only 1 H7-virus positive specimen was detected during March–September 2013 (in Meizhou in April), but detections of H7 viruses increased beginning in October: from 1 site in October, 3 in November, 8 in January, and 7 in February. H7 viruses were detected in the Pearl River Regions of Guangdong Province (Figure 1, panel B). Human cases were found in 10 of the 13 cities where environmental samples were positive for H7, and in 0 of the 8 cities where no H7 viruses were found in environmental samples (Figure 1).

Sequence Analysis

Internal Genes

Whole-genome sequences were determined for the H7N9 virus isolates from 16 patients and 6 environmental samples and for the 9 H9 viruses collected during environmental surveillance. Phylogenetic trees were constructed for each internal gene segment against all currently available H7N9 and H9N2 virus sequences from the National Center for Biotechnology Information and GISAID. Phylogenetic analysis of the whole-genome sequences showed the clear separation of PB2, PB1, and NS gene sequences of the Guangdong patient isolates from those detected from patients from eastern China (Figure 2).

Gene sequences on the same branch were reviewed to identify region of origin; these sequences matched internal genes from H9N2 viruses detected in southern China

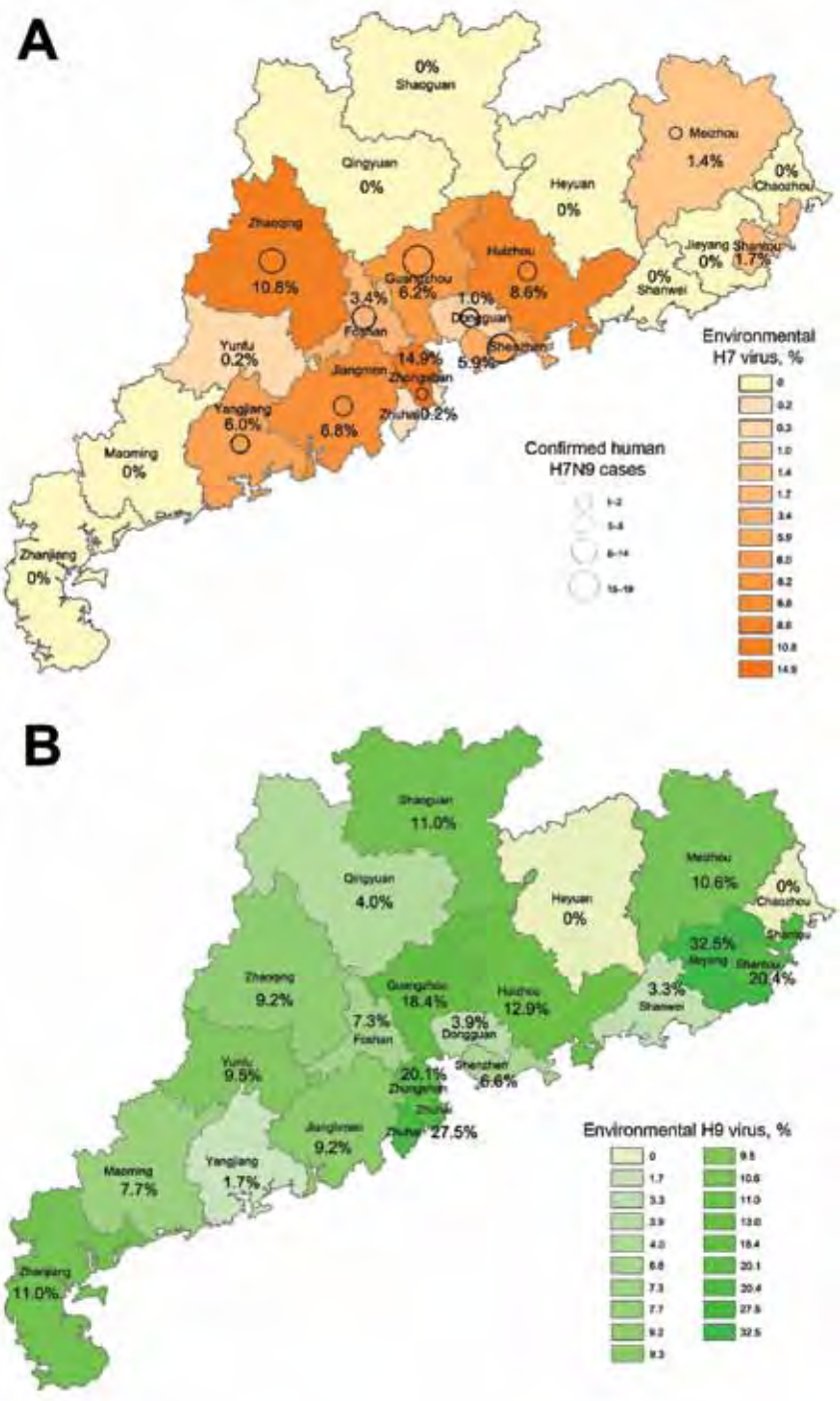

Figure 1. Distribution of influenza A H9 (A) and H7 (B) viruses, Guandong Province, China, 2013–2014. Shading indicates percentage of environmental swab specimens from live poultry markets in each region that were positive for each influenza subtype by reverse transcription PCR. Circles indicate locations of human cases; larger circles indicate higher numbers of cases.

(online Technical Appendix, http://wwwnc.cdc.gov/EID/article/20/12/14-0765-Techapp1.pdf). M genes of all viruses clustered with the genes detected in viruses from the main H7N9 virus cluster in 2013, whereas diversity was seen in the PA (main 2013 variant and 2 additional lineages) and NP (2 lineages) genes. Combined, the H7N9 virus isolates that were sequenced appeared to represent at least 4 different reassortants (Table 2).

HA and NA genes

The HA and NA genes of all H7N9 isolates from Guangdong Province we analyzed had high sequence identity (98.2%–99.7%) to viruses from other regions of China detected throughout 2013. However, the Guangdong Province isolates branched off and clustered with strains detected in Hong Kong during 2014 (online Technical Appendix).

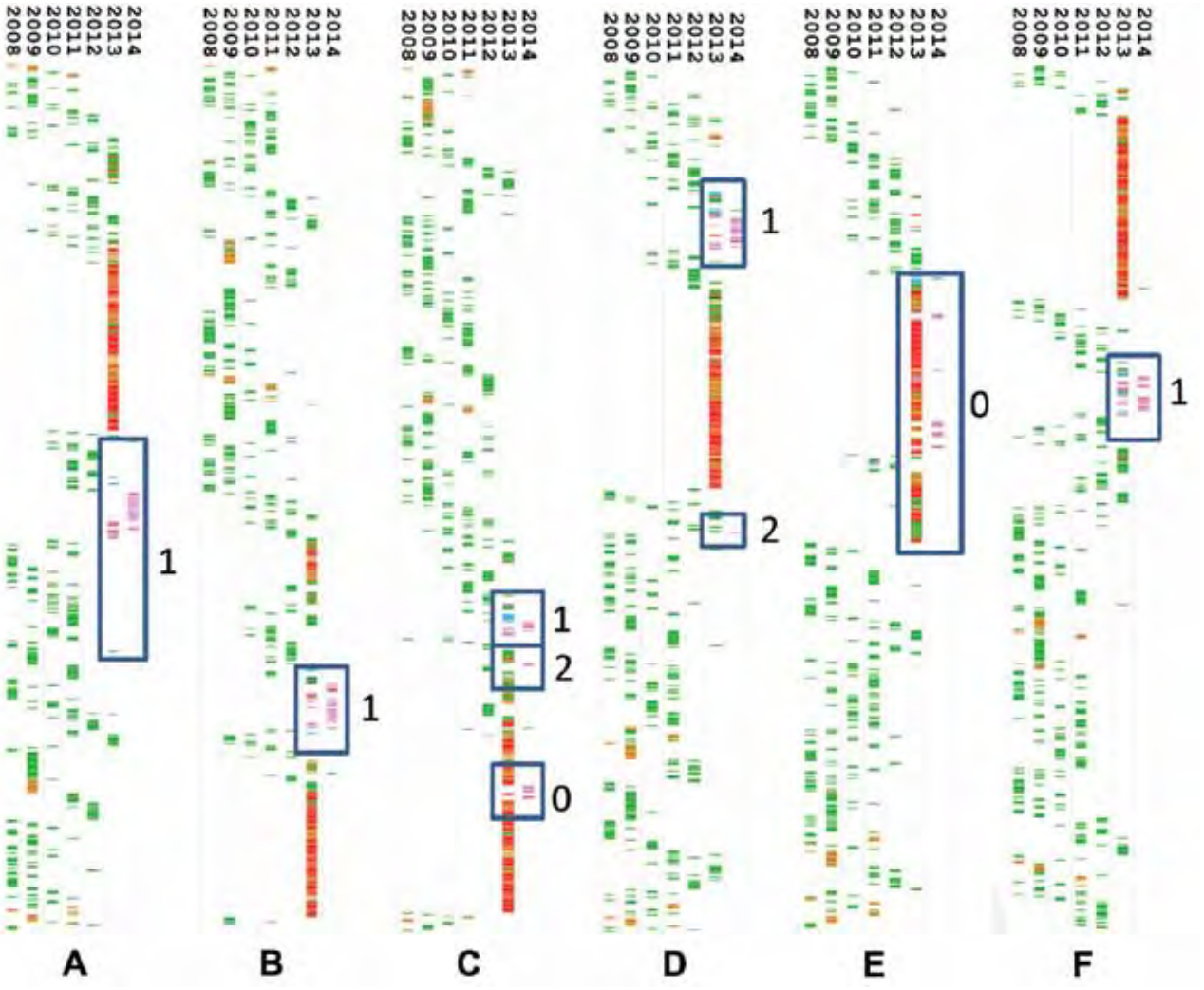

Figure 2. Timed phylogenies of internal gene segments of influenza A(H7N9) viruses detected in 16 patients from Guangdong Province, China, 2008–2014. A) Polymerase basic 2; B) polymerase basic 1; C) polymerase acidic; D) nucleoprotein; E) matrix; F) nonstructural. Avian H9N2 viruses are shown in green, avian H9N2 viruses from Guangdong Province in blue, human H7N9 sequences from Guangdong Province in pink, and human H7N9 sequences from the main case cluster in 2013 in eastern China in red. Blue boxes indicate clusters of patient sequences on separate branches; numbers correspond with the reassortant numbers listed in Table 2, where 0 indicates original genes from the 2013 cluster of influenza A(H7N9). Individual trees are shown in the online Technical Appendix (http://wwwnc.cdc.gov/EID/article/20/12/14-0765-Techapp1.pdf).

Discussion

The outbreak of influenza A(H7N9) virus infection in humans in Guangdong Province that started in late 2013 coincided with the emergence of influenza A H7 viruses in LPMs as determined by environmental surveillance. The strong association between detection of human H7N9 cases and presence of H7 viruses in LPMs confirms that these market environments are sources of human exposure (*8*,*13*). A key question is how the virus has been spreading in China since the initial emergence in eastern China. A risk-mapping approach taking into account LPM locations, human population density, cropland irrigation, and meteorologic conditions listed central Guangdong Province as a high-risk area (defined as probability of the presence of influenza A[H7N9] viruses) (*14*). Little is known, however, about how H7N9 virus spreads and the prevalence of infection in commercial poultry flocks.

The data from our study suggest sources of human infection in Guangdong Province are local. All sequenced viruses had evolved from the original strains through genetic reassortment with internal genes originating from influenza A(H9N2) viruses commonly found in southern China. The HA sequences of these viruses formed a distinct branch in phylogenetic trees, which indicates that reassortment occurred some time ago and suggests that local sources of virus transmission in Guangdong Province have not been

Table 2. Genomes of influenza A(H7N9) viruses detected in 16 patients and from environmental samples in Guangdong Province, China*

Sample identification	PB2 variant	PB1 variant	PA variant	NP variant	M variant	NS variant
Patient samples						
HZ-Y/01/2013	1	1	0	1	0	1
FS-Y/019/2014	1	1	0	1	0	1
FS2-Y/033/2014	1	1	0	1	0	1
FS2-T/034/2014	1	1	0	1	0	1
SZ-T/035/2014	1	1	0	1	0	1
SZ-Y/036/2014	1	1	0	1	0	1
A/Hong Kong/734/2014	1	1	0	1	0	1
DG-Y/02/2013	1	1	1	1	0	1
DG-T/03/2013	1	1	1	1	0	1
YJ-T/04/2013	1	1	1	1	0	1
YJ-T/05/2013	1	1	1	1	0	1
YJ2-T/012/2014	1	1	1	1	0	1
YJ2-Y/013/2014	1	1	1	1	0	1
FS-Y/029/2014	1	1	1	1	0	1
Hong Kong 2212982	1	1	1	1	0	1
GZ-T/010/2014	1	1	2	1	0	1
FS-Y/031/2014	1	1	2	1	0	1
SZ-T/026/2014	1	1	0	2	0	1
Environmental samples						
Guangdong/02620/2014	1	1	0	1	0	1
Guangdong/24997/2014	1	1	0	1	0	1
Guangdong/0092/2014	1	1	1	1	0	1
Guangdong/02124/2014	1	1	1	1	0	1
Guangdong/25003/2014	1	1	1	1	x	1
Guangdong/02125/2014	1	1	2	1	0	1
Variant origin	SC	SC	PA-1: SC PA-2: EC	NP-1: SC NP-2: EC		SC

*Lineages shown correlated with those shown Figure 2. Shading indicates grouping of 4 reassortant types. Variant origin (bottom rows) was derived from phylogenetic trees and is indicated as SC (southern China) and EC (eastern China). Three of the 4 reassortant genomes were also detected through environmental surveillance. M, matrix; NP, nucleoprotein; NS, nonstructural; PA, polymerase acidic; PB, polymerase basic.

detected by surveillance activities. However, available data are insufficient to determine how long influenza A(H7N9) viruses have been circulating in this region.

The results from environmental surveillance suggest a higher prevalence of H9N2 virus in Guangdong Province poultry environments than in poultry environments in other regions of China (*15*). Because live poultry is the primary source of H7N9 virus (*13*,*16*–*18*), the coexistence with H9N2 in the same susceptible population generates appropriate conditions for the emergence of novel reassortant variants such as those shown in this study.

In summary, our findings indicate that multiple strains of H7N9 and H9N2 influenza viruses are circulating in poultry in Guangdong Province, creating an environment that is rich for reassortment of these viruses and that poses an ongoing risk for human infection. Continued and uncontrolled co-circulation of multiple avian and other influenza viruses that can infect humans pose a potential pandemic threat; increased animal surveillance and further study of the ecology of influenza viruses are essential.

This work was supported by 12th five-year-major projects of China's Ministry of Public Health (grant no. 2012zx10004-213); the PREDICT Surveillance Animal Human Interface Project (grant no. Gvf: 06-09-057-02, to G.V.F.); and by the CASTELLUM grant, Dutch Ministry of Economic Affairs, Agriculture and Innovation (to M.K.).

Dr Ke is a senior scientist at Guangdong Provincial CDC, Guangdong, China, and is involved in the diagnosis and molecular epidemiology research of zoonoses and emerging infectious diseases.

References

1. Chen Y, Liang W, Yang S, Wu N, Gao H, Sheng J, et al. Human infections with the emerging avian influenza A H7N9 virus from wet market poultry: clinical analysis and characterisation of viral genome. Lancet. 2013;381:1916–25. http://dx.doi.org/10.1016/S0140-6736(13)60903-4
2. Gao R, Cao B, Hu Y, Feng Z, Wang D, Hu W, et al. Human infection with a novel avian-origin influenza A (H7N9) virus. N Engl J Med. 2013;368:1888–97. http://dx.doi.org/10.1056/NEJMoa1304459
3. Gao HN, Lu HZ, Cao B, Du B, Shang H, Gan JH, et al. Clinical findings in 111 cases of influenza A (H7N9) virus infection. N Engl J Med. 2013;368:2277–85. http://dx.doi.org/10.1056/NEJMoa1305584
4. Wu A, Su C, Wang D, Peng Y, Liu M, Hua S, et al. Sequential reassortments underlie diverse influenza H7N9 genotypes in China. Cell Host Microbe. 2013;14:446–52. http://dx.doi.org/10.1016/j.chom.2013.09.001
5. Lam TT, Wang J, Shen Y, Zhou B, Duan L, Cheung CL, et al. The genesis and source of the H7N9 influenza viruses causing human infections in China. Nature. 2013;502:241–4. http://dx.doi.org/10.1038/nature12515
6. Pantin-Jackwood MJ, Miller PJ, Spackman E, Swayne DE, Susta L, Costa-Hurtado M, et al. Role of poultry in spread of novel H7N9 influenza virus in China. J Virol. 2014;88:5381–90. http://dx.doi.org/10.1128/JVI.03689-13

7. Cui L, Liu D, Shi W, Pan J, Qi X, Li X, et al. Dynamic reassortments and genetic heterogeneity of the human-infecting influenza A (H7N9) virus. Nat Commun. 2014;5:3142. http://dx.doi.org/10.1038/ncomms4142
8. Ai J, Huang Y, Xu K, Ren D, Qi X, Ji H, et al. Case-control study of risk factors for human infection with influenza A(H7N9) virus in Jiangsu Province, China, 2013. Euro Surveill. 2013;18:20510. http://dx.doi.org/10.2807/1560-7917.ES2013.18.26.20510
9. Yu X, Jin T, Cui Y, Pu X, Li J, Xu J, et al. Coexistence of influenza H7N9 and H9N2 in poultry linked to human H7N9 infection and their genome characteristics. J Virol. 2014;88:3423–31. http://dx.doi.org/10.1128/JVI.02059-13
10. Huang K, Zhu H, Fan X, Wang J, Cheung CL, Duan L, et al. Establishment and lineage replacement of H6 influenza viruses in domestic ducks in southern China. J Virol. 2012;86:6075–83. http://dx.doi.org/10.1128/JVI.06389-11
11. Tamura K, Peterson D, Peterson N, Stecher G, Nei M, Kumar S. MEGA5: molecular evolutionary genetics analysis using maximum likelihood, evolutionary distance, and maximum parsimony methods. Mol Biol Evol. 2011;28:2731–9. http://dx.doi.org/10.1093/molbev/msr121
12. Guindon S, Dufayard JF, Lefort V, Anisimova M, Hordijk W, Gascuel O. New algorithms and methods to estimate maximum-likelihood phylogenies: assessing the performance of PhyML 3.0. Syst Biol. 2010;59:307–21. http://dx.doi.org/10.1093/sysbio/syq010
13. Han J, Jin M, Zhang P, Liu J, Wang L, Wen D, et al. Epidemiological link between exposure to poultry and all influenza A(H7N9) confirmed cases in Huzhou city, China, March to May 2013. Euro Surveill. 2013;18:pii:20481.
14. Fang LQ, Li XL, Liu K, Li YJ, Yao HW, Liang S, et al. Mapping spread and risk of avian influenza A (H7N9) in China. Sci Rep. 2013;3:2722. http://dx.doi.org/10.1038/srep02722
15. Song R, Pang X, Yang P, Shu Y, Zhang Y, Wang Q, et al. Surveillance of the first case of human avian influenza A (H7N9) virus in Beijing, China. Infection. 2014;42:127–33.
16. Li Q, Zhou L, Zhou M, Chen Z, Li F, Wu H, et al. Epidemiology of human infections with avian influenza A(H7N9) virus in China. N Engl J Med. 2014;370:520–32. http://dx.doi.org/10.1056/NEJMoa1304617
17. Bao CJ, Cui LB, Zhou MH, Hong L, Gao GF, Wang H. Live-animal markets and influenza A (H7N9) virus infection. N Engl J Med. 2013;368:2337–9. http://dx.doi.org/10.1056/NEJMc1306100
18. Zhang W, Wang L, Hu W, Ding F, Sun H, Li S, et al. Epidemiologic characteristics of cases for influenza A(H7N9) virus infections in China. Clin Infect Dis. 2013;57:619–20. http://dx.doi.org/10.1093/cid/cit277

Address for correspondence: Yonghui Zhang, Guangdong Provincial Center for Disease Control and Prevention, No.160, Qunxian Road, Dashi town, Panyu District, Guangzhou City, Guangdong Province, China; email: zyh@cdcp.org.cn

Effects of Knowledge, Attitudes, and Practices of Primary Care Providers on Antibiotic Selection, United States

Guillermo V. Sanchez, Rebecca M. Roberts, Alison P. Albert, Darcia D. Johnson, and Lauri A. Hicks

Appropriate selection of antibiotic drugs is critical to optimize treatment of infections and limit the spread of antibiotic resistance. To better inform public health efforts to improve prescribing of antibiotic drugs, we conducted in-depth interviews with 36 primary care providers in the United States (physicians, nurse practitioners, and physician assistants) to explore knowledge, attitudes, and self-reported practices regarding antibiotic drug resistance and antibiotic drug selection for common infections. Participants were generally familiar with guideline recommendations for antibiotic drug selection for common infections but did not always comply with them. Reasons for nonadherence included the belief that nonrecommended agents are more likely to cure an infection, concern for patient or parent satisfaction, and fear of infectious complications. Providers inconsistently defined broad- and narrow-spectrum antibiotic agents. There was widespread concern for antibiotic resistance; however, it was not commonly considered when selecting therapy. Strategies to encourage use of first-line agents are needed in addition to limiting unnecessary prescribing of antibiotic drugs.

Antibiotic prescribing guidelines establish standards of care, help focus efforts on quality improvement, and have been shown to improve patient outcomes (*1–3*). Many guidelines emphasize the importance of diagnostic certainty for the management of bacterial upper respiratory tract infections and promote β-lactam agents, such as amoxicillin or amoxicillin-clavulanate, as the preferred first-line therapy (*4–6*). Studies indicate that health care providers often do not adhere to established clinical practice guidelines for the management of common infections (*7–9*). Prescribing rates for second-line, broad-spectrum antibiotics among outpatients have increased, contributing to a growing problem of antibiotic-resistant infections (*10–14*). It is not clear whether nonadherence is related to lack of familiarity with clinical practice guidelines or if other factors influence antibiotic selection once a diagnosis is established.

Published qualitative studies that have examined antibiotic selection among primary care providers (PCPs) are outdated and focus on non-US–based physicians; they do not include nurse practitioners or physician assistants, who together comprise >25% of the US primary care workforce (*15–22*). The objectives of this study are to explore US PCP knowledge, attitudes, and self-reported practices (KAPs) concerning antibiotic therapy, assess factors that influence provider antibiotic choice, and provide an update on PCP attitudes regarding antibiotic resistance.

Methods

We conducted in-depth interviews by digitally recorded telephone calls, and transcribed the recordings to text to accurately and reliably assess PCP KAPs. The qualitative method of an open-ended interview by telephone was chosen to ensure candid and truthful answers from participants. We composed a screening questionnaire to recruit physicians, nurse practitioners (NPs), and physician assistants (PAs) from a nationwide marketing database in the United States. We initially contacted and screened potential participants (online Technical Appendix Section A, wwwnc.cdc.gov/EID/article/20/12/14-0331-Techapp1.pdf) using telephones, email, and fax transmission of documents. Inclusion criteria included self-reporting of spending ≥50% of medical practice time in direct patient contact in a primary care setting, ≥30 years of age, and fluency in the English language. Interviewees were excluded from this study if they had an immediate family member who was employed in an industry that could represent a conflict of interest, including advertising or public relations, the federal government, market research, news media, or the pharmaceutical industry; if they had board certification in a subspecialty outside of primary care; or if they had practiced medicine >30 years at the time of recruitment.

Author affiliation: Centers for Disease Control and Prevention, Atlanta, Georgia, USA

DOI: http://dx.doi.org/10.3201/eid2012.140331

Thirty-six PCPs were selected for the study. Specialties for the 27 physician participants selected included pediatrics (n = 9), family medicine (n = 9), and internal medicine (n = 9). Among PAs (n = 4) and NPs (n = 5), 6 practiced in family medicine settings and 3 practiced in pediatrics. Provider specialty, years in practice, and demographic information are described in Table 1.

Interviews were conducted during May 2013. One professional moderator who had >25 years of moderating experience conducted all interviews. Based on a discussion guide prepared by our research team (data not shown), participants were first informed of the sponsoring organization (Centers for Disease Control and Prevention, Atlanta, GA, USA), the planned use of data, and presence of listeners; they were then asked "warm-up" questions about the practice setting in which the participant worked and the patient populations whom they served. Next, each interview proceeded through an ordered list of open-ended questions on self-reported antibiotic prescribing practices, perceived prescribing practices of their peers, attitudes toward clinical practice guidelines for common bacterial infections, knowledge of narrow- versus broad-spectrum antibiotic agents, preferred resources and methods for medical education and antibiotic treatment, and attitudes toward antibiotic resistance.

Participants were provided a worksheet before the interview (online Technical Appendix, Section B) which asked them to rank each of 12 factors on the basis of its perceived influence on antibiotic selection when an antibiotic is indicated (e.g., illness severity, patient demand for an antibiotic, or clinical practice guidelines). Worksheet answers were discussed and recorded during the interview.

To assess compliance with clinical practice guidelines and to evaluate clinical decision-making, each participant was given a clinical vignette about a patient (online Technical Appendix, Section C) who had a diagnosis of an acute bacterial infection: acute otitis media (AOM) for pediatricians, acute bacterial rhinosinusitis for internists, acute uncomplicated cystitis for family practitioners, and group A streptococcal pharyngitis for PAs and NPs. The participant was asked to explain his or her rationale in choosing an antibiotic agent and why other PCPs might choose nonrecommended antibiotics. For the purposes of this study, antibiotics considered to be broad-spectrum include penicillins containing β-lactamase inhibitors (e.g., amoxicillin/clavulanate), second through fifth generation cephalosporins, macrolides, quinolones, and lincomycin derivatives. Narrow-spectrum agents include penicillins (e.g., amoxicillin), first generation cephalosporins, sulfonamides, and nitrofurantoin. Each participant received a cash incentive after the interview in exchange for participating.

Interviews were transcribed by project staff, and each member of the research team either listened to interview recordings or read corresponding interview transcripts. Relevant excerpts were coded into compilations of references to specific themes and were used to identify the most frequent responses to discussion topics outlined in the discussion guide. We identified common themes using both inductive and deductive methods that were reviewed by all authors. Author disagreement on theme selections were discussed until a consensus was met. If no consensus was met by most study authors, the theme was excluded from our results. We performed in-depth analyses of themes by reading and coding transcribed responses using Nvivo 9 (QSR International, Burlington, MA). This study was reviewed and approved for exemption status by the Human Research Protection Office of the Centers for Disease Control and Prevention.

Table 1. Characteristisc of primary care providers interviewed for knowledge, attitudes, and practices in antibiotic drug selection, United States*

Characteristic	Physician, n = 27	NP or PA, n = 9
Sex		
M	18	1
F	9	8
Race/ethnicity		
White	18	9
Black	4	0
Asian	3	0
Hispanic	1	0
Other	1	0
Years in practice		
<10	5	5
10–20	11	3
21–30	11	1
Medical specialty		
Pediatrics	9	3
Family medicine	9	6
Internal medicine	9	0

*NP, nurse practitioner; PA, physician assistant.

Results

We conducted 36 interviews, each lasting ≈45 minutes. Through analysis of provider in-depth interviews, several common themes regarding antibiotic prescribing and antibiotic resistance were identified (Table 2).

Antibiotic Selection

PCPs generally cited little difficulty selecting antibiotic treatments for common infections, but indicated that allergies, complicated medical histories, and recurrent infections regularly make antibiotic selection more challenging. Previous experience and familiarity with an agent were frequently cited as influential factors when choosing antibiotic therapy. Results from the ranking exercise suggest that illness severity, medical history, and clinical practice guidelines were important considerations across all specialties.

Table 2. Topics and quotations from in-depth interviews with primary care providers regarding antibiotic therapy and antibiotic resistance, United States

Topic	Quotation
Antibiotic selection	*"We as doctors are business people. We're no different than running a shoe store. If somebody comes in and wants black shoes, you don't sell them white shoes. And if you do, they get upset. You can convince a patient, look if I were you I wouldn't take this antibiotic… but patients in general don't understand that concept of not taking it if you don't need it… [and] if you don't give it to them, they don't come back to you."*
	"The patient [may] call you up and… tell you … call me in some X, Y or Z because everybody wants to hurry up and get better faster. Sometimes [you worry] about 1-800 call you-know-lawyer. [Maybe] you don't have a standing relationship with the patient and you don't know [if they will] come back if they are not getting better. All of those things [affect antibiotic selection]. But if you are pretty comfortable and have a good relationship [with a patient], you [may] not necessarily go straight to a broad-spectrum antibiotic."
	"[Broad-spectrum antibiotics] take the thinking out of it for me so that I am not trying to figure out what the organism is and [which] particular antibiotic treats the organism."
	"It's very simple. Patients come to the doctor and they want an antibiotic. If they don't get better, they get upset… I had a patient who came to me who had bronchitis and I started her on azithromycin… however, she did not get better. She came to see my colleague and [he] did not change the antibiotic, but gave her Prednisone and that got her better within 24 hours. She was mad at me, because I apparently did not give her 'the right antibiotic' and my partner did."
Broad- and narrow-spectrum definitions	*"If it's narrow, it [covers] one particular class of organism like gram-negative. If it's broad, it's going to be different types like gram-negative, gram-positive, anaerobes to treat a wider spectrum of infections."*
	"The more bacteria the antibiotic works …against, you call it broader. If this antibiotic only works against one or two types of bacteria, then that is a narrow-spectrum [antibiotic]."
	"The one thing no one's going to argue about is penicillin being narrow-spectrum."
	"Amoxicillin is a great example of a very broad-spectrum antibiotic."
	"I guess it is pretty subjective, the definition [of broad- versus narrow-spectrum antibiotics]."
Education and resources for antibiotic treatment	*"During residency…when you see patients with different conditions and decide how you want to treat them and see how the attending… chooses to treat them, I think that's when you learn the most."*
	"I think there needs to be more education to providers about the real dangers of antibiotic resistance. You get taught that in school and … you don't ever hear about it again, and you get busy in your practice, it's not your number one priority. And you… get to where you really don't think about it, but it is a huge issue."
	"I think [focusing education efforts only on students and residents] would be a mistake. I think that's the conclusion you would draw if you assume the rest of the system stayed unchanged. If you just focus on the young doctors you're still going to wait 15 years for that change to take place."
Changing prescribing habits	*"Habits are hard to change. I will say that. So if someone's used to writing Zithromax… they're not going to stop because it's easy, patients want it, and they want the patients to go away and be happy. But I think pushing the knowledge is helpful, and change takes time."*
	"[Physicians] tend to be rigid. That's it, really; a new generation that has learned its own rigid rules that come in and replace the previous… It's not that any new crop of doctors is any more malleable, it's the fact that everybody's not malleable… [they] resort to the way they were during residency."
	"Patients don't realize [antibiotic resistance could affect them] and some of them don't even care. You can say 'one day you're going to [have a resistant infection]' and they'll say 'oh, they'll make more [drugs]'."
Antibiotic resistance	*"It is very scary because we are seeing increasingly resistant germs. We had a lady in the office the other day [with] a urinary infection [resistant to] every single oral antibiotic on the entire list of the culture and sensitivity report. There wasn't a single oral medicine that could be used... It was resistant to everything."*
	"We haven't had a new antibiotic for at least 10 years and something is going to happen one of these days. We are going to get a big, big multi-drug resistant bacteria and we are going to end up with nothing to treat this thing… and then we are going to be in trouble. That is my main concern."

When asked why their peers made inappropriate choices regarding antibiotic selection, responses varied. The most common perceived reasons for inappropriate antibiotic prescribing were pressure from patients or parents; desire to prevent litigation as a result of complications of infections; concern for patient or parent satisfaction with the visit; and perceived decreases in visit length. Illnesses for which participants believed appropriate antibiotic selection was more difficult for their peers included sinus infections and recurrent urinary tract infections.

Broad-spectrum agents were widely thought to be more successful for curing an infection than narrow-spectrum antibiotics. One participant noted that broad-spectrum antibiotics are often chosen because less uncertainty exists regarding the adequacy of antimicrobial activity, which is why they may be commonly selected even if a narrow-spectrum agent is indicated. When asked whether antibiotic spectrum was a consideration when prescribing an antibiotic, participants indicated that it was generally not as important as choosing a drug known to successfully treat the infection. Choosing a narrow-spectrum agent was perceived to be a more attractive option when the diagnosis was more certain or when a patient was perceived to have a benign clinical condition.

PCPs commonly perceived that patients expect an antibiotic for clinical visits, contributing to a shared feeling of pressure among PCPs to satisfy patients. Concern

was further expressed that patient satisfaction scores are a common method by which providers are evaluated by hospital administration and insurance companies and that this may inadvertently contribute to more frequent antibiotic prescribing. Some participants believed that such evaluation methods could be a barrier to appropriate antibiotic use. PCPs in private practice said they were particularly sensitive to patient desires and were concerned that their patients might leave their practice in favor of another physician if their expectations were not met.

Several participants believed other health care providers' prescribing behaviors negatively affected their own. For example, if a patient sees a PCP and receives a course of antibiotics, and later visits another PCP for a separate infection with the same symptoms, they have the established expectation to receive another course of antibiotics. As a result, the new provider feels pressured by such expectations to prescribe antibiotics even if they may be inappropriate.

Responses to the clinical vignettes were generally in line with the recommended first-line therapies. Among 9 participants given a case describing acute bacterial sinusitis, 7 appropriately chose amoxicillin or amoxicillin/clavulanate. One participant chose to treat the patient with moxifloxacin, and another chose azithromycin. Sixteen of 18 PCPs given clinical vignettes of either AOM or group A streptococcal pharyngitis selected the recommended first-line treatments amoxicillin or penicillin. In response to the clinical vignette for acute cystitis, only 4 of 9 family practitioners selected the first-line agent nitrofurantoin; 4 others chose to treat the patient with a fluoroquinolone, and 1 chose to prescribe trimethoprim-sulfamethoxazole.

Broad- and Narrow-Spectrum Definitions

Participants had no shared definition of "broad-spectrum antibiotic" or "narrow-spectrum antibiotic" regardless of specialty or number of years in practice. When asked to define broad- versus narrow-spectrum antibiotics, responses varied (Table 2). Although many participants believed antibiotic spectrum referred to the classes of bacteria (gram-positive, gram-negative, or anaerobic) treated, others believed it referred to the number of pathogens addressed (e.g., a narrow-spectrum antibiotic might affect only 2 or 3 pathogens and a broad-spectrum antibiotic might affect many).

Although some participants correctly identified amoxicillin as a narrow-spectrum agent, and azithromycin as a broad-spectrum agent, many participants were uncertain of the spectrum of antimicrobial activity for these 2 widely used antibiotics. In general, participants were able to correctly identify fluoroquinolones and later-generation cephalosporins as broad-spectrum agents, especially in relation to other antibiotics. Many participants agreed that broad- and narrow-spectrum antibiotics were not uniformly defined among their colleagues.

Changing Prescribing Habits

Respondents believed that changing prescribing behaviors is a difficult task. When asked why some health care providers are reluctant to change their prescribing practices, many participants believed that health care providers are used to the way they have been practicing medicine for years. They believed that even when providers are familiar with established clinical practice guidelines, it may not matter because they seldom change their prescribing behaviors. Several respondents believed the best way to change antibiotic prescribing behavior is to change the expectations of patients so the pressure to prescribe antibiotics is reduced.

Respondents' preference of how they would like to receive information regarding antibiotic selection varied. Some participants suggested incorporating information in the electronic medical record to improve prescribing (e.g., a clinical decision support prompt would display on the computer in use if a physician entered an order for a prescription that is not standard for the diagnosis). One frequent suggestion to improve antibiotic prescribing was to have a quick reference guide for each major diagnosis, including antibiotic indications and causative pathogens. Another suggestion was to have a mobile telephone application available without Internet access. Several respondents saw value in having easy access to antibiotic resistance data for their local area.

Concern for Antibiotic Resistance

Participants generally agreed that antibiotic resistance is a concern for their patients and for public health; however, it was not commonly mentioned as a factor when considering which antibiotic to prescribe. Several participants expressed serious concerns about the availability of effective antibiotic therapies in the future related to increases in antibiotic resistance. Respondents also noted an increasing frequency of patients who were reluctant to begin antibiotics or complete their course of antibiotics because of concerns about antibiotic resistance.

Discussion

Our study shows that PCPs do not always adhere to guidelines because they believe broad-spectrum antibiotics may be more likely to cure an infection, a finding corroborated by the well-documented overuse of broad-spectrum antibiotics (*23*). However, the perception of better cure rates when using broad-spectrum agents is unfounded. For example, *Streptococcus pneumoniae,* a pathogen frequently implicated in bacterial respiratory infections, has a much higher prevalence of resistance

to macrolides than it does to amoxicillin (*24*,*25*). Nevertheless, azithromycin is often chosen over amoxicillin for the empiric treatment for AOM, sinusitis, and other respiratory infections (*25*,*26*). Similarly, for the treatment for acute uncomplicated cystitis, widespread use of fluoroquinolones has contributed to rising antimicrobial resistance, rendering ciprofloxacin far less active against urinary tract *Escherichia coli* infections than the more narrow-spectrum, first-line agent nitrofurantoin (*27*). The perceived association between broad-spectrum antibiotic use and better cure rates may regularly contribute to inappropriate antibiotic selection and warrants further attention from appropriate antibiotic use initiatives.

There is no widely accepted definition of broad- versus narrow-spectrum antibiotics among PCPs or their professional organizations. Although a list of "antibiotics of concern" has been published by the National Committee on Quality Assurance (*28*) and has been used in previous research to classify antibiotics as broad-spectrum (*29*,*30*), the list was not originally intended for this purpose. Clinical practice guidelines emphasize use of narrow-spectrum antimicrobial agents instead of their broad-spectrum counterparts (*4*,*5*,*31*,*32*). However, the effect of these messages may be limited because of lack of clarity regarding what constitutes a narrow- versus broad-spectrum antibiotic. For example, few participants in our study were able to confidently categorize macrolides and penicillins, which are among the most commonly prescribed classes of antibiotics (*33*), as broad or narrow spectrum. Although this issue is largely one of semantics, it has critical implications for medical education, public health messaging, and community antibiotic resistance. Communication to PCPs related to antibiotic choice should not focus on dichotomous narrow- versus broad-spectrum terminology, but rather promote specific recommended first-line and targeted antibiotic therapies for individual diagnoses.

Compared with results of previous qualitative studies, PCPs participating in this study expressed greater urgency regarding antibiotic resistance. For example, in a 1998 qualitative study exploring driving factors of antibiotic misuse, a principal barrier to change in antibiotic prescribing was the attitude that antibiotic resistance was not an important problem (*19*). Another study published in the same year noted similar findings (*21*). Conversely, not a single provider in this study dismissed antibiotic resistance as being a minor issue, and several expressed grave concerns about antibiotic resistance based on their own experiences.

Modifying prescriber behavior is a complex and difficult task. Multifaceted interventions that involve a combination of interactive group meetings, outreach visits to individual physicians, physician reminders, or patient-based interventions (e.g., delayed prescribing practices) have shown the most promise in changing prescribing behaviors in ambulatory care settings (*34*,*35*). Previous studies confirm that patients desire antibiotics less frequently than providers perceive and that inappropriate prescribing is a common result of this miscommunication (*21*,*36*,*37*). This finding suggests that an effective target for intervention is narrowing the gap between patient expectations and clinician perception of these expectations for antibiotics. Regardless of the intervention considered for promoting appropriate antibiotic use, the concerns of PCPs highlighted in this study should be addressed. This includes reassuring providers of the efficacy of first-line and targeted therapies, clarifying the role of antibiotic prescriptions in patient satisfaction, and providing resources that streamline patient education efforts in primary care settings.

This study has limitations, however. Although in-depth interviews are an effective method to explore individual providers' KAPs, we cannot generalize our findings to the PCP population as a whole because of the lack of external validity inherent in this type of qualitative research. Similarly, the clinicians who were screened, selected for participation, and agreed to be interviewed may hold stronger opinions about this topic than those who were excluded or declined to participate.

Our study suggests that inappropriate antibiotic selection among PCPs is not caused by lack of familiarity with guideline recommendations. Rather, this practice is the result of a complex interaction between perceived better cure rates for nonrecommended therapies and attempts to meet demands typical in primary care settings.

Future research efforts should be aimed at investigating effective incentives for appropriate antibiotic prescribing and determining alternative communication strategies to encourage use of first-line agents. Although most efforts have focused on reducing unnecessary antibiotic use, more research is needed to clarify which interventions improve antibiotic selection. Although awareness regarding antibiotic resistance appears to be improving, ongoing education efforts promoting appropriate antibiotic use among both patients and health care providers (e.g., CDC's Get Smart: Know When Antibiotics Work Program) are critical to addressing the growing threat of antibiotic resistance.

Acknowledgments

We thank staff of Oak Ridge Institute for Science and Education and Oak Ridge Associated Universities for their help in preparing for, conducting, and analyzing the interviews for this study.

Mr Sanchez is a board-certified physician assistant and a public health scientist for the Get Smart: Know When Antibiotics Work program. His research interests include outpatient antibiotic prescribing and antibiotic resistance within the United States.

References

1. Asadi L, Eurich DT, Gamble JM, Minhas-Sandhu JK, Marrie TJ, Majumdar SR. Impact of guideline-concordant antibiotics and macrolide/beta-lactam combinations in 3203 patients hospitalized with pneumonia: prospective cohort study. Clin Microbiol Infect. 2013;19:257–64. http://dx.doi.org/10.1111/j.1469-0691.2012.03783.x
2. Asadi L, Eurich DT, Gamble JM, Minhas-Sandhu JK, Marrie TJ, Majumdar SR. Guideline adherence and macrolides reduced mortality in outpatients with pneumonia. Respir Med. 2012;106:451–8. http://dx.doi.org/10.1016/j.rmed.2011.11.017
3. Garber AM. Evidence-based guidelines as a foundation for performance incentives. Health Aff. 2005;24:174–9. http://dx.doi.org/10.1377/hlthaff.24.1.174
4. Chow AW, Benninger MS, Brook I, Brozek JL, Goldstein EJ, Hicks LA, et al. IDSA clinical practice guideline for acute bacterial rhinosinusitis in children and adults. Clin Infect Dis. 2012;54:e72–112. http://dx.doi.org/10.1093/cid/cis370
5. Lieberthal AS, Carroll AE, Chonmaitree T, Ganiats TG, Hoberman A, Jackson MA, et al. The diagnosis and management of acute otitis media. Pediatrics. 2013;131:e964–99. http://dx.doi.org/10.1542/peds.2012-3488
6. Shulman ST, Bisno AL, Clegg HW, Gerber MA, Kaplan EL, Lee G, et al. Clinical practice guideline for the diagnosis and management of group A streptococcal pharyngitis: 2012 update by the Infectious Diseases Society of America. Clin Infect Dis. 2012;55:1279–82. http://dx.doi.org/10.1093/cid/cis847
7. Hong SY, Taur Y, Jordan MR, Wanke C. Antimicrobial prescribing in the USA for adult acute pharyngitis in relation to treatment guidelines. J Eval Clin Pract. 2011;17:1176–83. http://dx.doi.org/10.1111/j.1365-2753.2010.01495.x
8. Barnett ML, Linder JA. Antibiotic prescribing to adults with sore throat in the United States, 1997–2010. JAMA Intern Med. 2014;174:138–40. http://dx.doi.org/10.1001/jamainternmed.2013.11673
9. Crocker A, Alweis R, Scheirer J, Schamel S, Wasser T, Levingood K. Factors affecting adherence to evidence-based guidelines in the treatment of URI, sinusitis, and pharyngitis. J Community Hosp Intern Med Perspect. 2013;3. http://dx.doi.org/10.3402/jchimp.v3i2.20744
10. Steinman MA, Gonzales R, Linder JA, Landefeld CS. Changing use of antibiotics in community-based outpatient practice, 1991–1999. Ann Intern Med. 2003;138:525–33. http://dx.doi.org/10.7326/0003-4819-138-7-200304010-00008
11. Linder JA, Huang ES, Steinman MA, Gonzales R, Stafford RS. Fluoroquinolone prescribing in the United States: 1995 to 2002. Am J Med. 2005;118:259–68. http://dx.doi.org/10.1016/j.amjmed.2004.09.015
12. Shapiro DJ, Hicks LA, Pavia AT, Hersh AL. Antibiotic prescribing for adults in ambulatory care in the USA, 2007–09. J Antimicrob Chemother. Epub 2013 Jul 25. http://dx.doi.org/10.1093/jac/dkt301
13. Steinman MA, Landefeld CS, Gonzales R. Predictors of broad-spectrum antibiotic prescribing for acute respiratory tract infections in adult primary care. JAMA. 2003;289:719–25. http://dx.doi.org/10.1001/jama.289.6.719
14. Shehab N, Patel PR, Srinivasan A, Budnitz DS. Emergency department visits for antibiotic-associated adverse events. Clin Infect Dis. 2008;47:735–43. http://dx.doi.org/10.1086/591126
15. Cadieux G, Tamblyn R, Dauphinee D, Libman M. Predictors of inappropriate antibiotic prescribing among primary care physicians. CMAJ. 2007;177:877–83. http://dx.doi.org/10.1503/cmaj.070151
16. Björkman I, Erntell M, Roing M, Lundborg CS. Infectious disease management in primary care: perceptions of GPs. BMC Fam Pract. 2011;12:1. http://dx.doi.org/10.1186/1471-2296-12-1
17. Tonkin-Crine S, Yardley L, Coenen S, Fernandez-Vandellos P, Krawczyk J, Touboul P, et al. GPs' views in five European countries of interventions to promote prudent antibiotic use. Br J Gen Pract. 2011;61:e252–61. http://dx.doi.org/10.3399/bjgp11X572445
18. Linder JA, Schnipper JL, Tsurikova R, Volk LA, Middleton B. Self-reported familiarity with acute respiratory infection guidelines and antibiotic prescribing in primary care. Int J Qual Health Care. 2010;22:469–75. http://dx.doi.org/10.1093/intqhc/mzq052
19. Barden LS, Dowell SF, Schwartz B, Lackey C. Current attitudes regarding use of antimicrobial agents: results from physician's and parents' focus group discussions. Clin Pediatr. 1998;37:665–71. http://dx.doi.org/10.1177/000992289803701104
20. Wigton RS, Darr CA, Corbett KK, Nickol DR, Gonzales R. How do community practitioners decide whether to prescribe antibiotics for acute respiratory tract infections? J Gen Intern Med. 2008;23:1615–20. http://dx.doi.org/10.1007/s11606-008-0707-9
21. Butler CC, Rollnick S, Pill R, Maggs-Rapport F, Stott N. Understanding the culture of prescribing: qualitative study of general practitioners' and patients' perceptions of antibiotics for sore throats. BMJ. 1998;317:637–42. http://dx.doi.org/10.1136/bmj.317.7159.637
22. Agency for Healthcare Research and Quality. Primary care workforce and stats: overview. Rockville, MD: U.S. Department of Health and Human Services; January 2012 [cited 3Nov 1]. http://www.ahrq.gov/research/findings/factsheets/primary/pcworkforce/index.html
23. Shapiro DJ, Hicks LA, Pavia AT, Hersh AL. Antibiotic prescribing for adults in ambulatory care in the USA, 2007–09. J Antimicrob Chemother. 2014;69:234–40. http://dx.doi.org/10.1093/jac/dkt301
24. Hicks LA, Chien YW, Taylor TH Jr, Haber M, Klugman KP, Active Bacterial Core Surveillance T. Outpatient antibiotic prescribing and nonsusceptible *Streptococcus pneumoniae* in the United States, 1996–2003. Clin Infect Dis. 2011;53:631–9. http://dx.doi.org/10.1093/cid/cir443
25. Courter JD, Baker WL, Nowak KS, Smogowicz LA, Desjardins LL, Coleman CI, et al. Increased clinical failures when treating acute otitis media with macrolides: a meta-analysis. Ann Pharmacother. 2010;44:471–8. http://dx.doi.org/10.1345/aph.1M344
26. Fairlie T, Shapiro DJ, Hersh AL, Hicks LA. National trends in visit rates and antibiotic prescribing for adults with acute sinusitis. Arch Intern Med. 2012;172:1513–4. http://dx.doi.org/10.1001/archinternmed.2012.4089
27. Sanchez GV, Master RN, Karlowsky JA, Bordon JM. In vitro antimicrobial resistance of urinary *Escherichia coli* isolates among U.S. outpatients from 2000 to 2010. Antimicrob Agents Chemother. 2012;56:2181–3. http://dx.doi.org/10.1128/AAC.06060-11
28. Healthcare Effectiveness Data and Information Set. (HEDros Inf Serv.) & Quality Measurement: HEDros Inf Serv. 2014 National Drug Code List [cited 2014 June 23]. http://www.ncqa.org/HEDISQualityMeasurement/HEDISMeasures/HEDIS2014/HEDIS2014FinalNDCLists.aspx
29. Lee GC, Reveles KR, Attridge RT, Lawson KA, Mansi IA, Lewis JS II, et al. Outpatient antibiotic prescribing in the United States: 2000 to 2010. BMC Med. 2014;12:96. http://dx.doi.org/10.1186/1741-7015-12-96
30. Steinman MA, Yang KY, Byron SC, Maselli JH, Gonzales R. Variation in outpatient antibiotic prescribing in the United States. Am J Manag Care. 2009;15:861–8.
31. Gupta K, Hooton TM, Naber KG, Wullt B, Colgan R, Miller LG, et al. International clinical practice guidelines for the treatment of acute uncomplicated cystitis and pyelonephritis in women: A 2010 update by the Infectious Diseases Society of America and the European Society for Microbiology and Infectious Diseases. Clin Infect Dis. 2011;52:e103–20. http://dx.doi.org/10.1093/cid/ciq257
32. Mandell LA, Wunderink RG, Anzueto A, Bartlett JG, Campbell GD, Dean NC, et al. Infectious Diseases Society of America/American Thoracic Society consensus guidelines on the management of community-acquired pneumonia in adults. Clin Infect Dis. 2007;44 (Suppl 2):S27–72. http://dx.doi.org/10.1086/511159
33. Hicks LA, Taylor TH Jr, Hunkler RJUS. outpatient antibiotic prescribing, 2010. N Engl J Med. 2013;368:1461–2. http://dx.doi.org/10.1056/NEJMc1212055

34. Arnold SR, Straus SE. Interventions to improve antibiotic prescribing practices in ambulatory care. Cochrane Database Syst Rev. 2005;19. PubMed http://dx.doi.org/10.1002/14651858.CD003539.pub2
35. Weber JT. Antimicrobial resistance: beyond the breakpoint. Basel (Switzerland): Karger Books; 2010.
36. Stivers T, Mangione-Smith R, Elliott MN, McDonald L, Heritage J. Why do physicians think parents expect antibiotics? What parents report vs what physicians believe. J Fam Pract. 2003;52:140–8.
37. Vanden Eng J, Marcus R, Hadler JL, Imhoff B, Vugia DJ, Cieslak PR, et al. Consumer attitudes and use of antibiotics. Emerg Infect Dis. 2003;9:1128–35. http://dx.doi.org/10.3201/eid0909.020591

Address for correspondence: Guillermo V. Sanchez, Centers for Disease Control and Prevention, 1600 Clifton Rd NE, Mailstop C25, Atlanta, GA 30329, USA; email: gsanchez@cdc.gov

Accuracy of Herdsmen Reporting versus Serologic Testing for Estimating Foot-and-Mouth Disease Prevalence

Kenton L. Morgan, Ian G. Handel, Vincent N. Tanya, Saidou M. Hamman, Charles Nfon,[1] Ingrid E. Bergman, Viviana Malirat, Karl J. Sorensen, and Barend M. de C. Bronsvoort

Herdsman-reported disease prevalence is widely used in veterinary epidemiologic studies, especially for diseases with visible external lesions; however, the accuracy of such reports is rarely validated. Thus, we used latent class analysis in a Bayesian framework to compare sensitivity and specificity of herdsman reporting with virus neutralization testing and use of 3 nonstructural protein ELISAs for estimates of foot-and-mouth disease (FMD) prevalence on the Adamawa plateau of Cameroon in 2000. Herdsman-reported estimates in this FMD-endemic area were comparable to those obtained from serologic testing. To harness to this cost-effective resource of monitoring emerging infectious diseases, we suggest that estimates of the sensitivity and specificity of herdsmen reporting should be done in parallel with serologic surveys of other animal diseases.

Owner-, farmer-, or herdsman-reported disease prevalence is widely used in veterinary epidemiologic studies (*1*–*6*), especially for diseases that produce visible external lesions (e.g., ovine myiasis, foot-and-mouth disease [FMD]) (*1*,*5*) or characteristic clinical signs (e.g., scrapie) (*7*). For such interview- or questionnaire-based reporting, a common criticism is lack of external validation because questionnaires, like other measuring devices, need to be calibrated. External validation is usually approached by comparing questionnaire data with data measured by other methods such as visual inspection (*8*–*10*), photographs (*11*), selection of clinical signs (*2*,*4*), laboratory test results (*12*), or other (*4*,*13*). These approaches, however, are difficult to use in poorer countries and pastoral populations, where there are limited resources and no comparison data. We estimated sensitivity and specificity of herdsman-reported FMD prevalence in the Adamawa plateau, Cameroon, and compared herdsmen's estimates with serologic test results.

FMD is a highly contagious viral disease of even-toed ungulates, caused by FMD viruses in the family *Picornaviridae*. Globally, FMD is a major disease of livestock because it leads to production losses and restrictions on trade with FMD-free countries (*14*). Clinical signs in cattle are distinct: vesicles on the tongue, gums, coronary band, and occasionally, udder. Animals salivate and are febrile, lame, and inappetant. Ruptured vesicles leave ulcers with characteristic underrun epithelial tissue at the edges (*15*).

To assess herdsmen's ability to correctly identify FMD and to compare the sensitivity and specificity of herdsman reporting with that of serologic testing, we conducted a cross-sectional study of FMD on the Adamawa plateau, the major cattle-rearing area of Cameroon. We used a structured questionnaire, administered by interview, to determine whether herdsmen had seen FMD in their herds in the previous 1 and 2 years (*5*,*16*). Their ability to correctly identify FMD was also assessed by showing them color photographs of typical lesions. To estimate the sensitivity and specificity of the various estimates, we used Bayesian latent class models. These estimates were

Author affiliations: University of Liverpool, Neston, Wirral, UK (K.L. Morgan); University of Edinburgh, Roslin, Scotland, UK (I.G. Handel, B.M. de C. Bronsvoort); Institute of Agricultural Research for Development, Ngaoundéré, Cameroon (V.N. Tanya, S.M. Hamman, C. Nfon); Ministry of Scientific Research and Innovation, Yaoundé, Cameroon (V.N. Tanya); Pan American Foot and Mouth Disease Center, Rio de Janeiro, Brazil (I.E. Bergman, V. Malirat); Danish Veterinary Institute for Virus Research, Kalvehave, Denmark (K.J. Sorensen); and Instituto de Ciencia y Tecnología Dr. César Milstein, Buenos Aires, Argentina (I.E. Bergman, V. Malirat)

DOI: http://dx.doi.org/10.3201/eid2012.140931

[1]Current affiliation: Canadian Food Inspection Agency, Winnipeg, Manitoba, Canada.

arrived at by restricting the age of cattle analyzed by virus neutralization (VN) testing to <2 years and by adopting evidence that nonstructural protein (NSP) antibody titers fall more rapidly (over ≈1 year) than VN antibodies (*17*,*18*). The study was conducted in accordance with the Cameroonian Ministry of Research guidelines and with approval from the University of Liverpool ethics committee in 1999.

Materials and Methods

Study Population

The study population is described elsewhere (*5*). In brief, a database of 13,006 herds was constructed from rinderpest vaccination records from 88 veterinary centers across the Adamawa region. This region is ≈64,000 km^2, lies between latitudes 6°N and 8°N, and is divided into 5 administrative divisions (Vina, Mbere, Mayo Banyo, Djerem, and Faro and Deo).

Study Design

We used a cross-sectional study design and 2-stage stratified random cluster sample to select 147 herds in 2000. The sample size was chosen to enable a herd seroprevalence of 50% to be estimated with 9% accuracy and 90% confidence; we increased the number of samples selected by 10% (inflation) to allow for refusals (*5*).

From each herd, a minimum of 5 adult (>24 months) and 5 juvenile (8–24 months) cattle were randomly sampled (*5*,*16*). We used samples from juvenile cattle only. With a sample of this size, the probability of detecting at least 1 seropositive animal in a herd of 70 was 95%, assuming within-herd seroprevalence of 50% and test sensitivity and specificity of 100% each. The lower age limit was set at 8 months to minimize misclassification associated with maternal antibodies. In herds with <5 animals in the appropriate age group, all animals in that group were sampled. The number of animals presented for sampling from each herd was 7–81 (median 35, mean 37.4).

Sampling

Blood was collected by jugular venipuncture into 10-mL Vacutainer tubes (Becton Dickinson, Franklin Lakes, NJ, USA), allowed to clot, and then separated in a 12-volt portable field centrifuge (Vulcon Technologies, Grandview, MO, USA). Serum was collected into two 1.8-mL cryovials (Nunc. Roskilde, Denmark) and kept at 4°C in a portable gas refrigerator for up to 14 days before being frozen and stored at –20°C. Samples were transported on dry ice to the World Reference Laboratory for Foot-and-Mouth Disease in Pirbright, UK, and stored at –20°C.

Questionnaire

To collect data from herdsmen, we used a structured, interview-based questionnaire, administered in Fulfulde (the language of the Fulani people) (*5*,*19*). The questionnaire asked whether respondents had observed FMD in their herd in the previous year and (separate question) in the previous 2 years.

Photographs

Herdsmen were asked to identify the diseases shown in 3 A4-sized photographs: a bovine tongue with a ruptured FMD vesicle, a bovine foot with ruptured FMD vesicles, and a bovid with lumpy skin disease (*Capripoxviridae*, Poxviridae). The interviewer oriented the viewer as to what was on the photograph, pointing out relevant anatomic, but not pathologic, features. A herdsman was described as being able to recognize FMD if he identified at least 1 of the FMD photographs correctly and either identified or recognized lumpy skin disease as not being FMD.

VN Testing

VN testing was performed according to the World Organisation for Animal Health/World Reference Laboratory protocol (*20*). Details are described elsewhere (*21*). VN results for each herd were then combined so that if positive results were found for any of the 3 virus serotypes (O, A, SAT2), that animal was considered positive.

ELISA Testing

To test for antibodies against NSP, we used 3 ELISAs: indirect (I)–ELISA, CHEKIT-ELISA, and competitive (C)–ELISA. Each is described below.

For screening with the I-ELISA 3ABC (I-ELISA), aliquots of heat-treated serum (56°C for 2 h) were sent to Panaftosa, Brazil. This test is described elsewhere (*22*,*23*). Two samples had insufficient serum for the I-ELISA, so this testing was performed for 1,375 animals, 651 of which were 8–24 months of age.

The CHEKIT-3ABC-FMD ELISA (CHEKIT-ELISA) is described elsewhere (*23*). Testing was performed by author B.M.de C.B. at the World Reference Laboratory for Foot-and-Mouth Disease, according to the manufacturer's instructions.

The C-ELISA was performed as described (*24*,*25*). Testing was conducted by author K.J.S. at the Danish Institute for Food and Veterinary Research in Kalvehave, Denmark.

Comparison of Herdsman Reporting and Serologic Testing

First, herdsmen's reports of disease in their herd in the previous 2 years were compared with VN test results for cattle 8–24 months of age in the same herd. Second,

herdsmen's reports of disease in the previous year were compared with antibodies against NSP determined by all 3 NSP ELISAs.

Statistical Analyses

Prevalence estimates were conducted by using STATA version 6.0 (http://www.stata.com). To avoid bias in point and variance estimates, we incorporated stratification and cluster effects with *svymean* or *svyprop* commands and *strata* (administrative division), *psu* (veterinary center), and *pweight* (probability weightings) (*5*).

Sensitivity and specificity of serologic testing and herdsmen reporting were estimated by using a Bayesian latent class model (*24*,*26*,*27*) and the JAGS (Just Another Gibbs Sampler) (http://mcmc-jags.sourceforge.net/) software package in R. This technique requires use of at least 2 tests that are conditionally independent (i.e., that if the true disease status of an animal were known, the outcome of 1 test would not influence the probability of a positive or negative result in the other). This technique also requires that prior distributions are specified for test properties and prevalence. The serologic tests were assigned a prior distribution of β (3,1) according to previous estimates of sensitivity and specificity (*23*). Herdsmen's reports were assigned an uninformed distribution of β (1,1), which is equivalent to a uniform distribution between 0 and 1 and implies no prior knowledge of test performance.

Sensitivity and specificity were estimated by using a Markov chain Monte Carlo technique and Gibbs sampling (*28*,*29*), which involves sampling from the posterior distribution of interest and calculating the relevant measures (e.g., means, medians, and standard deviations of the parameters). This iterative procedure involves burn-in, checking for convergence of the sample chain, and then sampling from the posterior distribution. In this model, the first 50,000 iterations were discarded as burn-in, and every 100th of the following 200,000 iterations were kept for posterior inference. Convergence was assessed by visual inspection of the time-series plots for the parameters and by using Gelman and Rubin diagnostic plots from 3 sample chains with different starting values (*30*).

The posterior means, medians, and 95% credibility intervals (PCIs) for sensitivity, specificity, and prevalence were calculated. Because no differences between means and medians were found, means were reported; the primary results were 95% PCIs.

When comparing herdsmen's reports of FMD in the previous 2 years with VN test results, sensitivity and specificity could not be allowed to vary across populations because there were only 2 tests. However when 3 NSP tests were used, sensitivity and specificity of herdsmen's reports were allowed to vary across populations, depending on factors such as whether the herdsmen watched the animals daily, whether the owner was of Fulani or Mbororo ethnicity, or whether the herdsmen could recognize FMD lesions from pictures. To examine differences between prevalence and disease recognition in photographs, we used χ^2 testing.

.

Results

Response Rate

Of the 147 herds selected, 146 (99.3%) were sampled. Flooding prevented access to 1 herd. Blood was collected from 1,377 animals, 651 of which were 8–24 months of age (142 herds). One herd was excluded because antibody test results were missing, leaving 141 herds from which blood was collected.

FMD Prevalence during Previous 2 Years

Herdsmen reported that 78.2% herds had been infected with FMD at least once during the previous 2 years. VN testing results indicated an estimated 80.3% prevalence (Table 1). Prevalence estimated by both methods differed among administrative divisions. FMD in the previous 2 years was reported by all herdsmen in Faro and Deo but by

Table 1. Prevalence of FMD among cattle, Adamawa plateau, Cameroon, according to different surveillance methods, 2000*

Administrative division	Previous 2 years, % (95% CI)†		Previous 1 year, % (95% CI)†			
	Herdsmen's reports	VN testing	Herdsmen's reports	I-ELISA	CHEKIT-ELISA	C-ELISA
Vina	89.6 (83.0–96.1)	85.1 (76.4–93.8)	76.6 (66.4–86.8)	74.5 (64.9–84.0)	29.8 (16.3–43.2)	70.2 (58.6–81.8)
Mbere	72.0 (55.0–89.0)	76.0 (57.0–95.0)	54.4 (32.6–76.1)	50.8 (33.0–68.8)	15.8 (1.8–29.7)	56.1 (32.6–79.7)
Djerem	54.8 (34.7–74.9)	59.2 (48.0–70.6)	35.7 (19.1–52.3)	55.4 (45.0–65.7)	16.1 (1.7–30.4)	37.5 (24.1–50.9)
Mayo Banyo	78.6 (66.0–91.2)	85.7 (76.2–95.2)	43.9 (22.5–65.4)	59.1 (39.4–78.8)	12.1 (0.7–23.5)	63.6 (44.5–82.8)
Faro and Deo	100	100	73.3 (62.2–84.5)	73.3 (52.4–94.3)	40.0 (28.8–51.2)	73.3 (52.4–94.2)
Overall	78.2 (72.1–84.3)	80.3 (75.0–85.6)	57.4 (49.8–65.1)	63.0 (56.2–69.9)	21.8 (15.6–28.0)	60.4 (52.6–68.2)

*FMD, foot-and-mouth disease; VN, virus neutralization.
†CIs adjusted for stratification by administrative division and clustering of herds by veterinary center.

only 55% in Djerem. Prevalence estimates obtained by VN testing were similar (Table 1).

FMD Prevalence during Previous Year

For the previous year, ≈60% of herdsmen reported having noticed FMD in their herds. This prevalence estimate was similar to that obtained by I-ELISA and C-ELISA but considerably more than that estimated by CHEKIT-ELISA (Table 1). The differences in reported prevalence among administrative divisions for the previous 2 years were also found for the previous year. (Table 1.)

Sensitivity and Specificity

Overall sensitivity of herdsmen's reports of FMD in the past 2 years was 95.7% (95% PCI 88.7%–99.8%) and specificity was 60% (95% PCI 44.3%–77.5%). These rates were remarkably similar to those determined by VN testing for serum antibodies in juvenile cattle (sensitivity 95.2% [95% PCI 89.6%–99.1%] and specificity 59.9% [95% PCI 45.6%–77.2%]).

Overall sensitivity of herdsmen's reports of FMD in the previous year was 84.0% (95% PCI 75.1%–92.2%) and specificity was 75.1% (95% PCI 62.7%–85.1%). Sensitivity of herdsmen's reports was significantly lower than that of I-ELISA (97.1% [95% PCI 91.0%–99.9%]) and C-ELISA (97.5% [95% PCI 91.9%–99.9%]). Specificity of herdsmen's reports was also slightly lower than that of I-ELISA (79.6% [95% PCI 68.0%–89.6%]) and C-ELISA (86.5% [95% PCI 75.1%–95.7%]) but not significantly so. Sensitivity was poor for CHECKIT-ELISA (37.2% [95% PCI 27.0%–48.1%]), but specificity was high (92.8% [95% PCI 85.0%–98.1%]).

Differences among administrative divisions were marked. The sensitivity of herdsmen's reports was highest for Vina (94.3%) and lowest for Djerem (57.8%); specificity was highest for Mayo Banyo (92.0%) and lowest for Faro and Deo (33.1%) (Table 2.)

Sensitivity, but not specificity, of herdsmen's reports differed among ethnic groups. Sensitivity was greater for the Fulani (90.3% [795% PCI 8.7%–98.0%]) than for the Mbororo people (73.8% [95% PCI 57.5%–87.5%]); $p < 0.001$. Specificity for the Fulani was 72.4% (95% PCI 53.2%–88.2%) and for the Mbororo was 76.4% (95% PCI 60.4%–89.5%).

Reporting accuracy did not differ between herd owners and nonowners. Sensitivities were 79.3% (95% PCI 61.2%–92.8) and 82.9 (95% PCI 71.8%–92.2%), and specificities were 73.7% (95% PCI 52.0%–91.5%) and 74.4% (95% PCI 59.8%–86.8%), respectively.

Similarly, reporting accuracy did not differ between respondents who watched cattle daily and those who did not. Sensitivities were 88.5% (95% PCI 75.6%–97.3%) and 76.9% (95% PCI 63.9%–88.2%), and specificities were 71.9% (95% PCI 49.6%–89.7%) and 75.1% (95% PCI 60.6–87.5%), respectively.

Table 2. No–gold standard estimation of herd-level sensitivity and specificity of herdsman reporting of FMD in administrative divisions of the Adamawa plateau, Cameroon*

Administrative division	Sensitivity, % (95% PCI)	Specificity, % (95% PCI)
Vina	94.3 (84.2–99.4)	70.6 (44.6–91.3)
Mbere	77.2 (50.7–96.5)	69.3 (42.0–91.0)
Djerem	57.8 (29.0–84.6)	73.1 (51.4–90.3)
Mayo Banyo	76.3 (52.8–95.0)	92.0 (72.8–99.8)
Faro and Deo	69.1 (42.9–90.4)	33.1 (5.2–71.4)
Overall	84.0 (75.1–92.2)	74.6 (62.7–85.1)

*FMD, foot-and-mouth disease; PCI, posterior credibility interval.

Herdsmen Identification of FMD in Photographs

FMD was correctly identified on 1 of 2 photographs by more than two thirds (69.3% [95% CI 61.4%–77.2%]) of herdsmen; 60.4% (95% CI 53.2%–67.7%) correctly identified FMD tongue lesions, 65.2% (95% CI 57.6%–72.8%) FMD foot lesions, and 55.8% (95% CI 47.8%–63.8%) both. Only 20.9% (95% CI 12.9%–28.8%) correctly identified FMD lesions in all 3 photographs. Lumpy skin disease was recognized by 28.5% (95% CI 19.9. Almost a quarter (24.3% [95% CI 17.1%–31.6%]) were unable to recognize FMD or lumpy skin disease from photographs.

Herd ownership did not influence ability to recognize FMD from photographs. FMD was recognized in photographs by 68.5% (95% CI 60.0%–76.9%) of owners and 71.3% (95% CI 58.5%–84.1%) of nonowners ($p = 0.675$).

Ethnicity affected the ability to recognize FMD from photographs. FMD lesions were recognized by a greater proportion of Fulani (82.2% [95% CI 72.3%–92.3%]) than Mbororo (58.8 % [95% CI 44.1%–73.6%]) herdsmen; $p = 0.0143$.

Frequency of herd observation did not influence ability to recognize FMD from photographs. FMD lesions were recognized by 66.1% (95% CI 51.9%–80.2%) of those who watched the animals daily and by 70.7% (95% CI 61.2%–79.3%) of those who did not ($p = 0.537$).

Administrative region did affect ability to recognize FMD from photographs. Recognition of FMD lesions in photographs was highest for herdsmen in Vina (79.2% [95% CI 67.1%–91.2%]) and lowest for those in Faro and Deo (53.3% [95% CI 19.2%–87.5%]); these differences were not statistically significant ($p = 0.354$). FMD lesion recognition was 72.3% (95% CI 57.4%–89.3%) for herdsmen in Mbere, 59.4% (95% CI 38.9%–79.8%) in Djerem, and 68.2% (95% CI 51.6%–84.8%) in Mayo Banyo.

Sensitivity and Specificity of Photograph Identification

Compared with sensitivity for NSP antibody testing, sensitivity was higher for herdsmen recognition of FMD lesions in 1 photograph but specificity was lower for reporting of FMD in the previous year. The sensitivities and specificities were 90.0% (95% PCI 80.4%–97.3%) and 69.5% (95% PCI 54.3%–83.4%) for those able to identify a photograph of FMD compared with 63.5% (95% PCI 44.0%–90.9%) and 83.2% (95% PCI 64.0%–96.0%) for those who could not.

Discussion

With regard to estimating herd prevalence of FMD, herdsmen performed as well as laboratory-based VN testing. Estimates of prevalence in the previous 2 years were 78.2% (95% CI 72.1%–84.3%) according to herdsman's reports and 80.3% (95% CI 75.0%–85.6%) according to VN test results. Sensitivities of estimates for prevalence in the previous 2 years were 95.7% (95% PCI 88.7%–99.8%) and 95.2% (95% PCI 89.6%–99.1%) and specificities were 60.0% (95% PCI 44.3%–77.5%) and 59.9% (95% PCI 45.6%–77.2%), for herdsmen's reports and VN test results, respectively. These estimates were derived by restricting the age of cattle to <2 years and by using a no–gold standard Bayesian model (model to assess diagnostic test performance in the absence of a perfect reference test) to estimate sensitivity and specificity.

In addition to validating estimates of FMD prevalence in the previous 2 years, we also attempted to validate farmer reporting for the previous year by taking a different approach. The rationale behind using tests that detect antibodies against NSP was that the number of animals <1 year of age in the sample was insufficient to produce generalizable results and that NSP antibody titers fall more rapidly over time than do VN antibody titers (*17*,*18*). In an evaluation study in which we reported that the CHECKIT-ELISA performed less well than the I-ELISA and C-ELISA, we used 3 NSP ELISAs (*23*,*25*). The results of the CHECKIT-ELISA are included in the study reported here because they enable comparison with results in the only other publication in which herdsmen's estimates of FMD are compared with serologically derived estimates (*12*).

The 84.0% sensitivity of herdsmen's reports of FMD in the previous year was significantly lower than the sensitivity of I-ELISA (97.1%) and the C-ELISA (97.5%) results. The 75.1% specificity of herdsmen's reports was within the Bayesian credibility limits of the NSP test results. There are no published population-based estimates of NSP antibody persistence. In experimental studies, NSP antibodies have been detected in cattle for 229 (*31*), 304 (*32*), 365 (*33*), 395 (*24*), and 560 (*17*) days after infection, at which point the studies were terminated. It is possible that persistence of NSP antibody for >1 year accounted for the significantly lower sensitivity of herdsmen's reports compared with serum antibodies against NSP (i.e., NSP serum antibodies represented infection over the previous 2 years, but herdsmen reporting was confined to 1 year, when fewer herds would have been seropositive). However, the lower seroprevalence according to VN testing (80.3%) compared with NSP ELISA seroprevalence (60.0%–64.5%) would argue against this.

The only test previously used to validate herdsmen's reports of FMD is the CHEKIT-ELISA (*12*). When we used the results of this test as a reference standard, estimates of the sensitivity of reporting by pastoral Masai and Sukuma herdsmen in Tanzania were similar to those for herdsmen in Cameroon. Overall sensitivities were 90.9% (95% CI 75.7%–98.1%) and 72.7% (95% CI 49.8%–89.3%), respectively; however, specificities were lower at 35.2% (95% CI 14.2%–61.7%) and 35.1% (95% CI 20.2%–52.5%), respectively (*13*). The results of this and another study (*19*) suggest that the CHECKIT-ELISA was not the best choice of reference standard and that herdsmen's estimates are more reliable.

By restricting the age of cattle to 8–24 months, we focused on recent herd exposure. The lower limit was chosen to avoid misclassification associated with presence of maternal antibodies. The upper limit means that herds infected during the last 2 weeks of the 2-year period might not have had time to seroconvert, but given a random distribution of infection in these herds over the 24-month period, only 2% (2/104weeks) of herds would have been infected during these last 2 weeks.

In recent years, use of latent class models to estimate sensitivity and specificity of multiple tests in the absence of a reference standard has become common practice (*34*). A critical assumption of this technique is that test results must be independent within 2 classes (*35*,*36*), especially when a 2-class latent model is used. We used 2 biologically different and independent test approaches: herdsman reporting and VN testing. The assumption of conditional independence can be relaxed when there are >2 classes, but in our study, it was preserved even when 4 classes were compared; herdsmen reporting differed biologically from NSP ELISAs. A Bayesian approach to latent class models requires specification of prior distributions. The β (3,1) prior distributions given to NSP tests were based on previous findings. The uninformed β (1,1) prior distribution given to herdsman reporting is recommended when using this technique. Model fit was assessed by using Gelman-Rubin plots and statistics.

This study covered 64,000 km^2 and 5 administrative divisions. Differences in reports of FMD prevalence were found for herdsmen ethnic groups, ownership status, and amount of cattle contact. However, the only variable for which a statistically significant difference was found was

ethnic group; sensitivity of reporting by Fulani herdsmen was greater than that by Mbororo herdsmen. The Fulani and Mbororo are the major pastoralist groups on the Adamawa. They have a common language and cultural heritage, but the Mbororo are largely nomadic whereas the Fulani tend to be sedentary (*37*). The greater sensitivity of reporting by Fulani herdsmen is perhaps surprising because the nomadic group might be expected have more cattle contact. However, watching cattle on a daily basis was not associated with increased reporting accuracy. The differences between the Fulani and Mbororo might be a chance finding, or it might reflect differences in education or cattle ownership. A transethnic class of livestock owner seems to be emerging, in which sedentary Fulani employ non-Fulani herders, and non-Fulani owners employ poorer Mbororo who have lost their own herds. However, in this study, ownership was not associated with increased reporting accuracy.

With regard to the higher proportion of Fulani than Mbororo herdsmen who were able to identify FMD lesions from photographs, it is possible that Mbororo herdsmen might have less access to education and less experience interpreting 2-dimensional images (*38*). It is also possible that herdsmen rarely see vesicles in the mouth or coronary band and are more familiar with salivation and lameness. Recognition of lameness would be similar for sedentary and nomadic herdsmen because both groups spend each day slowly walking their cattle over a grazing area.

The finding of higher specificity for herdsmen recognition of FMD in at least 1 photograph and lower sensitivity of FMD reporting indicates a higher probability of reporting true-negative herds and a lower probability of reporting true-positive herds. This finding might represent a systematic reporting bias associated with herdsmen concerns about admitting that they had had FMD in their herds or a chance finding associated with seeing a familiar concept (FMD) in an unfamiliar way (photograph).

These results suggest that in FMD-endemic areas, an effective FMD surveillance method might be simply asking herdsmen if they have seen FMD in their herds. This concept is intuitive because FMD is a common disease and herdsmen are familiar with it. Whether herdsmen's reports of FMD prevalence would be effective in countries where FMD is sporadic or less prevalent remains to be determined.

If our findings are generalizable to other diseases that produce visible clinical signs in other populations, herdsmen's reports would provide a cost-effective surveillance mechanism that could extend to emerging diseases. In initial discussions, herdsmen reported that "Njobo" (Fulfulde word for FMD) had changed in recent years by causing death among adult cattle rather than just calves. The subsequent isolation of FMD virus serotype SAT2 in Cameroon provided a scientific explanation for this observation. Because of the potential usefulness of herdsmen's observations in surveillance and emerging disease identification, we suggest that studies of animal disease prevalence in developing countries should include estimates of sensitivity and specificity of reporting.

Acknowledgments

We thank all the herdsmen, heads of veterinary centers, and regional Ministère de l'Elevage, des Pêches et des Industries Animales delegates who made this study possible.

This work was supported by the Wellcome Trust (WT 053480). B.M. de C.B. held a Wellcome Trust Training Fellowship in Tropical Epidemiology but reports no conflict of interest. Cattle were sampled by a veterinary surgeon with the cattle owners' consent.

Dr Morgan is a veterinarian at the University of Liverpool. His research interests include racehorse injuries, exotic and endemic diseases of farmed animals, aquatic animal health, molecular epidemiology of rotavirus, and use of machine learning in epidemiology.

References

1. French NP, Wall R, Cripps PJ, Morgan KL. Prevalence, regional distribution and control of blowfly strike in England and Wales. Vet Rec. 1992;131:337–42. http://dx.doi.org/10.1136/vr.131.15.337.
2. Cetinkaya B, Erdogan HM, Morgan KL. Prevalence, incidence and geographical distribution of Johne's disease in cattle in England and the Welsh borders. Vet Rec. 1998;143:265–9. http://dx.doi.org/10.1136/vr.143.10.265.
3. Erdogan HM, Cetinkaya B, Green LE, Green LE, Cripps PJ, Morgan KL. Prevalence, incidence, signs and treatment of clinical listeriosis in dairy cattle in England. Vet Rec. 2001;149:289–93. http://dx.doi.org/10.1136/vr.149.10.289.
4. Bronsvoort BM, Tanya VN, Kitching RP, Nfon C, Hamman SM, Morgan KL. Foot and mouth disease and livestock husbandry practices in the Adamawa Province of Cameroon. Trop Anim Health Prod. 2003;35:491–507. http://dx.doi.org/10.1023/A:1027302525301.
5. Hermans PG, Morgan KL. Prevalence and associated risk factors of necrotic enteritis on broiler farms in the United Kingdom; a cross-sectional survey. Avian Pathol. 2007;36:43–51. http://dx.doi.org/10.1080/03079450601109991.
6. Inness CM, Morgan KL. Polo pony injuries: player-owner reported risk, perception, mitigation and risk factors. Equine Vet J. 2014 [cited 2014 Sep 29]. Epub ahead of print. http://onlinelibrary.wiley.com/doi/10.1111/evj.12298
7. Healy AM, Morgan KL, Hannon D, Collins JD, Weavers E, Doherty ML. Postal questionnaire survey of scrapie in sheep flocks in Ireland. Vet Rec. 2004;155:493–4. http://dx.doi.org/10.1136/vr.155.16.493.
8. Nespeca R, Vaillancourt JP, Morrow WE. Validation of a poultry biosecurity survey. Prev Vet Med. 1997;31:73–86. http://dx.doi.org/10.1016/S0167-5877(96)01122-1.
9. Vanderhaeghe C, Dewulf J, Ribbens S, de Kruif A, Maes D. A cross-sectional study to collect risk factors associated with stillbirths in pig herds. Anim Reprod Sci. 2010;118:62–8. http://dx.doi.org/10.1016/j.anireprosci.2009.06.012.
10. Knight-Jones TJ, Gibbens J, Wooldridge M, Stärk KD. Assessment of farm-level biosecurity measures after an outbreak of avian influenza in the United Kingdom. Transbound Emerg Dis. 2011;58:69–75. http://dx.doi.org/10.1111/j.1865-1682.2010.01183.x.

11. Kaler J, Green LE. Naming and recognition of six foot lesions of sheep using written and pictorial information: a study of 809 English sheep farmers. Prev Vet Med. 2008;83:52–64. http://dx.doi.org/10.1016/j.prevetmed.2007.06.003.
12. Catley A, Chibunda RT, Ranga E, Makungu S, Magayane FT, Magoma G, et al. Participatory diagnosis of a heat-intolerance syndrome in cattle in Tanzania and association with foot-and-mouth disease. Prev Vet Med. 2004;65:17–30. http://dx.doi.org/10.1016/j.prevetmed.2004.06.007.
13. Doherr MG, Carpenter TE, Wilson WD, Gardner IA. Application and evaluation of a mailed questionnaire for an epidemiologic study of *Corynebacterium pseudotuberculosis* infection in horses. Prev Vet Med. 1998;35:241–53. http://dx.doi.org/10.1016/S0167-5877(98)00070-1.
14. Perry B, Sones K. Science for development. Poverty reduction through animal health. Science. 2007;315:333–4. http://dx.doi.org/10.1126/science.1138614.
15. Kitching RP. Clinical variation in foot and mouth disease: cattle. Rev Sci Tech. 2002;21:499–504. .
16. de C. Bronsvoort BM, Nfon C, Hamman SM, Tanya VN, Kitching RP, Morgan KL. Risk factors for herdsman-reported foot-and-mouth disease in the Adamawa Province of Cameroon. Prev Vet Med. 2004;66:127–39. http://dx.doi.org/10.1016/j.prevetmed.2004.09.010.
17. Silberstein E, Kaplan G, Taboga O, Duffy S, Palma E. Foot-and-mouth disease virus-infected but not vaccinated cattle develop antibodies against recombinant 3AB1 nonstructural protein. Arch Virol. 1997;142:795–805. http://dx.doi.org/10.1007/s007050050119.
18. Brocchi E, Bergmann IE, Dekker A, Paton DJ, Sammin DJ, Greiner M, et al. Comparative evaluation of six ELISAs for the detection of antibodies to the non-structural proteins of foot-and-mouth disease virus. Vaccine. 2006 ;24:6966–79.
19. Lee JA, More SJ, Cotiwan BS. Problems translating a questionnaire in a cross-cultural setting. Prev Vet Med. 1999;41:187–94. http://dx.doi.org/10.1016/S0167-5877(99)00041-0.
20. Kitching RP, Barnett PV, Donaldson AI, Mackay D. Foot-and-mouth disease. In: Linnane S, editor. Manual of standards for diagnostic tests and vaccines. Paris: Office International des Epizooties; 2000. p. 77–92.
21. de C. Bronsvoort BM, Anderson J, Corteyn A, Hamblin P, Kitching RP, Nfon C, et al. Geographical and age-stratified distributions of foot-and-mouth disease virus-seropositive and probang-positive cattle herds in the Adamawa province of Cameroon. Vet Rec. 2006;159:299–308. http://dx.doi.org/10.1136/vr.159.10.299
22. Malirat V, Neitzert E, Bergmann IE, Maradei E, Beck E. Detection of cattle exposed to foot-and-mouth disease virus by means of an indirect ELISA test using bioengineered nonstructural polyprotein 3ABC. Vet Q. 1998;20(Suppl 2):S24–6. http://dx.doi.org/10.1080/01652176.1998.9694958.
23. Bronsvoort BM, Toft N, Bergmann IE, Sørensen KJ, Anderson J, Malirat V, et al. Evaluation of three 3ABC ELISAs for foot-and-mouth disease non-structural antibodies using latent class analysis. BMC Vet Res. 2006;2:30. http://dx.doi.org/10.1186/1746-6148-2-30.
24. Sørensen KJ, de Stricker K, Dyrting KC, Grazioli S, Haas B. Differentiation of foot-and-mouth disease virus infected animals from vaccinated animals using a blocking ELISA based on baculovirus expressed FMDV 3ABC antigen and a 3ABC monoclonal antibody. Arch Virol. 2005;150:805–14. http://dx.doi.org/10.1007/s00705-004-0455-z.
25. Bronsvoort BMC, Sørensen KJ, Anderson J, Corteyn A, Tanya VN, Kitching RP, et al. A comparison of two 3ABC enzyme-linked immunosorbent assays in a cattle population with endemic, multiple-serotype foot-and-mouth disease. J Clin Microbiol. 2004;42:2108–14. http://dx.doi.org/10.1128/JCM.42.5.2108-2114.2004.
26. Hui SL, Walter S. Estimating the error rates of diagnostic tests. Biometrics. 1980;36:167–71. http://dx.doi.org/10.2307/2530508.
27. Enøe C, Georgiadis MP, Johnson WO. Estimation of sensitivity and specificity of diagnostic tests and disease prevalence when the true disease state is unknown. Prev Vet Med. 2000;45:61–81. http://dx.doi.org/10.1016/S0167-5877(00)00117-3.
28. Johnson WO, Gastwirth JL, Pearson LM. Screening without a gold standard: the Hui–Walter paradigm revisited. Am J Epidemiol. 2001;153:921–4. http://dx.doi.org/10.1093/aje/153.9.921.
29. Toft N, Jørgensen E, Højsgaard S. Diagnosing diagnostic tests: evaluating the assumptions underlying the estimation of sensitivity and specificity in the absence of a gold standard. Prev Vet Med. 2005;68:19–33. http://dx.doi.org/10.1016/j.prevetmed.2005.01.006.
30. Gelman A, Rubin DB. Inference from iterative simulation using multiple sequences. Stat Sci. 1992;7:457–72. http://dx.doi.org/10.1214/ss/1177011136.
31. Fu Y, Cao Y, Sun P, Bao H, Bai X, Li P, et al. Development of a dot immunoblot method for differentiation of animals infected with foot-and-mouth disease virus from vaccinated animals using non-structural proteins expressed prokaryotically. J Virol Methods. 2011;171:234–40. http://dx.doi.org/10.1016/j.jviromet.2010.11.006.
32. Mackay DKJ. Forsyth MA, Davies PR, Berlinzani A, Belsham GJ, Flint M, et al. Differentiating infection from vaccination in foot-and-mouth disease using a panel of recombinant, non-structural proteins in ELISA. Vaccine. 1998;16:446–59.
33. Lubroth J, Brown F. Identification of native foot-and-mouth disease virus non-structural protein 2C as a serological indicator to differentiate infected from vaccinated livestock. Res Vet Sci. 1995;59:70–8. http://dx.doi.org/10.1016/0034-5288(95)90034-9.
34. van Smeden M, Naaktgeboren CA, Reitsma JB, Moons KG, de Groot JA. Latent class models in diagnostic studies when there is no reference standard—a systematic review. Am J Epidemiol. 2014;179:423–31. http://dx.doi.org/10.1093/aje/kwt286.
35. Torrance-Rynard VL, Walter SD. Effects of dependent errors in the assessment of diagnostic test performance. Stat Med. 1997;16:2157–75. http://dx.doi.org/10.1002/(SICI)1097-0258(19971015)16:19<2157::AID-SIM653>3.0.CO;2-X.
36. Spencer BD. When do latent class models overstate accuracy for diagnostic and other classifiers in the absence of a gold standard? Biometrics. 2012;68:559–66. http://dx.doi.org/10.1111/j.1541-0420.2011.01694.x.
37. Frantz C. Are the Mbororo'en boring and are the Fulani finished? In: Eguchi PK, Azarya V, editors. Unity and diversity. Senri ethnological studies 35. Osaka (Japan): National Museum of Ethnography; 1993. p. 11–34.
38. Deregowski JB. What about pictures? Behav Brain Sci. 1993;16:757–61. http://dx.doi.org/10.1017/S0140525X00032751.

Address for correspondence: Kenton L. Morgan, University of Liverpool, Leahurst Campus, Neston, Wirral, CH64 7TE, UK; email: k.l.morgan@liv.ac.uk

Residual Infestation and **Recolonization during** Urban *Triatoma infestans* **Bug Control Campaign, Peru**[1]

Corentin M. Barbu, Alison M. Buttenheim, Maria-Luz Hancco Pumahuanca, Javier E. Quintanilla Calderón, Renzo Salazar, Malwina Carrión, Andy Catacora Rospigliossi, Fernando S. Malaga Chavez, Karina Oppe Alvarez, Juan Cornejo del Carpio, César Náquira, and Michael Z. Levy

Chagas disease vector control campaigns are being conducted in Latin America, but little is known about medium-term or long-term effectiveness of these efforts, especially in urban areas. After analyzing entomologic data for 56,491 households during the treatment phase of a *Triatoma infestans* bug control campaign in Arequipa, Peru, during 2003–2011, we estimated that 97.1% of residual infestations are attributable to untreated households. Multivariate models for the surveillance phase of the campaign obtained during 2009–2012 confirm that nonparticipation in the initial treatment phase is a major risk factor (odds ratio [OR] 21.5, 95% CI 3.35–138). Infestation during surveillance also increased over time (OR 1.55, 95% CI 1.15–2.09 per year). In addition, we observed a negative interaction between nonparticipation and time (OR 0.73, 95% CI 0.53–0.99), suggesting that recolonization by vectors progressively dilutes risk associated with nonparticipation. Although the treatment phase was effective, recolonization in untreated households threatens the long-term success of vector control.

Chagas disease, an often deadly disease widespread in the Americas, is caused by the protozoan parasite *Trypanosoma cruzi* (*1*,*2*) and transmitted by hematophageous triatomine insects (*3*). In southern South America *Triatoma infestans* bugs are the primary vector (*2*). In 1991, the nations of this region created the Southern Cone Initiative to coordinate control efforts against *T. infestans* bugs. During the first decade of this initiative, 2.5 million households were treated with insecticide (*4*), which led to disruption of transmission of *T. cruzi* by *T. infestans* bugs in several countries and states (*2*). However, vector control efforts have at times failed unexpectedly, and repeatedly in some areas (*5*,*6*).

Across most of their range, *T. infestans* insects are found predominantly in rural areas (*2*). However, the vector has become an urban problem in Arequipa, Peru, a city of 850,000 inhabitants (*7*–*9*) where infected vectors have been observed since 1952 (*10*). Since 2003, municipal authorities and the regional ministry of health, in collaboration with the Pan American Health Organization, have worked to eliminate the vector from this city. The challenges to elimination in an urban area potentially differ from those in rural settings. Urban households have smaller peridomestic areas, fewer sources of blood, and fewer hiding places for the vector, thus mitigating some of the difficulties encountered in rural environments (*7*,*11*–*13*). However, whereas participation in control campaigns in rural areas is typically high (*5*,*7*), more affluent urban populations (*14*) might be more reluctant to participate (*15*). Thus, household level control might be easier in an urban household than in a rural household. However, at the community level, sustained control in an urban community might be more difficult.

We explored this hypothesis by using data obtained in Arequipa during the initial treatment phase or attack phase of the vector campaign and during the subsequent surveillance phase after insecticide application. We evaluated the effectiveness of the treatment phase in 3 ways. First, we estimated the reduction in the infestation prevalence resulting from the 2 insecticide applications

Author affiliations: University of Pennsylvania, Philadelphia, Pennsylvania, USA (C.M. Barbu, A.M. Buttenheim, M.Z. Levy); Universidad Peruana Cayetano Heredia, Arequipa, Peru (M.-L. Hancco Pumahuanca, J.E. Quintanilla Calderón, R. Salazar, M. Carrión, C. Náquira); Red de Salud Aequipa Caylloma, Arequipa (A. Catacora Rospigliossi); and Dirección Regional del Ministerio de Salud, Arequipa (F.S. Malaga Chavez, K. Oppe Alvarez, J. Cornejo del Carpio)

DOI: http://dx.doi.org/10.3201/eid2012.131820

[1]The authors have provided a Spanish version of this article online (http://www.spatcontrol.net/articles/Barbu2014/traduccionEspanol.pdf).

of the treatment phase. Second, we modeled recolonization (the colonization of new households after the initial treatment) as a function of treatment phase factors. Third, during the surveillance phase, we tested insects captured from households treated during the treatment phase for resistance to insecticide. We discuss converging results of these approaches in terms of their implications for continued efforts of the control campaign in Arequipa and, more generally, for design of strategies to control Chagas disease vectors in urban environments.

Materials and Methods

Campaign

The vector control campaign in Arequipa proceeded through the city district by district. Districts, local administrative subdivisions of the region, comprise 3,000–28,000 households. Within each district, treatment is organized on a locality level; localities vary in size from 50 to 2,000 households. Preliminary inspections in the months preceding the treatment phase identified localities (or city blocks within a locality) as sufficiently infested to warrant treatment (Figure 1; Table 1). However, the results of these preliminary inspections at the household level are available only for the most recent surveys.

After inspections, localities entered the treatment phase. Health promoters and vector control specialists visited every household in the targeted areas to apply insecticide (http://www.spatcontrol.net/articles/Barbu2014/suppMet.pdf) to all domestic and peridomestic structures. These visits occurred twice at 6-month intervals. All households in targeted areas were asked to participate in this phase. As houses were treated, trained personnel collected *T. infestans* specimens flushed out of their refuges by the insecticide. Six months after the second treatment, localities entered the surveillance phase, a community-based effort to identify residual and returning vector populations. All households in the district were eligible to participate in the surveillance phase, even if they were not targeted for the treatment phase. In the surveillance phase, households reported infestation, and campaign staff conducted inspections and treated areas in and around reporting households.

Inhabitants were asked to bring any *T. infestans* insects found in their households to community health workers or health posts located throughout the city. Trained entomologic technicians systematically searched for and collected *T. infestans* insects in indoor and peridomestic areas of reporting households and their immediate neighbors (1 person-hour search per household) by using aerosol spray containing tetramethrin (Mata Moscas 0.15% tetramethrin; Sapolio, Doral, FL, USA), which has a strong flushing out effect on triatomine insects but does not kill them. All captured insects were counted, staged, sexed, and microscopically examined for *T. cruzi* as described previously (*7*). Infested households and their immediate neighbors were treated with insecticide as in the treatment phase.

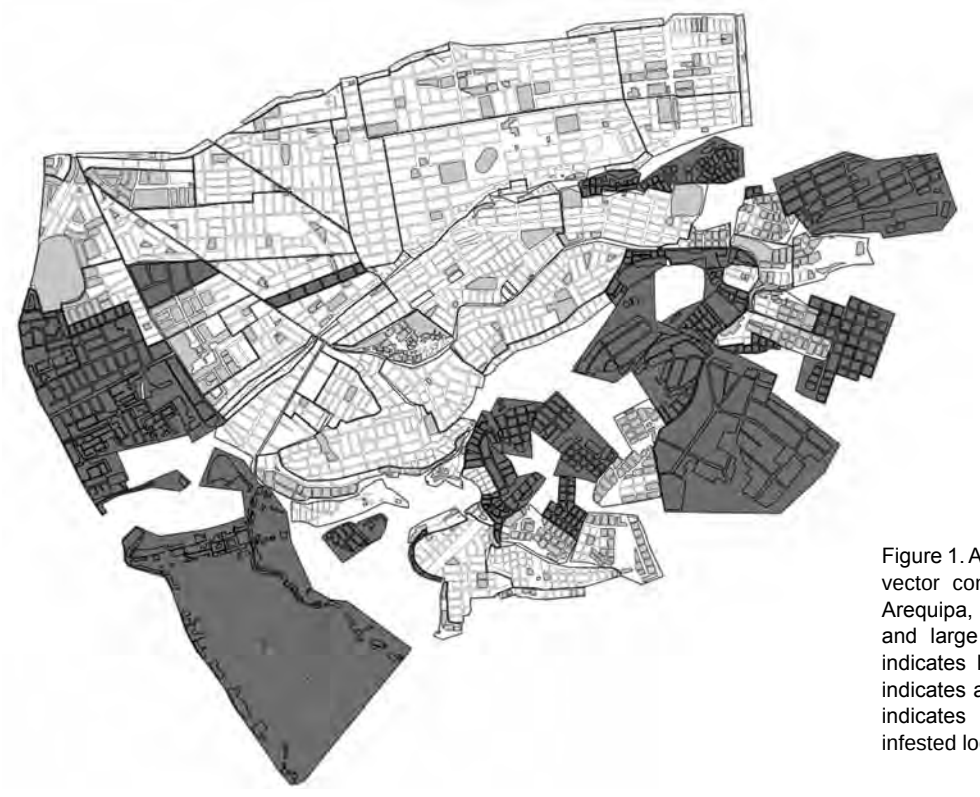

Figure 1. Areas targeted for Chagas disease vector control in the Paucarpata District, Arequipa, Peru. Small units are city blocks and large units are localities. Dark gray indicates localities not infested; light gray indicates areas targeted; and medium gray indicates nontargeted city blocks within infested localities.

Table 1. Targeted areas within districts and localities and distribution of reports, inspections, and uncovered infestation during surveillance phase of a Chagas disease vector control program, Arequipa, Peru, 2003–2011*

Nested units	City blocks	Households	Households reporting infestations	Households inspected	Households inspected and found infested
Participating districts, n = 8	5,955	79,972	301	785	145
Infested localities, n = 256	4,755	67,218	258	714	133
Targeted areas	3,727	56,491	225†	613	116‡

*Reporting and inspected households during surveillance are counted from January 2009 through end of December 2012.
†Households in targeted city blocks have a similar rate of report and risk of being positive during the surveillance phase as other households in their districts: odds ratio 1.12, p = 0.45; and 0.94, p = 0.77, controlling for diversity between districts.
‡Among these households, 77 were reporting households (35% of the 219 inspected reporting households).

For all phases of the campaign, a household with at least 1 observed *T. infestans* bug of any developmental stage was considered infested (eggs were not collected or reported) (http://www.spatcontrol.net/articles/Barbu2014/suppMet.pdf). For all control activities, a unique identifier code, participation (0/1), and infestation status (0/1) of each household were recorded. We mapped the exact positions of households and city blocks by using satellite imagery in Google Earth (*16*) and field maps drawn by Ministry of Health personnel. Household geographic unique identifier codes, coordinates, participation status, and *T. infestans* bug infestation status were stored for subsequent analysis (*17*).

Sample

During 2004–2011, eight urban districts participated in the treatment phase of the campaign (Jacobo Hunter, José Luis Bustamente y Rivero, La Joya, Paucarpata, Sachaca, Uchumayo, Tiabaya, and Socabaya); they encompassed 356 localities. These localities correspond to an urban-to-periurban environment as described by Delgado et al. (*17*). These districts comprised a total of 79,972 households in 5,955 city blocks (Table 1; Figure 1). However, 2,228 (37.4%) city blocks in these districts were not included in the treatment phase because no vectors were observed during preliminary inspections. The remaining 3,727 city blocks that were included contained 56,491 households. Because we aimed to find an association between treatment phase and infestation during the surveillance phase, we restricted our analysis to these city blocks and households. We report results of the surveillance phase inspections over a 4-year period (2009–2012) during which our study team collaborated with the Peru Ministry of Health to monitor infestation. Surveillance is still ongoing in these areas.

Statistical Analysis

Modeling Effectiveness of Treatment Phase and Residual Infestation

We included 3 parameters in our model of treatment phase effectiveness. The first parameter was *c*, the probability of clearing treated households of *T. infestans* bug colonies with 1 treatment. The second was *s*, the sensitivity of detection, defined as the probability that trained entomologic technicians performing house treatment would observe infestation when it is present. The third was $n_{I/II}$, the true number of infested households immediately before any treatment.

To estimate these parameters, we compared the infestation observed during the first and second treatments of the initial treatment phase in the 35,207 households that accepted both treatments (Table 2). Households were unlikely to become infested between the 2 treatments: the treatments were separated by only 6 months, the overall infestation is severely reduced by the first treatment, and treated households are protected by the residual effect of the insecticide for several months (*18*). Assuming that households did not become infested between the 2 treatments, we jointly estimated *c*, *s*, and $n_{I/II}$ by modeling the observed infestation as a system of 3 equations (observed infested twice, infested only during treatment I, and infested only during treatment II) (Table 3) that we solved analytically. In addition, we considered this model from a stochastic perspective to compute CIs for our estimates; further details are available online (http://www.spatcontrol.net/articles/Barbu2014/suppMet.pdf).

We extrapolated infestation prevalence before treatment in households treated only once by using the estimated sensitivity of the infestation detection (*s*) (Table 2). For households that were never treated with insecticide, and on

Table 2. Estimations of initial and residual infestation for treatment phase of a Chagas disease vector control program, Arequipa, Peru, 2003–2011*

Treatment received	No. households	Initial prevalence, %		Estimated residual infestation	
		Observed	Estimated	Prevalence, %	No. (%) infested households
I and II	35,207	20.1	35.6	0.006	2 (0.3)
I only	7,521	7.0	12.2	0.16	14 (2.1)
II only	4,169	4.0	6.9	0.09	4 (0.5)
Not treated	9,594	ND	6.9†	6.9	666 (97.1)
Total	56,491	16.2	25.8	1.2	686 (100)

*Estimates are calculated by using equations in Table 3 (estimated sensitivity of inspectors p = 57% [range 46%–66%] and probability of clearing households of infestation through 1 treatment c = 98.7% [range 98.4%–98.9%]). ND, no data.
†Extrapolation of the prevalence in households participating only in the second treatment to households that were never treated.

Table 3. Household level model of observation, initial infestation, treatment, and residual infestation during treatment phase of a Chagas disease vector campaign, Arequipa, Peru, 2003–2011*

Treatment received	Observed infestation	Estimated initial prevalence	Estimated residual prevalence
I and II	$\begin{cases} O_{I+II+} = n_{I/II} \times s(1-c) \times s \\ O_{I+II-} = n_{I/II} \times s\left(c + (1-c) \times (1-s)\right) \\ O_{I+II+} = n_{I/II} \times (1-s) \times (1-c) \times s \end{cases}$	$p_{I/II} = n_{I/II}/T_{I//II}$	$r_{I/II} = p_{I/II} \times (1-c)^2$
I only	$O_{I+II\emptyset} = n_I \times s$	$p_I = n_I/T_I$	$r_I = p_I \times (1-c)$
II only	$O_{I\emptyset II+} = n_{II} \times s$	$p_{II} = n_{II}/T_{II}$	$r_{II} = p_{II} \times (1-c)$
None	Not observed	$p_\emptyset = p_{II}$	$r_\emptyset = p_\emptyset$

*Upper case letters refer to observed quantities. Lower case letters refer to estimated quantities. $O_{Ix/Iy}$, number of infested households observed in the first (*Ix*) and second (*Iy*) step of the treatment phase, with *x* and *y* taking the following values: ∅, no treatment and infestation could not be observed; +, treated and observed infested; –, treated and observed noninfested. For n_z, p_z, T_z, and r_z, the subscript z corresponds to the participation in treatments: *I*, only first; *II*, only second; *I/II*, both; n_z, estimated number of infested households; p_z, estimated initial prevalence of infestation; T_z, total number of households; r_z, estimated residual prevalence of infestation post treatment phase; *s*, sensitivity of technicians performing treatment to household infestation; *c*, probability of clearing infestation when treated. Further details and the solved system of equations have been provided by the authors (http://www.spatcontrol.net/articles/Barbu2014/suppMet.pdf).

the basis of other data (http://www.spatcontrol.net/articles/Barbu2014/suppMet.pdf), we used the prevalence found in households that were only treated during the second insecticide treatment.

Finally, we estimated residual infestation (number of households still infested after the treatment phase), assuming that the effects of the first and second insecticide spraying of the treatment phase are comparable and independent. We applied the clearing rate estimated during the first treatment, *c*, to the estimated initial infestation once or twice according to the number of treatments (Table 3). We examine the validity of this assumption below; other details are available online (http://www.spatcontrol.net/articles/Barbu2014/suppMet.pdf).

Logistic Mixed Effect Models of Infestation during Surveillance

We used univariate and multivariate mixed effect logistic regressions (*19*) to describe the correlations between treatment phase and surveillance observations. Unless otherwise noted, we used a random effect term to control for potential similarity of households in a locality (*20*,*21*).

Our first multivariate logistic model describes the probability that households targeted during the treatment phase were infested at least once during the surveillance phase as a function of observed infestation of the household during the treatment phase, participation of the household in the treatment phase, and number of years the household had been under surveillance as of January 1, 2013. We also considered the interaction between time and the other risk factors. The outcome assessed in the first model consists of 2 processes: selection of inspected households (reporting households and their neighbors) and individual infestation status of inspected households. We investigated these processes separately in the second and third logistic models.

In our second logistic model, we estimated the probability that an infestation report was generated on a city block given the number of infested and participating households on the block during the treatment phase. In our third logistic model, we estimated the probability of infestation among inspected households given the household infestation and participation status during the treatment phase; we used a random effect term to control for potential similarity of households around a household that generated a report. A total of 225 reports were generated. Because some households had been inspected multiple times during the study, we limited our sample to the first inspection following the treatment phase. Because sensitivity and specificity of our surveillance program rely on community reports, we assessed their reliability (http://www.spatcontrol.net/articles/Barbu2014/suppMet.pdf). We estimated the goodness-of-fit for these models by using Nagelkerke pseudo R^2 (*22*). All computations were performed by using R (*23*).

Evaluation of Susceptibility of Residual Populations to Pyrethroid Insecticide

During the surveillance phase, we collected triatomine insects from infested households that had been treated during the treatment phase to evaluate resistance to deltamethrin. We followed guidelines for wall bioassays of the World Health Organization/Special Programme for Research and Training in Tropical Diseases (*24*). In brief, we applied 5% deltamethrin suspension concentrate (K-Othrine SC; Bayer, Leverkuesen, Germany) with an X-Pert compression sprayer (Hudson Manufacturing Co., Chicago, IL, USA) at the target dose of 25 mg/m^2 to a cemented wall and allowed it to dry for 24 h. From each household, we placed 10 F_1 progeny fifth instar nymphs in a petri dish on the wall for 72 h. We evaluated the status of the insects 3 days after the exposure. The insects used in the bioassay had molted 15–20 days before the experiment, and had fasted for 7 days. Throughout the experiment, insects were kept under ambient conditions in our field laboratory (19–28°C, humidity 24%–51%).

Results

Treatment Phase Effectiveness and Estimated Residual Infestation

Among the 56,491 households targeted for the initial treatment phase in Arequipa, 46,897 (83%) participated in at least 1 of the treatments. A total of 35,207 (62%) households targeted for the treatment phase were treated twice, 11,690 (21%) were treated only once, and 9,594 (17%) were not treated in either step of the treatment phase (Table 2). Participation in the 2 treatments showed a strong correlation (odds ratio [OR] 1.56, 95% CI 1.54–1.57).

Our model comparing the infestation observed during the first and second insecticide treatments suggested that a single treatment was successful in 98.7% (95% CI 98.4%–98.9%) of infested households (Table 2) (http://www.spatcontrol.net/articles/Barbu2014/suppMet.pdf). Among households treated twice, estimated prevalence of infestation decreased from 35.6% before the treatment phase to 0.006% after the second treatment. Estimated initial prevalence of infestation in households participating in a single treatment (range 6.9%–12.2%) was lower than that of households that participated twice (35.6%), which suggested a strong correlation between infestation status and participation. Estimated probability of detecting infestation in an infested household during a treatment (*s*) was 57% (95% CI 0.46–0.66) (Table 2) (http://www.spatcontrol.net/articles/Barbu2014/suppMet.pdf), which is comparable to previous estimates obtained by using other methods (*25*).

Similar results were found for the district of Mariano Melgar (treated during 2011–2012) by using a difference-in-difference approach (http://www.spatcontrol.net/articles/Barbu2014/suppMet.pdf). We observed a strong reduction in infestation attributable to the treatment (OR 0.02, 95% CI 0.006–0.09]) and a strong effect of infestation on participation in the treatment (OR 4.4, 95% CI 3.5–4.5). These 2 analyses suggest that after the initial treatment phase, households that received no treatment represent >90% of infested households.

Surveillance Phase Infestations and Their Relationship to Treatment Phase

During 2009–2012, surveillance authorities received 225 reports of vector infestations within the area targeted by the treatment phase (Table 1). A total of 613 houses (including reporting houses and their immediate neighbors) were inspected during the surveillance phase. Of these 613 households, 116 (19%) were infested (http://www.spatcontrol.net/articles/Barbu2014/suppMet.pdf). Of the 116 infested houses, 29 (25%) had never been treated, 18 (16%) had been treated only once, and most (69, 59%), had been treated twice, which indicated that recolonization can occur in treated households. Among the 87 households found to be infested after treatment, most (49, 56%), had no history of infestation before treatment. No houses were observed to be continuously infested during the 2 steps of the treatment and during the surveillance phase (http://www.spatcontrol.net/articles/Barbu2014/suppMet.pdf), which suggested that treatment was highly effective.

Maps of infestation as observed during the surveillance phase and treatment histories of 2 representative districts treated during 2003–2005 and 2007–2009, respectively, show different patterns of vector presence (Figure 2). In the more recently treated district, most households (13/18, 72%) that were found to be infested during the surveillance phase had not been treated during the treatment phase; in the district treated earlier, infestation was present mainly in treated households (30/32, 94%). In the more recently treated area, infestation of a treated household was usually (3/5, 60%) associated with at least 1 neighboring nontreated infested household, whereas in the area treated earlier, such infestations were rare; only 3 (9%) of 34 were associated with neighboring nontreated households.

Among 116 households identified as infested by the surveillance program in areas targeted by the treatment phase, we found 16 households with *T. cruzi*–infected *T. infestans* bugs. These 16 households were in 5 districts and showed a strong spatial positive autocorrelation <50 m (http://www.spatcontrol.net/articles/Barbu2014/suppMet.pdf). Most (75%) of these households were treated at least once during the treatment phase.

Risk Factors for Infestation during Surveillance

Our first logistic model (Table 4) suggests that nonparticipation in, and infestation before, the treatment phase affected the observation of infestation in households during the surveillance phase. Nonparticipation and initial infestation were associated with the probability of inspection through generation of reports at the city block level (Table 5) and with the probability of infestation among inspected households (Table 5). The strong effect of time in the surveillance phase on infestation (Tables 4, 5) suggests a dynamic pattern of recolonization. The negative interaction between time since treatment and nonparticipation in the treatment phase suggests recolonization from nonparticipating households to their neighbors. The recolonization progressively dilutes the association between infestation and untreated houses. The lack of a strong interaction between time and nonparticipation at the city block level suggests less dispersal of the vectors between city blocks. Infestation before treatment is also a strong predictor of infestation during surveillance. The persistence of this association over time, combined with the progression of infestation, suggests that previous infestation is a risk factor for recolonization. This interpretation is also consistent with equally likely alternative models (http://www.spatcontrol.net/articles/Barbu2014/suppMet.pdf).

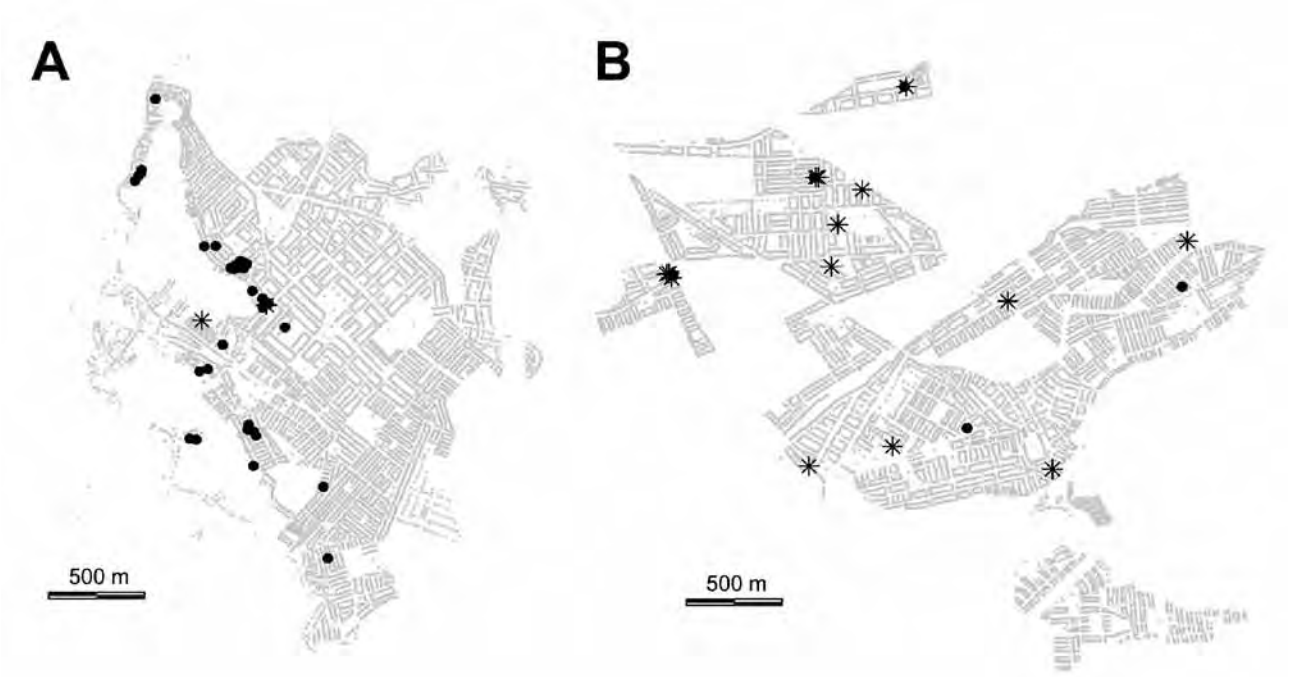

Figure 2. Infestation during the surveillance phase of a Chagas disease vector control program shown by history of treatment during the treatment phase for A) Jacobo Hunter District (treatment phase during 2003–2005) and B) Paucarpata District (treatment phase during 2006–2009, Arequipa, Peru. Stars indicate households infested during surveillance phase and not treated during treatment phase; black circles indicate households infested during surveillance phase but treated during the treatment phase; and light gray dots indicate other households (their alignment produces what appears as the background pattern of streets).

Insecticide Bioassays

We tested 21 vector populations from 12 localities from 6 of the 8 study districts for deltamethrin resistance. All insects exposed were found dead as defined by the World Health Organization (*24*) three days after the end of the exposure, which suggested that residual populations did not have complete resistance to the insecticide.

Discussion

Our results provide a consistent picture of the control of *T. infestans* bugs in Arequipa. After the treatment phase, infesting insects were successfully eliminated in nearly all participating households. Immediately thereafter, most infestations were attributable to the households that never participated in the campaign. In the years after treatment, these untreated households served as sources of insects that recolonized their neighbors. Recolonization disproportionately affects households that were infested before control activities, probably because of the continued presence of risk factors for infestation (e.g., poor quality of buildings) (*7*,*11*,*12*,*26*).

Similar studies in rural areas emphasize the role of residual populations of vectors in the recolonization of communities following vector control (*26–30*). Recolonization in urban areas was perhaps predictable because insects rapidly move between households (*25*,*31*). However, the problem of residual vector populations is different in our urban study area. In the city, residual infestation is caused mainly by lack of participation; in rural settings, by contrast, participation rates are typically high, and residual vector populations generally originate from locations that are difficult to treat (*26–30*).

Recently, insecticide-resistant populations of *T. infestans* bugs have been detected in the Gran Chaco of Argentina, Bolivia, and Paraguay, and many authors have highlighted the possibility that these resistant populations might contribute to the failure of vector control efforts (*32–34*). Persistent populations have also been observed following the treatment phase in Cochabamba, Bolivia; however, the reason for this persistence is not understood (*35*). Our study suggests that resistance is not a major cause of residual infestation in Arequipa. This result is reassuring, but partial resistance to insecticides might still be present (*36*).

There are various limitations to our study. Our analysis of the treatment phase assumes independence and similar effectiveness of the 2 treatments. If we relax this assumption, 78% of residual infestations would still have occurred in untreated households, only marginally decreasing the overall effectiveness of the treatment phase (http://www.spatcontrol.net/articles/Barbu2014/suppMet.pdf). In practice, no household was observed to be infested during both treatments of the initial treatment phase and surveillance

Table 4. Predictors of infestation among all households by *Triatoma infestans* bugs during the surveillance phase (2009–2012) in areas of Arequipa, Peru, treated during 2003–2011)*

Predictor	OR	2.5% CI	97.5% CI
Intercept	2.1×10^{-5}†	3.2×10^{-6}	1.4×10^{-4}
Infested during treatment phase	3.21†	1.96	5.24
Untreated during treatment phase	21.5‡	3.35	138
Time, y	1.55‡	1.15	2.09

*Time corresponds to the number of years after the end of the initial treatment phase in the locality as of January 1, 2013. A locality level random effect is included. CIs assume asymptotic normality. n = 56,491 (116 infested), Nagelkerke pseudo-R^2 = 0.16. OR, odds ratio.
†p<0.001.
‡p<0.01.

inspections, which suggested effectiveness of the second treatment. In addition, because there is a strong correlation between infestation and participation (*15*,*21*), households that never participated might have initially a lower prevalence of infestation than those that participated once, in contrast to the equal prevalence we assumed in our analysis. Assuming an overly conservative 5-fold lower prevalence among never-treated houses relative to once-treated households, the never-treated households would still represent >85% of the residual infestation after the treatment phase (http://www.spatcontrol.net/articles/Barbu2014/supp Met. pdf). To date, we have not observed any evidence of clustering of infestation during the surveillance phase around nontargeted areas. However, the presence of these areas, similar to that of untreated households in targeted areas, poses a potential risk for recolonization; consequently, surveillance efforts should continue to include these areas.

Despite the efficiency of treatment, we observed a strong effect of previous infestation. The permanence of factors known to favor infestation (e.g., presence of guinea pigs and building materials) might explain the higher recolonization rate. However, we could not quantify the contribution of different factors to this risk. We also did not assess the risk for transmission of the parasite. Although it appears that treated areas of the city are not under an immediate threat of transmission, a recolonization of the city would create fertile ground for reintroduction of *T. cruzi* infections. The observation during the surveillance phase of *T. cruzi* infection in several households that participated in the initial treatment phase highlights this risk. Finally, although this study covered only 1 city, it encompasses a large part of what comprises one of the main infested urban areas in Latin America and is characterized by diverse landscapes ranging from semi-rural/periurban (*37*) to urban (*25*).

For long-term control of *T. infestans* bugs, the rate of detection and elimination of vector populations in surveillance must exceed that of recolonization. The preponderant role of untreated households in maintaining infestation suggests that when a household reports the presence of a vector during surveillance, we should identify houses in the vicinity that did not participate in the control campaign and target them for inspections and treatment. The higher risk for recolonization of previously infested households also suggests that active surveillance of initially highly infested areas might be useful.

After confirmed absence of vector-borne transmission of *T. cruzi* in Chile, Uruguay, Brazil, eastern Paraguay, and parts of Argentina, southern Peru and the Gran Chaco region represent the last bastions of domestic infestation by *T. infestans* bugs (*2*,*38*,*39*). It is too early to tell whether long-term control will be achieved more or less easily in cities than in rural areas. However, our results confirm our core hypothesis: lower participation in cities such as Arequipa is the main obstacle to the effectiveness of treatment. Identification of nonparticipating households as the main reservoir for residual infestation

Table 5. Predictors of confirmed reports at the city block level and predictors of observed infestation by *Triatoma infestans* bugs among infested households during surveillance phase of vector control campaign in urban districts of Arequipa, Peru, 2009–2012*

Confirmed reports at city blocks level				Infestation among inspected households			
Predictor	OR	2.5% CI	97.5% CI	Predictor	OR	2.5% CI	97.5% CI
Intercept	8.2×10^{-5}†	4.5×10^{-6}	1.5×10^{-3}	Intercept	0.08†	0.05	0.12
Log(no. infested + 1)	2.08†	1.42	3.04	Infested	2.24‡	1.28	3.91
Time, y	1.69§	1.10	2.58	–	–	–	–
Log(no. untreated + 1)	4.85§	1.34	17.49	Untreated	5.88†	3.18	10.88
Time × log(no. untreated + 1)	0.82¶	0.66	1.02	–	–	–	–

*For confirmed reports at city blocks level, outcome is the existence of ≥1 confirmed report on the city block: reports leading to observing ≥1 infested household on the city block in subsequent inspections. Infested is number of households observed to be infested at least once during the treatment phase. Untreated is number of households not treated in the treatment phase in the city block. Time corresponds to number of years as of 2012 since the end of the initial treatment phase for the locality. A locality level random effect is included for the city block level analysis. OR, odds ratio. N = 3,727 city blocks (80 with confirmed reports) Nagelkerke pseudo-R^2 = 0.71. For infestation among inspected households, outcome is the infestation status during the first inspection during the surveillance phase. Infested is households infested in ≥1 inspection of the treatment phase. Untreated is households not treated during the treatment phase. We used a random effect on inspections batches around a reporting house. –, because all houses in a batch are inspected at the same time, time is not included as a predictor. CIs are ± values and assume asymptotic normality. n = 613 inspected (102 infested). Nagelkerke pseudo-R^2 = 0.91.
†p<0.001.
‡p<0.01.
§p<0.05.
¶p<0.1.

after the treatment phase opens new options for long-term sustainable control.

Acknowledgments

We thank the Ministerio de Salud del Peru, the Dirección General de Salud de las Personas through the Estrategia Sanitaria Nacional de Prevención y Control de Enfermedades Metaxénicas y Otras Transmitidas por Vectores, the Dirección General de Salud Ambiental, the Gobierno Regional de Arequipa, the Gerencia Regional de Salud de Arequipa, the Red de Salud Arequipa Caylloma, the Pan American Health Organization, the Canadian International Development Agency, and the Gobierno Regional de Arequipa for organizing and conducting the Chagas disease control campaign in Arequipa; and Sébastien Gourbière, Yage Wu, Daniel Rivera Lana, Karthik Sethuraman, and Dylan Tracy for providing editing suggestions for the manuscript.

This study was supported by National Institutes of Health grants NIH-NIAID R01AI101229, P50 AI074285, and K01 AI079162, and a University of Pennsylvania Global Engagement grant.

Dr Barbu is a postdoctoral fellow in epidemiology at the University of Pennsylvania, Philadelphia, Pennsylvania. His primary research interest is applying computational and statistical methods to understand and control populations of Chagas disease vectors.

References

1. Maguire JH, Hoff R, Sherlock I, Guimarães AC, Sleigh AC, Ramos NB, et al. Cardiac morbidity and mortality due to Chagas' disease: prospective electrocardiographic study of a Brazilian community. Circulation. 1987;75:1140–5. http://dx.doi.org/10.1161/01.CIR.75.6.1140
2. Moncayo A. Chagas disease: current epidemiological trends after the interruption of vectorial and transfusional transmission in the Southern Cone countries. Mem Inst Oswaldo Cruz. 2003;98:577–91. http://dx.doi.org/10.1590/S0074-02762003000500001
3. Gourbière S, Dorn P, Tripet F, Dumonteil E. Genetics and evolution of triatomines: from phylogeny to vector control. Heredity. 2012;108:190–202. http://dx.doi.org/10.1038/hdy.2011.71
4. Levine R. Case 12: controlling Chagas disease in the southern cone of South America. In: Center for global development, editor. Case studies in global health. Millions saved case studies. Burlington (MA): Jones & Bartlett Learning; 2007. p. 95–102.
5. Porcasi X, Catalá S, Hrellac H, Scavuzzo M, Gorla D. Infestation of rural houses by *Triatoma infestans* (Hemiptera: Reduviidae) in southern area of Gran Chaco in Argentina. J Med Entomol. 2006;43:1060–7. http://dx.doi.org/10.1603/0022-2585(2006)43[1060:IORHBT]2.0.CO;2
6. Gurevitz JM, Gaspe MS, Enriquez GF, Provecho YM, Kitron U, Gürtler RE. Intensified surveillance and insecticide-based control of the Chagas disease vector *Triatoma infestans* in the Argentinean Chaco. PLoS Negl Trop Dis. 2013;7:e2158. http://dx.doi.org/10.1371/journal.pntd.0002158
7. Levy MZ, Bowman NM, Kawai V, Waller LA, Cornejo del Carpio JG, Benzaquen EC, et al. Periurban *Trypanosoma cruzi*–infected *Triatoma infestans*, Arequipa, Peru. Emerg Infect Dis. 2006;12:1345–52. http://dx.doi.org/10.3201/eid1209.051662
8. Bayer AM, Hunter GC, Gilman RH, Cornejo del Carpio JG, Naquira C, Bern C, et al. Chagas disease, migration and community settlement patterns in Arequipa, Peru. PLoS Negl Trop Dis. 2009;3:e567. http://dx.doi.org/10.1371/journal.pntd.0000567
9. Oficina Técnica de Difusión INEI. IV Censo nacional agropecuario, nota de prensa. Lima, Peru: Instituto Nacional de Estadística e Informática. July 10, 2012 [cited 2013 Jul 8]. http://www.inei.gob.pe/web/NotaPrensa/Attach/14584.pdf
10. Lumbreras Cruz H. Epidemiology of Chagas disease during the urbanization of Miraflores de Arequipa [in Spanish]. Archivos Patologia. 1952;6:191–200.
11. Cecere MC, Canale DM, Gürtler RE. Effects of refuge availability on the population dynamics of *Triatoma infestans* in central Argentina. Journal of Applied Ecology. 2003;40:742–56. http://dx.doi.org/10.1046/j.1365-2664.2003.00825.x
12. Gürtler RE, Kitron U, Cecere MC, Segura EL, Cohen JE. Sustainable vector control and management of Chagas disease in the Gran Chaco, Argentina. Proc Natl Acad Sci U S A. 2007;104:16194–9. http://dx.doi.org/10.1073/pnas.0700863104
13. Saunders M, Small A, Dedicoat M, Roberts L. The development and validation of a risk score for household infestation by *Triatoma infestans*, a Bolivian vector of Chagas disease. Trans R Soc Trop Med Hyg. 2012;106:677–82. http://dx.doi.org/10.1016/j.trstmh.2012.07.006
14. Escobal J. The determinants of nonfarm income diversification in rural Peru. World Development. 2001;29:497–508. http://dx.doi.org/10.1016/S0305-750X(00)00104-2
15. Buttenheim AM, Paz-Soldan V, Barbu C, Skovira C, Calderón JQ, Riveros LM, et al. Is participation contagious? Evidence from a household vector control campaign in urban Peru. J Epidemiol Community Health. 2014;68:103–9. http://dx.doi.org/10.1136/jech-2013-202661
16. Google Earth. Arequipa, Peru, metropolis. Mountain View (CA): Google Inc. Aug 17, 2009 [cited 2010 Apr 1]. http://www.google.com/earth/index.html.
17. Delgado S, Ernst KC, Pumahuanca ML, Yool SR, Comrie AC, Sterling CR, et al. A country bug in the city: urban infestation by the Chagas disease vector *Triatoma infestans* in Arequipa, Peru. Int J Health Geogr. 2013;12:48. http://dx.doi.org/10.1186/1476-072X-12-48
18. Palomino M, Villaseca P, Cárdenas F, Ancca J, Pinto M. Efficiency and residuality of two insecticide pyrethroids against *Triatoma infestans* in three types of housing: field evaluation in Arequipa, Peru [in Spanish]. Perú Revista Peruana de Medicina Experimental y Salud Publica. 2008;25:9–16.
19. Bates D, Maechler M, Bolker B. lme4: linear mixed-effects models using S4 classes, 2013. R package version 0.999999–2 [cited 2014 Jul 25]. http://CRAN.R-project.org/package=lme4.
20. Levy MZ, Barbu CM, Castillo-Neyra R, Quispe-Machaca VR, Ancca-Juarez J, Escalante-Mejia P, et al. Urbanization, land tenure security and vector-borne Chagas disease. Proc Biol Sci. 2014;281:20141003. http://dx.doi.org/10.1098/rspb.2014.1003
21. Hong A, Barbu C, Small D, Levy M. Mapping the spatial distribution of a disease transmitting insect in the presence of surveillance error and missing data.. J R Stat Soc [Ser A]. 2014 [cited 2014 Sep 22]. http://onlinelibrary.wiley.com/enhanced/doi/10.1111/rssa.12077/
22. Nagelkerke NJ. A note on a general definition of the coefficient of determination. Biometrika. 1991;78:691–2. http://dx.doi.org/10.1093/biomet/78.3.691
23. R Core Team. R: a language and environment for statistical computing. Vienna: R Foundation for Statistical Computing, 2014 [cited 2014 Jul 25]. http://www.R-project.org.
24. Centro de Investigaciones de Plagas e Insecticidas/ Centro Institucional de Investigaciones Cientificas y Técnicas de las Fuerzas Armadas/Consejo Nacional de Investigaciones Científicas y

Técnicas (CIPEIN/CITEFA/CONICET). Protocolo de evaluación de efecto insecticida en *Triatoma infestans*. Buenos Aires, Argentina: CIPEIN/WHO/TDR, 2005 [cited 2013 Jul 15]. http://www.anmat.gov.ar/webanmat/Protocolo_Traitoma.asp.

25. Barbu CM, Hong A, Manne JM, Small DS, Quintanilla Calderón JE, Sethuraman K, et al. The effects of city streets on an urban disease vector. PLOS Comput Biol. 2013;9:e1002801. http://dx.doi.org/10.1371/journal.pcbi.1002801
26. Gürtler RE, Petersen RM, Cecere MC, Schweigmann NJ, Chuit R, Gualtieri JM, et al. Chagas disease in north-west Argentina: risk of domestic reinfestation by *Triatoma infestans* after a single community-wide application of deltamethrin. Trans R Soc Trop Med Hyg. 1994;88:27–30. http://dx.doi.org/10.1016/0035-9203(94)90483-9
27. Gürtler RE, Cecere M, Canale D, Castañera M, Chuit R, Cohen J. Monitoring house reinfestation by vectors of Chagas disease: a comparative trial of detection methods during a four-year follow-up. Acta Trop. 1999;72:213–34. http://dx.doi.org/10.1016/S0001-706X(98)00096-5
28. Cecere MC, Vazquez-Prokopec GM, Gürtler RE, Kitron U. Spatio-temporal analysis of reinfestation by *Triatoma infestans* (Hemiptera: Reduviidae) following insecticide spraying in a rural community in northwestern Argentina. Am J Trop Med Hyg. 2004;71:803–10.
29. Pérez de Rosas AR, Segura EL, García BA. Microsatellite analysis of genetic structure in natural *Triatoma infestans* (Hemiptera: Reduviidae) populations from Argentina: its implication in assessing the effectiveness of Chagas' disease vector control programmes. Mol Ecol. 2007;16:1401–12. http://dx.doi.org/10.1111/j.1365-294X.2007.03251.x
30. Gaspe MS, Gurevitz JM, Gürtler RE, Dujardin J-P. Origins of house reinfestation with *Triatoma infestans* after insecticide spraying in the Argentine Chaco using wing geometric morphometry. Infect Genet Evol. 2013;17:93–100. http://dx.doi.org/10.1016/j.meegid.2013.03.044
31. Levy MZ, Quíspe-Machaca VR, Ylla-Velasquez JL, Waller LA, Richards JM, Rath B, et al. Impregnated netting slows infestation by *Triatoma infestans*. Am J Trop Med Hyg. 2008;79:528–34.
32. Picollo MI, Vassena C, Orihuela PS, Barrios S, Zaidemberg M, Zerba E. High resistance to pyrethroid insecticides associated with ineffective field treatments in *Triatoma infestans* (Hemiptera: Reduviidae) from northern Argentina. J Med Entomol. 2005;42:637–42. http://dx.doi.org/10.1603/0022-2585(2005)042[0637:HRTPIA]2.0.CO;2
33. Toloza AC, Germano M, Cueto GM, Vassena C, Zerba E, Picollo MI. Differential patterns of insecticide resistance in eggs and first instars of *Triatoma infestans* (Hemiptera: Reduviidae) from Argentina and Bolivia. J Med Entomol. 2008;45:421–6. http://dx.doi.org/10.1603/0022-2585(2008)45[421:DPOIRI]2.0.CO;2
34. Germano MD, Acevedo GR, Cueto GA, Toloza A, Vassena C, Picollo M. New findings of insecticide resistance in *Triatoma infestans* (Heteroptera: Reduviidae) from the Gran Chaco. J Med Entomol. 2010;47:1077–81. http://dx.doi.org/10.1603/ME10069
35. Espinoza N, Borrás R, Abad-Franch F. Chagas disease vector control in a hyperendemic setting: the first 11 years of intervention in Cochabamba, Bolivia. PLoS Negl Trop Dis. 2014;8:e2782. http://dx.doi.org/10.1371/journal.pntd.0002782
36. Adelman ZN, Kilcullen KA, Koganemaru R, Anderson MAE, Anderson TD, Miller DM. Deep sequencing of pyrethroid-resistant bed bugs reveals multiple mechanisms of resistance within a single population. PLoS ONE. 2011;6:e26228. http://dx.doi.org/10.1371/journal.pone.0026228
37. Levy MZ, Kawai V, Bowman NM, Waller LA, Cabrera L, Pinedo-Cancino VV, et al. Targeted screening strategies to detect *Trypanosoma cruzi* infection in children. PLoS Negl Trop Dis. 2007;1:e103. http://dx.doi.org/10.1371/journal.pntd.0000103
38. Noireau F. Wild *Triatoma infestans*, a potential threat that needs to be monitored. Mem Inst Oswaldo Cruz. 2009;104:60–4. http://dx.doi.org/10.1590/S0074-02762009000900010
39. Ceballos LA, Piccinali RV, Marcet PL, Vazquez-Prokopec GM, Cardinal MV, Schachter-Broide J, et al. Hidden sylvatic foci of the main vector of Chagas disease *Triatoma infestans*: threats to the vector elimination campaign? PLoS Negl Trop Dis. 2011;5:e1365. http://dx.doi.org/10.1371/journal.pntd.0001365

Address for correspondence: Corentin M. Barbu or Michael Z. Levy, Center for Clinical Epidemiology and Biostatistics, Perelman School of Medicine, University of Pennsylvania, 715 Blockley Hall, 423 Guardian Dr, Philadelphia, PA 19104-6021, USA; email: corentin.barbu@gmail.com or mzlevy@mail.med.upenn.edu

Two *Anaplasma phagocytophilum* Strains in *Ixodes scapularis* Ticks, Canada

Chantel N. Krakowetz, Antonia Dibernardo, L. Robbin Lindsay, and Neil B. Chilton

We developed PCR-based assays to distinguish a human pathogenic strain of *Anaplasma phagocytophilum*, Ap-ha, from Ap-variant 1, a strain not associated with human infection. The assays were validated on *A. phagocytophilum*–infected black-legged ticks (*Ixodes scapularis*) collected in Canada. The relative prevalence of these 2 strains in *I. scapularis* ticks differed among geographic regions.

The gram-negative bacterium *Anaplasma phagocytophilum* is the causative agent of human granulocytic anaplasmosis (HGA) in the United States (*1*). More than 90% of HGA cases occur in the Upper Midwest and Northeast (*2*). In these regions, black-legged ticks (*Ixodes scapularis*) are the vectors of a human pathogenic strain (Ap-ha) and a variant strain (Ap-variant 1) of *A. phagocytophilum* (*3*–*7*), the latter of which appears not to be associated with human infection (*1*,*3*). HGA represents an emerging disease in southern Canada because populations of *I. scapularis* ticks have become established or are in the process of becoming established (*8*,*9*). However, there is limited information on the occurrence of *A. phagocytophilum* in these ticks (*10*–*12*) and the proportion of ticks infected with the Ap-ha strain.

The most commonly used method to distinguish the human pathogenic strain of *A. phagocytophilum* from those not associated with human infection is to sequence the 16S rRNA gene (*3*–*7*,*13*). The Ap-ha strain differs from the Ap-variant 1 strain by 2 nucleotide differences at the 5′ end of the gene sequence (*1*,*3*). However, there is a need for an alternative to currently used PCR-based methods for strain identification that are reliable, but faster and more cost-effective. Therefore, the objectives of the current study were to determine the proportion of black-legged ticks infected with *A. phagocytophilum* in different geographic regions of Canada, and to develop restriction fragment length polymorphism (RFLP) and single nucleotide polymorphism (SNP) genotyping assays, targeting the 16S rRNA gene, to differentiate the Ap-ha strain from the Ap-variant 1 strain. We assessed the usefulness of these assays and determined the prevalence of the Ap-ha strain in *I. scapularis* ticks from different geographic regions of Canada.

Author affiliations: University of Saskatchewan, Saskatoon, Saskatchewan, Canada (C.N. Krakowetz, N.B. Chilton); and Public Health Agency of Canada, Winnipeg, Manitoba, Canada (A. Dibernardo, L.R. Lindsay)

DOI: http://dx.doi.org/10.3201/eid2012.140172

The Study

We conducted real-time PCR analyses targeting the *msp2* gene on genomic (g) DNA of 12,606 *I. scapularis* ticks collected across Canada (online Technical Appendix 1, http://wwwnc.cdc.gov/EID/article/20/12/14-0172-Techapp1.pdf). Of these, 169 (1.3%) ticks were PCR-positive (Table 1). There were significant differences (χ^2_5 = 129.7, p<0.001) in the proportions of ticks infected with *A. phagocytophilum* among geographic regions; with a greater proportion of PCR-positive ticks in Manitoba than in Ontario, Quebec, and the Atlantic provinces.

We developed PCR-based assays to distinguish the Ap-ha strain from the Ap-variant 1 strain of *A. phagocytophilum* based on DNA sequence comparisons of the 16S rRNA gene of each strain (online Technical Appendix 1) over a much larger region (875 bp) than in previous studies (*1*,*3*). In addition to the 2 nucleotide differences described previously (*1*,*3*), a third difference (at position 536) was detected in the aligned sequences (online Technical Appendix 2, http://wwwnc.cdc.gov/EID/article/20/12/14-0172-Techapp2.pdf). This nucleotide alteration in the DNA sequence of the Ap-variant 1 strain was associated with a restriction site for the endonuclease *Kpn2I* (T/CCGGA) that was absent in the sequence of the Ap-ha strain. Two PCR-RFLP assays (online Technical Appendix 1), developed at different laboratories, were designed on the basis of this sequence difference and tested on 22 amplicons derived from *A. phagocytophilum*–infected ticks collected in Minnesota, USA (n = 17) and Manitoba (n = 5). Identical results were obtained for both assays. Three different RFLP patterns were produced. Eighteen amplicons remained undigested (i.e., a single band of ≈920 bp), and 3 amplicons had 2 bands (≈360 and ≈550 bp), representing the expected patterns for the Ap-ha strain and Ap-variant 1 strain, respectively (Figure 1). These results were confirmed on the basis of comparisons of the DNA sequences of representative samples. The RFLP pattern of 1 amplicon, derived from the gDNA of a female tick from Itasca State Park, Minnesota, consisted of 3 bands (≈360, ≈550, and ≈920 bp) (online Technical Appendix 2), suggesting a mixture of the 2 strains. Additional analyses of another 125 amplicons from *A. phagocytophilum*–infected ticks revealed that 79 (63%) had RFLP patterns consistent with the Ap-variant 1 strain, and 46 (37%) had RFLP patterns of the Ap-ha strain. The DNA sequences of a subset of these samples (n = 58)

Table 1. *Anaplasma phagocytophilum* PCR–positive black-legged ticks collected from various provinces during 2007–2010, Canada

Location	2007		2008		2009		2010		2007–2010	
	No. ticks	No. +	No. ticks	No. +	No. ticks	No. +	No. ticks	No. +	No. ticks	No. + (%)
Prairie Provinces										
Alberta*	9	0	25	0	13	0	42	3	89	3 (3.4)
Saskatchewan*	5	2	3	1	1	1	1	0	10	4 (40.0)
Manitoba	35	2	156	4	119	6	260	20	570	32 (5.6)
Central Canada										
Ontario	1,187	4	1,402	3	856	3	962	3	4,407	13 (0.3)
Quebec	982	13	1,687	26	1,026	8	1,002	24	4,697	71 (1.5)
Atlantic Provinces										
New Brunswick	129	1	174	0	189	4	271	10	763	15 (2.0)
Nova Scotia	201	2	394	4	378	4	676	9	1,649	19 (1.2)
Prince Edward Island	54	3	76	1	107	3	122	3	359	10 (2.8)
Newfoundland*	11	0	9	0	15	1	27	1	62	2 (3.2)
Total	2,613	27	3,926	39	2,704	30	3,363	73	12,606	169 (1.3)

*Data from these provinces were not included in the statistical analyses because sample sizes (2007–2010) were <100 ticks.

showed 100% agreement between RFLP pattern and strain type of *A. phagocytophilum* (i.e., 24 of the Ap-ha strain and 34 of the Ap-variant 1 strain).

We also designed a custom TaqMan SNP genotyping assay (https://www.lifetechnologies.com/order/custom-genomic-products/tools/genotyping) to differentiate the two *A. phagocytophilum* strains on the basis of a nucleotide difference at the 5′ end of the 16S rRNA gene sequence (online Technical Appendix 1). The SNP assay clearly discriminated between ticks infected with the Ap-ha and/or Ap-variant 1 strains (Figure 2). Of the 142 amplicons tested by this assay, 82 (58%) contained the Ap-variant 1 strain, 59 (42%) contained the Ap-ha strain, and 1 contained a mixture of both strains, which was in 100% agreement with the results of the RFLP analyses and DNA sequencing. The results of the SNP analyses also revealed a significant difference ($\chi^2_2 = 40.48$, $p<0.001$) in the proportions of *I. scapularis* ticks infected with the Ap-ha strain among geographic regions (Table 2). A smaller proportion of ticks from Central Provinces were infected with the Ap-ha strain when compared with those from the Prairie and Atlantic Provinces.

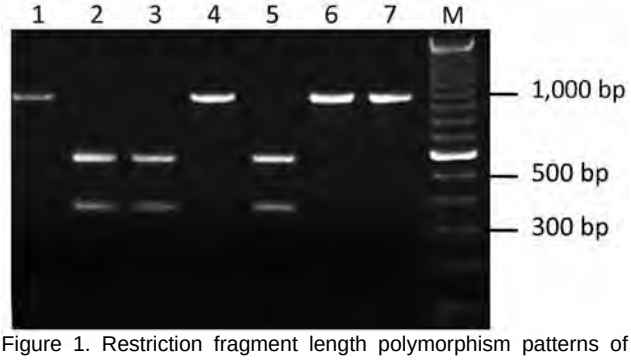

Figure 1. Restriction fragment length polymorphism patterns of 16S DNA for 7 *Anaplasma phagocytophilum* PCR–positive *Ixodes scapularis* ticks. All amplicons were produced by semi-nested PCR and digested with the restriction enzyme *Kpn2I*. Lane M, molecular mass marker.

Conclusions

A small proportion (1.3%) of *I. scapularis* ticks collected in Canada were infected with *A. phagocytophilum*. The prevalence of *A. phagocytophilum*–infected ticks differed among geographic regions, but the potential significance of this finding needs to be explored further. Although knowledge of the prevalence of *A. phagocytophilum*–infected *I. scapularis* ticks provides some information for determining the public health risks for HGA, the prevalence of the Ap-ha strain of *A. phagocytophilum* in black-legged

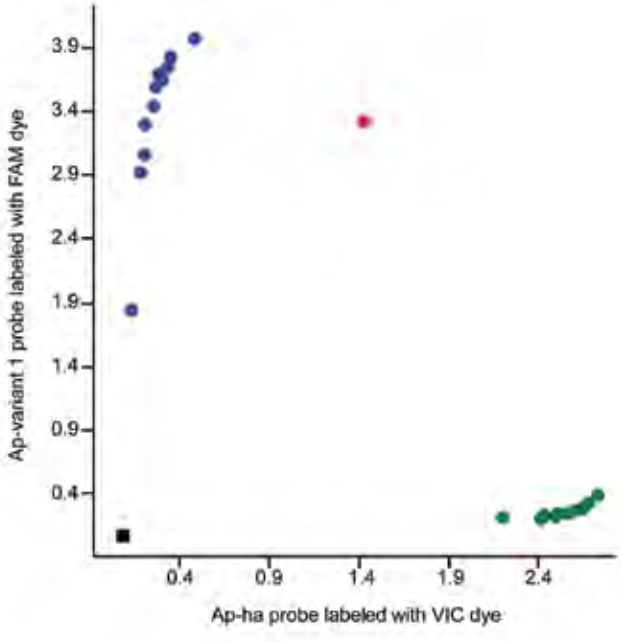

Figure 2. Allelic discrimination plot for the *Anaplasma* single nucleotide polymorphism assay based on the 16S RNA gene. Blue circles represent samples that contain the Ap-ha strain; green circles represent samples that contain the Ap-variant 1 strain. The red circle represents a sample containing a mixture of both strains. The black square represents the control (no template).

Table 2. Black-legged ticks infected with the Ap-ha or Ap-variant 1 strain of *Anaplasma phagocytophilum* based on analyses using the TaqMan SNP genotyping assay,* Canada

Province	No. ticks	Ap-ha (%)	Ap-variant 1 (%)
Prairie Provinces			
Alberta	1	1 (100)	0 (0)
Saskatchewan†	2	2 (100)	0 (0)
Manitoba	17	15 (88.2)	2 (11.8)
Central Canada			
Ontario	24†	2 (8.3)	22 (91.7)
Quebec	47	9 (19.1)	38 (80.9)
Atlantic Provinces			
Prince Edward Island	7	3 (42.9)	4 (57.1)
New Brunswick	10	6 (60.0)	4 (40.0)
Nova Scotia	17	8 (47.1)	9 (52.9)
Total	125	46 (36.8)	79 (63.2)

*http://www.lifetechnologies.com/search/global/searchAction.action?query=SNP&resultPage=1&resultsPerPage=15&autocomplete.
†Includes 13 ticks listed in Table 1 and an additional 11 *A. phagocytophilum*–infected ticks collected by drag sampling at 2 sites in Ontario.

ticks should be considered for risk assessment, since the Ap-ha strain, and not the Ap-variant 1 strain, is most often associated with clinical cases of HGA (*4*).

For the current study, 3 PCR-based assays were developed to distinguish the Ap-ha strain from the Ap-variant 1 strain. DNA sequencing of representative samples confirmed the reliability of these assays. Each of the 3 assays detected the presence of both strains in the gDNA of a female tick. Mixed infections of both strains in *I. scapularis* ticks have been reported (*4*), but appear to be uncommon. Results of these assays also were 100% concordant with the results of 2 RFLP assays (developed at different laboratories) that were tested on the same gDNA samples. Similarly, there was total concordance in the identifications of the *A. phagocytophilum* strains present within 125 infected ticks collected across Canada by using the seminested PCR-RFLP assay and the TaqMan SNP genotyping assay. The results of these analyses revealed significant differences in the proportion of black-legged ticks infected with the Ap-ha strain among geographic regions ($p<0.001$). The public health implications of these findings need to be examined in more detail, using the molecular assays developed in this study.

The TaqMan SNP genotyping assay is ideal for clinical and epidemiologic use where it may be essential to distinguish between the 2 strains of *A. phagocytophilum* in *I. scapularis* to assess the potential risk for human infection. However, in a clinical setting, it remains to be established how this assay would be incorporated into or supplement the current diagnostic approach for detecting *A. phagocytophilum* infections in humans. This test is less technically demanding and takes less time to perform than nested/seminested PCR-RFLPs and DNA sequencing analyses. Moreover, this method eliminates the need for postamplification manipulations and technical problems that are sometimes associated with RFLP analyses of amplicons produced by nested PCR (*14*,*15*). Nonetheless, given the 100% concordance in the results of the different analytical methods, the PCR-RFLP assays provide a reliable and cost-effective approach for distinguishing the Ap-ha strain from the Ap-variant 1 strain of *A. phagocytophilum*. The PCR-RFLP assays will be particularly useful in research laboratories that lack the capacity to conduct real-time PCRs providing an independent and relatively inexpensive method to confirm the results of the SNP assay.

Acknowledgments

We thank David Nietzel and Melissa Kemperman (Minnesota Department of Health) for providing the black-legged ticks from Minnesota, and Tim Kurtti (University of Minnesota) for supplying the equine isolate of *A. phagocytophilum* [MN-93]. We also thank Shaun Dergousoff and Allison Sproat for laboratory assistance.

Funding for this work was provided by the Natural Sciences and Engineering Research Council of Canada (Discovery Grant to N.B.C., CGSM and Vanier Canada Graduate Scholarships to C.N.K.), the Canadian Foundation for Innovation (to N.B.C.), and the Provincial Government of Saskatchewan and the University of Saskatchewan (Saskatchewan Innovation and Opportunity Scholarship (to C.N.K.).

Ms Krakowetz is a PhD candidate in the Biology Department at the University of Saskatchewan. Her research focus is on the population genetics and bacteria of black-legged ticks in Canada.

References

1. Chen SM, Dumler JS, Bakken JS, Walker DH. Identification of a granulocytotropic *Ehrlichia* species as the etiologic agent of human disease. J Clin Microbiol. 1994;32:589–95.
2. Dahlgren FS, Mandel EJ, Krebs JW, Massung RF, McQuiston JH. Increasing incidence of *Ehrlichia chaffeensis* and *Anaplasma phagocytophilum* in the United States, 2000–2007. Am J Trop Med Hyg. 2011;85:124–31. http://dx.doi.org/10.4269/ajtmh.2011.10-0613
3. Massung RF, Slater K, Owens JH, Nicholson WL, Mather TN, Solberg VB, et al. Nested PCR assay for detection of granulocytic ehrlichiae. J Clin Microbiol. 1998;36:1090–5.
4. Massung RF, Mauel MJ, Owens JH, Allan N, Courtney JW, Stafford KC, et al. Genetic variants of *Ehrlichia phagocytophila*, Rhode Island and Connecticut. Emerg Infect Dis. 2002;8:467–72. http://dx.doi.org/10.3201/eid0805.010251
5. Courtney JW, Dryden RL, Wyleto P, Schneider BS, Massung RF. Characterization of *Anaplasma phagocytophila* and *Borrelia burgdorferi* genotypes in *Ixodes scapularis* ticks from Pennsylvania. Ann N Y Acad Sci. 2003;990:131–3. http://dx.doi.org/10.1111/j.1749-6632.2003.tb07351.x
6. Michalski M, Rosenfield C, Erickson M, Selle R, Bates K, Essar D, et al. *Anaplasma phagocytophilum* in central and western Wisconsin: a molecular survey. Parasitol Res. 2006;99:694–9. http://dx.doi.org/10.1007/s00436-006-0217-9
7. Steiner FE, Pinger RR, Vann CN, Grindle N, Civitello D, Clay K, et al. Infection and co-infection rates of *Anaplasma phagocytophilum* variants, *Babesia* spp., *Borrelia burgdorferi*, and the

rickettsial endosymbiont in *Ixodes scapularis* (Acari: Ixodidae) from sites in Indiana, Maine, Pennsylvania, and Wisconsin. J Med Entomol. 2008;45:289–97. http://dx.doi.org/10.1603/0022-2585(2008)45[289:IACROA]2.0.CO;2
8. Ogden NH, Lindsay LR, Morshed M, Sockett PN, Artsob H. The emergence of Lyme disease in Canada. CMAJ. 2009;180:1221–4. http://dx.doi.org/10.1503/cmaj.080148
9. Bouchard C, Beauchamp G, Nguon S, Trudel L, Milord LF, Lindsay LR, et al. Associations between *Ixodes scapularis* ticks and small mammal hosts in a newly endemic zone in southeastern Canada: implications for *Borrelia burgdorferi* transmission. Ticks Tick Borne Dis. 2011;2:183–90. http://dx.doi.org/10.1016/j.ttbdis.2011.03.005
10. Ogden NH, Lindsay RL, Hanincova K, Barker IK, Bigras-Poulin M, Charron DF, et al. Role of migratory birds in introduction and range expansion of *Ixodes scapularis* ticks and of *Borrelia burgdorferi* and *Anaplasma phagocytophilum* in Canada. Appl Environ Microbiol. 2008;74:1780–90. http://dx.doi.org/10.1128/AEM.01982-07
11. Bouchard C, Leighton PA, Beauchamp G, Nguon S, Trudel L, Milord LF, et al. Harvested white-tailed deer as sentinel hosts for early establishing *Ixodes scapularis* populations and risk from vector-borne zoonoses in southeastern Canada. J Med Entomol. 2013;50:384–93. http://dx.doi.org/10.1603/ME12093
12. Dibernardo A, Cote T, Ogden NH, Lindsay RL. The prevalence of *Borrelia miyamotoi* infection, and co-infections with other *Borrelia* spp. in *Ixodes scapularis* ticks collected in Canada. Parasites & Vectors. 2014 7:183. http://dx.doi.org/10.1186/1756-3305-7-183
13. Massung RF, Courtney JW, Hiratzka SL, Pitzer VE, Smith G, Dryden RL. *Anaplasma phagocytophilum* in white-tailed deer. Emerg Infect Dis. 2005;11:1604–6. http://dx.doi.org/10.3201/eid1110.041329
14. Kim E-J, Bauer C, Grevelding CG, Quack T. Improved PCR/nested PCR approaches with increased sensitivity and specificity for the detection of pathogens in hard ticks. Ticks Tick Borne Dis. 2013;4:409–16. http://dx.doi.org/10.1016/j.ttbdis.2013.04.004
15. Campsall PA, Au NHC, Prendiville JS, Speert DP, Tan R, Thomas EE. Detection and genotyping of varicella-zoster virus by Taqman allelic discrimination real-time PCR. 2004;42:109–13.

Address for correspondence: Neil Chilton, Department of Biology, University of Saskatchewan, 112 Science Pl, Saskatoon, SK, S7N 5E2, Canada; email: neil.chilton@usask.ca

Francisella tularensis Bacteria Associated with Feline Tularemia in the United States

Marilynn A. Larson, Paul D. Fey, Steven H. Hinrichs, and Peter C. Iwen

Tularemia in the United States was examined by reviewing 106 *Francisella tularensis* isolates, mostly from Nebraska, collected during 1998–2012: 48% of Nebraska cases were cat-associated; 7/8 human cases were caused by subtype A.I. A vaccine is needed to reduce feline-associated tularemia, and cat owners should protect against bites/scratches and limit their pet's outdoor access.

Francisella tularensis, a Tier 1 select agent, is one of the most pathogenic bacteria known and the etiologic agent of the zoonotic disease tularemia (*1*,*2*). Although the various subspecies of *F. tularensis* share considerable genomic content (>97% nt identity), they exhibit different degrees of virulence (*3*). *F. tularensis* subspecies *tularensis* (also known as type A) and subspecies *holarctica* (also known as type B) infections can be life-threatening if untreated (*1*). Type A is further subdivided into subtypes A.I and A.II; clade A.I contains strains that are associated with considerably higher death rates among humans than are the other members of this pathogenic species (*4*). Type B infections occur throughout the Northern Hemisphere, whereas type A infections occur primarily in North America (*3*).

Fatal and nonfatal cases of tularemia in domestic cats (*Felis catus*) have been reported, as has the transmission of this disease from cats to humans (*5*–*7*). Previous serologic surveys from several geographic regions determined that 12% of the domestic cats examined had antibodies to *F. tularensis* (*8*). Cases of feline-associated tularemia in humans continue to appear in the literature. However, the relative contribution of this source of *F. tularensis* transmission to humans is unknown and may be underrecognized. This study was conducted to examine the relative proportion and characteristics of feline-associated *F. tularensis* isolates within the repository at the University of Nebraska Medical Center (UNMC).

Author affiliations: University of Nebraska Medical Center, Omaha, Nebraska, USA

DOI: http://dx.doi.org/10.3201/eid2012.131101

The Study

A review was conducted of the 106 wild-type *F. tularensis* isolates voluntarily deposited in the UNMC collection during 1998–2012. These isolates were obtained from infected humans, animals, or ticks predominantly residing in Nebraska; however, isolates from several other regions were also included. Wild-type *F. tularensis* isolates had been transferred to UNMC from other locations, according to requirements of the national Select Agent Program (*2*). None of these isolates had been solicited from veterinary or environmental reference laboratories. Species identity for locally detected wild-type *F. tularensis* isolates to which humans had been exposed was confirmed by the Nebraska Public Health Laboratory in Omaha. Viable culture material was manipulated by authorized persons following select agent–approved Biosafety Level 3 criteria. For genotyping, we used the PCR-based differential insertion sequence amplification (DISA) method with the CR10 C+L+S primer set and pulsed-field gel electrophoresis (PFGE) of *Pme*I-digested *Francisella* spp. DNA, as previously described (*9*).

Of the 106 wild-type *F. tularensis* isolates in the repository, 54 (51%) were from humans for whom the source of exposure was unknown or undocumented, 29 (27%) were from cats (21) or from humans (8) with tularemia linked to infected cats, 5 (5%) were from humans with tularemia linked to infected ticks, 1 (1%) was from a human with tularemia linked to an infected rabbit, 16 (15%) were from animals with tularemia, and 1 (1%) was from an unknown host. Of the 29 isolates derived from feline-associated cases, 28 were associated with domestic cats and 1 involved a feral cat (Figure). Eight cases of human tularemia occurred through a cat bite: 7 of these cases involved adults and 1 involved a 6-year-old child. In 2 cases, the person was bitten while taking a rabbit from a cat. None of the 8 humans died.

We also analyzed a subset of the 29 *F. tularensis* isolates obtained from cats or humans bitten by cats. All but 2 of the 29 isolates were available for genotyping. DISA and PFGE results showed that 1 type B and 26 subtype A.I strains were responsible for the 27 cases of tularemia (Figure). Of the 8 cat bite–associated human tularemia cases, 1 was caused by a type B and 7 by subtype A.I strains. None of the feline-associated tularemia cases were caused by a subtype A.II strain.

PFGE demonstrated that the feline-derived *F. tularensis* A.I strains could be further divided into 4 subpopulations. For strains in 1 of these subpopulations, DISA results showed chromosomal polymorphisms in which a

1.2-kbp or a 1.5-kbp amplicon was produced. This finding is consistent with 2 unique origins for the strains, even though they were obtained from the same geographic area.

Subset analysis of Nebraska cases showed that 48% (24/50) of the wild-type *F. tularensis* isolates were feline-associated, and most of those 24 isolates (71%, 17/24) were associated with tularemia cases that occurred in 1 city in eastern Nebraska. The highest number of tularemia cases in Nebraska was reported in 2012, a year noted for extreme heat and drought conditions with warm weather beginning in early January and lasting through December. No feline-associated tularemia cases in Nebraska were reported during 1998–2004; however, 18 were reported during 2005–2011.

Conclusions

Two different molecular methods demonstrated that *F. tularensis* subtype A.I was responsible for most of the tularemia cases in cats (96%, 26/27); 1 of the 27 cases was caused by a type B strain. This finding is consistent with subtype A.I strains being found predominantly east of the 100th meridian in the United States, whereas A.II strains appear to be restricted to the west of this meridian

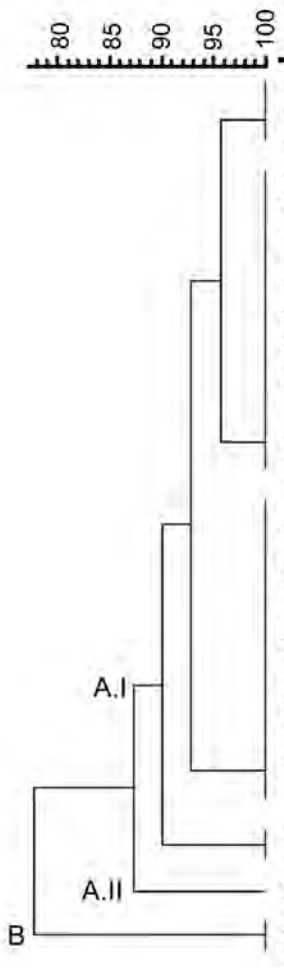

Strain	Geographic location	Host (specimen)	Year isolated	Infected source	Genotype	Amplicon size, kbp
NE-081405	NE	Human (hand)	2005	Domestic cat	A.I	1.5
NE-120312B	NE	Cat (lymph node)	2012	Domestic cat	A.I	1.5
NE-120312A	NE	Cat (lymph node)	2012	Domestic cat	A.I	1.5
SCHU S4	OH	Human (unknown)	1941	Unknown	A.I	1.2
OK-FelineNC	OK	Cat (unknown)	Unknown	Domestic cat	A.I	1.2
NE-081205	NE	Human (hand)	2005	Domestic cat	A.I	1.2
NE-050707	NE	Cat (brain)	2007	Domestic cat	A.I	1.2
NE-073007	NE	Human (finger)	2007	Domestic cat	A.I	1.2
NE-092107	NE	Cat (lymph node)	2007	Domestic cat	A.I	1.2
NE-120707	NE	Cat (liver and spleen)	2007	Domestic cat	A.I	1.2
NE-060309	NE	Cat (unknown)	2009	Feral cat	A.I	1.2
NE-050611	NE	Cat (unknown)	2011	Domestic cat	A.I	1.2
NE-090712	NE	Human (unknown)	2012	Domestic cat	A.I	1.2
NE-102412	NE	Cat (spleen and lymph node)	2012	Domestic cat	A.I	1.2
OK-98041035	OK	Cat (unknown)	1998	Domestic cat	A.I	1.2
OK-00101504	OK	Cat (unknown)	2000	Domestic cat	A.I	1.2
NC-54558-01	NC	Cat (lung)	2001	Domestic cat	A.I	1.2
NC-554559-01	NC	Cat (lymph node)	2001	Domestic cat	A.I	1.2
NE-102105	NE	Cat (blood)	2005	Domestic cat	A.I	1.2
NE-121905	NE	Human (hand)	2005	Domestic cat	A.I	1.2
NE-062008	NE	Human (hand)	2008	Domestic cat	A.I	1.5
NE-071408	NE	Cat (throat)	2008	Domestic cat	A.I	1.5
NE-083010	NE	Cat (unknown)	2010	Domestic cat	A.I	1.2
NE-041912	NE	Cat (unknown)	2012	Domestic cat	A.I	1.2
NE-101912	NE	Cat (salivary gland)	2012	Domestic cat	A.I	1.2
NE-110607	NE	Human (hand)	2007	Domestic cat	A.I	1.2
NE-061608	NE	Cat (liver and spleen)	2008	Domestic cat	A.I	1.2
WY96-3418	WY	Human	1996	Unknown	A.II	1.3
ATCC 29684	Russia	Vole	Unknown	Unknown	B	2.1
NE-061705	NE	Human (hand)	2005	Domestic cat	B	2.1

Figure. Molecular genotyping of *Francisella tularensis* isolates obtained from infected cats or humans bitten by an infected cat, United States, 1998–2012. Genotyping was performed by using pulsed-field gel electrophoresis (PFGE) and the PCR-based differential insertion sequence amplification (DISA) assay. A dendrogram of PFGE patterns obtained with *Pme*I-digested *F. tularensis* isolates is shown on the left; the scale bar at the top indicates distance in relative units. The genotype-specific amplicon lengths obtained with the DISA CR10 C+L+S primer set are shown on the right. Migration profiles of the *Pme*I restriction fragments from *F. tularensis* chromosomal DNA were normalized to *Sma*I-digested *Staphylococcus aureus* NCTC 8325 by using BioNumerics software (Applied Maths, Inc., Austin, TX, USA). Cluster analysis was performed by using the Dice correlation coefficient and the unweighted pair group mathematical average (UPGMA) clustering algorithm in the BioNumerics software. The DISA CR10 C+S primer pair identified the subtype A.I strains, whereas the CR10 C+L primer pair differentiated the subtype A.II and type B strains by the size of the amplicon produced. Underlining indicates *F. tularensis* strains SCHU S4 (subtype A.I), WY96–3418 (subtype A.II), and ATCC 29684 (type B), which were included as references. *F. tularensis* isolates NE-062508 and NE-073009 were no longer viable after storage and therefore not genotyped; these pathogens were isolated from domestic cats from eastern Nebraska (NE) in 2008 and 2009, respectively. ATCC, American Type Culture Collection; NC, North Carolina; OH, Ohio; OK, Oklahoma; WY, Wyoming.

(*4*). More importantly, this study confirms that the highly virulent A.I strains are frequent causes of tularemia in cats and humans, a finding that is in agreement with those in a previous report (*4*), and that the type B clade can cause disease in these hosts.

Although cats are a well-known vector of *F. tularensis*, the strikingly high percentage of disease associated with cats in Nebraska was unexpected (48% in Nebraska vs. 27% in the UNMC repository). Of note, the highest number of feline-derived tularemia cases occurred in a city known to have multiple feral cat colonies and during a year with extended warm weather and extreme drought conditions. Warmer temperatures can accelerate the tick life cycle, augmenting the potential for transmission of vector-borne diseases (*10*,*11*), and droughts can contribute to impaired host immunity, thereby increasing the likelihood for the transmission of zoonotic pathogens at the limited sources of water (*12*). Therefore, although the natural reservoir of *F. tularensis* is unknown, we speculate that these environmental conditions exacerbated the spread of tularemia by increasing the abundance of ticks harboring and transmitting *F. tularensis* to outdoor animals. Nevertheless, the high relative contribution of cats to disease may be due to underrecognition of an existing problem, a new emerging threat caused by environmental factors, and/or reporting or other biases.

A 2012 systematic review reported that free-ranging domestic cats are probably responsible for the greatest percentage of bird and mammal deaths (*13*). This information and the findings from the current study support the supposition that although cats are considered incidental hosts for *F. tularensis*, their inherent predatory behavior increases the likelihood that they will acquire tularemia through the consumption of infected animals and exposure to contaminated ticks, animals, or water harboring this pathogen. A vaccine for tularemia is not available in the United States, and the overall prognosis for infected persons is poor if antibiotic drug treatment is not administered early in the infection process. Therefore, cat owners should protect themselves against potential bites and/or scratches and consider limiting outdoor access for domestic cats. In addition, because tularemia is often initially misdiagnosed (*14*), confirmatory testing by public health laboratories is important and will provide critical surveillance information regarding *F. tularensis* in the environment.

The high percentage of feline-associated tularemia cases reported in this study demonstrates that outdoor domestic cats are frequent vectors of *F. tularensis*, particularly in areas where the bacterium is endemic. The cases reported in this study were primarily from urban areas with nearby access to veterinarians and with cat owners/caretakers motivated to treat infected animals; therefore, our findings may not accurately estimate the prevalence of this pathogen within the feral and rural domestic cat populations. These findings do emphasize the importance of taking appropriate measures to reduce the transmission of feline-associated tularemia to humans and the need for a vaccine that protects against the highly virulent pathogen *F. tularensis*.

Acknowledgments

We thank the Nebraska Public Health Laboratory for providing the bacterial isolates.

This study was funded in part by the Department of Pathology and Microbiology at the University of Nebraska Medical Center.

Dr Larson is an assistant professor in the Pathology and Microbiology Department at the University of Nebraska Medical Center in Omaha. Her research interests include the development of diagnostics and therapeutics for pathogen identification and treatment, respectively, as well as determining the molecular mechanisms that allow pathogens to replicate and persist.

References

1. Sjöstedt A. Tularemia: history, epidemiology, pathogen physiology, and clinical manifestations. Ann N Y Acad Sci. 2007;1105:1–29. http://dx.doi.org/10.1196/annals.1409.009
2. Centers for Disease Control and Prevention, Department of Health and Human Services (HHS). Possession, use, and transfer of select agents and toxins; final rule. Fed Regist. 2012;77:61083–115.
3. Pechous RD, McCarthy TR, Zahrt TC. Working toward the future: insights into *Francisella tularensis* pathogenesis and vaccine development. Microbiol Mol Biol Rev. 2009;73:684–711. http://dx.doi.org/10.1128/MMBR.00028-09
4. Kugeler KJ, Mead PS, Janusz AM, Staples JE, Kubota KA, Chalcraft LG, et al. Molecular epidemiology of *Francisella tularensis* in the United States. Clin Infect Dis. 2009;48:863–70. http://dx.doi.org/10.1086/597261
5. Arav-Boger R. Cat-bite tularemia in a seventeen-year-old girl treated with ciprofloxacin. Pediatr Infect Dis J. 2000;19:583–4. http://dx.doi.org/10.1097/00006454-200006000-00024
6. Capellan J, Fong IW. Tularemia from a cat bite: case report and review of feline-associated tularemia. Clin Infect Dis. 1993;16:472–5. http://dx.doi.org/10.1093/clind/16.4.472
7. Liles WC, Burger RJ. Tularemia from domestic cats. West J Med. 1993;158:619–22.
8. Magnarelli L, Levy S, Koski R. Detection of antibodies to *Francisella tularensis* in cats. Res Vet Sci. 2007;82:22–6. http://dx.doi.org/10.1016/j.rvsc.2006.06.003
9. Larson MA, Fey PD, Bartling AM, Iwen PC, Dempsey MP, Francesconi SC, et al. *Francisella tularensis* molecular typing using differential insertion sequence amplification. J Clin Microbiol. 2011;49:2786–97. http://dx.doi.org/10.1128/JCM.00033-11
10. Tabachnick WJ. Challenges in predicting climate and environmental effects on vector-borne disease episystems in a changing world. J Exp Biol. 2010;213:946–54. http://dx.doi.org/10.1242/jeb.037564
11. Estrada-Peña A, Gray JS, Kahl O, Lane RS, Nijhof AM. Research on the ecology of ticks and tick-borne pathogens—methodological principles and caveats. Front Cell Infect Microbiol. 2013;3:29. http://dx.doi.org/10.3389/fcimb.2013.00029

12 Altizer S, Dobson A, Hosseini P, Hudson P, Pascual M, Rohani P. Seasonality and the dynamics of infectious diseases. Ecol Lett. 2006;9:467–84. http://dx.doi.org/10.1111/j.1461-0248.2005.00879.x

13. Loss SR, Will T, Marra PP. The impact of free-ranging domestic cats on wildlife of the United States. Nat Commun. 2013;4:1396. http://dx.doi.org/10.1038/ncomms2380

14. Weber IB, Turabelidze G, Patrick S, Griffith KS, Kugeler KJ, Mead PS. Clinical recognition and management of tularemia in Missouri: a retrospective records review of 121 cases. Clin Infect Dis. 2012;55:1283–90. http://dx.doi.org/10.1093/cid/cis706

Address for correspondence: Marilynn A. Larson, Department of Pathology and Microbiology, University of Nebraska Medical Center, 985900 Nebraska Medical Center, Omaha, NE 68198-5900, USA; email: malarson@unmc.edu

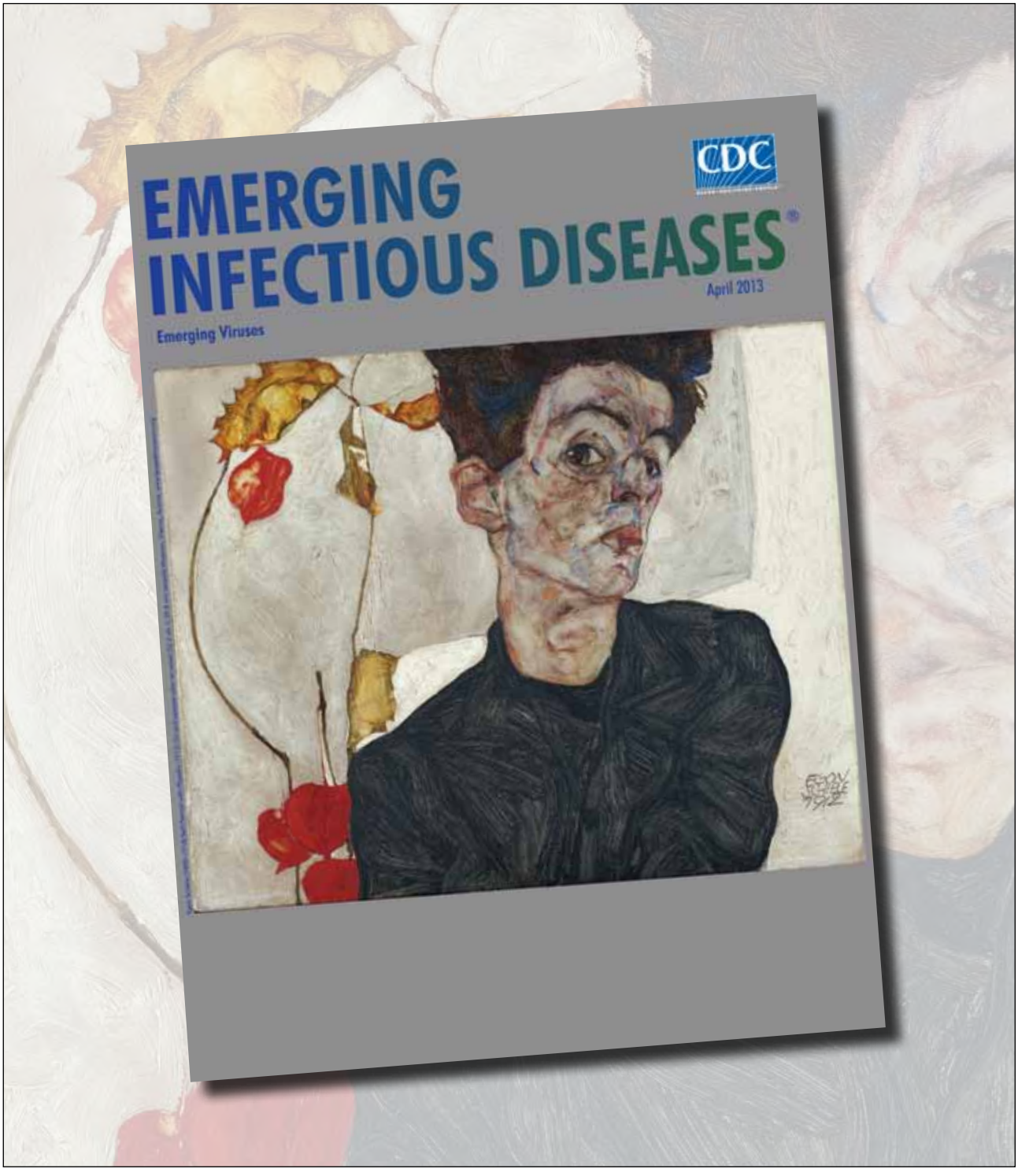

Gouleako and Herbert Viruses in Pigs, Republic of Korea, 2013

Hee Chun Chung, Van Giap Nguyen, Dane Goede, Chang Hoon Park, A. Reum Kim, Hyoung Joon Moon, Seong Jun Park, Hye Kwon Kim, and Bong Kyun Park

Several viruses in the family *Bunyaviridae* are pathogenic to animals and cause vector-borne zoonoses. In 2013, investigation of cause of death of 9 pigs on 1 farm in the Republic of Korea found infection with Gouleako and Herbert viruses. Subsequent investigation revealed high prevalence of these viruses among pigs throughout the country.

Several viruses in the family *Bunyaviridae*, such as severe fever thrombocytopenia syndrome virus, sandfly fever Naples virus, and La Crosse virus, cause vector-borne zoonotic problems (*1–7*). Recently, outbreaks of severe disease caused by Rift Valley fever virus and Schmallenberg virus produced abortion storms, resulting in a high mortality rate among newborn lambs and calves (*4*,*8*). Gouleako virus (GOLV) and Herbert virus (HEBV) have been isolated from mosquitoes (*Culex* spp.) trapped in Côte d'Ivoire (*9*,*10*); however, their infectivity or virulence have not been proven. Investigation of the cause of death of pigs in the Republic of Korea identified GOLV and HEBV infection.

The Study

In March 27, 2013, a piglet, ≈8 weeks of age, on a 150-sow farm in Gyeonggi, Republic of Korea, died after onset of high fever (40°C), wasting, respiratory disease, and diarrhea. The carcass was sent to the Department of Veterinary Medicine Virology Laboratory, Seoul National University, Seoul, Republic of Korea, for diagnostics. Necropsy and microscopic examinations revealed greenish lung tissue with lymphoid depletion, consistent with severe bronchopneumonia. Despite the presence of multiple clinical signs, the results of routine tests for major pathogens in pigs (e.g., porcine reproductive and respiratory syndrome virus, porcine circovirus type 2, transmissible gastroenteritis virus, porcine epidemic diarrhea virus, *Escherichia coli*, *Streptococcus* spp., and *Salmonella* spp.) were negative.

To further explore cause of the death, we used the particle-associated nucleic acid –random PCR method (online Technical Appendix, http://wwwnc.cdc.gov/EID/article/20/12/13-1742-Techapp1.pdf). Sequencing and BLAST analysis (http://www.ncbi.nlm.nih.gov/blast/Blast.cgi) of the agent-specific amplicon simultaneously detected 2 viruses in lung tissue RNA samples. One partial sequence had 100% identity with 63 nt of the GOLV strain F23/CI/2004 glycoprotein gene (GenBank accession no. FJ765411). Another sequence had 97% similarity with 66 nt of the HEBV strain F23-K4 RNA-dependent RNA polymerase (*RdRp*) gene (GenBank accession no. EF423168).

Results were validated with reverse transcription PCR (RT-PCR) (online Technical Appendix). We obtained partial sequences of 235 nt of GOLV and 324 nt of HEBV. These sequences had 97.1% and 96.9% similarity with GOLV and HEBV, respectively, previously isolated from mosquitoes (*9*,*10*). The sequences were registered as GenBank accession nos. KF361520 and KF361522 and designated as GOLV/P1 and HEBV/P1, respectively.

During March–May 2013, we received a total of 9 dead pigs from the same farm; they had displayed various clinical signs. We further screened these pigs for the presence of GOLV and HEBV by using the same primer sets (online Technical Appendix) selective for their glycoprotein and *RdRp* genes, respectively. The results showed that the pigs were infected with GOLV and HEBV at a prevalence of 83.3% and 100%, respectively, mostly in lung samples (Table 1). The sequences obtained from this assay were registered as GenBank accession nos. KF361521 and KF361523 and designated GOLV/P8 and HEBV/P9, respectively.

Because of the high rate of GOLV positivity, we conducted a histopathologic RNA in situ hybridization study (online Technical Appendix). Hybridization signal was positive in lung and lymph node tissues and negative in intestine and control tissues. Hybridization was strong in the cytoplasm of mononuclear cells (deep blue color) (online Technical Appendix Figure 1).

Using the same RT-PCR method (online Technical Appendix), we investigated the prevalence of GOLV and HEBV in other swine populations in the Republic of Korea; we used the existing primer sets: (GOLV-NCF and GOLV-NCR) and (HEBV-F and HEBV-R). During March–September 2013, a total of 461 serum samples were randomly collected from 40 commercial swine farms in 9 provinces. Of these, 204 (44.3%) samples were positive for GOLV

Author affiliations: Seoul National University, Seoul, Republic of Korea (H.C. Chung, C.H. Park, A.R. Kim, B.K. Park); Vietnam National University of Agriculture, Hanoi, Vietnam (V.G. Nguyen); University of Minnesota, St. Paul, Minnesota, USA (D. Goede); Green Cross Veterinary Products, Yongin, Republic of Korea (H.J. Moon); Korea Research Institute of Bioscience and Biotechnology, Daejeon, Republic of Korea (S.J. Park); National Forensic Service, Chilgok, Republic of Korea (S.J. Park); and Institute for Basic Science, Daejeon (H.K. Kim)

DOI: http://dx.doi.org/10.3201/eid2012.131742

Table 1. GOLV and HEBV screening results for dead pigs on 1 farm in Gyeonggi Province, Republic of Korea, 2013*

Pig no.	Clinical signs	Age group†	Month sample collected	Sample no.	Sample type	GOLV RT-PCR	GOLV qRT-PCR, copies/μL‡	HEBV RT-PCR	HEBV qRT-PCR, copies/μL‡	Other pathogens
1	None	Finisher	Mar	P0	Lung	–	NA	+	2.57×10^3	
2	Wasting, cyanosis, fever, respiratory disorders, diarrhea	Weaned	Mar	P1	Lung§	+¶	2.03×10^3	+#	1.26×10^2	NA
				P2	Intestine	+	1.27×10^4	+	1.16×10^2	NA
3	Diarrhea, respiratory disorders	Finisher	Mar	P3	Lung	+	1.11×10^2	+	1.37×10^3	PRRSV, PCV2
				P4	Intestine	–	NA	–	.	
4	Diarrhea, respiratory disorders	Gilt	Mar	P5	Lung	+	2.53×10^3	+	5.45×10^4	PRRSV, PCV2
				P6	Intestine	–	NA	–	NA	Rotavirus, *E. coli*
5	Respiratory disorders	Weaned	Apr	P7	Lung	+	2.04×10^3	+	2.78×10^3	PRRSV, PCV2
				P8	Intestine	+¶	1.82×10^2	–	NA	
6	Diarrhea, respiratory disorders	Grower	Apr	P9	Lung	+	$5.10 \times 1\ 0^5$	+#	5.46×10^3	PRRSV
				P10	Intestine	–	NA	–	NA	
7	Diarrhea	Finisher	Mar	P11	Intestine	–	NA	–	NA	*E. coli*
8	Diarrhea	Sow	Mar	P12	Intestine	+	6.52×10^2	–	NA	Rotavirus, *E. coli*
9	None	Finisher	Mar	P13	Intestine	–	NA	–	NA	NA

*_E. coli_, _Escherichia coli_; GOLV, Gouleako virus; HEBV, Herbert virus; NA, not applicable; qRT-PCR, quantitative reverse transcription PCR; PCV2, porcine circovirus type 2; PRRSV, porcine reproductive and respiratory syndrome virus, Rota, rotavirus.
†Samples were sorted into 6 groups: female (gilt and sow), suckling (<30 d), weaned (30–60 d), grower (60–90 d); and finisher (≥90 d).
‡Amount of virus from qRT-PCR results, copies/μL (online Technical Appendix, http://wwwnc.cdc.gov/EID/article/20/12/13-1742-Techapp1.pdf).
§First sample in which virus was detected by particle-associated nucleic acid–random PCR.
¶GenBank, GOLV (P1, KF361520; P8, KF361521).
#GenBank, HEBV (P1, KF361522; P9, KF362523).

and 26 (5.6%) samples were positive for HEBV (Table 2). The rates of positivity for the investigated provinces are shown in Figure 1. When examined according to season, positive samples were more frequently found in the summer than in spring. For example, during July–August, rates were ≈65% (for GOLV) and 10% (for HEBV), but in March, rates for each virus were <10%. Rates for GOLV and HEBV positivity were higher among sows (1–4 years of age) than among pigs in other age groups (Table 2).

The study was extended to include sows on other farms in the Republic of Korea because of the major

Table 2. Pig samples positive for GOLV or HEBV by RT-PCR, Republic of Korea, 2013*

Variable	No. (%) positive GOLV	HEBV
Pig age group		
Gilt, n = 49	23 (46.9)	3 (6.1)
Sow, n = 76	42 (55.3)	12 (15.8)
Suckling, n = 90	20 (22.2)	5 (5.6)
Weaned, n = 90	44 (48.8)	2 (2.2)
Grower, n = 77	37 (48.1)	3 (3.9)
Finisher, n = 79	38 (48.1)	1 (1.3)
Total, n = 461	204 (44.3)	26 (5.6)
Sample collection		
Mar, n = 40	3 (7.5)	0
Apr, n = 40	5 (12.5)	1 (2.5)
May, n = 64	22 (34.4)	3 (4.7)
Jun, n = 72	27 (37.5)	3 (4.2)
Jul, n = 79	39 (49.4)	5 (6.3)
Aug, n = 82	66 (80.5)	10 (12.2)
Sep, n = 84	42 (50.0)	4 (4.8)
Total, n = 461	204 (44.3)	26 (5.6)

*GOLV, Gouleako virus; HEBV, Herbert virus; RT-PCR, reverse transcription PCR.

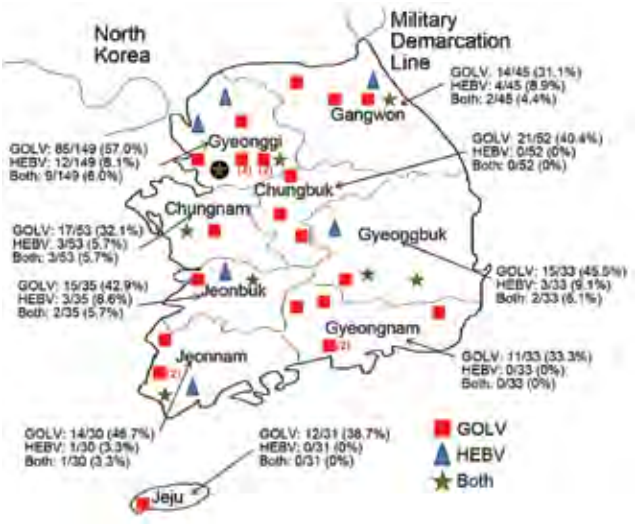

Figure 1. Distribution of swine farms investigated to determine cause of death of pigs, 9 provinces, Republic of Korea, 2013. The locations of farms are indicated, and the numbers and percentages of positive farms are shown in parentheses. Black dot indicates location of first case discovered. GOLV, Gouleako virus; HEBV, Herbert virus.

role of sows on a commercial swine farm. Pigs were divided into 3 groups and the following samples were collected: blood from healthy sows >1 year of age (n = 76), blood from abortion-problem sows (n = 13), and tissue from aborted fetuses (n = 42). Rates of virus positivity for GOLV and HEBV were higher for the 42 fetuses (33 [78.6%] and 11 [26.2%]) than for pigs in the healthy group (42 [55.3%] and 12 [15.8%]), respectively. Of the 13 abortion-problem sows, GOLV and HEBV, respectively, were found in 10 (76.9%) and 3 (23%) samples. The rates of GOLV and HEBV positivity among the healthy and abortion groups (abortion-problem sows and fetuses) were statistically compared by using the Pearson χ^2 test in SPSS version12.0 (SPSS Inc., Chicago, IL, USA). The only significant correlation found was for HEBV infection in the abortion group; $p \leq 0.05$.

Within the abortion group, pooled tissues from the 42 fetuses were screened for other pathogens (online Technical Appendix Table). The highest rate of positivity for the fetuses was for GOLV; 17 (40.5%) of the 42 samples were positive for GOLV only. Concurrent GOLV and HEBV infection was found in 9 (21.4%) samples and GOLV and swine influenza virus in 4 (9.5%) samples; no specific pathogens were detected in 7 (16.7%) samples (Technical Appendix Table).

The phylogenetic relationships of GOLV and HEBV isolated from swine in the Republic of Korea (online Technical Appendix) with the other members of family *Bunyaviridae* were analyzed; analyses were based on genes that encode the nucleocapsid protein (for GOLV) and *RdRp* (for HEBV). Of the GOLVs, the result showed that samples from the swine farms examined (KJ830623, KJ830624) clustered with GOLV strains from Africa (*9*) and showed high similarities (98.34%–98.98%) with a strain of GOLV from mosquitoes in western Africa (HQ541736) (Figure 2, panel A). Of the HEBV viruses, samples from swine farms examined (KJ830625, KJ830626) formed a branch with existing strains (KF590583, JQ659256) from mosquitoes in Côte d'Ivoire (*10*) (Figure 2, panel B). Similarities with each other were 94.46%–97.23%.

Two field GOLV strains (CP-1/2013 and CP-2/2013) used in this study were isolated from pig kidney (PK15) cells. Detailed information about the methods used to prove the results are shown in online Technical Appendix Figure 2.

Conclusions

We demonstrated that GOLV and HEBV are prevalent on swine farms in the Republic of Korea. Prevalence of these viruses was first suspected after particle-associated

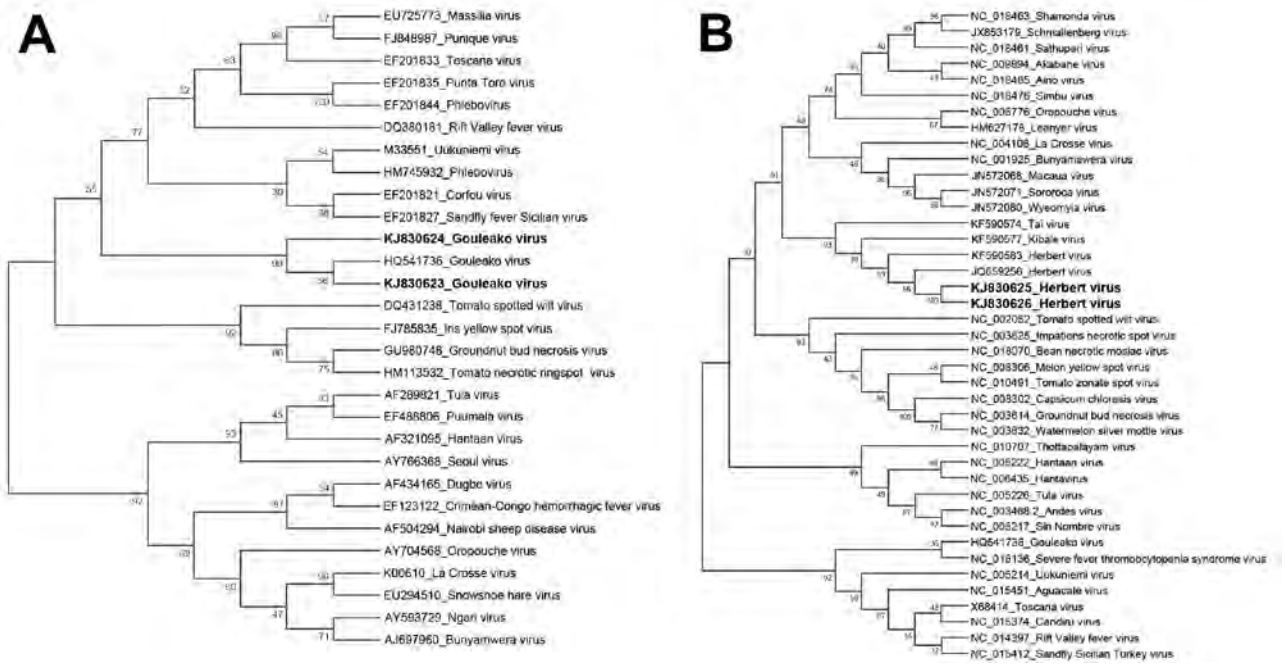

Figure 2. Phylogenetic analyses of Gouleako virus (GOLV) and Herbert virus (HEBV) collected from swine in the Republic of Korea, 2013 (KJ830623–J830626, in boldface), and other family *Bunyaviridae* viruses. The bootstrap consensus trees were constructed by using the maximum-likelihood method based on the general time-reversible model, implemented in MEGA version 6.06 (http://www.megasoftware.net). The phylogenetic trees for GOLV (A) and HEBV (B) were inferred on the basis of nucleotide sequences of the gene encoding nucleocapsid protein (GOLV) or RNA-dependent RNA polymerase (HEBV). The bootstrap values are shown next to the branches. *Bunyaviridae* virus sequences from previous studies (*9*,*10*) were used as reference sequences.

nucleic acid–random PCR of tissue from dead pigs, and it was proven by RT-PCR screening of a large collection of samples (serum, fetal tissue) from healthy and sick pigs throughout the country. The in situ hybridization method detected GOLV RNA in pig tissues and provided evidence in support of the presence of GOLV in the infected tissues of pigs. The findings of this study indicate that GOLV and HEBV may be associated with disease in pigs; investigation of the pathogenicity of the viruses in pigs, as well as their relation to other emerging viruses of swine, is needed.

Acknowledgments

We thank Su Hee Yun for expert technical assistance.

This study was supported by a grant (PJ009015) from BioGreen 21 Program, Republic of Korea.

Mr Chung is a virologist at the Department of Veterinary Medicine Virology Lab, College of Veterinary Medicine, Seoul National University, Republic of Korea. His research interests include human infectious diseases, zoonoses, vector-borne diseases, novel viruses, swine virology, transgenic pigs, endogenous retroviruses, viral enteritis of pigs, and viral diseases of animals.

References

1. Wu Y, Gao GF. Severe fever with thrombocytopenia syndrome virus expands its borders. Emerging Microbes & Infections. 2013;2:e36. http://dx.doi.org/10.1038/emi.2013.36
2. Chang MS, Woo JH. Severe fever with thrombocytopenia syndrome: tick-mediated viral disease. J Korean Med Sci. 2013;28:795–6. http://dx.doi.org/10.3346/jkms.2013.28.6.795
3. Lambert AJ, Blair CD, D'Anton M, Ewing W, Harborth M, Seiferth R, et al. La Crosse virus in *Aedes albopictus* mosquitoes, Texas, USA, 2009. Emerg Infect Dis. 2010;16:856–8. http://dx.doi.org/10.3201/eid1605.100170
4. Coetzer JA. The pathology of Rift Valley fever. II. Lesions occurring in field cases in adult cattle, calves and aborted foetuses. Onderstepoort J Vet Res. 1982;49:11–7.
5. Zhioua E, Moureau G, Chelbi I, Ninove L, Bichaud L, Derbali M, et al. Punique virus, a novel phlebovirus, related to sandfly fever Naples virus, isolated from sandflies collected in Tunisia. J Gen Virol. 2010;91:1275–83. http://dx.doi.org/10.1099/vir.0.019240-0
6. Hoffmann B, Scheuch M, Höper D, Jungblut R, Holsteg M, Schirrmeier H, et al. Novel orthobunyavirus in cattle, Europe, 2011. Emerg Infect Dis. 2012;18:469–72. http://dx.doi.org/10.3201/eid1803.111905
7. Kim KH, Yi J, Kim G, Choi SJ, Jun KI, Kim NH, et al. Severe fever with thrombocytopenia syndrome, South Korea, 2012. Emerg Infect Dis. 2013;19:1892–4. http://dx.doi.org/10.3201/eid1911.130792
8. Bilk S, Schulze C, Fischer M, Beer M, Hlinak A, Hoffmann B. Organ distribution of Schmallenberg virus RNA in malformed newborns. Vet Microbiol. 2012;159:236–8. http://dx.doi.org/10.1016/j.vetmic.2012.03.035
9. Marklewitz M, Handrick S, Grasse W, Kurth A, Lukashev A, Drosten C, et al. Gouleako virus isolated from West African mosquitoes constitutes a proposed novel genus in the family *Bunyaviridae*. J Virol. 2011;85:9227–34. http://dx.doi.org/10.1128/JVI.00230-11
10. Marklewitz M, Zirkel F, Rwego IB, Heidemann H, Trippner P, Kurth A, et al. Discovery of a unique novel clade of mosquito-associated bunyaviruses. J Virol. 2013;87:12850–65. http://dx.doi.org/10.1128/JVI.01862-13

Addresses for correspondence: Bong Kyun Park, Department of Veterinary Medicine Virology Laboratory, College of Veterinary Medicine and Research Institute for Veterinary Science, Seoul National University, Seoul 151-742, Republic of Korea; email: parkx026@snu.ac.kr

Human Infection with Influenza Virus A(H10N8) from Live Poultry Markets, China, 2014

Tao Zhang,[1] Yuhai Bi,[1] Huaiyu Tian,[1] Xiaowen Li,[1] Di Liu, Ying Wu, Tao Jin, Yong Wang, Quanjiao Chen, Ze Chen, Jianyu Chang, George F. Gao, and Bing Xu

Human infection with avian influenza virus A(H10N8) was initially reported in China in December 2013. We characterized H10N8 strains from a human patient and from poultry in live markets that infected persons had visited. Results of genome sequencing and virus characterization suggest that the virus strains that infected humans originated from these markets.

Avian influenza virus (AIV) is classified into 16 subtypes on the basis of hemagglutinin (HA) and 9 subtypes on the basis of neuraminidase (NA); additional bat-derived influenza-like genomes, H17N10 and H18N11, have recently been reported (*1*). Birds can be infected with AIV through direct contact with infected hosts or through contact with contaminated surfaces or materials, including water and food. In China, H10N8 virus was isolated from the environment of Dongting Lake in Hunan Province in 2007 (*2*) and from a duck in a live poultry market (LPM) in Guangdong Province in 2012 (*3*). This AIV was not then known to directly infect humans or other mammals.

In December 2013, H10N8 virus infection in a person was reported in Nanchang, Jiangxi Province, China (*4*); 2 more human cases followed. The initial reported case was in a 73-year-old woman who visited a local LPM 4 days before the onset of her illness (*4*). Because genetic information on AIV is essential for understanding of the biology of these viruses, their spread among avian species, and their potential transmission to humans, in January 2014, we conducted surveillance of several LPMs in Nanchang, including those visited by the 3 reported case-patients, to determine the source of these infections.

Author affiliations: Ministry of Education Key Laboratory for Earth System Modelling, Center for Earth System Science and School of Environment, Tsinghua University, Beijing, China (T. Zhang, Y. Wang, B. Xu); Chinese Academy of Sciences Institute of Microbiology, Beijing (Y. Bi, D. Liu, Y. Wu, G.F. Gao); Beijing Normal University, Beijing (H. Tian, X. Li, B. Xu); BGI-Shenzhen, Shenzhen, China (T. Jin); Wuhan Institute of Virology, Chinese Academy of Sciences, Wuhan, China (Q. Chen, Z. Chen); China Agricultural University, Beijing (J. Chang); and Chinese Center for Disease Control and Prevention, Beijing (G.F. Gao)

DOI: http://dx.doi.org/10.3201/eid2012.140911

The Study

During January 2014, we collected 226 pairs of cloacal and oropharyngeal swab specimens from apparently healthy poultry in several LPMs in Nanchang, China. The samples were stored in viral medium at 4°C until they were transported to the laboratory and then stored at –80°C until analysis. Virus material was injected into 10-day-old specific pathogen free embryonated chicken eggs; we then genetically analyzed all HA-positive samples. Viral RNA from allantoic fluid was extracted with the RNeasy Mini Kit (QIAGEN, Hilden, Germany), and cDNAs were synthesized from the viral RNA by reverse transcription PCR by using a SuperScript First-Strand Synthesis System for RT-PCR Kit (Invitrogen, Carlsbad, CA, USA). All gene segments were amplified by using a Phusion High-Fidelity PCR Kit (New England Biolabs, Ipswich, MA, USA). The PCR products were sequenced and the sequences were edited and aligned by using BioEdit software (http://www.mbio.ncsu.edu/bioedit/bioedit.html).

Two H10N8 viruses, A/chicken/Jiangxi/77/2014 (JX77) and A/chicken/Jiangxi/B15/2014 (JXB15), were isolated from the 226 pairs of swab specimens from healthy chickens. JXB15 and JX77 grew well in embryonated eggs and caused the specific pathogen free chicken embryos to die 48–72 h after inoculation; hemagglutination titers were 2^{6-7}. Genomic analysis showed that these isolates had sequence identity of ≥99% in each of the 8 genes tested with human isolate A/Jiangxi-Donghu/346/2013 (H10N8) (JX346), which was derived from the case-patient who became ill in December 2013. This finding indicates that the H10N8 virus that infected humans might have been derived from local poultry or the environments of LPMs. All 8 genes of JXB15 and JX77 were adjacent to the corresponding genes of JX346 on phylogenetic trees (Figures 1, 2). JXB15 and JX77 also shared high nucleotide sequence identity (99.3%–99.9%) with JX346 (Table 1). Phylogenetic analysis showed that the HA genes of JXB15 and JX77 belong to the Eurasian avian lineage, whereas the NA genes belong to the North American avian lineage (Figure 1). When compared with JX346, the avian isolates JXB15 and JX77 contained nucleotide differences resulting in only 5 amino acid substitutions in the HA protein: Met80Tyr, Asn116Asp, Thr188Ile, Lys415Met, and Phe536Val (Table 2). All 3 isolates shared 100% identity in their NA amino acid sequences.

[1]These authors contributed equally to this article.

Phylogenetic trees constructed from the 6 internal genes (polymerase basic [PB] 1 and 2, polymerase acidic, nucleoprotein, matrix [M], and nonstructural [NS]) showed that JXB15, JX77, and JX346 clustered closely with H9N2 viruses isolated from Jiangxi in 2010 and 2011 (Figure 2). The internal genes of JXB15 and JX77 also showed high nucleotide sequence identity with those of 5 H9N2 virus isolates collected from local poultry environments during 2010–2013, with highest similarity to those of A/environment/Jiangxi/00449/2013 (H9N2) (96.4%–99.5%) (Table 1). These findings suggest that the 6 internal genes of these 3 H10N8 viruses originated from local H9N2 viruses that have been circulating for years. The 6 internal genes of JXB15 and JX77 shared 95.9%–98.9% identity with those of the H9N2 viruses from chickens but only 69.4%–91.1% with those of H9N2 viruses from ducks (Table 1). Phylogenetic analysis showed that the PB2 genes of JXB15, JX77, and JX346 belong to the DE113-like lineage; the PB1, polymerase, and nucleoprotein genes belong to the SH/F/98-like lineage; the M genes belong to the G1-like lineage; and the NS genes belong to the BJ94-like lineage (Figure 2).

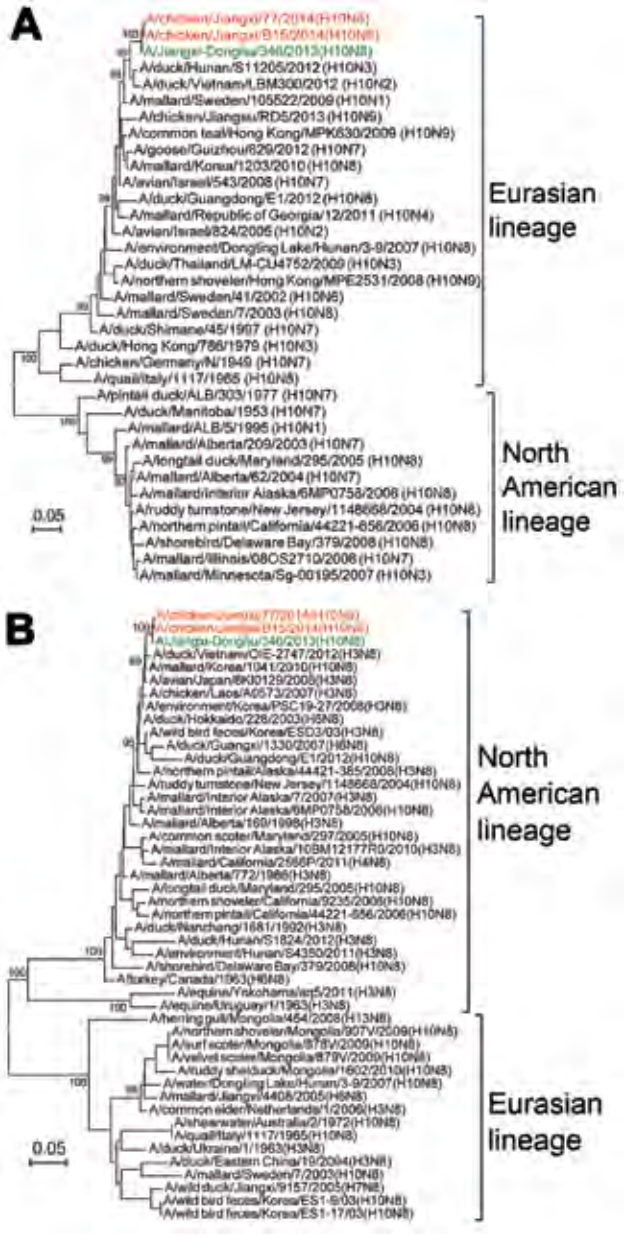

Figure 1. Phylogenetic trees of hemagglutinin (A) and neuraminidase (B) gene segments of influenza virus A(H10N8) isolates from Jiangxi Province, China, 2013–2014, compared with other closely related influenza viruses. Red indicates the novel H10N8 isolates A/chicken/Jiangxi/77/2013 (H10N8) and A/chicken/Jiangxi/B15/2014 (H10N8) that were identified in this study from poultry from live poultry markets; green indicates the human-source H10N8 virus isolate A/Jiangxi/346/2014 (H10N8). Scale bars indicate nucleotide substitutions per site.

Amino acid sites 591K, 627K, and 701N in the internal protein PB2 are key amino acids required for the mammalian adaptation of the virus (*5*). JXB15, JX77, and JX346 have 591Q and 701D in protein PB2; however, although the human JX346 virus has 627K in protein PB2, 627E is found in the poultry isolates. This substitution suggests that the mammalian-adaptation mutation to 627K might have occurred in the human body after infection. For all 3 isolates, amino acids 473V and 598L were also observed in the viral PB1 protein in mammalian cells and are assumed to enhance the replicative capacity of the virus (*6*). Deletions of the PDZ motif and 42Ser in the NS1 protein were observed; these changes have been shown to increase pathogenicity in mice (*7*). The M2 protein contained the Ser31Asn substitution, indicating resistance to adamantanes, as has been consistently observed in recent seasonal influenza virus isolates.

Conclusions

Our results provide evidence that the novel avian influenza virus A(H10N8) that infected humans in Nanchang, Jiangxi Province, China, could have derived from strains circulating in LPMs. In the LPMs, the sale of freshly slaughtered poultry, live poultry transportation, and mixed trading of different domestic animals provide environments conducive to genome segment reassortment, gene mutation, and interspecies transmission of AIVs (*8*,*9*). Human-infecting H7N9 virus strains are believed to be directly related to those found in the live poultry traded in LPMs (*10*,*11*); closure of LPMs has been shown to partly control the spread of these infections (*8*). Moreover, serologic evidence recently confirmed the infection of dogs with an H10 subtype influenza virus in close proximity to LPMs in Guangdong Province (*12*). Other recent research has shown that the internal genes of the H5N1, H7N9, and H10N8 viruses are constantly reacquired from poultry H9N2 viruses (*9*,*13*,*14*). Taken together, these data suggest that LPMs act as gene sources, facilitating reassortment of AIV genome segments (*15*).

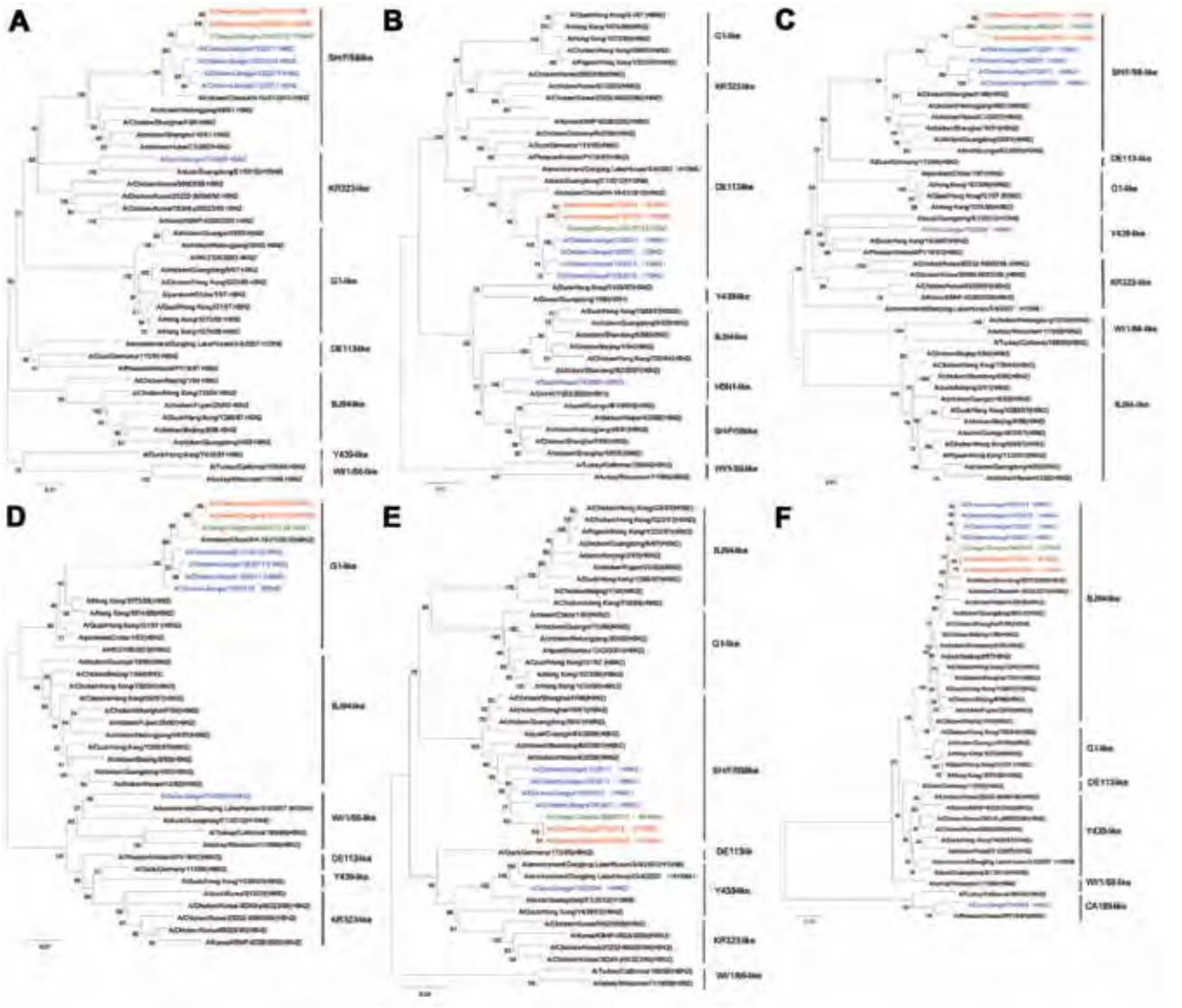

Figure 2. Phylogenetic trees of the internal genes of influenza virus A(H10N8) isolates from Jiangxi Province, China, 2013–2014, compared with other closely related influenza viruses. A) Polymerase basic 1; B) polymerase basic 2; C) nucleoprotein; D) matrix; E) polymerase acidic; F) nonstructural. Red indicates the novel H10N8 isolates A/chicken/Jiangxi/77/2013 (H10N8) and A/chicken/Jiangxi/B15/2014 (H10N8) that were identified in this study from poultry from live poultry markets; green indicates the human-source H10N8 virus isolate A/Jiangxi/346/2014 (H10N8); blue indicates the 5 H9N2 virus isolates used for comparison, A/environment/Jiangxi/00449/2013 (H9N2), A/chicken/Jiangxi/103/2010 (H9N2), A/chicken/Jiangxi/12/2011(H9N2), A/chicken/Jiangxi/19/2011 (H9N2), and A/chicken/Jiangxi/13/2011 (H9N2). Scale bars indicate nucleotide substitutions per site.

In summary, exposure to infected and/or virus-carrying poultry or to contaminated environments in LPMs and the emergence of mammal-adapted and drug-resistant viruses puts humans at high risk for infection with novel influenza viruses. Measures to improve poultry farming practices must be enforced, including strict biosecurity measures for the trade and transport of live birds, proper disposal of diseased and dead birds, and even closure of LPMs.

This research was supported by the Ministry of Science and Technology, the National Research Program (nos. 2010CB530300, 2012CB955501, 2012AA12A407, 2013AA122003), and the National Natural Science Foundation of China (nos. 41271099, 31101830). G.F.G. is a leading principal investigator of the NSFC Innovative Research Group (no. 81321063). The funding sources had no role in the study design, data collection and analysis, decision to publish, or preparation of the manuscript.

Mr Zhang is a PhD student at Tsinghua University. His primary research interest is the virologic and molecular characterization of avian influenza viruses.

Table 1. Nucleotide identity of influenza A(H10N8) and A(H9N2) viruses isolated in Jiangxi Province, China, during 2009–2014, compared with human isolate A/Jiangxi-Donghu/346/2013 (H10N8)*

Strain	Collection date	Nucleotide identity, %							
		HA	NA	PB2	PB1	PA	NP	M	NS
A/Jiangxi/346/2013 (H10N8)	2013 Dec								
A/chicken/Jiangxi/77/2014 (H10N8)	2014 Jan	99.5	99.8	99.5	99.9	99.9	99.3	99.4	99.9
A/chicken/Jiangxi/B15/2014 (H10N8)	2014 Jan	99.5	99.8	99.5	99.9	99.9	99.7	99.4	99.9
A/environment/Jiangxi/00449/2013 (H9N2)	2013 Feb	NT	NT	98.6	96.4	98.6	99.5	99.4	98.8
A/chicken/Jiangxi/103/2010 (H9N2)	2010 Dec	NT	NT	97.8	96.3	98.1	96.3	98.6	98.6
A/chicken/Jiangxi/12/2011 (H9N2)	2011 Jan	NT	NT	97.2	97.3	97.3	97.7	98.8	98.8
A/chicken/Jiangxi/13/2011 (H9N2)	2011 Jan	NT	NT	97.4	97.4	97.6	95.9	98.6	98.5
A/chicken/Jiangxi/19/2011 (H9N2)	2011 Jan	NT	NT	97.1	98.1	97.6	96.1	98.9	98.9
A/duck/Jiangxi/79/2009 (H9N2)	2009 Sep	NT	NT	87.0	90.0	89.8	91.1	90.7	69.4

*Isolates were from mixed cloacal and oropharyngeal swab specimens collected in Nachang city, Jiangxi Province. Nucleotide identity was calculated by using DNAStar software (http://www.dnastar.com) from the complete coding sequence of each gene segment. HA, hemagglutinin; M, matrix protein; NA, neuraminidase; NP, nucleoprotein; NS, nonstructural protein; NT, not tested; PA, polymerase acidic protein; PB, polymerase basic protein.

References

1. Wu Y, Wu Y, Tefsen B, Shi Y, Gao GF. Bat-derived influenza-like viruses H17N10 and H18N11. Trends Microbiol. 2014;22:183–91. http://dx.doi.org/10.1016/j.tim.2014.01.010
2. Zhang H, Xu B, Chen Q, Chen J, Chen Z. Characterization of an H10N8 influenza virus isolated from Dongting lake wetland. Virol J. 2011;8:42. http://dx.doi.org/10.1186/1743-422X-8-42
3. Jiao P, Cao L, Yuan R, Wei L, Song Y, Shen D, et al. Complete genome sequence of an H10N8 avian influenza virus isolated from a live bird market in southern China. J Virol. 2012;86:7716. http://dx.doi.org/10.1128/JVI.00959-12
4. Chen H, Yuan H, Gao R, Zhang J, Wang D, Xiong Y, et al. Clinical and epidemiological characteristics of a fatal case of avian influenza A H10N8 virus infection: a descriptive study. Lancet. 2014;383:714–21. http://dx.doi.org/10.1016/S0140-6736(14)60111-2
5. Yamada S, Hatta M, Staker BL, Watanabe S, Imai M, Shinya K, et al. Biological and structural characterization of a host-adapting amino acid in influenza virus. PLoS Pathog. 2010;6:e1001034. http://dx.doi.org/10.1371/journal.ppat.1001034
6. Xu C, Hu W-B, Xu K, He Y-X, Wang T-Y, Chen Z, et al. Amino acids 473V and 598P of PB1 from an avian-origin influenza A virus contribute to polymerase activity, especially in mammalian cells. J Gen Virol. 2012;93:531–40. http://dx.doi.org/10.1099/vir.0.036434-0
7. Jiao P, Tian G, Li Y, Deng G, Jiang Y, Liu C, et al. A single-amino-acid substitution in the NS1 protein changes the pathogenicity of H5N1 avian influenza viruses in mice. J Virol. 2008;82:1146–54. http://dx.doi.org/10.1128/JVI.01698-07
8. Gao GF. Influenza and the live poultry trade. Science. 2014;344:235. http://dx.doi.org/10.1126/science.1254664
9. Cui LB, Liu D, Shi WF, Pan JC, Qi X, Li XB, et al. Dynamic reassortments and genetic heterogeneity of the human-infecting influenza A (H7N9) virus. Nat Commun. 2014;5:3142. http://dx.doi.org/10.1038/ncomms4142
10. Wu Y, Gao GF. Lessons learnt from the human infections of avian-origin influenza A H7N9 virus: live free markets and human health. Sci China Life Sci. 2013;56:493–4. http://dx.doi.org/10.1007/s11427-013-4496-y
11. Bao CJ, Cui LB, Zhou MH, Hong L, Gao GF, Wang H. Live-animal markets and influenza A (H7N9) virus infection. N Engl J Med. 2013;368:2337–9. http://dx.doi.org/10.1056/NEJMc1306100
12. Su S, Qi W, Zhou P, Xiao C, Yan Z, Cui J, et al. First evidence of H10N8 avian influenza virus infections among feral dogs in live poultry markets in Guangdong Province, China. Clin Infect Dis. 2014 May 7; [Epub ahead of print].
13. Webster RG. Wet markets—a continuing source of severe acute respiratory syndrome and influenza? Lancet. 2004;363:234–6. http://dx.doi.org/10.1016/S0140-6736(03)15329-9
14. Liu D, Shi W, Shi Y, Wang D, Xiao H, Li W, et al. Origin and diversity of novel avian influenza A H7N9 viruses causing human infection: phylogenetic, structural, and coalescent analyses. Lancet. 2013;381:1926–32. http://dx.doi.org/10.1016/S0140-6736(13)60938-1
15. Wang Y, Jiang Z, Jin Z, Tan H, Xu B. Risk factors of infectious diseases for backyard poultry farms in the Poyang Lake area, China. PLoS ONE. 2013;8:e67366. http://dx.doi.org/10.1371/journal.pone.0067366

Address for correspondence: Bing Xu, Tsinghua University, Beijing 100084, China; email: bingxu@tsinghua.edu.cn

Molecular Epidemiology of **Influenza A(H1N1)** pdm09 Virus among Humans and Swine, Sri Lanka

Harsha K.K. Perera, Dhanasekaran Vijaykrishna, Akuratiya G. Premarathna, Chrishan J.S. Jayamaha, Geethani Wickramasinghe, Chung L. Cheung, Ming F. Yeung, Leo L.M. Poon, Aluthgama K.C. Perera, Ian G. Barr, Yi Guan, and Malik Peiris

After multiple discrete introductions of influenza A(H1N1)pdm09 virus into Sri Lanka, the virus was transmitted among humans, then swine. The spread of virus between geographically distant swine farms is consistent with virus dispersal associated with a vehicle used for swine transportation, although this remains unproven.

The first known transmission of influenza A(H1N1) pdm09 virus to humans from swine was in 2009. As the virus spread among humans worldwide, it was transmitted from humans to swine repeatedly (*1*), changing the global genetic landscape of swine influenza viruses. We previously reported the spillover of H1N1pdm from humans to swine and absence of North American triple reassortant, classical, and European avian-like swine viruses in swine herds in Sri Lanka during August 2009–May 2012 (*2*). Here, we extend these studies through August 2013 with the analysis of paired nasal and tracheal swab samples collected from 4,683 animals and serum samples from 3,351 animals (online Technical Appendix Table 1, wwwnc.cdc.gov/EID/article/20/12/14-0842-Techapp1.pdf) and comprehensively analyze full genomes of viruses isolated from samples from 26 swine (11 isolated in 2009, 4 in 2010, and 11 in 2011) and 35 humans (6 isolated in 2009, 17 in 2010, 9 in 2011, and 3 in 2012) and 2 publicly available hemagglutinin sequences of human H1N1pdm viruses from Sri Lanka. Sequences generated in this study are available in GenBank (KJ856002–KJ856446).

Author affiliations: University of Hong Kong, Hong Kong, China (H.K.K. Perera, C.L. Cheung, M.F. Yeung. L.L.M. Poon, Y. Guan, M. Peiris); University of Kelaniya, Kelaniya, Sri Lanka (H.K.K. Perera, A.G. Premarathna); Duke-National University of Singapore Graduate Medical School, Singapore (D. Vijaykrishna), Medical Research Institute, Colombo, Sri Lanka (C.J.S. Jayamaha, G. Wickramasinghe); Colombo Municipal Council, Colombo (A.K.C. Perera); and WHO Collaborating Centre for Reference and Research on Influenza, Melbourne, Australia (I.G.Barr)

DOI: http://dx.doi.org/10.3201/eid2012.140842

The Study

To understand the molecular epidemiology and spatial and temporal dynamics of spillover events, we compared our data with full-genome sequences of H1N1pdm available in public databases as of August 28, 2013. These include all available full genome sequences from swine H1N1pdm viruses (n = 82), all human H1N1pdm viruses from outside of the USA (n = 957), and 100 randomly selected full genome sequences from 1,500 human H1N1pdm sequences from the United States. Reassorted swine or human viruses containing H1N1pdm virus genes were excluded from this analysis. Our final dataset included the full genomes of 35 human and 26 swine samples from Sri Lanka and a global sample of 1,057 human and 82 swine virus sequences.

The single breakpoint recombination and genetic algorithm for recombination detection methods (*3*) excluded the presence of reassortants in our dataset; hence, we used concatenated genomes of 8 gene segments for all subsequent analyses. We conducted multiple-sequence alignment using MUSCLE (*4*) and optimized the sum of all of the pairs of characters manually. Phylogenetic trees and bootstrap supports were estimated by using the GTR+I+Γ nucleotide substitution model as identified by using JModeltest (*5*) and the maximum likelihood method in RaXML (*6*). We inferred dates of introduction of major Sri Lankan human and swine lineages using the relaxed clock method under a Bayesian Markov chain Monte Carlo approach (BEAST v1.7) (*7*).

Figure 1 illustrates independent introductions of at least 8 H1N1pdm sublineages into Sri Lanka during 2009–2012. Six of these were exclusively detected in humans: hu1 (2009), hu2 (2009), hu3 (2009), hu5 (2010/11), hu6 (2011), and hu7 (2011). One was exclusively from swine (sw1; 2009/10) and 1 sublineage was detected in both humans (hu4; 2011) and swine (sw2; 2011) (Figures 1, 2). Similar multiple discrete introductions of human H1N1pdm viruses have been reported in the United Kingdom and India (*8*,*9*).

In Sri Lanka, swine H1N1pdm clusters sw1 (2009/10) and sw2 (2011) were genetically distinct from each other and from other swine viruses isolated globally, indicating 2 separate introductions to local swine that circulated among swine for 11 and 4 months, respectively, for each cluster. The sw1 and sw2 lineages did not appear to establish long-term sustained transmission within pigs. However, the

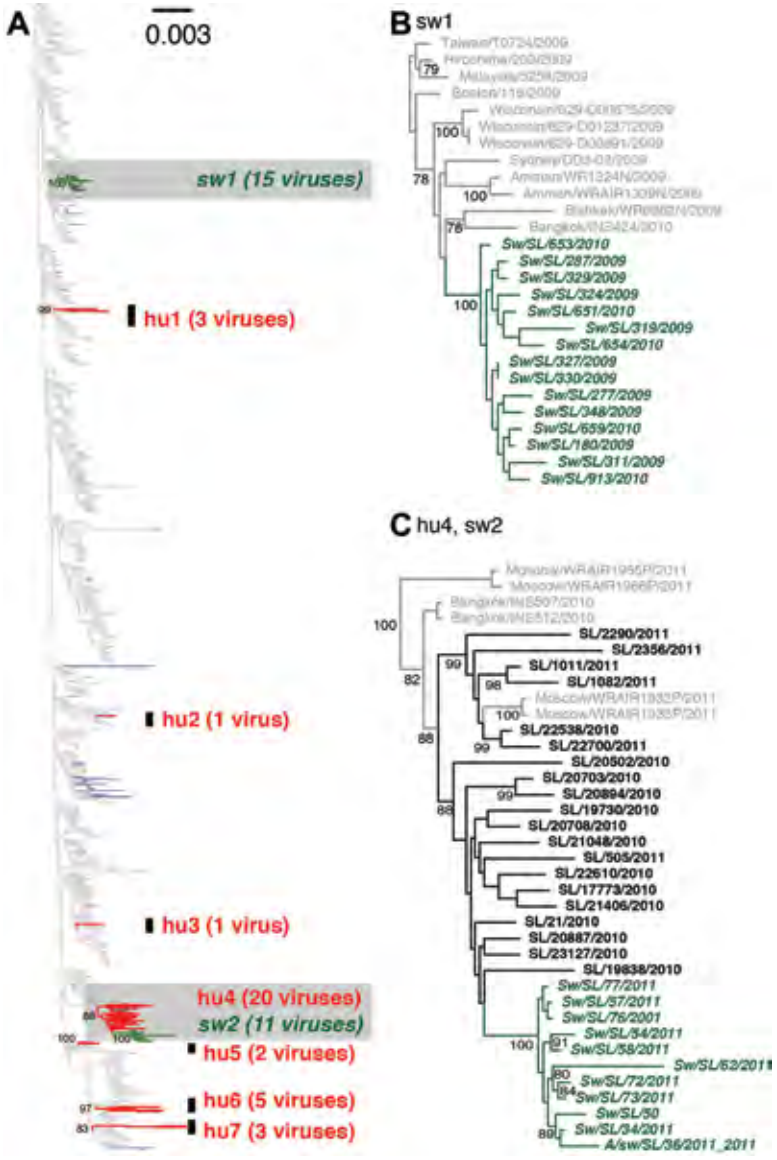

Figure 1. Phylogenetic relationships of influenza A H1N1pdm viruses isolated from human and swine during 2009–2012 in Sri Lanka. (A) Maximum likelihood tree generated from a concatenated dataset of 8 gene segment sequences from 1,057 human and 82 swine H1N1pdm viruses isolated globally during 2009–2012, and 35 human and 26 swine H1N1pdm viruses isolated in Sri Lanka in 2009–2012. Red and green branches represent human (hu) and swine (sw) viruses isolated in Sri Lanka, respectively; gray and blue branches represent globally sampled human and swine viruses, respectively. Highlighted regions (gray) are shown with virus names in (B) and (C), respectively. Support values estimated from 500 maximum likelihood bootstrap replicates are shown along the node for each swine and human clusters identified in Sri Lanka in (A) and for each node with >70% support for (B) and (C).

reduced surveillance of farms during the period 2012–2013 (online Technical Appendix Table 1) means that this conclusion has to be qualified in regard to the sw2 lineage. We did not identify ancestors of sw1 in Sri Lanka, however sw2 appears to have been directly derived from hu4, which included the majority of the human viruses (20/35) sequenced from Sri Lanka. The lack of identification of a human ancestor for sw1 may be related to insufficient human influenza genomic data obtained from Sri Lanka during 2009–2010 (Figures 1, 2). Although the 11 sw2 viruses were isolated from pigs on farms A, C, and G, which were separated by >25 km from each other (Table, Figure 2), they form a monophyletic clade with no human isolates within this cluster. Even though the paucity of human viruses sampled is a limitation in this study, the data suggest a single introduction of human viruses into swine followed by transmission within and between swine farms for >4 months (Figure 2).

To clarify transmission patterns between affected swine farms in Sri Lanka, we obtained contact patterns by interviewing pig farmers using a structured questionnaire (online Technical Appendix) with approval from the Ethics Review Committee, Faculty of Medicine, Ragama, Sri Lanka. There was no evidence of movement of persons or fomites between farms. However, during the peak demand period (November–December) of each year that surveillance was performed, a common truck owned by farm M (Table), driven by a single driver and an assistant, provided transportation from multiple farms to the abattoir, including from affected farms A, C, and G (Table). On some occasions, animals taken to the abattoir for slaughter were returned to the farm. Pools of water or body fluids were often noted within this

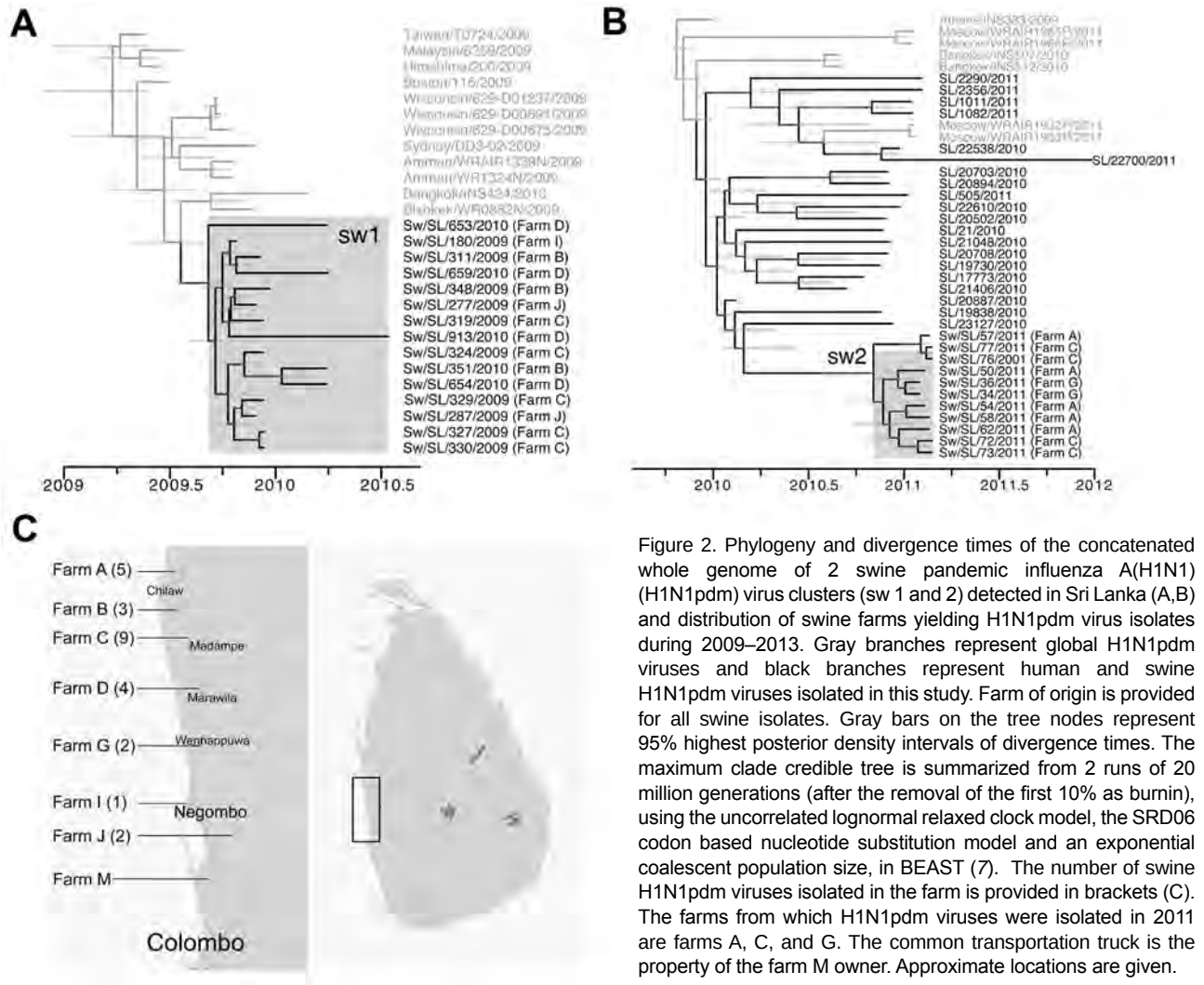

Figure 2. Phylogeny and divergence times of the concatenated whole genome of 2 swine pandemic influenza A(H1N1) (H1N1pdm) virus clusters (sw 1 and 2) detected in Sri Lanka (A,B) and distribution of swine farms yielding H1N1pdm virus isolates during 2009–2013. Gray branches represent global H1N1pdm viruses and black branches represent human and swine H1N1pdm viruses isolated in this study. Farm of origin is provided for all swine isolates. Gray bars on the tree nodes represent 95% highest posterior density intervals of divergence times. The maximum clade credible tree is summarized from 2 runs of 20 million generations (after the removal of the first 10% as burnin), using the uncorrelated lognormal relaxed clock model, the SRD06 codon based nucleotide substitution model and an exponential coalescent population size, in BEAST (*7*). The number of swine H1N1pdm viruses isolated in the farm is provided in brackets (C). The farms from which H1N1pdm viruses were isolated in 2011 are farms A, C, and G. The common transportation truck is the property of the farm M owner. Approximate locations are given.

truck, and it is possible that viable swine influenza viruses may have survived for varying periods. We did not test these fluids from the common transportation truck for influenza viruses; this is also a limitation of the study.

Of the 15 farms on which the common truck was used, swine on 3 (20%) were infected by a sw2 clade virus; on 2 farms on which the common truck was not used, no swine were infected. This association was not statistically significant (p = 1.0), however, given the small numbers of farms investigated. Our findings are consistent with dispersal of sw2 clade viruses in association with the truck to infect multiple farms that were geographically distant, but this remains unproven. It was previously documented that influenza viruses can remain viable for prolonged periods of time in water at a temperature of ≈28°C (comparable ambient temperature in the Western Province, Sri Lanka) (*10*) and are reported to survive longer periods on nonporous surfaces (*11*). Influenza virus has been detected in air samples from rooms of experimentally infected pigs (*12*) and in the exhaust air samples collected up to 1 mile away from the index farm (*13*), indicating the possibility of aerosol transmission for some distance. Notably, studies of the swine populations in the United States have demonstrated spatial dissemination of swine influenza viruses of human origin to match long-distance swine movements (*14*).

Despite widespread inter-farm transmission of sw1 and sw2, our results show that only animals on farm C were infected in both spillover events. Farms A and G, on which swine were infected by sw2 in 2011, appeared not to have had infected swine during 2009–2010, as shown by both virus isolation and serologic testing (online Technical Appendix Table 1). Maternally derived antibodies transferred through colostrum from dams infected during 2009–2011 may have provided passive protection to offspring born in 2010–2011. On swine farms in Sri Lanka, female swine are used for breeding for ≈2–3 years. In experimental challenge, maternally derived antibodies provided some protection against disease, but not complete protection from infection (*15*).

Table. Demographic data, internal and external biosecurity measures practice by swine farms, Sri Lanka, 2009–2013*

Farm	Pig replacement source	Used specific clothing and footwear	Used disinfectants for wheel and foot baths	Dedicated employees for fattening and nursery units	Type of truck used to transport pigs to the GSHD	Visitor restriction grade	Service provider visits	Cats and/or dogs allowed in the facility	H1N1pdm detection
A	Internal	No	Yes	Yes	Hired/farm M	M	Nil	Yes	Clade 2
B	Internal	Yes	Yes	Yes	Dedicated	A	No	Yes	Clade 1
C	Internal	No	No	No	Hired/farm M	N	Occasionally	Yes	Clades1/2
D	Internal	No	No	Yes	Dedicated	M	Occasionally	Yes	Nil
E	Internal	No	No	No	Hired/farm M	N	Occasionally	Yes	Nil
F	Internal	No	No	No	Hired/farm M	M	Nil	Yes	Nil
G	Internal	No	No	No	Hired/farm M	M	Nil	Yes	Clade 2
H	Internal	No	No	No	Hired/farm M	M	Nil	Yes	Nil
I	Internal	No	No	No	Hired/farm M	M	Occasionally	Yes	Clade 1
J	Internal	No	No	No	Hired/farm M	N	Occasionally	Yes	Clade 1
K	Internal	No	No	No	Hired/farm M	M	Nil	Yes	Nil
L	ND	No	ND	ND	Hired/farm M	ND	ND	ND	Nil
M	External	No	No	No	Self-owned	M	Yes	Yes	Nil
N	Internal	No	No	No	Hired/farm M	N	Nil	Yes	Nil
O†	NA	No	No	No	NA	N	Nil	Yes	Nil
P	Internal	No	No	No	Hired/farm M	N	Nil	Yes	Nil
Q‡	Internal	Yes	No	Yes	NA	A	Yes	Yes	Nil
R	Internal	No	No	No	Hired/farm M	M	Occasionally	Yes	Nil
S	Internal	No	No	No	Hired/farm M	N	Occasionally	Yes	Nil

*None of the swine farms housed domestic poultry in the facility. Farms are listed in alphabetical order, A being in the northernmost location and S the southernmost farm in this study. GSHD, Government Slaughter House Dematagoda. The common transportation truck is the property of the farm M owner. Visitor restriction is scored as M-moderate, and A-absolute restriction, N-nil, on the basis of level of visitor restrictions (absolute/moderate/nil) and selection of veterinary surgeons (designated/freelance); service providers are veterinary surgeons, drug, and vaccine providers. NA, not applicable; ND, no data available.
†Backyard slaughterhouse.
‡Pigs not slaughtered at the GSHD.

Conclusions

This study demonstrates natural independent spillover events of H1N1pdm influenza viruses from humans to swine. H1N1pdm viruses appear to be spread by multiple, discrete introductions to swine, after which clonal expansion occurs within the swine. The spread of such virus lineages across multiple farms is consistent with virus dispersal by breaches of external biosecurity measures, including the manner of swine transportation, although this remains unproven given the small sample size. Unlike classical swine influenza, North American triple reassortant, and European avian swine viruses that have persistently circulated among swine for several decades in other countries (*15*), H1N1pdm does not appear to establish long-term lineages in swine in the absence of further reassortment. This observation requires confirmation in other geographic settings.

Acknowledgments

We acknowledge the excellent technical assistance of T.Y Lung, G.D.W.S. Gunathilaka and Preethimala Liyanage.

This research was supported by contracts HHSN266200700005C and HHSN272201400006C from the National Institute of Allergy and Infectious Disease, National Institutes of Health, Department of Health and Human Services, USA; an Area of Excellence Scheme of the University Grants Committee [AoE/M-12/06] of the Hong Kong Special Administrative Region Government; PhD studentship from The University of Hong Kong, Ministry of Education Academic Research Fund grant (MOE2011-T2-2-049); the Duke-NUS Signature Research Program, Agency of Science, Technology and Research, Singapore, the Ministry of Health, Singapore; and the Melbourne WHO Collaborating Centre for Reference and Research on Influenza, Department of Health, Australia.

Dr Perera, formerly a postdoctoral research assistant in the School of Public Health, The University of Hong Kong, is senior lecturer in Department of Medical Microbiology at University of Kelaniya, Sri Lanka. His research focuses on the ecology and evolution of influenza viruses and emerging viral infections.

References

1. Vijaykrishna D, Poon LL, Zhu HC, Ma SK, Li OT, Cheung CL, et al. Reassortment of pandemic H1N1/2009 influenza A virus in swine. Science. 2010;328:1529. http://dx.doi.org/10.1126/science.1189132
2. Perera HK, Wickramasinghe G, Cheung CL, Nishiura H, Smith DK, Poon LL, et al. Swine influenza in Sri Lanka. Emerg Infect Dis. 2013;19:481–4. http://dx.doi.org/10.3201/eid1903.120945
3. Pond SLK, Frost SDW, Muse SV. HyPhy: hypothesis testing using phylogenies. Bioinformatics. 2005;21:676–9. http://dx.doi.org/10.1093/bioinformatics/bti079
4. Edgar RC. MUSCLE: A multiple sequence alignment method with reduced time and space complexity. BMC Bioinformatics. 2004;5:113. http://dx.doi.org/10.1186/1471-2105-5-113

5. Posada D. jModelTest: phylogenetic model averaging. Mol Biol Evol. 2008;25:1253–6. http://dx.doi.org/10.1093/molbev/msn083
6. Stamatakis A. RAxML-VI-HPC: maximum likelihood-based phylogenetic analyses with thousands of taxa and mixed models. Bioinformatics. 2006;22:2688–90. http://dx.doi.org/10.1093/bioinformatics/btl446
7. Drummond AJ, Suchard MA, Xie D, Rambaut A. Bayesian phylogenetics with BEAUti and the BEAST 1.7. Mol Biol Evol. 2012;29:1969–73. http://dx.doi.org/10.1093/molbev/mss075
8. Baillie GJ, Galiano M, Agapow PM, Myers R, Chiam R, Gall A, et al. Evolutionary dynamics of local pandemic H1N1/2009 influenza virus lineages revealed by whole-genome analysis. J Virol. 2012;86:11–8. http://dx.doi.org/10.1128/JVI.05347-11
9. Sharma S, Joshi G, Dash PK, Thomas M, Athmaram TN, Kumar JS, et al. Molecular epidemiology and complete genome characterization of H1N1pdm virus from India. PLoS ONE. 2013;8:e56364. http://dx.doi.org/10.1371/journal.pone.0056364
10. Stallknecht DE, Kearney MT, Shane SM, Zwank PJ. Effects of pH, temperature, and salinity on persistence of avian influenza viruses in water. Avian Dis. 1990;34:412–8. http://dx.doi.org/10.2307/1591429
11. Bean B, Moore BM, Sterner B, Peterson LR, Gerding DN, Balfour HH Jr. Survival of influenza viruses on environmental surfaces. J Infect Dis. 1982;146:47–51. http://dx.doi.org/10.1093/infdis/146.1.47
12. Corzo CA, Romagosa A, Dee S, Gramer M, Morrison RB, Torremorell M. Relationship between airborne detection of influenza A virus and the number of infected. Vet J. 2013;196:171–175.
13. Torremorell M, Allerson M, Corzo C, Diaz A, Gramer M. Transmission of Influenza A Virus in Pigs. Transbound Emerg Dis. 2012:59(Suppls1):68–84. http://dx.doi.org/10.1111/j.1865-1682.2011. 01300.x
14. Nelson MI, Lemey P, Tan Y, Vincent A, Lam TT, Detmer S, et al. Spatial dynamics of human-origin H1 influenza A virus in North American swine. PLoS Pathog. 2011;7:e1002077. http://dx.doi.org/10.1371/journal.ppat.1002077
15. Loeffen WL, Heinen PP, Bianchi AT, Hunneman WA, Verheijden JH. Effect of maternally derived antibodies on the clinical signs and immune response in pigs after primary and secondary infection with an influenza H1N1 virus. Vet Immunol Immunopathol. 2003;92:23–35. http://dx.doi.org/10.1016/S0165-2427(03)00019-9

Address for correspondence: Malik Peiris, School of Public Health, 21, Sassoon Road, University of Hong Kong, Pokfulam, Hong Kong, China; email: malik@hku.hk

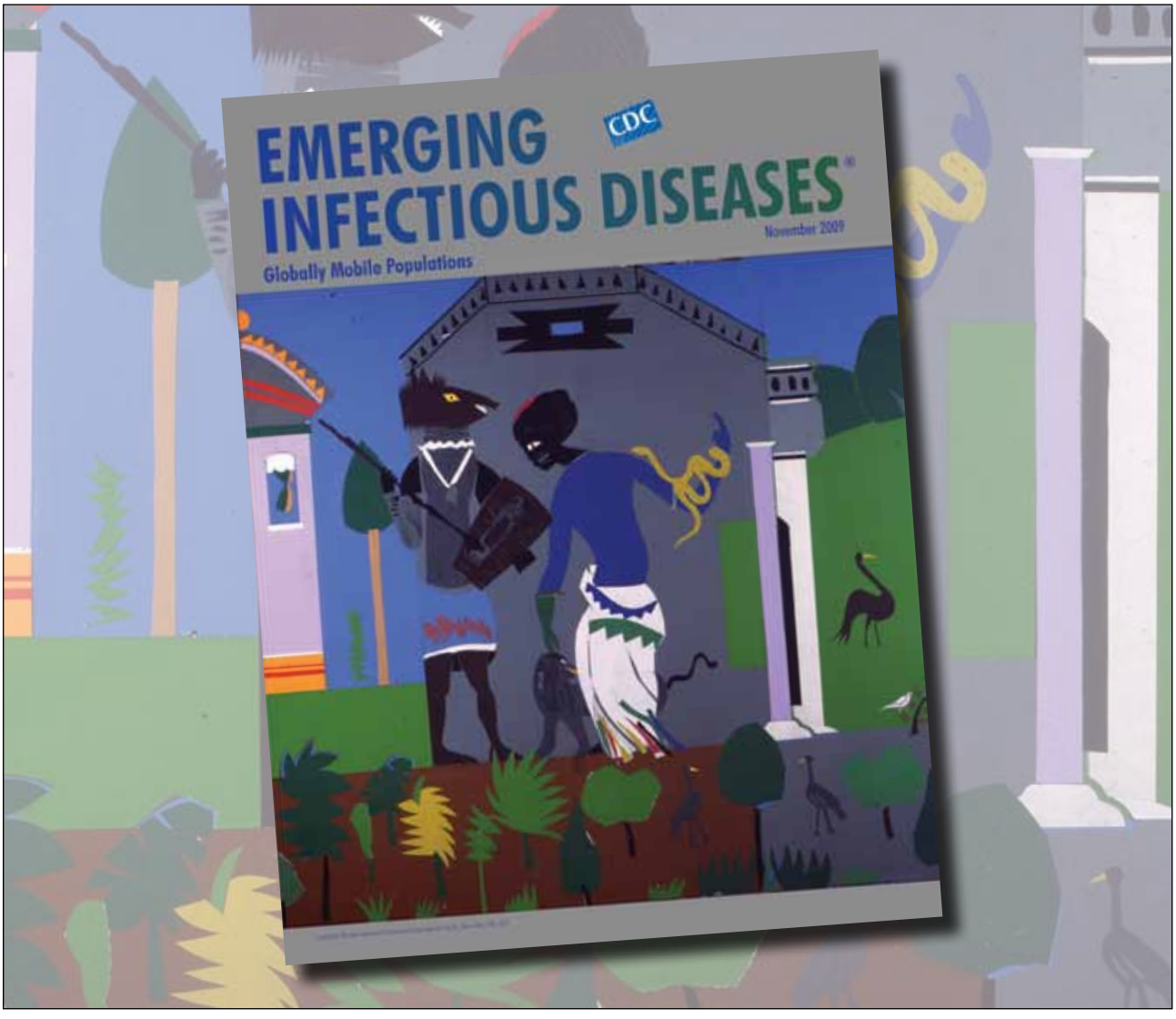

Novel Amdoparvovirus Infecting Farmed Raccoon Dogs and Arctic Foxes

Xi-Qun Shao, Yong-Jun Wen, Heng-Xing Ba, Xiu-Ting Zhang, Zhi-Gang Yue, Ke-Jian Wang, Chun-Yi Li, Jianming Qiu, and Fu-He Yang

A new amdoparvovirus, named raccoon dog and fox amdoparvovirus (RFAV), was identified in farmed sick raccoon dogs and arctic foxes. Phylogenetic analyses showed that RFAV belongs to a new species within the genus *Amdoparvovirus* of the family *Parvoviridae*. An RFAV strain was isolated in Crandell feline kidney cell culture.

Amdoparvoviruses, members of the autonomous parvoviruses, belong to the genus family *Parvovirdae*, subfamily *Parvovirinae*, genus *Amdoparvovirus* (*1*). Only 2 distant species have been reported: *Carnivore amdoparvovirus 1*, which comprises only Aleutian mink disease virus (AMDV), and *C. amdoparvovirus 2*, which comprises only gray fox amdovirus (*1*,*2*). Natural AMDV infection mainly occurs in the *Mustelidae* family (*3*) and causes immune complex–mediated disease (*4*). However, to our knowledge, natural amdoparvovirus infection in raccoon dogs or arctic foxes has not been reported. We describe the identification, isolation, and infection of a novel amdoparvovirus in canids, which represents a new viral species (*C. amdoparvovirus 3*), named raccoon dog and fox amdoparvovirus (RFAV), within the *Amdoparvovirus* genus.

The Study

During July–December 2012 and 2013, sick raccoon dogs and arctic foxes, which were farmed for fur products on 6 farms (farms A–F) in Jilin and Liaoning provinces, China, were received for quarantine inspection at the Fur Animal Disease Laboratory, Institute of Special Animal and Plant Sciences, Chinese Academy of Agricultural Sciences. Several infant raccoon dogs from 1 litter became ill 40 days after birth, and the numbers of sick animals increased by the time they were 3 months of age. Clinical signs included anorexia, emaciation, growth retardation, thirst, chronic diarrhea, and unkempt fur; necropsy often revealed cyanosed splenomegaly, enlargement of mesenteric lymph nodes, and renal cortex congestion and brittleness. For the raccoon dogs showing similar clinical signs, rate of illness was 4%–8%; death rate was ≈60% before the age of 4 months; and rate of illness increased by years on the farms that initially had sick animals. Among arctic foxes, signs varied: emaciation and growth retardation in 3-month-old cubs with pale and swelling kidneys in dead foxes; and severe diarrhea or intermittent tar-like feces in 3–7-month-old cubs. Antibacterial drug treatment was ineffective in these diseased animals.

Because signs in the sick animals sent for quarantine inspection were similar to those in Aleutian mink disease, we first used AMDV-specific counter-immunoelectrophoresis (CIEP) (*5*) to test serum samples of six 3-month-old sick raccoon dogs from farm A. All 6 were positive. Next, we designed conserved amdoparvovirus primers (AV7; Table 1) for PCR detection. Viral nucleic acids were extracted by using a MiniBest Viral RNA/DNA Extraction Kit (TaKaRa, Dalian, China). DNA extracted from spleen, kidney, mesenteric lymphonodus, and mucosal tissue and blood of the 4 sick raccoon dogs was all RFAV DNA positive. After 10 days, the 4 raccoon dogs remained RFAV DNA PCR positive in blood and CIEP positive in serum. DNA extracted from blood of two 3–7-month-old sick raccoon dogs from farm C was RFAV DNA PCR positive, and serum samples from these animals were CIEP positive. Two 7-month-old raccoon dogs from farm D appeared healthy but on necropsy showed cyanosed splenomegaly. Their blood and spleens were RFAV DNA positive, and serum was CIEP positive. The overall positive rates of RFAV DNA and CEIP antibody in sick raccoon dogs were 90% and 100%, respectively.

Serum iodine agglutination test (IAT) (*6*) was positive or strongly positive in 20 sick raccoon dogs that were 7 and 19 months old but was negative in healthy animals. Of the 29 sick raccoon dogs, two 3–7-month-old animals were both canine parvovirus 2 and RFAV DNA positive by PCR in blood or spleen samples. However, canine distemper virus was not detected in spleen samples from any sick raccoon dogs.

In arctic foxes raised together with sick raccoon dogs on farm B, intestinal mucosa samples from 3 of 7 foxes that died of diarrhea-associated dehydration were RFAV DNA PCR positive. One kidney sample from a 3-month-old fox of 3 tested on farm F showed renal enlargement and was RFAV DNA PCR positive. Blood, urine, and feces of

Author affiliations: State Key Laboratory for Molecular Biology of Special Economical Animals, Institute of Special Animal and Plant Sciences, Chinese Academy of Agricultural Sciences, Changchun, China (X.Q. Shao, Y.J. Wen, H.X. Ba, X.T. Zhang, Z.G. Yue, C.Y. Li, F.H. Yang); State Key Laboratory of Marine Environmental Science, Xiamen University, Xiamen, China (K.J. Wang); and University of Kansas Medical Center, Kansas City, Kansas, USA (J Qiu)

DOI: http://dx.doi.org/10.3201/eid2012.140289

Table 1. Oligonucleotide primer pairs used for PCR amplification of amdoparvovirus*

Gene, name	Primer (5' → 3')	Ta,† amplicon	Use
VP2			
AV7-F	CCAACAAGTAATGACACCTTGGT	52°C	Detection
AV7-R	CCTGCTGGTATTATCCATTCAGGA	≈786 bp	Sequencing
AV3-F	CCAACAAGTAATGACACCTTGGT	53°C	Detection
AV3-R	GGTTGGTTTGGTTGCTCTCCAAGGA	316 bp	
NS1			
ANS-F	GTAACATGGCTCAGGCTCA	52°C	
ANS-R	CTCATGCCGAGGTCTCTTGTG	2,008 bp	Sequencing
VP1			
AVP-F1	CACAAGAGACCTCGGCATGAGTA	52°C	
AVP-R1	CCTGCTGGTATTATCCATTCAGGA	≈1,297 bp	Sequencing
AVP-F2	GGCTTTGTTCCTTGGAGAGCAAC	52°C	
AVP-R2	TGGTAGAATRAGGAAGTACACAK	≈1,443 bp	Sequencing

*NS, nonstructural protein; VP, viral structural protein.
†Annealing temperature.

two 7-month-old arctic foxes on farm C, which had tar-like feces, were RFAV DNA PCR positive. Serum samples of these 2 foxes were CIEP positive. Both PCR and CIEP remained positive for at least 2 months. Results of all samples tested by PCR, CIEP, and IAT are summarized in Table 2.

We next applied a semiquantitative PCR to quantify the level of RFAV DNA in the blood and spleens of four 7-month-old sick raccoon dogs (3 from farm D, 1 from farm C). Briefly, DNA samples were diluted from 10^1 to 10^7 viral genomic copies (vgc)/mL by using a quantified RFAV DNA template and were amplified by using AV3 primers with the detection threshold of ≈100 vgc in a volume of 15 mL. Virus titer was determined on the basis of the maximum dilution at which viral DNA was detected by agarose gel electrophoresis. RFAV DNA ranged from ≈2×10^5 to ≈5×10^7 vgc/mL in blood and ≈7×10^7 vgc/g in spleen. In spleen and kidney tissues of 2 raccoon dogs euthanized at 3 months of age (from farm A) and four 7-month-old sick raccoon dogs (from farm D), bacterial infections, performed by standard methods, were not found. Collectively, these results demonstrate that blood or tissues from the 2 sick animals contained RFAV DNA, and the DNA levels were high in some samples.

We used indirect immunofluorescence assay (IFA) to probe RFAV antigens in spleen and kidney of the 2 RFAV PCR–positive 3-month-old sick raccoon dogs from farm A. Tissues of the sick raccoon dogs were AMDV-G antigen IFA positive, but the healthy animal tissues were not (Figure 1, panel A). This result indicates that the spleen and kidney of the sick raccoon dogs contained viral antigens that share immunogenicity with AMDV-G. More importantly, we isolated an RFAV strain, named XQ-JLR, by

Table 2. Detection of raccoon dog and fox amdoparvovirus in sick and healthy animals using PCR, CIEP, and IAT, China*

Animal, health status	Age, mo	Year	Farm†	No.	Rate			
					PCR+‡	CIEP+	IAT+	CIEP+PCR+
Raccoon dog								
Diseased	3–7		Total	10	8/10	8/8	2/2	6/8
		2012	A	6	4/6	6/6	ND	4/6
		2012	B	2	2/2	ND	ND	NA
		2013	C	2	2/2	2/2	2/2	2/2
	7, 19		Total	18, 1	18/19	18/18	18/18	17/18
		2013	D	12, 1	12/13	13/13	13/13	12/13
		2012	A	5	5/5	5/5	5/5	5/5
		2012	E	1	1/1	ND	ND	NA
Healthy§	3	2013	Total	10	0/10	0/10	ND	0/10
	7	2013	Total	5	0/5	2/5	0/5	0/5
Arctic fox								
Diseased	3		Total	10	4/10	ND	ND	NA
		2012	B	7	3/7	ND	ND	NA
		2012	F	3	1/3	ND	ND	NA
	7–9	2012	C	2	2/2	2/2	ND	2/2
Healthy	7	2012	Total	5	0/5	0/5	0/5	0/5

*CIEP, counter-immunoelectrophoresis; IAT, serum iodine agglutination test; NA, samples not available; ND, assays not done; +, positive.
†Farm: A, Heishan County; B, Qian'an County; C, Jilin County; D, Panjin County; E, Haicheng County; F, Nong'an County. Qian'an, Jilin, and Nong'an are located in Jilin province; Heishan, Panjin and Haicheng are located in Liaoning province.
‡For raccoon dogs, PCR+ for all the tested tissues (blood, spleen, kidney and mesenteric lymphonodus). For arctic foxes, PCR+ results only for 1 of the tested tissues (blood, kidney, or intestinal mucosae).
§Blood and spleen samples were tested separately by PCR from healthy animals except for the blood samples from the 3-month-old healthy raccoon dogs.

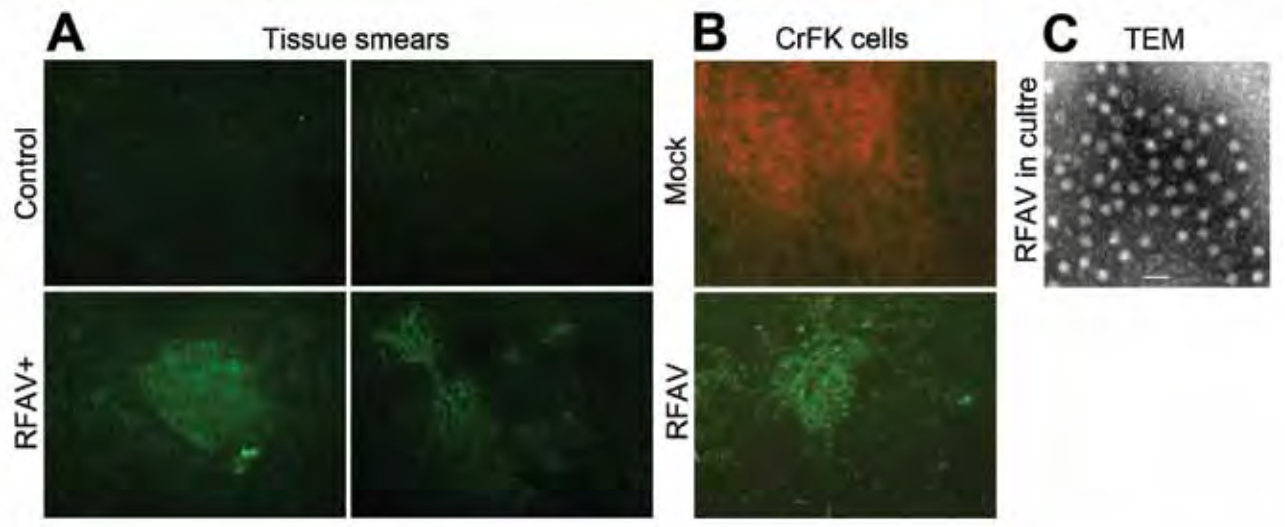

Figure 1. Detection of amdoparvovirus antigens in sick raccoon dogs and infected cells. A) Detection of amdoparvovirus antigens in tissues of sick raccoon dogs. Tissue smears, as described below, were prepared from spleen and kidney samples of sick raccoon dogs and detected with a control mouse serum or anti-AMDV-G serum by using an IFA (*8*). (a) Mock smear of a spleen tissue from a sick raccoon dog, detected with normal mouse serum as a primary antibody; (b) Control smear of a spleen tissue from a healthy raccoon dog; (c,d) amdoparvovirus antigen-positive smears of spleen tissue (c) and kidney tissue (d) from a sick raccoon dog, detected with anti-AMDV-G serum. Original magnification ×200. B,C) Detection of amdoparvovirus antigens and virions in infected CrFK cells. B) One milliliter filtered (0.22 μm) pathological spleen samples collected from a sick raccoon dog that had a virus titer of ≈7×10^7 vgc/mL, was inoculated to confluent CrFK cells in a T25 flask. Infected cells of the fourth passage were fixed and analyzed with IFA by using anti-AMDV serum (mock- or RFAV-infected CrFK cells). C) Twenty-five milliliter supernatant (≈2×10^9 vgc/mL) of RFAV(XQ-JLR)–infected CrFK cell cultures were concentrated. Virions were agglutinated with an anti-RFAV raccoon dog serum and were visualized under a transmission electron microscope (TEM). AMDV, Aleutian mink disease virus; RFAV, raccoon dog and fox amdoparvovirus; IFA, indirect immunofluorescence assay; vgc, viral genome copies. Scale bar = 50 nm.

infecting CrFK cells. IFA using anti-AMDV serum showed positive green cells in RFAV-infected CrFK cells but not in mock-infected cells (Figure 1, panel B). Under a transmission electron microscoe, virus particles at ≈23 nm in diameter were visualized in a concentrated supernatant of infected CrFK cells (Figure 1, panel C).

We further proved that RFAV is the predominant virus in the lesion tissues of sick animals. A modified SISPA (*7*) was performed for high-throughput sequencing with mixed lesion tissues of 3 spleens and 3 kidneys from 3 sick raccoon dogs. By using Illumina MiSeq sequencing (Illumina, San Diego, CA, USA), we obtained 478,813 high-quality reads, and 668 contigs were assembled, including 17 contigs for new amdoparvovirus. Amdoparvovirus sequences, except for a difficult-to-sequence high guanine–cytosine nucleotide content of 62-bp gap, were recovered, which are consistent with the sequences acquired by Sanger sequencing of viral DNA amplified from tissues. There were 865 reads, by BLASTn (http://www.blast.ncbi.nlm.nih.gov/Blast.cgi), in alignment with amdoparvovirus sequences but only 16 reads with sequences of other non-mammal viruses, such as phage and baculovirus. The identities were <91% of the reads aligning with AMDV sequences in GenBank by BLASTn (E value $<10^{-5}$).

We sequenced AV7 primer-amplified PCR products of RFAV DNA from the tissues of 32 animals (GenBank accession nos. KJ396347– KJ396358). Four representative strains of nearly full-length genome sequences (GenBank accession nos. KJ396347–KJ396350) only share a similarity of 82% and 76.7% in the nonstructural protein (NS) 1–encoding sequence and NS1 aa sequence, respectively, with AMDV. Phylogenetic analyses of 2 neighbor-joining trees of either NS1 or major structural protein (VP2) strongly suggest that RFAV strains cluster into a unique clade between AMDV and gray fox amdovirus species (Figure 2).

Conclusions

We identified a new virus species, RFAV, from farmed raccoon dogs and arctic foxes in Jilin and Liaoning provinces, China. Raccoon dogs are naturally susceptible to RFAV infection, and RFAV is most likely the etiologic agent responsible for the disease manifestations of the sick raccoon dogs.

The study was supported by the Special Fund for Public Welfare Technology Research of Agricultural Industry (200903014) and the Agricultural Science and Technology Innovation Fund (2014) from the Ministry of Agriculture of China, and the Special Economic Animal Germplasm Resources of Domesticated Animal Germplasm Platform (2013) from the National Science and Technology Infrastructure Foundation.

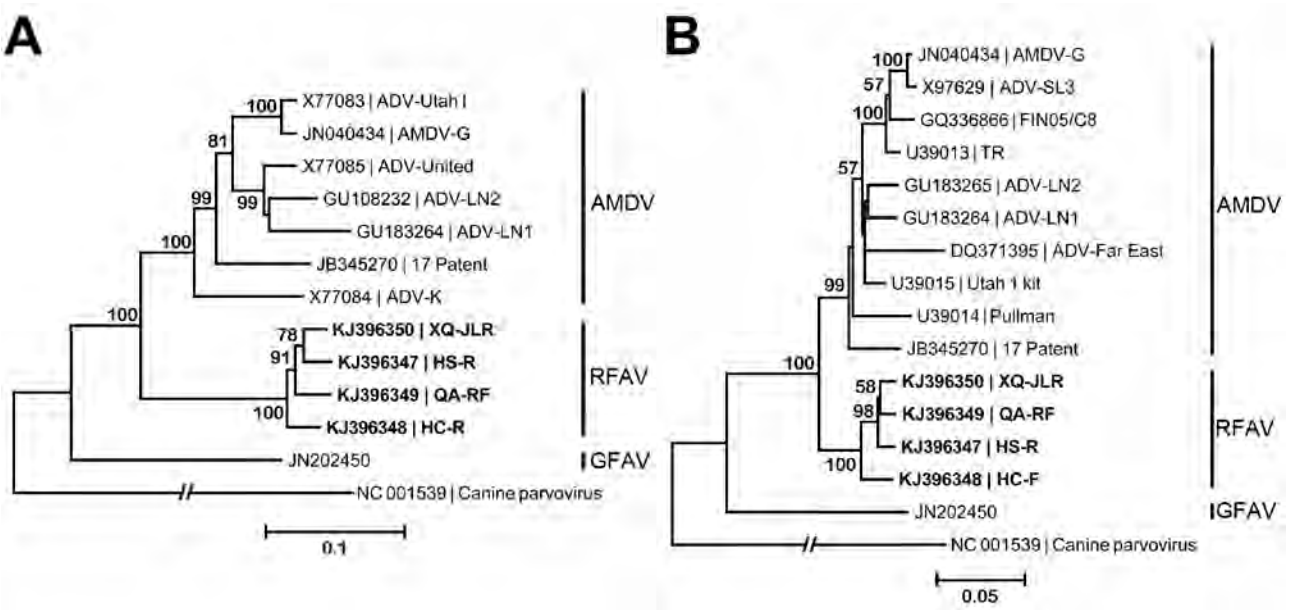

Figure 2. Phylogenetic analyses of amdoparvoviruses. A) Phylogenetic tree based on the viral NS1 gene. B) A phylogenetic tree based on the major capsid VP2. RFAV and other published amdoparvovirus sequences were aligned by using the MUSCLE program in MEGA5.2 (*9*), which used a P-distance model with 1,000 bootstrap replicates to generate phylogenetic trees of NS1 and VP2 aa sequences. GenBank accession numbers of isolates or strains are shown on the tree. Canine parvovirus was used as an outgroup. AMDV, Aleutian mink disease virus; GFAV, gray fox amdoparvovirus; RFAV, raccoon dog and fox amdoparvovirus; NS, nonstructural protein; VP, viral structural protein. Sequences obtained from this study are shown in bold. Scale bars indicate nucleotide substitutions per site.

Dr Shao is an associate professor in the Division of Special Animal Infectious Disease, Institute of Special Animal and Plant Sciences, Chinese Academy of Agricultural Sciences. His research interests include epidemiology of animal infectious diseases and novel pathogens.

References

1. Cotmore SF, Agbandje-McKenna M, Chiorini JA, Mukha DV, Pintel DJ, Qiu J, et al. The family *Parvoviridae*. Arch Virol. 2014;159:1239–47. http://dx.doi.org/10.1007/s00705-013-1914-1
2. Li L, Pesavento PA, Woods L, Clifford DL, Luff J, Wang C, et al. Novel amdovirus in gray foxes. Emerg Infect Dis. 2011;17:1876–8. http://dx.doi.org/10.3201/eid1710.110233
3. Farid AH. Aleutian mink disease virus in furbearing mammals in Nova Scotia, Canada. Acta Vet Scand. 2013;55:10–55 http://dx.doi.org/10.1186/1751-0147-55-10.
4. Porter DD, Larsen AE, Porter HG. The pathogenesis of Aleutian disease of mink. 3. Immune complex arteritis. Am J Pathol. 1973;71:331–44.
5. Cho HJ, Greenfield J. Eradication of Aleutian disease of mink by eliminating positive counterimmunoelectrophoresis test reactors. J Clin Microbiol. 1978;7:18–22.
6. Henson JB, Gorham JR, Leader RW. A field test for Aleutian disease. Natl.Fur.News. 1962;34:8–9.
7. Djikeng A, Halpin R, Kuzmickas R, Depasse J, Feldblyum J, Sengamalay N, et al. Viral genome sequencing by random priming methods. BMC Genomics. 2008;9:5–9 http://dx.doi.org/10.1186/1471-2164-9-5.
8. Oleksiewicz MB, Costello F, Huhtanen M, Wolfinbarger JB, Alexandersen S, Bloom ME. Subcellular localization of Aleutian mink disease parvovirus proteins and DNA during permissive infection of Crandell feline kidney cells. J Virol. 1996;70:3242–7.
9. Tamura K, Peterson D, Peterson N, Stecher G, Nei M, Kumar S. MEGA5: molecular evolutionary genetics analysis using maximum likelihood, evolutionary distance, and maximum parsimony methods. Mol Biol Evol. 2011;28:2731–9. http://dx.doi.org/10.1093/molbev/msr121

Address for correspondence: Xi-Qun Shao, Division of Special Animal Infectious Disease, Institute of Special Animal and Plant Sciences, Chinese Academy of Agricultural Sciences, Changchun 130112, Jilin, China; email: shaoxiqun@caas.cn; Fu-He Yang, State Key Laboratory for Molecular Biology of Special Economical Animals, Institute of Special Animal and Plant Sciences, Chinese Academy of Agricultural Sciences, Changchun 130112, Jilin, China; email: yangfh@126.com

Novel Porcine Epidemic Diarrhea Virus Variant with Large Genomic Deletion, South Korea

Seongjun Park, Sanghyun Kim, Daesub Song,[1] and Bongkyun Park[1]

Since 1992, porcine epidemic diarrhea virus (PEDV) has been one of the most common porcine diarrhea–associated viruses in South Korea. We conducted a large-scale investigation of the incidence of PEDV in pigs with diarrhea in South Korea and consequently identified and characterized a novel PEDV variant with a large genomic deletion.

Porcine epidemic diarrhea virus (PEDV) (family *Coronaviridae*, subfamily *Coronavirinae*, genus *Alphacoronavirus*) is an enveloped, positive-sense, single-stranded RNA virus. PEDV causes an acute and highly contagious enteric disease characterized by severe diarrhea, dehydration, and a high death rate in pigs that results in substantial economic losses in the swine industry (*1*). PEDV was first reported in Belgium and the United Kingdom in 1978; since then, it has been identified in many swine-raising countries in Europe and Asia, notably Belgium, Hungary, Italy, South Korea, Thailand, Japan, and China (*1*,*2*). PEDV was not reported in North and South America until 2013, when it was officially confirmed in the United States; it is spreading rapidly across the country (*3*). We report the emergence and genetic characterization of a novel PEDV variant with a large genomic deletion, which was serendipitously recognized in fecal and intestinal samples of suckling pigs with diarrhea in South Korea as a result of a systematic surveillance program to monitor activity for porcine diarrhea–associated viruses.

The Study

A total of 2,634 fecal and intestinal samples were collected from pigs exhibiting diarrhea from 569 swine farms in all 9 provinces of South Korea, during January 1–December 31, 2008; age groups of the pigs are defined in the Table. All samples were processed as 10% (vol/vol) suspensions with phosphate-buffered saline (PBS; 0.1 M, pH 7.2), and viral RNA was extracted from them. Subsequently, reverse transcription PCR (RT-PCR) was performed by using 3 primer pairs as described previously (*4*). To determine complete spike (S) gene sequence, we purified, cloned, and sequenced PCR products on an automated DNA sequencer by using T7, SP6 primers, and newly designed S gene–specific primers (primer sequences available on request). Sequences were analyzed by ClustalX version 1.83 program (http://www.clustal.org) and MegAlign software (DNAStar Inc., Madison, WI, USA), and compared with those of reference strains in GenBank. Phylogenetic analysis was conducted with MEGA version 5.22 (*5*). The complete S gene sequence of the PEDV variant with a large genomic deletion (strain MF3809/2008/South Korea) described here has been deposited in GenBank under accession no. KF779469.

Of the 2,634 samples, 205 (7.8%; 49/569 [8.6%] farms) were positive for PEDV: 116 (16.8%) of 692, 12 (2.4%) of 504, 29 (3.6%) of 808, 34 (24.1%) of 141, 1 (16.7%) of 6, and 13 (2.7%) of 483 samples from the 6 age groups tested (Table); however, when SF2/SR2 primers were subjected to PCR, a strong and single band of unexpected size (≈1,000 bp) was found in each PCR product from 3 diarrhea samples of the suckling pigs on 1 farm. Exact length of the band was 981 nt, and the band was much shorter than that of intact fragment because of 612-nt deletion at positions 22777–23388 (1,593 vs 981 nt for PEDV reference strains and PEDV variant, respectively; online Technical Appendix Figure 1, http://wwwnc.cdc.gov/EID/article/20/12/13-1642-Techapp1.pdf). Sequence similarity of the 981-nt fragment of MF3809 was found to be in PEDV S gene region in GenBank by BLAST analysis (http://blast.ncbi.nlm.nih.gov/Blast.cgi). The complete S gene (3549-nt segment, corresponding to 1182 aa) of MF3809 had high (93.3%–98.5% nt, 92.0%–98.0% aa) sequence identity to all known PEDV strains for which full-length S gene sequences were available in GenBank, except that MF3809 has the large deletion in its S gene. Phylogenetic analysis confirmed that MF3809 belonged to a cluster containing a PEDV reference strain, not a cluster that included any other coronaviruses, and showed the closest genetic relationship with PEDV strains from South Korea in 2009 (Figure).

MF3809 had numerous sequence variations in the S protein (online Technical Appendix Table). Besides a large (204-aa) deletion at positions 713–916, a 2-aa (D/NI) deletion was identified at positions 163–164. We also discovered 2 separate insertions: a 4-aa (QGVN) insertion at

Author affiliations: Korea Research Institute of Bioscience and Biotechnology, Daejeon, South Korea (S. Park, S. Kim, D. Song); National Forensic Service, Chilgok, South Korea (S. Park); and Seoul National University, Seoul, South Korea (B. Park)

DOI: http://dx.doi.org/10.3201/eid2012.131642

[1]These authors were co-principal investigators for this study.

Table. Incidence of PEDV RNA in diarrhea samples from pigs, South Korea, January 1–December 31, 2008*

Pig age	No. specimens positive/no. tested (%).		
	Feces	Intestine	Total
Suckling pigs, ≤3 wk	90/526 (17.1)	26/166 (15.7)	116/692 (16.8)
Weaned pigs, >3 wk to 6 wk	12/388 (3.1)	0/116 (0)	12/504 (2.4)
Grower/finisher pigs, >6 wk to 22 wk	29/600 (4.8)	0/208 (0)	29/808 (3.6)
Sows, ≥1 y	34/140 (24.3)	0/1 (0)	34/141 (24.1)
Boars, ≥8 mo	1/6 (16.7)	0	1/6 (16.7)
Unknown	13/402 (3.2)	0/81 (0)	13/483 (2.7)
Total	179/ 2062 (8.7)	26/572 (4.5)	205/2634 (7.8)

*All animals showed signs of diarrhea at the time of sample collection. The PEDV variant with a large deletion in the S gene was found in 3 samples (2 fecal and 1 intestinal) of the suckling pigs with diarrhea at 1 farm in Chungnam Province. Other pigs on the same farm were infected with PEDV with the full-length S gene; however, in no instance were both the PEDV variant and PEDV with the full-length S gene observed in 1 pig. PEDV, porcine epidemic diarrhea virus; S gene, spike gene.

positions 59–62 and a 1-aa (N) insertion at position 140. A total of 15 separate substitutions were identified, and the number(s) of replaced amino acids ranged from 1 through 5. These sequence variations were similar to those in highly virulent isolates recently reported in China (*6*) and the United States (*3*), as well as in South Korea.

To further characterize the virus, we conducted RT-PCR with respect to the membrane (M) gene using the protocol described previously (*7*). The complete M gene sequence was determined and then submitted, together with the complete S gene sequence, to GenBank under accession no. KF779470. The entire M gene of MF3809 had 96.6%–100% nt (96.0%–100% aa) sequence identity to all known PEDV strains available in GenBank, and phylogenetic analysis showed that MF3809 belonged to a cluster containing PEDV reference strain and showed the closest genetic relationship with 2007 Korean PEDV strains (data not shown).

The filtered samples positive for PEDV variant were inoculated onto Vero cells. After 3 serial passages, no

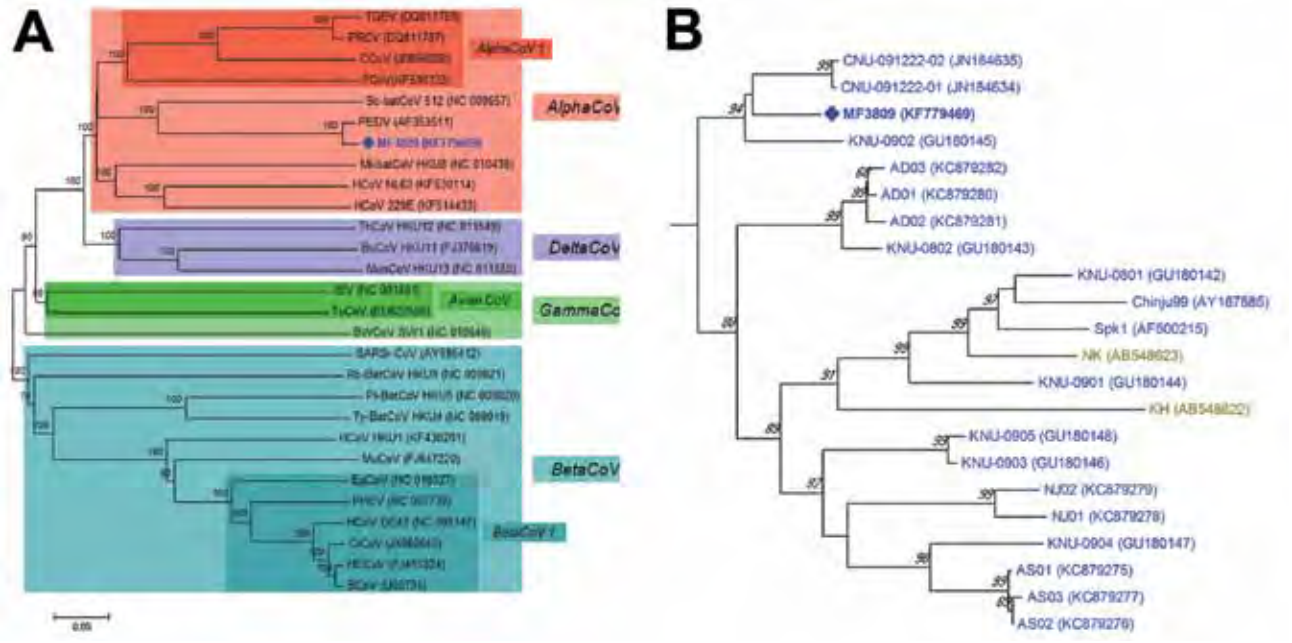

Figure. A) Relationships between the PEDV variant (MF3809/2008/South Korea) and other coronaviruses based on the full-length spike gene. PEDV, porcene epidemic diarrhea virus; TGEV, transmissible gastroenteritis virus; PRCV, porcine respiratory coronavirus; CCoV, canine coronavirus; FCoV, feline coronavirus; HCoV, human coronavirus; Mi-batCoV, *Miniopterus* bat coronavirus; Sc-batCoV, *Scotophilus* bat coronavirus; HECoV, human enteric coronavirus; BCoV, bovine coronavirus; PHEV, porcine hemagglutinating encephalomyelitis virus; EqCoV, equine coronavirus; CrCoV, canine respiratory coronavirus; MuCoV, murine coronavirus; Pi-BatCoV, *Pipistrellus* bat coronavirus; Ro-BatCoV, Rousettus bat coronavirus; SARSr-CoV, severe acute respiratory syndrome-related coronavirus; Ty-BatCoV, Tylonycteris bat coronavirus; IBV, infectious bronchitis virus; TuCoV, turkey coronavirus; BWCoV, Beluga whale coronavirus; BuCoV, bulbul coronavirus; ThCoV, thrush coronavirus; MunCoV, munia coronavirus. B) Phylogenetic tree of the entire spike genes of the PEDV variant and all known PEDV strains available in GenBank. The phylogenetic tree was constructed using the neighbor-joining clustering method in MEGA version 5.22 with a pairwise distance (5). Bootstrap values (based on 1,000 replicates) for each node are given if >60%. Scale bar indicates nucleotide substitutions per site. PEDV strains isolated from various countries are marked with colors as follows: Europe (black), China (red), Japan (olive green), USA (bright magenta) and South Korea (blue). PEDV, porcine epidemic diarrhea virus.

obvious cytopathic effect in Vero cells was noted. Cells and supernatants in every passage were collected separately for RNA extraction and used to detect the virus and determine the amount of the viral RNA in the medium with real-time RT-PCR (*8*). The cells and supernatants of the 3 passages were positive for the virus, and the control inoculated with PBS was negative; however, the amount of viral RNA in the medium decreased with each passage. Whether the positive result was attributed to residual viruses of the initial inoculation or to the decreased propagation of the virus in the cells is not clear. Further studies, such as continuous serial passages and neutralization assays, are needed to determine the final activity of the virus in Vero cells.

Conclusions

Our large-scale study of the incidence of PEDV in pigs with diarrhea in South Korea found that 7.8% of animals were infected with the virus. Moreover, our investigation identified and characterized a new PEDV variant with a 612-nt deletion in S gene, corresponding to a 204-aa deletion. The coronavirus S protein plays a pivotal role in regulating interactions with specific host cell receptor glycoproteins to mediate viral entry and stimulate induction of neutralizing antibodies in the natural host (*1*,*2*,*9*). Mutations or deletions in the coronavirus S gene affect its pathogenicity and tissue tropism (*10*–*12*). Porcine respiratory coronavirus (PRCV), a naturally occurring deletion mutant of transmissible gastroenteritis virus (TGEV), is an example of pathogenic change and tropism switching, apparently associated with S gene change. PRCV has a 224-aa deletion at positions 21–244 in the N terminal region, which is needed for the enteric tropism of TGEV and comprises antigenic sites C and B (*13*–*15*), of S1 compared with TGEV. In other words, TGEV, a highly enteropathogenic porcine coronavirus, is turned into PRCV, a respiratory pathogen with reduced pathogenicity, as a consequence of a large deletion in the S gene. Unlike PRCV, the PEDV variant has a 204-aa deletion at positions 713–916 in the C-terminus of S1 and N terminus of S2, destroying 4 N-linked glycosylation sites at positions 728, 745, 783, and 875, as well as 2 neutralizing epitopes, SS2 (753–760) and SS6 (769–776) (online Technical Appendix Figure 2). These amino acid mutations might cause the conformational change of S protein and result in antigenicity/immunogenicity alteration of the PEDV variant. However, how the PEDV variant was generated and has evolved is not clear. Further studies should be conducted to analyze extensive genomic sequences and determine biological properties, such as pathogenicity, tissue tropism, and transmissibility of the new PEDV variant.

This study was supported by a grant (PJ009015) from BioGreen 21 Program, South Korea. This work was supported by a National Agenda Project grant from the Korea Research Council of Fundamental Science and Technology and the KRIBB Initiative program (KGM3121322).

Dr Seongjun Park is a virologist at the Viral Infectious Disease Research Center, Korea Research Institute of Bioscience and Biotechnology and the Forensic Medicine Division, Daegu Institute, National Forensic Service. His research interests include diagnosis, molecular virology, and epidemiology of emerging viral pathogens of public health significance.

References

1. Song D, Park B. Porcine epidemic diarrhoea virus: a comprehensive review of molecular epidemiology, diagnosis, and vaccines. Virus Genes. 2012;44:167–75. http://dx.doi.org/10.1007/s11262-012-0713-1
2. Saif LJ, Pensaert MB, Sestak K, Yeo SG, Jung K. Coronaviruses. In: Zimmerman JJ, Karriker LA, Ramirez A, Schwartz KJ, Stevenson GW, editors. Disease of swine. Hoboken (NJ): Wiley-Blackwell; 2012. p. 501–24.
3. Stevenson GW, Hoang H, Schwartz KJ, Burrough ER, Sun D, Madson D, et al. Emergence of porcine epidemic diarrhea virus in the United States: clinical signs, lesions, and viral genomic sequences. J Vet Diagn Invest. 2013;25:649–54. http://dx.doi.org/10.1177/1040638713501675
4. Park SJ, Song DS, Ha GW, Park BK. Cloning and further sequence analysis of the spike gene of attenuated porcine epidemic diarrhea virus DR13. Virus Genes. 2007;35:55–64. http://dx.doi.org/10.1007/s11262-006-0036-1
5. Tamura K, Peterson D, Peterson N, Stecher G, Nei M, Kumar S. MEGA5: Molecular evolutionary genetics analysis using maximum likelihood, evolutionary distance, and maximum parsimony methods. Mol Biol Evol. 2011;28:2731–9. http://dx.doi.org/10.1093/molbev/msr121
6. Tian Y, Yu Z, Cheng K, Liu Y, Huang J, Xin Y, et al. Molecular characterization and phylogenetic analysis of new variants of the porcine epidemic diarrhea virus in Gansu, China in 2012. Viruses. 2013;5:1991–2004. http://dx.doi.org/10.3390/v5081991
7. Park SJ, Kim HK, Song DS, Moon HJ, Park BK. Molecular characterization and phylogenetic analysis of porcine epidemic diarrhea virus (PEDV) field isolates in Korea. Arch Virol. 2011;156:577–85. http://dx.doi.org/10.1007/s00705-010-0892-9
8. Kim SH, Kim IJ, Pyo HM, Tark DS, Song JY, Hyun BH. Multiplex real-time RT-PCR for the simultaneous detection and quantification of transmissible gastroenteritis virus and porcine epidemic diarrhea virus. J Virol Methods. 2007;146:172–7. http://dx.doi.org/10.1016/j.jviromet.2007.06.021
9. Masters PS. The molecular biology of coronaviruses. Adv Virus Res. 2006;66:193–292. http://dx.doi.org/10.1016/S0065-3527(06)66005-3
10. Laude H, Van Reeth K, Pensaert M. Porcine respiratory coronavirus: molecular features and virus–host interactions. Vet Res. 1993;24:125–50.
11. Bernard S, Laude H. Site-specific alteration of transmissible gastroenteritis virus spike protein results in markedly reduced pathogenicity. J Gen Virol. 1995;76:2235–41. http://dx.doi.org/10.1099/0022-1317-76-9-2235
12. Gallagher TM, Buchmeier MJ. Coronavirus spike proteins in viral entry and pathogenesis. Virology. 2001;279:371–4. http://dx.doi.org/10.1006/viro.2000.0757

13. Callebaut P, Correa I, Pensaert M, Jimenez G, Enjuanes L. Antigenic differentiation between transmissible gastroenteritis virus of swine and a related porcine respiratory coronavirus. J Gen Virol. 1988;69:1725–30. http://dx.doi.org/10.1099/0022-1317-69-7-1725
14. Reguera J, Ordono D, Santiago C, Enjuanes L, Casasnovas JM. Antigenic modules in the N-terminal S1 region of the transmissible gastroenteritis virus spike protein. J Gen Virol. 2011;92:1117–26. http://dx.doi.org/10.1099/vir.0.027607-0
15. Sánchez CM, Gebauer F, Suñé C, Mendez A, Dopazo J, Enjuanes L. Genetic evolution and tropism of transmissible gastroenteritis coronaviruses. Virology. 1992;190:92–105. http://dx.doi.org/10.1016/0042-6822(92)91195-Z

Addresses for correspondence: Bongkyun Park, Department of Veterinary Medicine Virology Laboratory, College of Veterinary Medicine and Research Institute for Veterinary Science, Seoul National University, Gwanak-gu, Seoul, 151-742, South Korea; email: parkx026@snu.ac.kr

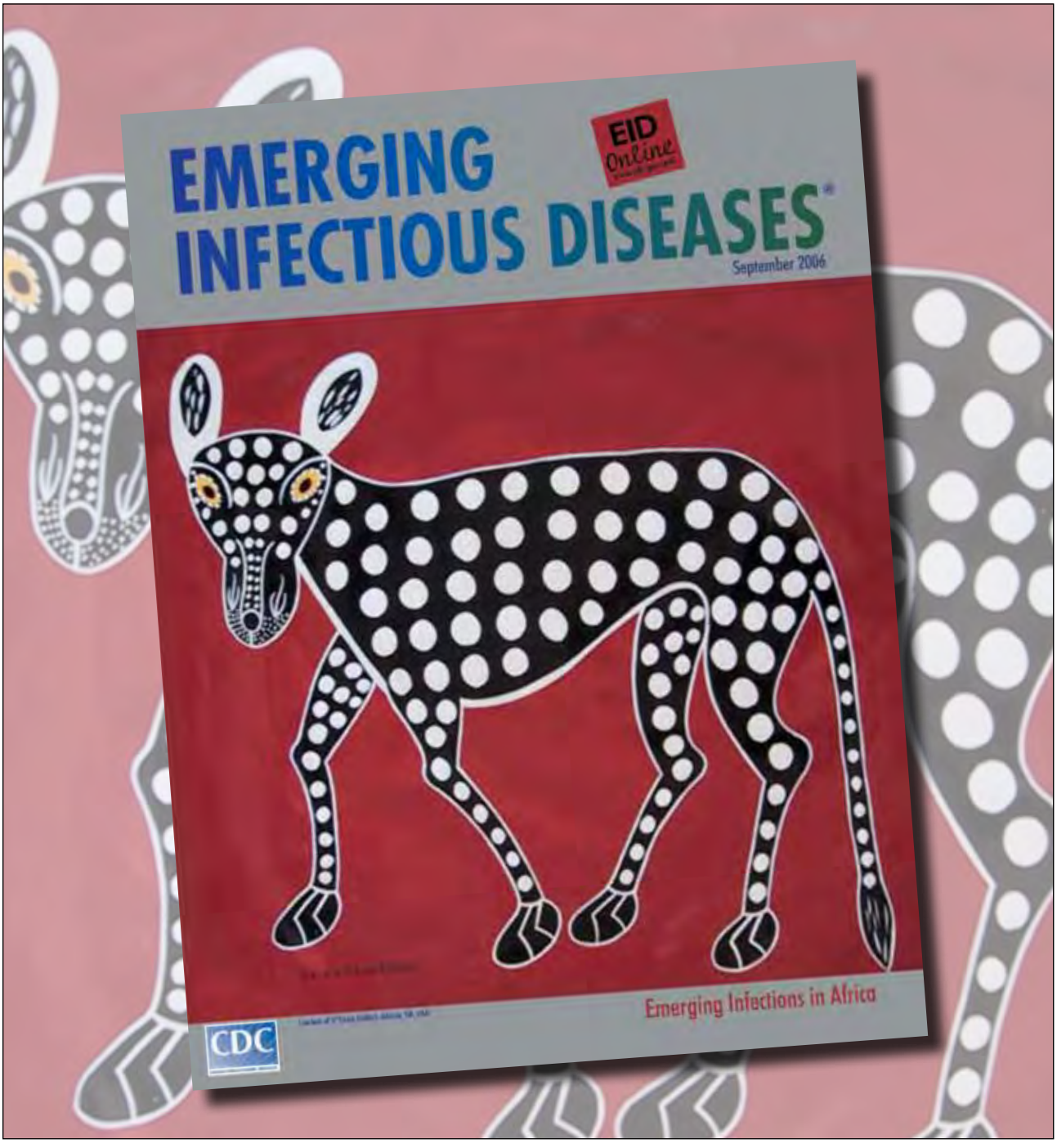

MERS Coronavirus **Neutralizing** Antibodies in Camels, Eastern Africa, 1983–1997

Marcel A. Müller,[1] Victor Max Corman,[1] Joerg Jores, Benjamin Meyer, Mario Younan, Anne Liljander, Berend-Jan Bosch, Erik Lattwein, Mosaad Hilali, Bakri E. Musa, Set Bornstein, and Christian Drosten

To analyze the distribution of Middle East respiratory syndrome coronavirus (MERS-CoV)–seropositive dromedary camels in eastern Africa, we tested 189 archived serum samples accumulated during the past 30 years. We identified MERS-CoV neutralizing antibodies in 81.0% of samples from the main camel-exporting countries, Sudan and Somalia, suggesting long-term virus circulation in these animals.

Since 2012, a newly emerged human pathogenic coronavirus (CoV) has caused an ongoing epidemic on the Arabian Peninsula. The designated Middle East respiratory syndrome (MERS)-CoV belongs to the *Betacoronavirus* genus lineage C and causes severe respiratory disease in humans (*1*). As of July 2, 2014, MERS-CoV has caused ≈842 human infections, including 322 deaths (*2*). Dromedary camels are a putative source for MERS-CoV infection in humans. Dromedaries from countries in Africa (Egypt, Tunisia, Nigeria, Sudan, Ethiopia, and Kenya) and Arabia (United Arab Emirates, Saudi Arabia, Oman, Qatar, and Jordan) have shown high rates of MERS-CoV seropositivity in serum samples collected during the past 2 decades (*3*–*9*). In addition, MERS-CoV nucleotide sequences and virus were detected in respiratory swab samples, predominantly from juvenile dromedaries (*5*,*10*). Transmission between humans and camels has been described in Qatar and Saudi Arabia (*11*,*12*). No autochthonous MERS-CoV infections in humans have been reported in Africa. Most dromedary camels traded in the Middle East are bred in the Greater Horn of Africa, primarily in Ethiopia, Sudan, Somalia, and Kenya (*13*). To further analyze the spatial and temporal distribution of MERS-CoV–seropositive camels, we tested archived camel serum samples originating in Egypt, Sudan, and Somalia, accumulated during the past 30 years, for MERS-CoV antibodies.

The Study

A serum sample from each of 189 dromedary camels was collected by trained personnel as previously described (*14*). Blood samples were taken by jugular vein puncture. The blood was allowed to clot and subsequently centrifuged to obtain serum, or serum was separated from the coagulated blood during slaughter. All serum samples were heat-inactivated at 56°C for 30 min (*14*). Serum from Somalia was collected during 1983 and 1984; samples from Sudan were collected during June and July 1984, and samples from Egypt were collected during June and July 1997. All camels from Sudan were female (>6 years of age) and belonged to the Anafi breed. They were kept locally and used as a means of transport and a source of milk. The camels from Somalia were sampled at slaughterhouses in Afgoi and Mogadishu. Most camels were adults; however, detailed information about sex and age was not available. The camels from Somalia were bred predominantly for milk and meat. No background information was available for the camels from Egypt. Our study fully complied with national regulations and was approved by the ethics committee of the International Livestock Research Institute accredited by the National Council of Science and Technology in Kenya (approval no. ILRI-IREC2013–12).

We tested all serum samples for MERS-CoV antibodies at a 1:100 dilution by a recombinant MERS-CoV spike protein subunit 1–based ELISA (rELISA) as previously described (*3*,*12*). To determine the assay-specific cutoff value, we tested 124 confirmed MERS-CoV antibody–negative and 106 MERS-COV antibody–positive camel serum samples from previous studies (*3*). For inter-assay calibration, we used the same selected positive serum samples in all applications. The optical density (OD) was measured at 450/605 nm. We determined the OD ratio by dividing the OD of each sample by the OD of the positive serum. The cutoff was defined as the 3-fold mean OD ratio of all tested MERS-CoV antibody–negative serum samples (online Technical Appendix Figure 1, http://wwwnc.cdc.gov/EID/article/20/12/14-1026-Techapp1.pdf). To confirm antibody specificity and rule out possible cross-reactivity with other livestock-associated CoVs, we conducted a highly specific MERS-CoV

Author affiliations: University of Bonn Medical Centre, Bonn, Germany (M.A. Müller, V.M. Corman, B. Meyer, C. Drosten); German Centre for Infection Research, Bonn (V.M. Corman); International Livestock Research Institute, Nairobi, Kenya (J. Jores, A. Liljander); Vétérinaires Sans Frontières Germany, Nairobi (M. Younan); Utrecht University, Utrecht, the Netherlands (B.-J. Bosch); EUROIMMUN AG, Lübeck, Germany (E. Lattwein); Cairo University, Giza, Egypt (M. Hilali); Ministry of Science and Communication, Khartoum, Sudan (B.E. Musa); and National Veterinary Institute, Uppsala, Sweden (S. Bornstein)

DOI: http://dx.doi.org/10.3201/eid2012.141026

[1]These authors contributed equally to this article.

microneutralization test (*3*,*6*). All serum samples were tested at a 1:80 dilution and at a 1:800 dilution to identify MERS-CoV neutralizing antibodies. Serum without neutralizing activity at 1:80 was rated MERS-CoV antibody negative.

A total of 159 (84.1%; range among countries 80.0%–86.7%) of 189 dromedary camels were positive for MERS-CoV antibodies in the rELISA (Figure, Table 1). The highly specific neutralization test confirmed that 153 (81.0%; range 68.0%–86.9%) of camels had neutralizing activity with reciprocal titers of >80 (Table 1). Whereas most samples (124 [65.6%; range 56.0%–73.8%]) had reciprocal neutralizing titers of 80–800, we detected high neutralizing titers of >800 in 29 (15.3%; range 11.6%–21.7%) samples (Table 2). Neutralizing titers correlated significantly ($p<0.001$, Kruskal-Wallis 1-way analysis of variance) with the determined OD ratios of the rELISA. The rELISA was 99.0% specific when correlated with the results of the microneutralization test (online Technical Appendix Figure 2).

MERS-CoV antibody–carrying dromedaries were present in all 3 countries in 1983, 1984, and 1997 (Figure; Tables 1, 2). The high seropositivity in camels from Egypt (35 [81.4%] of 43), a country that imports camels from Sudan and Somalia, was consistent with previous studies (*7*,*10*). Strikingly, camels sampled in Somalia and Sudan >30 years ago were identified as MERS-CoV antibody positive with seropositivity of up to 86.7% in Sudan in 1983.

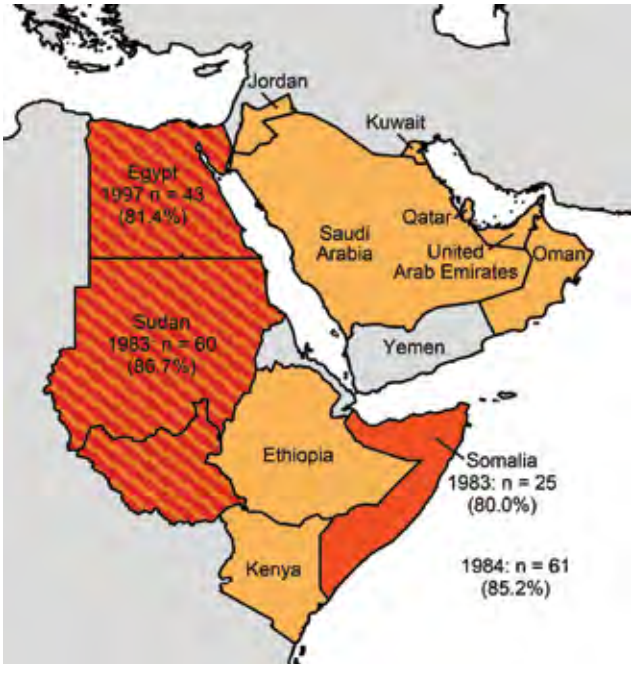

Figure. Arabian Peninsula and neighboring countries of the Greater Horn of Africa in 2014. The study sites Egypt, Sudan (separated into Sudan and South Sudan), and Somalia are in dark orange and labeled with the year the camels were sampled, the number of samples, and the percentage of samples that were reactive in the MERS-CoV ELISA. Countries with previously reported MERS-CoV seropositive dromedaries are in light orange (overlap shown in stripes).

Conclusions

Our study complements and supports the latest findings on long-term and widespread circulation of MERS-CoV or MERS-like CoV in dromedaries in Africa (*3*,*7*,*9*,*10*). By identifying neutralizing antibodies for MERS-CoV in Somalia dromedaries, we provided data for the country lodging the world's largest camel population and from which many camels are exported to Saudi Arabia (*13*). The large proportion of adult animals tested in this study explains the high seropositivity (>80%) and agrees with previous observations (*3*,*6*,*12*). Earlier reports provided evidence for seropositive camels in Kenya and Saudi Arabia dating to the early 1990s (*3*,*4*). Here we describe the presence of anti-MERS-CoV antibodies in archived serum collected >30 years ago, increasing the timescale for detection by an additional decade. Long-term circulation of MERS-CoV or MERS-like CoV in dromedaries can therefore be hypothesized. As suggested, an important factor possibly contributing to continuous virus maintenance in camels could be a high camel population density combined with nomadic husbandry, including frequent contact among camel herds in the Greater Horn of Africa (*3*).

MERS-CoV sequences from camels in Saudi Arabia and Qatar were closely related to sequences found in humans and did not show major genetic variability that would support long-term evolution of MERS-CoV in camels (*10*,*11*). The MERS-CoV sequence from a camel in Egypt was phylogenetically most distantly related to all other known camel-associated MERS-CoVs but closely related to the early human MERS-CoV isolates (*10*). An urgent task would be to characterize the diversity of MERS-related CoV in other camels in Africa to elucidate whether the current epidemic MERS-CoV strains have evolved toward more efficient human transmissibility.

The existence of unrecognized human infections in African or Arabian countries in the past cannot be ruled out. Resource-limited African countries that have been exposed to civil unrest, such as Somalia and Sudan, are not likely to diagnose and report diagnostically challenging infections

Table 1. MERS-CoV antibodies in dromedary camels from eastern Africa*

Country, date	No. samples	No. rELISA positive (%)†	No. mNT positive (%)‡
Egypt, 1997 Jul	43	35 (81.4)	34 (79.1)
Somalia			
1983 Jan–Nov	25	20 (80.0)	17 (68.0)
1984 Feb–Dec	61	52 (85.2)	53 (86.9)
Sudan, 1983 Jun	60	52 (86.7)	49 (81.7)
Total	189	159 (84.1)	153 (81.0)

*MERS-CoV, Middle East respiratory syndrome coronavirus; mNT, microneutralization test; rELISA, recombinant ELISA based on the MERS-CoV subunit 1 spike protein.
†Serum was tested at a dilution of 1:100.
‡mNT for MERS-CoV was done in a microtiter plate format in duplicate at dilutions 1:80 and 1:800. Serum with reciprocal titers >80 were considered MERS-CoV antibody positive.

Table 2. MERS-CoV neutralizing antibody titers in dromedary camels from eastern Africa*

Country, date	No. samples	mNT titer, no. (%) samples†		
		<80	80–800	>800
Egypt, 1997 Jul	43	9 (20.9)	29 (67.4)	5 (11.6)
Somalia				
1983 Jan–Nov	25	8 (32.0)	14 (56.0)	3 (12.0)
1984 Feb–Dec	61	8 (13.1)	45 (73.8)	8 (13.1)
Sudan, 1983 Jun	60	11 (18.3)	36 (60.0)	13 (21.7)
Total	189	36 (19.0)	124 (65.6)	29 (15.3)

*MERS-CoV, Middle East respiratory syndrome coronavirus; mNT, microneutralization test.
†mNT for MERS-CoV was done in a microtiter plate format in duplicate at dilutions 1:80 and 1:800. Serum with reciprocal titers >80 were considered MERS-CoV antibody positive.

resembling other diseases. The lack of MERS-CoV antibodies in a small cohort serosurvey in Saudi Arabia did not suggest the long-term circulation of MERS-CoV in humans on the Arabian Peninsula (*15*). Large serosurveys in countries where camels are bred and traded, especially in eastern Africa, are needed to explore the general MERS-CoV seroprevalence in camels and humans, particularly humans who have close contact with camels. Such serosurveys could provide the data needed to ascertain whether MERS-CoV has been introduced into, but unrecognized in, the human population on the African continent.

Acknowledgments

We thank Stephan Kallies, Monika Eschbach-Bludau, Sebastian Brünink, Tobias Bleicker, and Andrea Sieberg for excellent technical assistance. We are grateful to Tasnim Suliman for critical reading of the manuscript. We thank Fatuma M. Jama and all camel owners and herdsmen for their support during field work.

The work was funded by the European Commission (FP7-EMPERIE no. 223498, FP7-ANTIGONE no. 278976) and the German Research Foundation (DFG grant DR772/3-1 to C.D.). This work was supported by the Consultative Group for International Agricultural Research (CGIAR) program on Agriculture for Nutrition and Health. The Centrum of International Migration (CIM) supported A.L. The funders had no role in study design, data collection and analysis, decision to publish, or preparation of the manuscript.

Dr Müller is staff scientist at the Institute of Virology, University of Bonn Medical Centre. His current research is dedicated to developing serologic detection methods for emerging viruses and in-depth molecular studies focusing on virus–host interactions.

References

1. Zaki AM, van Boheemen S, Bestebroer TM, Osterhaus AD, Fouchier RA. Isolation of a novel coronavirus from a man with pneumonia in Saudi Arabia. N Engl J Med. 2012;367:1814–20. http://dx.doi.org/10.1056/NEJMoa1211721
2. European Centre for Disease Prevention and Control. Epidemiological update: Middle East respiratory syndrome coronavirus (MERS-CoV). 02 July 2014 [cited 2014 Jul 3]. http://www.ecdc.europa.eu/en/press/news/_layouts/forms/News_DispForm.aspx?List=8db7286c-fe2d-476c-9133-18ff4cb1b568&ID=1029
3. Corman VM, Jores J, Meyer B, Younan M, Liljander A, Said MY, et al. Antibodies against MERS coronavirus in dromedary camels, Kenya, 1992–2013. Emerg Infect Dis [Internet]. 2014 Aug [cited 2014 Jul 21]. http://dx.doi.org/10.3201/eid2008.140596
4. Hemida M, Perera R, Al Jassim R, Kayali G, Siu L, Wang P, et al. Seroepidemiology of Middle East respiratory syndrome (MERS) coronavirus in Saudi Arabia (1993) and Australia (2014) and characterisation of assay specificity. Euro Surveill. 2014;19:20828. http://dx.doi.org/10.2807/1560-7917.ES2014.19.23.20828
5. Hemida MG, Chu DK, Poon LL, Perera RA, Alhammadi MA, Ng HY, et al. MERS coronavirus in dromedary camel herd, Saudi Arabia. Emerg Infect Dis. 2014;20.
6. Meyer B, Muller MA, Corman VM, Reusken CB, Ritz D, Godecke GJ, et al. Antibodies against MERS coronavirus in dromedaries, United Arab Emirates, 2003 and 2013. Emerg Infect Dis. 2014;20:552–9. http://dx.doi.org/10.3201/eid2004.131746
7. Perera RA1, Wang P, Gomaa MR, El-Shesheny R, Kandeil A, Bagato O, et al. Seroepidemiology for MERS coronavirus using microneutralisation and pseudoparticle virus neutralisation assays reveal a high prevalence of antibody in dromedary camels in Egypt, June 2013. Euro Surveill. 2013;18:20574. http://dx.doi.org/10.2807/1560-7917.ES2013.18.36.20574
8. Reusken CB, Haagmans BL, Muller MA, Gutierrez C, Godeke GJ, Meyer B, et al. Middle East respiratory syndrome coronavirus neutralising serum antibodies in dromedary camels: a comparative serological study. Lancet Infect Dis. 2013;13:859–66. http://dx.doi.org/10.1016/S1473-3099(13)70164-6
9. Reusken CBEM, Messadi L, Feyisa A, Ularamu H, Godeke GJ, Danmarwa A, et al. Geographic distribution of MERS coronavirus among dromedary camels, Africa. Emerg Infect Dis [Internet]. 2014 Dec [cited 2014 Jul 21]. http://dx.doi.org/10.3201/eid2008.140590
10. Chu DK, Poon LL, Gomaa MM, Shehata MM, Perera RA, Abu Zeid D, et al. MERS coronaviruses in dromedary camels, Egypt. Emerg Infect Dis. 2014;20:1049–53. http://dx.doi.org/10.3201/eid2006.140299
11. Haagmans BL, Al Dhahiry SH, Reusken CB, Raj VS, Galiano M, Myers R, et al. Middle East respiratory syndrome coronavirus in dromedary camels: an outbreak investigation. Lancet Infect Dis. 2014;14:140–5. http://dx.doi.org/10.1016/S1473-3099(13)70690-X
12. Memish ZA, Cotten M, Meyer B, Watson SJ, Alsahafi AJ, Al Rabeeah AA, et al. Human infection with MERS coronavirus after exposure to infected camels, Saudi Arabia, 2013. Emerg Infect Dis. 2014;20:1012–5. http://dx.doi.org/10.3201/eid2006.140402
13. Food and Agriculture Organisiation of the United Nations. FAOSTAT [cited 2014 Jul 21]. http://faostat3.fao.org/faostat-gateway/go/to/home/E
14. Bornstein S, Musa BE. Prevalence of antibodies to some viral pathogens, *Brucella abortus* and *Toxoplasma gondii* in serum from camels (*Camelus dromedarius*) in Sudan. Zentralbl Veterinarmed B. 1987;34:364–70.
15. Aburizaiza AS, Mattes FM, Azhar EI, Hassan AM, Memish ZA, Muth D, et al. Investigation of anti–Middle East respiratory syndrome antibodies in blood donors and slaughterhouse workers in Jeddah and Makkah, Saudi Arabia, fall 2012. J Infect Dis. 2014;209:243–6. http://dx.doi.org/10.1093/infdis/jit589

Address for correspondence: Marcel A. Müller, Institute of Virology, University of Bonn Medical Centre, Sigmund-Freud-Str. 25, 53105 Bonn, Germany; email: muller@virology-bonn.de

Equine Influenza A(H3N8) Virus Infection in Cats

Shuo Su,[1] Lifang Wang,[1] Xinliang Fu, Shuyi He, Malin Hong, Pei Zhou, Alexander Lai, Gregory Gray, and Shoujun Li

Interspecies transmission of equine influenza A(H3N8) virus has resulted in establishment of a canine influenza virus. To determine if something similar could happen with cats, we experimentally infected 14 cats with the equine influenza A(H3N8) virus. All showed clinical signs, shed virus, and transmitted the virus to a contact cohort.

Equine influenza A(H3N8) virus (EIV) remains a major cause of acute respiratory infections in horses (*1*). Epizootics are highly explosive and spread rapidly within and among equine premises. Virus transmission is by direct contact and inhalation. First isolated in 1963, EIV has evolved and diverged into American and Eurasian lineages (*2*,*3*). The American lineage has further diverged into multiple clades: Florida-1 clade predominates in North America and Florida-2 clade in Eurasia (*4*).

In Florida, USA, the etiologic agent of an outbreak of acute respiratory disease among greyhounds in 2004 was identified as EIV. Virologic and serologic analyses indicated that this virus had been circulating among greyhounds for several years before. Serologic evidence of infection was also found for pet dogs (*5*). In Great Britain, retrospective analysis showed that an outbreak of respiratory disease among English foxhounds in 2002 was caused by an EIV (*6*). Likewise, this virus was found to have circulated among greyhounds in the United States before 2004 (*7*). The virus has now been established as canine influenza virus and has spread to other breeds and pet dogs; the virus evolved independently from EIV as a monophyletic lineage (*8*).

During the 2003–2004 outbreak of highly pathogenic avian influenza virus (H5N1) infection in Asia, infections in feline species, including cats, were reported. (*9*). Previously, given the lack of circulating feline influenza virus, feral cats had been believed to be resistant to influenza virus, although an earlier report described susceptibility to A/Hong Kong/68 (H3N2) virus infection and prolonged virus shedding (*10*). Recent serologic and virus isolation studies have shown that cats are susceptible to multiple influenza viruses, e.g., avian-origin canine influenza (H3N2) (*11*), seasonal influenza A(H1N1), and influenza A/H1N1) pdm09 (*12*) viruses. To investigate cats' susceptibility to EIV infection and virus transmissibility among cats, we conducted an infection and transmission experiment.

The Study

During 2013–2014, a total of 14 specific pathogen–free domestic shorthair cats, 9–12 weeks of age, were purchased and housed in an accredited Biosafety Level 2 facility at South China Agricultural University, Guangzhou. Results of virus isolation in eggs (nasal and rectal swab samples) and serologic testing determined that these cats were influenza virus free. Experiments were approved by the Institutional Animal Care and Use Committee and monitored by veterinarians.

The virus used was A/equine/Heilongjiang/SS1/2013, which had been isolated from a mule in northern China (S. Su et al., unpub. data). For virus inoculation, 6 cats were anesthetized with xylazine hydrochloride (30 mg/kg intraperitoneally), after which they were inoculated with virus (10 $TCID_{50}$ [median tissue culture infective dose]) in 1.0 mL of phosphate-buffered saline (0.5 mL in each nostril). One day after inoculation, 5 specific pathogen–free cats (contact cohort) were introduced into the same cages. Three noninfected cats (control cohort) were housed in a different room. Clinical monitoring began 1 day before virus inoculation and continued daily for the next 14 days. Nasal swab samples were collected daily for virus titration in MDCK cells. Serum was collected on postinoculation days 5, 7, 9, 12, and 14 and titrated by hemagglutination-inhibition assay with a 1% horse erythrocyte suspension. On postinoculation day 5, a total of 2 cats from the inoculated group were euthanized by intravenous pentobarbital, and on postinfection day 7, another 2 cats from the inoculated group plus 2 cats from the contact cohort were euthanized. Necropsies were performed, and trachea and lung sections were stained with hematoxylin and eosin and by an immunocytochemistry technique that involved a murine monoclonal antibody specific to EIV hemagglutinin.

The cats were susceptible to EIV infection; they showed overt clinical signs, virus shedding, and corresponding histopathologic changes in trachea and lung. Infected cats transmitted the virus to cats in the contact cohort. Overt clinical signs characteristic of acute influenza infection developed in inoculated cats during postinfection days 2–9 (peaking at day 4) and in contact cohort cats during days 4–9 (peaking at

Author affiliations: South China Agricultural University, Guangzhou, China (S. Su, L. Wang, X. Fu, S. He, M. Hong, P. Zhou, S. Li); Kentucky State University, Frankfort, Kentucky, USA (A. Lai); University of Florida, Gainesville, Florida, USA (G. Gray); and Key Laboratory of Comprehensive Prevention and Control for Severe Clinical Animal Diseases of Guangdong Province, Guangzhou (S. Su, M. Hong, P. Zhou, S. Li)

DOI: http://dx.doi.org/10.3201/eid2012.140867

[1]These authors contributed equally to this article.

day 5); however, average clinical scores were lower for cats in the contact cohort than in the inoculated cohort (Table). Virus shedding was detected for cats in the inoculated group on days 2–5 and in the contact cohort on days 5–6 (Figure 1). This shift of virus shedding correlated with the shift in clinical signs, suggesting that the cohort group was infected by the virus shed from inoculated cats. Likewise, an antibody response was detected for cats in both groups, again 2–3 days later for the contact cohort.

Productive viral infection was evidenced by histopathologic and immunocytochemical examinations. Characteristic lymphocytic infiltration was observed in samples from cats in the inoculated and contact cohorts; intensity was less for cats in the contact cohort (Figure 2). Likewise, EIV antigen was detected in cats in the inoculated and contact cohorts but not in the control cohort. These results indicated productive viral infection in cats in both cohorts. Because specimens were obtained from euthanized animals on the same date (postinfection day 7), the lower intensity of lymphocyte infiltration corresponded to the shift in virus titer (Figure 1) and clinical signs (Table).

Conclusions

That cats are susceptible to EIV by direct inoculation is not surprising because infection of cats with various influenza A viruses has been reported. Feline respiratory tract epithelial cells contain sialic acid α-2,3-galactose β-1,3-N-acetyl galactosamine (SA α2,3 gal) receptors for avian and equine influenza viruses and SA α2,6 gal receptors for mammalian influenza virus (*13*). However, our finding of horizontal transmission of EIV among cats is significant. If transmission occurs outside the laboratory, and if the basic reproduction rate is higher than 1.0, then EIV could potentially establish itself and circulate in this new host species. Why it has not yet happened naturally, as it did for canine influenza virus (H3N8), remains to be determined. Possibilities include lower transmission efficiency, lower probability of horse–cat contact, less virus shedding than in a laboratory, or feline behavior (less social contact than dogs).

Because cats in the inoculated and contact cohorts were housed in the same cages, our study could not delineate the route of transmission (direct contact or inhalation). Experiments to elucidate the transmission mechanism are being conducted.

Because we had used a contemporary strain of EIV, to rule out the possibility that the ability to cause clinical infection is unique to this strain, we repeated the experiment with the prototype EIV, A/equine/Miami/63 (H3N8). Although 6 of 6 infected cats showed no overt clinical signs, and virus shedding was not detectable (<1:10), susceptibility was evidenced by seroconversion for 2 of the 6 inoculated cats, although at a low hemagglutination-inhibition titer (1:40 on postinoculation day 14), thereby ruling out the possibility that A/equine/Heilongjiang/SS1/2013 is an aberrant virus. None of the 3 cats in the contact cohort showed clinical signs, shed virus, or had detectable hemagglutination-inhibition titers. This strain-dependent variation in virulence is not unusual for influenza virus. Interspecies transmission of EIV to dogs and establishment of a new lineage of equine influenza virus in dogs were probably a function of that particular EIV strain, as evidenced by finding that so far only 1 EIV-originated canine influenza virus lineage is circulating. However, transmission of EIV to dogs has occasionally occurred, including during the epizootic of EIV in Australia (*14*). Of note, the prototype canine influenza virus

Table. Clinical progression for cats in experimental equine influenza A(H3N8) virus inoculation study*

Cohort, cat	No. days after inoculation															
	–1	0	1	2	3	4	5	6	7	8	9	10	11	12	13	14
Inoculated																
A1	0	0	0	2	2.5	3.5	0.5	†								
A2	0	0	0.5	2.5	2.5	3	2	1.5	0.5	0.5	0.5	0	0	0	0	0
A3	0	0	0	2	2.5	2.5	2	0.5	0	†						
A4	0	0	1	2	2	2.5	1.5	0.5	0.5	†						
A5	0	0	0	2	2.5	3	2	†								
A6	0	0	0	2.5	3	3	1	1.5	1.5	0.5	0	0	0	0	0	0
Contact																
B1	0	0	0	0	0	0	2.5	3	2.5	†						
B2	0	0	0	0	0	0	0	0	0	0.5	0	0	0	0	0	0
B3	0	0	0	0	0	1.5	2.5	1.5	1.5	1	1	0	0	0	0	0
B4	0	0	0	0	0	0.5	3	2.5	1.5	†						
B5	0	0	0	0	0	0	0	0.5	0	0	0	0	0	0	0	0
Control																
C1	0	0	0	0	0	0	0	0	0	0	0	0	0	0	0	0
C2	0	0	0	0	0	0	0	0	0	0	0	0	0	0	0	0
C3	0	0	0	0	0	0	0	0	0	0	0	0	0	0	0	0

*Data indicate the sum of clinical scores, as follows: ocular and nasal discharge (0 = no discharge, 0.5 = serous, 1.0 = mild mucopurulent, 2.0 = severe mucopurulent); cough (0 = absent, 0.5 = mild, 1.0 = moderate, 1.5 = persistent, 2.0 = severe with choking or retching); sneezing, dyspnea, and depression (0 = absent, 2 = present); and body temperature (0 = <39.58°C, 2 = ≥39.58°C). Shading indicates days on which some animals had a clinical score ≥1, showing the shift between the 2 cohorts.
†Euthanized on the day indicated.

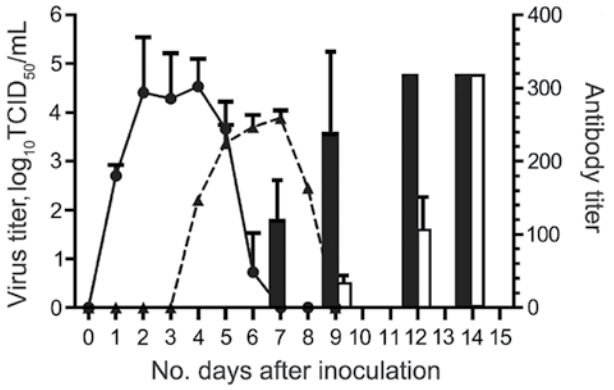

Figure 1. Results of virus titration and hemagglutination-inhibition assay for the cohort of cats inoculated with equine influenza A(H3N8) virus and the contact cohort. Virus shedding was titrated in MDCK cells. Virus titer is shown as $\log_{10}$ median tissue culture infective dose ($TCID_{50}$) (solid line and circles, inoculated cohort; dashed line and triangles, contact cohort). Hemagglutination-inhibition assay of serum samples was conducted by using 1% horse erythrocytes (black bars, inoculated; white bars, contact cohort). Error bars indicate SEM.

is phylogenetically related to the Florida-1 clade of EIV. Whether viruses in this clade have characteristics considered to be "promiscuous" and "plastic" (*15*) remains to be determined. On the basis of our results, we conclude that cats are susceptible to EIV and that the infection can be transmitted by close contact.

Acknowledgment

We thank Wenhua Xiang for providing EIV A/equine/Miami/63 (H3N8) virus and monoclonal antibodies for this study.

This project was supported in part by the National Natural Science Foundation of China (grant no. 31372448), the National Key Basic Research Program (project 973) of China (grant no. 2011CB504700-G), the Natural Science Foundation of Guangdong Province (no. 8251064201000008, S2012020011111), the Basic Conditions for Science and Technology Projects of Guangdong Province (no. 2011B060400015), and the Special Fund for Agro-Scientific Research in the Public Interest (grant No. 201303042).

Dr Su is a researcher at the College of Veterinary Medicine, South China Agricultural University. His research interests include the epidemiology of acute respiratory infections, influenza, and porcine viruses.

References

1. Cullinane A, Newton JR. Equine influenza—a global perspective. Vet Microbiol. 2013;167:205–14. http://dx.doi.org/10.1016/j.vetmic.2013.03.029
2. Daly JM, Lai AC, Binns MM, Chambers TM, Barrandeguy M, Mumford JA. Antigenic and genetic evolution of equine H3N8 influenza A viruses. J Gen Virol. 1996;77:661–71. http://dx.doi.org/10.1099/0022-1317-77-4-661
3. Lai AC, Chambers TM, Holland RE Jr, Morley PS, Haines DM, Townsend HG, et al. Diverged evolution of recent equine-2 influenza (H3N8) viruses in the Western Hemisphere. Arch Virol. 2001;146:1063–74. http://dx.doi.org/10.1007/s007050170106
4. Bryant NA, Rash AS, Russell CA, Ross J, Cooke A, Bowman S, et al. Antigenic and genetic variations in European and North American equine influenza virus strains (H3N8) isolated from 2006 to 2007. Vet Microbiol. 2009;138:41–52. http://dx.doi.org/10.1016/j.vetmic.2009.03.004
5. Crawford PC, Dubovi EJ, Castleman WL, Stephenson I, Gibbs EP, Chen L, et al. Transmission of equine influenza virus to dogs. Science. 2005;310:482–5. http://dx.doi.org/10.1126/science.1117950

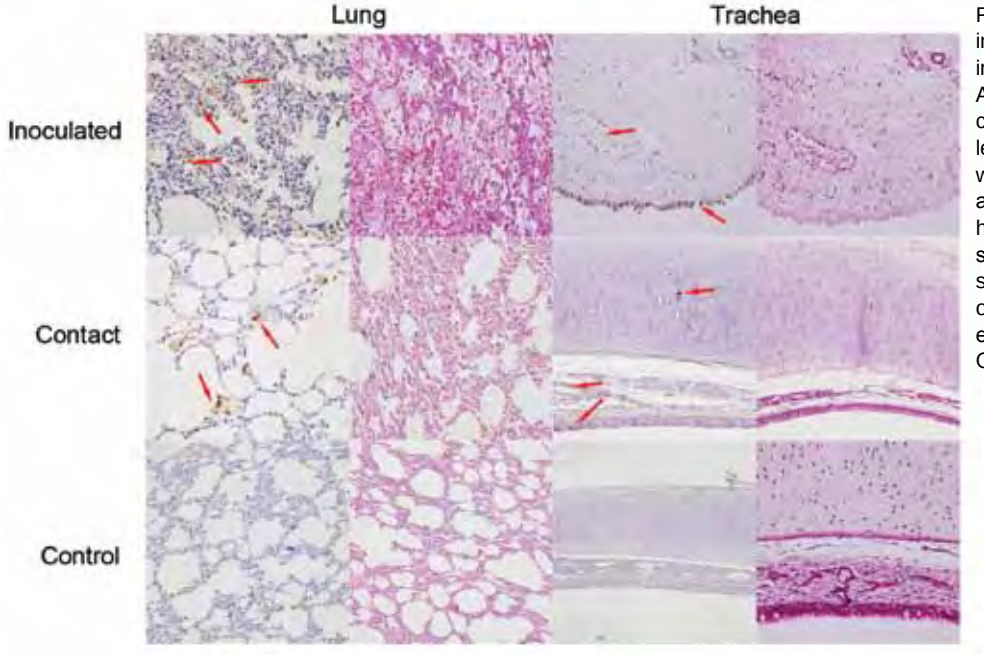

Figure 2. Detection of viral antigens in the respiratory tract of cats inoculated with equine influenza A(H3N8) virus and from a contact cohort. For each tissue type, the left column shows incubation with a monoclonal antibody against equine influenza virus hemagglutinin and the right column shows hematoxylin and eosin staining. Arrows indicate detection of viral antigen (hemagglutinin) expression (brownish staining). Original magnification ×100.

6. Daly JM, Blunden AS, Macrae S, Miller J, Bowman SJ, Kolodziejek J, et al. Transmission of equine influenza virus to English foxhounds. Emerg Infect Dis. 2008;14:461–4. http://dx.doi.org/10.3201/eid1403.070643
7. Anderson TC, Bromfield CR, Crawford PC, Dodds WJ, Gibbs EP, Hernandez JA. Serological evidence of H3N8 canine influenza-like virus circulation in USA dogs prior to 2004. Vet J. 2012;191:312–6. http://dx.doi.org/10.1016/j.tvjl.2011.11.010.
8. Rivailler P, Perry IA, Jang Y, Davis CT, Chen LM, Dubovi EJ, et al. Evolution of canine and equine influenza (H3N8) viruses co-circulating between 2005 and 2008. Virology. 2010;408:71–9. http://dx.doi.org/10.1016/j.virol.2010.08.022.
9. Kuiken T, Rimmelzwaan G, van Riel D, van Amerongen G, Baars M, Fouchier R, et al. Avian H5N1 influenza in cats. Science. 2004;306:241. http://dx.doi.org/10.1126/science.1102287
10. Paniker CK, Nair CM. Infection with A2 Hong Kong influenza virus in domestic cats. Bull World Health Organ. 1970;43:859–62.
11. Song DS, An DJ, Moon HJ, Yeom MJ, Jeong HY, Jeong WS, et al. Interspecies transmission of the canine influenza H3N2 virus to domestic cats in South Korea, 2010. J Gen Virol. 2011;92:2350–5. http://dx.doi.org/10.1099/vir.0.033522-0.
12. McCullers JA, Van De Velde LA, Schultz RD, Mitchell CG, Halford CR, Boyd KL, et al. Seroprevalence of seasonal and pandemic influenza A viruses in domestic cats. Arch Virol. 2011;156:117–20. http://dx.doi.org/10.1007/s00705-010-0809-7.
13. Wang H, Wu X, Cheng Y, An Y, Ning Z. Tissue distribution of human and avian type sialic acid influenza virus receptors in domestic cat. Acta Vet Hung. 2013;61:537–46. http://dx.doi.org/10.1556/AVet.2013.030.
14. Kirkland PD, Finlaison DS, Crispe E, Hurt AC. Influenza virus transmission from horses to dogs, Australia. Emerg infect Dis.2010;16:699–702. DOI: 10.3201/eid1604.091489
15. Gibbs EP, Anderson TC. Equine and canine influenza: a review of current events. Anim Health Res Rev. 2010;11:43–51. http://dx.doi.org/10.1017/S1466252310000046.

Address for correspondence: Alexander Lai, Kentucky State University, Math & Sciences, 208D Carver Hall, 400 E. Main St, Frankfort, KY 40601, USA: email: alexander.lai@kysu.edu; Shoujun Li, College of Veterinary Medicine, South China Agricultural University, 483 Wushan Rd, Tianhe District, Guangzhou, China 510642; email: shoujunli@scau.edu.cn

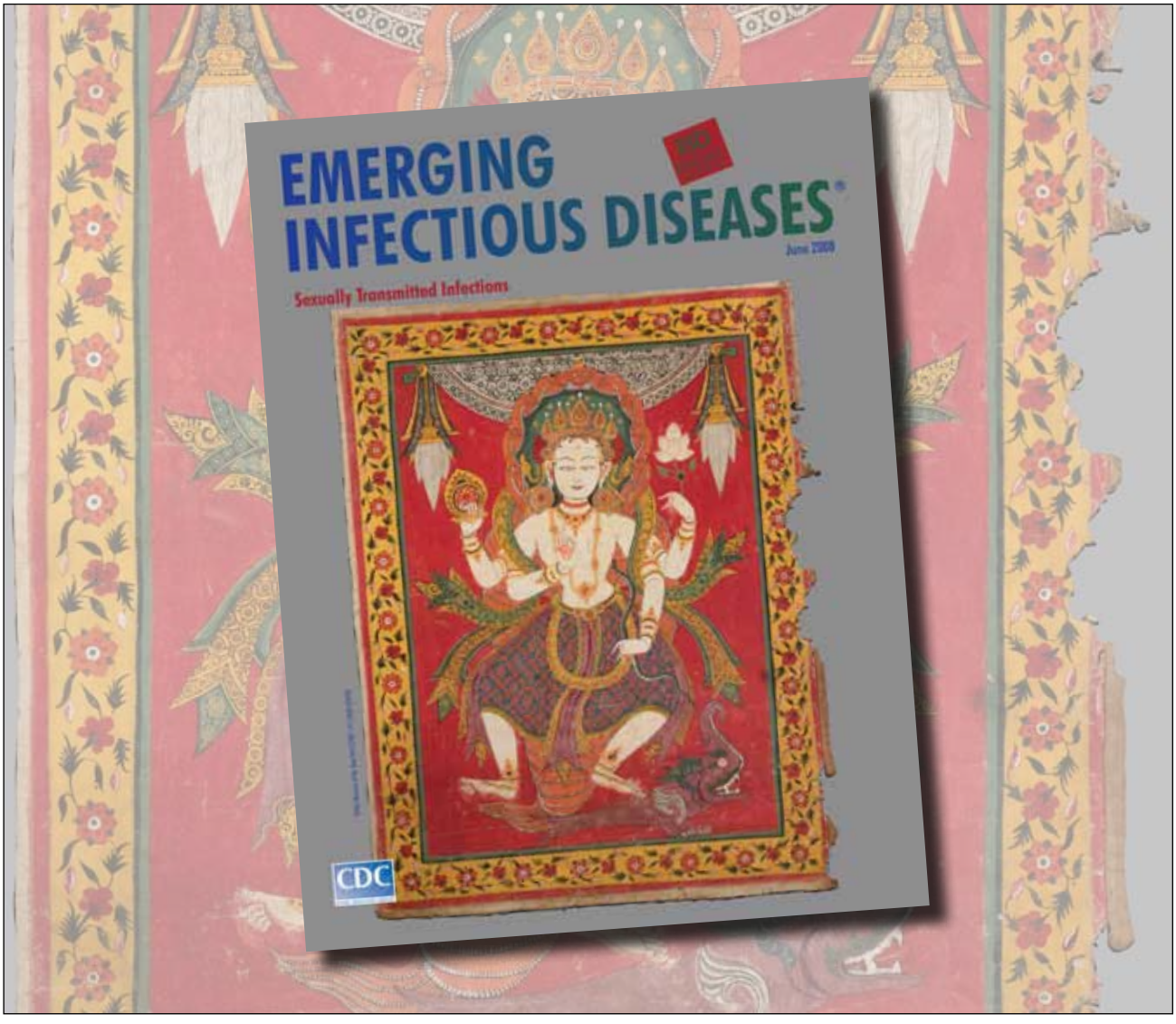

Echinococcus ortleppi Infections in Humans and Cattle, France

Frédéric Grenouillet,[1] Gérald Umhang,[1] Francine Arbez-Gindre, Georges Mantion, Eric Delabrousse, Laurence Millon, and Franck Boué

In 2011 and 2012, liver infections caused by *Echinococcus ortleppi* tapeworms were diagnosed in 2 humans in France. In 2012, a nationwide slaughterhouse survey identified 7 *E. ortleppi* infections in cattle. The foci for these infections were spatially distinct. The prevalence of *E. ortleppi* infections in France may be underestimated.

Cystic echinococcosis (CE) is a zoonotic disease caused by the taeniid tapeworm *Echinococcus granulosus* sensu lato (*1*). This neglected disease is distributed worldwide and causes illnesses in humans and animals (*2*). During the past few decades, the taxonomic status of *E. granulosus* has been uncertain; varying classifications have been proposed for its species, subspecies, and genotypes. This taxon is now recognized as a complex of at least 5 distinct species that encompass 10 genotypes with different host specificities: *E. granulosus* sensu stricto (genotypes G1–G3), *E. equinus* (G4), *E. ortleppi* (G5), and *E. canadensis* (G6–G10) (*3*). *E. ortleppi*, first described in South Africa (*4*,*5*), has a dog/cattle life cycle and is reported to have low pathogenicity for humans. This species is prevalent in South America but has been reported only sporadically on other continents (*6*,*7*).

In France, the annual incidence rate of CE was stable during 2005–2012 at ≈0.18 cases per 100,000 inhabitants, or 110 new cases per year (D. Van Cauteren, unpub. data). A nationwide slaughterhouse survey in 1989 revealed an average infection rate of 0.13% in cattle and 0.42% in sheep and goats (*8*). More recently, low prevalence in slaughterhouses was described in southern France (3 and 4 cases per 100,000 in cattle and sheep, respectively), and only *E. granulosus* sensu stricto larval tapeworms were identified (*9*). We provide evidence of infection with *E. ortleppi* larval tapeworms in France in humans and in cattle and delineate 4 distinct spatial localizations for these infections.

Author affiliations: World Health Organization Collaborating Center for Prevention and Treatment of Human Echinococcosis and French National Reference Center on Alveolar Echinococcosis, Besançon, France (F. Grenouillet, F. Arbez-Gindre, G. Mantion, E. Delabrousse, L. Millon); Chrono-Environnement Unité Mixte de Recherche 6249, Centre National de la Recherche Scientifique et Université de Franche-Comté, Besançon (F. Grenouillet, L. Millon); and Agence Nationale de Sécurité Sanitaire de l'Alimentation National Reference Laboratory for *Echinococcus* spp., Malzéville, France (G. Umhang, F. Boué)

DOI: http://dx.doi.org/10.3201/eid2012.140641

The Cases

In 2011, a 63-year-old man from the Jura *département* (eastern France) sought treatment for moderate pain in the right hypochondrium. Ultrasound examination revealed 2 hyperechoic liver nodules (6 and 3 cm in diameter) in segment V. Computed tomography (CT) scan of the abdomen showed atypical lesions, suggesting a tumor, but magnetic resonance imaging revealed well-defined cysts with internal structure suggestive of CE, with detached endocysts (Figure 1, panels A, B). CE had initially been ruled out because of a negative result from serologic testing for *Echinococcus* (ELISA using *E. granulosus* vesicular fluid). A right hepatectomy was performed, and histopathologic examination of the operative specimen revealed many protoscoleces and detached layers (Figure 1, panels C, D), confirming CE. Retrospective re-analysis of the patient's serum sample showed evidence of antibodies against *Echinococcus*, demonstrated by *E. granulosus* hemagglutination (Fumouze, Levallois, France) at 1:80 and by Western blot (LDBio Products, Lyon, France) showing the typical 7-kDa band. The patient's medical history indicated that he had probably been infected ≈10 years previously through contact with his son's dog in a cattle-breeding, middle-altitude mountainous region (the Haute-Savoie *département* in the French Alps). Ultrasound and serologic screening excluded other CE cases in the patient's family.

In 2012, a 39-year-old woman in the Vendée *département* (western France) sought treatment for abdominal pain and fever; testing showed a typical 7-cm diameter, well-defined liver cyst in segment VII, pathognomonic of CE, despite negative results for *Echinococcus* on serologic testing (ELISA for *E. granulosus*, e.g., hemagglutination Fumouze, Western blot, LDBio). Pericystectomy and cholecystectomy were performed. Histopathologic examination of the liver cyst revealed calcified content with protoscoleces. The patient had been living near farms for >20 years in an area with many stray dogs and where livestock carcasses are not disposed of quickly. Ultrasound screening excluded CE in her husband and children.

During 2012, a nationwide slaughterhouse survey for CE was conducted in France identified *E. ortleppi* infections in 7 cattle. During meat inspection, cysts were

[1]These authors contributed equally to this article.

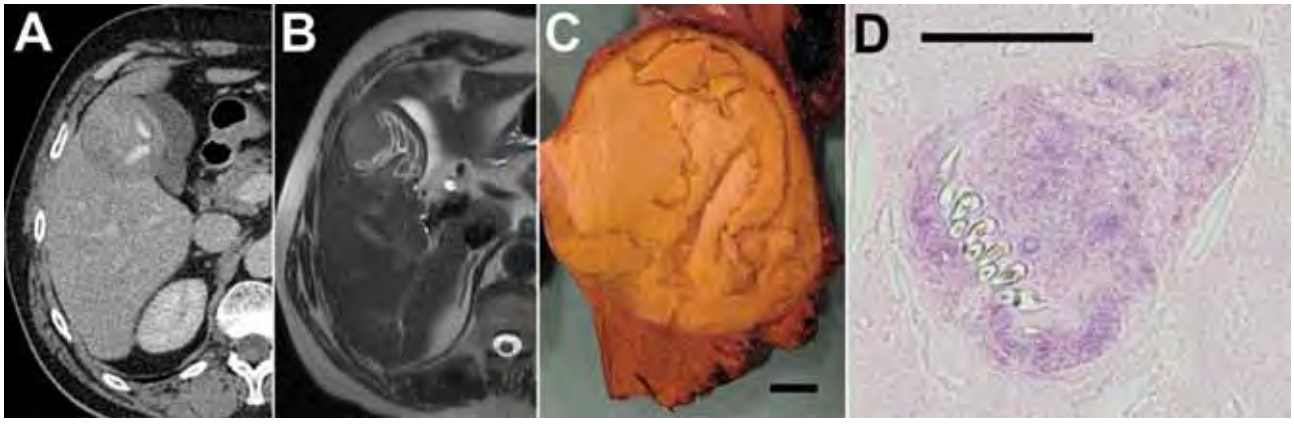

Figure 1. Results of testing in a 63-year-old man from the Jura *département* (eastern France), who was diagnosed with infection with *Echinococcus ortleppi* larval tapeworms in 2001. A) Abdominal computed tomography scan; B) magnetic resonance imaging; and C) macroscopic morphologic examination of operative specimen. All show lesions with a detached endocyst and calcified matrix; scale bar in panel C indicates 1 cm. D) Microscopic examination shows evidence of protoscoleces in the matrix (hematoxylin and eosin stain; scale bar indicates 50 μm).

systematically sampled, then stored for genotyping. Molecular methods identified *E. ortleppi* tapeworms in 7 cattle that had lung cysts. All cases except 1 showed fertile cysts with numerous protoscoleces. Mean age of the animals was 10 (range 3–14) years. The cattle were of 4 breeds; 6 were meat animals, and 1 was a dairy animal. All 7 animals came from 2 foci, 1 in central France (n = 4) and 1 in southwestern France (n = 3); the diameters of these foci were 130 and 160 km, respectively (Figure 2). None of the animals originated from the same herd, but in each focus area, 2 animals came from herds <10 km apart. Three animals had lived on another farm, but in each case, the farm was in the same focus area.

We conducted molecular analyses of fresh cyst tissue samples from the 2 patients and the 7 cattle using PCR-based DNA sequencing of 2 genes, the mitochondrial cytochrome *c* oxidase 1 (*cox1*) and ATPase subunit 6 (*ATP6*), as previously described (*10*,*11*). Samples from all cattle and the female patient showed the same sequences of the *cox1* gene (GenBank accession no. KC430087) and 100% identity with reference *E. ortleppi* gene sequences available in the GenBank database, determined by using BLAST software (http://www.ncbi.nlm.nih.gov/blast). The sample from the male patient, however, had a different *cox1* sequence (GenBank accession no. KJ624625), with 1 substitution. All cattle and human lesions had the same *ATP6* sequence (GenBank accession no. KC430091), showing 100% identity with a reference sequence from GenBank (accession no. DQ318953). All findings were consistent with *E. ortleppi* infection.

Conclusions

Infection with *E. ortleppi* larval tapeworms is rarely diagnosed in humans; a literature search found only 8 reported cases worldwide (*7*). Since 1984, in Europe, infections have been reported in 1 human in the Netherlands (*12*) and in 1 bovid from Italy (*13*). The 2 foci of cattle infections we found did not spatially correspond to the human cases or to the major cattle foci of CE previously identified in France (*8*). Close proximity to cattle and dogs suggests autochthonous infection for the human cases. For the suspected infection area of the male patient (Haute-Savoie), only *E. granulosus* sensu stricto infection had previously been reported in cattle (*9*).

False-negative serologic results are frequent in patients with CE; 10%–20% of patients with hepatic cysts,

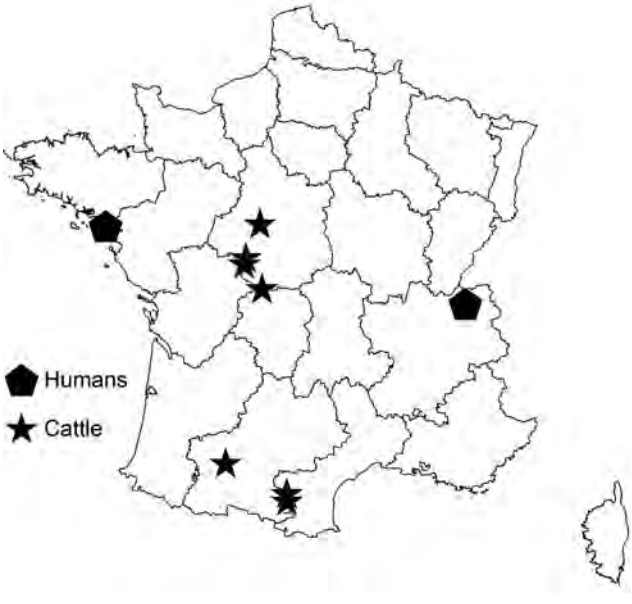

Figure 2. Geographic locations of human and cattle cases of *Echinococcus ortleppi* infection, France, 2011–2012.

especially old and devolving lesions, do not produce detectable specific serum antibodies (*1*). Moreover, antigens used for serologic tests are manufactured from *E. granulosus* sensu stricto G1, which may be antigenically different from *E. ortleppi*. The lack of immunoreactivity in patients with *E. ortleppi* infection has led, and may lead, to underdiagnosis.

E. ortleppi tapeworms are called the "Swiss cattle strain," but some authors have suggested that this species may become extinct in Europe as a result of fewer opportunities for transmission between cattle and dogs (*14*,*15*). However, the fertile lesions observed in cattle and humans in our study may attest to the ability of the parasite to adapt to its hosts. Because home slaughter and deaths of animals without appropriate carcass disposal are rare events in Western European countries, this fertility may compensate for the decreased probability of interactions between cattle-infected viscera and dogs. Because molecular data are scarce, it is difficult to determine how widespread *E. ortleppi* tapeworms are in France or to evaluate the potential for human infection with this parasite.

In summary, our findings of *E. ortleppi* larval tapeworm infections in France highlight the need to enhance national surveillance efforts. *E. ortleppi* tapeworms found in cases of human CE should be systematically genotyped to determine patterns of infection, and meat from slaughterhouses in the 4 identified foci should be inspected carefully. In addition, information on dog infection status and livestock production practices at local cattle farms should be compiled to help identify anomalies in the regulated procedures for carcass treatment and disposal that help maintain the *E. ortleppi* tapeworm life cycle.

Acknowledgments

We thank the General Directorate for Food and the Departmental Directorate for Social Cohesion and Protection of the Population for organizing the nationwide slaughterhouse survey. We are also grateful to Florence Grenouillet, Vanessa Hormaz, Jean-Marc Boucher, and Carine Peytavin de Garam for their excellent technical support and to Lois Rose, Carolyn Engel-Gautier, Dana Pottratz, Jean-Baptiste Aupet, and Michel Gaudron for their editorial assistance.

Dr Grenouillet is a microbiologist at the Besançon University Hospital. His areas of interest include epidemiology, optimization of diagnosis, and follow-up of echinococcosis and invasive fungal diseases.

References

1. Eckert J, Deplazes P. Biological, epidemiological, and clinical aspects of echinococcosis, a zoonosis of increasing concern. Clin Microbiol Rev. 2004;17:107–35. http://dx.doi.org/10.1128/CMR.17.1.107-135.2004
2. Cardona GA, Carmena D. A review of the global prevalence, molecular epidemiology and economics of cystic echinococcosis in production animals. Vet Parasitol. 2013;192:10–32. http://dx.doi.org/10.1016/j.vetpar.2012.09.027
3. Nakao M, Yanagida T, Okamoto M, Knapp J, Nkouawa A, Sako Y, et al. State-of-the-art *Echinococcus* and *Taenia*: phylogenetic taxonomy of human-pathogenic tapeworms and its application to molecular diagnosis. Infect Genet Evol. 2010;10:444–52. http://dx.doi.org/10.1016/j.meegid.2010.01.011
4. Verster AJ. Review of *Echinococcus* species in South Africa. Onderstepoort J Vet Res. 1965;32:7–118.
5. Ortlepp RJ. *Echinococcus* in dogs from Pretoria and vicinity. Onderstepoort J Vet Res. 1934;3:97–108.
6. Balbinotti H, Santos GB, Badaraco J, Arend AC, Graichen DA, Haag KL, et al. *Echinococcus ortleppi* (G5) and *Echinococcus granulosus sensu stricto* (G1) loads in cattle from Southern Brazil. Vet Parasitol. 2012;188:255–60. http://dx.doi.org/10.1016/j.vetpar.2012.04.007
7. Alvarez Rojas CA, Romig T, Lightowlers MW. *Echinococcus granulosus* sensu lato genotypes infecting humans—review of current knowledge. Int J Parasitol. 2014;44:9–18. http://dx.doi.org/10.1016/j.ijpara.2013.08.008
8. Soule C, Fabien J-F, Maillot E. Enquête échinococcose-hydatidose. DGAL–CNEVA–LCRV, Maison Alfort; 1989.
9. Umhang G, Richomme C, Boucher JM, Hormaz V, Boue F. Prevalence survey and first molecular characterization of *Echinococcus granulosus* in France. Parasitol Res. 2013;112:1809–12. http://dx.doi.org/10.1007/s00436-012-3245-7
10. Bowles J, Blair D, McManus DP. Genetic variants within the genus *Echinococcus* identified by mitochondrial DNA sequencing. Mol Biochem Parasitol. 1992;54:165–73. http://dx.doi.org/10.1016/0166-6851(92)90109-W
11. Lavikainen A, Lehtinen MJ, Laaksonen S, Agren E, Oksanen A, Meri S. Molecular characterization of *Echinococcus* isolates of cervid origin from Finland and Sweden. Parasitology. 2006;133:565–70. http://dx.doi.org/10.1017/S0031182006000667
12. Bowles J, van Knapen F, McManus D. Cattle strain of *Echinococcus granulosus* and human infection. Lancet. 1992;339:1358. http://dx.doi.org/10.1016/0140-6736(92)92003-X
13. Casulli A, Manfredi MT, La Rosa G, Cerbo AR, Genchi C, Pozio E. *Echinococcus ortleppi* and *E. granulosus* G1, G2 and G3 genotypes in Italian bovines. Vet Parasitol. 2008;155:168–72. http://dx.doi.org/10.1016/j.vetpar.2008.04.004
14. Thompson RC, Kumaratilake LM, Eckert J. Observations on *Echinococcus granulosus* of cattle origin in Switzerland. Int J Parasitol. 1984;14:283–91. http://dx.doi.org/10.1016/0020-7519(84)90079-1
15. Romig T, Dinkel A, Mackenstedt U. The present situation of echinococcosis in Europe. Parasitol Int. 2006;55(Suppl):S187–91. http://dx.doi.org/10.1016/j.parint.2005.11.028

Address for correspondence: Frédéric Grenouillet, WHO Collaborating Center for Prevention and Treatment of Human Echinococcosis, French National Reference Center for Alveolar Echinococcosis—Parasitology-Mycology Department, Besançon University Hospital, Boulevard Fleming, 25030 Besançon, France; email: fgrenouillet@chu-besancon.fr

Avian Bornavirus in Free-Ranging Psittacine Birds, **Brazil**

Nuri Encinas-Nagel, Dirk Enderlein, Anne Piepenbring, Christiane Herden, Ursula Heffels-Redmann, Paulo A.N. Felippe, Clarice Arns, Hafez M. Hafez, and Michael Lierz

Avian bornavirus (ABV) has been identified as the cause of proventricular dilatation disease in birds, but the virus is also found in healthy birds. Most studies of ABV have focused on captive birds. We investigated 86 free-ranging psittacine birds in Brazil and found evidence for natural, long-term ABV infection.

Proventricular dilatation disease (PDD) is a fatal disease in birds worldwide, mainly affecting psittacines but also other species (*1*). This disease is characterized by gastrointestinal dysfunction with or without neurologic symptoms. In 2008, two independent research groups identified a novel virus in PDD-affected birds and named it avian bornavirus (ABV) (*2*,*3*); the researchers suggested ABV as the most likely cause of PDD. Subsequent studies have confirmed the association between ABV infection and PDD (*2*–*7*). However, ABV has also been found in healthy birds, indicating that additional factors may be required to cause clinical disease (*4*,*7*).

To date, 12 genotypes of ABV have been detected from birds in Africa, Europe, North America, Japan, and Australia (*1*–*3*,*6*,*8*–*11*). All recent studies have involved psittacine birds originating from captivity. Villanueva et al. used Western blot assays to test 8 free-ranging psittacine birds from the Peruvian Amazon for the presence of ABV antibodies, but all results were negative (*12*). A literature search yielded no reports of PDD or ABV infection in free-ranging psittacine birds. In this study, we tested apparently healthy, free-ranging psittacine birds captured in Brazil to identify ABV infections or PDD.

The Study

During December 2009–January 2010, we collected samples from psittacine birds brought to rehabilitation centers (Centro de Rehabilitação de Animais Silvestres [CRAS]) in the federal states of São Paulo (CRAS Parque ecológico Tietê–SP) and Mato Grosso do Sul (CRAS Campo Grande–MS) in Brazil. The birds had been rescued or confiscated from illegal animal trade or holding by environmental police. The 86 birds came from 7 species: *Amazona aestiva* (n = 29), *Aratinga leucophthalmus* (n = 22), *Arara ararauna* (n = 14), *Brotogeris tirica* (n = 10), *Amazona amazonica* (n = 8), *Amazona xanthops* (n = 2), and *Brotogeris chiriri* (n = 1).

The 49 birds from CRAS do Parque ecológico do Tietê–SP were euthanized for humanitarian reasons because of severe lesions that impeded reintroduction into the wild. The 37 birds from CRAS Campo Grande–MS were in good condition and were submitted for sampling purposes; however, 1 bird died suddenly. These birds had no signs of digestive or neurologic diseases and were anesthetized with inhalational isoflurane before organ sampling or euthanasia.

From dead birds (n = 50), we collected tissue samples from brain, eye, crop, proventriculus, ventriculus, adrenal gland, and heart. From live birds (n = 36), we collected crop biopsy samples from 30. Blood samples (n = 77) and tracheal (n = 78) and cloacal swab (n = 83) specimens were also collected. The collected tissue samples were rapidly embedded in RNALater RNA Stabilizations Reagent (QIAGEN, Hilden, Germany) for further molecular analysis. Real-time reverse transcription PCR (rRT-PCR) was used to detect ABV RNA from cloacal swab and crop biopsy specimens from live birds and from brain or proventriculus samples from dead birds (*3*). Cycle threshold (C_t) values >36 were considered negative. Genotyping was done according to the method described by Kistler et al. (*2*). Indirect immunofluorescence assay (IIFA) was performed to detect antibodies against ABV in serum samples (*13*). For histopathologic evaluation, collected tissue samples were fixed in 10% buffered formalin. Samples from brain, proventriculus, and ventriculus were embedded in paraffin wax, sectioned at 4 μm, and stained with hematoxylin and eosin. The primary criteria used to diagnose PDD histologically were perivascular or periganglionar mononuclear infiltrates in crop, proventriculus, or both.

We detected ABV RNA in tissue samples or cloacal swab specimens from 26 (30.2%) sampled psittacine birds; all were identified as type ABV-4. Of these birds, 12 originated from CRAS Tietê and 14 from CRAS Campo Grande. Most (84.6%) of the infected birds were adults, but nestlings (15.4%) were also affected. Antibodies against ABV were found in 19 psittacine birds, but for 15 of them, titers were low (1:10–1:20) and thus the birds were classified as probably, but not clearly, positive. The remaining 4 birds had titers >1:40 and were classified as ABV-antibody positive.

By evaluating hematoxylin and eosin–stained sections from the crop, brain, and proventriculus of 50 birds and crop biopsy specimens from 30 birds, we determined that

Author affiliations: Freie Universitaet Berlin, Berlin, Germany (N.M. Encinas-Nagel, H.M. Hafez); Justus Liebig Universitaet, Giessen, Germany (D. Enderlein, A. Piepenbring, U. Heffels-Redmann, C. Herden); and Universidade Estadual de Campinas, São Paulo, Brazil (P.A.N. Felippe, C. Arns)

DOI: http://dx.doi.org/10.3201/eid2012.140920

11 (14%) birds had mononuclear infiltrates in the ganglia of the proventriculus or crop, which were diagnosed as suspected PDD (Figure). Seven of these birds also had ABV RNA in tissue samples or cloacal swab specimens or antibodies against ABV in blood samples.

Conclusions

Brazil is known for its variety in free-ranging psittacine birds and is the origin country of endangered species such as the critically endangered Spix's macaw (*Cyanopsitta spixii*) and the Lear's macaw (*Anodorhychus leari)*. The spread of infectious pathogens such as ABV is a constant threat for the survival of these species in the wild and to species conservation projects. Hence, identification of disease agents and prevention of infection is critical.

In this surveillance study, we investigated 86 birds of the family *Psittacidae* originating from the wild from 2 regions of Brazil and found that 40 had signs of ABV infection, PDD, or both (Tables 1, 2). Four birds of 2 species (1 *B. tirica*, bird no. 12; and 3 *A. leucophthalmus*, birds no. 69, 70, and 71) had ABV antibodies in blood and ABV RNA in tissue samples (n = 2), cloacal swab specimens (n = 1), or both (n = 1). Other authors have reported ABV RNA and antibodies against ABV in birds without signs of disease (*4*,*5*,*12*,*14*), which suggests a persistent (*5*,*14*) or a subclinical (*4*,*5*,*9*) course of infection for an indefinite period (*9*,*14*). In our study, 50% of the ABV RNA–positive birds did not show antibodies against ABV by IIFA. Similar findings have also been observed by other authors (*4*,*5*,*14*), which suggests the infection might be at an early stage (*5*,*12*,*13*) or that the virus may escape the immune system (*5*,*15*). Because ABV is unstable in the environment or in fecal material, the virus does not seem to be highly contagious (*14*). Sampling for this study was conducted only once, and because ABV shedding in urofeces is intermittent (*9*), it is possible that some of the tested birds were undetected carriers of ABV and that the prevalence of ABV infection is even wider than supposed.

ABV RNA in cloacal swab specimens reinforces the suggestion of a gastrointestinal/urogenital location for the virus in the free-ranging psittacine bird population in these areas of Brazil. Unless infection during captivity in the rehabilitation centers can be proven, infection in the wild must be considered. We found ABV RNA by rRT-PCR in a white-eyed conure nestling (*Aratinga leucophthalmus*; bird no. 76) that was introduced into the CRAS Mato Grosso do Sul rehabilitation center 1 day before sampling. Likewise, 6 birds of 3 species (*B. tirica*, birds no. 5, 8, and 12; *A. leucophthalmus*, birds no. 50 and 55; and *A. ararauna*, bird no. 86) that arrived in the centers 2 months to 1 week before sampling showed either antibodies against ABV or ABV RNA (Table 1).

In summary, our findings indicate the apparent existence of ABV infection in the free-ranging psittacine bird population in 2 areas of Brazil. The presence of antibodies in the birds we tested may indicate long-term infection in which ABV viral shedding and transmission are not unusual. Our findings provide evidence of natural infection with ABV in free-ranging psittacine birds, the development of histopathologic lesions typical of PDD, and the occurrence of this disease in the natural habitat of these birds in South America.

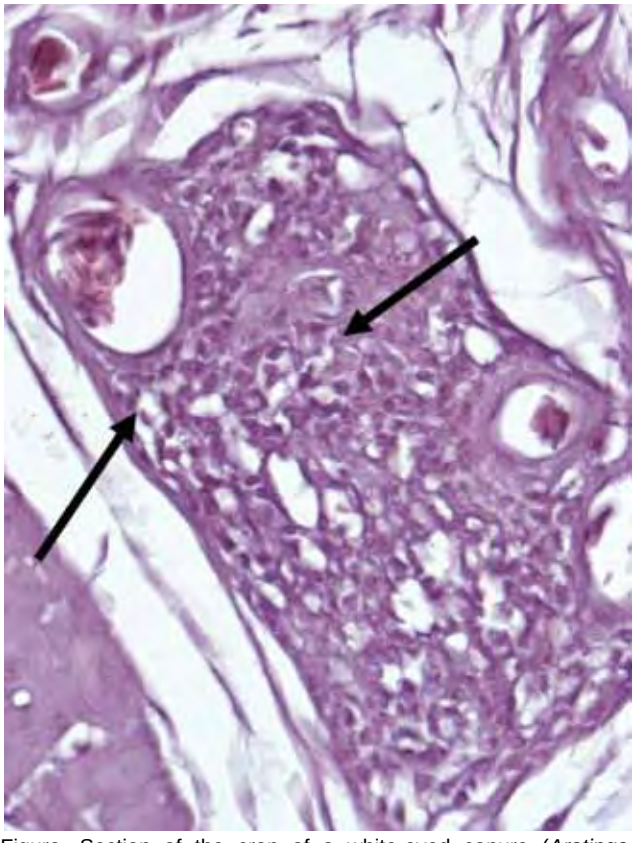

Figure. Section of the crop of a white-eyed conure (*Aratinga leucophthalmus*; bird no. 70 [Table 1]) from Brazil that was infected with avian bornavirus genotype 4. Stain shows mononuclear infiltration typical of proventricular dilatation disease (arrows). Hematoxylin and eosin stain; original magnification ×1,000.

Acknowledgments

We thank the teams from CRAS Tiete São Paulo and CRAS Campo Grande Mato Grosso do Sul who enabled this research study. We also are grateful to Marcela Saragiotto for support in field work.

The research was supported by the German Academic Exchange Service.

Mrs Encinas-Nagel is a veterinarian in a small animal practice and a doctoral student at the Institute for Poultry Diseases of the Freie Universitaet Berlin. During this research study, she worked in cooperation with the biology institute from the

Table 1. Results of testing of serum and tissue samples from 40 free-ranging psittacine birds that showed signs of ABV infection or PDD disease, Brazil, December 2009–January 2010*

Bird no.	Species	CRAS admission date	Sampling date†	ABV RNA in tissue samples‡	ABV antibody titer in serum sample§	ABV RNA in cloacal swab specimens	Histopathologic signs of PDD¶
1	*Aratinga leucophthalmus*	2008 Dec 9	2009 Dec 17	–	1:10	–	Cr
2	*Brotogeris tirica*	2008 Oct 14	2009 Dec 17	–	1:10	–	–
4	*A. leucophthalmus*	2008 Aug 2	2009 Dec 17	–	–	–	Cr, Pr
5	*B. tirica*	2009 Oct 22	2009 Dec 17	–	1:20	–	–
6	*B. tirica*	2008 Aug 8	2009 Dec 17	–	–	–	Cr, Pr
8	*B. tirica*	2009 Nov 6	2009 Dec 17	–	1:20	–	–
12	*B. tirica*	2009 Oct 21	2009 Dec 17	33.72	1:160	–	–
18	*Amazona aestiva*	2009 May 15	2009 Dec 17	32.29	–	–	–
19	*A. aestiva*	2009 Jan 15	2009 Dec 17	38.38	–	–	–
16	*Amazona amazonica*	2009 Aug 20	2009 Dec 17	32.50	–	–	–
20	*A. aestiva*	2009 Aug 18	2009 Dec 17	31.22	1:20	–	–
21	*A. aestiva*	2009 Aug 13	2009 Dec 17	34.34	1:20	–	Cr, Br
14	*Brotogeris chiriri*	2009 Mar 6	2009 Dec 17	32.58	–	–	–
17	*A. aestiva*	2008 Dec 12	2009 Dec 17	32.25	–	–	Br
15	*Ara ararauna*	2008 Jun 17	2009 Dec 17	31.44	–	–	Pr
28	*A. aestiva*	2008 Jul 4	2010 Jan 19	33.77	–	–	–
29	*A. aestiva*	2008 Jun 17	2010 Jan 19	–	1:20	–	–
26	*A. amazonica*	2008 Jan 11	2010 Jan 19	33.49	–	–	–
50	*Aratinga leucophthalmus*	2010 Jan 12	2010 Feb 1	35.00	–	–	–
55	*A. leucophthalmus*	2010 Jan 25	2010 Feb 1	–	–	28.85	–
61	*A. leucophthalmus*	2010 Jan 25	2010 Feb 1	–	ND	ND	Pr
67	*Amazona xanthops*	2009 Sep 10	2010 Feb 2	–	–	34.16	–
68	*A. leucophthalmus*	2008 Sep 26	2010 Feb 3	–	1:10	–	–
69	*A. leucophthalmus*	2008 Aug 28	2010 Feb 3	33.44	1:160	–	–
70	*A. leucophthalmus*	2009 Nov 19	2010 Feb 3	34.00	1:160	32.72	Cr
71	*A. leucophthalmus*	2009 Feb 17	2010 Feb 3	–	1:40	34.99	–
73	*A. leucophthalmus*	2008 Mar 19	2010 Feb 3	–	–	34.55	–
75	*A. amazonica*	2009 Jun 19	2010 Feb 3	35.71	–	–	–
76	*A. leucophthalmus*	2010 Feb 2	2010 Feb 3	–	ND	34.17	–
78	*A. aestiva*	2009 Nov 17	2010 Feb 3	–	–	34.01	Cr
79	*A. aestiva*	2009 Jul 8	2010 Feb 3	–	–	34.16	–
80	*A. amazonica*	2008 Dec 5	2010 Feb 3	35.13	1:20	34.38	–
82	*A. aestiva*	NA	2010 Feb 3	–	–	–	Pr
44	*Ara ararauna*	2007 Aug 15	2010 Jan 19	–	1:10	–	–
47	*A. ararauna*	2008 Jun 17	2010 Jan 19	35.11	–	–	Cr, Br
37	*A. aestiva*	2008 Oct 23	2010 Jan 19	–	1:10	–	–
35	*A. aestiva*	2008 Aug 13	2010 Jan 19	–	1:10	–	–
83	*A. aestiva*	2009 Jun 19	2010 Feb 3	ND	1:10	–	ND
85	*A. ararauna*	2009 Oct 29	2010 Feb 4	ND	1:20	32.90	ND
86	*A. ararauna*	2010 Jan 4	2010 Feb 4	ND	1:10	34.59	ND

*–, negative; ABV, avian bornavirus; Br, brain; Cr, crop; CRAS, Centro de Rehabilitação de Animais Silvestres; PDD, proventricular dilatation disease; Pr, proventriculus; NA, not available; ND, not done.
†Birds sampled in December and January were from CRAS São Paulo, and birds sampled in February were from CRAS Mato Grosso do Sul.
‡If available, brain samples were used; otherwise crop samples or biopsy samples were tested. RNA from ABV detected by real-time reverse-transcription PCR. Cycle threshold values <36 were considered positive.
§Antibodies against ABV in serum sample, detected by indirect immunofluorescence assay. Titers >1:20 were considered positive; titers 1:10–1:20 were considered probably positive.
¶Hematoxylin and eosin staining was used to test all available organ samples from crop, brain, and proventriculus or crop biopsy samples. PDD was diagnosed in birds with ABV RNA, antibodies against ABV, or both and mononuclear infiltrates in or near the ganglia of the crop or proventriculus.

Universidade Estadual de Campinas, São Paulo, Brazil, and the Clinic for Birds, Reptiles, Amphibians and Fish from the Justus-Liebig Universitaet, Giessen, Germany.

References

1. Delnatte P, Ojkic D, Delay J, Campbell D, Crawshaw G, Smith DA. Pathology and diagnosis of avian bornavirus infection in wild Canada geese (*Branta canadensis*), trumpeter swans (*Cygnus buccinator*) and mute swans (*Cygnus olor*) in Canada: a retrospective study. Avian Pathol. 2013;42:114–28. http://dx.doi.org/10.1080/03079457.2013.769669
2. Kistler AL, Gancz A, Clubb S, Skewes-Cox P, Fischer K, Sorber K, et al. Recovery of divergent avian bornaviruses from cases of proventricular dilatation disease: identification of a candidate etiologic agent. Virol J. 2008;5:88. http://dx.doi.org/10.1186/1743-422X-5-88
3. Honkavuori KS, Shivaprasad HL, Williams BL, Quan PL, Hornig M, Street C, et al. Novel bornavirus in psittacine birds with proventricular dilatation disease. Emerg Infect Dis. 2008;14:1883–6. http://dx.doi.org/10.3201/eid1412.080984
4. Lierz M, Hafez HM, Honkavuori KS, Gruber AD, Olias P, Abdelwhab EM, et al. Anatomical distribution of avian bornavirus in parrots, its occurrence in clinically healthy birds and ABV-antibody detection. Avian Pathol. 2009;38:491–6. http://dx.doi.org/10.1080/03079450903349238

Table 2. Detection of ABV RNA, antibodies against ABV, and PDD lesions among free-ranging psittacine birds, by species, Brazil, December 2009–January 2010*

Species	No. birds				
	Total	With ABV RNA in organ sample†	With ABV antibodies in serum sample	With ABV RNA in cloacal swab specimen†	With suspected PDD lesions‡
Amazona aestiva	29	6	0	2	4
Aratinga leucophthalmus	22	3	3	5	4
Ara ararauna	14	2	0	2	2
Brotogeris tirica	10	1	1	0	1
Amazona amazonica	8	4	0	1	0
Amazona xanthops	2	0	0	1	0
Brotogeris chiriri	1	1	0	0	0
Total	86	17	4	11	11

*ABV, avian bornavirus; PDD, proventricular dilatation disease.
†By real-time reverse transcription PCR.
‡By hematoxylin and eosin stain.

5. Heffels-Redmann U, Enderlein D, Herzog S, Herden C, Piepen-bring A, Neumann D, et al. Occurrence of avian bornavirus infection in captive psittacines in various European countries and its association with proventricular dilatation disease. Avian Pathol. 2011;40:419–26. http://dx.doi.org/10.1080/03079457.2011.589825
6. Weissenböck H, Bakonyi T, Sekulin K, Ehrensperger F, Doneley RJ, Dürrwald R, et al. Avian bornaviruses in psittacine birds from Europe and Australia with proventricular dilatation disease. Emerg Infect Dis. 2009;15:1453–9. http://dx.doi.org/10.3201/eid1509.090353
7. Piepenbring AK, Enderlein D, Herzog S, Kaleta EF, Heffels-Redmann U, Ressmeyer S, et al. Pathogenesis of avian bornavirus in experimentally infected cockatiels. Emerg Infect Dis. 2012;18:234–41. http://dx.doi.org/10.3201/eid1802.111525
8. Last RD, Weissenböck H, Nedorost N, Shivaprasad HL. Avian bornavirus genotype 4 recovered from naturally infected psittacine birds with proventricular dilatation disease in South Africa. J S Afr Vet Assoc. 2012;83:938. http://dx.doi.org/10.4102/jsava.v83i1.938
9. Payne S, Shivaprasad HL, Mirhosseini N, Gray P, Hoppes S, Weissenbock H, et al. Unusual and severe lesions of proventricular dilatation disease in cockatiels (*Nymphicus hollandicus*) acting as healthy carriers of avian bornavirus (ABV) and subsequently infected with a virulent strain of ABV. Avian Pathol. 2011;40:15–22. http://dx.doi.org/10.1080/03079457.2010.536978
10. Rubbenstroth D, Schmidt V, Rinder M, Legler M, Corman VM, Staeheli P. Discovery of a new avian bornavirus genotype in estrildid finches (*Estrildidae*) in Germany. Vet Microbiol. 2014;168:318–23. http://dx.doi.org/10.1016/j.vetmic.2013.11.032
11. Sassa Y, Horie M, Fujino K, Nishiura N, Okazaki S, Furuya T, et al. Molecular epidemiology of avian bornavirus from pet birds in Japan. Virus Genes. 2013;47:173–7. http://dx.doi.org/10.1007/s11262-013-0913-3
12. Villanueva I, Gray P, Mirhosseini N, Payne S, Hoppes S, Honkavuori KS, et al. The diagnosis of proventricular dilatation disease: use of a Western blot assay to detect antibodies against avian Borna virus. Vet Microbiol. 2010;143:196–201. http://dx.doi.org/10.1016/j.vetmic.2009.11.041
13. Herzog S, Enderlein D, Heffels-Redmann U, Piepenbring A, Neumann D, Kaleta EF, et al. Indirect immunofluorescence assay for intra vitam diagnosis of avian bornavirus infection in psittacine birds. J Clin Microbiol. 2010;48:2282–4. http://dx.doi.org/10.1128/JCM.00145-10
14. De Kloet SR, Dorrestein GM. Presence of avian bornavirus RNA and anti-avian bornavirus antibodies in apparently healthy macaws. Avian Dis. 2009;53:568–73. http://dx.doi.org/10.1637/8828-040209-Reg.1
15. Reuter A, Ackermann A, Kothlow S, Rinder M, Kaspers B, Staeheli P. Avian bornaviruses escape recognition by the innate immune system. Viruses. 2010;2:927–38. http://dx.doi.org/10.3390/v2040927

Address for correspondence: Michael Lierz, Clinic for Birds, Reptiles, Amphibians and Fish, Justus-Liebig-University Giessen, Frankfurter Str 91-93, 35392 Giessen, Germany; email: michael.lierz@vetmed.unigiessen.de

Human Hantavirus Infections in the Netherlands

Jussi Sane, Johan Reimerink, Margriet Harms, Jacinta Bakker, Lapo Mughini-Gras, Barbara Schimmer, and Wilfrid van Pelt

We report the recent epidemiology and estimated seroprevalence of human hantavirus infections in the Netherlands. Sixty-two cases were reported during December 2008–December 2013. The estimated seroprevalence in the screened municipalities in 2006–2007 was 1.7% (95% CI 1.3%–2.3%). Findings suggest that hantavirus infections are underdiagnosed in the Netherlands.

Hantaviruses (family *Bunuyaviriade*, genus *Hantavirus*) are primarily rodent-borne pathogens that are a suspected cause of hemorrhagic fever with renal syndrome (HFRS) in Eurasia (*1*). They are transmitted to humans mainly through aerosolized rodent excreta (*1*). Five hantaviruses circulate among rodents in Europe, but most human HFRS cases are caused by Puumala virus (PUUV) (*1,2*). The reservoir for PUUV is bank voles (*Myodes glareolus*), which are widespread in Europe (*1,2*). HFRS is a reportable disease in most countries in Europe, and cases are reported mostly from Finland, Sweden, and forest-rich regions of Belgium and Germany (*1,3,4*).

In the Netherlands, hantavirus infections have been reportable since December 2008, although voluntary laboratory surveillance has been in place since 1989. An earlier study in the Netherlands reported a seroprevalence of 0.7% among blood donors but higher prevalences in forest workers and animal trappers (*5*). Antibodies to PUUV, Tula virus (TULV), and Seoul virus (SEOV) have been found in rodent populations in the Netherlands, and TULV has been isolated from common voles (*Microtus arvalis*) (*5,6*). The purpose of this study was to report recent trends in human hantavirus infection and estimate seroprevalence in the Netherlands.

The Study

We analyzed reported data for the Netherlands for December 2008–December 2013. Reporting criteria included ≥1 hantavirus-associated symptom (fever, renal insufficiency, or thrombocytopenia) and virus detection in blood, or a major increase in IgG titers or increases in IgM or IgA titers against hantavirus. For the seroprevalence study, a subset of samples from a large serum bank established for population-based serologic studies (Pienter 2), particularly immunization program evaluations, was used. Pienter 2 is a cross-sectional serosurvey conducted during 2006–2007 with a representative sample (n = 7,904) of the population of the Netherlands (*7*).

Participants also completed a questionnaire that included basic demographic characteristics and behaviors and activities related to increased risk for acquiring infectious diseases. Variables possibly related to hantavirus infection from the literature, such as age, sex, outdoor activities, and animal contact, were selected from the Pienter 2 questionnaire. A total of 2,933 serum samples from 19 municipalities distributed across the country, including known high-risk areas, were included in the study and screened for antibodies against hantavirus (Figure 1).

An ELISA (Hantavirus IgG Dx Select; Focus Diagnostics, Cypress, CA, USA) that detects all known circulating hantaviruses in Europe was used for initial screening of all serum samples. For confirmation, all ELISA-positive samples were analyzed by using a PUUV-specific indirect immunofluorescence assay (IFA) (Progen, Heidelberg, Germany). Samples with reactivity at a dilution of 1:32 were considered positive for hantavirus infection. Manufacturer's recommendations were followed for both assays. A randomly selected subset of ELISA-negative samples were screened by IFA to correct for possible false-negative ELISA results.

We calculated odds ratios (ORs) and 95% CIs for variables putatively associated with hantavirus seropositivity by using mixed-effects logistic regression that included municipality as a random effect to account for clustering of samples. All estimates were adjusted for age and sex. A p value ≤0.15 was used in the single-variable analysis to select variables for the multivariable model built in backward stepwise fashion. Statistical significance was considered at the 5% level.

A total of 62 cases were reported during December 2008–December 2013 (Figure 2). Most cases (63.0%) were in men (median age 48 y, range 16–72 y). The highest number of cases (n = 26) occurred in the region of Twente (Figure 1) in the eastern Netherlands. Fifty-two case-patients (85.0%) were hospitalized and seven (12.0%) required dialysis. Most cases (90.0%) were acquired domestically.

A total of 154 (5.3%) serum samples were positive by ELISA. Of the ELISA-positive samples, 27 (17.5%) were also positive for PUUV IgG by IFA and therefore considered samples with positive results. One of the 119 ELISA-negative samples was also positive by IFA. After

Author affiliations: National Institute for Public Health and the Environment, Bilthoven, the Netherlands (J. Sane, J. Reimerink, M. Harms, J. Bakker, L. Mughini-Gras, B. Schimmer, W. van Pelt); and European Centre for Disease Prevention and Control, Stockholm, Sweden (J. Sane)

DOI: http://dx.doi.org/10.3201/eid2012.131886

Figure 1. Municipalities sampled in the Pienter 2 study and subset of municipalities included in the seroprevalence study of hantavirus infections, the Netherlands.

we corrected for false-negative results, the overall seroprevalence was 1.7% (95% CI 1.3%–2.3%).

Selected factors associated with PUUV infection are shown in the Table. Seroprevalence (uncorrected) in women was higher than that in men, albeit, not significantly. Age was not associated with PUUV infection. Owning ≥1 or more dogs or any livestock was associated with PUUV infection in a multivariable model (Table). Variables reflecting other outdoor activities were not associated with higher seroprevalence. The municipality-level random effect was significant ($p = 0.001$, by log-likelihood ratio test). Most positive samples (n = 10) were from the municipality of Enschede (Twente Region) in which seroprevalence was 3.2% (10/309) (Figure 1). Seroprevalence was lower (0.8%–1.8%) or 0% in all the other municipalities surveyed.

Conclusions

We report that hantavirus seroprevalence in the Netherlands is 1.7% for the years analyzed on the basis of a subset of samples from a large population-based serum bank. This seroprevalence was similar to estimates for neighboring countries (1.5% for Belgium and 1%–3% for Germany) (*2*,*4*). However, comparing prevalences is challenging because of different methods used and populations studied.

The number of reported cases in the Netherlands was low. Given our seroprevalence estimate, although not entirely representative of the population of the Netherlands, and the proportion of symptomatic PUUV-infected persons (20%–30%), some of whom seek medical care (*1*), the number of cases in the Netherlands (≈16.5 million resident population) is expected to be higher. Many cases with milder symptoms probably go unnoticed because of low awareness of hantavirus infection among physicians in the Netherlands. Hantavirus infections in the Netherlands are most likely caused by PUUV, although SEOV- or TULV-associated infections cannot be excluded; clinical SEOV infections have been reported from France and the United Kingdom (*8*,*9*).

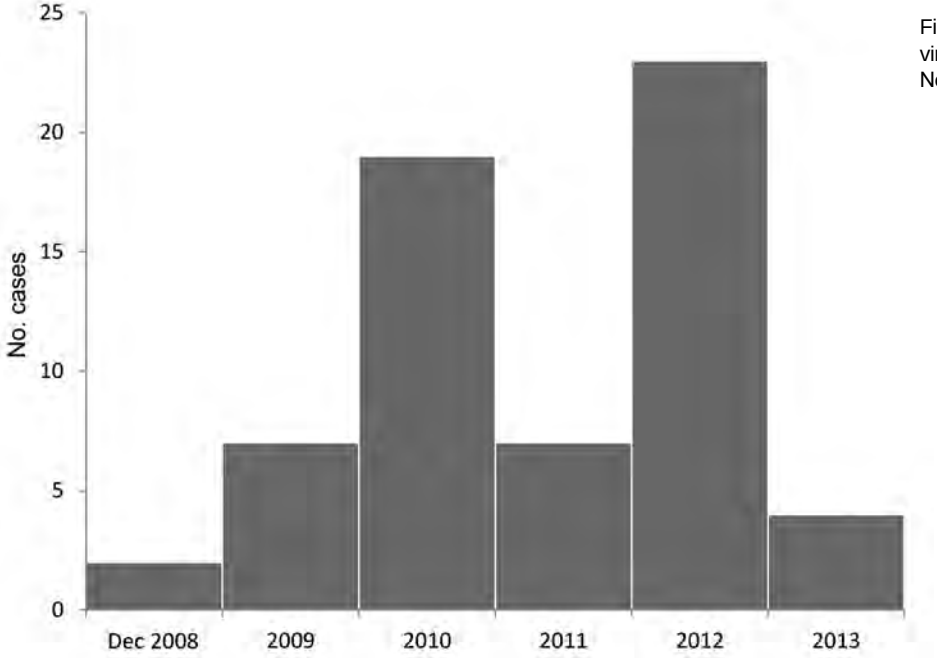

Figure 2. Reported cases of hantavirus infection (n = 62) by year, the Netherlands, December 2008–2013.

Table. Selected factors associated with positivity for IgG against Puumala virus, the Netherlands, December 2008–December 2013*

Factor	No. persons IFA positive/no. tested (%)	Single variable		Multivariable	
		aOR (95% CI)†	p value	aOR (95% CI)‡	p value
Sex					
M	9/1,368 (0.66)	Reference		Reference	NA
F	18/1,565 (1.15)	1.79 (0.89–3.57)	0.10	1.87 (0.97–3.61)	0.06
Age, y					
0–15	7/824 (0.84)	Reference		Reference	NA
16–40	7/822 (0.85)	1.03 (0.36–2.93)	0.96	1.0 (0.33–3.07)	0.99
41–60	5/585 (0.85)	0.91 (0.26–3.19)	0.88	0.86 (0.22–3.32)	0.82
>60	8/702 (1.14)	1.32 (0.48–3.62)	0.59	1.69 (0.51–5.56)	0.39
Owning ≥1 dog					
No	12/2147 (0.56)	Reference		Reference	NA
Yes	15/786 (1.53)	4.51 (1.81–11.30)	0.001	3.49 (1.50–8.14)	0.004
Owning any livestock§					
No	19/2,706 (0.70)	Reference		Reference	NA
Yes	8/227 (3.52)	6.97 (2.45–19.82)	<0.001	4.79 (1.69–13.57)	0.003
Net monthly income, Euros					
<1,150	11/426 (2.58)	Reference		NA	NA
1,151–3,050	9/1,539 (5.84)	0.27 (0.05–1.47)	0.13	NA	NA
>3,501	1/242 (0.41)	0.21 (0.03–1.79)	0.15	NA	NA
Occupational exposure to any animal					
No	25/2794 (0.89)	Reference		NA	NA
Yes	2/139 (1.43)	1.72 (0.25–11.77)	0.58	NA	NA

*IFA, indirect immunofluorescence assay; aOR, adjusted odds ratio; NA, not applicable. The municipality-level random effect was significant (p = 0.001, by log-likelihood ratio test).
†Adjusted for age, sex, and clustering at municipality level (random effect).
‡Adjusted for age, sex, clustering at municipality level (random effect), and the other covariates included in the multivariable model.
§Cattle, pigs, sheep, goats, poultry, and other livestock.

The proportions of hospitalizations and persons requiring dialysis were much higher than those reported in other countries. In Finland, 52.0% of PUUV-infected persons required hospitalization (*10*). In Germany, 64.0% of persons with reported cases of infection in 2010 required hospitalization (*11*). The difference in hospitalization rates is probably associated with reporting bias because only the most severe cases are reported due to strict reporting criteria and possible higher thresholds for testing. This finding also suggests that a large number of milder cases are being underreported.

Bank voles are a forest-dwelling species, and risk for PUUV infection is associated with vicinity of forests and the proportion of forested land cover (*1*,*12*,*13*). Seroprevalence and number of cases were highest in the Twente Region, a region to which PUUV is endemic. This region borders areas in Germany in which incidence is high (*11*) and is located near forests, which are scarce in the Netherlands. The only variables associated with PUUV infection were dog and livestock ownership. However, it is highly unlikely that these factors reflect direct virus transmission from such domestic animals to humans, but represent proxies for lifestyle characteristics of dog owners and persons engaged in farming activities that predispose them to more frequent or more substantial contact with rodents.

Seroprevalence was higher in women, but the disease was most often reported in men. Similar male:female ratios among persons with clinical PUUV infection have been reported from other countries (*10*,*14*). These data suggest that women have a higher proportion of subclinical or mild infections, although a recent study suggested that disease severity does not differ between men and women (*15*).

In conclusion, higher seroprevalence relative to the number of reported cases calls for further awareness of hantavirus infection among physicians in the Netherlands. Seroprevalence studies of persons with unresolved renal problems could further increase our understanding of the true incidence of hantavirus infection in the Netherlands.

Acknowledgments

We thank Chantal Reusken for contributing to the study design and manuscript preparation.

J.S. was supported by the European Programme for Intervention Epidemiology Training, European Centre for Disease Prevention and Control.

Dr Sane is a fellow in the European Programme for Intervention Epidemiology Training, European Centre for Disease Prevention and Control, at National Institute for Public Health and the Environment, Bilthoven, the Netherlands. His primary research interests include epidemiology of viral diseases, especially vaccine-preventable and vector-borne infections.

References

1. Vaheri A, Henttonen H, Voutilainen L, Mustonen J, Sironen T, Vapalahti O. Hantavirus infections in Europe and their impact on public health. Rev Med Virol. 2013;23:35–49. http://dx.doi.org/10.1002/rmv.1722

2. Olsson GE, Leirs H, Henttonen H. Hantaviruses and their hosts in Europe: reservoirs here and there, but not everywhere? Vector Borne Zoonotic Dis. 2010;10:549–61. http://dx.doi.org/10.1089/vbz.2009.0138
3. Ahlm C, Linderholm M, Juto P, Stegmayr B, Settergren B. Prevalence of serum IgG antibodies to Puumala virus (haemorrhagic fever with renal syndrome) in northern Sweden. Epidemiol Infect. 1994;113:129–36. http://dx.doi.org/10.1017/S0950268800051542
4. Zöller L, Faulde M, Meisel H, Ruh B, Kimmig P, Schelling U, et al. Seroprevalence of hantavirus antibodies in Germany as determined by a new recombinant enzyme immunoassay. Eur J Clin Microbiol Infect Dis. 1995;14:305–13. http://dx.doi.org/10.1007/BF02116523
5. Groen J, Gerding MN, Jordans JG, Clement JP, Nieuwenhuijs JH, Osterhaus AD. Hantavirus infections in The Netherlands: epidemiology and disease. Epidemiol Infect. 1995;114:373–83. http://dx.doi.org/10.1017/S0950268800058003
6. Reusken C, de Vries A, Adema J, Vos W, van der Giessen J, Bekker D, et al. First genetic detection of Tula hantavirus in wild rodents in the Netherlands. J Infect. 2008;57:500–3. http://dx.doi.org/10.1016/j.jinf.2008.09.032
7. van der Klis FR, Mollema L, Berbers GA, de Melker HE, Coutinho RA. Second national serum bank for population-based seroprevalence studies in the Netherlands. Neth J Med. 2009;67:301–8.
8. Jameson LJ, Logue CH, Atkinson B, Baker N, Galbraith SE, Carroll MW, et al. The continued emergence of hantaviruses: isolation of a Seoul virus implicated in human disease, United Kingdom, October 2012. Euro Surveill. 2013;18:4–7.
9. Macé G, Feyeux C, Mollard N, Chantegret C, Audia S, Rebibou JM, et al. Severe Seoul hantavirus infection in a pregnant woman, France, October 2012. Euro Surveill. 2013;18:20464.
10. Makary P, Kanerva M, Ollgren J, Virtanen MJ, Vapalahti O, Lyytikainen O. Disease burden of Puumala virus infections, 1995–2008. Epidemiol Infect. 2010;138:1484–92. http://dx.doi.org/10.1017/S0950268810000087
11. Faber MS, Ulrich RG, Frank C, Brockmann SO, Pfaff GM, Jacob J, et al. Steep rise in notified hantavirus infections in Germany, April 2010. Euro Surveill. 2010;15:pii:19574.
12. Schwarz AC, Ranft U, Piechotowski I, Childs JE, Brockmann SO. Risk factors for human infection with Puumala virus, southwestern Germany. Emerg Infect Dis. 2009;15:1032–9. http://dx.doi.org/10.3201/eid1507.081413
13. Voutilainen L, Savola S, Kallio ER, Laakkonen J, Vaheri A, Vapalahti O, et al. Environmental change and disease dynamics: effects of intensive forest management on Puumala hantavirus infection in boreal bank vole populations. PLoS ONE. 2012;7:e39452. http://dx.doi.org/10.1371/journal.pone.0039452
14. Hjertqvist M, Klein SL, Ahlm C, Klingstrom J. Mortality rate patterns for hemorrhagic fever with renal syndrome caused by Puumala virus. Emerg Infect Dis. 2010;16:1584–6. http://dx.doi.org/10.3201/eid1610.100242
15. Krautkrämer E, Grouls S, Urban E, Schnitzler P, Zeier M. No gender-related differences in the severity of nephropathia epidemica, Germany. BMC Infect Dis. 2013;13:457. http://dx.doi.org/10.1186/1471-2334-13-457

Address for correspondence: Jussi Sane, Epidemiology and Surveillance Unit, National Institute for Public Health and the Environment, PO Box 1, Bilthoven 3720 BA, the Netherlands; email: jussi.sane@rivm.nl

Mycobacterium Species Related to *M. leprae* and *M. lepromatosis* from Cows with Bovine Nodular Thelitis

Didier Pin, Véronique Guérin-Faublée, Virginie Garreau, Franck Breysse, Oana Dumitrescu, Jean-Pierre Flandrois, and Gerard Lina

Bovine nodular thelitis is a granulomatous dermatitis associated with infection with acid-fast bacteria. To identify the mycobacterium responsible for this infection, we conducted phylogenetic investigations based on partial sequencing of 6 genes. These bacteria were identified as an undescribed *Mycobacterium* species that was phylogenetically related to *M. leprae* and *M. lepromatosis*.

The genus *Mycobacterium* contains >100 species. Except for the *Mycobacterium tuberculosis* complex and *M. leprae*, which are parasitic bacteria, mycobacteria are considered saprophytic and found in soil, water, and sediments. Humans and wild and domestic animals can be infected by nontuberculous mycobacteria (NTM) from environmental sources, and several species are emerging as opportunistic pathogens in humans. NTM are often present on the skin surface after exposure to aqueous environments, and NTM skin diseases are of particular concern in humans (*1*).

Bovine nodular thelitis is a chronic and enzootic cutaneous disease that was first described in France in 1963 and then in Japan and Switzerland (*2*–*4*). This granulomatous dermatitis is associated with acid-fast bacilli and believed to have a mycobacterial origin of infection (*2*,*4*). However, cultivation and characterization of the causal bacteria have not been successful (*3*). We used a multigene sequencing phylogenetic approach described previously (*5*) to identify the mycobacterium responsible for bovine nodular thelitis.

Author affiliations: VetAgro Sup Campus Vétérinaire de Lyon, Marcy l'Étoile, France (D. Pin, V. Guérin-Faublée); Clinique Vétérinaire, Saint Bénigne, France (V. Garreau); Centre Hospitalier Lyon Sud, Pierre Bénite, France (F. Breysse); and Université Lyon 1, Lyon, France (O. Dumitrescu, J.-P. Flandrois, G. Lina)

DOI: http://dx.doi.org/10.3201/eid2012.140184

The Study

In 2013, we visited a dairy herd in Jura, France, on 3 occasions. The herd contained ≈30 lactating cows. During physical examination of all teats, one third of the cows had lesions. In most cases, only 1 teat/cow had a lesion, which was a single, painless nodule of variable size that was localized in the dermis (Figure 1, panel A). Early-stage lesions, which had a well-demarcated indurated area, were observed only in a few cows. A few nodules evolved to ulcers, and most ulcers showed cicatrization and fibrosis.

To establish a diagnosis, we obtained 3 biopsy specimens from 3 cows (1 specimen/cow) under local anesthesia (lidocaine) from intact nodules by using a skin biopsy punch (diameter 8 mm). Each biopsy specimen was divided into 2 parts: half was placed in formalin, and half was placed in sterile 0.9% NaCl.

During histopathologic examination, superficial and deep dermis showed nodular and interstitial dermatitis (Figure 1, panel B) and an infiltrate composed predominantly of large, pale, foamy macrophages mixed with lymphocytes and few plasma cells (Figure 1, panel C). Some macrophages contained 2 or 3 nuclei and a granular cytoplasm. Multinucleated giant cells were rarely observed. There were large foci of necrosis. Ziehl-Neelsen staining indicated acid-fast bacteria deposited in clumps and resembling globi of leprosy within macrophages and necrotic foci exclusively on samples 1 and 2 (Figure 1, panel D). These observations resulted in the diagnosis of bovine nodular thelitis. Mycobacterial culture was not attempted because of its inherent difficulty (*3*). A molecular approach was used to characterize bacteria from the 3 biopsy specimens.

Biopsy specimens were washed 3 times with DNA-free sterile water, and epidermis was removed from the dermis and hypodermis to avoid contamination with cutaneous flora. The dermis and hypodermis were homogenized at 7,400 rpm for 70 s in a proteinase K solution (1 mg/mL) (Sigma, St. Louis, MO, USA) by using a MagNA Lyser (Roche Molecular Diagnostics, Mannheim, Germany), followed by incubation for 18 h at 55°C in a shaking dry bath incubator. Whole DNA was extracted from the lysed tissue by using the MagnaPure Compact Kit (Roche Molecular Diagnostics).

For the phylogenetic investigations, a multigene sequencing approach was used (*5*). Double-stranded partial sequences of the genes for 65-kDa heat shock protein (*hsp65* [*groEL2*]), the β-subunit of RNA polymerase gene (*rpoB*), superoxide dismutase (*sodA*), elongation factor Tuf (*tuf*), 16S rRNA, and transfer–messenger (tmRNA) were obtained by real-time PCR by using primers (Table) designed for this study (*rpoB*) or described previously (*5*,*6*). For each gene, chromatograms corresponding to the 2 strands of the 3 amplified products (only 2 amplified

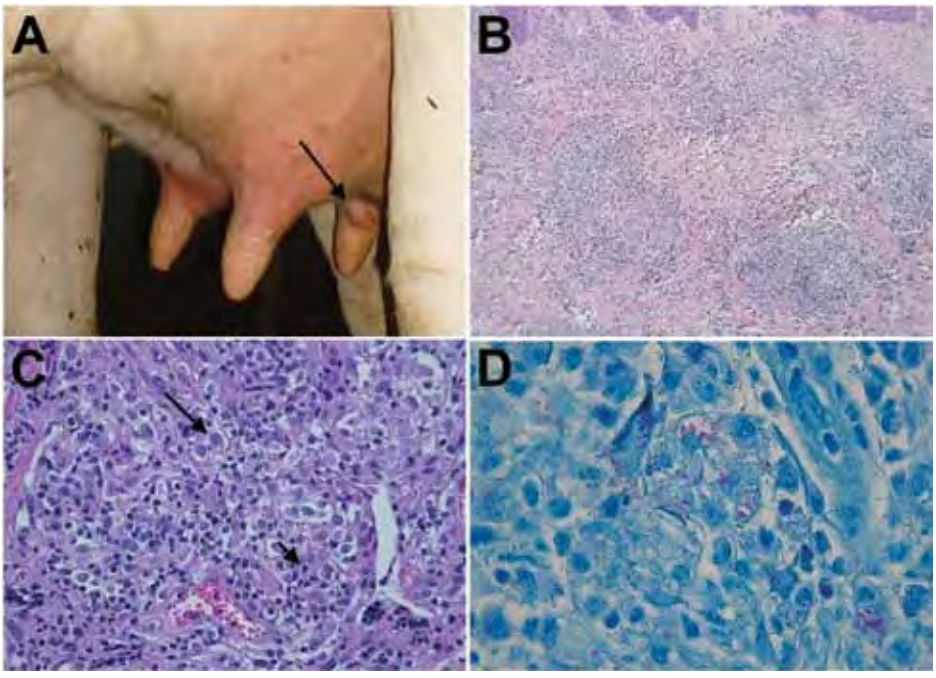

Figure 1. Lesions of cows with bovine nodular thelitis, Jura, France. A) Nodule on a bovine teat (arrow). B) Nodular granulomatous dermatitis, hematoxylin and eosin stained, original magnification ×100). C) Nodular granulomatous dermatitis, showing foamy macrophages (large arrow) and lymphocytes (small arrow) in an inflammatory infiltrate, original magnification ×400. D) Acid-fast bacteria. Ziehl-Neelsen stained, original magnification ×1,000.

products for the 16S rRNA gene) were compared by using Staden software (http://staden.sourceforge.net/) and edited to remove ambiguous bases (*7*).

For each gene, no differences were detected among 3 sequences (2 sequences for the 16S rRNA gene), and a consensus sequence was subsequently used for each gene (392 bp for *hsp65* [KJ095005], 951 bp for *rpoB* [KJ095009], 442 bp for *sodA* [KJ095006], 718 bp for *tuf* [KJ095008], 359 bp for the tmRNA gene [KJ095007], and 369 bp for the 16S rRNA gene [KJ095004]). To make phylogenetic comparisons, we selected a subset of *Mycobacterium* spp. sequences for each gene to obtain a good representation of the genomic diversity among the slow-growing mycobacteria by using data from Mignard and Flandrois (*5*). Sequences were obtained from GenBank/European Molecular Biology Laboratory/DNA Data Bank of Japan databases. The MAFFT program (http://mafft.cbrc.jp/alignment/software/) was used to align

Table. Primers used for PCR detection of *Mycobacterium* species, Jura, France

Gene*	Sequence, 5′→3′†
16S rRNA gene (*6*)	F-TCAAAKgAATTgACgggggC
	R-ggTTACCTTgTTACgACTT
hsp65 (*5*)	F-ACCAACgATggTgTgTCCAT
	R-CTTgTCgAACCgCATACCCT
rpoB (designed for this study)	2F-TCAACgggACCgAgCgTgTC
	2R-gTgTTgTCCTTCTCCAgCgT
	3F-TCAACgggACCgAgCgTgTC
	4R-gTCTCgATCgggCACATC
	9F-gTgggCACCggCATggAgTT
	9R-ATgTTCATCCgTCgCggC
	8F-ATGAAgCTgCACCACTTggT
	8R-gCCGATTCgTTgCgggACA
sodA (*5*)	F-AgCTTCACCACAgCAAgCACCA
	R-TCggCCAgTTCACgACgTTCCA
tuf (*5*)	F-CACgCCgACTACATCAAgAA
	R-gAACTgCggACggTAgTTgT
tmRNA (*5*)	F-ggggCTgAAACggTTTCgAC
	R-TggAgCTgCCgggAATCgAAC

**hsp65*, heat shock protein 65; *rpoB*, β-subunit of RNA polymerase; *sodA*, superoxide dismutase A; *tuf*, elongation factor Tuf; tmRNA, transfer–messenger RNA.

†F, forward; R, revrse. DNA was amplified by using a LightCycler 2.0 instrument (Roche Molecular Diagnostics, Indianapolis, IN, USA) and a ready-to-use hot start reaction mixture (TAKARA, Tokyo, Japan). For all PCRs, parameters were denaturation 95°C for 30 s; and amplification (45 cycles) at 95°C for 15 s, 65°C for 20 s, and 72°C for 40 s (slope, 2°C/s); melting curve, 0 s at 95°C, 15 s at 75°C, and 0 s at 98°C (slope, 0.05°C/s).

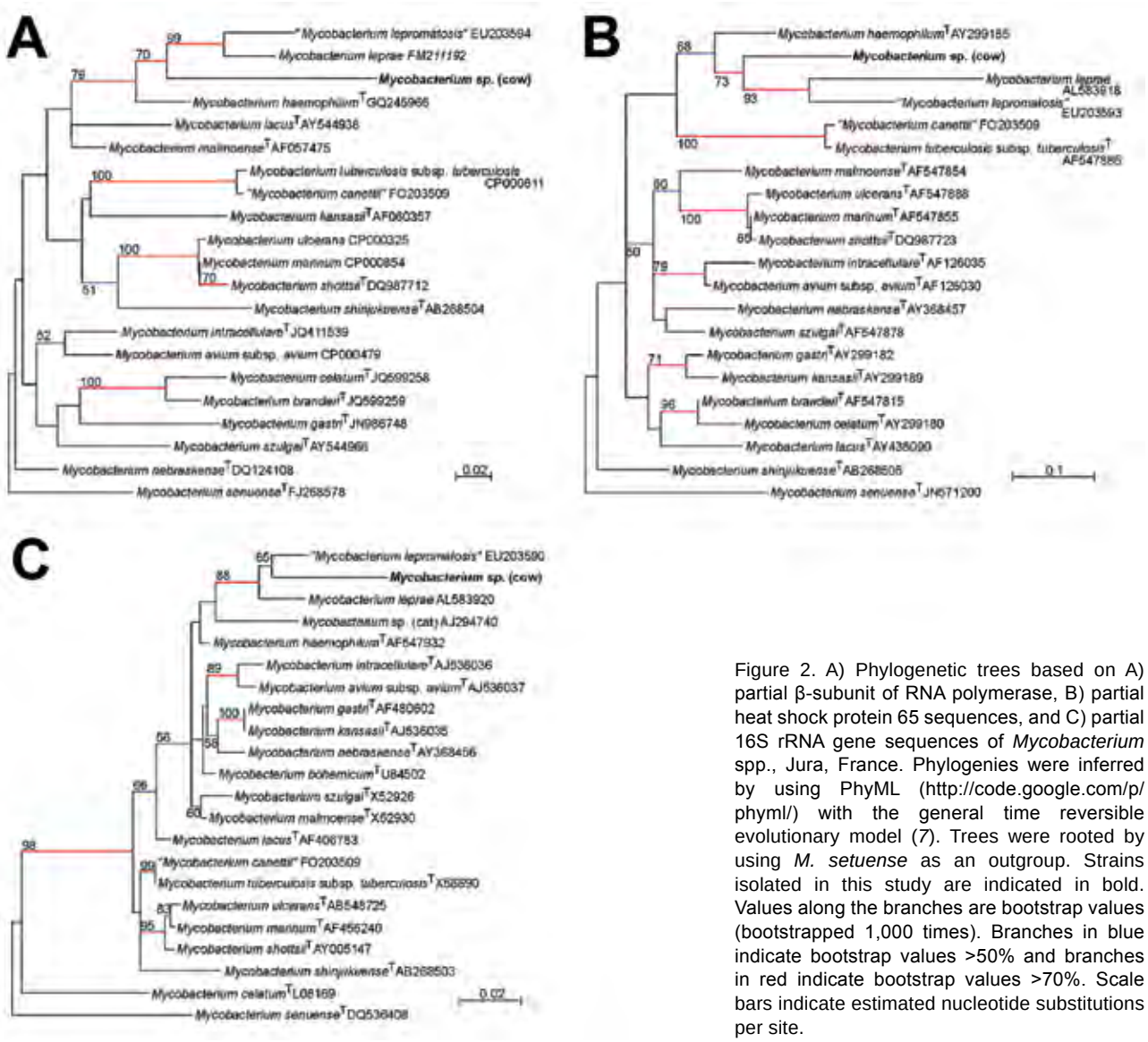

Figure 2. A) Phylogenetic trees based on A) partial β-subunit of RNA polymerase, B) partial heat shock protein 65 sequences, and C) partial 16S rRNA gene sequences of *Mycobacterium* spp., Jura, France. Phylogenies were inferred by using PhyML (http://code.google.com/p/phyml/) with the general time reversible evolutionary model (*7*). Trees were rooted by using *M. setuense* as an outgroup. Strains isolated in this study are indicated in bold. Values along the branches are bootstrap values (bootstrapped 1,000 times). Branches in blue indicate bootstrap values >50% and branches in red indicate bootstrap values >70%. Scale bars indicate estimated nucleotide substitutions per site.

nucleotide sequences. Alignments were verified by using SeaView (http://www.molecularevolution.org/software/alignment/seaview). Divergent and ambiguously aligned blocks were removed by using Gblocks (http://molevol.cmina.csic.es/castresana/Gblocks_server.html) to ensure an accurate alignment before phylogenetic reconstructions. Phylogenies were inferred from sequences by calculating observed genetic distances by using PhyML (http://code.google.com/p/phyml/) with the general time reversible evolutionary model (*7*). *Mycobacterium setuense* was used as an outgroup because it is a species that is borderline to the slow-growing mycobacteria (*8*). Resulting tree topologies were evaluated by bootstrap analysis with 1,000 resamples.

The phylogenetic tree based on *rpoB* sequences (Figure 2, panel A) was consistent with that obtained for *hsp65* sequences (Figure 2, panel B). On the basis of *rpoB* and *hsp65* phylogenies, the unidentified organism was phylogenetically similar to *M. leprae* and *M. lepromatosis* but belonged to a clearly distinct branch. Similar to these species, it shares a common ancestor with *M. haemophilum*. The same well-sustained relationship with *M. leprae* and separation from *M. haemophilum* was inferred from *sodA*, *tuf*, and tmRNA gene phylogenies, but the lack of corresponding sequences for *M. lepromatosis* impaired this analysis.

On the basis of 16S rRNA gene phylogeny (Figure 2, panel C), the unknown organism was a member of the *M. leprae* cluster and was related to *M. lepromatosis* and an unknown feline *Mycobacterium* sp. that causes leprosy-like symptoms in cats (*9*). This organism was phylogenetically related to *M. lepromatosis*, and the 2 species constituted

a separate branch from that of *M. leprae* (bootstrap value 88%). The absence of congruence between the phylogenetic trees inferred from the 16S rRNA gene and the *hsp65* and *rpoB* genes could be related to a short consensus sequence (369 bp) in a position that is not optimal for mycobacteria discrimination.

Conclusions

Phylogenetic investigations strongly supported the conclusion that an undescribed species of the genus *Mycobacterium* that is related to *M. leprae* and *M. lepromatosis*, the causative agents of tuberculoid and lepromatous leprosy, and a diffuse form of lepromatous leprosy (*10*,*11*), respectively, was characterized in cows with bovine nodular thelitis. *M. leprae* and *M. lepromatosis* are not cultivable on artificial media. *M. haemophilum*, which is closely related to *M. leprae* and *M. lepromatosis* (*11*,*12*), is a slow-growing mycobacterium that requires hemin and a low temperature for growth (*12*). Attempts to cultivate mycobacteria from cows with bovine nodular thelitis were mostly unsuccessful and necessitated multiple samples (*3*).

M. leprae strains were found to be clonal (*13*,*14*). In accordance with reductive evolution of its genome (*15*), this species is an obligate parasite that infects humans and armadillos (*13*). In contrast, the environment could be a reservoir of *M. haemophilum* (*12*). The natural habitat of the causative agent of bovine nodular thelitis is unknown, and zoonotic transmission had never been observed in breeder cows.

The *M. leprae* cluster might have an animal origin. Genetic studies of multiple bovine and feline mycobacteria characterized from animals with nodular thelitis and leprosy-like syndromes, respectively, are currently in progress and should provide useful information.

Acknowledgments

We thank Jérôme Frasson and the farmers for assistance with fieldwork and Catherine Pichat for technical assistance.

This study was supported by Unité Mixte de Recherche 558–Laboratoire Biométrie et Biologie Évolutives, Dermatology and Dermatopathology Unit–VetAgro Sup and Institut National de la Santé et de la Recherche Médicale Unité 1111.

Dr Pin is an associate professor in the Dermatology and Dermatopathology Unit in VetAgro Sup of the University of Lyon, Marcy l'Étoile, France. His research interests focus on large animal dermatology and the skin barrier.

References

1. Elston D. Nontuberculous mycobacterial skin infections. Am J Clin Dermatol. 2009;10:281–5. http://dx.doi.org/10.2165/00128071-200910050-00001
2. Thorel M-F, Morand M, Fontaine J-J, Gourreau J-M. Bovine nodular thelitis: a clinicopathological study of 20 cases. Vet Dermatol. 1990;1:165–70. http://dx.doi.org/10.1111/j.1365-3164.1990.tb00095.x
3. Yachida S, Shimizu K, Hirose T, Sato M. Studies on mycobacteria isolated from skin lesion tuberculosis of the bovine udder. Nihon Juigaku Zasshi. 1973;35:357–65. http://dx.doi.org/10.1292/jvms1939.35.357
4. Rüsch P, Corboz L, Ossent P, Berchtold M, Ehrensperger F. Enzootic nodular-ulcerative mamillitis in dairy cows caused by unclassified mycobacteria [in German]. Schweiz Arch Tierheilkd. 1984;126:467–78.
5. Mignard S, Flandrois J-P. A seven-gene, multilocus, genus-wide approach to the phylogeny of mycobacteria using supertrees. Int J Syst Evol Microbiol. 2008;58:1432–41. http://dx.doi.org/10.1099/ijs.0.65658-0
6. Relman DA. Universal bacterial 16S rDNA amplification and sequencing. In: Persing DH, Smith TF, Tenover FC, White TJ, editors. Diagnostic molecular microbiology: principles and applications. Washington (DC): American Society for Microbiology; 1993. p. 489–95.
7. Guérin-Faublée V, Flandrois J-P, Pichat C, Boschiroli ML, Lamy B. *Mycobacterium bourgelatii* sp. nov., a rapidly growing, non-chromogenic species isolated from the lymph nodes of cattle. Int J Syst Evol Microbiol. 2013;63:4669–74. http://dx.doi.org/10.1099/ijs.0.051979-0
8. Tortoli E. Phylogeny of the genus *Mycobacterium*: many doubts, few certainties. Infect Genet Evol. 2012;12:827–31. http://dx.doi.org/10.1016/j.meegid.2011.05.025
9. Malik R, Hughes MS, James G, Martin P, Wigney DI, Canfield PJ, et al. Feline leprosy: two different clinical syndromes. J Feline Med Surg. 2002;4:43–59. http://dx.doi.org/10.1053/jfms.2001.0151
10. Han XY, Sizer KC, Thompson EJ, Kabanja J, Li J, Hu P, et al. Comparative sequence analysis of *Mycobacterium leprae* and the new leprosy-causing *Mycobacterium lepromatosis.* J Bacteriol. 2009;191:6067–74. http://dx.doi.org/10.1128/JB.00762-09
11. Han XY, Seo Y-H, Sizer KC, Schoberle T, May GS, Spencer JS, et al. A new *Mycobacterium* species causing diffuse lepromatous leprosy. Am J Clin Pathol. 2008;130:856–64. http://dx.doi.org/10.1309/AJCPP72FJZZRRVMM
12. Lindeboom JA, Bruijnesteijn van Coppenraet LES, van Soolingen D, Prins JM, Kuijper EJ. Clinical manifestations, diagnosis, and treatment of *Mycobacterium haemophilum* infections. Clin Microbiol Rev. 2011;24:701–17. http://dx.doi.org/10.1128/CMR.00020-11
13. Monot M, Honoré N, Garnier T, Araoz R, Coppée J-Y, Lacroix C, et al. On the origin of leprosy. Science. 2005;308:1040–2. http://dx.doi.org/10.1126/science/1109759
14. Schuenemann VJ, Singh P, Mendum TA, Krause-Kyora B, Jäger G, Bos KI, et al. Genome-wide comparison of medieval and modern *Mycobacterium leprae.* Science. 2013;341:179–83. http://dx.doi.org/10.1126/science.1238286
15. Cole ST, Eiglmeier K, Parkhill J, James KD, Thomson NR, Wheeler PR, et al. Massive gene decay in the leprosy bacillus. Nature. 2001;409:1007–11. http://dx.doi.org/10.1038/35059006

Address for correspondence: Didier Pin, VetAgro Sup Campus Vétérinaire de Lyon, Unité de Recherche Interactions Cellule Environnement, 69280 Marcy l'Étoile, France; email: didier.pin@vetagro-sup.fr

Human Metapneumovirus Infection in **Chimpanzees,** United States

Owen M. Slater,[1] Karen A. Terio, Yange Zhang, Dean D. Erdman, Eileen Schneider, Jane M. Kuypers, Steven M. Wolinsky, Kevin J. Kunstman, Jennifer Kunstman, Michael J. Kinsel, and Kathryn C. Gamble

Zoonotic disease transmission and infections are of particular concern for humans and closely related great apes. In 2009, an outbreak of human metapneumovirus infection was associated with the death of a captive chimpanzee in Chicago, Illinois, USA. Biosecurity and surveillance for this virus in captive great ape populations should be considered.

Zoological facilities in North America house endangered species of great apes with annual visitation rates of >100 million persons (*1*). Because humans and great apes are related genetically, interspecies transmission of infectious pathogens is a concern. Consequently, procedures are instituted to limit the potential spread of infectious pathogens (*2*).

Reports of outbreaks of human metapneumovirus (HMPV) infection with respiratory symptoms have been documented in wild great ape populations (*3*–*5*). All of these outbreaks have been attributed to exposure to humans because of the suspected HMPV-negative status of these populations. However, disease caused by HMPV has not been previously documented in North American zoo populations, despite the close proximity of humans and great apes. We report an outbreak of HMPV infection in 2009 in a troop of previously HPMV-negative chimpanzees (*Pan troglodytes*) in Chicago, Illinois, USA, that resulted in 1 death and an illness rate of 100%.

Author affiliations: Lincoln Park Zoo, Chicago, Illinois, USA (O.M. Slater, K.C. Gamble); University of Illinois, Maywood, Illinois, USA (K.A. Terio, M.J. Kinsel); Battelle, Atlanta, Georgia, USA (Y. Zhang); Centers for Disease Control and Prevention, Atlanta (D.D. Erdman, E. Schneider); University of Washington, Seattle, Washington, USA (J.M. Kuypers); and Northwestern University, Chicago (S.M. Wolinsky, K.J. Kunstman, J. Kunstman)

DOI: http://dx.doi.org/10.3201/eid2012.140408

The Study

Two chimpanzee and 2 western lowland gorilla (*Gorilla gorilla gorilla*) troops were housed in separate areas within 1 building with shared airspace at a zoological facility in Chicago, Illinois, USA. Animals had periodic contact with keepers during daily feeding, cage cleaning, and training sessions. Biosecurity for staff in the great ape area included wearing gloves, dedicated footwear and clothing, handwashing, and use of footbaths when entering and exiting the facility and during movement between troops. Staff members were required to notify management if they had a confirmed or suspected respiratory infection so that they were removed from direct interaction with animals. No outside personnel were allowed direct contact; indirect contact was considered rare and only possible if visitors tossed objects into outdoor enclosures.

Within 1 week before the outbreak in chimpanzees, staff members at the great ape facility had respiratory disease (coughing and nasal discharge), which coincided with peak HMPV season in the United States (Figure 1). The affected chimpanzee troop consisted of 7 chimpanzees; the initial clinical sign (coughing) on March 18, 2009, was observed in 1 adult female (Table, http://wwwnc.cdc.gov/EID/article/20/12/14-0408-T1.htm).

Within 96 hours, all 7 chimpanzees had moderate-to-severe respiratory disease (≥2 characteristic clinical signs), and their intake of oral fluids was increased. One juvenile male with pectus excavatum had marked mucopurulent rhinorrhea, coughing, lethargy, tachypnea, dyspnea, and partial anorexia; he was also given an intramuscular broad-spectrum antimicrobial drug (ceftiofur, 25 mg/kg). Within 24 hours, the condition of this animal worsened, which necessitated sedation for rehydration and diagnostic assessment. Radiographs showed marked bronchointerstitial pneumonia. An additional antimicrobial drug (cefazolin, 25 mg/kg) and fluids (0.9% NaCl, 40 mL/kg/h) were administered, but the animal died the next morning.

The remaining animals in the troop were given antimicrobial drugs (cefazolin, 25 mg/kg; enrofloxacin, 5 mg/kg) and anti-inflammatory medication (flunixin meglumine, 0.25 mg/kg). Within 48 hours, all animals showed mild improvement. Antimicrobial drugs were given for 10 days. Fifteen days post-onset, clinical resolution had occurred. The other troops showed no signs of respiratory disease.

Necropsy of the animal that died showed that the lungs were firm, had not collapsed, and surrounding airways were mottled red-to-purple. Histologic analysis showed that lesions were similar to those observed in humans and indicated necrotizing bronchointerstitial pneumonia with type II pneumocyte hyperplasia, abundant fibrin, and streaming mucus in airways. Cilia were absent from many bronchial epithelial cells, and rare epithelial cells lacked

[1]Current affiliation: University of Calgary, Calgary, Alberta, Canada.

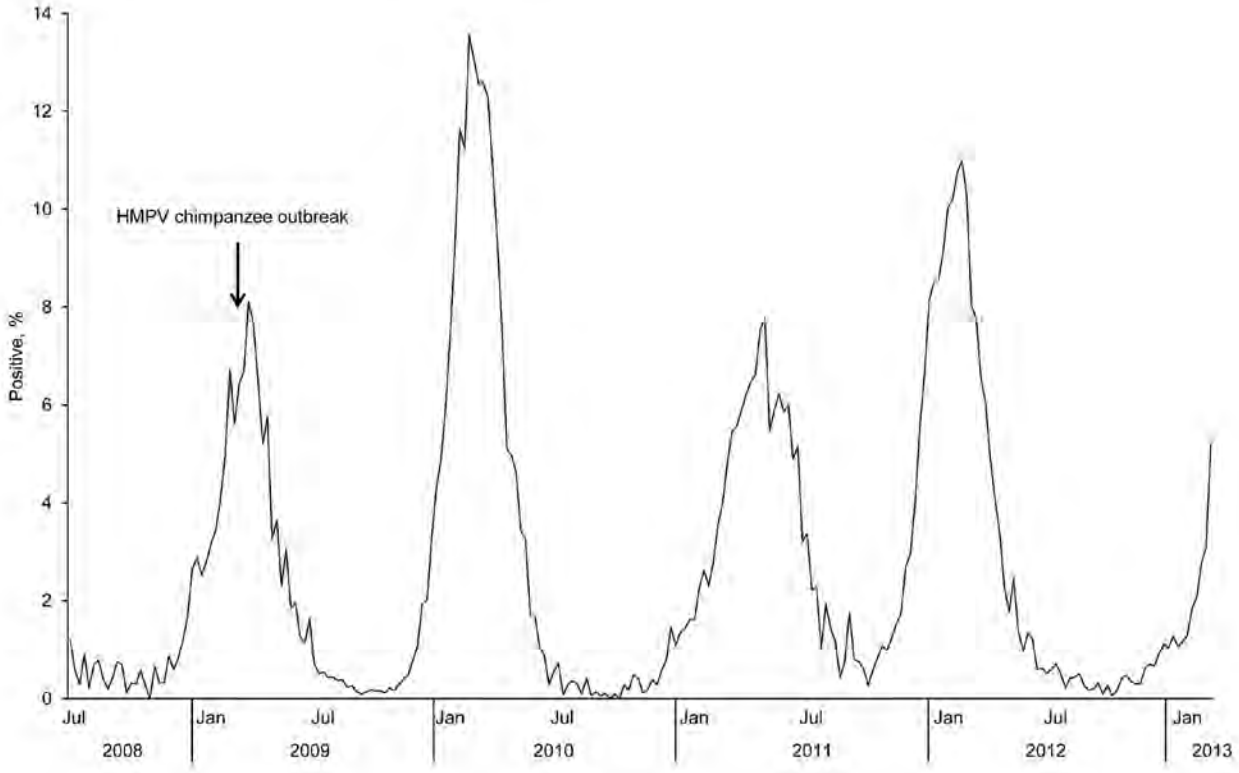

Figure 1. Percentage of human metapneumovirus (HMPV)–positive test results, by week of report, National Respiratory and Enteric Virus Surveillance System, United States, July 2008–January 2013.

any identifiable cytoplasmic membrane or nuclear structure, suggestive of the smudge cells commonly found in human HMPV infection (*6*) (Figure 2).

Only rare gram-positive cocci were observed, and the lack of extensive suppurative inflammation suggested that these findings were not a major contributing factor. Bacterial lung tissue cultures were negative. Lung tissue was screened for viral respiratory pathogens by real time reverse transcription PCR by using published methods (*7*). Sections were positive for HMPV and negative for adenoviruses, coronaviruses, influenza viruses A and B, human parainfluenza viruses 1–4, bocavirus, rhinovirus, and respiratory syncytial virus.

The complete HMPV nucleoprotein gene was sequenced and deposited in GenBank (accession no. KF891365). The HMPV strain sequence showed 99% nucleotide identity with group A, subgroup A2 reference strain CAN97–83 (accession no. AY297749.1).

To assess troop HMPV exposure, we conducted a serologic study by measuring IgG against HMPV in available serum samples collected at various times before and after the outbreak (Table) (*8*). Serum samples were usually collected opportunistically, often not during clinical illness. Unlike samples from other troops, serum samples from chimpanzee troop 1 showed that these animals were seronegative for HMPV before the outbreak; 100% seroconversion was observed 1–3 years later. Serum samples obtained before 2009 from the other troops had stable levels of IgG against HMPV, and these troops had experienced 12 episodes in which a ≥4-fold increase in titer or seroconversion were noted, indicating exposure within the testing interval. Overall, HMPV seroprevalence in the year before the outbreak for the chimpanzee and gorilla troops were 42% and 75%, respectively. Seroprevelance 3 years post-outbreak was 100% and 92%, respectively.

Conclusions

We report an outbreak of HMPV infection producing illness and death in chimpanzees in a North American zoo. Although the human source of the infection remains unknown, staff members in the great ape area had respiratory disease just before the outbreak in chimpanzees. Serologic testing of staff for respiratory viruses could not be performed. Post-outbreak, in addition to biosecurity measures already in place, all staff working with primates have been required to wear facemasks during direct primate interactions.

Unlike this situation, chimpanzees experimentally infected with HMPV have shown only mild cold-like clinical signs in seronegative animals and no clinical signs in seroconverted animals (*9*). Seroconverted, naturally

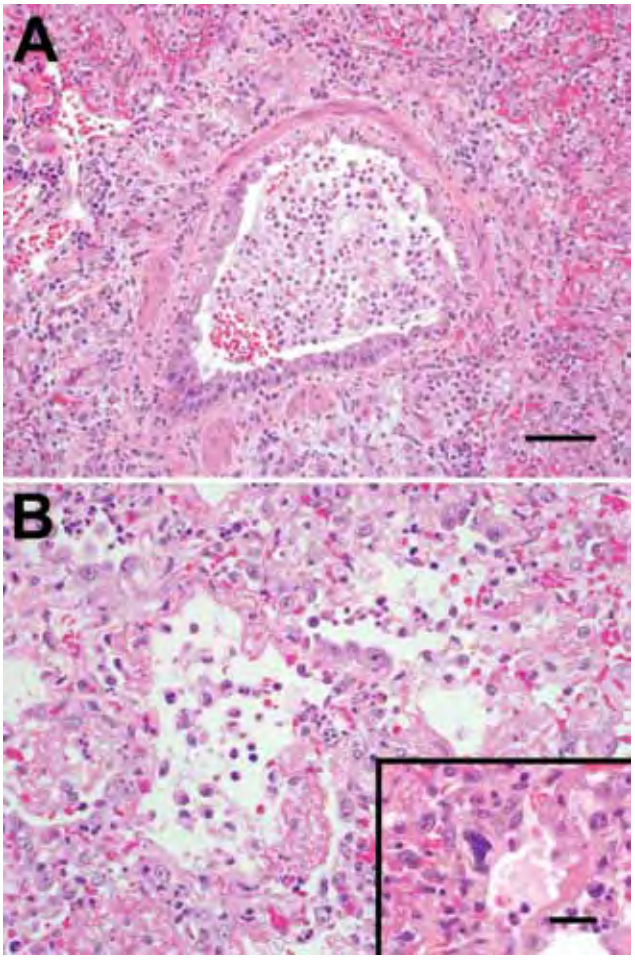

Figure 2. A) Bronchiolar epithelium of chimpanzees infected with human metapneumovirus, United States, 2009, showing cell variation from attenuated to piled and disorganized. Epithelial cells lack cilia, and lumens contain foamy macrophages, neutrophils, and hemorrhage. Adjacent air spaces are filled with similar inflammatory cells. Scale bar = 70 μm. B) Alveoli lined with plump type II pneumocytes and fibrin. Inset: Rare, deeply basophilic, smudged nuclei are present in some areas. Scale bar = 20 μm. Hematoxylin and eosin stain.

infected, captive-bred chimpanzees represented 61% of the laboratory population, which demonstrated that captive animals are readily infected with HMPV (*9*). Worldwide, nearly 100% of the human population has seroconverted to HMPV by 10 years of age, and most illness and death occurs in young, elderly, and immunocompromised persons, although persons in any age group can become infected (*10*,*11*). Immunity is transient, and reinfections with the same or different strains are common, but illness is reduced (*10*,*11*). Recent evidence suggests these findings are also found in captive and wild chimpanzees (*9*,*12*) and other primates (*13*). In this instance, the congenital thoracic defect may have affected the ability of the chimpanzee to survive. In contrast to other cases in which apes were infected with *Streptococcus pneumoniae* (*3*–*5*), only rare lung bacteria were observed histologically and lung bacterial cultures were negative. These findings, in combination with the absence of major suppurative inflammation, suggest that HMPV was the primary pathogen.

Given the ubiquitous nature of this human virus in North America and the frequency with which it infects humans, it is notable that all members of the affected chimpanzee troop were born in captivity and had contact with humans throughout their lives, yet still remained negative for this virus until March 2009. Because HMPV is a recently discovered virus that closely resembles other respiratory viruses in its clinical course and few animal facilities specifically test for it, the degree of illness associated with this disease in the captive great ape population is unknown. Therefore, enhanced biosecurity and disease surveillance measures for HMPV should be considered for great apes. In addition to the commonly tested viral respiratory pathogens of great apes, surveillance for HMPV by serologic analysis at quarantine or preventative medical examinations would provide additional benefits. These procedures would enable management to tailor biosecurity protocols and procedures to limit the risk for exposure of HMPV-negative animals or troops, particularly during the height of the HMPV season.

Acknowledgments

We thank the staff at the Lincoln Park Zoo for providing help during and after the disease outbreak, and the Histology Laboratory at the University of Illinois Veterinary Diagnostic Laboratory (Champaign, Illinois) for providing excellent technical assistance.

Dr Slater is an instructor of zoo, wildlife and exotic animal veterinary medicine at the University of Calgary, Calgary, Alberta, Canada. His primary research interests are in infectious diseases of zoo and wildlife species and wildlife transport.

References

1. Association of Zoos and Aquariums [cited 2013 Feb 1]. http://www.aza.org/zoo-aquarium-statistics/
2. Unwin S, Chatterton J, Chantrey J. Management of severe respiratory tract disease caused by human respiratory syncytial virus and *Streptococcus pneumoniae* in captive chimpanzees (*Pan troglodytes*). J Zoo Wildl Med. 2013;44:105–15. http://dx.doi.org/10.1638/1042-7260-44.1.105
3. Kaur T, Singh J, Tong S, Humphrey C, Clevenger D, Tan W, et al. Descriptive epidemiology of fatal respiratory outbreaks and detection of a human-related metapneumovirus in wild chimpanzees (*Pan troglodytes*) at Mahale Mountains National Park, Western Tanzania. Am J Primatol. 2008;70:755–65. http://dx.doi.org/10.1002/ajp.20565
4. Köndgen S, Kuhl H, N'Goran PK, Walsh PD, Schenk S, Ernst N. Pandemic human viruses cause decline of endangered great apes. Curr Biol. 2008;18:260–4. http://dx.doi.org/10.1016/j.cub.2008.01.012
5. Palacios G, Lowenstine LJ, Cranfield MR, Gilardi KV, Spelman L, Lukasik-Braum M, et al. Human metapneumovirus infection in wild mountain gorillas, Rwanda. Emerg Infect Dis. 2011;17:711–3.

6. Sumino KC, Agapoc E, Pierce RA, Trulock EP, Pfeifer JD, Ritter JH, et al. Detection of severe human metapneumovirus infection by real-time polymerase chain reaction and histopathological assessment. J Infect Dis. 2005;192:1052–60. http://dx.doi.org/10.1086/432728
7. Kuypers J, Wright N, Corey L, Morrow R. Detection and quantification of human metapneumovirus in pediatric specimens by real time RT-PCR. J Clin Virol. 2005;33:299–305. http://dx.doi.org/10.1016/j.jcv.2004.11.023
8. Erdman DD, Anderson LJ, Adams DR, Stewart JA, Markowitz LE, Bellini WJ. Evaluation of monoclonal antibody-based capture enzyme immunoassays for detection of specific antibodies to measles virus. J Clin Microbiol. 1991;29:1466–71.
9. Skiadopoulos MH, Biacchesi S, Buchholz UJ, Riggs JM, Surman SR, Amaro-Carambot E, et al. The two major human metapneumovirus genetic lineages are highly related antigenically, and the fusion (F) protein is a major contributor to this antigenic relatedness. J Virol. 2004;78:6927–37. http://dx.doi.org/10.1128/JVI.78.13.6927-6937.2004
10. Feuillet F, Lina B, Rosa-Calatrava M, Boivin G. Ten years of human metapneumovirus research. J Clin Virol. 2012;53:97–105. http://dx.doi.org/10.1016/j.jcv.2011.10.002
11. Peret TC, Boivin G, Li Y, Couillard M, Humphrey C, Osterhaus AD, et al. Characterization of human metapneumoviruses isolated from patients in North America. J Infect Dis. 2002;185:1660–3. http://dx.doi.org/10.1086/340518
12. Köndgen S, Schenk S, Pauli G, Boesch C, Leendertz FH. Noninvasive monitoring of respiratory viruses in wild chimpanzees. EcoHealth. 2010;7:332–41. http://dx.doi.org/10.1007/s10393-010-0340-z
13. van den Hoogen BG, Herfst S, de Graaf M, Sprong L, van Lavieren R, van Amerongen G, et al. Experimental infection of macaques with human metapneumovirus induces transient protective immunity. J Gen Virol. 2007;88:1251–9. http://dx.doi.org/10.1099/vir.0.82663-0

Address for correspondence: Owen M. Slater, Faculty of Veterinary Medicine, University of Calgary, 1-202 11th Ave NW, Calgary, Alberta T2M 0B8, Canada; email: owenslater@yahoo.com

Putative New West Nile Virus Lineage in *Uranotaenia unguiculata* Mosquitoes, Austria, 2013

Karin Pachler,[1] Karin Lebl, Dominik Berer, Ivo Rudolf, Zdenek Hubalek, and Norbert Nowotny

West Nile virus (WNV) is becoming more widespread and markedly effecting public health. We sequenced the complete polyprotein gene of a divergent WNV strain newly detected in a pool of *Uranotaenia unguiculata* mosquitoes in Austria. Phylogenetic analyses suggest that the new strain constitutes a ninth WNV lineage or a sublineage of WNV lineage 4.

West Nile virus (WNV), the most widespread flavivirus, is distributed throughout Africa, Asia, Europe, and Australia, and since 1999, WNV has also been present in the Americas (*1*). Within the last 2 decades, WNV infection has caused an increasing number of cases of neuroinvasive disease in humans and become a substantial public health problem (*1*).

Up to 8 lineages of WNV, based on genetic differences, have been proposed (*1*,*2*) (Table 1). Lineage 1 is widely distributed and further divided into lineage 1a, which includes the American strains; lineage 1b, which is also referred to as Kunjin virus and mainly described in Australia; and lineage 1c, which is also referred to as lineage 5 and comprises isolates from India. Lineage 2 has been detected in Africa and several parts of Europe, lineage 3 (Rabensburg virus) has been isolated only in the Czech Republic, and lineage 4 has been reported from Russia (*3*). A putative sixth lineage, based on a small genome fragment, has been described from Spain (*4*), and putative lineages 7 (Koutango virus) and 8 have been reported from Senegal (*2*).

WNV is maintained in an enzootic cycle between mosquitoes and wild birds (*1*). In 2013, ≈100 *Uranotaenia unguiculata* Edwards, 1913, mosquitoes were trapped during mosquito-monitoring projects at Lake Neusiedl-Seewinkel National Park in Austria and near Sedlec in the Czech Republic. In Russia, *Ur. unguiculata* mosquitoes have been described as hosting lineage 4 WNV strains (A. Platonov, unpub. data) (GenBank accession nos. FJ154906–49 and FJ159129–31). To determine whether *Ur. unguiculata* mosquitoes in Austria and the Czech Republic also host WNV, we investigated the mosquitoes collected in 2013 for the presence of WNV, focusing on lineage 4 viruses.

The Study

During May–October 2013, ≈11,300 female mosquitoes belonging to 13 species were trapped at 4 sites in Lake Neusiedl-Seewinkel National Park in Burgenland State, Austria. Mosquito species were determined according to morphologic criteria (*5*). Individual mosquitoes were pooled by species and collection site and date. A total of 47 *Ur. unguiculata* mosquitoes were collected in Austria (12 pools, 1–12 mosquitoes/pool). The relative abundance of *Ur. unguiculata* mosquitoes among the total collected in Austria was 0.42%. During August 2013, ≈39,000 mosquitoes were trapped at 2 fish ponds (Nesyt and Novy) in Sedlec, Czech Republic, near the border with northeastern Austria. A total of 47 female *Ur. unguiculata* mosquitoes were grouped into 4 pools (2 with 1 mosquito each, 1 with 4 mosquitoes, and 1 with 41 mosquitoes). The relative abundance of *Ur. unguiculata* mosquitoes among the total collected in the Czech Republic was 0.12%.

The mosquito pools were homogenized in RNase-free water, and RNA was extracted by using the QIAamp Viral RNA Mini Kit (QIAGEN, Valencia, CA, USA). The samples were screened for the presence of flavivirus nucleic acid by reverse transcription PCR, using universal flavivirus primers MAMD (*6*) and CFD2 (*6*,*7*) for amplification of a partial nonstructural protein (NS) 5 sequence. Results were negative for the samples from Czech Republic. One pooled sample from Austria was positive; the pool contained 9 mosquitoes that had been captured in late August in Illmitz, a village east of Lake Neusiedl (47.769997°N, 16.752887°E). We obtained the complete polyprotein coding sequence and partial 5′ and 3′ noncoding ends of this novel WNV strain (GenBank accession no. KJ831223), which was designated West Nile virus-*Uranotaenia unguiculata*-Lake Neusiedl-Austria-2013 (WNV-Uu-LN-AT-2013). Primer sequences and amplification protocols are available upon request.

The complete polyprotein gene sequence of WNV-Uu-LN-AT-2013 shares a maximum identity of ≈83% with lineage 4 WNV strains isolated from *Ur. unguiculata* mosquitoes and *Dermacentor marginatus* ticks in Russia (*3*). At the amino acid level, the entire polyproteins of WNV-

Author affiliations: University of Veterinary Medicine Vienna, Vienna, Austria (K. Pachler, K. Lebl, D. Berer, N. Nowotny); Academy of Sciences, Brno, Czech Republic (I. Rudolf, Z. Hubalek); and Sultan Qaboos University, Muscat, Oman (N. Nowotny)

DOI: http://dx.doi.org/10.3201/eid2012.140921

[1]Current affiliation: Paracelsus Medical University, Salzburg, Austria.

Table 1. Overview of West Nile virus lineages

Lineage	Representative strain, location	GenBank accession no.
1a	NY 2000-crow3356, New York, USA	AF404756
1b	Kunjin virus, Australia	D00246
1c/5	804994, India	DQ256376
2	Goshawk-Hungary/04, Hungary	AAZ91684
3	Rabensburg virus 97–103, Czech Republic	AY765264
4/4a	LEIV-Krnd88–190, Russia	AY277251
6/4b, putative*	HU2925/06, Spain	GU047875
7 (Koutango virus), putative	Dak-Ar-D-5443, Senegal	EU082200
8, putative*	ArD94343, Senegal	KJ131502
9/4c, putative	WNV-Uu-LN-AT-2013, Austria	KJ831223

*Only partial sequence available.

Uu-LN-AT-2013 and the lineage 4 strains from Russia share ≈96% identity (Table 2). Compared with the Russian lineage 4 strains, a 1,813-nt fragment of the NS5-coding sequence for the putative lineage 6 WNV, isolated from *Culex pipiens* mosquitoes in Spain (*4*), shares slightly higher nucleotide and amino acid identities with WNV-Uu-LN-AT-2013 (Table 2).

Phylogenetic neighbor-joining trees were generated with MEGA5 software, using ClustalW alignments, 1,000 replicates for bootstrap testing, and evolutionary distances computation with the p-distance model (*8*). One phylogenetic tree was constructed on the basis of the complete polyprotein-encoding nucleotide sequences of 32 WNV strains representing all previously described lineages for which complete polyprotein-encoding sequences are available. This tree also showed a close relationship between WNV-Uu-LN-AT-2013 and the lineage 4 WNV strains from Russia; however, the newly identified strain forms a distinct branch (Figure, panel A). A second phylogenetic analysis that included the proposed lineage 6 virus from Spain and that was based on 1,813-nt fragments of NS5 showed a close grouping of WNV-Uu-LN-AT-2013 virus from Austria, the virus from Spain, and the lineage 4 viruses from Russia; similarity was slightly higher between the viruses from Austria and Spain (Figure, panel B).

WNV-Uu-LN-AT-2013 encodes a polyprotein of 3,432 aa. The envelope protein carries 1 putative *N*-linked glycosylation site at asparagine residue N-154, which has been associated with increased WNV pathogenicity and neuroinvasiveness (*9*). The 3 highly conserved *N*-linked glycosylation sites at NS1 positions N-130, N-175, and N-207 in WNV strains were also calculated for WNV-Uu-LN-AT-2013 by using NetNGlyc 1.0 software (http://www.cbs.dtu.dk/services/NetNGlyc/). Glycosylation of NS1 at these 3 positions has been implicated in neuroinvasiveness (*10*), as has proline at NS1 aa position 250 (*11*), which is also present in WNV-Uu-LN-AT-2013. The NS2A-encoding nucleotide region contains a *foo* motif, which can mediate production of NS1′, a variant of NS1 that plays a role in neuroinvasiveness (*12*). A *fifo* motif, which has been described for the nonpathogenic mosquito-specific flaviviruses (*13*), could not be determined for WNV-Uu-LN-AT-2013.

Table 2. Sequence identities between the newly identified WNV strain from Austria, WNV-Uu-LN-AT-2013, and other strains representing different WNV lineages*

	Nucleotide identity or amino acid identity, %, by strain/lineage†‡										
Strain/lineage†	WNV-Uu-LN-AT-2013	1a	1b	1c/5	2	3	4	6 (Spain)§	7 (Koutango virus)	8¶	Usutu virus
WNV-Uu-LN-AT-2013		88.3	87.9	87.0	88.8	86.7	96.2	95.9	85.3	81.2	75.5
1a	76.2		97.6	93.4	94.0	90.4	88.6	91.7	89.2	92.4	76.3
1b	75.4	88.2		92.7	93.5	89.8	88.3	91.2	88.8	92.0	76.1
1c/5	76.3	80.5	79.7		92.1	88.8	87.4	89.1	87.7	91.2	76.1
2	77.0	79.8	79.6	79.1		90.9	89.2	92.6	89.3	92.0	76.0
3	75.9	78.3	77.3	77.3	78.7		87.0	91.4	86.6	89.2	75.5
4	82.8	76.6	76.0	76.2	76.9	76.5		95.0	85.5	81.0	74.7
6 (Spain)§	83.2	78.1	78.1	77.7	78.6	79.5	81.7		88.6	–	80.8
7 (Koutango virus)	75.1	77.7	77.4	77.0	77.8	76.3	75.6	78.0		86.8	75.3
8¶	72.7	78.4	78.0	77.3	78.4	77.7	72.6	–	77.4		76.3
Usutu virus	71.2	72.4	72.6	72.4	71.3	71.0	70.1	73.6	72.4	72.5	

*Alignments were performed by using ClustalW2 (http://www.ebi.ac.uk/Tools/msa/clustalw2/). WNV, West Nile virus; WNV-Uu-LN-AT-2013, West Nile virus strain *Uranotaenia unguiculata*-Lake Neusiedl-Austria-2013; –, comparison between lineages 6 and 8 was not possible because the available partial sequences do not cover the same nucleotide regions.

†GenBank accession nos. are as follows for the polyprotein genes/polyproteins: WNV-Uu-LN-AT-2013 (KJ831223), lineage 1a (AF404756/AAM81752), lineage 1b (D00246/BAA00176), lineage 1c (DQ256376/ABC40712), lineage 2 (DQ116961/AAZ91684), lineage 3 (AY765264/AAW81711), lineage 4 (FJ159129/ACH99530), lineage 6 (Spain) (GU047875/ADD69956), lineage 7 (Koutango virus) (EU082200/ABW76844), lineage 8 (KJ131502/AHV83443), Usutu virus (AY453411/AAS59402).

‡Amino acid sequences (above the diagonal) and nucleotide sequences (below the diagonal) are based on complete polyprotein genes, with the exception of lineage 6 and 8 strains, for which only partial sequences were available.

§Comparison was based only on partial NS5 gene sequences.

¶Comparison was based only on complete envelope protein gene sequences.

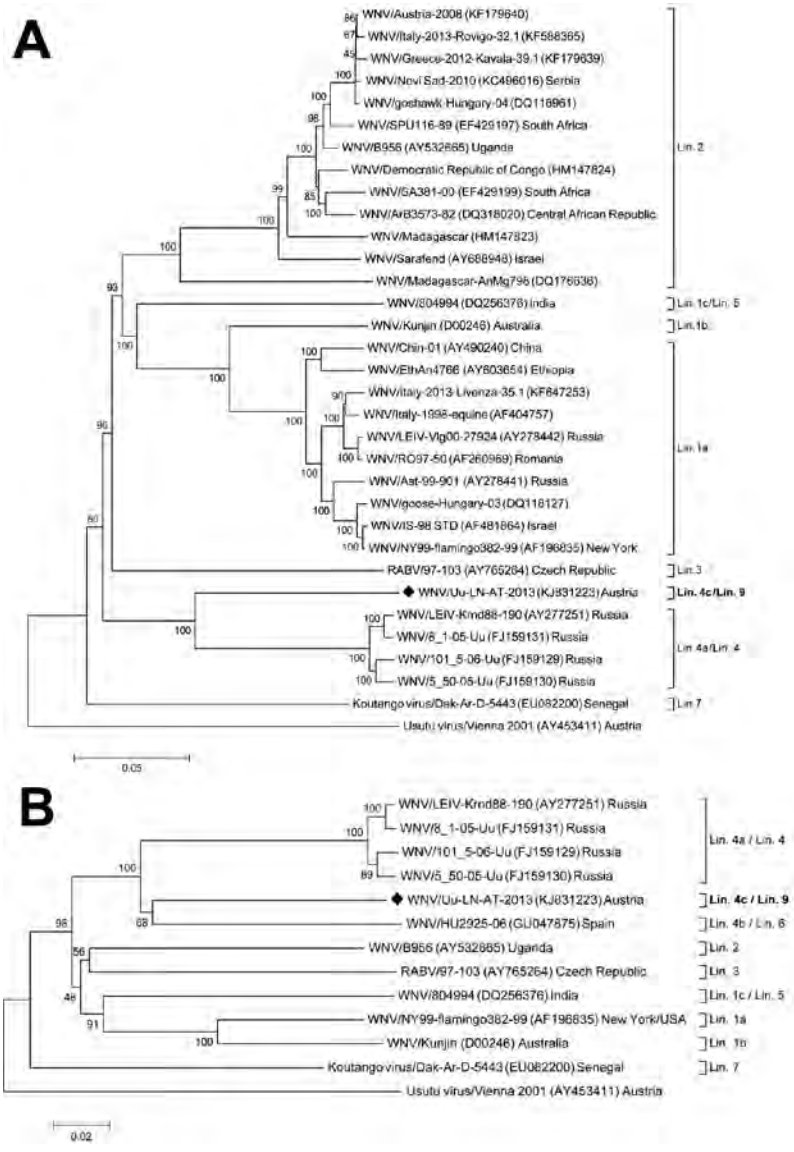

Figure. Phylogenetic positioning of WNV-Uu-LN-AT-2013, a West Nile virus (WNV) strain newly identified in Austria, within the species *West Nile virus*. A) Phylogenetic position as determined on the basis of the full-length polyprotein-coding nucleotide sequences. B) Phylogenetic position as determined on the basis of 1,813-nt fragments of NS5, which enabled inclusion of the proposed lineage 6 virus. The evolutionary history was inferred by using the neighbor-joining method of MEGA5 (*8*) with 1,000-fold bootstrap analysis, rooted against the respective sequence of Usutu flavivirus. Numbers next to the branches indicate the percentage of replicates in the bootstrap analysis. Black diamond indicates the WNV sequence determined in this study. GenBank accession numbers are shown in parentheses with the virus names. Scale bars indicate nucleotide substitutions per site. Lin., lineage; RABV, Rabensburg virus.

Conclusions

WNV lineages 1–4 and putative lineage 6 have been detected in Europe, but only WNV lineage 1a has spread across the American continents. Circulation of such a genetically diverse group of WNV strains in Europe may partly explain the epidemiologic differences observed between WNV disease in Europe and the Americas. In Europe, the presence of less pathogenic WNV strains may inhibit the spread of more pathogenic strains.

We propose that the WNV-Uu-LN-AT-2013 strain from Austria either constitutes a new lineage (lineage 9) or can be grouped into lineage 4 as sublineage 4c, with the strains from Russia and Spain as sublineages 4a and 4b, respectively. However, the short sequence available for the strain from Spain does not allow a clear-cut conclusion to be drawn with regard to lineage 4. We suggest that future designation of new WNV lineages should be restricted to viruses for which at least the complete polyprotein gene sequences have been determined. In addition, rules for defining virus lineages should be established by the International Committee on Taxonomy of Viruses.

Strain WNV-Uu-LN-AT-2013 has been detected only in *Ur. unguiculata* mosquitoes. These mosquitoes are mainly distributed in the southern half of Europe (*5*); in eastern Europe, they have spread from southern Ukraine and the Volga Delta through middle and southwestern Asia to Iran and Pakistan (*5*). In the Lake Neusiedl area of Austria, *Ur. unguiculata* mosquitoes seem to be an indigenous species, which was first reported in 1970 (*14*). In the Czech Republic, *Ur. unguiculata* mosquitoes have been detected only in Moravia, in the southern part of the country (*15*). Although there are anecdotal reports of *Ur. unguiculata* mosquitoes feeding on mammals, including humans, they feed mainly on amphibians and reptiles (*5*).

The pathogenicity of strain WNV-Uu-LN-AT-2013 in humans and animals has not been elucidated. Genetic data show that the strain carries typical WNV pathogenicity markers and suggest that WNV-Uu-LN-AT-2013 is not restricted to mosquitoes. Additional monitoring studies involving cell culture and animal isolation experiments are necessary to evaluate the pathogenic potential of this virus for humans and animals.

Acknowledgments

We thank Oldřich Šebesta for collecting and identifying mosquitoes in the Czech Republic and Jolanta Kolodziejek for her support.

This study was partially funded by support from the European Commission (grants HEALTH.2010.2.3.3-3 Project 261391 EuroWestNile [http://www.eurowestnile.org] and FP7-261504 EDENext [http://www.edenext.eu], and is catalogued by the EDENext Steering Committee as EDENext228).

Dr Pachler is a postdoctoral researcher at the Institute of Virology, University of Veterinary Medicine, Vienna, Austria. Her research interests include the molecular biology of emerging and vectorborne viruses.

References

1. Gray TJ, Webb CE. A review of the epidemiological and clinical aspects of West Nile virus. Int J Gen Med. 2014;7:193–203. http://dx.doi.org/10.2147/IJGM.S59902
2 Fall G, Diallo M, Loucoubar C, Faye O, Sall AA. Vector competence of *Culex neavei* and *Culex quinquefasciatus* (*Diptera*: *Culicidae*) from Senegal for lineages 1, 2, Koutango and a putative new lineage of West Nile virus. Am J Trop Med Hyg. 2014;90:747–54. http://dx.doi.org/10.4269/ajtmh.13-0405
3. Lvov DK, Butenko AM, Gromashevsky VL, Kovtunov AI, Prilipov AG, Kinney R, et al. West Nile virus and other zoonotic viruses in Russia: examples of emerging–reemerging situations. Arch Virol Suppl. 2004;18:85–96.
4. Vázquez A, Sánchez-Seco MP, Ruiz S, Molero F, Hernández L, Moreno J, et al. Putative new lineage of West Nile virus, Spain. Emerg Infect Dis. 2010;16:549–52. http://dx.doi.org/10.3201/eid1603.091033
5. Becker N, Petrič D, Zgomba M, Boase C, Madon M, Dahl C, et al. Mosquitoes and their control, 2nd ed. Heidelberg (Germany): Springer Verlag; 2010. p. 91–111, 312–4.
6. Scaramozzino N, Crance J-M, Jouan A, DeBriel DA, Stoll F, Garin D. Comparison of *Flavivirus* universal primer pairs and development of a rapid, highly sensitive heminested reverse transcription–PCR assay for detection of flaviviruses targeted to a conserved region of the NS5 gene sequences. J Clin Microbiol. 2001;39:1922–7. http://dx.doi.org/10.1128/JCM.39.5.1922-1927.2001
7. Kuno G, Chang GJ, Tsuchiya KR, Karabatsos N, Cropp CB. Phylogeny of the genus *Flavivirus.* J Virol. 1998;72:73–83.
8. Tamura K, Peterson D, Peterson N, Stecher G, Nei M, Kumar S. MEGA5: Molecular Evolutionary Genetics Analysis using maximum likelihood, evolutionary distance, and maximum parsimony methods. Mol Biol Evol. 2011;28:2731–9. http://dx.doi.org/10.1093/molbev/msr121
9. Shirato K, Miyoshi H, Goto A, Ako Y, Ueki T, Kariwa H, et al. Viral envelope protein glycosylation is a molecular determinant of the neuroinvasiveness of the New York strain of West Nile virus. J Gen Virol. 2004;85:3637–45. http://dx.doi.org/10.1099/vir.0.80247-0
10. Whiteman MC, Wicker JA, Kinney RM, Huang CYH, Solomon T, Barrett ADT. Multiple amino acid changes at the first glycosylation motif in NS1 protein of West Nile virus are necessary for complete attenuation for mouse neuroinvasiveness. Vaccine. 2011;29:9702–10. http://dx.doi.org/10.1016/j.vaccine.2011.09.036
11. Hall RA, Khromykh AA, Mackenzie JM, Scherret JH, Khromykh TI, Mackenzie JS. Loss of dimerisation of the nonstructural protein NS1 of Kunjin virus delays viral replication and reduces virulence in mice, but still allows secretion of NS1. Virology. 1999;264:66–75. http://dx.doi.org/10.1006/viro.1999.9956
12. Melian EB, Hinzman E, Nagasaki T, Firth AE, Wills NM, Nouwens AS, et al. NS1′ of flaviviruses in the Japanese encephalitis virus serogroup is a product of ribosomal frameshifting and plays a role in viral neuroinvasiveness. J Virol. 2010;84:1641–7. http://dx.doi.org/10.1128/JVI.01979-09
13. Firth AE, Blitvich BJ, Wills NM, Miller CL, Atkins JF. Evidence for ribosomal frameshifting and a novel overlapping gene in the genomes of insect-specific flaviviruses. Virology. 2010;399:153–66. http://dx.doi.org/10.1016/j.virol.2009.12.033
14. Aspöck H, Kunz C, Pretzmann G. Seasonal distribution of mosquitoes and its relation to the appearance of mosquito-borne viruses in the eastern part of the Neusiedlersee area (eastern Austria) [in German]. Zentralbl Bakteriol Orig. 1970;214:160–73.
15. Šebesta O, Halouzka J, Hubálek Z, Juřicová Z, Rudolf I, Šikutová S, et al. Mosquito (*Diptera: Culicidae*) fauna in an area endemic for West Nile virus. J Vector Ecol. 2010;35:156–62. http://dx.doi.org/10.1111/j.1948-7134.2010.00072.x

Address for correspondence: Norbert Nowotny, Viral Zoonoses, Emerging and Vector-Borne Infections Group, Institute of Virology, University of Veterinary Medicine Vienna, Veterinaerplatz 1, 1210 Vienna, Austria; email: norbert.nowotny@vetmeduni.ac.at and nowotny@squ.edu.om

Novel Bluetongue Virus in Goats, Corsica, France, 2014

Stéphan Zientara, Corinne Sailleau, Cyril Viarouge, Dirck Höper, Martin Beer, Maria Jenckel, Bernd Hoffmann, Aurore Romey, Labib Bakkali-Kassimi, Aurore Fablet, Damien Vitour, and Emmanuel Bréard

During 2000–2013, 4 genotypes of bluetongue virus (BTV) were detected in Corsica, France. At the end of 2013, a compulsory BTV-1 vaccination campaign was initiated among domestic ruminants; biological samples from goats were tested as part of a corresponding monitoring program. A BTV strain with nucleotide sequences suggestive of a novel serotype was detected.

Bluetongue is an infectious, noncontagious, arthropod-borne viral disease of domestic and wild ruminants (*1*). Twenty-six distinct bluetongue virus (BTV) serotypes have been identified (*2*).

The first detection of bluetongue virus (BTV) on the island of Corsica, France, was in 2000, when sheep were found to be infected with BTV genotype 2 (BTV-2); the virus most likely originated from Sardinia (*3*). In 2003 and 2004, BTV-4 and BTV-16 were detected on Corsica (*4*). Since 2004, no other outbreaks of BTV had been reported on the island until September 2, 2013, when BTV-1 was isolated from 3 flocks of sheep in southern Corsica (*5*). In the following weeks, the virus spread across the island, and by March 2014, 169 outbreaks had been reported.

The Study

During September–December 2013, a total of 1,097 blood and spleen samples were collected from diseased or dead animals on Corsica; the samples were sent to the French National Reference Laboratory at Agence Nationale de Sécurité Sanitaire (Maisons-Alfort, France) to be tested for the presence of BTV. RNA was extracted from the samples and then amplified by using a real-time reverse transcription PCR (RT-qPCR). The ADIAVET BTV Real-time PCR Kit (bioMérieux, Saint Brieuc, France) was used for BTV group (i.e., *Orbivirus Bluetongue virus*) and serotype 1 detection. The LSI VetMAX European BTV Typing (1-2-4-6-8-9-11-16) Real-time PCR Kit (Life Technologies, Lissieu, France) was used for BTV-2, -4, -9, and -16 serotyping. A total of 531 samples from sheep, cattle, and goats had RT-qPCR results positive for BTV. All genotyped samples were positive only for BTV-1.

At the end of 2013, a compulsory vaccination program of domestic sheep, cattle, and goats was initiated by veterinary authorities in France. During the campaign, testing of ruminants with clinical signs of BTV was continued as part of a corresponding monitoring program.

During January–April 2014, we analyzed 436 samples from goats; 86 (19.7%) had positive BTV group RT-qPCR results. This method detects the BTV RNA genome segment 10. Of the 86 BTV-positive samples, 73 with a cycle threshold (C_t) value of <35 were genotyped: 57 (78.0%) of the samples were classified as BTV-1, and 10 (13.7%) were classified as non–BTV-1, -2, -4, -9, -16, and -25. By using various primers (Table) with a conventional in-house RT-PCR that amplifies a region of the BTV RNA genome segment 2, we obtained an amplicon for each of the 10 samples that were negative for BTV-1, -2, -4, -9, -16, and -25 (segment 2 encodes viral protein 2 and determines the serotype). The animals from which these samples came were in 5 herds that were sampled in January and February 2014. One of the 10 amplified products (806 bp) was sequenced directly and compared with homologous sequences available in the GenBank database; Blast 2.2.28 (http://blast.ncbi.nlm.nih.gov/Blast.cgi) was used for the comparison. Because the genome sequence was similar to that of the BTV-25 segment 2, we selected different primers, and by gene walking, we obtained the full coding sequence of the gene.

BLASTN 2.2.29 (http://blast.ncbi.nlm.nih.gov/Blast.cgi) was used to align sequences: the virus showed highest identity with the BTV-25 and BTV-26 serotypes circulating in Switzerland and Kuwait, respectively (*6*,*7*) (Figure). The complete segment 2 sequence of this new virus from Corsica (termed BTV-n; GenBank accession no. KM200718) shared 73% nt and 75% aa identify with BTV-25 sequences and 65% nt and 60% aa identity with BTV-26 sequences.

We developed a conventional in-house RT-PCR and an RT-qPCR that enabled specific detection of BTV-n by selection of BTV-n–specific primers and probe (Table). We could not detect BTV-n virus genome in any cattle or sheep samples tested in 2014, and we did not detect any coinfections with BTV-1 and BTV-n.

We attempted to isolate BTV-n from blood samples of the 10 BTV-n–positive goats; BTV-group C_t values for

Author affiliations: ANSES (French Agency for Food, Environmental and Occupational Health and Safety), Maisons-Alfort, France (S. Zientara, C. Sailleau, C. Viarouge, A. Romey, L. Bakkali-Kassimi, A. Fablet, D. Vitour, E. Bréard); and Friedrich-Loeffler-Institut, Greifswald-Insel Riems, Germany (D. Höper, M. Beer, M Jenckel, B. Hoffmann)

DOI: http://dx.doi.org/10.3201/eid2012.140924

Table. Primers and probe used to detect the BTV strain BTV-n in samples from goats, Corsica, France, 2014*

PCR type	Target	Probe and primer names	Primer sequence, 5′ → 3′	Nucleotide location
Conventional BTV RT-PCR	Segment 2	PF	YRWTTGATTTTGARAARGA	1549–1566
		PR	GAAYCGACCACTGCCTATG	2355–2337
Conventional RT-PCR	BTV-n segment 2	BTV-n F	CAGATCTGGTTTTACCGAG	1546–1564
		BTV-n R	ATGATCCATCGGACTTAACT	1949–1927
Real-time RT-PCR	BTV-n segment 2	BTV-n F3	TGGATCATGATGGTTATGAACACC	1942–1966
		BTV-n R3	CGCCTCTCCAATCTCACGTATT	2102–2081
		BTV-n	FAM-TGACTATGCGAGGTTGG-MGB	1987–2004

*BTV, bluetongue virus; RT, reverse transcription; PF, forward primer; PR, reverse primer.

the samples ranged from 28.6 to 34.2. After many isolation attempts using embryonated chicken eggs as well as KC cells (a *Culicoides sonorensis*–derived cell line), Vero cells, and BHK (baby hamster kidney) cells, we isolated 1 virus strain by using BSR (a clone of BHK-21) cells. We used supernatants to conduct a BTV-n–specific RT-qPCR (primers shown in Table); the resulting C_t value of <17, indicated efficient virus replication. The virus was not neutralized by the reference antisera raised against BTV genotypes 1–24 and 26 or by an anti–BTV-25 serum (a titrated anti–BTV-25 serum is not available).

During May 2014, blood samples were collected from 56 goat bucks on a breeding farm located in the same area as the farms with the 4 previously sampled BTV-n–positive herds. Of the 56 sampled bucks, 51 were BTV-n positive by the BTV group–specific RT-qPCR (C_t value range 27.7–37.8). No buck was BTV-1 positive by the RT-qPCR, but 43 were positive by the BTV-n RT-qPCR; for the other 8 bucks, C_t values were beyond the positive range. Many of the bucks had not been vaccinated against BTV and showed no clinical signs of infection.

Conclusions

We report the detection and identification of a new BTV, BTV-n, that is circulating among goats on Corsica. BLAST analysis of the BTV-n RNA segment 2 suggests that this virus most likely belongs to the BTV serogroup. However, full-genome segment 2 sequence identity between BTV-n and its closest BTV relative, BTV-25, was low (73.0% homologous); thus, BTV-n may be a novel serotype.

Some criteria for defining serotype/nucleotype have been defined by Maan et al. (*6*) and Hofmann et al. (*7*). Comparison of the segment 2 nucleotide sequences of the 26 BTV serotypes enabled definition of 12 nucleotypes; members of the same segment 2 nucleotype are characterized by at least 66.9% identity in their segment 2 nucleotide sequences (*7*). Our findings show that BTV-n shares 73.0% identity with the full genome segment 2 sequence of

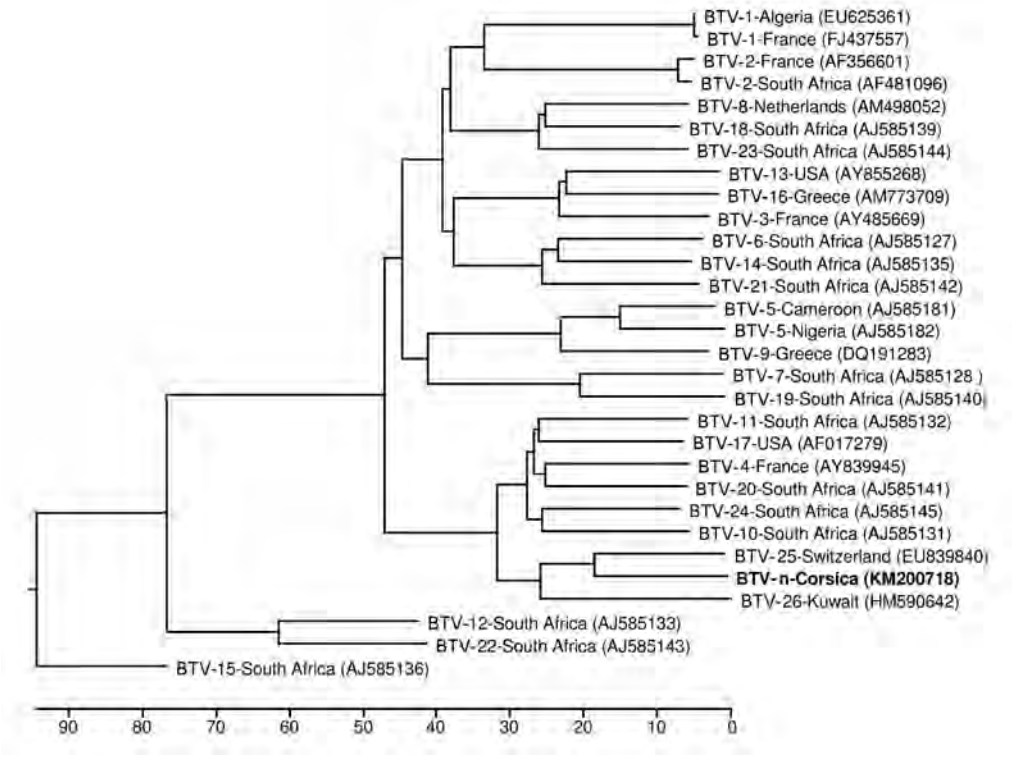

Figure. Phylogenetic tree of segment 2, showing relationships between BTV-n (boldface) and other BTV strains available in GenBank (accession nos. are shown in parentheses). Scale bar represents the percentage of nucleotide substitutions. BTV, bluetongue virus.

BTV-25. According to criteria defined by Maan et al. (*6*), BTV-n cannot be considered a new nucleotype and seems to belong to the BTV-25 nucleotype. Maan et al. (*8*) also showed that the differences in segment 2 sequences correspond to differences in serotypes. They reported overall interserotype variations in segment 2 of 29.0% (BTV-8 and BTV-18) to 59.0% (BTV-16 and BTV-22); the deduced amino acid sequence of VP2 varied from 22.4% (BTV-4 and BTV-20) to 73.0% (BTV-6 and BTV-22) (*8*). However, unlike BTV-25, BTV-n can grow in BSR cells (*7*,9).

Like BTV-25 (*9*) and BTV-26 strains, BTV-n has been detected in goats without clinical signs and symptoms of infection. All of the samples positive for BTV-n by RT-qPCR were from healthy bucks, and most BTV samples from clinically affected goats were negative for BTV group by RT-qPCR. Thus, it is also likely that BTV-n is not pathogenic for goats.

We suggest, on the basis of the following findings, that the newly detected BTV-n strain could be a new serotype: the differences between BTV-n sequences and other BTV sequences were as high as those described by Maan et al. (*8*); BTV-n is genetically diverse from other BTVs; BTV-n could not be amplified by the BTV-25–specific RT-PCR; anti–BTV-25 serum could not neutralize BTV-n; and, unlike BTV-25, BTV-n can be cultivated on BSR cells (*7*,*10*). No information is available about the origin of this new BTV strain; more in-depth investigation is needed to determine when and how the virus arrived in Corsica. Additional genome sequencing and experiments in various ruminant species are planned. These studies will help characterize this new BTV strain and evaluate the duration of viremia, humoral immune response, and pathogenicity of this serotype.

Acknowledgments

We thank veterinarians in Corsica and the French veterinary services and departmental laboratories in Bastia and Ajaccio, Corsica, for sending samples and the diagnostic department of the Institute of Virology and Immunology, Mittelhausern, Switzerland, for the BTV-25 antiserum.

This work was supported by Agence Nationale de Sécurité Sanitaire, Friedrich Loeffler Institute, and the EMIDA ERA-Net Project "Orbinet" (BMBF FKZ031 5858).

Dr Zientara is a research scientist at the Animal Health Laboratory, Agence Nationale de Sécurité Sanitaire. His research focuses on viral emerging diseases in Europe, such as orbiviruses and orthobunyaviruses.

References

1. Verwoerd D, Erasmus BJ. Bluetongue. In : Coetzer JAW, Tustin RC, editors. Infectious diseases of livestock. 2nd ed. Cape Town (South Africa): Oxford University Press; 2004. p. 1201–20.
2. Maan S, Maan NS, Nomikou K, Veronesi E, Bachanek-Bankowska K, Belaganahalli MN, et al. Complete genome characterisation of a novel 26th bluetongue virus serotype from Kuwait. PLoS ONE. 2011;6:e26147. http://dx.doi.org/10.1371/journal.pone.0026147
3. Zientara S, Sailleau C, Dauphin G, Roquier C, Rémond EM, Lebreton F, et al. Identification of bluetongue virus serotype 2 (Corsican strain) by reverse-transcriptase PCR reaction analysis of segment 2 of the genome. Vet Rec. 2002;150:598–601. http://dx.doi.org/10.1136/vr.150.19.598
4. Zientara S, MacLachlan NJ, Calistri P, Sanchez-Vizcaino JM, Savini G. Bluetongue vaccination in Europe. Expert Rev Vaccines. 2010;9:989–91. http://dx.doi.org/10.1586/erv.10.97
5. Sailleau C,, Viarouge C, Bréard E, Perrin JB, Doceul V, Vitour D, Zientara S. Emergence of bluetongue virus serotype 1 in French Corsica Island in September 2013 [cited 2014 Jul 18]. Transboundary and Emerging Dis. Epub ahead of print 2014Jan 24.
6. Maan S, Maan NS, Nomikou K, Batten C, Antony F, Belaganahalli MN, et al. Novel bluetongue virus serotype from Kuwait. Emerg Infect Dis. 2011;17:886–9. http://dx.doi.org/10.3201/eid1705.101742
7. Hofmann MA, Renzullo S, Mader M, Chaignat V, Worwa G, Thuer B. Genetic characterization of Toggenburg orbivirus, a new bluetongue virus, from goats, Switzerland. Emerg Infect Dis. 2008;14:1855–61. http://dx.doi.org/10.3201/eid1412.080818
8. Maan S, Maan NS, Samuel AR, Rao S, Attoui H, Mertens PP. Analysis and phylogenetic comparisons of full-length VP2 genes of the 24 bluetongue virus serotypes. J Gen Virol. 2007;88:621–30. http://dx.doi.org/10.1099/vir.0.82456-0
9. Hofmann MA, Renzullo S, Planzer J, Mader M, Chaignat V, Thuer B. Detection of Toggenburg orbivirus by a segment 2–specific quantitative RT-PCR. J Virol Methods. 2010;165:325–9. http://dx.doi.org/10.1016/j.jviromet.2010.02.027
10. Planzer J, Kaufmann C, Worwa G, Gavier-Widen D, Hofmann MA, Chaignat V, et al. In vivo and in vitro propagation and transmission of Toggenburg orbivirus. Res Vet Sci. 2011;91:e163–8. http://dx.doi.org/10.1016/j.rvsc.2011.03.007

Address for correspondence: Stéphan Zientara, UPE, ANSES Maisons-Alfort–UMR ANSES/INRA/ENVA, 23 Ave du Génral de Gaulle, Maisons-Alfort 94703, France; email: szientara@vet-alfort.fr

Prevalence of SFTSV among Asian House Shrews and Rodents, China, January–August 2013

Jian-Wei Liu,[1] Hong-Ling Wen,[1] Li-Zhu Fang, Zhen-Tang Zhang, Shu-Ting He, Zai-Feng Xue, Dong-Qiang Ma, Xiao-Shuang Zhang, Tao Wang, Hao Yu, Yan Zhang, Li Zhao, and Xue-jie Yu

To evaluate the role of small mammals as hosts of severe fever with thrombocytopenia syndrome virus (SFTSV), we tested serum samples from rodents and shrews in China, collected in 2013. SFTSV antibodies and RNA were detected, suggesting that rodents and shrews might be hosts for SFTSV.

Severe fever with thrombocytopenia syndrome (SFTS) is an emerging hemorrhagic fever caused by SFTS virus (SFTSV), a recently discovered phlebovirus in the family *Bunyaviridae* (*1*). SFTS has been reported in humans in China, South Korea, and Japan since 2010 (*1*–*3*). During 2011–2012, an outbreak with 2,047 reported SFTS cases occurred in China (*4*). The disease has a high case-fatality rate (12%–30%) (*1*).

SFTSV has been detected in *Haemaphysalis longicornis* ticks, the probable source of transmission to humans (*1*), and person-to-person transmission of SFTSV through contact with an infected person's blood or mucus has been reported (*5*,*6*). SFTSV has been detected in domestic animals, including goats, cattle, dogs, and chickens (*7*–*10*). Small mammals, such as rodents and shrews, are the major hosts of *H. longicornis* tick larvae and nymphs (*11*); however, the role of small mammals as hosts of SFTSV is not well defined. In this study, we determined the seroprevalence of SFTSV and the prevalence of SFTSV viral RNA among rodents and shrews captured in rural areas of eastern China.

Authors affiliations: School of Public Health, Shandong University, Jinan, China (J.-W. Liu, H.-L. Wen, L.-Z. Fang, S.-T. He, X.-S. Zhang, L. Zhao, X.-j. Yu); Huangdao District Center for Disease Control and Prevention, Qingdao City, China (Z.-T. Zhang, Z.-F. Xue, D.-Q. Ma); Zibo Municipal Center for Disease Control and Prevention, Zibo, China (T. Wang); University of Texas Medical Branch, Galveston, Texas, USA (H. Yu, X-j. Yu); and College of Medicine and Nursing, Dezhou University, Dezhou City, China (Y. Zhang)

DOI: http://dx.doi.org/10.3201/eid2012.141013

The Study

During January–August 2013, we collected rodents and shrews in Jiaonan County, Shandong Province, China (119°30′–120°30′E, 35°35′–36°08′ N). The animals were trapped once a month by using mouse traps baited with peanuts; a different trap site was used each month. The traps were set before sunset outside human dwellings in rural areas and collected the next morning. We classified the rodents and shrews according to appearance (hair color) and body structures (i.e., shape of mouth, teeth, tail, ratio of tail length to body length, cheek pouch). After the animals were euthanized, we collected blood samples from their hearts onto absorbent paper strips (10 mm × 30 mm). Spleens were collected aseptically and frozen at –80°C. Animal use and sample collection protocols were approved by the bioethics committee of the School of Public Health, Shandong University.

Before testing the serum samples for the presence of SFTSV, we evaluated the sensitivity and specificity of a double-antigen sandwich ELISA kit (Wuxi Xnlianxin Biotech Co, Wuxi City, China) for detecting SFTSV in rodent serum. To do this, we used an indirect immunofluorescence assay (IFA) as a standard to test rodent serum samples for SFTSV and compared the results with those from the ELISA. A total of 68 Kunming albino mice (Shandong University Experimental Animal Center, Jinan, China) were used for the tests: 36 were injected with SFTSV, and 32 (controls) were injected intraperitoneally with saline solution. On days 7, 12, 17, and 21 after injection, 9 infected and 8 control mice were euthanized, and serum samples from the mice were tested for SFTSV antibody by IFA and ELISA. Of the 36 serum samples from the SFTSV-inoculated mice, 33 were positive for SFTSV by IFA and ELISA and 3 were positive by IFA only. All 32 serum samples from the control mice were negative for SFTSV by IFA and ELISA. Thus, under these laboratory conditions and compared with the IFA, the ELISA had a sensitivity of 91.7% and specificity of 100%, suggesting that the ELISA could be used to test serum samples from the field-collected rodents. Kits for shrews were not commercially available in China, so we were unable to test the sensitivity and specificity of the ELISA for detecting SFTSV in serum from shrews.

We collected 89 Asian house shrews (*Suncus murinus*) and 666 rodents in the field during January–August 2013. The rodents included 186 striped field mice (*Apodemus agrarius*), 182 house mice (*Mus musculus*), 156 brown rats (*Rattus norvegicus*), 125 greater long-tailed hamsters

[1]These authors contributed equally to this article.

(*Cricetulus tyiton*), and 17 Chinese hamsters (*Cricetulus barabensis*). Serum samples from the rodents and shrews were tested for IgG and IgM to SFTSV by using the ELISA as described previously (*8–10*). Serum samples on absorbent paper were each reconstituted by adding 150 mL of phosphate-buffered saline, and 75 mL of each sample was added to a well of the ELISA plate.

ELISA results showed that SFTSV seroprevalence was higher among Asian house shrews (4.5%, 4/89) than among rodents (0.9%, 6/666) (p = 0.014). Among the rodents, SFTSV seropositivity was higher in house mice (1.1%, 2/182) and striped field mice (1.1%, 2/186) than in other rodent species (Table). However, the seropositivity rate was not significantly different among the rodent species (p = 0.691). In addition, the seropositivity rate did not differ significantly by month (p = 0.411). Statistical analyses were performed by using the Fisher exact test.

Total RNA was extracted from homogenized animal spleens by using the RNeasy Mini Kit (QIAGEN, Hilden, Germany), which was used as a template for SFTSV amplification performed by using the Access RT-PCR System (Promega, Madison, WI, USA). Primers for reverse transcription PCR (RT-PCR) were designed from the M segments of the SFTSV genome. Outside PCR primers were 5′-TCTGCAGTTCAGACTCAGGGA-3′ and 5′-GACGTGTATTGCTGTTTTCCC-3′; nested PCR primers were 5′-TGTTGCTTGTCAGCCTATGAC-3′ and 5′-CAACCAATGATCCTGAGTGGA-3′. The PCR products (674 bp) were cloned and sequenced for both strands at least 3 times. Amplification results showed that the SFTSV positivity rate was higher among shrews (2.6%, 2/77) than among rodents (0.7%, 3/440), but the difference was not significant (p = 0.162) (Table). The PCR positivity rate differed by month: the rate was 4.7% (4/86) for animals trapped in March, 1.6% (1/62) for animals trapped in June, and 0 for animals collected during the other 6 months (p = 0.043).

Phylogenetic analysis indicated that the SFTSV sequences from the rodents and shrews were closely related to each other (98.5%– 99.7% homology) and highly homologous (95.3% to 99.7%) to the corresponding sequences of SFTSV from a human (GenBank accession no. KC505127), a dog (GenBank accession no. JF267784), and ticks (GenBank accession nos. KC473541 and JQ684872) (Figure). DNA sequences were deposited in GenBank (accession nos. KF770995–9).

Conclusions

Two previous studies demonstrated that rodents in China were seronegative for SFTSV (*7*,*12*). However, negative results might have been caused by small sample sizes or by using rodents that were collected from sites where SFTSV was not endemic. The serologic and RT-PCR results in our study show that rodents and shrews in eastern China are seropositive for SFTSV. These findings suggest that these animals are potential hosts for SFTSV. We also attempted to amplify S segments of the genomes of SFTSV isolates, but results were positive for only 1 animal. It is possible that in our study, the primer for the S segment was not as sensitive as that for the M segment.

Most animal species that have been investigated for the presence of SFTSV have been positive for the virus, including rodents, shrews, goats, cattle, dogs, and chickens (*5*,*8–10*). Thus, there may be numerous animal hosts for SFTSV. Goats have usually shown high seroprevalence to SFTSV but very low virus loads and short periods of SFTSV viremia (*9*). Rodents experimentally infected with SFTSV usually have long periods of viremia and high virus loads in the blood (*13*,*14*).

Cross-sectional analysis indicated that the SFTSV infection rate among rodents and shrews did not differ substantially by month during the 8-month study period, but the PCR positivity rate was highest for animals collected during March. The variation between months can probably be explained by the fact that the animals were collected from different sites each month; the rates of infection among animals at the different sites may have differed.

In conclusion, our findings show that the Asian house shrew and different varieties of rodents are potential animal hosts of SFTSV. Further studies are needed to determine which of the many animal hosts of SFTSV can most effectively transmit the virus to ticks, the probable vector of SFTSV transmission to humans.

Acknowledgments

We are grateful to the Huangdao District Center for Disease Control and Prevention, Qingdao City, China, for organizing the fieldwork to trap rodents.

Table. Severe fever with thrombocytopenia syndrome virus seroprevalence rate and PCR positivity rate among rodents and shrews, Jiaonan County, Shandong Province, China, January–August 2013

Animal	No. seropositive/no. total (%)	No. PCR positive/no. total (%)
Mus musculus mice	2/182 (1.1)	1/103 (1.0)
Rattus norvegicus rats	0/156	1/116 (0.9)
Cricetulus tyiton hamsters	1/125 (0.8)	1/83 (1.2)
Apodemus agrarius mice	2/186 (1.1)	0/129
Cricetulus barabensis hamsters	0/17	0/9
Suncus murinus shrews	4/89 (4.5)	2/77 (2.6)
Total	9/755 (1.2)	5/517 (1.0)

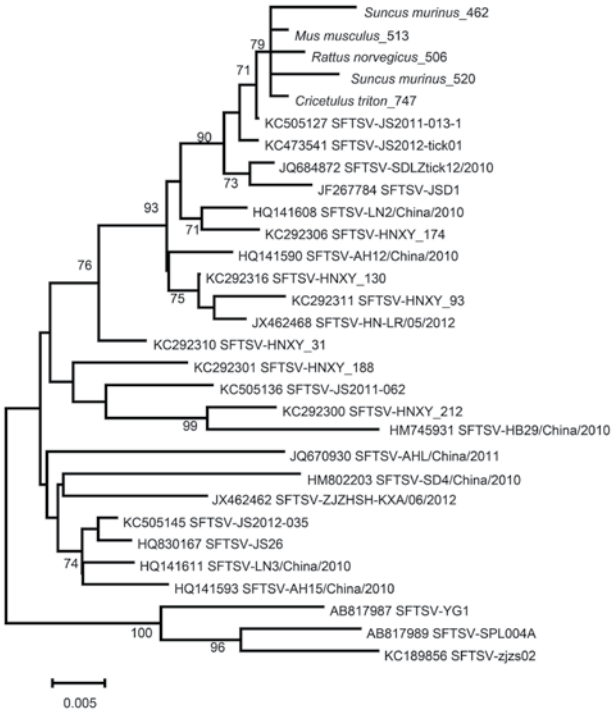

Figure. Phylogenetic analysis of severe fever with thrombocytopenia syndrome virus (SFTSV) amplified from the spleens of Asian house shrew and rodents. The neighbor-joining phylogenetic tree was constructed by using MEGA 5.2 software(http://www.megasoftware.net/).GenBank accession numbers precede isolate names on the right side of the figure. Numbers at nodes represent bootstrap values. Scale bar represents nucleotide substitutions per site.

This study was supported by Shandong University and a pilot grant from the Institute for Human Infections and Immunity, University of Texas Medical Branch (to X.-j.Y).

Mr Liu is a PhD student in the School of Public Health, Shandong University, Jinan, China. His research interests include epidemiology and mechanism of the pathogenesis of bunyaviruses.

References

1. Yu XJ, Liang MF, Zhang SY, Liu Y, Li JD, Sun YL, et al. Fever with thrombocytopenia associated with a novel bunyavirus in China. N Engl J Med. 2011;364:1523–32. http://dx.doi.org/10.1056/NEJMoa1010095
2. Kim KH, Yi J, Kim G, Choi SJ, Jun KI, Kim NH, et al. Severe fever with thrombocytopenia syndrome, South Korea, 2012. Emerg Infect Dis. 2013;19:1892–4. http://dx.doi.org/10.3201/eid1911.130792
3. Takahashi T, Maeda K, Suzuki T, Ishido A, Shigeoka T, Tominaga T, et al. The first identification and retrospective study of severe fever with thrombocytopenia syndrome in Japan. J Infect Dis. 2014;209:816–27. http://dx.doi.org/10.1093/infdis/jit603
4. Ding F, Zhang W, Wang L, Hu W, Soares Magalhaes RJ, Sun H, et al. Epidemiologic features of severe fever with thrombocytopenia syndrome in China, 2011–2012. Clin Infect Dis. 2013;56:1682–3. http://dx.doi.org/10.1093/cid/cit100
5. Bao CJ, Guo XL, Qi X, Hu JL, Zhou MH, Varma JK, et al. A family cluster of infections by a newly recognized bunyavirus in eastern China, 2007: further evidence of person-to-person transmission. Clin Infect Dis. 2011;53:1208–14. http://dx.doi.org/10.1093/cid/cir732
6. Liu Y, Li Q, Hu W, Wu J, Wang Y, Mei L, et al. Person-to-person transmission of severe fever with thrombocytopenia syndrome virus. Vector Borne Zoonotic Dis. 2012;12:156–60. http://dx.doi.org/10.1089/vbz.2011.0758
7. Cui F, Cao HX, Wang L, Zhang SF, Ding SJ, Yu XJ, et al. Clinical and epidemiological study on severe fever with thrombocytopenia syndrome in Yiyuan County, Shandong Province, China. Am J Trop Med Hyg. 2013;88:510–2. http://dx.doi.org/10.4269/ajtmh.11-0760
8. Jiao Y, Zeng X, Guo X, Qi X, Zhang X, Shi Z, et al. Preparation and evaluation of recombinant severe fever with thrombocytopenia syndrome virus nucleocapsid protein for detection of total antibodies in human and animal sera by double-antigen sandwich enzyme-linked immunosorbent assay. J Clin Microbiol. 2012;50:372–7. http://dx.doi.org/10.1128/JCM.01319-11
9. Niu G, Li J, Liang M, Jiang X, Jiang M, Yin H, et al. Severe fever with thrombocytopenia syndrome virus among domesticated animals, China. Emerg Infect Dis. 2013;19:756–63.
10. Zhao L, Zhai S, Wen H, Cui F, Chi Y, Wang L, et al. Severe fever with thrombocytopenia syndrome virus, Shandong Province, China. Emerg Infect Dis. 2012;18:963–5. http://dx.doi.org/10.3201/eid1806.111345
11. Tenquist JD, Charleston WAG. A revision of the annotated checklist of ectoparasites of terrestrial mammals in New Zealand. J R Soc N Z. 2001;31:481–542. http://dx.doi.org/10.1080/03014223.2001.9517666
12. Lu YN, Dou XF, Wang XM, Tian LL, Yang YS, Wang HY, et al. Preliminary investigation on the carriage status of the novel bunyavirus among animals and ticks in Beijing area. Int J Virol. 2011;18:33–6.
13. Jin C, Liang M, Ning J, Gu W, Jiang H, Wu W, et al. Pathogenesis of emerging severe fever with thrombocytopenia syndrome virus in C57/BL6 mouse model. Proc Natl Acad Sci U S A. 2012;109:10053–8. http://dx.doi.org/10.1073/pnas.1120246109
14. Liu Y, Wu B, Paessler S, Walker DH, Tesh RB, Yu XJ. The pathogenesis of severe fever with thrombocytopenia syndrome virus infection in alpha/beta interferon knockout mice: insights into the pathologic mechanisms of a new viral hemorrhagic fever. J Virol. 2014;88:1781–6. http://dx.doi.org/10.1128/JVI.02277-13

Address for correspondence: Li Zhao, Department of Laboratory Microbiology, School of Public Health, Shandong University, Jinan, Shandong Province 250012, China; email: dlzhl@sdu.edu.cn; Xue-jie Yu, Department of Pathology, University of Texas Medical Branch, 301 Univ. Blvd. Galveston, TX, 77555-0609, USA; email: xuyu@utmb.edu

Evaluation of Commercially Available Serologic Diagnostic Tests for Chikungunya Virus

Christine M. Prat, Olivier Flusin, Amanda Panella, Bernard Tenebray, Robert Lanciotti, and Isabelle Leparc-Goffart

Chikungunya virus (CHIKV) is present or emerging in dengue virus–endemic areas. Infections caused by these viruses share some common signs/symptoms, but prognosis, patient care, and persistent symptoms differ. Thus, accurate diagnostic methods are essential for differentiating the infections. We evaluated 4 CHIKV serologic diagnostic tests, 2 of which showed poor sensitivity and specificity.

Disease caused by chikungunya virus (CHIKV), a mosquitoborne arbovirus (family *Togaviridae* family, genus *Alphavirus*), is clinically characterized by sudden-onset fever and severe arthralgia, which may persist for weeks, months, or years after the acute phase of the infection (*1*). Other symptoms of CHIKV infection (headache, fatigue, and rash) are common among many arboviral infections, including dengue.

CHIKV is endemic to some parts of Africa and causes recurrent epidemic waves in Asia and the Indian subcontinent. In 2005, CHIKV emerged in the Indian Ocean region (*2*), and at the end of 2013, the virus emerged in the Americas. The latter emergence occurred on St. Martin Island in the Caribbean, where autochthonous cases were confirmed in early December 2013; thereafter, the virus rapidly expanded to neighboring islands and territories (*3*). *Aedes aegypti* and *Ae. albopictus* mosquitoes, the vectors of CHIKV and dengue virus (DENV), are established in tropical and temperate regions of the world. The vulnerability of Europe to transmission of CHIKV and other arboviruses has been shown: autochthonous cases of CHIKV infection occurred in Italy in 2007 (*4*) and in France in 2010 (*5*), and cases of autochthonous dengue occurred in France in 2010 and 2013 (*6*,*7*).

Author affiliations: French Armed Forces Biomedical Research Institute (IRBA), Marseille, France (C.M. Prat, O. Flusin, B. Tenebray, I. Leparc-Goffart); and Centers for Disease Control and Prevention, Fort Collins, Colorado, USA (A. Panella, R. Lanciotti)

DOI: http://dx.doi.org/10.3201/eid2012.141269

The rate of CHIKV and DENV co-infections during the recent epidemic of CHIKV infections on St. Martin was 2.8% (*8*). It can be challenging to differentiate clinically between CHIKV and DENV infections, but it is crucial to do so because prognosis and patient care differ for these diseases.

The increasing threat of CHIKV emergence in temperate regions and the need to anticipate possible outbreaks of CHIKV infection are presenting a challenge to the current level of diagnostic preparedness. In France, a National Public Health plan for stopping the spread of CHIKV and DENV has been developed. The plan calls for detecting possible infections by obtaining clinical samples from patients with suspected cases and using vector control measures if needed. The diagnostic strategy (*9*) is twofold: for serum collected 1–7 days after the onset of symptoms, real-time PCR is used to detect viral genome; and for serum collected >5 days after onset of symptoms, serologic techniques are used to detect IgM and/or IgG responses to the virus. Real-time PCR testing can differentiate between DENV and CHIKV infections; however, a certain proportion of infected persons seek medical care at a time when real-time PCR is no longer effective for diagnosis. Thus, we evaluated commercially available serologic test kits that could be used widely.

One serologic testing method is the indirect fluorescent antibody (IFA) technique. Although IFA tests have good sensitivity and specificity (*10*) for CHIKV, this method requires specific material that may not be available in diagnostic laboratories worldwide. Furthermore, a previous study showed variability in IFA results between laboratories (*11*). Thus, we focused our analysis on 2 other serologic CHIKV detection methods: ELISA and immunochromatography test for rapid detection (RDT).

The Study

We evaluated 4 commercially available serologic tests that are approved for CHIKV testing by the European Commission. Two of the tests were RDTs for CHIKV IgM: SD Bioline Chikungunya IgM (Standard Diagnostics Inc., Yongin-si, South Korea) and *OnSite* Chikungunya IgM Combo Rapid Test (CTK Biotech Inc., San Diego, CA, USA). The 2 other tests were ELISAs for the detection of CHIKV IgM and IgG: Chikungunya IgM m-capture ELISA and Chikungunya IgG Capture ELISA (both from IBL International, Hamburg, Germany) and Anti-Chikungunya Virus ELISA IgM test and Anti-Chikungunya Virus ELISA IgG test (Euroimmun, Lübeck, Germany).

We obtained 2 sets of serum samples for testing: panel A (23 samples) and panel B (30 samples). The samples had been submitted to the French Armed Forces Biomedical Research Institute (IRBA; Marseille, France) for arbovirus testing during 2005–2014. We chose the serum samples on

the basis of their reactivity against CHIKV and other genetically or clinically related arboviruses.

Panel A was characterized in the laboratories of 2 National Reference Centers for Arboviruses by using in-house ELISAs as previously described (*12*,*13*) and a neutralization test (*14*). One reference laboratory was at IRBA and the other was at the Centers for Disease Control and Prevention (Fort Collins, CO, USA). Both laboratories used an ELISA positivity threshold that was 3 times the reactivity of a negative control serum against viral antigens. Results from the 2 laboratories were 100% concordant (Tables 1, 2).

Panel B was tested by using in-house techniques at IRBA. Because sample volumes were limited, we used panel A to test the commercial kits and used panel B only if the specificity and sensitivity of tests on panel A were >70%. Commercial tests were performed according to manufacturers' protocols.

We used SD Bioline and CTK Biotech RDTs to process panel A samples plus serum samples (1 each) infected with Mayaro virus and o'nyong-nyong virus (Tables 1, 2). Neither Mayaro virus nor o'nyong-nyong virus was detected by the RDTs. The SD Bioline RDT showed poor sensitivity (30%) and specificity (73%) for CHIKV in panel A samples, and 39% and 57% of the results were false negative and false positive, respectively. The CTK kit showed 93% specificity and 20% sensitivity for CHIKV in panel A samples, and 36% and 33% of the results were false negative and false positive, respectively. The

Table 1. Results of serologic diagnostic testing of 23 serum samples (panel A) in a study evaluating the accuracy of commercially available CHIKV test kits*

	In-house ELISA					Commercially available RDT		Commercially available ELISA			
	IRBA†		CDC‡		In-house CHIKV neutralization,	SD Bioline Chikungunya	OnSite Chikungunya IgM Combo	Chikungunya IgM/IgG Capture**		Anti-Chikungunya Virus ELISA IgM/IgG††	
Virus tested, sample no.	IgM	IgG	IgM	IgG	IRBA and CDC§	IgM¶	Rapid Test#	IgM	IgG	IgM	IgG
CHIKV											
IgG											
1	–	+	–	+	5,120	+	–	–	+	–	–
2	–	+	–	+	1,280	–	–	–	–	–	+
3	–	+	–	+	>320	+	+	–	+	+	+
IgM + IgG											
4	+	+	+	+	320	–	–	+	+	+	+
5	+	+	+	+	40	–	–	+	+	+	–
6	+	+	+	+	2,560	+	–	+	+	+	+
7	+	+	+	+	1,280	–	+	+	+	NA	NA
8	+	+	+	+	640	+	+	+	+	+	+
9	+	+	+	+	320	+	–	+	–	+	+
10	+	+	+	+	80	–	–	+	–	+	+
IgM											
11	+	–	+	–	<10	–	–	+	–	+	–
12	+	–	+	–	<10	–	–	+	–	+	–
13	+	–	+	–	80	–	–	+	–	+	–
DENV											
IgM + IgG											
14	–	–	–	–	<10	–	–	–	–	–	–
15	–	–	–	–	<10	–	–	–	–	–	–
Negative samples‡‡											
16	–	–	–	–	<10	–	–	–	–	–	–
17	–	–	–	–	<10	+	–	–	–	–	–
18	–	–	–	–	<10	–	–	-	–	–	–
19	–	–	–	–	<10	+	–	+	–	–	–
20	–	–	–	–	<10	–	–	+	–	+	NA
21	–	–	–	–	<10	–	–	–	–	–	–
22	–	–	–	–	<10	–	–	–	–	–	–
23	–	–	–	–	<10	–	–	–	–	–	–

*The serum samples were obtained from IRBA (Marseille, France). CDC, Centers for Disease Control and Prevention; CHIKV, chikungunya virus; DENV, dengue virus; IRBA, French Armed Forces Biomedical Research Institute; NA, not applicable; RDT, immunochromatography test for rapid detection.
†National Reference Center for Arboviruses at IRBA.
‡National Reference Center for Arboviruses at CDC (Fort Collins, CO, USA).
§Data are CHIKV neutralization titers of serum.
¶From Standard Diagnostics Inc., Yongin-si, South Korea.
#From CTK Biotech Inc., San Diego, CA, USA.
**From IBL International, Hamburg, Germany.
††From Euroimmun, Lübeck, Germany.
‡‡Depending on the patient's recent travel history, these samples were tested for various other viruses. Test results were negative for following arboviruses: DENV, CHIKV, West Nile virus, Toscana virus, Japanese encephalitis virus, Rift Valley fever virus, St. Louis encephalitis virus, Mayaro virus.

Table 2. Results of serologic diagnostic testing of 23 serum samples (panel B) in a study evaluating the accuracy of commercially available CHIKV test kits*

Virus tested, sample no.	In-house ELISA				In-house CHIKV neutralization, IRBA and CDC§	Commercially available RDT		Commercially available ELISA			
	IRBA†		CDC‡			SD Bioline Chikungunya IgM	OnSite Chikungunya IgM Combo Rapid Test#	Chikungunya IgM/IgG Capture**		Anti-Chikungunya Virus ELISA IgM/IgG††	
	IgM	IgG	IgM	IgG				IgM	IgG	IgM	IgG
CHIKV											
IgG											
24	–	+	NA	NA	NA	NA	NA	–	–	+	+
25	–	+	NA	NA	NA	NA	NA	–	–	+	+
26	–	+	NA	NA	NA	NA	NA	–	–	–	+
27	–	+	NA	NA	NA	NA	NA	–	–	–	+
28	–	+	NA	NA	NA	NA	NA	–	–	–	+
29	–	+	NA	NA	NA	NA	NA	–	+	–	+
IgM + IgG											
30	+	+	NA	NA	NA	NA	NA	+	+	NA	NA
31	+	+	NA	NA	NA	NA	NA	+	+	+	+
32	+	+	NA	NA	NA	NA	NA	+	+	+	+
33	+	+	NA	NA	NA	NA	NA	–	–	+	+
34	+	+	NA	NA	NA	NA	NA	+	–	+	+
35	+	+	NA	NA	NA	NA	NA	+	–	+	+
36	+	+	NA	NA	NA	NA	NA	–	–	–	+
37	+	+	NA	NA	NA	NA	NA	+	+	+	–
38	+	+	NA	NA	NA	NA	NA	+	–	+	+
39	+	+	NA	NA	NA	NA	NA	+	+	+	+
40	+	+	NA	NA	NA	NA	NA	+	+	+	NA
41	+	+	NA	NA	NA	NA	NA	+	+	+	+
IgM											
42	+	–	NA	NA	NA	NA	NA	+	–	+	NA
43	+	–	NA	NA	NA	NA	NA	–	–	–	–
44	+	–	NA	NA	NA	NA	NA	–	–	+	–
45	+	–	NA	NA	NA	NA	NA	+	–	+	–
46	+	–	NA	NA	NA	NA	NA	–	–	–	–
47	+	–	NA	NA	NA	NA	NA	–	–	–	–
DENV											
IgM + IgG											
48	–	–	NA	NA	NA	NA	NA	–	–	–	–
49	–	–	NA	NA	NA	NA	NA	–	–	–	–
50	–	–	NA	NA	NA	NA	NA	–	–	–	+
RVRV‡‡											
IgG, 51	–	+	NA	NA	<10	NA	NA	–	–	NA	NA
MAYV‡‡											
IgM + IgG, 52	–	+	NA	NA	<10	–	–	–	–	–	+
ONNV‡‡											
IgM + IgG, 53	+	+	NA	NA	<10	–	–	+	+	+	+

*The serum samples were obtained from IRBA (Marseille, France). CDC, Centers for Disease Control and Prevention; CHIKV, chikungunya virus; DENV, dengue virus; IRBA, French Armed Forces Biomedical Research Institute; MAYV, Mayaro virus; NA, not applicable; ONNV o'nyong-nyong virus; RDT, immunochromatography test for rapid detection; RVRV, Rift Valley fever virus.
†National Reference Center for Arboviruses at IRBA.
‡National Reference Center for Arboviruses at CDC (Fort Collins, CO, USA).
§Data are CHIKV neutralization titers of serum.
¶From Standard Diagnostics Inc., Yongin-si, South Korea.
#From CTK Biotech Inc., San Diego, CA, USA.
**From IBL International,Hamburg, Germany.
††From Euroimmun, Lübeck, Germany.
‡‡These samples were characterized by neutralization techniques against 4 viruses in parallel: RRV, MAYV, ONNV, and CHIKV.

ineffectiveness of the RDT kits was demonstrated by panel A test results, so panel B was not tested.

Commercially Available IgM and IgG ELISAs

We used chikungunya IgM/IgG ELISAs from Euroimmun and IBL International (Tables 1, 2) to process panel A samples plus serum samples (1 each) infected with Mayaro virus and o'nyong-nyong virus. The specificity and sensitivity of the ELISAs for this set of samples were >70%, so we also tested panel B.

ELISAs from both companies detected o'nyong-nyong virus IgM and IgG. The Euroimmun ELISA detected Mayaro virus IgG but not IgM; the IBL International ELISA did not detect Mayaro virus IgG or IgM. This cross-reactivity

highlights the fact that seroneutralization is necessary to differentiate between viruses in the same serogroup. The IBL ELISA had a specificity of 88% (IgM) and 96% (IgG) and a sensitivity of 79% (IgM) and 52% (IgG). For IgM detection, 12% of the IBL ELISA results were false positive and 21% were false negative. The Euroimmun ELISA had a specificity of 82% (IgM) and 95% (IgG) and a sensitivity of 85% (IgM) and 88% (IgG). For IgM detection, 18% of the Euroimmun ELISA results were false positive and 15% were false negative.

Conclusions

In our evaluation, the commercial RDTs that we compared with in-house ELISAs from 2 National Reference Centers for Arboviruses performed poorly. A previous evaluation study that used the same RDTs to process serum samples from residents of Indonesia had results in the same range as our results (*15*); together, these findings show that the kits should not be used in clinical settings, regardless of the geographic origin of the infection. The 2 ELISAs that we tested had better sensitivity and specificity than the RDTs; however, they had a non-negligible number of false-negative and false-positive results.

If the current outbreak of CHIKV infection in the Americas follows the same trend as that seen in the 2005 Réunion Island outbreak, increased circulation of the virus can be expected, and diagnostic laboratories must be prepared. A 2009 international evaluation of the diagnostic quality of 30 expert laboratories showed that most of the laboratories needed more sensitive CHIKV IgM detection assays; results for IgM were correct in only 50.7% of cases (*11*). Our evaluation was a pilot study using a small number of samples, but the findings show the importance of evaluating commercial diagnostic kits and published protocols before using such tools in clinical settings.

This work was financed by the French National Reference Center for Arboviruses.

Dr Prat is deputy director of the French National Reference Center for Arboviruses at IRBA. Her research interests include arboviruses epidemiology and viral infections of the brain.

References

1. Pialoux G, Gaüzère BA, Jauréguiberry S, Strobel M. Chikungunya, an epidemic arbovirosis. Lancet Infect Dis. 2007;7:319–27. http://dx.doi.org/10.1016/S1473-3099(07)70107-X
2. Staikowsky F, Talarmin F, Grivard P, Souab A, Schuffenecker I, Le Roux K, et al. Prospective study of chikungunya virus acute infection in the island of La Réunion during the 2005–2006 outbreak. PLoS ONE. 2009;4:e7603. http://dx.doi.org/10.1371/journal.pone.0007603
3. Van Bortel W, Dorleans F, Rosine J, Blateau A, Rousset D, Matheus S, et al. Chikungunya outbreak in the Caribbean region, December 2013 to March 2014, and the significance for Europe. Euro Surveill. 2014;19:20759.
4. Rezza G, Nicoletti L, Angelini R, Romi R, Finarelli AC, Panning M, et al. Infection with chikungunya virus in Italy: an outbreak in a temperate region. Lancet. 2007;370:1840–6. http://dx.doi.org/10.1016/S0140-6736(07)61779-6
5. Grandadam M, Caro V, Plumet S, Thiberge JM, Souarès Y, Failloux AB, et al. Chikungunya virus, southeastern France. Emerg Infect Dis. 2011;17:910–3. http://dx.doi.org/10.3201/eid1705.101873
6. La Ruche G, Souarès Y, Armengaud A, Peloux-Petiot F, Delaunay P, Desprès P, et al. First two autochthonous dengue virus infections in metropolitan France, September 2010. Euro Surveill. 2010;15:19676.
7. Marchand E, Prat C, Jeannin C, Lafont E, Bergmann T, Flusin O, et al. Autochthonous case of dengue in France, October 2013. Euro Surveill. 2013;18:20661.
8. Omarjee R, Prat C, Flusin O, Boucau S, Tenebray B, Merle O, et al. Importance of case definition to monitor ongoing outbreak of chikungunya virus on a background of actively circulating dengue virus, St Martin, December 2013 to January 2014. Euro Surveill. 2014;19:20753.
9. Paty MC, Six C, Charlet F, Heuzé G, Cochet A, Wiegandt A, et al. Large number of imported chikungunya cases in mainland France, 2014: a challenge for surveillance and response. Euro Surveill. 2014;19:20856.
10. Yap G, Pok KY, Lai YL, Hapuarachchi HC, Chow A, Leo YS, et al. Evaluation of chikungunya diagnostic assays: differences in sensitivity of serology assays in two independent outbreaks. PLoS Negl Trop Dis. 2010;4:e753. http://dx.doi.org/10.1371/journal.pntd.0000753
11. Niedrig M, Zeller H, Schuffenecker I, Drosten C, Emmerich P, Rumer L, et al. International diagnostic accuracy study for the serological detection of chikungunya virus infection. Clin Microbiol Infect. 2009;15:880–4. http://dx.doi.org/10.1111/j.1469-0691.2009.02851.x
12. Peyrefitte CN, Pastorino BA, Bessaud M, Gravier P, Tock F, Couissinier-Paris P, et al. Dengue type 3 virus, Saint Martin, 2003–2004. Emerg Infect Dis. 2005;11:757–61. http://dx.doi.org/10.3201/eid1105.040959
13. Martin DA, Muth DA, Brown T, Johnson AJ, Karabatsos N, Roehrig JT. Standardization of immunoglobulin M capture enzyme-linked immunosorbent assays for routine diagnosis of arboviral infections. J Clin Microbiol. 2000;38:1823–6.
14. Lindsey HS, Calisher CH, Mathews JH. Serum dilution neutralization test for California group virus identification and serology. J Clin Microbiol. 1976;4:503–10.
15. Kosasih H, Widjaja S, Surya E, Hadiwijaya SH, Butarbutar DP, Jaya UA, et al. Evaluation of two IgM rapid immunochromatographic tests during circulation of Asian lineage chikungunya virus. Southeast Asian J Trop Med Public Health. 2012;43:55–61.

Address for correspondence: Christine M. Prat, French National Reference Centre, Armed Forces Biomedical Research Institute, Tropical Medicine Research Team, Marseille, France; email: christine.prat.irba@gmail.com

Zoonotic *Bartonella* Species in Cardiac Valves of Healthy Coyotes, California, USA

Spencer P. Kehoe, Bruno B. Chomel, Matthew J. Stuckey, Rickie W. Kasten, Nandhakumar Balakrishnan, Benjamin N. Sacks, and Edward B. Breitschwerdt

We investigated whether *Bartonella* spp. could cause endocarditis in coyotes or localize to cardiac valves before lesions develop. *Bartonella* DNA was amplified more often from coyote cardiac valves than spleen. *Bartonella* infection apparently leads to cardiac valve tropism, which could cause endocarditis, an often lethal complication in mammals, including humans.

Bartonellae are vector-borne gram-negative, aerobic, intracellular bacteria with a tropism for erythrocytes and endothelial cells (*1*). These bacteria, many of which are zoonotic, infect a wide range of domestic and wild animal species, causing a spectrum of disease manifestations and pathologies (*2*). Bartonellae, especially *Bartonella vinsonii* subsp. *berkhoffii* (*B. v. berkhoffii*), cause valvular endocarditis, especially of the aortic valve in mammals, including humans, dogs, cats, and cattle (*1*,*3*). Fleas and possibly ticks can vector *B. v. berkhoffii* (*4*). *Bartonella* species, typically observed in 5- to 7-year-old mid-sized to large dogs, account for ≈28% of endocarditis in dogs (*3*,*5*). Bartonellae, including *B. v. berkhoffii*, account for ≈3% of human endocarditis cases (*1*,*6*). In dogs and humans, these bacteria appear to have a specific tropism for aortic and mitral valves (*1*). Similar to lesions that develop with *Coxiella burnetii* endocarditis (*7*), valvular vegetative lesions can result from chronic *Bartonella* infection.

In California, coyotes (*Canis latrans*) are a major reservoir for *B. v. berkhoffii* (*8*). Natural *Bartonella* reservoir hosts are often asymptomatic, but to our knowledge, the possible role of *Bartonella*-induced endocarditis in coyotes has never been investigated. We hypothesized that *B. v. berkhoffii* or other *Bartonella* species could cause endocarditis in coyotes. We also hypothesized that bartonellae might preferentially localize to the aortic and/or mitral valves before vegetative lesions develop. Hence, coyotes served as a naturally occurring epidemiologic and physiologic sentinel model for studying infection kinetics and pathology induced by this bacterium in a reservoir host (coyotes).

Author affiliations: University of California, Davis, Davis, California, USA (S.P. Kehoe, B.B. Chomel, M.J. Stuckey, R.W. Kasten, B.N.Sacks); and North Carolina State University, Raleigh, North Carolina, USA (N. Balakrishnan, E.B. Breitschwerdt)

DOI: http://dx.doi.org/10.3201/eid2012.140578

The Study

During the early 2000s, a total of 70 coyotes trapped in 9 northern California counties as part of a depredation control program were assessed for zoonotic heartworm (*Dirofilaria immitis*) disease (*9*). Coyote hearts and spleens were collected at that time and stored at –70°C in a manner to avoid DNA carryover during handling, storage, and processing. In 2012 and 2013, the hearts were dissected for macroscopic evidence of aortic and mitral valve vegetative endocarditis lesions. A board-certified veterinary pathologist examined possible valvular lesions or thickened regions; however, because the samples had been frozen, microscopic histopathologic examination was not conducted. We extracted DNA from aortic and mitral valves and spleens using DNeasy Blood and Tissue Kits (QIAGEN, Hilden, Germany). *B. v. berkhoffii*–spiked rabbit blood was the DNA extraction positive control. We tested extracted samples by PCR for *Bartonella* DNA targeting the citrate synthase gene (*glt*A) (*10*). PCR of spleen tissue was a substitute for blood culture detection of bacteremia. *B. henselae* DNA and distilled water were PCR-positive and -negative controls, respectively. Partial gene sequencing was performed on PCR-positive tissues. Nineteen aortic valve, mitral valve, and splenic DNA samples from 14 coyotes (*B. v. berkhoffii* PCR-positive animals by *gltA* PCR and sequencing) were genotyped by using primers targeting 16–23S intergenic transcribed spacer (ITS) region, as previously described (*11*) with minor modifications in annealing temperature (68°C for 15 s) and extension (72°C for 18 s). We conducted statistical analysis for differences in tissue tropism using Epi Info version 6 (Centers for Disease Control and Prevention, Atlanta, GA, USA).

Of the 70 coyotes collected from 9 counties (Figure), 45 (64%) were male. Coyotes' ages ranged from ≤1 year (57 [81%]) to >5 years (3 [4%]). Nine (20%) male and 6 (24%) female coyotes were PCR positive for *Bartonella* species. Fourteen (93%) of the 15 *Bartonella*-positive coyotes were ≤3 years old, of which 13 (87%) were ≤1 year old. Prevalence by county ranged from 0% to 33% (Figure).

We found no gross vegetative aortic or mitral valvular endocarditis lesions. Fifteen (21%) coyotes tested

Figure. Molecular prevalence of *Bartonella* species in 70 coyotes from 9 counties, California, USA. Shaded areas are counties where coyotes were trapped during the early 2000s. *Bartonella*-positive coyotes were identified from the 9 counties as follows: Yuba, 6 (33%) of 18 trapped coyotes; Santa Clara, 3/22 (14%); Mendocino, 2/11 (18%); Napa, 2/6 (33%); Sonoma, 1/5 (20%); Glenn, 1/4 (25%); Yolo, 0/1; Butte, 0/1; Solano, 0/2.

positive by PCR for *Bartonella gltA* gene. Overall, 8 aortic valves, 5 mitral valves, and 4 spleens were PCR positive. Aortic and mitral cardiac valves of 1 coyote (no. 93) tested positive by PCR for *B. v. berkhoffii,* and the aortic valve and spleen of another coyote (no. 110) were PCR positive (Table). Although a higher percentage of positive cardiac valves were aortic (53%) than mitral (33%), the difference was not significant. However, when we compared the number of *Bartonella*-infected cardiac valves (11 valves) with *Bartonella*-infected spleens (3 spleens), we found that *Bartonella* DNA was amplified 4.16 times (95% CI 1.02–24.12) more often from cardiac valves than from spleens.

Partial DNA sequencing showed that aortic valves from 8 (53%) of 15 coyotes were *B. v. berkhoffii* positive, compared with mitral valves from 4 (27%) and spleens from 3 (20%) coyotes. *B. rochalimae* was amplified from the spleen of coyote no. 99, and *B. henselae* DNA was amplified from the mitral valve of coyote no. 137 (Table). Of 14 coyotes tested for *B. v. berkhoffii* genotypes by 16–23S ITS PCR, 8 were positive, whereas *Bartonella* DNA was not amplified from the remaining 6 tissue DNA samples by using ITS primers. By sequence analyses, 4 coyotes were infected with *B. v. berkhoffii* genotype I, 3 with genotype II, and 1 with genotype III.

Conclusions

Our study documents the presence of 3 zoonotic *Bartonella* species in heart valves and/or spleen of free-ranging coyotes from northern California. Despite the absence of gross vegetative endocardial lesions, *Bartonella* DNA was amplified and sequenced from >20% of the coyotes, mainly from cardiac valves; only 4 (6%) coyotes had PCR-positive spleens, compared with 12 (17%) coyotes with PCR-positive cardiac valves. We hypothesize that *Bartonella* in the spleen indicated early or ongoing bacteremia, whereas

Table. Coyotes (*Canis latrans*) positive for *Bartonella* species by PCR, California, USA

Coyote no.	Sex/estimated age, y	Weight, kg	County	*Bartonella* PCR-positive tissue	*Bartonella* species by DNA sequencing
91	F/1	11.7	Yuba	Aortic valve	*B. vinsonii* subsp. *berkhoffii* type III
92	M/1	13	Yuba	Aortic valve	*B. vinsonii* subsp. *berkhoffii* type I
93	M/1	10.5	Mendocino	Aortic valve	*B. vinsonii* subsp. *berkhoffii* type I
				Mitral valve	*B. vinsonii* subsp. *berkhoffii**
99	M/<1	10.6	Yuba	Spleen	*B. rochalimae*
101	M/1	12.3	Yuba	Mitral valve	*B. vinsonii* subsp. *berkhoffii**
102	M/<1	10	Glenn	Spleen	*B. vinsonii* subsp. *berkhoffii* type II
106	F/1	12	Yuba	Aortic valve	*B. vinsonii* subsp. *berkhoffii**
110	M/<1	11	Yuba	Aortic valve, spleen	*B. vinsonii* subsp. *berkhoffii* type II
121	F/<1	8.6	Santa Clara	Aortic valve	*B. vinsonii* subsp. *berkhoffii**
124	F/9	10.4	Santa Clara	Aortic valve	*B. vinsonii* subsp. *berkhoffii**
137	M/<1	10.7	Mendocino	Mitral valve	*B. henselae*
146	M/3	16.6	Sonoma	Aortic valve	*B. vinsonii* subsp. *berkhoffii* type I
152	M/<1	9.7	Napa	Spleen	*B. vinsonii* subsp. *berkhoffii* type II
156	F/<1	8.1	Santa Clara	Mitral valve	*B. vinsonii* subsp. *berkhoffii**
164	F/<1	10.1	Napa	Mitral valve	*B. vinsonii* subsp. *berkhoffii* type I

*Type not amplified.

bartonellae in the heart valves, in their absence in the spleen, indicated valvular bacterial localization, possibly facilitating persistent infection that could evolve through time to endocarditis. This evolution has been observed for *C. burnetii* infection in humans (*12*), for which the mean reported interval from illness onset to endocarditis diagnosis is 12–24 months (*7*). *Bartonella* endocarditis is usually seen in middle-aged dogs (mean age 6.3 years ± 2.8) (*3*,*5*) and in adult humans (mean age 54 years ± 16) (*6*). Because 93% of the PCR-positive coyotes were ≤3 years old, they were very likely too young for vegetative endocarditis to have developed.

Nevertheless, the fact that ≈20% of the cardiac valve tissues were PCR positive for *Bartonella* perhaps indicates that the bacteria had localized to the valves of infected coyotes. *B. v. berkhoffii* can induce vasoproliferative lesions in animals (*13*); thus, cases of *Bartonella* endocarditis might represent only a small fraction of infected animals that have chronic cardiac valvular localization. All 3 *B. v. berkhoffii* genotypes identified in these coyotes have been previously involved in humans or dogs with endocarditis (*14*,*15*). To our knowledge, *B. henselae* and *B. v. berkhoffii* genotype III have not been previously identified in coyotes; thus, these mammals can be added to the list of susceptible species. Coyotes might be a natural reservoir for *B. v. berkhoffii* genotype III, which so far has been mainly described in California gray foxes (*14*).

In conclusion, *Bartonella* infection of a natural reservoir appears to lead to cardiac valve tropism. This tropism could result in development of endocarditis, a severe and often lethal complication of *Bartonella* infection.

Mr Kehoe is a fourth-year veterinary student at the University of California, Davis. His primary research interests include zoologic and wildlife medicine and health and emerging zoonotic infections.

References

1. Chomel BB, Kasten RW, Williams C, Wey AC, Henn JB, Maggi R, et al. *Bartonella* endocarditis: a pathology shared by animal reservoirs and patients. Ann N Y Acad Sci. 2009;1166:120–6. http://dx.doi.org/10.1111/j.1749-6632.2009.04523.x
2. Boulouis HJ, Chang CC, Henn JB, Kasten RW, Chomel BB. Factors associated with the rapid emergence of zoonotic *Bartonella* infections. Vet Res. 2005;36:383–410. http://dx.doi.org/10.1051/vetres:2005009
3. MacDonald KA, Chomel BB, Kittleson MD, Kasten RW, Thomas WP, Pesavento P. A prospective study of canine infective endocarditis in northern California (1999–2001): emergence of *Bartonella* as a prevalent etiologic agent. J Vet Intern Med. 2004;18:56–64.
4. Yore K, Digangi B, Brewer M, Balakrishnan N, Breitschwerdt EB, Lappin M. Flea species infesting dogs in Florida and *Bartonella* spp. prevalence rates. Vet Parasitol. 2014;199:225–9. http://dx.doi.org/10.1016/j.vetpar.2013.10.017
5. Sykes JE, Kittleson MD, Pesavento PA, Byrne BA, MacDonald KA, Chomel BB. Evaluation of the relationship between causative organisms and clinical characteristics of infective endocarditis in dogs: 71 cases (1992–2005). J Am Vet Med Assoc. 2006;228:1723–34. http://dx.doi.org/10.2460/javma.228.11.1723
6. Houpikian P, Raoult D. Diagnostic methods. Current best practices and guidelines for identification of difficult-to-culture pathogens in infective endocarditis. Cardiol Clin. 2003;21:207–17. http://dx.doi.org/10.1016/S0733-8651(03)00028-6
7. Stein A, Raoult D, Q fever endocarditis. Eur Heart J. 1995;16 Suppl B:19.
8. Chang CC, Kasten RW, Chomel BB, Simpson DC, Hew CM, Kordick DL, et al. Coyotes (*Canis latrans*) as the reservoir for a human pathogenic *Bartonella* sp.: molecular epidemiology of *Bartonella vinsonii* subsp. *berkhoffii* infection in coyotes from central coastal California. J Clin Microbiol. 2000;38:4193–200.
9. Sacks BN, Chomel BB, Kasten RW, Chang CC, Sanders RK, Leterme SD. Validation for use with coyotes (*Canis latrans)* of a commercially available enzyme-linked immunosorbent assay for *Dirofilaria immitis.* Vet Parasitol. 2002;109:45–58. http://dx.doi.org/10.1016/S0304-4017(02)00254-6
10. Norman AF, Regnery R, Jameson P, Greene C, Krause DC. Differentiation of *Bartonella*-like isolates at the species level by PCR-restriction fragment length polymorphism in the citrate synthase gene. J Clin Microbiol. 1995;33:1797–803.

11. Varanat M, Maggi RG, Linder KE, Breitschwerdt EB. Molecular prevalence of *Bartonella*, *Babesia*, and hemotropic *Mycoplasma* sp. in dogs with splenic disease. J Vet Intern Med. 2011;25:1284–91. http://dx.doi.org/10.1111/j.1939-1676.2011.00811.x
12. Fenollar F, Fournier PE, Carrieri MP, Habib G, Messana T, Raoult D. Risks factors and prevention of Q fever endocarditis. Clin Infect Dis. 2001;33:312–6. http://dx.doi.org/10.1086/321889
13. Beerlage C, Varanat M, Linder K, Maggi RG, Cooley J, Kempf VA, et al. *Bartonella vinsonii* subsp. *berkhoffii* and *Bartonella henselae* as potential causes of proliferative vascular diseases in animals. Med Microbiol Immunol (Berl). 2012;201:319–26. http://dx.doi.org/10.1007/s00430-012-0234-5
14. Maggi RG, Chomel B, Hegarty BC, Henn J, Breitschwerdt EB. A *Bartonella vinsonii berkhoffii* typing scheme based upon 16S–23S ITS and Pap31 sequences from dog, coyote, gray fox, and human isolates. Mol Cell Probes. 2006;20:128–34. http://dx.doi.org/10.1016/j.mcp.2005.11.002
15. Cadenas MB, Bradley J, Maggi RG, Takara M, Hegarty BC, Breitschwerdt EB. Molecular characterization of *Bartonella vinsonii* subsp. *berkhoffii* genotype III. J Clin Microbiol. 2008;46:1858–60. http://dx.doi.org/10.1128/JCM.02456-07

Address for correspondence: Bruno B. Chomel, Department of Population Health and Reproduction, School of Veterinary Medicine, VM3B, 1089 Veterinary Medicine Dr, University of California, Davis, Davis, CA 95616, USA; email: bbchomel@ucdavis.edu

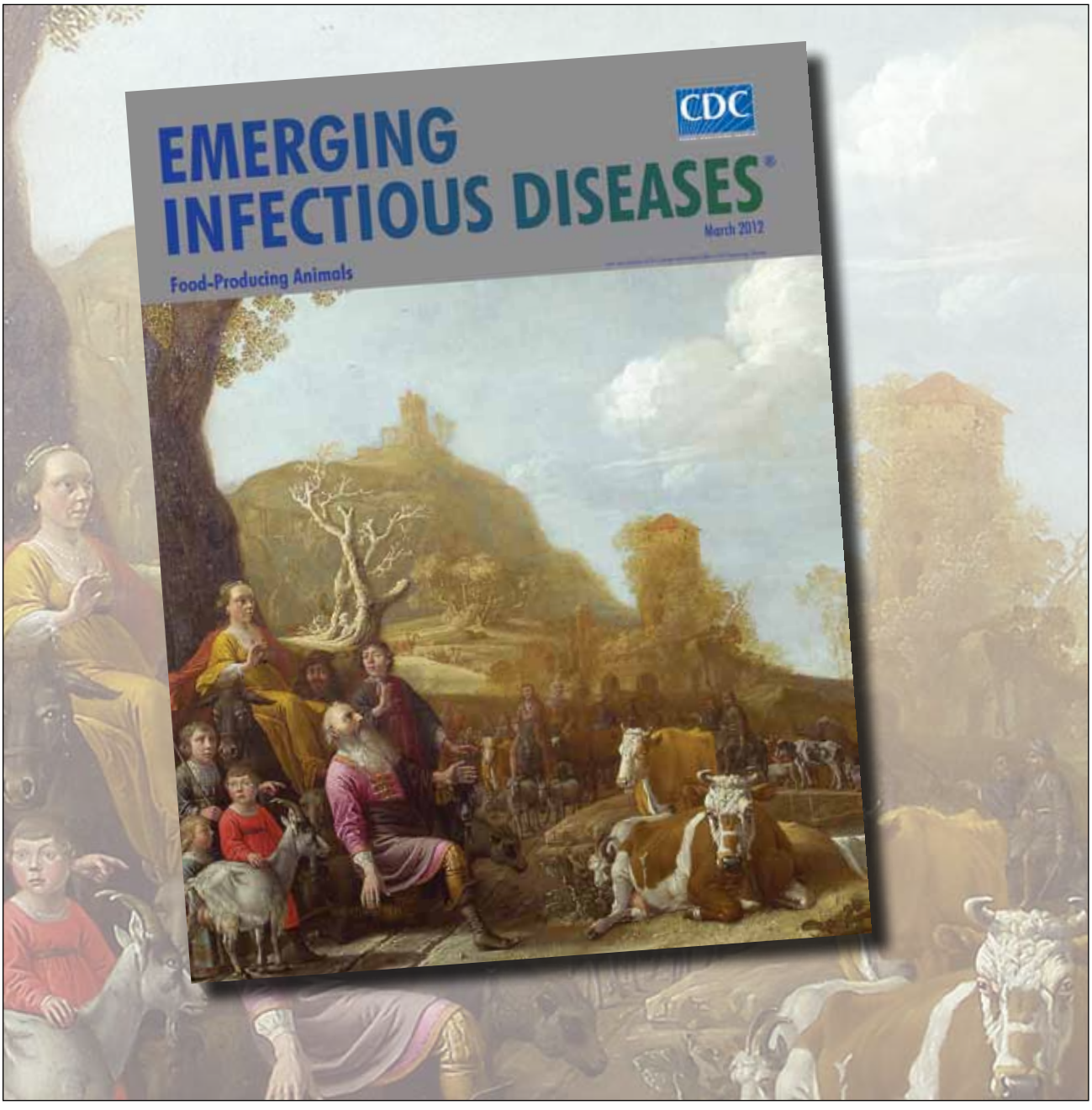

Reduction of *Baylisascaris procyonis* Eggs in Raccoon Latrines, Suburban Chicago, Illinois, USA

Kristen Page, Timothy J. Smyser, Elise Dunkerton, Emily Gavard, Bruce Larkin, and Stanley Gehrt

Baylisascaris procyonis, a common roundworm of raccoons, causes severe or fatal human infections, often in suburban areas. To evaluate the effectiveness of a baiting strategy requiring minimal labor, we distributed medicated baits near raccoon latrines in suburban Chicago, Illinois, USA. This strategy lowered *B. procyonis* prevalence in raccoons, possibly reducing risk to humans.

Modification of landscapes resulting in human-dominated ecosystems is one of the most important drivers of emerging diseases (*1*). In human-dominated landscapes, the transmission dynamics of diseases often change as host and pathogen population dynamics respond to loss or creation of habitat (*1*). As a result, contact rates can increase, and humans can be infected (*2*). Public health officials, veterinarians, and wildlife ecologists increasingly are focusing on mitigation strategies to decrease the potential for human disease in such landscapes (*2*).

Baylisascaris procyonis roundworms are ubiquitous ascarid parasites of raccoons; prevalence of infection can reach 82% (*3*). Infected raccoons can shed thousands of eggs daily; transmission generally occurs at raccoon latrines where fecal material accumulates (*4*). *B. procyonis* eggs are highly resistant and can remain viable in the environment for years (*3*). Thirty severe or fatal human cases of baylisascariasis have been reported (*5–7*; K.R. Kazacos, pers. comm), many of which occurred in human-dominated landscapes (K.R. Kazacos, pers. comm). Therefore, mitigation strategies appropriate for urban and suburban landscapes need to be developed.

Author affiliations: Wheaton College, Wheaton, Illinois, USA (K. Page, E. Dunkerton, E. Gavard, B. Larkin); Purdue University, West Lafayette, Indiana, USA (T.J. Smyser); State University of New York College of Environmental Science and Forestry, Syracuse, New York, USA (E. Gavard); and The Ohio State University, Columbus, Ohio, USA (S. Gehrt)

DOI: http://dx.doi.org/10.3201/eid2012.140977

Anthelmintic bait distribution has been evaluated for managing *B. procyonis* (*5*,*6*); however, to our knowledge, no *B. procyonis* mitigation study has been conducted in urban or suburban landscapes, where the risk for transmission to humans is highest. Additionally, previous studies implemented a regimen of latrine removal and substrate sterilization that might not be feasible for resource-restricted wildlife management officials. Furthermore, raccoon core habitat within suburban environments is fragmented with raccoon populations concentrated in preserves interspersed among residential areas (*8*). As a result, raccoons frequently move throughout adjacent residential areas, creating latrines in close proximity to homes and placing humans at risk to *B. procyonis* exposure (*9*). The ability of raccoons to exploit both natural and human-dominated landscapes can present challenges for *B. procyonis* mitigation, given that bait distribution is generally restricted to natural habitats (*10*). Our objective was to evaluate the effectiveness of a baiting strategy requiring minimal labor investment in a highly developed suburban region of Chicago, Illinois, USA. By modifying an existing mitigation strategy (*5*) and implementing it in a suburban landscape, we hope to provide wildlife managers and public health officials with a feasible strategy to decrease *B. procyonis* infection risks for children living in suburban landscapes.

The Study

We conducted this study in Cook and McHenry Counties, Illinois, within the Chicago metropolitan area, a landscape characterized as 45% developed, 12% forested and open, 31% agricultural, 10% vacant or wetland, and 2% water (*11*) (Figure). Our experiment was conducted throughout 6 study sites associated with 6 forest preserves, 3 each in Cook and McHenry Counties. In September and October 2012, we sampled sixty-three 200-m^2 quadrats across the 6 study sites. We sampled 8–16 quadrats per study site; the number of quadrats per site were related to the amount of forested habitat within each site (*12*). All fecal deposits were collected individually for analysis from each latrine within sampling quadrats (*13*). In contrast to previous studies (*5*,*6*), latrine substrates were not sterilized with a propane torch, nor were all latrines located and removed from the treatment sites. Similar to previous studies (*5*,*6*), we distributed anthelmintic baits monthly at 1.5 baits/hectare at each of the 3 randomly selected treatment sites for the duration (12 months) of the study. Baits were similar to oral rabies vaccine baits and consisted of a hollow fishmeal polymer food attractant (15 g, 33 mm × 32 mm × 21 mm) in which we placed 180 mg (base) of pyrantel pamoate mixed with marshmallow creme, which was sealed within the hollow chamber with paraffin wax. We distributed baits by hand along transects through forested portions of each site to achieve a relatively even distribution of 1.5/hectare.

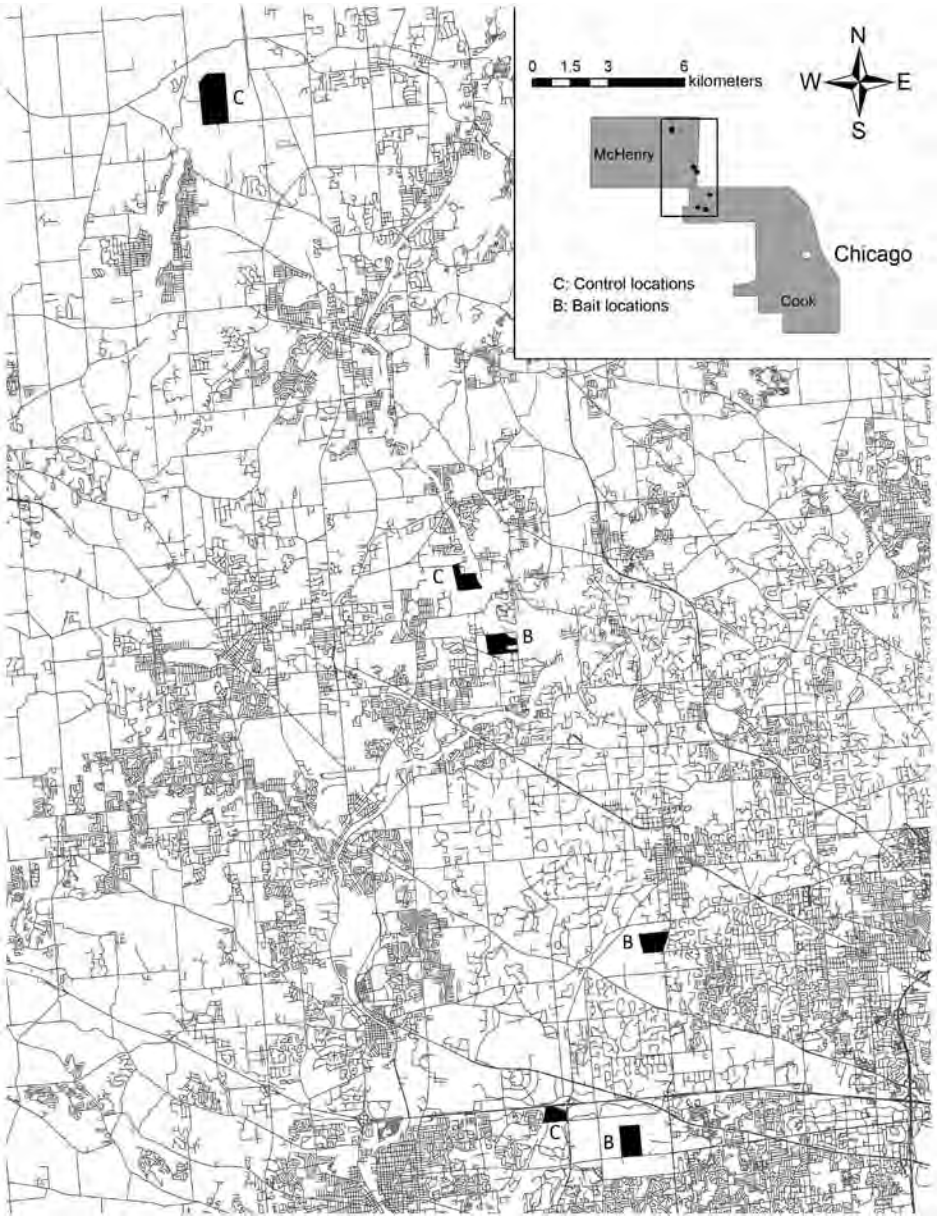

Figure. Location of study areas within the metropolitan area of Chicago, Illinois, USA, showing treatment and control sites. Insert indicates location of metropolitan Chicago counties where baits were placed.

After 1 year of monthly bait distribution, we repeated latrine sampling in September and October 2013, using an equal sampling effort (sixty-three 200-m^2 quadrats) during surveys before and after treatment. All fecal samples were stored at –20°C until they were examined for *B. procyonis* eggs. We used centrifugal fecal flotation in Sheather sugar solution and microscopic examination to evaluate all samples for eggs (*3*). Each fecal sample was determined to be positive or negative, and prevalence (proportion positive) was determined for each year, site, and treatment type. We evaluated differences in prevalence by year, site, and treatment type using χ^2 analysis with a Fisher exact test. The Wheaton College Institutional Animal Care and Use committee approved this study.

We sampled 63 latrines ($2.5 \times 10^{-5}/m^2$) in 2012, and 59 latrines ($2.0 \times 10^{-5}/m^2$) in 2013. Latrine density did not differ between sampling years ($F = 0.124$, df = 1, p = 0.725). Pretreatment (2012) sampling of latrines resulted in 209 fecal samples, and a prevalence of 13% ± 4.56% across sites. The prevalence of *B. procyonis* roundworms did not differ between treatment (14% ± 6.91%) and control (12% ± 6.02%) sites before placement of anthelmintic baits ($\chi^2 = 0.368$, d.f. = 1, p = 0.544) (Table). Posttreatment sampling of latrines resulted in 124 fecal samples, and a prevalence of 11% ± 5.28% across sites. Prevalence across sites did not differ between years ($\chi^2 = 0.44$, d.f. = 1, p = 0.602) (Table); however, prevalence differed significantly between treatment (3% ± 3.94%) and control

Table. Findings for baited and control locations in a study of prevalence of *Baylisascaris procyonis* eggs at raccoon latrines, suburban Chicago, Illinois, USA*

Location	2012 (before treatment)		2013 (after treatment)	
	Fecal samples, no. positive/total	Positive ± 95% CI, %	Fecal samples, no. positive/total	Positive ± 95% CI, %
All	27/209	13 ± 4.56	13/124	11 ± 5.28
Control areas	14/97	14 ± 6.91	11/52	21± 11.07
Baited areas	13/112	12 ± 6.02	2/72	3 ± 3.94

*Prevalence was determined as the proportion of positive fecal samples among all fecel sampled at a location. Baited locations received 1.5 baits/hectare.

(21% ±1 1.07%) sites after treatment (χ^2 = 11.28, d.f. = 1, p<0.001) (Table).

Conclusions

Previous strategies to decrease prevalence of *B. procyonis* roundworms required removing all latrines and heat sterilizing latrine substrates (*5*,*6*). Wildlife managers in urban or suburban settings often do not have the resources to implement such a labor-intensive strategy. We found that a modified strategy that eliminates latrine removal and sterilization but retains the monthly distribution of baits effectively reduced environmental contamination with *B. procyonis* eggs.

Implementation of this anthelmintic baiting strategy in suburban green spaces might significantly reduce risk for exposure by humans who use green spaces for recreation or live in close proximity to forested areas (*9*). However, both material and distribution costs can be substantial when such management action is implemented at landscapes scales. This study shows that the monthly distribution of baits and subsequent consumption by raccoons would keep reinfections from reaching patency (32–38 days) (*3*). For initial disease control, it is recommended that intervals between consecutive bait distributions not exceed the prepatency period (*14*). Once prevalence is reduced, interbaiting intervals can be extended while reduced prevalence is maintained (*14*). Although we implemented labor-intensive hand baiting, implementation of bait stations (*10*) could maintain management efficacy while reducing labor required for bait distribution. Bait stations have been used successfully for oral rabies vaccination in raccoons (*10*) and may enable more targeted bait distribution in areas of high raccoon density. Our study demonstrated that anthelmintic baiting successfully reduced environmental contamination with *B. procyonis* eggs; prevalence among treatment sites decreased nearly 80% with 1 year of treatment; however, further study is needed to identify optimal long-term bait distribution frequencies and bait distribution strategies to make anthelmintic baiting a viable and sustainable management solution for *B. procyonis* control.

Acknowledgments

We thank Chris Anchor, the Cook County Forest Preserve District, and Tom Simpson for facilitating access to the study sites. We also thank Drew Dickelman for providing valuable field assistance.

The Wheaton College Faculty Achievement Award program provided financial support for this study.

Dr Page is a professor of biology at Wheaton College, Wheaton, Illinois. Her research interests include the transmission ecology of *B procyonis* roundworms and the link between human land use and disease transmission.

References

1. Patz JA, Graczyk TK, Geller N, Vittor AY. Effects of environmental change on emerging parasitic diseases. Int J Parasitol. 2000;30:1395–405. http://dx.doi.org/10.1016/S0020-7519(00)00141-7
2. Ryser-Degiorgis MP. Wildlife health investigations: needs, challenges and recommendations. BMC Vet Res. 2013;9:223. http://dx.doi.org/10.1186/1746-6148-9-223
3. Kazacos KR. *Baylisascaris procyonis* and related species. In: Samuel WM, Pybus MJ, Kocan AA, editors. Parasitic diseases of wild mammals. Ames (IA): Iowa State University Press; 2001. p. 301–41.
4. Page LK, Swihart RK, Kazacos KR. Implications of raccoon latrines in the epizootiology of baylisascariasis. J Wildl Dis. 1999;35:474–80. http://dx.doi.org/10.7589/0090-3558-35.3.474
5. Page K, Beasley JC, Olson ZH, Smyser TJ, Downey M, Kellner KF, et al. Reducing *Baylisascaris procyonis* roundworm larvae in raccoon latrines. Emerg Infect Dis. 2011;17:90–3. http://dx.doi.org/10.3201/eid1701.100876
6. Smyser TJ, Page LK, Johnson SA, Hudson CM, Kellner KF, Swihart RK, et al. Management of raccoon roundworm in free-ranging raccoon populations via anthelmintic baiting. J Wildl Manage. 2013;77:1372–9. http://dx.doi.org/10.1002/jwmg.585
7. Hernandez SM, Glabreath B, Riddle DF, Moore AP, Palamar MB, Levy MG, et al. *Baylisascaris procyonis* in raccoons (*Procyon lotor*) from North Carolina and current status of the parasite in the USA. Parasitol Res. 2013;112:693–8. http://dx.doi.org/10.1007/s00436-012-3186-1
8. Prange S, Gehrt SD, Wiggers EP. Demographic factors contributing to high raccoon densities in urban landscapes. J Wildl Manage. 2003;67:324–33. http://dx.doi.org/10.2307/3802774
9. Page LK, Anchor C, Luy E, Kron S, Larson G, Madsen L, et al. Backyard raccoon latrines and risk for *Baylisascaris procyonis* transmission to humans. Emerg Infect Dis. 2009;15:1530–1. http://dx.doi.org/10.3201/eid1509.090128
10. Boulanger JR, Bigler LL, Curtis PD, Lein DH, Lembo AJ Jr. Comparison of suburban vaccine distribution strategies to control raccoon rabies. J Wildl Dis. 2008;44:1014–23. http://dx.doi.org/10.7589/0090-3558-44.4.1014
11. Chicago Metropolitan Agency for Planning. Data bulletin: 2001 land-use inventory for northeastern Illinois. Chicago: Northeastern Illinois Planning Commission; 2006.
12. Page LK, Swihart RK, Kazacos KR. Raccoon latrine structure and its potential role in transmission of *Baylisascaris procyonis* to vertebrates. Am Midl Nat. 1998;140:180–5. http://dx.doi.org/10.1674/0003-0031(1998)140[0180:RLSAIP]2.0.CO;2
13. Smyser TJ, Page LK, Rhodes OE Jr. Optimization of raccoon latrine surveys for quantifying exposure to *Baylisacaris procyonis.* J Wildl Dis. 2010;46:929–33. http://dx.doi.org/10.7589/0090-3558-46.3.929

14. Hegglin D, Deplazes P. Control of *Echinococcus multilocularis*: strategies, feasibility and cost-benefit analyses. Int J Parasitol. 2013;43:327–37. http://dx.doi.org/10.1016/j.ijpara.2012.11.013

Address for correspondence Kristen Page, 501 College Ave, Biology Department, Wheaton College, Wheaton, IL 60187, USA; email: kristen.page@wheaton.edu

Triatoma sanguisuga Blood Meals and Potential for Chagas Disease, Louisiana, USA

Etienne Waleckx,[1] Julianne Suarez, Bethany Richards, and Patricia L. Dorn

To evaluate human risk for Chagas disease, we molecularly identified blood meal sources and prevalence of *Trypanosoma cruzi* infection among 49 *Triatoma sanguisuga* kissing bugs in Louisiana, USA. Humans accounted for the second most frequent blood source. Of the bugs that fed on humans, ≈40% were infected with *T. cruzi*, revealing transmission potential.

Chagas disease, caused by the parasite *Trypanosoma cruzi*, is mainly transmitted to humans and other mammals by blood-sucking insects called triatomines (also known as kissing bugs). In the United States, 24 species of wild mammals have been found to be naturally infected with *T. cruzi*, but only a few (<25) autochthonous cases of vectorial transmission to humans have been described (*1*,*2*). This number is probably an underestimate, and there is concern that vectorial transmission to humans in the United States may increase because of the following factors: 1) loss of sylvan blood sources because of habitat destruction, forcing the bugs to seek other (possibly human) blood sources; 2) climate change that could extend the range of the vectors northward; and 3) introduction of parasites by migrants from disease-endemic countries (*3*–*5*). Among the 11 triatomine species in the United States, the most widely distributed and the only 2 found in Louisiana are *Triatoma lecticularia* and *T. sanguisuga* (*5*). Bugs of the species *T. sanguisuga* are responsible for the first described autochthonous case of *T. cruzi* transmission in Louisiana (*6*), but little is known about their feeding habits in natural conditions. To evaluate the risk for Chagas disease (based on human/vector/parasite contact) and determine the feeding behavior of *T. sanguisuga* bugs, we molecularly identified the blood meal sources and *T. cruzi* infection in *T. sanguisuga* kissing bugs.

Author affiliation: Loyola University New Orleans, New Orleans, Louisiana, USA

DOI: http://dx.doi.org/10.3201/eid2012.131576

The Study

In 2007, at the site of the first autochthonous case of transmission of Chagas disease in Louisiana, 49 *T. sanguisuga* (16 male and 33 female) bugs were collected and identified (*6*–*8*). DNA was isolated from the abdomen of each bug by using the DNeasy Blood and Tissue Kit (QIAGEN, Valencia, CA, USA), and presence of *T. cruzi* was assessed by PCR (*9*). *T. cruzi* infection was found in 27 (55.1%) bugs; prevalence did not differ significantly between males (50.0%, 8/16) and females (57.6%, 19/33) (Fisher exact test; p = 0.76) (online Technical Appendix Table, http://wwwnc.cdc.gov/EID/article/20/12/13-1576-Techapp1.pdf).

Blood meals were detected by using PCR with universal vertebrate primers targeting the 12S ribosomal RNA gene (*10*). The PCR products were purified and cloned to enable detection of multiple blood sources in a single bug. For cloning, the p-GEM-T Easy Vector System (Promega, Madison, WI, USA) was used; for the ligation step, the DNA-to-vector ratio was 3:1. After transformation, up to 8 transformants per bug were randomly selected and sequenced. Blood meals were detected in 45 (92%) of 49 bugs, and 43 (96%) of the 45 detected blood meals were successfully cloned (online Technical Appendix Table).

Blood meal sources were inferred by using BLAST (http://www.ncbi.nlm.nih.gov/blast/Blast.cgi); ≥97% identity was considered a match. From the 43 bugs, 201 vertebrate 12S sequences were obtained. In all, 8 vertebrate blood-source species were identified. Multiple blood source species were identified in 21 (48.8%) of 43 bugs; the maximum number of blood meal sources was 4 (online Technical Appendix Table), confirming the ability of the cloning approach to identify multiple blood meals. The average number of blood source species detected per bug was 1.6. The predominant blood source was the American green tree frog (*Hyla cinerea*), found in 53.5% of triatomines; the second most predominant was the human (*Homo sapiens*), found in 48.8%, followed by the raccoon (*Procyon lotor*), found in nearly 30% of triatomines (Figure). Less prevalent blood sources included cow (*Bos taurus*), dog/wolf (*Canis lupus*), squirrel (*Sciurus carolinensis*), cat (*Felis domesticus*), and woodrat (*Neotoma floridana*), each found in <15% of bugs.

In total, 33 different vertebrate 12S haplotypes were found at an average of 2.1 per bug (online Technical Appendix Table, Figure). We found 8 human haplotypes, indicating that bugs had fed on at least 8 persons, assuming that multiple haplotypes did not result from heteroplasmy. More female than male bugs had fed on frogs (Fisher exact test, p = 0.005). Neither the average number of blood

[1]Current affiliation: Universidad Autónoma de Yucatán, Mérida, México

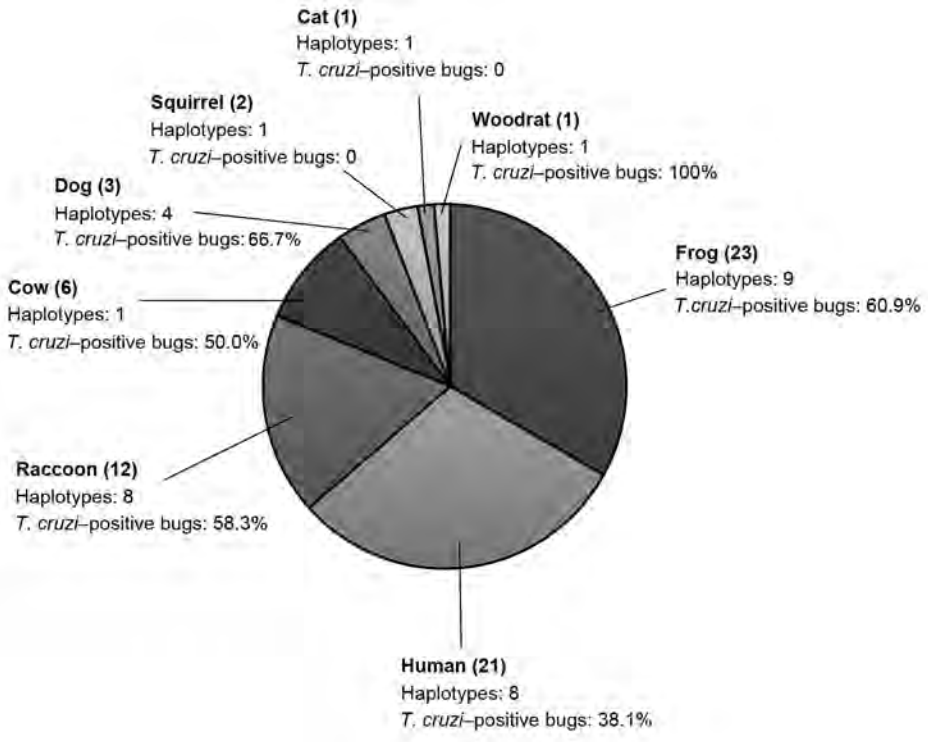

Figure. Vertebrate blood meal sources of *Triatoma sanguisuga* kissing bugs detected by 12S rDNA assay (*10*). The numbers of triatomines containing each vertebrate blood source are indicated in parenthesis. The numbers of haplotypes of each vertebrate source and the *Trypanosoma cruzi* infection prevalence in the triatomines containing this vertebrate blood source are indicated.

sources detected (females 1.7 ± 0.8 vs. males 1.4 ± 0.6, *t*-test; p = 0.23) nor the average number of vertebrate haplotypes found (females 2.0 ± 0.9 vs. males 2.1 ± 0.9, *t*-test; p = 0.75) differed significantly between bugs of each sex.

Of the 55% of bugs that were infected with *T. cruzi*, 61.9% had fed on frogs (incompetent *T. cruzi* host) and 38.1% on humans. We found 3 human haplotypes in *T. cruzi*–infected bugs, suggesting, in the absence of heteroplasmy, that at least 3 persons were bitten by an infected bug (online Technical Appendix Table). Because only 2 persons lived at the location sampled, some bugs may have fed on visiting persons or migrated from nearby houses. No significant association was found between infection and a particular blood source, even after we removed from analysis all insects that had fed on at least 1 frog or had fed on frogs only.

Conclusions

Our results indicate that *T. sanguisuga* kissing bugs pose an epidemiologic threat to humans and animals in Louisiana. Human/vector/*T. cruzi* contact is frequent; 55% of bugs were infected, of which nearly 40% had fed on humans.

In addition to humans, the bugs fed on a wide variety of vertebrates; multiple blood sources were detected in about half of the bugs. These observations support catholic and opportunistic feeding habits for *T. sanguisuga*, which probably feed on any available animal. The high occurrence of the American green tree frog as a blood source is not surprising because these frogs are abundant in this region (*11*). Although amphibians are incompetent *T. cruzi* hosts, frogs contribute to the epidemiology because as a blood source, they help maintain large populations of bugs near human dwellings. Further investigation could determine whether frogs also control the bug population by eating them, as do *Neotoma* spp. rats, the traditional hosts of kissing bugs in North America (*5*). Raccoons serve as sylvatic *T. cruzi* reservoirs in the southeastern United States and play an epidemiologic role because they are frequently found close to humans and, as do woodrats, they link the sylvatic cycle of the parasite with a domestic cycle (*5*). Dogs also serve as reservoirs and are at high risk for Chagas disease; many dogs in the southern United States die of this disease (*1*,*12*,*13*). In addition to the loss of companion animals, Chagas disease in animals has an evident economic effect (*13*).

Results of our study, as well as those of Stevens et al. (*10*) and Kjos et al. (*14*), reject the assertion that kissing bugs in North America prefer blood from wild animals, which has been one explanation for the low prevalence of Chagas disease in the United States. Our study provides evidence of frequent vector/human/*T. cruzi* contact in Louisiana and reveals the potential for transmission in the United States. Even if this finding does not apply to all localities (e.g., human blood has rarely been detected in triatomines from Texas [*15*]), the risk for vectorial transmission of *T. cruzi* in the United States may increase because of expansion of human settlements into formerly sylvatic

areas. Moreover, the low number of Chagas disease cases reported in the United States is probably caused, at least in part, by a lack of awareness (*4*,*5*). Because knowledge of the feeding behavior of triatomines is critical for the implementation of efficient control measures, more studies of the blood sources of triatomines in North America are needed. In addition, awareness of Chagas disease and surveillance of insect vectors and human disease should be improved.

Acknowledgments

We thank Leon Perniciaro, Gabriela Estrada, Laura Duncan, Paula Mischler, and Dawn Wesson for technical and field assistance.

Funding was provided by National Institutes of Health grant 1R15 A1079672–01A1, Supervised Undergraduate Research Experiences from the Louisiana Board of Regents, National Science Foundation grant BCS-1216193, and the Mullahy, S.J. Fund for Undergraduate Research from Loyola University New Orleans.

Dr Waleckx is a research professor in medical entomology at the Laboratory of Parasitology of the "Dr. Hideyo Noguchi" Regional Research Center, Autonomous University of Yucatán, in Mexico. His research interests are focused on the ecology, population genetics, and control of tropical disease vectors.

References

1. Bern C, Kjos S. Yabsley MJ, Montgomery SP. *Trypanosoma cruzi* and Chagas' disease in the United States. Clin Microbiol Rev. 2011;24:655–81. http://dx.doi.org/10.1128/CMR.00005-11
2. Cantey PT, Stramer SL, Townsend RL, Kamel H, Ofafa K, Todd CW, et al. The United States *Trypanosoma cruzi* Infection Study: evidence for vector-borne transmission of the parasite that causes Chagas disease among United States blood donors. Transfusion. 2012;52:1922–30. http://dx.doi.org/10.1111/j.1537-2995.2012.03581.x
3. Waleckx E, Depickere S, Salas R, Aliaga C, Monje M, Calle H, et al. New discoveries of sylvatic *Triatoma infestans* (Hemiptera: Reduviidae) throughout the Bolivian Chaco. Am J Trop Med Hyg. 2012;86:455–8. http://dx.doi.org/10.4269/ajtmh.2012.11-0205
4. Click Lambert R, Kolivras KN, Resler LM, Brewster CC, Paulson SL. The potential for emergence of Chagas disease in the United States. Geospat Health. 2008;2:227–39.
5. Zeledon R, Beard CB, Diaz JCP, Leiby DA, Dorn PL, Coura JR. An appraisal of the status of Chagas disease in the United States. Oxford (UK): Elsevier; 2012.
6. Dorn PL, Perniciaro L, Yabsley MJ, Roellig DM, Balsamo G, Diaz J, et al. Autochthonous transmission of *Trypanosoma cruzi*, Louisiana. Emerg Infect Dis. 2007;13:605–7. http://dx.doi.org/10.3201/eid1304.061002
7. Lent H, Wygodzinsky P. Revision of the triatominae (Hemiptera, Reduviidae), and their significance as vectors of Chagas' disease. American Museum of Natural History. 1979;163:321–4.
8. Cesa K, Caillouet KA, Dorn PL, Wesson DM. High *Trypanosoma cruzi* (Kinetoplastida: Trypanosomatidae) prevalence in *Triatoma sanguisuga* (Hemiptera: Redviidae) in southeastern Louisiana. J Med Entomol. 2011;48:1091–4. http://dx.doi.org/10.1603/ME10195
9. Moser DR, Kirchhoff LV, Donelson JE. Detection of *Trypanosoma cruzi* by DNA amplification using the polymerase chain reaction. J Clin Microbiol. 1989;27:1477–82.
10. Stevens L, Dorn PL, Hobson J, de la Rua NM, Lucero DE, Klotz JH, et al. Vector blood meals and Chagas disease transmission potential, United States. Emerg Infect Dis. 2012;18:646–9. http://dx.doi.org/10.3201/eid1804.111396
11. Dundee HA, Rossman DA. The amphibians and reptiles of Louisiana. Baton Rouge (LA): Louisiana State University Press; 1989. p. 91–2.
12. Kjos SA, Snowden KF, Craig TM, Lewis B, Ronald N, Olson JK. Distribution and characterization of canine Chagas disease in Texas. Vet Parasitol. 2008;152:249–56. http://dx.doi.org/10.1016/j.vetpar.2007.12.021
13. Nieto PD, Boughton R, Dorn PL, Steurer F, Raychaudhuri S, Esfandiari J, et al. Comparison of two immunochromatographic assays and the indirect immunofluorescence antibody test for diagnosis of *Trypanosoma cruzi* infection in dogs in south central Louisiana. Vet Parasitol. 2009;165:241–7. http://dx.doi.org/10.1016/j.vetpar.2009.07.010
14. Klotz SA, Schmidt JO, Dorn PL, Ivanyi C, Sullivan KR, Stevens L. Free-roaming kissing bugs, vectors of Chagas disease, feed often on humans in the Southwest. Am J Med. 2014;127:421–6. http://dx.doi.org/10.1016/j.amjmed.2013.12.017
15. Kjos SA, Marcet PL, Yabsley MJ, Kitron U, Snowden KF, Logan KS, et al. Identification of blood meal sources and *Trypanosoma cruzi* infection in triatomine bugs (Hemiptera: Reduviidae) from residential settings in Texas, the United States. J Med Entomol. 2013;50:1126–39. http://dx.doi.org/10.1603/ME12242

Address for correspondence: Etienne Waleckx, Centro de Investigaciones Regionales Hideyo Noguchi, Universidad Autónoma de Yucatán, Calle 96 x Av. Jacinto Canek y Calle 47, Col. Paseo de Las Fuentes, C.P. 97225, Mérida, Yucatán, México; email: etienne.waleckx@ird.fr

Equine Influenza A(H3N8) Virus Isolated from Bactrian Camel, Mongolia

Myagmarsukh Yondon, Batsukh Zayat, Martha I. Nelson, Gary L. Heil, Benjamin D. Anderson, Xudong Lin, Rebecca A. Halpin, Pamela P. McKenzie, Sarah K. White, David E. Wentworth, and Gregory C. Gray

Because little is known about the ecology of influenza viruses in camels, 460 nasal swab specimens were collected from healthy (no overt illness) Bactrian camels in Mongolia during 2012. One specimen was positive for influenza A virus (A/camel/Mongolia/335/2012[H3N8]), which is phylogenetically related to equine influenza A(H3N8) viruses and probably represents natural horse-to-camel transmission.

Since the first isolation in 1963 of an avian-origin influenza A(H3N8) virus from horses (*1*), subtype H3N8 influenza viruses have continued to circulate panzootically among horses, causing severe outbreaks of equine influenza respiratory disease. In the United States, these viruses jumped from horses to dogs and continue to circulate among dogs (*2*,*3*). In Mongolia, the site of some of the world's largest epizootics of equine influenza A(H3N8) virus (EIV) infection, transmission of this virus is sustained among 2.1 million free-ranging horses, causing significant economic losses among rural herders. Major epizootics of EIV infection occurred in Mongolia during 2007–2008 (459,000 cases, 24,600 deaths) and again in 2011 (74,608 cases, 40 deaths) (*4*).

Over previous decades in Mongolia, outbreaks of respiratory disease, thought to be influenza, among camels have been reported, In the 1980s, the virus was characterized, and researchers speculated that it was related to a reassortant influenza A(H1N1) virus vaccine strain, A/PR-8/34 + A/USSR/77, generated in a Soviet laboratory and administered to humans in Mongolia and possibly transmitted from vaccinated humans to camels in a reactivated form (*5*,*6*). However, only 1 genetic sequence from this outbreak among camels is available in GenBank: A/camel/Mongolia/1982/H1N1. Despite reports of serologic activity against influenza A virus among camels in several African countries (*7*,*8*), the lack of isolated virus from these populations highlights how little is known about the ecology of influenza viruses in camels. Questions about the potential role of camels in human cases of Middle East respiratory syndrome (*9*) further highlight our lack of knowledge of infectious diseases in camels and the merits of increased surveillance at this unique human–animal interface.

Since January 2011, surveillance of equine influenza viruses has been enhanced in 3 Mongolian aimags (provinces). Surveillance among camels was also initiated in response to anecdotal reports of signs of respiratory illness in Bactrian camels (*Camelus bactrianus*). We describe the isolation, full-genome sequencing, and phylogenetic characterization of an influenza A(H3N8) virus of equine lineage isolated from a Bactrian camel, thereby identifying a novel route of influenza virus interspecies transmission and raising further questions about influenza A virus ecology in understudied regions such as Mongolia.

The Study

During January–January 2013, a total of 460 nasal swab specimens were collected through active surveillance of horses and camels in 3 Mongolian aimags (Figure 1) known for high densities of free-ranging horses and camels (Table). Specimens were collected monthly, as weather permitted, from 50 free-ranging horses and 20 free-ranging Bactrian camels that were safely and carefully restrained with halters, ropes, and by hand, according to a protocol approved by the Department of Veterinary and Animal Breeding, Government of Mongolia. During sampling, camels were in a crouched or take-down position. Horse and camel specimens were carefully stored and shipped in separate containers; to prevent cross-contamination with EIV, specimens were separated during laboratory analyses.

All specimens were first screened at the Institute of Veterinary Medicine laboratory (Ulaanbaatar, Mongolia) by using the World Health Organization (WHO) influenza A quantitative reverse transcription PCR (qRT-PCR) protocol (*10*). Six specimens collected from camels without respiratory signs were positive for influenza A and were double-blind passaged in embryonated chicken eggs. Subsequent testing revealed hemagglutination activity in all 6 specimens. Allantoic fluid of the 6 cultured specimens was then shipped to the University of Florida for confirmation testing and sequencing.

Author affiliations: Institute of Veterinary Medicine, Ulaanbaatar, Mongolia (M. Yondon, B. Zayat); National Institutes of Health, Bethesda, Maryland, USA (M.I. Nelson); University of Florida, Gainesville, Florida, USA (G.L. Heil, B.D. Anderson, S.K. White, G.C. Gray); J. Craig Venter Institute, Rockville, Maryland, USA (X. Lin, R.A. Halpin, D.E. Wentworth); and St. Jude Children's Research Hospital, Memphis, Tennessee, USA (P.P. McKenzie)

DOI: http://dx.doi.org/10.3201/eid2012.140435

Figure 1. The 3 aimags from which nasal swab specimens were collected from healthy Bactrian camels, for influenza A virus testing, Mongolia, 2012. 1, Töv; 2, Khentii; 3, Dundgovi.

Only 1 specimen was confirmed positive by influenza A–specific qRT-PCR (cycle threshold [C_t]<35), suggesting possible virus degradation during shipment, despite specimens being shipped on dry ice and carefully handled upon receipt (*10*). The original swab specimen from a camel was later shared with the Mongolia National Influenza Center for confirmation in an anonymized panel of 10 camel swab specimens. Using WHO qRT-PCR procedures, staff identified the specimen as having the strongest evidence (by C_t) of influenza A virus. Staff further studied the specimen with conventional RT-PCR primers and probes for the hemagglutinin and neuraminidase genomes. These reactions yielded amplicons of the expected size, which were sequenced and found to be 100% identical to the corresponding portions of the J. Craig Venter Institute (Rockville, MD, USA) sequences described below.

Sanger sequence data for the hemagglutinin and neuraminidase genes of this isolate demonstrated extremely high levels of identity with recent EIV from Asia isolated under this project in 2011 (*4*). Full-genome sequencing of the 8 genome segments amplified by multisegment RT-PCR (*11*) was performed at the J. Craig Venter Institute by using Ion Torrent PGM technology (Life Technologies, Grand Island, NY, USA) with a 314v2 chip, and the sequences were validated by using the MiSeq platform (Illumina, Inc., San Diego, CA, USA). Full-genome sequence data for this virus, named A/camel/Mongolia/335/2012(H3N8), were deposited in GenBank (accession nos. CY164120.1, CY164121.1, CY164122.1, CY164123.1, CY164124.1, CY164125.1, CY164126.1 and CY164127.1). The isolate should soon (summer 2014) become available for other research use through BEI Resources (Manassas, VA, USA).

For each of the 8 viral genome segments, phylogenetic trees were inferred separately by use of the maximum-likelihood methods available in RAxML version 7.2.6 (*12*), a general time-reversible model of nucleotide

Table. Number of specimens collected from camels, by aimag, each month, and result of testing for influenza A virus, Mongolia, January 2012–January 2013*

	Aimag (province)					
	Töv		Khentii		Dundgovi	
Date	Positive	Total	Positive	Total	Positive	Total
2012						
January	0	20	–	–	–	–
February	–	–	–	–	0	20
March	0	20	–	–	–	–
April	0	20	0	20	–	–
May	0	20	–	–	0	20
June	0	20	–	–	0	20
July	–	–	0	20	0	20
August	0	20	–	–	0	20
September	0	20	–	–	0	20
October	0	20	0	20	–	–
November	–	–	0	20	4	20
December	0	20	–	–	0	20
2013						
January	2	20	0	20	–	–
Total	2	200	0	100	4	160

*Testing was performed by quantitative reverse transcription PCR. A total of 460 specimens were collected across all aimags. – denotes when sampling did not occur because of poor weather or road conditions.

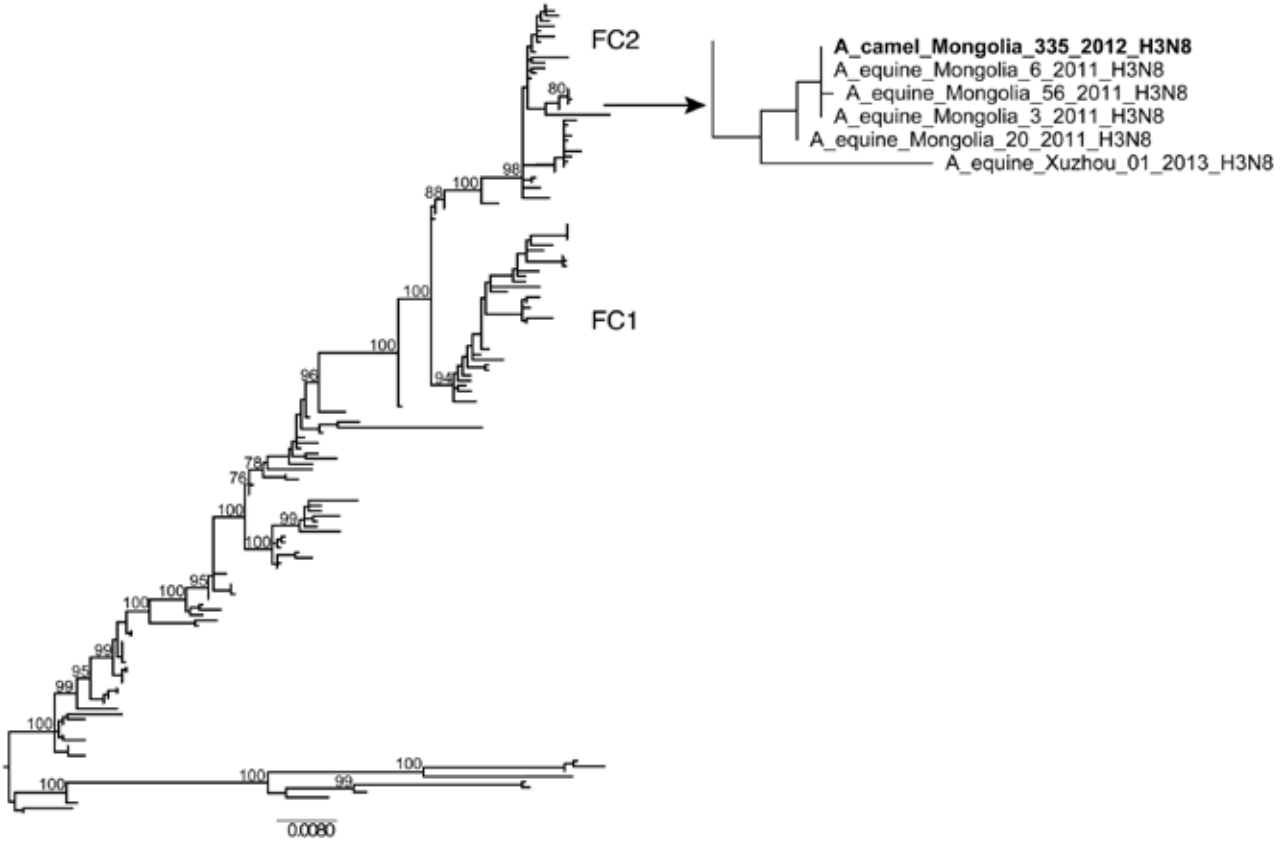

Figure 2. Evolutionary relationships of 155 full-length hemagglutinin sequences from equine A(H3N8)viruses collected globally and A/camel/Mongolia/335/2012 (arrow). The 2 clades associated with most recent equine influenza A(H3N8) viruses, Florida clade 1 and Florida clade 2, are denoted as FC1 and FC2, respectively, and with nomenclature adopted previously (*13*). The maximum-likelihood tree is midpoint rooted for clarity, and all branch lengths are drawn to scale. High (>70) bootstrap values are provided for key nodes. Hemagglutinin sequences containing a 2aa insertion are identified with a solid black circle. Scale bar indicates nucleotide substitutions per site. An expanded version of this figure is available online (http://wwwnc.cdc.gov/EID/article/20/12/14-0435-F2.htm).

substitution, and a gamma-distributed rate variation among sites, with a bootstrapping resampling process (500 replicates). All 8 viral genome segments (polymerase basic protein [PB] 2, PB1, polymerase acidic protein (PA), hemagglutinin (HA) , nucleocapsid protein (NP), neuraminidase (NA), matrix protein (MP), and nonstructural protein (NS) are closely related to the equine influenza A(H3N8) viruses that have recently been circulating among the horse population in Asia; this lineage is evolutionarily distinct from the influenza A(H3N8) viruses circulating among birds in Asia (online Technical Appendix Figures 1–7, http://wwwnc.cdc.gov/EID/article/20/12/14-0435-Techapp1.pdf). A more detailed phylogenetic analysis of the hemagglutinin segment performed by using the additional background sequence data representing the global diversity of influenza A(H3N8) viruses in horses indicates that A/camel/Mongolia/335/2012 is positioned within Florida clade 2 (FC2) (Figure 2) (*13*) and, more specifically, within a bootstrap-supported clade that contains 3 influenza A(H3N8) viruses isolated from horses in Mongolia in 2011: A/equine/Mongolia/6/2011 (100% nt similarity), A/equine/Mongolia/56/2011 (99.9% nt similarity), and A/equine/Mongolia/3/2011 (100% nt similarity). A/camel/Mongolia/335/2012 also contains an insertion of 2 aa (I and F) near the beginning of the hemagglutinin sequence (hemagglutinin positions 8–9, online Technical Appendix) that was first detected among FC2 equine viruses in 2005 (A/equine/Bari/2005/H3N8) and has been detected in most FC2 viruses, including all viruses that are closely related to A/camel/Mongolia/335/2012.

Conclusions

The phylogeny indicates that A/camel/Mongolia/335/2012 probably represents a relatively recent horse-to-camel transmission event. Without additional isolates from camels or corresponding epidemiologic data, and given the close genetic relationship between A/camel/Mongolia/335/2012 and related equine viruses, it is impossible to determine at this time whether the virus has been successfully transmitted from camel to camel.

In recent years, enhanced surveillance has detected influenza A viruses across a wider range of mammalian hosts, including horses, swine, dogs (*14*), seals (*15*), cats, and now camels, providing a more complete picture of the ecology of influenza A viruses beyond their presence in birds. How influenza A viruses successfully jump from 1 host species to another, and what the constraints on interspecies transmission are, remain key questions about influenza virus ecology and assessments of pandemic threats. Our findings highlight the need to further elucidate the ecology of influenza viruses and other pathogens in free-ranging camel populations.

Acknowledgments

We thank Badarch Darmaa for her help with validating the influenza culture work.

This research was supported by multiple grants: contracts HHSN266200700005C (St. Jude Children's Research Hospital) and HHSN272200900007C (J. Craig Venter Institute) from the National Institute of Allergy and Infectious Diseases, National Institutes of Health, Department of Health and Human Services, USA; R01 AI068803-ARRA supplement (G.C.G.) from the National Institute of Allergy and Infectious Diseases; and multiple grants (G.C.G.) from the US Department of Defense Armed Forces Health Surveillance Center, Global Emerging Infections Surveillance and Response Program. This research was conducted within the context of the Multinational Influenza Seasonal Mortality Study, an ongoing international collaborative effort to understand influenza epidemiology and evolution, led by the Fogarty International Center, National Institutes of Health, with funding from the Office of Global Affairs at the Department of Health and Human Services (M.I.N.).

Dr Yondon is a researcher in the Virology Laboratory at the Institute of Veterinary Medicine, Ulaanbaatar, Mongolia. His research interests include the development of new methods and technology for diagnosing, controlling, and preventing viral diseases in animals and their application in veterinary medical practice.

References

1. Waddell GH, Teigland MB, Sigel MM. A new influenza virus associated with equine respiratory disease. J Am Vet Med Assoc. 1963;143:587–90.
2. Crawford PC, Dubovi EJ, Castleman WL, Stephenson I, Gibbs EP, Chen L, et al. Transmission of equine influenza virus to dogs. Science. 2005;310:482–5. http://dx.doi.org/10.1126/science.1117950
3. Hayward JJ, Dubovi EJ, Scarlett JM, Janeczko S, Holmes EC, Parrish CR. Microevolution of canine influenza virus in shelters and its molecular epidemiology in the United States. J Virol. 2010;84:12636–45. http://dx.doi.org/10.1128/JVI.01350-10
4. Yondon M, Heil GL, Burks JP, Zayat B, Waltzek TB, Jamiyan BO, et al. Isolation and characterization of H3N8 equine influenza A virus associated with the 2011 epizootic in Mongolia. Influenza Other Respir Viruses. 2013;7:659–65. http://dx.doi.org/10.1111/irv.12069
5. Anchlan D, Ludwig S, Nymadawa P, Mendsaikhan J, Scholtissek C. Previous H1N1 influenza A viruses circulating in the Mongolian population. Arch Virol. 1996;141:1553–69. http://dx.doi.org/10.1007/BF01718254
6. Yamnikova SS, Mandler J, Bekh-Ochir ZH, Dachtzeren P, Ludwig S, Lvov DK, et al. A reassortant H1N1 influenza A virus caused fatal epizootics among camels in Mongolia. Virology. 1993;197:558–63. http://dx.doi.org/10.1006/viro.1993.1629
7. Caffar Elamin MA, Kheir SA. Detection of influenza antibody in animal sera from Kassala region, Sudan, by agar gel diffusion test. Rev Elev Med Vet Pays Trop. 1985;38:127–9.
8. Olaleye OD, Baba SS, Omolabu SA. Preliminary survey for antibodies against respiratory viruses among slaughter camels (*Camelus dromedarius*) in north-eastern Nigeria [in French]. Revue Scientifique et Technique de l'OIE. 1989;8:779–83.
9. Haagmans BL, Al Dhahiry SH, Reusken CB, Raj VS, Galiano M, Myers R, et al. Middle East respiratory syndrome coronavirus in dromedary camels: an outbreak investigation. Lancet Infect Dis. 2014;14:140–5. http://dx.doi.org/10.1016/S1473-3099(13)70690-X
10. World Health Organization. WHO information for molecular diagnosis of influenza virus in humans—update. 2011 [cited 2013 Jun 10]. http://www.who.int/influenza/resources/documents/molecular_diagnosis_influenza_virus_humans_update_201108.pdf
11. Zhou B, Donnelly ME, Scholes DT, St George K, Hatta M, Kawaoka Y, et al. Single-reaction genomic amplification accelerates sequencing and vaccine production for classical and swine origin human influenza A viruses. J Virol. 2009;83:10309–13. http://dx.doi.org/10.1128/JVI.01109-09
12. Stamatakis A. RAxML-VI-HPC: maximum likelihood-based phylogenetic analyses with thousands of taxa and mixed models. Bioinformatics. 2006;22:2688–90. http://dx.doi.org/10.1093/bioinformatics/btl446
13. Murcia PR, Wood JL, Holmes EC. Genome-scale evolution and phylodynamics of equine H3N8 influenza A virus. J Virol. 2011;85:5312–22. http://dx.doi.org/10.1128/JVI.02619-10
14. Song D, Moon HJ, An DJ, Jeoung HY, Kim H, Yeom MJ, et al. A novel reassortant canine H3N1 influenza virus between pandemic H1N1 and canine H3N2 influenza viruses in Korea. J Gen Virol. 2012;93:551–4. http://dx.doi.org/10.1099/vir.0.037739-0
15. Anthony SJ, St Leger JA, Pugliares K, Ip HS, Chan JM, Carpenter ZW, et al. Emergence of fatal avian influenza in New England harbor seals. mBio. 2012;3:e00166-12.

Address for correspondence: Gregory C. Gray, College of Public Health and Health Professions, University of Florida, Box 100188, Gainesville, FL 32610, USA: email: gcgray@phhp.ufl.edu

Health Care Worker Contact with MERS Patient, Saudi Arabia

Aron J. Hall, Jerome I. Tokars, Samar A. Badreddine, Ziad Bin Saad, Elaine Furukawa, Malak Al Masri, Lia M. Haynes, Susan I. Gerber, David T. Kuhar, Congrong Miao, Suvang U. Trivedi, Mark A. Pallansch, Rana Hajjeh, and Ziad A. Memish

To investigate potential transmission of Middle East respiratory syndrome coronavirus (MERS-CoV) to health care workers in a hospital, we serologically tested hospital contacts of the index case-patient in Saudi Arabia, 4 months after his death. None of the 48 contacts showed evidence of MERS-CoV infection.

Middle East respiratory syndrome coronavirus (MERS-CoV) was initially isolated in September 2012 from a 60-year-old man from Bisha, Saudi Arabia (*1*). In June 2012, this index case-patient was hospitalized for severe respiratory disease in Jeddah at Dr. Soliman Fakeeh Hospital and subsequently died (*1*). As of November 3, 2014, a total of 897 laboratory-confirmed cases of MERS-CoV infection, including 325 deaths, had been reported to the World Health Organization; >85% of reported MERS-CoV cases and deaths have occurred in Saudi Arabia (*2*). The clinical syndrome among hospitalized MERS-CoV patients includes severe acute respiratory illness, sometimes associated with hypoxemic respiratory failure and extrapulmonary organ dysfunction (*3*); however, milder illness and asymptomatic infections have been identified through contact investigations (*4*–6). Transmission of MERS-CoV to health care workers (HCWs) has been reported (*5*,*6*), although no sustained community transmission has been identified.

A zoonotic origin of MERS-CoV has been hypothesized; camels potentially play a role in transmission (*7*), although the specific types of exposure associated with primary cases remain unknown. There remains a dearth of information on how MERS-CoV is spread and on transmission risks to HCW or other close contacts. Our objectives were to evaluate the degree and nature of HCW contact with the MERS-CoV index case-patient and to serologically assess HCWs for MERS-CoV infection. The field investigation was performed in October 2012; we awaited development and validation of MERS-CoV serologic assays before completing the study.

Author affiliations: Centers for Disease Control and Prevention, Atlanta, Georgia, USA (A.J. Hall, J.I. Tokars, L.M. Haynes, S.I. Gerber, D.T. Kuhar, C. Miao, S.U. Trivedi, M.A. Pallansch, R. Hajjeh); Dr. Soliman Fakeeh Hospital, Jeddah, Saudi Arabia (S.A. Badreddine); and Ministry of Health, Riyadh, Saudi Arabia (Z. Bin Saad, E. Furukawa, M. Al Masri, Z.A. Memish)

DOI: http://dx.doi.org/10.3201/eid2012.141211

The Study

The index case-patient was hospitalized on June 13, 2012, with a 7-day history of fever, cough, sputum expectoration, and shortness of breath. Precautions to prevent airborne transmission were taken by placing the patient in a private room with negative pressure for the first 2 days of hospitalization. After an infectious disease consultation on day 2, airborne-transmission precautions were replaced with droplet-transmission precautions; after a multidrug-resistant organism was isolated on day 4, contact-transmission precautions were implemented (*8*). The case-patient remained in a private room, under standard and contact-transmission precautions, throughout hospitalization until he died on day 11.

Using dates and units in which the case-patient received care, hospital staff initially identified HCWs who had had contact with the case-patient (came within 2 meters of the case-patient or his bedding, equipment, or body fluids). A comparison group of approximately equal numbers of HCWs (preferentially with similar job responsibilities) was selected from HCWs who had had no known contact with the case-patient. Hospital infection control staff administered a brief, standardized questionnaire to both groups of HCWs. Information was collected on HCW demographics, job duties, and symptoms of respiratory disease during June 15–July 4, 2012, which corresponds to the period when the case-patient was hospitalized and an incubation period of 2–10 days, based on MERS-CoV natural history information available at the time of investigation. Specific information about circumstances of case-patient contact and potential for MERS-CoV exposure was collected from HCWs who had had contact with the case-patient.

In October 2013 (4 months after the case-patient's death), a blood specimen (<20 mL) was collected from each HCW and transported first to the Ministry of Health Western Regional Laboratory in Saudi Arabia and then to the US Centers for Disease Control and Prevention for MERS-CoV testing. Upon receipt, specimens were gamma-irradiated on dry ice and stored at –70°C. All specimens were tested by HKU5.2N nucleocapsid enzyme immunoassay (EIA) (*9*); incubations and substrate development were conducted at 37°C. MERS-CoV antibody positivity was defined as positive HKU5.2N screening EIA results and confirmed by MERS-CoV immunofluorescence or microneutralization assay (*9*,*10*); specimens with negative EIA results were considered antibody negative.

Of 56 HCWs identified as having had contact with the MERS-CoV case-patient, 5 were unavailable for interview and 3 refused serum collection, leaving 48 for the final analysis. Among HCWs who had had case-patient contact, median age was 30.5 (range 22–57) years; 29 (60%) were female; 24 (50%) were nurses; 14 (29%) were physicians; 7 (15%) were respiratory technicians; and 1 each was a housekeeping, radiology, or infection control staff member. Six (13%) HCWs reported having a chronic medical condition (e.g., asthma, diabetes, hypertension), and 6 (13%) reported smoking tobacco. According to body mass index (BMI) calculations from self-reported height and weight, nearly half of HCWs were overweight (BMI 25.0–29.9, n = 11 [23%]) or obese (BMI ≥30.0, n = 12 [25%]).

Most of the 48 HCWs had reportedly come within 1 meter of the case-patient (89%); touched the case-patient (85%); or touched the case-patient's bedding, equipment, or body fluids (62%) (Table). During a single shift, most (60%) HCWs reported <1 hour of case-patient contact, but 23% reported ≥5 hours of contact. HCWs reported having been present during airway suction (50%), nebulizer treatment (30%), sputum induction (23%), bronchoscopy (9%), and intubation (6%). Infection control precautions reportedly used by HCWs during contact with the case-patient included hand hygiene (100%) and/or wearing of gloves (94%), surgical mask (87%), and gown (40%); however, among those reporting use of these precautions, some admitted to <100% compliance and none used eye protection.

Table. Contact characteristics for 48 health care workers who had contact with Middle East respiratory syndrome coronavirus index case-patient, Jeddah, Saudi Arabia, June 2012

Characteristic	No. (%)
Unit where contact occurred	
Intensive care unit	21 (43.8)
Consult	7 (14.6)
Respiratory treatment	7 (14.6)
Respiratory disease unit	4 (8.3)
Emergency department	3 (6.3)
Bronchoscopy	2 (4.2)
Infectious disease unit	2 (4.2)
Virology laboratory	1 (2.1)
Infection control	1 (2.1)
Type of contact*	
Came within 1 m of patient	43 (89.6)
Touched patient	41 (85.4)
Touched patient's bedding, equipment, or body fluids	30 (62.5)
Collected clinical specimens	19 (39.6)
Emptied bedpan	11 (22.9)
Maximum contact duration during any shift	
<1 h	28 (58.3)
1–2 h	4 (8.3)
3–4 h	4 (8.3)
≥5 h	12 (25.0)
Care provided to patient*	
Physical examination	24 (50.0)
Assessment of vital signs	19 (39.6)
Lifting or positioning	15 (31.3)
Medication administration	14 (29.2)
Blood collection	14 (29.2)
Linen change	12 (25.0)
Bathing	11 (22.9)
Feeding	11 (22.9)
Intravenous catheter placement	11 (22.9)
Radiography	5 (10.4)
Present during medical procedures*	
Airway suction	24 (50.0)
Nebulizer treatment	14 (29.2)
Sputum induction	11 (22.9)
Bronchoscopy	4 (8.3)
Intubation	3 (6.3)
Infection control precautions used during patient contact*	
Hand hygiene	48 (100)
Gloves	45 (93.8)
Surgical mask	42 (87.5)
Gown	19 (39.6)
N95 mask	16 (33.3)
Eye protection	0

*Because >1 response could be selected for these characteristics, percentages may total >100%.

Respiratory disease symptoms during June 15–July 4 were reported by 10 (21%) HCWs who had had case-patient contact. Among these, symptoms included cough (40%), sore throat (30%), myalgia (30%), rhinorrhea (20%), self-reported fever (10%), diarrhea (10%), and sneezing (10%); 2 (20%) of these 10 HCWs sought medical care and received a diagnosis of pharyngitis. For comparison, respiratory symptoms were reported during the same period by 16 (33%) HCWs who had not had case-patient contact. Results of EIA testing of serum collected during October 14–17, 2012, from all 48 HCWs who had and all 48 who had not had case-patient contact were negative for MERS-CoV. Immunofluorescence assay of 13 randomly selected serum specimens also gave negative MERS-CoV results, supporting interpretation of EIA-negative specimens as antibody negative.

Conclusions

This investigation provides indicators of transmission potential during the initial emergence of MERS-CoV. The lack of MERS-CoV transmission among HCWs in this study is similar to results of some published contact investigations (*11*,*12*) but different from others that reported transmission to HCW contacts (*5*,*6*). Recovery of cultivable virus from the sputum of the case-patient reported here (*1*) and the severity of illness suggest some potential for virus transmission. We did not assess use of recommended personal protective equipment during each episode of case-patient contact; however, the reported lack of use during every episode of patient contact suggests that some HCWs might have been exposed to MERS-CoV. Nonetheless, the infection control precautions that were used might have contributed to the demonstrated lack of transmission.

Serologic assays to determine past infections are useful for assessing the risk for MERS-CoV transmission (*13*). The assays used in this study have previously detected MERS-CoV–specific antibodies ≤2 weeks and ≥13 months after illness onset with ≥97% specificity (*9*,*14*). Although no severely ill HCWs were identified during this investigation, real-time reverse transcription PCR detection of MERS-CoV in respiratory tract specimens from asymptomatic or mildly ill HCWs during other contact investigations has been described (*5*,*15*). The timing of this investigation 4 months after hospitalization of the case-patient precluded use of real-time reverse transcription PCR and potentially introduced recall bias during HCW interviews.

Despite numerous case-patient contact episodes among HCWs, we found no serologic evidence suggesting health care–associated transmission of MERS-CoV from the index case-patient. Rapid identification of potentially infected patients and implementation of infection control precautions can help protect HCWs. US Centers for Disease Control and Prevention recommendations for management of hospitalized patients with known or suspected MERS-CoV infection include implementing standard, contact- and airborne transmission precautions (*15*).

Acknowledgments

We are extremely grateful for the collaboration of the participating HCW in this investigation. Additionally, we thank Idris Sulemann for assistance with data entry and management and Jennifer L. Harcourt, Hayat Caidi, and Azaibi Tamin for performing the serologic evaluations.

This work was supported by the US Global Disease Detection Operations Center Outbreak Response Contingency Fund.

Dr Hall is a veterinarian and an epidemiologist in the Division of Viral Diseases of the National Center for Immunization and Respiratory Diseases at the US Centers for Disease Control and Prevention. His research interests focus on the epidemiology of emerging viral diseases, specifically caliciviruses and coronaviruses.

References

1. Zaki AM, van Boheemen S, Bestebroer TM, Osterhaus AD, Fouchier RA. Isolation of a novel coronavirus from a man with pneumonia in Saudi Arabia. N Engl J Med. 2012;367:1814–20. http://dx.doi.org/10.1056/NEJMoa1211721.
2. World Health Organization. Middle East respiratory syndrome coronavirus (MERS-CoV)— update. Disease Outbreak News. 2014 Nov 3 [cited 2014 Nov 4]. http://www.who.int/csr/don/2014_07_14_mers/en/
3. Assiri A, Al-Tawfiq JA, Al-Rabeeah AA, Al-Rabiah FA, Al-Hajjar S, Al-Barrak A, et al. Epidemiological, demographic, and clinical characteristics of 47 cases of Middle East respiratory syndrome coronavirus disease from Saudi Arabia: a descriptive study. Lancet Infect Dis. 2013;13:752–61. http://dx.doi.org/10.1016/S1473-3099(13)70204-4.
4. Health Protection Agency UK Novel Coronavirus Investigation Team. Evidence of person-to-person transmission within a family cluster of novel coronavirus infections, United Kingdom, February 2013. Euro surveillance. 2013;18: pii: 20427.
5. Assiri A, McGeer A, Perl TM, Price CS, Al Rabeeah AA, Cummings DA, et al. Hospital outbreak of Middle East respiratory syndrome coronavirus. N Engl J Med. 2013;369:407–16. http://dx.doi.org/10.1056/NEJMoa1306742.
6. Memish ZA, Zumla AI, Assiri A. Middle East respiratory syndrome coronavirus infections in health care workers. N Engl J Med. 2013;369:884–6. http://dx.doi.org/10.1056/NEJMc1308698.
7. Memish ZA, Cotten M, Meyer B, Watson SJ, Alsahafi AJ, Al Rabeeah AA, et al. Human infection with MERS coronavirus after exposure to infected camels, Saudi Arabia, 2013. Emerg Infect Dis. 2014;20:1012–5. http://dx.doi.org/10.3201/eid2006.140402.
8. Centers for Disease Control and Prevention. 2007 Guideline for isolation precautions: preventing transmission of infectious agents in healthcare settings [cited 2014 Jun 30]. http://www.cdc.gov/hicpac/2007IP/2007isolationPrecautions.html
9. Al-Abdallat MM, Payne DC, Alqasrawi S, Rha B, Tohme RA, Abedi GR, et al. Hospital-associated outbreak of Middle East respiratory syndrome coronavirus: a serologic, epidemiologic, and clinical description. Clin Infect Dis. 2014; May 14. pii: ciu359 [cited 2014 Jul 8]. [Epub ahead of print]. http://dx.doi.org/10.1093/cid/ciu359

10. Payne DC, Iblan I, Alqasrawi S, Al Nsour M, Rha B, Tohme RA, et al. Stillbirth during infection with Middle East respiratory syndrome coronavirus. J Infect Dis. 2014;209:1870–2. http://dx.doi.org/10.1093/infdis/jiu068.
11. Pebody RG, Chand MA, Thomas HL, Green HK, Boddington NL, Carvalho C, et al. The United Kingdom public health response to an imported laboratory-confirmed case of a novel coronavirus in September 2012. Euro Surveill. 2012;17:20292.
12. Mailles A, Blanckaert K, Chaud P, van der Werf S, Lina B, Caro V, et al. First cases of Middle East respiratory syndrome coronavirus (MERS-CoV) infections in France, investigations and implications for the prevention of human-to-human transmission, France, May 2013. Euro Surveill. 2013;18:20502.
13. Consortium for the Standardization of Influenza Seroepidemiology. Novel coronavirus (MERS-CoV) [cited 2014 Aug 12]. https://consise.tghn.org/articles/novel-coronavirus-ncov/
14. Kapoor M, Pringle K, Kumar A, Dearth S, Liu L, Lovchik J, et al. Clinical and laboratory findings of the first imported case of Middle East respiratory syndrome coronavirus (MERS-CoV) into the United States. Clin Infect Dis. 2014 Aug 6. pii: ciu635 [cited 2014 Aug 6]. http://dx.doi.org/10.1093/cid/ciu635
15. Bialek SR, Allen D, Alvarado-Ramy F, Arthur R, Balajee A, Bell D, et al. First confirmed cases of Middle East respiratory syndrome coronavirus (MERS-CoV) infection in the United States, updated information on the epidemiology of MERS-CoV infection, and guidance for the public, clinicians, and public health authorities—May 2014. MMWR Morb Mortal Wkly Rep. 2014;63:431–6.

Address for correspondence: Aron J. Hall, Centers for Disease Control and Prevention, 1600 Clifton Rd NE, Mailstop A34, Atlanta, GA 30329-4027, USA; email: ajhall@cdc.gov; Ziad Memish, Ministry of Health, Riyadh 11176, Saudi Arabia; email: zmemish@yahoo.com

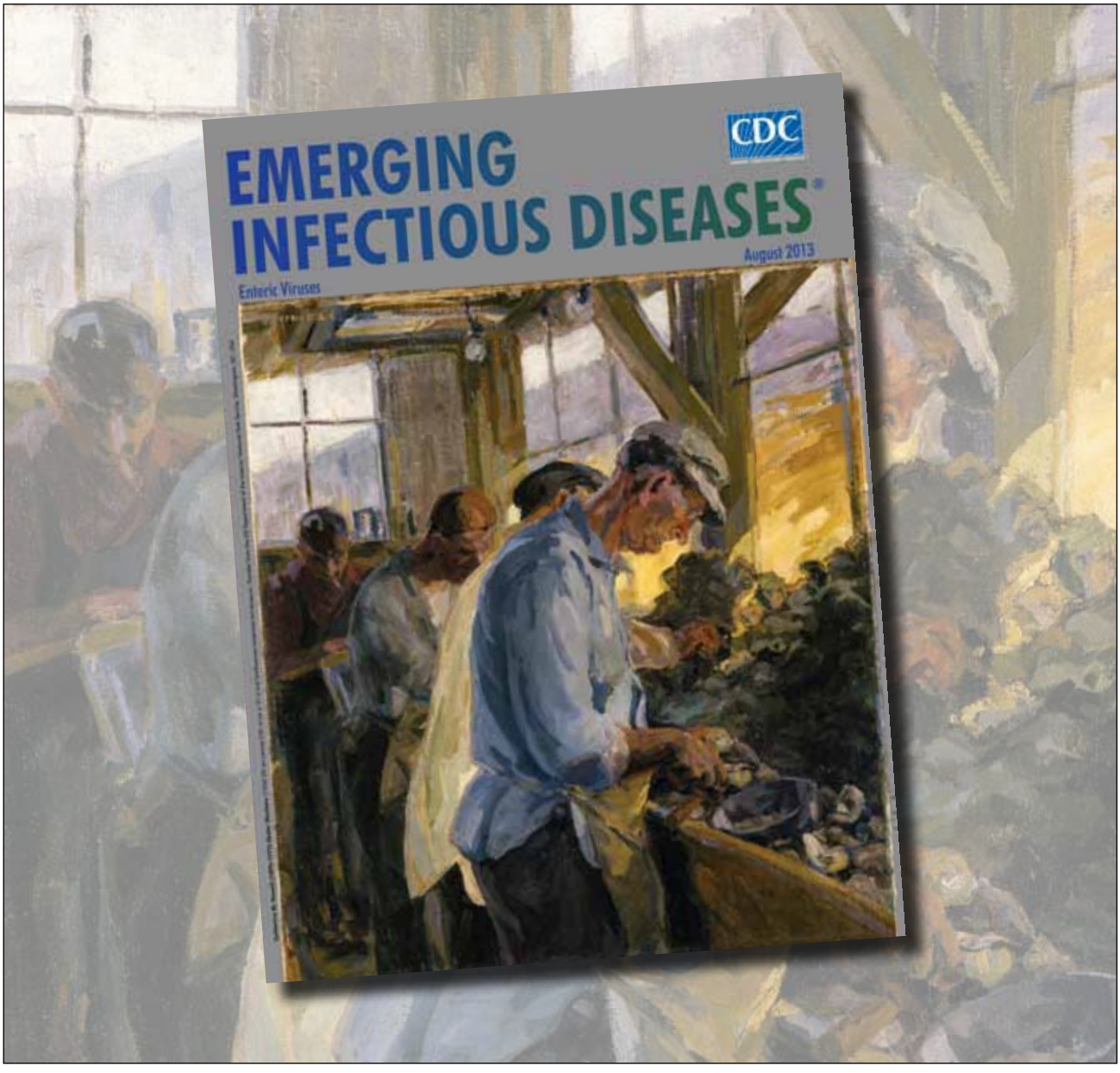

Subclinical Highly Pathogenic Avian **Influenza Virus** Infection in Vaccinated Chickens, China

Qing-Xia Ma, Wen-Ming Jiang, Shuo Liu, Su-Chun Wang, Qing-Ye Zhuang, Guang-Yu Hou, Xiang-Ming Liu, Zheng-Hong Sui, and Ji-Ming Chen

Subclinical infection of vaccinated chickens with a highly pathogenic avian influenza A(H5N2) virus was identified through routine surveillance in China. Investigation suggested that the virus has evolved into multiple genotypes. To better control transmission of the virus, we recommend a strengthened program of education, biosecurity, rapid diagnostics, surveillance, and elimination of infected poultry.

Highly pathogenic avian influenza (HPAI) type A viruses of the subtype H5 have been circulating among poultry in several countries of Asia and Africa for many years. HPAI viruses of this subtype have also caused hundreds of infections among humans and presented a substantial threat to public health (*1*,*2*). China is one of the countries deeply affected by zoonotic viruses of this subtype (*3*). The government of China decided during 2005 to use a comprehensive strategy to control this zoonosis involving mass vaccination of poultry and strict culling of infected flocks (*2*). Although this strategy has played a successful role in guaranteeing safety of food supplies, maintaining the poultry system, and minimizing human infections, governmental agencies in China are considering how to exit from mass vaccination programs, mainly because of the tremendous cost of this intervention. We report here an investigation of recent subclinical circulation of the HPAI virus among egg-laying chickens on a farm in China, to provide novel data and views on the evolution of the virus and improvement of HPAI control in China.

Author affiliations: College of Marine Life Sciences, Ocean University of China, Qingdao, China (Q.-X. Ma, Z.-H Sui); China Animal Health and Epidemiology Center, Qingdao (W.-M. Jiang, S. Liu, S.-C. Wang, Q.-Y. Zhuang, G.-Y. Hou, X.-M. Liu, J.-M. Chen); and Qingdao Center for Control of Animal Infectious Diseases, Qingdao (Q.-X. Ma)

DOI: http://dx.doi.org/10.3201/eid2012.140733

The Study

During routine surveillance in January 2014, we collected 30 swab samples from chickens on an egg-laying chicken farm populated by 12,000 320-day-old and 6,000 150-day-old chickens without any clinical signs, in Qingdao, Shandong Province, China. Of those, 5 were positive by real-time reverse transcription PCR for detection of the hemagglutinin (HA) gene of H5 HPAI viruses. The flock was culled immediately after the diagnosis, and an H5N2 subtype HPAI virus was isolated by inoculating specific-pathogen-free embryonated eggs with the collected samples. The entire viral genome of the virus, A/chicken/Qingdao/1/2014(H5N2), abbreviated as H5N2qd14, was sequenced and analyzed as described (*4*). The sequences were deposited in GenBank under accession nos. KJ683877–KJ683884. We used the full-length sequences for each gene in phylogenetic analyses.

The HA protein of the H5N2qd14 virus has multiple basic amino acid residues (PQIEGRRRKR↓GLF) at the cleavage site, categorizing it as an HPAI virus. Its intravenous pathogenicity index is 2.84, determined by intravenously inoculating 10 chickens, which were 6 weeks old and specific pathogen–free, with 0.1 mL of a 1:10 dilution of the H5N2qd14 allantoic fluid. Phylogenetic analysis of the HA gene suggested that H5N2qd14 is a variant of clade 7.2 (Figure); this variant has become predominant in clade 7.2 in China since 2011 (*5*). Re-4, the vaccine strain which corresponds to this clade, was generated in 2006 through reverse genetics: the HA gene was derived from the virus A/chicken/Shanxi/2/2006 (*2*). As compared with the vaccine strain, 47 aa mutations occurred in the HA protein of H5N2qd14, of which 9 (I124V, H126R, G154E, K155N, L162V, I166T, T182A, V189I, D198N) were located on the antigenic epitopes of the viral protein, suggesting that H5N2qd14 is likely distinct in antigenicity from the vaccine strain (*6*,*7*). This conclusion is supported by our epidemiologic investigation, which revealed that the affected flock had been vaccinated 3 times with the vaccine strain Re-4. Moreover, we collected 30 serum samples from the flock simultaneously with the swab samples, and analyzed them using the hemagglutination inhibition (HI) assay. The geometric mean and standard deviation of the HI titers of these 30 serum samples were 250.51 ± 2.93 against the vaccine strain Re-4 and 10.83 ± 2.79 against H5N2qd14, showing a 23-fold difference. Additionally, the geometric mean and standard deviation of the HI titers of 20 standard serum specimens specifically against the vaccine strain Re-4, which we prepared in-house using specific pathogen–free chickens, were 388.02 ± 1.92 against the vaccine strain Re-4 and only 4.92 ± 1.48 against H5N2qd14, with a 78-fold difference.

Phylogenetic analysis of the genomic sequences further suggested that the 2 genomic segments of H5N2qd14 coding the HA and matrix protein genes were likely from

recent H5N1 HPAI viruses in clade 7.2, and the remaining 6 genomic segments of H5N2qd14 likely reassorted from subtype H9N2 avian influenza virus (Figure, online Technical Appendix Figures 1–7 [wwwnc.cdc.gov/EID/article/20/12/14-0733-Techapp.pdf]). Moreover, analysis of the viral genomic sequences available in the Global Initiative on Sharing Avian Influenza Data (http://platform.gisaid.org/epi3/frontend#216031) suggested that H5N2 HPAI viruses have evolved into ≥2 HA clades (clades 7.2 and 2.3.4) and 6 genotypes in China in recent years (Table, online Technical Appendix Figures 1–7). The genotype corresponding to H5N2qd14 has been identified in 2 other provinces, Henan and Jiangsu, in China during 2013 (Table). The H5N2 HPAI viruses in clade 2.3.4 are also likely vaccine-escape variants as suggested by the similar phylogenetic and antigenic analysis given above (data not shown).

No mutations in the viral HA protein that confer binding to human-like receptors were identified, suggesting that this virus likely cannot bind efficiently to human-like receptors (*8*). No mutations in the viral polymerase basic 2 protein, which are associated with high pathogenicity of the virus in mammals, were identified (*9*). No mutations in the viral neuraminidase protein (NA), which confers resistance to oseltamivir, were identified (*10*). However, a mutation of S31N occurred in the viral matrix 2 protein, which could render the virus resistant to amantadine (*11*,*12*).

Our epidemiologic investigation revealed that the farm of the affected flock had multiple biosecurity deficiencies. For example, the farm was 80 meters from a road on which a high volume of garbage trucks traveled. Additionally, the farm had neither procedures for control and disinfection of vehicles and pedestrians entering the property, nor facilities to exclude rodents and wild birds, and many sparrows shared the feed with the egg-laying chickens in the poultry house.

Conclusions

HPAI mass vaccination played a crucial role in HPAI control in China. However, this study demonstrated multiple disadvantages of HPAI mass vaccination, which had been suspected (*13*,*14*). For example, this study showed that H5N1 subtype HPAI virus has evolved into multiple H5N2 genotypes, which are all likely vaccine-escape variants, suggesting that this virus can easily evolve into vaccine-escape variants. This observation suggests that HPAI mass vaccination, which is highly effective in the beginning of an outbreak, may lose its effectiveness with time unless the vaccine strains are updated. Moreover, this study showed that vaccinated chicken flocks can be infected with vaccine-escape variants without signs of illness. Thus HPAI mass vaccination may increase shedding of the virus by infected chickens that otherwise would likely exhibit signs of illness and die soon after infection; therefore, HPAI mass vaccination may increase spread of a virus that otherwise would be easily identified by observation of clinical signs.

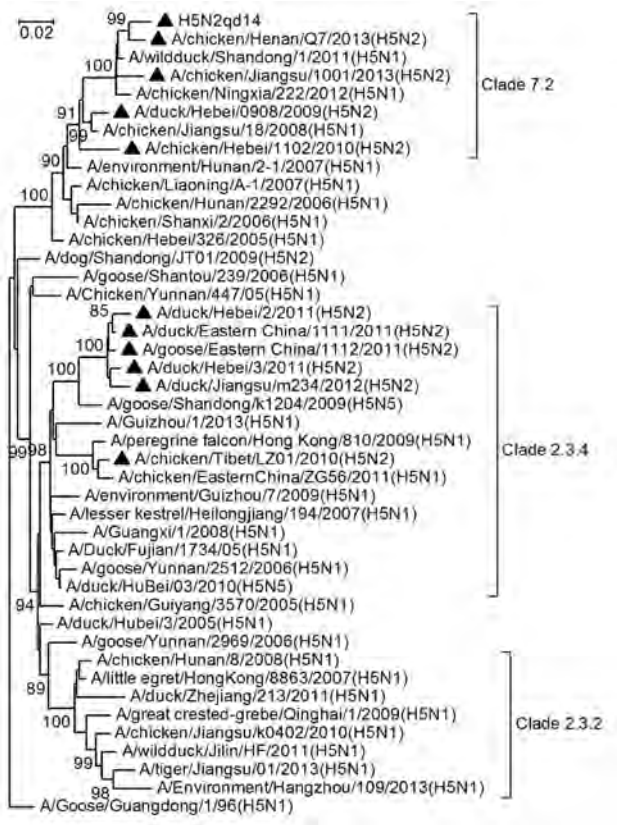

Figure. The phylogenetic relationships among some subtype H5 highly pathogenic influenza viruses based on their heamagluttinin sequences. The H5N2 subtype viruses identified in China in recent years are marked with black triangles. Bootstrap values are given at relevant nodes.

Currently, HPAI mass vaccination in poultry should not be stopped; otherwise, many HPAI outbreaks could likely occur in poultry farms with limited biosecurity. Conversely, HPAI mass vaccination in China cannot be expected to have a progressive effect because the practice leads to silent spread of vaccine-escape variants selected in the host immunologicpressure induced against vaccine strains. We propose that the only way out of this dilemma is to strengthen the strategy published previously, which covers the following components: education, biosecurity, rapid diagnostics and surveillance, and elimination of infected poultry (*14*). Mass vaccination should be used as an additional tool within this 4-component strategy, not in place of the 4 components.

This work was supported by the Sci-tech Basic Work Project of Ministry of Science and Technology (SQ2012FY3260033).

Dr Ma is a veterinary researcher at Qingdao Center for Control of Animal Infectious Diseases. Her research interests are epidemiology and control of animal infectious diseases.

Table. Six genotypes of highly pathogenic avian influenza type A identified during 2009–2014 calculated through phylogenetic analysis, China

Genotype	Representative virus	Clade	Lineage of gene*							
			PB2	PB1	PA	HA	NP	NA	M	NS
1	H5N2qd14	7.2	A	A	A	B	A	A	B	A
	A/chicken/Jiangsu/1001/2013(H5N2)	7.2	A	A	A	B	A	A	B	A
	A/chicken/Henan/Q7/2013(H5N2)	7.2	A	A	A	B	A	A	B	A
2	A/chicken/Hebei/1102/2010(H5N2)	7.2	A	A	A	B	A	A	A	A
3	A/duck/Hebei/0908/2009(H5N2)	7.2	B	B	B	B	B	B	C	B
4	A/duck/Hebei/2/2011(H5N2)	2.3.4	C	C	C	C	C	C	D	C
5	A/duck/Jiangsu/m234/2012(H5N2)	2.3.4	C	B	C	C	C	B	D	C
6	A/chicken/Tibet/LZ01/2010(H5N2)	2.3.4	D	A	A	D	A	A	A	D

*Lineages of each gene are partially shown in online Technical Appendix Figures 1–7 (wwwnc.cdc.gov/EID/article/20/12/14-0733-Techapp.pdf). Lineage A of each gene is likely from H9N2 subtype avian influenza virusess. Any 2 viruses with ≥1 gene of different lineages belong to different genotypes. PB, polymerase basic protein; PA, polymerase acidic protein; HA, hemagglutinin; NP, nucleocapsid protein; NA, neuraminidase; M, matrix protein; NS, nonstructural protein.

References

1. Chen JM, Chen JW, Dai JJ, Sun YX. A survey of human cases of H5N1 avian influenza reported by the WHO before June 2006 for infection control. Am J Infect Control. 2007;35:467–9. http://dx.doi.org/10.1016/j.ajic.2006.12.001
2. Chen H. H5N1 avian influenza in China. Sci China C Life Sci. 2009;52:419–27. http://dx.doi.org/10.1007/s11427-009-0068-6
3. Li Y, Shi J, Zhong G, Deng G, Tian G, Ge J, et al. Continued evolution of H5N1 influenza viruses in wild birds, domestic poultry, and humans in China from 2004 to 2009. J Virol. 2010;84:8389–97. http://dx.doi.org/10.1128/JVI.00413-10
4. Hoffmann E, Stech J, Gu Y, Webster RG, Perez DR. Universal primer set for the full-length amplification of all influenza A viruses. Arch Virol. 2001;146:2275–89. http://dx.doi.org/10.1007/s007050170002
5. Liu H, Wang X, Wang J, Zhao Y, Zheng D, Chen J, et al. Genome sequences of an H5N1 highly pathogenic avian influenza virus isolated from vaccinated layers in China in 2012. Genome Announc. 2013;1:e00936–13. http://dx.doi.org/10.1128/genomeA.00936-13
6. Kaverin NV, Rudneva IA, Govorkova EA, Timofeeva TA, Shilov AA, Kochergin-Nikitsky KS, et al. Epitope mapping of the hemagglutinin molecule of a highly pathogenic H5N1 influenza virus by using monoclonal antibodies. J Virol. 2007;81:12911–7. http://dx.doi.org/10.1128/JVI.01522-07
7. Velkov T, Ong C, Baker MA, Kim H, Li J, Nation RL, et al. The antigenic architecture of the hemagglutinin of influenza H5N1 viruses. MolImmunol. 2013;56:705–19. http://dx.doi.org/10.1016/j.molimm.2013.07.010
8. Tharakaraman K, Raman R, Viswanathan K, Stebbins NW, Jayaraman A, Krishnan A, et al. Structural determinants for naturally evolving H5N1 hemagglutinin to switch its receptor specificity. Cell. 2013;153:1475–85. http://dx.doi.org/10.1016/j.cell.2013.05.035
9. Hatta M, Gao P, Halfmann P, Kawaoka Y. Molecular basis for high virulence of Hong Kong H5N1 influenza A viruses. Science. 2001;293:1840–2. http://dx.doi.org/10.1126/science.1062882
10. Yen HL, Ilyushina NA, Salomon R, Hoffmann E, Webster RG, Govorkova EA. Neuraminidase inhibitor-resistant recombinant A/Vietnam/1203/04 (H5N1) influenza viruses retain their replication efficiency and pathogenicity in vitro and in vivo. J Virol. 2007;81:12418–26. http://dx.doi.org/10.1128/JVI.01067-07
11. Yan J, Lu Y, Mao H, Feng Y, Xu C, Shi W, et al. Pathogenic and molecular characterization of the H5N1 avian influenza virus isolated from the first human case in Zhejiang province, China. Diagn Microbiol Infect Dis. 2007;58:399–405. http://dx.doi.org/10.1016/j.diagmicrobio.2007.03.004
12. He G, Qiao J, Dong C, He C, Zhao L, Tian Y. Amantadine-resistance among H5N1 avian influenza viruses isolated in Northern China. Antiviral Res. 2008;77:72–6. http://dx.doi.org/10.1016/j.antiviral.2007.08.007
13. Savill NJ, St Rose SG, Keeling MJ, Woolhouse ME. Silent spread of H5N1 in vaccinated poultry. Nature. 2006;442:757. http://dx.doi.org/10.1038/442757a
14. Swayne DE. Impact of vaccines and vaccination on global control of avian influenza. Avian Dis. 2012;56:818–28. http://dx.doi.org/10.1637/10183-041012-Review.1

Address for correspondence: Ji-Ming Chen, Laboratory of Surveillance for Avian Diseases, China Animal Health and Epidemiology Center, No. 369 Nanjing Rd, Qingdao 266032, China; email: chenjiming@cahec.cn

Two Outbreaks of *Listeria monocytogenes* Infection, Northern Spain

Emilio Pérez-Trallero, Carmen Zigorraga, Junkal Artieda, Miriam Alkorta, and José M. Marimón

In the province of Gipuzkoa, Spain (≈700,000 inhabitants), 7–12 episodes of human listeriosis were recorded annually during 2009–2012. However, during January 2013–February 2014, 27 episodes were detected, including 11 pregnancy-associated cases. Fifteen cases in 2 epidemiologically unrelated outbreaks were caused by a rare type of *Listeria monocytogenes*, sequence type 87 serotype 1/2b.

Listeriosis is a bacterial zoonotic infection caused by *Listeria monocytogenes*. Most human listeriosis episodes are sporadic, but outbreaks affecting a large number of persons can distort the usual annual incidence of infection in a region. Several *L. monocytogenes* serotypes have been identified, and not all have the same capacity to infect humans; most human cases are caused by serotypes 1/2a, 1/2b, and 4b (*1*). Although the circulating serotypes have been well defined, little is known about the genetic diversity of *L. monocytogenes*.

During January 2009–December 2012, the province of Gipuzkoa in Basque Country, northern Spain (≈700,000 inhabitants), recorded 7–12 annual episodes of listeriosis. However, during January 2013–February 2014, a total of 27 human listeriosis episodes were detected in this region. Most of the isolates identified were sequence type (ST) 87 and serotype 1/2b. To date, ST87 represents a rare ST from lineage I that had previously been reported in food (*2*,*3*) but had not been shown to cause human infections. We describe 2 epidemiologically unrelated outbreaks of listeriosis caused by ST87 that occurred at the same time in the same region. For 1 of these outbreaks, the causative agent was found in contaminated food.

Author affiliations: Hospital Universitario Donostia, Instituto de Investigación Sanitaria Biodonostia and Centros de Investigación Biomédica en Red, San Sebastián, Spain (E. Pérez-Trallero, M. Alkorta, J.M. Marimón); Public Health Division of Gipuzkoa, Basque Government, San Sebastián (C. Zigorraga, J. Artieda); and University of the Basque Country Faculty of Medicine, San Sebastián (E. Pérez-Trallero)

DOI: http://dx.doi.org/10.3201/eid2012.140993

The Study

In Gipuzkoa, 27 human listeriosis episodes were reported during January 2013–February 2014. All cases produced sepsis in the patients, except 1 case that produced diarrheal disease in a 34-year-old parturient woman who had undergone a splenectomy. Eleven episodes (40.7%) occurred in pregnant or parturient women, and 8 of the children of these patients were affected: 5 newborns (4 of them premature infants) became ill, 2 pregnancies ended in miscarriage, and 1 infant was stillborn. (For this study, a pregnancy-associated episode was counted only once, whether the causative strain was isolated from mother, child, or both.) Ten cases (37.0%) occurred among the elderly (>70 years of age) and 6 (22.2%) in adults 45–60 years of age. Of the 6 patients in the 45- to 60-year age group, 3 were apparently healthy and 3 immunocompromised. Three of the 10 elderly patients died.

Human *L. monocytogenes* isolates were obtained by using routine microbiological procedures. A total of 29 human *L. monocytogenes* isolates were available for microbiological characterization: 22 from blood, 3 from placental membranes, 2 from cerebrospinal fluid, and 1 each from stool and dermal exudate. Serotypes were established by agglutination (Listeria-O-antisera, Difco; BD Diagnostics, Sparks, MD, USA) and by multiplex-PCR (*4*). The predominant serotypes identified were 1/2b (n = 17, 58.6%) and 4b (n = 8, 27.6%); 4 isolates were serotype 1/2a (13.8%).

Pulsed-field gel electrophoresis (PFGE) was performed by using the restriction endonucleases *Sma*I and *Asc*I (*5*). The STs of *L. monocytogenes* isolates were determined by using the multilocus sequence typing (MLST) primers and conditions described by the Pasteur Institute (*6*). MLST showed that 16 of 17 serotype 1/2b isolates we tested were ST87; the remaining serotype 1/2b isolate was ST3. Only 2 human *L. monocytogenes* ST87 serotype 1/2b isolates, both from Japan, were listed in the Pasteur Institute MLST database (*6*). Further, PFGE showed 2 large clusters within serotype 1/2b, and epidemiologic research detected 2 main outbreaks. All listeriosis episodes during the study period that were caused by isolate types other than serotype 1/2b and ST87 were sporadic.

In the first case cluster (first outbreak), 5 episodes were detected during August–September 2013; of these, 3 were pregnancy associated. All isolates from 1 woman at 28 weeks' gestation, 1 parturient woman and her newborn child, and 2 newborn twins (no samples from the mother were available) showed the same PFGE pattern with the restriction enzyme *Asc*I (arbitrarily named as pattern A) and were ST87 (Figure). Another 2 *L. monocytogenes* isolates from cases apparently not related to this first outbreak, isolated in January 2012 and in April 2013 from a 53-year-old man with meningitis and an 84-year-old woman, respectively, showed the same PFGE pattern.

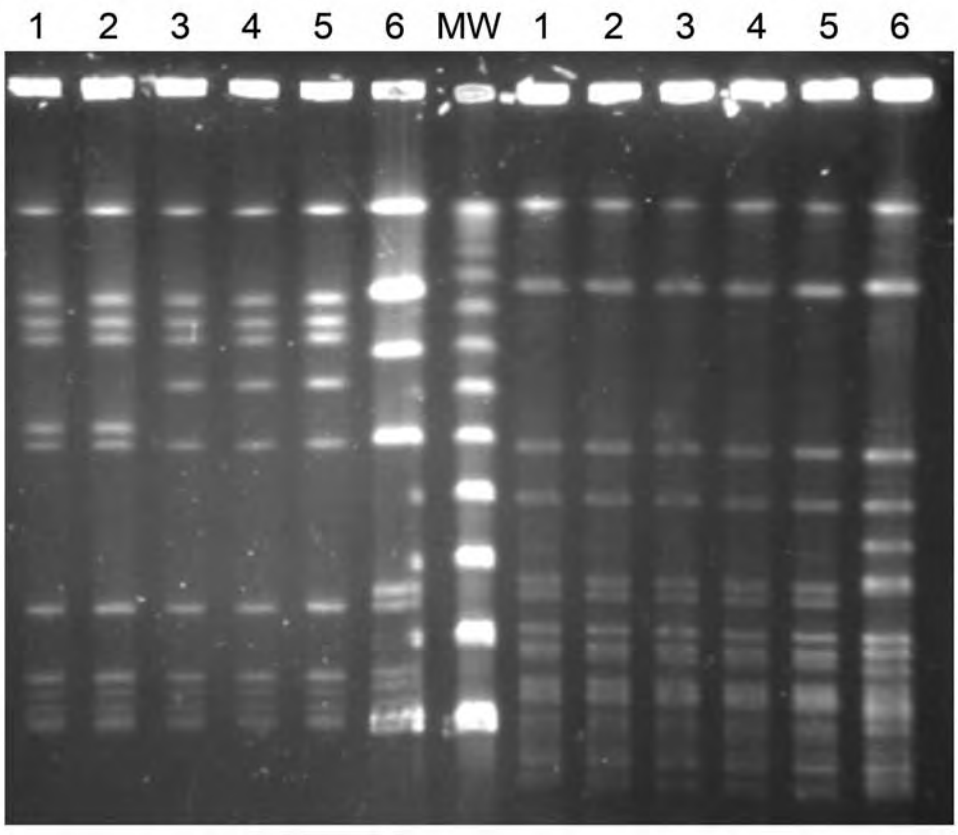

Figure. Pulsed-field gel electrophoresis patterns of 6 *Listeria monocytogenes* serotype 1/2b isolates collected from listeriosis patients in Gipuzkoa, northern Spain, during January 2013–February 2014. Left side, after *Asc*I restriction; right side, after *Sma*I restriction. Lanes 1 and 2, isolates from first outbreak (pattern A); lanes 3, 4, and 5, isolates from second outbreak (pattern B), including (lane 5) 1 isolate from a food product of foie gras; lane 6, *L. monocytogenes* sequence type 3 serotype 1/2b isolate, unrelated to outbreaks. MW, DNA molecular weight marker (50-kbp ladder).

For this first outbreak, epidemiologic interviews were conducted starting with the cases observed during September 2013. Patients were asked about their alimentary habits, focusing on consumption of raw or semicooked animal or animal derivate products. Although no specific food was identified as the possible source of the outbreak, all but 1 of the patients remembered eating cooked ham bought in the butcher's department of a certain supermarket chain located in different villages of the province. *Listeria* spp. in food products were investigated by PCR and culture after selective enrichment (24 Listeria Enrichment Broth; Oxoid, Basingstoke, UK)). In the microbiological investigation (*7*), 1 of 6 brands of cooked ham studied grew *L. monocytogenes* at a low level, but the sample strain was not the serotype 1/2b identified in the outbreak. No *Listeria* spp. were identified in the remaining 5 brands of cooked ham studied.

In the second outbreak, 10 episodes were reported during early November 2013 through late February 2014; patients were 5 elderly persons, 4 previously healthy parturient women, and 1 parturient women who had undergone a splenectomy. No isolates could be obtained from the mother of an infected newborn and from a miscarriage. The 10 isolates available for study (1 per episode) were of the same serotype and sequence type, 1/2b and ST87, as isolates from the first outbreak, but these isolates differed in PFGE *Asc*I pattern (this pattern arbitrarily named pattern B). Isolates from these 2 outbreaks had the same PFGE pattern when the *Sma*I enzyme was used (Figure).

After the epidemiologic survey for this outbreak, we conducted microbiological analysis of several foods. A foie gras product kept by a patient in his refrigerator yielded a positive culture of *L. monocytogenes* that had the same phenotype and molecular profile as isolates from the second outbreak. The presence of the outbreak strain was confirmed in high amounts (5.2×10^4 CFU/g) by several other cultures from 3 unopened samples from the same brand of foie gras. After this food source was identified as the source of this second outbreak, all patients from the first outbreak were specifically interviewed again about the consumption of this product, but none remembered having eaten it.

Conclusions

L. monocytogenes infection is serious and has high fatality rates. Among the 35 persons infected in this region of Spain since 2013, a total of 6 deaths have occurred: 3 adults, 2 fetuses (miscarriages), and 1 child (stillbirth). Without rapid case detection and early treatment, the lethality of these infections could have been much higher.

L. monocytogenes infections mainly affect elderly persons, pregnant women, newborns, and immunocompromised

adults (*8–10*). Humans are usually infected after eating contaminated food, although the source of the infection is infrequently detected in sporadic cases. For outbreaks, after the epidemiologic survey, a food is usually implicated as the source of infection, but it is not always possible to obtain microbiological confirmation (*11*). In this study, the strain (same phenotype and genotype) that caused the second outbreak was obtained from a recently consumed food in the home and in several unopened samples from the same batch of food. However, this source could not be identified as related to the first outbreak.

Pregnant women were frequently infected during these outbreaks; epidemic clones infected 8 pregnant women and their offspring. However, during 2012 and 2013, serotype 4b isolates of different genotypes also infected 5 pregnant women, resulting in 1 miscarriage, 3 premature newborns, and 1 stillborn infant and 1 premature newborn in a twin pregnancy.

In summary, we defined 2 epidemiologically unrelated outbreaks of listeriosis caused by a rare type of *L. monocytogenes* that occurred at the same time in a small region of Spain. Management of this frequently fatal disease requires careful investigation of the source of infection to stop its spread and prompt treatment of infected persons to prevent severe illness and death.

Acknowledgments

We thank the team of curators of the Institut Pasteur MLST system (Paris, France) for importing novel alleles, profiles and/or isolates.

Dr Pérez-Trallero is a clinical microbiologist and infectious disease consultant. He is head of the Department of Microbiology at Donostia University Hospital and professor of preventive medicine and public health at the Faculty of Medicine at Basque Country University. His research focuses on antimicrobial resistance and epidemiology of transmissible diseases.

References

1. Schuchat A, Swaminathan B, Broome C. Epidemiology of human listeriosis. Clin Microbiol Rev. 1991;4:169–83.
2. Chenal-Francisque V, Lopez J, Cantinelli T, Caro V, Tran C, Leclercq A, et al. Worldwide distribution of major clones of *Listeria monocytogenes*. Emerg Infect Dis. 2011;17:1110–2. http://dx.doi.org/10.3201/eid/1706.101778
3. Wang Y, Zhao A, Zhu R, Lan R, Jin D, Cui Z, et al. Genetic diversity and molecular typing of *Listeria monocytogenes* in China. BMC Microbiol. 2012;12:119. http://dx.doi.org/10.1186/1471-2180-12-119
4. Doumith M, Buchrieser C, Glaser P, Jacquet C, Martin P. Differentiation of the major *Listeria monocytogenes* serovars by multiplex PCR. J Clin Microbiol. 2004;42:3819–22. http://dx.doi.org/10.1128/JCM.42.8.3819-3822.2004
5. Standard PulseNet Listeria PFGE–One-Day (24–28 h). Standardized laboratory protocol for molecular subtyping of *Listeria monocytogenes* by pulsed field gel electrophoresis (PFGE) [cited 2014 Jun 6]. http://www.pulsenetinternational.org/SiteCollectionDocuments/pfge/5.3_2009_PNetStandProtLMonocytogenes.pdf
6. *Listeria monocytogenes* MLST database [cited 2014 Jun 6]. http://www.pasteur.fr/recherche/genopole/PF8/mlst/Lmono.html
7. European Commission (EC). Commission Regulation (EC) No 1441/2007 of 5 December 2007 amending Regulation (EC) No 2073/2005 on microbiological criteria for foodstuffs. EC; 2007. Official Journal of the European Union [cited 2014 Jun 6]. http://eur-lex.europa.eu/LexUriServ/LexUriServ.do?uri=OJ:L:2007:322:0012:0029:EN:PDF
8. European Food Safety Authority and European Centre for Disease Prevention and Control. The European Union summary report on trends and sources of zoonoses, zoonotic agents and food-borne outbreaks in 2012. EFSA Journal. 2014;12:3547.
9. Centers for Diseases and Control and Prevention. *Listeria* (listeriosis) [cited 2014 Jun 6]. http://www.cdc.gov/listeria/
10. Denny J, McLauchlin J. Human *Listeria monocytogenes* infections in Europe—an opportunity for improved European surveillance. Euro Surveill. 2008;13:pii=8082 [cited 2014 Jun 6]. http://www.eurosurveillance.org/ViewArticle.aspx?ArticleId=8082
11. European Commission Health & Consumer Protection Directorate-General. Opinion of Scientific Committee on Veterinary Measures relating to public health on *Listeria monocytogenes* (23 September 1999) [cited 2014 Jun 6]. http://ec.europa.eu/food/fs/sc/scv/out25_en.pdf

Address for correspondence: Emilio Pérez-Trallero, Hospital Donostia—Microbiology, Paseo Dr, Beguiristain s/n San Sebastian Gipuzkoa 20014, Spain; email: mikrobiol@terra.com

Reemergence of Foot-and-Mouth Disease, South Korea, 2000–2011

Jong-Hyeon Park, Kwang-Nyeong Lee, Su-Mi Kim, Hyang-Sim Lee, Young-Joon Ko, Dong-Seob Tark, Yeun-Kyung Shin, Min-Goo Seo, and Byounghan Kim

Five outbreaks of foot-and-mouth disease have occurred in South Korea during 2000–2011. Macro-analysis of these outbreaks showed a correlation with outbreaks in countries in eastern Asia. Genetic analyses of food-and-mouth disease viruses in South Korea showed a correlation with viruses that are prevalent in neighboring countries.

Foot-and-mouth disease is an infectious viral disease that occurs in animals and is easily transmissible. Outbreaks of this disease affect international trade (*1*). Since 2000, five outbreaks (in March 2000, May 2002, January 2010, April 2010, and November 2010–April 2011) have occurred in South Korea; the outbreak in 2000 was the first in 66 years (*2–8*).

To better understand the risks associated with reemergence of this disease in South Korea, we examined characteristics of these outbreaks and those occurring in neighboring countries by using macroscopic analysis. We describe the outbreak patterns to enable prediction and prevention of this disease in South Korea.

The Study

Spatiotemporal analyses used data obtained from the World Organisation for Animal Health Information Database (http://www.oie.int), the Food and Agriculture Organization World Reference Laboratory for foot-and-mouth disease (http://www.wrlfmd.org), the Southeast Asia and China Foot-and-Mouth Disease Campaign (http://www.seafmd-rcu.oie.int), national reports for international meetings (Southeast Asia and China Foot-and-Mouth Disease Campaign 2013, World Organisation for Animal Health/Japan Trust Fund on foot-and-mouth disease control in Asia 2013), and previously reported data (*9–11*) for Southeast Asia (Vietnam, Cambodia, Myanmar, Thailand, Laos, Malaysia, and the Philippines) and eastern Asia (South Korea, Japan, China, Mongolia, Russia, North Korea, Hong Kong, and Taiwan) regions for 1999–2013. Statistical analysis was performed by using paired or unpaired *t*-tests, and correlation were made by using GraphPad InStat version 3.05 (Graph Pad Software, La Jolla, CA, USA). A phylogenetic tree was inferred by using the neighbor-joining method, and analysis was conducted by using MEGA version 6 (http://www.megasoftware.net/).

Comparative analysis of outbreaks in neighboring countries over the past 15 years showed a high incidence of outbreaks at 2- to 5-year intervals (2000, 2005, 2010–2011, and 2013) (Figure 1, panels A and F, http://wwwnc.cdc.gov/EID/article/20/12/13-0518-F1.htm). Analysis of outbreak serotypes and cases in neighboring countries (Figure 1, panels A–C) showed that type O foot-and-mouth disease virus has been predominant every year for the past 15 years. Outbreaks in eastern Asia and South Korea over the past 15 years showed a strong relationship with each other ($r = 0.725$) (Figure 1, panels D–H). Given the overall trend in Asia, serotype Asia 1 was predominant in 2005 (Figure 1, panels A, B). The situation for foot-and-mouth disease in Asia was regarded as serious during 2010–2011 because of the increased numbers of outbreaks (Figure 1, panels A, C–F). In 2013, the number of type A outbreaks increased, and outbreaks caused by types O and A viruses were still considered a threat (Figure 1, panels A, B).

Of 5 outbreaks in South Korea during 2000–2011, 4 were caused by type O virus, 2 were caused by the Middle East–South Asia topotype, and 2 were caused by the Southeast Asia topotype. One of the 5 outbreaks was caused by type A virus (ASIA topotype, Sea-97 lineage) (Table; Figure 1, panel I). Middle East–South Asia topotype viruses that caused outbreaks in 2000 and 2002 were related to PanAsia lineage viruses, which were detected during 1999–2000 in China, Taiwan, Japan, and Thailand; the causative viruses had high genetic similarity (*12*). We assume that these viruses, which have predominated in these regions since 1998 (*12*), were introduced to South Korea in 2000 and 2002. Serotype O viruses that caused outbreaks in 2010 were identified as SEA type, Mya-98 lineage. This virus type was detected in 2010 in Asia, including Russia, Japan, China, Hong Kong, and Vietnam, and the genetic similarity of these viruses was high (Figure 1, panel I). Type A virus (ASIA topotype, Sea-97 lineage) was detected in South Korea in January 2010. This virus is similar to those detected in 2009 in China and Vietnam. Genetic analyses of all viruses detected in South Korea showed a correlation with viruses that predominated in neighboring countries (Figure 1, panel I).

Major putative factors for inter-regional or inter-farm virus transmission during the 5 foot-and-mouth disease outbreaks in South Korea were movement of humans or

Author affiliation: Animal and Plant Quarantine Agency, Gyeonggi-do, South Korea

DOI: http://dx.doi.org/10.3201/eid2012.130518

Table. Characteristics of 5 outbreaks of foot-and mouth-disease, South Korea, 2000–2011*

Characteristic	2000 Mar	2002 May	2010 Jan	2010 Apr	2010 Nov–2011 Apr
Disease status					
No. cases	15	16	7	13	153
No. virus-positive cases	15	16	7	29	3,700
Duration virus detected, d	22	52	28	29	145
Period of virus detection	Mar 24–Apr 15	May 2–Jun 23	Jan 2–Jan 29	Apr 8–May 6	Nov 28–2011 Apr 21
Host tropism	Ruminant	Pig (cattle)	Ruminant	Ruminant, pig	Ruminant, pig
Serotype (topotype/lineage)	O (ME-SA/PanAsia)	O (ME-SA/PanAsia)	A (ASIA/SEA-97)	O (SEA/Mya-98)	O (SEA/Mya-98)
No. affected provinces (cities or counties)	3 (6)	2 (4)	1 (2)	4 (4)	11 (75)
Economic losses, US$, millions	300	143	29	124	3,000
Date of disease-free status	2001 Sep 16	2002 Nov 29	2010 Sep 27	2010 Sep 27	2014 May 29
Control measures					
Eradication policy	Culling, vaccination	Culling	Culling	Culling	Culling, vaccination
No. cattle culled	2,021	1,372	2,905	10,858	150,864
No. pigs culled	63	158,708	2,953	38,274	3,318,298
No. other animals culled	132	75	98	742	10,800
Total culled	2,216	160,155	5,956	49,874	3,479,962
Area of culling, km radius	0.5 (all)	0.5 (all), 3 (pigs)	0.5	0.5, 3 (on 2 farms)	0.5
Vaccine strain	O Manisa	NA	NA	NA	O Manisa
No. animals vaccinated	1st: 860,700, booster: 661,700	NA	NA	NA	All susceptible animals
Vaccination range, km radius	10	NA	NA	NA	Nationwide
Serosurveillance area, km radius	20	10	10	10	10
Restricted zones, km radius					
Management	NA	NA	10–20	10–20	10–20
Surveillance	10–20	3–10	3–10	3–10	3–10
Protection	0–10	0–3	0–3	0–3	0–3
Putative sources					
Regions in Asia as possible sources	Northeastern	Northeastern	Northeastern	Northeastern	Southeastern
Major sources of first outbreak	International travelers, imported hay	Overseas travel, foreign workers	Foreign workers, international parcels	Overseas travel	Overseas travel
Low possibility sources of first outbreak	Windborne spread of contaminated yellow sand, wild birds	Swill, saw dust, wild animals and birds, yellow sand	Overseas travel, imported forage, TMR feed, saw dust	Imported forage, TMR feed	Foreign workers, illegal livestock products
Possible transmission factor for domestic regions	Imported hay	Humans and vehicles	Humans (veterinarians, meetings, animal feeding)	Vehicles, humans	Vehicles, humans
References†	(*2*,*8*)	(*3*)	(*4*)	(*6*)	(*5*,*7*)

*ME-SA, Middle East–South Asia; USD, US dollars; TMR, total mixed ration; NA, not applicable.
†Data were obtained from national epidemiology investigation reports on the 5 foot-and-mouth disease outbreaks in South Korea and the references.

vehicles (Table). The 5 outbreaks that occurred since 2000 were analyzed by province (Figure 2, panel A). The disease occurred most frequently in Gyeonggi Province (5 times), followed by Chungbuk Province (4 times) and Chungnam Province (3 times). Therefore, these 3 provinces, which had the highest risk for infection, were characterized by a high density of pig and cattle farms. On the basis of analysis of 4 outbreaks, the second round of outbreaks occurred 8.0 ± 2.0 days after the first infected group had been identified (Figure 2, panel B). In the most recent outbreak in November 2010, the initial diagnosis was delayed for 1 week; many concurrent infections were detected, and no unique aspects of transmission after the first detection of the disease had been identified (Figure 2, panel B). Most infections occurred ≤25 days after the initial case, after which occurrence was intermittent (Figure 2, panel B).

Conclusions

International trade and globalization have recently been indicated as major factors for transmission of infectious diseases associated with livestock (*6*). Multiple sources of serotypes O, A, and Asia 1 of foot-and-mouth

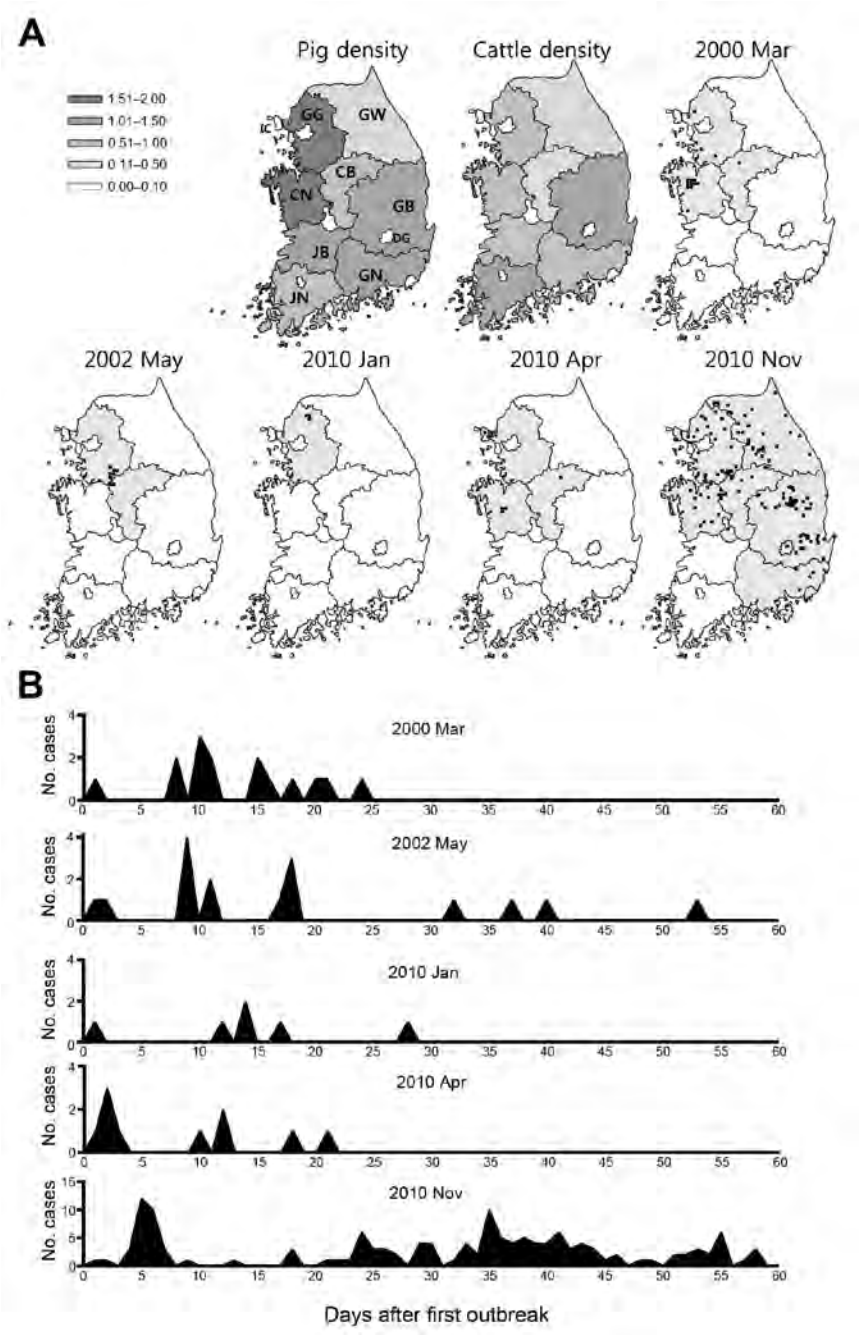

Figure 2. Affected regions and detection time points during 5 foot-and-mouth disease outbreaks, South Korea, 2000–2010. A) Affected provinces and regions and the densities of livestock (pigs and cattle) in 2010 on the basis of data from the Korean Statistical Information Service (http://kosis.kr). Values in the key are in millions. IC, Incheon; GG, Gyeonggi; GW, Gangwon; CN, Chungnam; CB, Chungbuk; GB, Gyeongbuk; GN, Gyeongnam; JN, Jeonnam; JB, Jeonbuk; DG, Daegu. B) Comparison of detection time points of cases of foot-and-mouth disease.

disease viruses, which have caused recent outbreaks in eastern Asia, are endemic to Southeast Asia (*13*). Incursion of these viruses from Southeast Asia into eastern Asia has been suggested because of the porous nature of borders (*13*). However, the Korean Peninsula is surrounded by water on 3 sides and shares its only land border with North Korea. We believe that inflow of illegal live animals and livestock products, which is generally the highest risk factor for foot-and-mouth disease (*14*), is negligible in the regions around South Korea. Access to suspected infectious materials from countries with outbreaks is fundamentally blocked by shipping regulations.

Although no evidence for confirmation of introduction is available, results of epidemiologic investigations have indicated that the 5 foot-and-mouth disease outbreaks in South Korea were related primarily to indirect transmission by humans who came into contact with suspected infectious animals or livestock products from countries in Asia to which the virus is endemic (Table) (*2–7*). In addition, imported hay or other imported animal products were

probable sources of virus in March 2000 and January 2010 (Table) (*2*,*4*,*8*), and the viruses were transmitted to persons who had contact with these materials directly or indirectly. On the basis of the national mandatory reporting system for foreign workers (http://www.kahis.go.kr), we found that the number of persons from Vietnam, Cambodia, Thailand, and China who work on farms in South Korea has been increasing since 2005. The recent situation can be regarded as conducive for an increased risk for foot-and-mouth disease.

The outbreak pattern of foot-and-mouth disease in South Korea was more strongly correlated with outbreaks in countries in eastern Asia than with outbreaks in Southeast Asia. Outbreaks every 15 years caused by type O foot-and-mouth disease virus are predominant in Asia. The greatest risk for infection is currently by type O and A viruses, followed by type Asia 1 virus.

In summary, type O foot-and-mouth disease virus was responsible for 4 outbreaks in South Korea and type A virus accounted for 1 outbreak. South Korea might be at risk for foot-and mouth disease, given the high incidence of this disease at 2- to 5-year intervals (2000, 2005, 2010–2011, and 2013) in eastern Asia. Foot-and-mouth disease outbreaks in neighboring countries were a probable major source of introduction of this disease into South Korea. Once this disease is introduced, prevention of domestic transmission should include extensive restriction of movement of humans or vehicles during an outbreak.

Acknowledgments

We thank the staff of the Animal and Plant Quarantine Agency for providing assistance during the study.

This study was supported by a grant from the Animal and Plant Quarantine Agency National Animal Disease Research Project.

Dr Park is a research scientist at the Animal and Plant Quarantine Agency, Gyeonggi-do, South Korea. His research interests are diagnosis and surveillance of foot and mouth disease, and development of vaccines and antiviral agents against this disease.

References

1. Callis JJ. Evaluation of the presence and risk of foot and mouth disease virus by commodity in international trade. Rev Sci Tech. 1996;15:1075–85.
2. Sakamoto K, Yoshida K. Recent outbreaks of foot and mouth disease in countries of east Asia. Rev Sci Tech. 2002;21:459–63.
3. Wee SH, Yoon H, More SJ, Nam HM, Moon OK, Jung JM, et al. Epidemiological characteristics of the 2002 outbreak of foot-and-mouth disease in the Republic of Korea. Transbound Emerg Dis. 2008;55:360–8. http://dx.doi.org/10.1111/j.1865-1682.2008.01045.x
4. Park JH, Lee KN, Ko YJ, Kim SM, Lee HS, Park JY, et al. Diagnosis and control measures of the 2010 outbreak of foot-and-mouth disease A type in the Republic of Korea. Transbound Emerg Dis. 2013;60:188–92. http://dx.doi.org/10.1111/j.1865-1682.2012.01333.x
5. Park JH, Lee KN, Ko YJ, Kim SM, Lee HS, Shin YK, et al. Control of foot-and-mouth disease during 2010–2011 epidemic, South Korea. Emerg Infect Dis. 2013;19:655–9. http://dx.doi.org/10.3201/eid1904.121320
6. Park JH, Lee KN, Ko YJ, Kim SM, Lee HS, Park JY, et al. Outbreaks and diagnosis of foot-and-mouth disease serotype O in the Republic of Korea, April–June 2010. Transbound Emerg Dis. 2014;61:277–84. http://dx.doi.org/10.1111/tbed.12029
7. Yoon H, Yoon SS, Kim YJ, Moon OK, Wee SH, Joo YS, et al. Epidemiology of the foot-and-mouth disease serotype O epidemic of November 2010 to April 2011 in the Republic of Korea. Transbound Emerg Dis. 2013. [Epub ahead of print]. http://dx.doi.org/10.1111/tbed.12109
8. Shin JH, Sohn HJ, Choi KS, Kwon BJ, Ko YJ, An DJ, et al. Molecular epidemiological investigation of foot-and-mouth disease virus in Korea in 2000. J Vet Med Sci. 2003;65:9–16. http://dx.doi.org/10.1292/jvms.65.9
9. Di Nardo A, Knowles NJ, Paton DJ. Combining livestock trade patterns with phylogenetics to help understand the spread of foot and mouth disease in sub-Saharan Africa, the Middle East and Southeast Asia. Rev Sci Tech. 2011;30:63–85.
10. Valdazo-González B, Timina A, Scherbakov A, Abdul-Hamid NF, Knowles NJ, King DP. Multiple introductions of serotype O foot-and-mouth disease viruses into east Asia in 2010–2011. Vet Res. 2013;44:76. http://dx.doi.org/10.1186/1297-9716-44-76
11. Madin B. An evaluation of foot-and-mouth disease outbreak reporting in mainland South-East Asia from 2000 to 2010. Prev Vet Med. 2011;102:230–41. http://dx.doi.org/10.1016/j.prevetmed.2011.07.010
12. Knowles NJ, Samuel AR, Davies PR, Midgley RJ, Valarcher JF. Pandemic strain of foot-and-mouth disease virus serotype O. Emerg Infect Dis. 2005;11:1887–93. http://dx.doi.org/10.3201/eid1112.050908
13. Knowles NJ, He J, Shang Y, Wadsworth J, Valdazo-Gonzalez B, Onosato H, et al. Southeast Asian foot-and-mouth disease viruses in eastern Asia. Emerg Infect Dis. 2012;18:499–501. http://dx.doi.org/10.3201/eid1803.110908
14. Pharo HJ. Foot-and-mouth disease: an assessment of the risks facing New Zealand. N Z Vet J. 2002;50:46–55. http://dx.doi.org/10.1080/00480169.2002.36250

Address for correspondence: Jong-Hyeon Park, Animal and Plant Quarantine Agency, 175 Anyang-ro, Manan gu, Anyang City, Gyeonggi-do 430-757, South Korea; email: parkjhvet@korea.kr

Third Strain of Porcine Epidemic Diarrhea Virus, United States

To the Editor: In April 2013, porcine epidemic diarrhea virus (PEDV) was first reported (*1*). Since PEDV was detected, the virus has continued to spread throughout the United States and has now been reported in Mexico and Canada (*2*). PEDV was first reported in Europe in the 1970s and was later reported in Asia during the 1980s (*3*,*4*). PEDV outbreaks in Asia were more acute and severe than the PEDV outbreaks in Europe (*4*). In 2010, an increase, up to 100%, in illness and deaths in piglets was reported in China associated with PEDV infection (*4*–*6*). The original North American PEDV strains identified in 2013 caused severe illness and deaths in piglets and had a 99.5% nucleotide identity with Chinese strain AH2012 (*1*,*7*,*8*).

Recently, a North American PEDV variant-INDEL strain was identified, which has been previously described (*9*). This spike gene deletion has been described in global PEDV strains, which may correlate with a less severe clinical presentation of PEDV. Although the PEDV variant-INDEL strain (OH851) was first reported in February 2014 by the Ohio Department of Agriculture, the PEDV variant-INDEL strains were first detected in June 2013, which suggests that the original PEDV strain mutated or that 2 different PEDV strains were introduced concurrently into the United States (*2*).

The University of Minnesota Veterinary Diagnostic Laboratory has tested clinical samples from thousands of case-patients to determine the presence of PEDV by real-time reverse transcription PCR. Some of the PEDV-positive samples from case-patients were selected for PEDV spike gene sequencing per veterinarian's request, whereas other samples were selected for complete genome sequencing to fulfill a grant objective. When PEDV was first detected in the United States, the University of Minnesota Veterinary Diagnostic Laboratory was only sequencing the PEDV spike gene segment to clarify the phylogenetic relationship between PEDV strains.

In February 2014, after the identification and analysis of PEDV variant-INDEL strains, we decided to sequence the complete PEDV genome by using next generation sequencing to clarify the phylogenetic relationship of the US PEDV strains (*7*). In January 2014, intestines from a deceased neonatal piglet, which had severe diarrhea, were positive for PEDV by real-time reverse transcription PCR, and PEDV was sequenced per request of the veterinarian. The sample was processed for next generation sequencing and analyzed by mapping to reference strain USA/Colorado/2013 (*7*). During the assembly of PEDV strain USA/Minnesota188/2014 (GenBank accession no. KM077139), a region of the spike only had 5× coverage and ambiguity bases in the consensus contig whereas the coverage across the remaining PEDV genome was 50×. The consensus contig was separated at this region, and the 2 separate contigs were created. After remapping, the 2 contigs were aligned back into a new consensus contig, and the new consensus contig was remapped to verify the accuracy of the contig, which had 50× coverage.

The PEDV strain Minnesota188 was aligned with the other complete genome of PEDV available in GenBank (n = 113); it had a 99.9% nucleotide percentage identity to Colorado/2013 and clustered in the North American clade II (Figure, panel A, http://wwwnc.cdc.gov/EID/article/20/12/14-0908-F1.htm). The spike gene segment had a 99.7% nucleotide percentage identity (99.4% amino acid identity) with Colorado/2013 and clustered with the non–North American INDEL strains (Figure, panel B). The alignment indicated a spike gene nucleotide deletion at positions 164–169 (TTG-GTG), which corresponded to amino acid deletion at positions 55 and 56. The spike gene amino acid alignment identified substitution at positions 23 (I), 31 (H), 57 (K), and 59 (E), which have not been identified in the complete PEDV genomes available from North America.

Thus far, 3 naturally occurring US PEDV strains have been identified: the original PEDV, the PEDV with changes in the spike gene (INDEL), and the PEDV strain (S2aa-del) reported in this article. The role of genetic changes in the US PEDV strains to clinical disease has yet to be reported. The clinical presentation of diarrhea in this case was reported as equally or more severe than such presentation in cases caused by the prototype PEDV Colorado/2013. Other factors such as concurrent infections and the rate of group exposure, which is rapid in most PEDV cases affecting neonatal piglets, may influence the clinical presentation.

Documenting PEDV variation is vital to understanding the natural evolution of the virus and possibly identifying portions of the genome associated with different clinical disease features. Animal studies are required to define the effects of these mutations on clinical disease, pathogenesis, immunity; these studies will be conducted in the future with the S2aa-del strain. A consistent model to properly evaluate these differences is required to control PEDV infection. The most compelling need is to understand how exposure by sows to different PEDV strains correlates with protection of piglets from clinical disease. Whether the PEDV S2aa-del strain will circulate in the North American swine population is not known.

Funding was provided by the Swine Vet Center and the University of Minnesota Veterinary Diagnostic Laboratory.

Douglas Marthaler, Laura Bruner, James Collins, and Kurt Rossow

Author affiliations: University of Minnesota Veterinary Diagnostic Laboratory, Saint Paul, Minnesota, USA (D. Marthaler, J. Collins, K. Rossow); and Swine Vet Center, Saint Peter, Minnesota, USA (L. Bruner)

DOI: http://dx.doi.org/10.3201/eid2012.140908

References

1. Stevenson GW, Hoang H, Schwartz KJ, Burrough ER, Sun D, Madson D, et al. Emergence of porcine epidemic diarrhea virus in the United States: clinical signs, lesions, and viral genomic sequences. J Vet Diagn Invest. 2013;25:649–54d http://dx.doi.org/10.1177/1040638713501675
2. Vlasova AN, Marthaler D, Wang Q, Culhane MR, Rossow KD, Rovira A, et al. Distinct characteristics and complex evolution of PEDV, North America, May 2013–February 2014. Emerg Infect Dis. 2014;20:1620–8.
3. Pensaert MB, de Bouck P. A new coronavirus-like particle associated with diarrhea in swine. Arch Virol. 1978;58:243–7d http://dx.doi.org/10.1007/BF01317606
4. Song D, Park B. Porcine epidemic diarrhoea virus: a comprehensive review of molecular epidemiology, diagnosis, and vaccines. Virus Genes. 2012;44:167–75d http://dx.doi.org/10.1007/s11262-012-0713-1
5. Luo Y, Zhang J, Deng X, Ye Y, Liao M, Fan H. Complete genome sequence of a highly prevalent isolate of porcine epidemic diarrhea virus in South China. J Virol. 2012;86:9551d http://dx.doi.org/10.1128/JVI.01455-12
6. Fan H, Zhang J, Ye Y, Tong T, Xie K, Liao M. Complete genome sequence of a novel porcine epidemic diarrhea virus in south China. J Virol. 2012;86:10248–9d http://dx.doi.org/10.1128/JVI.01589-12
7. Marthaler D, Jiang Y, Otterson T, Goyal S, Rossow K, Collins J. Complete genome sequence of porcine epidemic diarrhea virus strain USA/Colorado/2013 from the United States. Genome Announc. 2013;1: http://dx.doi.org/10.1128/genomeA.00555-13
8. Jung K, Wang Q, Scheuer KA, Lu Z, Zhang Y, Saif LJ. Pathology of US porcine epidemic diarrhea virus strain PC21A in gnotobiotic pigs. Emerg Infect Dis. 2014;20:662–5d http://dx.doi.org/10.3201/eid2004.131685
9. Wang L, Byrum B, Zhang Y. New variant of porcine epidemic diarrhea virus, united states, 2014. Emerg Infect Dis. 2014;20:917–9d http://dx.doi.org/10.3201/eid2005.140195

Address for correspondence: Douglas Marthaler, Veterinary Diagnostic Laboratory, College of Veterinary Medicine, University of Minnesota, 1333 Gortner Ave, Saint Paul, MN 55108, USA; email: marth027@umn.edu

Schistosomiasis in Cattle in Corsica, France

To the Editor: The origin of the human cases of urinary schistosomiasis observed in France was recently identified (*1*,*2*). None of these patients had traveled to a disease-endemic area, but all had vacationed in Corsica and had swum in the Cavu River, near Porto-Vecchio in southern Corsica. The letter by Berry et al. to Emerging Infectious Diseases (*2*) reminded us that bovine schistosomiasis had been reported in Corsica in the past, up through the 1960s, in the same area.

In cattle, *Schistosoma bovis* has been found in Africa and the Middle East (Iraq, Israel), as well as in the Mediterranean Basin, especially in Sicily and Sardinia in Italy, and Corsica, France, where cases were reported as early as 1929 by Emile Brumpt (*3*,*4*). In addition, certain *Schistosoma* blood fluke species, especially *S. haematobium* and *S. bovis*, can share the same definitive hosts (humans or animals) and the same intermediate hosts, i.e., *Bulinus contortus* snails. Cattle, sheep and goats, horses, wild ruminants and rodents can all be definitive hosts of *S. bovis*.

In cattle, the clinical manifestations of infestation are poorly documented. In experimental animals, intermittent diarrhea has been observed, sometimes containing blood or mucus, in addition to a loss of appetite, progressive anemia, and, especially, blood eosinophilia, a sign which, as in humans, indicates that the infestation is recent. Under natural conditions, the disease is believed to be mainly subclinical and chronic. It should be noted that the acute form of the disease is more common in sheep (*5*). With regard to lesions, the disease is closer to intestinal schistosomiasis (caused by *S. mansoni*) than to urinary schistosomiasis. The lesions are characterized by the formation of gray-white granulomas ³5 mmin diameter, or by polyps, and intestinal hemorrhaging due to bleeding of the granulomas formed during migration of the parasite's eggs to the intestinal lumen. In the liver, granulomas may also be observed, as well as fibrosis of the portal vein. Hepatomegaly and cirrhosis may also be present. These lesions are caused by adult parasites in the mesenteric vessels and the portal vein.

The presence of *Bulinus truncatus contortus* (Michaud) (*Mollusca, Gastropoda, Hygrophila*) snails was mentioned as early as 1832, and the species was formally identified in 1922 in Corsica. Since that time it has been assumed that this mollusc could be a potential intermediate host for human (*6*) or bovine (*3*,*7*) schistosomiasis.

In 1963, Gretillat studied bovine schistosomiasis in Corsica (*8*). Investigations of *Bulinus* snails were conducted solely in the southern part of the island, in the area where Brumpt had described their presence 30 years earlier. *Bulinus* snails were identified in 4 rivers, the Rizzanese, Baraci, Ortolo and Spartano, especially in residual ponds of waterways sometimes quite close to the sea. At 2 sites, unidentifiable cercaria larvae were revealed through dissection (5 of 70 *Bulinus* snails in the Rizzanese, 26 of 50 in the Baraci). As part of the same study, slaughterhouse examination of 15 cattle from regions where *Bulinus* snails had been discovered revealed adult *Schistosoma* in the mesenteric

and vesical veins, as well as in the liver and the portal system.

In a more comprehensive study (*9*), *Bulinus* snails were found in all of Corsica's coastal rivers, except for those in the northwestern-most part of the island. However, of the 55 bodies of water where *Bulinus* snails were found, only 1 contained gastropods with *Schistosoma* cercariae, and results of a search for blood flukes in 220 small rodents (known for being susceptible to *S. bovis* and captured near bodies of water where *Bulinus* snails had been observed) were negative.

We have found no other documentation on bovine schistosomiasis in Corsica between 1966 and the present time. Has this disease disappeared since the 1960s? Is it still present as an enzootic disease with silent transmission? It should be noted that the disease produces few or no clinical signs and that slaughterhouse detection requires dissection of the circulatory system of the abdominal cavity. In any case, the discovery of human cases of schistosomiasis proves that a human–*Bulinus* parasitic cycle exists in Corsica, and therefore an animal–*Bulinus* cycle may exist as well. For the sake of scientific interest, an investigation into the presence of *S. bovis* in ruminants in Corsica would be worthwhile. Moreover, the fact that both *Schistosoma* species use the same intermediate host, *Bulinus contortus* snails, could cause problems with differential diagnosis.

Didier Calavas and Paul M.V. Martin

Author affiliation: Agence Nationale de Sécurité Sanitaire, Lyon Laboratory, Lyon, France

DOI: http://dx.doi.org/10.3201/eid2012.141474

References

1. Holtfreter MC, Moné H, Müller-Stöver I, Mouahid G, Richter J. *Schistosoma haematobium* infections acquired in Corsica, France, August 2013. Euro Surveill. 2014;19:20821 http://www.eurosurveillance.org/ViewArticle.aspx?ArticleId=20821.
2. Berry A, Moné H, Iriart X, Mouahid G, Abbo O, Boissier J, et al. Schistosomiasis haematobium, Corsica, France [letter]. Emerg Infect Dis. 2014;20:1595–7. http://dx.doi.org/10.3201/eid2009.140928.
3. Brumpt E. Cycle évolutif du *Schistosoma bovis* (*Bilharzia crassa*); infection spontanée de *Bulinus contortus* en Corse C.-R. Acad. Sci. 1929;CLXXXXI:879.
4. Brumpt E. Cycle évolutif complet de *Schistosoma bovis*. Infection naturelle en Corse et infection expérimentale de *Bulinus contortus*. Ann Parasitol Hum Comp. 1930;VIII:17–50.
5. Pandey VS, Ziam H. Helminthoses circulatoires. In: Lefèvre P-C, Blancou J, Charmette R, editors. Principales maladies infectieuses et parasitaires du bétail, Europe et régions chaudes. Paris: Tec & Doc Editions Lavoisier; 2003. p. 1485–99.
6. Dollfus PH. Sur la présence en France et en Corse du *Bullinus contortus* (Michaud), hôte intermédiaire de *Schistosoma hæmatobium* (Bilharz): note préliminaire. Bull Soc Pathol Exot. 1922;15:208–12.
7. Arfaa F, Massoud J, Chu KY. Susceptibility of Portuguese *Bulinus contortus* to Iranian strains of *Schistosoma haematobium* and *S. bovis*. Bull World Health Organ. 1967;37:165–6.
8. Gretillat S. Epidémiologie de certaines affections à trématodes des animaux domestiques en Corse (bilharziose bovine et distomatose bovine et ovine). Ann Parasitol Hum Comp. 1963;38:471–81.
9. Doby J-M, Rault S, Deblock S, Chabaud A. Bulins et bilharzioses en Corse. Répartition, fréquence et biologie de "*Bulinus truncates*" [in French]. Annal. Parasitol. 1966;4:337–49.

Address for correspondence: Paul M.V. Martin, Anses - Lab de Lyon, 31, ave Tony Garnier, Lyon 69009, France; email: paul.martin@anses.fr

HIV-Associated Disseminated Emmonsiosis, Johannesburg, South Africa

To the Editor: *Emmonsia* spp., dimorphic fungi found worldwide, cause disease mainly among lower-order mammals (*1*). Although emmonsia rarely infect humans, the fungi can cause localized granulomatous pulmonary disease (adiaspiromycosis) in immunocompetent persons (*1–4*). Before 2013, no association was known between emmonsia and HIV, and there was no indication that emmonsia were endemic to sub-Saharan Africa.

In 2013 a novel *Emmonsia* sp. that is closely related to *E. pasteuriana* was described. The fungus caused disseminated disease in 13 HIV-infected persons in South Africa (12 in Cape Town, 1 in Bloemfontein) (*5*). Two additional cases of disseminated emmonsiosis caused by this novel species were identified in HIV-uninfected persons (1 immunocompetent, the other immunosuppressed for renal transplantation) in Cape Town (*6*). Because these cases clustered geographically, it was suggested that this novel *Emmonsia* sp. occupies a microenvironment around Cape Town (*7*). We report 3 additional cases of disseminated emmonsiosis from Johannesburg, South Africa, 403 km from Bloemfontein and 1,400 km from Cape Town. All patients were HIV-infected and reported no travel to Bloemfontein or Cape Town.

The 3 patients were admitted to Helen Joseph Hospital between August 2012 and August 2014; all patients were male and had CD4 counts of ≤5 cells/μL at admission. Patient 1 had never received antiretroviral therapy; patients 2 and 3 had defaulted antiretroviral treatment for several months before admission. All patients had disseminated skin rash, pneumonia, anemia, and substantial weight loss; chest radiographs suggested pulmonary tuberculosis. The rash appeared as disseminated hyperpigmented scaly papules and plaques (online Technical Appendix Figure 1, http://wwwnc.cdc.gov/EID/article/20/12/14-0902-Techapp1.pdf). Patients 1 and 2 also had diarrhea and exhibited delirium.

Laboratory investigations for patient 1 showed normocytic anemia,

hyponatremia, renal insufficiency, and elevated liver enzyme levels. Patients 2 and 3 had pancytopenia, hyponatremia, metabolic acidosis, and elevated liver enzyme levels. Lumbar puncture results were unremarkable for patients 1 and 3; patient 2 had normal lumbar puncture results during a previous admission (online Technical Appendix Table 1). Automated laboratory identification systems initially misidentified the *Emmonsia* sp. on blood culture as *Trichosporon* spp. (patients 1 and 3) and *Histoplasma capsulatum* (patient 2). Co-infection with *Mycobacterium avium* (patients 1 and 2) and *M. tuberculosis* (patient 2) was observed (online Technical Appendix Table 2). Subsequent histologic examination of skin biopsy specimens from all patients showed granulomas and yeast-like organisms.

Antifungal drug therapy consisted of fluconazole for patient 1 and conventional amphotericin B for patients 2 and 3; itraconazole was co-administered to patient 2 (online Technical Appendix Table 3). Clinical and biochemical parameters improved for all patients during the first 2 weeks of hospitalization. However, hospital-acquired pneumonia developed in patient 1, who subsequently died on hospitalization day 21, and patient 2 died of an unknown cause on day 17. Permission for autopsy was not granted for either patient. At the time of this report, patient 3 was recovering well.

The fungal isolates were not identified molecularly before patients 1 and 2 died. Sequencing of the ribosomal DNA internal transcribed spacer region of isolates from all 3 patients showed 97%–99% homology with the previously described novel *Emmonsia* sp. (GenBank accession nos. KM199781–83 and KM492927) (*5*). At admission, clinical features for patients in our study were similar to those for patients with the previously reported cases of HIV-associated emmonsiosis (*5*): all patients had rash, anemia, low CD4 count, abnormal liver enzyme levels, and chest radiographs compatible with pulmonary tuberculosis.

The patients in our study received an initial misdiagnosis. Kenyon et al. (*5*) also encountered diagnostic ambiguity in invasive fungal infection cases: over an 8-year period in South Africa, 39 cases were diagnosed as histoplasmosis on the basis of histologic findings, and only 1 was confirmed by using molecular techniques. Because laboratory services in Africa are generally weak (*8*), this trend of misdiagnosis could continue. The high death rate among patients with HIV-associated emmonsiosis (31%, 5/16 patients) may partly be explained by misdiagnoses (*5*), and it also raises questions regarding optimal treatment. Amphotericin B will likely remain the optimal empiric induction therapy for suspected cases of disseminated fungal infection among HIV-infected persons in sub-Saharan Africa, given the phylogenetic proximity of *Emmonsia* spp. to *Histoplasma* spp., the antifungal minimum inhibitory concentrations of emmonsia reported thus far (*5*), and the potential for laboratory misdiagnosis of fungal infection cases. Supplementary itraconazole may be beneficial if dimorphic fungal infection, specifically emmonsia, is clinically suspected. Regardless, early confirmatory diagnoses based on culture and histopathologic results should be aggressively pursued.

Although HIV-associated emmonsiosis was suggested to be geographically isolated to the Western Cape Province, South Africa (*7*), the ecologic niche occupied by this novel *Emmonsia* sp. probably extends throughout southern Africa. Of the 13 previously reported patients (*5*), 12 lived near Cape Town (Western Cape Province) and 1 lived in Bloemfontein (Free State Province; in the center of the country) at the time of diagnosis. The 3 additional patients reported in our study resided in Johannesburg, a geographic setting distinctly separate from the other locations. A region-wide surveillance program is needed to enhance disease identification within South Africa and to determine the environmental presence of this organism beyond South Africa's borders.

Acknowledgments

We acknowledge Tsidiso Maphanga for technical assistance and Sarolda Keresztes for assistance in retrieving the laboratory samples.

This work was supported by the Fogarty International Center; the National Cancer Institute; the National Heart, Lung, and Blood Institute; the Office of the Director Office of Research on Women's Health, National Institutes of Health; and the Office of the Director Office of AIDS Research, National Institutes of Health (grant no. R25 TW009340 to C.K.L.).

Wesley G. van Hougenhouck-Tulleken, Nectarios S. Papavarnavas, Jeremy S. Nel, Lauren Y. Blackburn, Nelesh P. Govender, David C. Spencer, and Christopher K. Lippincott

Author affiliations: Helen Joseph Hospital, Johannesburg, South Africa (W.G. van Hougenhouck-Tulleken, N.S. Papavarnavas, J.S. Nel. D.C. Spencer); University of the Witwatersrand, Johannesburg (W.G. van Hougenhouck-Tulleken, N.P. Govender); Right to Care, Johannesburg (N.S. Papavarnavas, C.K. Lippincott, D.C. Spencer); National Health Laboratory Service, Johannesburg (L.Y. Blackburn); National Institute for Communicable Diseases, Johannesburg (N.P. Govender); and University of North Carolina, Chapel Hill, North Carolina, USA (C.K. Lippincott)

DOI: http://dx.doi.org/10.3201/eid2012.140902

References

1. Anstead GM, Sutton DA, Graybill JR. Adiaspiromycosis causing respiratory failure and a review of human infections due to *Emmonsia* and *Chrysosporium* spp. J Clin Microbiol. 2012;50:1346–54. http://dx.doi.org/10.1128/JCM.00226-11

2. Dot JM, Debourgogne A, Champigneulle J, Salles Y, Brizion M, Puyhardy JM, et al. Molecular diagnosis of disseminated adiaspiromycosis due to *Emmonsia crescens*. J Clin Microbiol. 2009;47:1269–73. http://dx.doi.org/10.1128/JCM.01885-08
3. Peterson SW, Sigler L. Molecular genetic variation in *Emmonsia crescens* and *Emmonsia parva*, etiologic agents of adiaspiromycosis, and their phylogenetic relationship to *Blastomyces dermatitidis* (*Ajellomyces dermatitidis*) and other systemic fungal pathogens. J Clin Microbiol. 1998;36:2918–25.
4. Wellinghausen N, Kern WV, Haase G, Rozdzinski E, Kern P, Marre R, et al. Chronic granulomatous lung infection caused by the dimorphic fungus *Emmonsia* sp. Int J Med Microbiol. 2003;293:441–5. http://dx.doi.org/10.1078/1438-4221-00281
5. Kenyon C, Bonorchis K, Corcoran C, Meintjes G, Locketz M, Lehloenya R, et al. A dimorphic fungus causing disseminated infection in South Africa. N Engl J Med. 2013;369:1416–24. http://dx.doi.org/10.1056/NEJMoa1215460
6. Heys I, Taljaard J, Orth H. An *Emmonsia* species causing disseminated infection in South Africa. N Engl J Med. 2014;370:283–4. http://dx.doi.org/10.1056/NEJMc1314277
7. Latgé JP. Oh, to be new. N Engl J Med. 2013;369:1464–6. http://dx.doi.org/10.1056/NEJMe1309132
8. Petti CA, Polage CR, Quinn TC, Ronald AR, Sande MA. Laboratory medicine in Africa: a barrier to effective health care. Clin Infect Dis. 2006;42:377–82. http://dx.doi.org/10.1086/499363

Address for correspondence: Wesley van Hougenhouck-Tulleken, Helen Joseph Hospital, 1 Perth Road, Johannesburg, South Africa; email: westulleken@gmail.com

Ecosystem Effects of Variant Rabbit Hemorrhagic Disease Virus, Iberian Peninsula

To the Editor: In this investigation, we found evidence for the apparent effects that a new variant of the rabbit hemorrhagic disease virus (RHDV) is having on native wild European rabbit (*Oryctolagus cuniculus*) populations on the Iberian Peninsula, and how this virus could threaten the conservation of endangered predators.

Historically, European rabbits were extremely abundant on the Iberian Peninsula, which is in their native range. However, during the 20th century, the number of rabbits on the peninsula has declined >90%, mainly because of diseases (*1*). The first notable crisis among rabbits occurred during the 1950s concurrent with the arrival of myxomatosis among rabbit populations, which caused mortality rates of ≈90% (*1*), as registered in other regions. During the late 1980s, a calicivirus, RHDV, caused infections that made a strong impact on rabbit populations, causing initial mortality rates of 55%–75% in Iberia (*1*). Since their initial outbreaks, both diseases have become enzootic, and related mortality rates have decreased, in part because of increased host resistance, although the infections still play a major role in the dynamics of rabbit populations (*2*).

In 2011, a new variant of RHDV, which appears to be closely related to an isolate originating in France that was described in 2010 (*3*), caused high mortality rates in some rabbit farms in Spain (*4*) and was also identified in an experimental wild rabbit plot in northern Spain (*5*). Since 2012, the new variant of RHDV has been detected in most rabbit farms in Spain (*6*), and in several wild populations distributed across Spain and Portugal (*7*), suggesting that it has rapidly spread throughout the Iberian Peninsula. This variant affects both of the wild rabbit subspecies (*O. cuniculus cuniculus* and *O. c. algirus*), and unlike the classical form of RHDV, it kills rabbits as young as 11 days of age and rabbits that have been vaccinated against classic RHDV (*6*,*7*). This scenario has raised concern for the survival of wild rabbit populations and its predators in this region.

Data regarding rabbit trends seem to sustain this concern. For example, a long-term monitoring program in Aragón in northern Spain shows a notable decline in rabbit numbers during 2013 in populations that showed both long-term increasing and decreasing trends over the monitoring period (Figure, panels A, B, respectively). A similar trend has been observed in the main areas inhabited by the highly endangered Iberian lynx (*Lynx pardinus*). The lynx relies on rabbits for survival, because they represent >85% of the lynx's diet (*9*). For instance, in Coto del Rey, the area within Doñana National Park in southern Spain that traditionally held the highest rabbit densities and therefore represents the core of Iberian lynx populations in this national park, there was a decline in rabbits of >80% during 2012–2013 (Figure, panel C). Similar declines have been detected in low-density rabbit populations surveyed within Doñana National Park (Figure, panel C). Rabbit numbers have also been progressively dropping in the proximity of the Yeguas River in Andújar and Cardeña Natural Parks in southern Spain, where the largest Iberian lynx population currently lives: rabbit density was >3.5 rabbits/hectare in 2010 and <1 rabbit/hectare in 2013, a decline of ≈75% (*10*). In accordance with field surveys, hunters throughout Iberia claim that the number of rabbits harvested this season has decreased dramatically, pointing to a 70%–80% decline compared to the previous hunting season in some estates (A. Linares, pers. comm.).

The European rabbit is a multifunctional keystone species of the Iberian Mediterranean ecosystem, where it serves as prey for >30 predatory animals, alters plant species composition and vegetation structure through grazing and seed dispersal, its excrement and urine have an effect on soil fertility and plant growth and provide feeding resources for invertebrates, and its burrows provide shelter for different

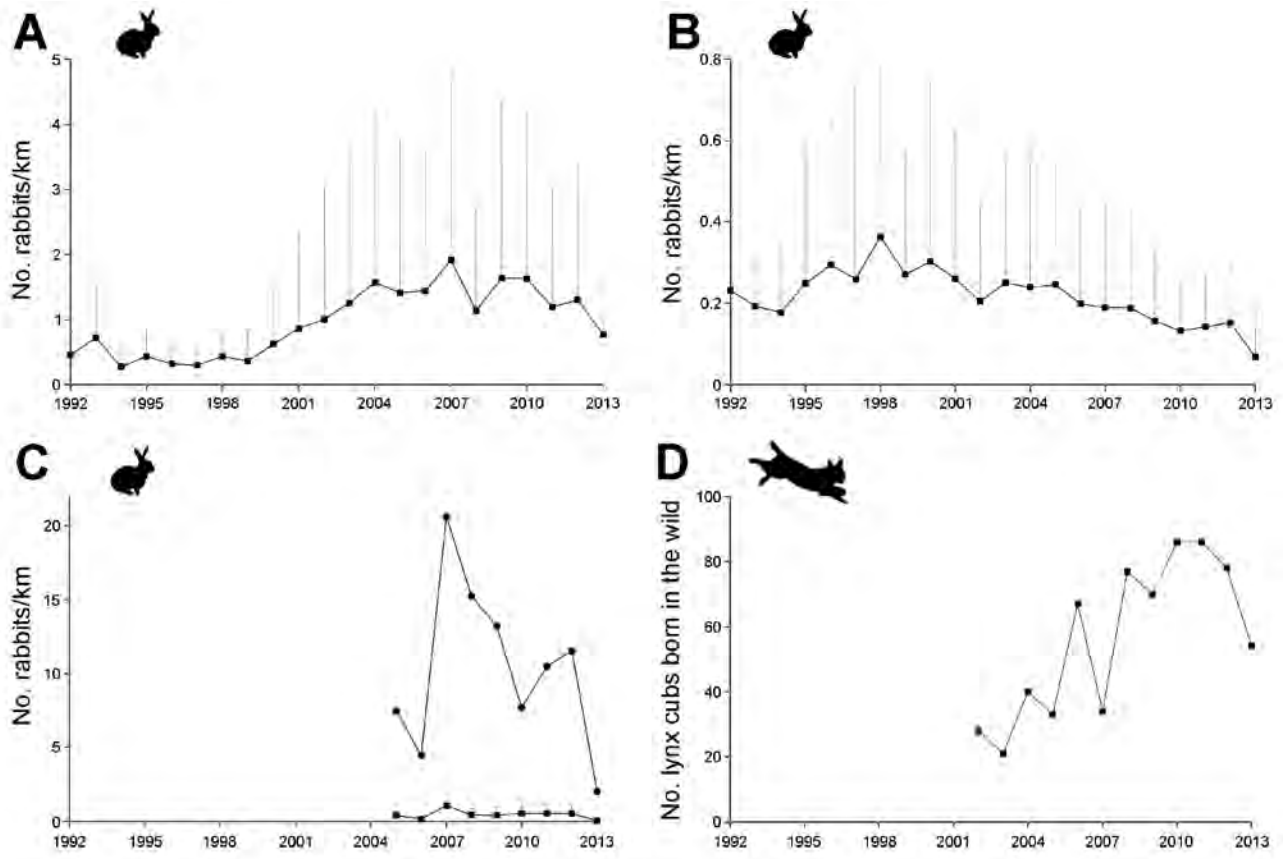

Figure. Trends in rabbit abundance (number of rabbits/km) in Aragón and Doñana National Park, northern and southern Spain, respectively, and in the number of Iberian lynx cubs born in the wild in Spain. A) Average rabbit abundance (+SD) of populations showing long-term increasing trend over the whole sampling period (n = 18) in Aragón (*8*); B) average rabbit abundance (+SD) of populations showing long-term decreasing trend over the whole sampling period (n = 25) in Aragón (*8*); C) rabbit abundance over the study period in Coto del Rey (circles), which is likely the main area for rabbits and lynxes within Doñana National Park; and average rabbit abundance (+SD) over the study period of 7 low-density populations (squares) within Doñana National Park (see details about methods in http://www-rbd.ebd.csic.es/Seguimiento/mediobiologico/conejo/pnd/ProtocoloCensoConejosPND.pdf); and D) total number of lynx cubs born in the wild during 2002–2013 in Spain (data available at http://www.lifelince.org and http://www.juntandeandalucia.es).

species (*9*). Therefore, the decline in rabbit numbers could have potential cascading effects on ecosystem function. In fact, some of these effects may already be apparent on rabbit-reliant animals. On one hand, the sharp reduction in rabbit numbers observed in 2013 in the main lynx distribution area has been accompanied by a notable decrease in the number of lynx cubs born in the wild (Figure, panel D). On the other hand, the number of lynxes killed on roads doubled in 2013 (n = 14) in relation to 2012 (n = 7), and this has been linked to increased lynx displacements related to rabbit scarcity potentially associated with the impact of the new variant of RHDV (http://www.juntadeandalucia.es).

The situation described exemplifies how emerging diseases can affect biodiversity conservation. It also highlights the importance of using wildlife monitoring schemes as detection tools for monitoring the impact of stochastic factors, such as the variant RHDV, on wildlife populations. Urgent management actions, designed within an Iberian rabbit conservation strategy that relies on a multidisciplinary framework, are needed to ensure the conservation of this keystone member of the Iberian Peninsula ecosystem and that of rabbit-reliant predators.

Acknowledgments

We thank Olga Ceballos, David Paz, Isidro Román, Luis Alfonso, Rocío López, and other members of the Doñana Biological Station Monitoring Team, Miguel Pineda, and 2 anonymous reviewers for their comments on the manuscript.

The Aragón monitoring scheme is run by the Fish and Game Department, Government of Aragón. M.D.M. was supported by a JAE-DOC contract (Programa Junta para la Ampliación de Estudios), funded by CSIC and the European Social Fund. C.F. was supported by a Post-Doctoral Fellowship funded by NSERC, Government of Canada. C.G. acknowledges EU-FP7 grant ANTIGONE (#278976)

and the EMIDA ERA-NET and INIA grant APHAEA.

Miguel Delibes-Mateos, Catarina Ferreira, Francisco Carro, Marco A. Escudero, and Christian Gortázar

Author affiliations: Instituto de Investigación en Recursos Cinegéticos, a collaborative agency of the Consejo Superior de Investigaciones Científicas, Universidad de Castilla-La Mancha, and Junta de Comunidades de Castilla-La Mancha, Ciudad Real, Spain (M. Delibes-Mateos, C. Gortázar); Trent University, Peterborough, Ontario, Canada (C. Ferreira); Estación Biológica de Doñana, Seville, Spain (F. Carro); and Ebronatura, Zaragoza, Spain (M.A. Escudero)

DOI: http://dx.doi.org/10.3201/eid2012.140517

References

1. Delibes-Mateos M, Ferreras P, Villafuerte R. European rabbit population trends and associated factors: a review of the situation in the Iberian Peninsula. Mammal Review. 2009;39:124–40. http://dx.doi.org/10.1111/j.1365-2907.2009.00140.x
2. Calvete C. Modeling the effect of population dynamics on the impact of rabbit hemorrhagic disease. Conserv Biol. 2006;20:1232–41. http://dx.doi.org/10.1111/j.1523-1739.2006.00371.x
3. Le Gall-Reculé G, Zwingelstein F, Boucher S, Le NB, Plassiart G, Portejoie Y, et al. Detection of a new variant of rabbit haemorrhagic disease virus in France. Vet Rec. 2011;168:137–8. http://dx.doi.org/10.1136/vr.d697
4. Dalton KP, Nicieza I, Balseiro A, Muguerza MA, Rosell JM, Casais R, et al. Variant rabbit hemorrhagic disease virus in young rabbits, Spain. Emerg Infect Dis. 2012;18:2009–12. http://dx.doi.org/10.3201/eid1812.120341
5. Calvete C, Calvo JH, Sarto P. Detección de una nueva variante del virus de la enfermedad hemorrágica en conejos silvestres en España. In: Abstracts of the 37th symposium de cunicultura de ASESCU, 2012 May 24–25. Barbastro (Spain): Asociación Española de Cunicultura; 2012.
6. Dalton KP, Nicieza I, Abrantes J, Esteves PJ, Parra F. Spread of new variant of RHDV in domestic rabbits on the Iberian Peninsula. Vet Microbiol. 2014;169:67–73. http://dx.doi.org/10.1016/j.vetmic.2013.12.015
7. Abrantes J, Lopes AM, Dalton KP, Melo P, Correia JJ, Ramada M, et al. New variant of rabbit hemorrhagic disease virus, Portugal, 2012–2013. Emerg Infect Dis. 2013;19:1900–2. http://dx.doi.org/10.3201/eid1911.130908
8. Williams D, Acevedo P, Gortázar C, Escudero MA, Labarta JL, Marco MA, et al. Hunting for answers: rabbit (*Oryctolagus cuniculus*) population trends in northeastern Spain. European Journal of Wildlife Research. 2007;53:19–28. http://dx.doi.org/10.1007/s10344-006-0056-0
9. Delibes-Mateos M, Delibes M, Ferreras P, Villafuerte R. Key role of European rabbits in the conservation of the western Mediterranean Basin hotspot. Conserv Biol. 2008;22:1106–17. http://dx.doi.org/10.1111/j.1523-1739.2008.00993.x
10. Garrote G. Repoblaciones del conejo de monte en gran escala para la conservación del lince Ibérico. In: Abstracts of the First International Wild Rabbit Seminar, 2013 Oct. 23–25. Beja (Portugal): Associação IBERLINX, Instituto da Conservação da Naturaleza e das Florestas, and Junta de Andalucía; 2013, p. 6.

Address for correspondence: Miguel Delibes-Mateos. Instituto de Investgación en Recursos Cinegéticos, IREC-CSIC-UCLM-JCCM, Ronda de Toledo s/n 13071 Ciudad Real, Spain; email: mdelibesmateos@gmail.com

Molecular Characterization of *Borrelia burgdorferi* from Case of Autochthonous Lyme Arthritis

To the Editor: The first Lyme borreliosis (LB) case reported to be acquired in California occurred in 1978 (*1*). During the past 10 years, 744 confirmed LB cases were reported in California; 419 (56.2%) were likely acquired in-state. The highest incidence of this disease occurs in northern coastal California, in locations such as Santa Cruz County (*2*), where habitat supports yearlong activity of the tick vector *Ixodes pacificus* (*3*,*4*).

Existing data describe the genetic diversity of the LB agent *Borrelia burgdorferi* among ticks in California (*5*,*6*), but few instances of direct detection and genetic characterization of *B. burgdorferi* sensu stricto in samples from humans are documented in California. *B. burgdorferi* has been isolated from skin biopsy samples of 3 patients in California in whom LB was diagnosed (*1*). Seinost et al. genotyped strains isolated in the United States, including 7 isolates identified in California from skin, blood, or cerebrospinal fluid, but no documented exposure information was available (*7*). Girard et al. genotyped *B. burgdorferi* in 10- to 12-year-old stored serum samples collected from 22 northern California residents, some of whom were asymptomatic at time of collection. Of 22 PCR-positive specimens, 21 had the single laboratory type strain B31 genotype (*3*).

A 12-year-old resident of Santa Cruz County, California, came to the emergency department of Dominican Hospital in September 2012 with a swollen, painful right knee and mildly painful right hip. The patient's family reported that LB had been diagnosed by a local physician. Illness onset was in May 2010; symptoms consisted of recurrent knee swelling and pain lasting several days every 4–5 months and positive serologic test results for *B. burdorferi* (not available). The patient had not traveled outside of California during the preceding 6 years. In May 2011, an IgG Western blot of the patient's serum that was processed at a commercial laboratory showed immunoreactive bands of 18, 23, 28, 30, 39, 41, 45, 58, 66, and 93 kDa. In both 2010 and 2011, the patient's family had chosen to give the patient unspecified herbal treatments instead of antibacterial drugs.

On physical examination in the emergency department, the patient's right knee was swollen; knee flexion

was reduced to 30°. The right hip was painful on rotation. Serum laboratory values included a leukocyte count of 7,000/mL, hematocrit 33%, and erythrocyte sedimentation rate of 73mm/h. Plain radiograph images of the right hip did not show any abnormalities; the radiograph of the right knee showed suprapatellar effusion (Figure). Right knee aspiration yielded 115 mL of cloudy yellow fluid; laboratory tests showed a leukocyte count of 59,750/mL and protein level 5 g/dL; no crystals were noted. Results of routine bacterial culture of synovial fluid were negative. Amoxicillin was prescribed for a suspected septic joint and was taken for 1 week. Nine months later, the patient was reportedly asymptomatic and had returned to normal activity.

Right knee synovial fluid was sent to ARUP Laboratories (Salt Lake City, UT, USA); results were positive for the *B. burgdorferi* sensu lato *recA* gene by use of a proprietary qualitative PCR procedure. At the University of California, Irvine, we thawed another aliquot of synovial fluid, which had been frozen without cryoprotectant, and inoculated samples into BSK II medium (*8*). After incubation for 2 weeks at 34°C, no spirochetes were noted. We subjected another 100 mL aliquot to DNA extraction using DNeasy Blood and Tissue Kit and the QIAcube apparatus (QIAGEN, Valencia, CA, USA). We used multiplex quantitative PCR (qPCR) and primers and specific probes for the 16S ribosomal RNA genes of LB group species and for relapsing fever group species of *Borrelia* in 2 replicates as described by Barbour et al. (*9*). By qPCR, there were 18 gene copies of an LB group species in 1 replicate and 23 copies in the other. The qPCR results for relapsing fever group species, including *B. miyamotoi* and *B. hermsii*, which are enzootic in parts of California, were negative. We genotyped the *ospC* allele and 16S–23S intergenic spacer (IGS) using PCR amplification of each locus and direct sequencing as described by Travinsky et al. (*6*). Sequencing of the targeted PCR products showed that the *ospC* allele was type Hb and the IGS genotype was 13.

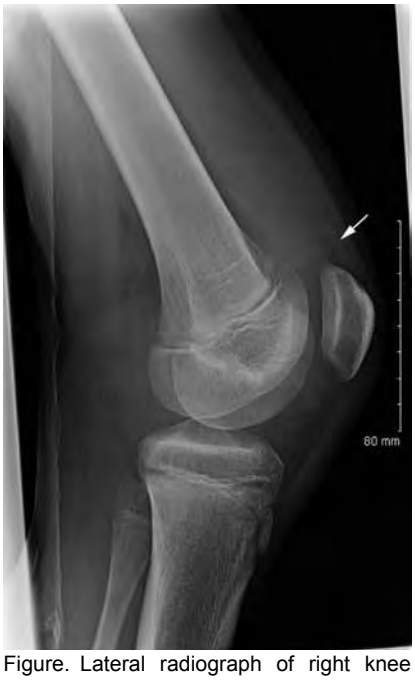

Figure. Lateral radiograph of right knee demonstrating suprapatellar effusion without acute osseous injury (arrow).

Two years of untreated relapsing pauciarticular arthritis of the knee and hip, a *B. burgdorferi*–positive Western blot, and laboratory detection of *B. burgdorferi* from synovial fluid by PCR in 2 different laboratories leads us to conclude that the patient had Lyme arthritis. This patient likely acquired the infection locally. The prevalence of *B. burgdorferi* in nymphal *I. pacificus* ticks (range 4%–10%) in Santa Cruz County, and >10% of the geographic area of the county is categorized as being at high acarologic risk for LB (*4*). To our knowledge, the combination of *ospC* allele Hb and IGS genotype 13 has been identified only in California to date (*6*,*8*). A type "H" *osp*C type was reported from synovial fluid from LB patients from the eastern United States (*10*), but in the absence of IGS determination, this was probably type Ha, which is more typical of that region (*8*). The addition of the IGS locus to *ospC* alleles provides a precise approach to characterize genetic diversity and potential origin of *B. burgdorferi* in human tissue.

Acknowledgments

We thank the staff of Dominican Hospital, Santa Cruz, California, for facilitating access to case information; the staff of the County of Santa Cruz communicable disease division for their continued support; and California Epidemiologic Investigation Services for their suggestions for this manuscript and the work of their fellow, Sharon I. Brummitt.

The project described was supported by the Preventive Health Services Block Grant from the Centers for Disease Control and Prevention. Laboratory work at University of California Irvine was supported by the National Institutes of Health grant AI-065359. This work was determined exempt by The Committee for the Protection of Human Subjects, California Office of State Health and Planning.

Sharon I. Brummitt, Alan G. Barbour, Fong Hue, and Anne M. Kjemtrup

Author affiliations: Santa Cruz Communicable Disease, Santa Cruz, California, USA (S.I. Brummitt); California Department of Public Health, Sacramento, California, USA (S.I. Brummitt, A.M. Kjemtrup); County of and University of California Irvine, Irvine, California, USA (A.G. Barbour, F. Hue)

DOI: http://dx.doi.org/10.3201/eid2012.140655

References

1. Fritz CL, Vugia DJ. Clinical issues in Lyme borreliosis: a California perspective. Infectious Disease Review 2001;3:111–22.
2. California Department of Public Health, Vector-Borne Disease Section. California: information for health professionals: tick-borne disease of interest in California (updated 2014 Mar 10; cited 2014 Mar 11). http://www.cdph.ca.gov/HealthInfo/discond/Documents/EpiandPreventionofTBDInterestinCa.ppsx
3. Girard YA, Fedorova N, Lane RS. Genetic diversity of *Borrelia burgdorferi* and detection of *B. bissettii*-like DNA in serum of north-coastal California residents.

J Clin Microbiol. 2011;49:945–54. http://dx.doi.org/10.1128/JCM.01689-10
4. Lane RS, Manweiler SA, Stubbs HA, Lennette ET, Madigan JE, Lavoie PE. Risk factors for Lyme disease in a small rural community in northern California. Am J Epidemiol. 1992;136:1358–68.
5. Girard YA, Travinsky B, Schotthoefer A, Fedorova N, Eisen RJ, Eisen L, et al. Population structure of the Lyme borreliosis spirochete *Borrelia burgdorferi* in the Western black-legged tick (*Ixodes pacificus*) in northern California. Appl Environ Microbiol. 2009;75:7243–52. http://dx.doi.org/10.1128/AEM.01704-09
6. Travinsky B, Bunikis J, Barbour AG. Geographic differences in genetic locus linkages for *Borrelia burgdorferi*. Emerg Infect Dis. 2010;16:1147–50. http://dx.doi.org/10.3201/eid1607.091452
7. Seinost G, Dykhuizen DE, Dattwyler RJ, Golde WT, Dunn JJ, Wang IN, et al. Four clones of *Borrelia burgdorferi* sensu stricto cause invasive infection in humans. Infect Immun. 1999;67:3518–24.
8. Barbour AG, Travinsky B. Evolution and distribution of the *ospC* gene, a transferable serotype determinant of *Borrelia burgdorferi*. MBio. 2010;1:10.1128/mBio.00153-10.
9. Barbour AG, Bunikis J, Travinsky B, Gatewood HA, Diuk-Wasser M, Fish D, et al. Niche partitioning of *Borrelia burgdorferi* and *Borrelia miyamotoi* in the same reservoir host and arthropod vector. Am J Trop Med Hyg. 2009;81:1120–31. http://dx.doi.org/10.4269/ajtmh.2009.09-0208
10. Strle K, Jones KL, Drouin EE, Li X, Steere AC. *Borrelia burgdorferi* RST 1 (OspC Type A) Genotype is associated with greater inflammation and more severe Lyme disease. Am J Pathol. 2011;178:2726–39. http://dx.doi.org/10.1016/j.ajpath.2011.02.018

Address for correspondence: Anne M. Kjemtrup, California Department of Public Health, 1616 Capitol Ave, MS 7307, PO Box 997377, Sacramento, CA 95899-9730. USA; email: Anne.Kjemtrup@cdph.ca.gov

Zoonotic *Baylisascaris procyonis* Roundworms in Raccoons, China

To the Editor: *Baylisascaris procyonis*, an intestinal roundworm that infects raccoons (*Procyon lotor*), causes fatal or severe neural larva migrans in animals and humans (*1*,*2*). Globally, ≈130 species of wild and domesticated animals are susceptible (*2*). Infections in humans typically occur in children who have the disorders pica or geophagia and ingest *B. procyonis* eggs in items contaminated with raccoon feces (*3*). Clinical manifestations include ocular disease, eosinophilic encephalitis, and eosinophilic cardiac pseudotumors; severe infection can lead to death. Since 1984, ≈24 cases of *B. procyonis*–related human neural larva migrans have been reported, mainly in the United States (*1*,*3*–*5*; K.R. Kazacos, pers. comm.). Despite few cases among humans, lack of effective treatment and widespread distribution of infected raccoons in close association with humans make *B. procyonis* a potentially serious public health threat (*2*,*6*). The current distribution of *B. procyonis* is poorly recorded in Asia (*2*,*7*), except for Japan (*8*). We describe *B. procyonis* infections among raccoons in China as part of a series of ongoing surveys of helminthic zoonoses linked to captive exotic animals in zoologic gardens (ZGs) in China.

More than 90% of raccoons in China (n >320) are raised as exotic ornamental animals in 18 ZGs. During 2011–2013, we collected 2×308 fecal samples (i.e., 1 repeat within each sampling) from 277 raccoons in 12 randomly selected ZGs (online Technical Appendix Figure 1, wwwnc.cdc.gov/EID/article/20/12/14-0970-Techapp1.pdf). Samples were stored in individual plastic bags at –20°C until use. We examined raccoons (n = 31) at the Sichuan ZGs twice, in June 2012 and May 2013. We identified *B. procyonis* eggs in feces using morphologic and molecular analyses (*1*,*2*,*9*). The nuclear first internal transcribed spacer (428 bp) and mitochondrial cytochrome c oxidase subunit 1 (*cox-1*, 938 bp) genes in each sample were PCR-amplified and sequenced. *B. procyonis* infection was confirmed by sequencing and phylogenetic analyses of both genes (*7*,*9*). We reexamined ≈60% of fecal samples to validate results. Prevalence (95% CI) was calculated for the overall population and independently for female, male, juvenile, and adult raccoons. We determined differences between the tested ZG prevalence and prevalence by sex or age of raccoons using χ^2 or Fisher exact tests in SAS (SAS Institute, Cary, NC, USA); p values <0.05 were considered significant.

Building on egg-based morphologic characterization and internal transcribed spacer 1 and *cox-1* gene-based phylogenies using neighbor-joining trees (online Technical Appendix Figure 2), we found *B. procyonis* in raccoon feces from 5/12 ZGs (42%; 95% CI 14%–70%), including 2 in the most densely populated provinces, Henan and Sichuan. More infections were found in western than central and eastern ZGs (4/6 and 1/6, respectively; Table, online Technical Appendix Figure 1) (p = 0.079). Fecal samples of 35 raccoons (13%; 95% CI 9%–17%) tested positive for *B. procyonis*. The mean intensity of egg shedding was 5,000 eggs per gram (range 800–11,200 eggs per gram; data not shown). No significant difference was observed in the intensity of shedding by comparing sex and age of animals, and no significant differences were noted in the mean prevalence between female and male raccoons (12% versus 14%; p = 0.677) or between adult and juvenile animals (13% versus 10%; p = 0.536).

This investigation documents the presence and prevalence of *B. procyonis*

Table. Prevalence of *Baylisascaris procyonis* roundworm infections among captive raccoons, China, 2011–2013*

Location, zoological gardens	No. *B. procyonis*–positive samples/total no. samples (%)				
	Sex		Age group		
	M	F	Adult	Juvenile	Total
Western region					33/146 (23)
Chongqing	–	0/4	0/4	–	0/4
Bifengxia	0/8	0/14	0/13	0/9	0/22, 0/22
Chengdu	0/4	1/5 (20)	0/6	1/3 (33)	1/9 (11), 0/9
Xi'an Wildlife	0/9	1/27 (4)	0/28	1/8 (13)	1/36 (3)
Kunming	12/12 (100)	15/15 (100)	22/22 (100)	5/5 (100)	27/27 (100)
Kunming Wildlife	1/24 (4)	3/24 (13)	4/48 (8)	–	4/48 (8)
Central region					2/56 (4)
Harbin Northern Forest	0/12	0/18	0/21	0/9	0/30
Zhengzhou	1/5 (20)	1/11 (9)	2/12 (17)	0/4	2/16 (13)
Changsha	0/3	0/7	0/5	0/5	0/10
Eastern region					0/75
Beijing	0/16	0/24	0/22	0/18	0/40
Guangzhou	0/5	0/15	0/20	–	0/20
Shanghai Wildlife	0/4	0/11	0/9	0/6	0/15
Total	14/102 (14)	21/175 (12)	28/210 (13)	7/67 (10)	35/277 (13)
p value	0.677		0.536		–

*Raccoons, considered to be exotic ornamental animals, are mainly kept in 18 zoologic gardens (ZGs) in China; 12 ZGs were examined for *B. procyonis* prevalence during the study period. Sichuan ZGs, including Bifengxia ZG and Chengdu ZG, were tested twice during this surveillance period. –, no raccoons in the group or no data available.

among raccoons in China. The findings imply that raccoons harboring this parasite have the potential for spreading it to humans. One reason is that captive raccoons adapt readily to humans and easily take food offered by hand; another is that communal raccoon latrine sites in ZGs are usually close to areas where humans gather, so ZG visitors may be exposed to large numbers of eggs (online Technical Appendix Figure 3). These eggs can remain viable and infective for years (*2*), and latrines are recognized as primary sources of transmission of *B. procyonis* to humans (*4*). Current public health initiatives to prevent *B. procyonis* infections in humans rely on the education of veterinary and human health care professionals, who in turn inform the public (*1*,*6*,*10*). Thus, veterinarians, clinicians, and public health officials in China should be more informed about this pathogen, especially in regions with large raccoon populations.

Because of a lack of clinical awareness of this illness and subsequent lack of early diagnosis and effective treatment, prevention of *B. procyonis* infection by education is essential. In addition, a strategy for eradication is needed. Heat, in the form of boiling water, steam-cleaning, or fire, is the optimal tool for killing *B. procyonis* eggs (*2*) and therefore can be used to decontaminate areas surrounding latrines. Within heavily contaminated areas, removing and then sterilizing the top few inches of surface soil with heat would be effective and practical (*1*,*2*). Among captive raccoon populations, particularly in China, regular deworming is also likely to be helpful in reducing novel and existing sources of infection (*1*–*3*).

Finally, although no cases of human infection have been reported in China to our knowledge, physicians should consider including *B. procyonis* infections in their differential diagnoses of patients with indicative features: clinical (eosinophilic encephalitis, ocular disease), epidemiologic (raccoon exposure), radiologic (white matter disease), and laboratory results (blood and CNS eosinophilia) (*1*,*10*). This study lays the foundation for future steps to educate the population of China about *B. procyonis* infection and to create programs to prevent the spread of this disease to humans.

Acknowledgments

We thank Bo Zhao and Lili Niu for their coordination and help in collecting fecal samples from zoologic gardens of China. We also thank Kevin R. Kazacos for reviewing the manuscript and providing helpful comments.

This study was supported by grants from the Program for Changjiang Scholars and Innovative Research Team in University (PCSIRT) (grant no. IRT0848) and the Research Fund for the Chengdu Research of Giant Panda Breeding (project no. CPF2012-13).

Yue Xie, Xuan Zhou, Mei Li, Tianyu Liu, Xiaobin Gu, Tao Wang, Weimin Lai, Xuerong Peng, and Guangyou Yang

Author affiliation: Sichuan Agricultural University, Ya'an, Sichuan, China

DOI: http://dx.doi.org/10.3201/eid2012.140970

References

1. Gavin PJ, Kazacos KR, Shulman ST. Baylisascariasis. Clin Microbiol Rev. 2005;18:703–18. http://dx.doi.org/10.1128/CMR.18.4.703-718.2005
2. Kazacos K. *Baylisascaris procyonis* and related species. In: Samuel W, Pybus M, Kocan A, editors. Parasitic diseases of wild mammals. 2nd ed. Ames (IA): Iowa State University Press; 2001. p. 301–41.
3. Murray WJ, Kazacos KR. Raccoon roundworm encephalitis. Clin Infect Dis. 2004;39:1484–92. http://dx.doi.org/10.1086/425364

4. Page LK, Anchor C, Luy E, Kron S, Larson G, Madsen L, et al. Backyard raccoon latrines and risk for *Baylisascaris procyonis* transmission to humans. Emerg Infect Dis. 2009;15:1530–1. http://dx.doi.org/10.3201/eid1509.090128
5. Kelly TG, Madhavan VL, Peters JM, Kazacos KR, Silvera VM. Spinal cord involvement in a child with raccoon roundworm (*Baylisascaris procyonis*) meningoencephalitis. Pediatr Radiol. 2012;42:369–73. http://dx.doi.org/10.1007/s00247-011-2151-y
6. Wise ME, Sorvillo FJ, Shafir SC, Ash LR, Berlin OG. Severe and fatal central nervous system disease in humans caused by *Baylisascaris procyonis*, the common roundworm of raccoons: a review of current literature. Microbes Infect. 2005;7:317–23. http://dx.doi.org/10.1016/j.micinf.2004.12.005
7. Blizzard EL, Yabsley MJ, Beck MF, Harsch S. Geographic expansion of *Baylisascaris procyonis* roundworms, Florida, USA. Emerg Infect Dis. 2010;16:1803–4. http://dx.doi.org/10.3201/eid1611.100549
8. Miyashita M. Prevalence of *Baylisascaris procyonis* in raccoons in Japan and experimental infections of the worm in laboratory animals. Journal of Urban Living and Health Association. 1993;37:137–51.
9. Xie Y, Zhang Z, Niu L, Wang Q, Wang C, Lan J, et al. The mitochondrial genome of *Baylisascaris procyonis*. PLoS ONE. 2011;6:e27066. http://dx.doi.org/10.1371/journal.pone.0027066
10. Sorvillo F, Ash LR, Berlin OGW, Tatabe J, Degiorgio C, Morse SA. *Baylisascaris procyonis*: an emerging helminthic zoonosis. Emerg Infect Dis. 2002;8:355–9. http://dx.doi.org/10.3201/eid0804.010273

Address for correspondence: Guangyou Yang, Department of Parasitology, College of Veterinary Medicine, Sichuan Agricultural University, 46 Xinkang Rd, Ya'an, Sichuan, 625014, People's Republic of China; email: guangyouyang@hotmail.com

Novel Divergent Rhabdovirus in Feces of Red Fox, Spain

To the Editor: Rhabdoviruses (family *Rhabdoviridae*) are enveloped single-stranded negative-sense RNA viruses belonging to the Mononegavirales order. The International Committee on Taxonomy of Viruses recognizes 11 genera (*Cytorhabdovirus*, *Ephemerovirus*, *Lyssavirus*, *Novirhabdovirus*, *Nucleorhabdovirus*, *Perhabdovirus*, *Sigmavirus*, *Sprivivirus*, *Tibrovirus*, *Tupavirus*, *Vesiculovirus*) (*1*). In addition, many recently described rhabdoviruses remain unassigned. Rhabdoviruses contain 5 major genes, encoding for nucleoprotein (N), phosphoprotein (P), matrix (M), glycoprotein (G), and RNA-dependent RNA polymerase (L). The *Rhabdoviridae* family includes pathogens of various animal species, humans, and plants. Viruses of the genus *Lyssavirus* are the most relevant to public health because they can cause rabies. Bats are the driving force within this genus; foxes and various other species of wild carnivores also can be infected with lyssaviruses and transmit them to humans and dogs (*2*).

During a viral metagenomic survey, conducted as described previously (*3*), of fecal samples collected from 4 red foxes (*Vulpes vulpes*) that were found dead in Álava, Basque Country, Spain, we identified the complete coding sequence and the partial leader and trailer sequence of a novel rhabdovirus, tentatively called red fox fecal rhabdovirus (RFFRV; 15,541 nt, GenBank accession no. KF823814; online Technical Appendix, http://wwwnc.cdc.gov/EID/article/20/12/14-0236-Techapp1.pdf) by mapping 8,287 of the 56,519 sequence reads in the sample of a red fox. A proportion of obtained reads contained sequences that were ≥99% identical to mitochondrial DNA of *V. vulpes*, which confirmed that the sample was collected from a red fox.

The obtained sequence of RFFRV was partially confirmed by specific primers and Sanger sequencing of PCR amplicons. Five major and 3 minor open reading frames (ORFs) were identified that had a genome organization similar to that of other rhabdoviruses (Figure, panel A). No significant hits were obtained by BLAST analysis (http://blast.ncbi.nlm.gov/Blast.cgi) of N, P, M, and G nucleotide and amino acid sequences, which was reported previously for novel divergent rhabdoviruses (*4*).

Predicted N, P, and M genes of RFFRV consist of 1,629, 2,490, and 813 nt, respectively, encoding for 543, 830, and 271 aa (online Technical Appendix Table 1). In addition to the absence of significant hits observed by BLAST analysis, no significant sequence homology was observed with known rhabdovirus proteins in pairwise alignments. Furthermore, no conserved motifs were detected in N, P, and M genes of RFFRV that are commonly observed in rhabdoviruses. However, intergenic regions between all major ORFs contained relatively conserved motifs that could be transcription termination/polyadenylation sequences (A/U) CU_7, similar to other rhabdoviruses (*5*). Adjacent to this termination signal was a stretch of conserved nucleotides that might function as a transcription initiation signal (online Technical Appendix Table 1).

The amino acid sequence of the G protein consisted of 669 aa and contained an N terminal signal peptide (1-MYHLIVLLVMLGQRAVA-17), a noncytoplasmic domain (aa 18–646), a transmembrane domain (647-ITAILMPLLSLAVVVGIIMCC-667), and a cytoplasmic tail of 2 aa, similar to other rhabdovirus G proteins as predicted by using Phobius and TMHMM (http://www.cbs.dtu.dk/services/TMHMM) (*6*,*7*). We predicted 3 potential glycosylation sites in the ectodomain at positions 38–40

(NKT), 554–556 (NAS), and 592–594 (NIS) using NetNGlyc 1.0 (http://www.cbs.dtu.dk/services/NetNGlyc).

Between the G and L genes, a complex intergenic region was present that contained 3 ORFs of 246 nt (7,413–7,658 aa), 231 nt (7,716–7,946 aa), and 459 nt (7,893–8,355 aa), of which 2 were overlapping frames (U1–3). Additional ORFs between G and L genes were detected previously in other rhabdoviruses (*8*,*9*). We detected transmembrane domains in the amino acid sequences of all 3 additional ORFs, suggesting they might act as viroporin (*8*,*9*).

The L gene of RFFRV contained 6,591 nt (2,197 aa). We detected several conserved domains and motifs, including RNA-dependent RNA polymerase, mRNA-capping region, mRNA capping enzyme, and virus-capping methyltransferase. Alignment of the deduced amino acid sequence of the L gene with the L gene of various other viruses belonging to the Mononegavirales order by using MAFFT version 7 (http://mafft.cbrc.jp/alignment/software/) and subsequent phylogenetic reconstruction by using a maximum-likelihood tree (WAG+F+I+G model with 100 bootstrap replicates in MEGA5 [http://www.megasoftware.net]) suggested that this virus belongs to a novel genus of the *Rhabdoviridiae* family. In addition, pairwise identities of the deduced amino acid sequence of the L gene of RFFRV with that of other rhabdoviruses of the *Rhabdoviridae* family were only ≤35% (online Technical Appendix Table 2).

Because the fox was found dead and no tissue samples were collected, whether RFFRV played a role in the animal's death is unknown. In addition, multiple attempts to isolate this virus on various cell lines of eukaryotes (Vero E6, MDCK, CRFK, N2a, and BHK cells, primary fox kidney cells) failed because of the absence of cytopathic effects and viral replication by quantitative reverse transcription PCR, despite a high number of reads in the original sample. The fox might have acquired the virus through spillover from a small prey, such as a bat, and additional studies are required to elucidate the prevalence, original host, and pathogenic potential of this novel virus.

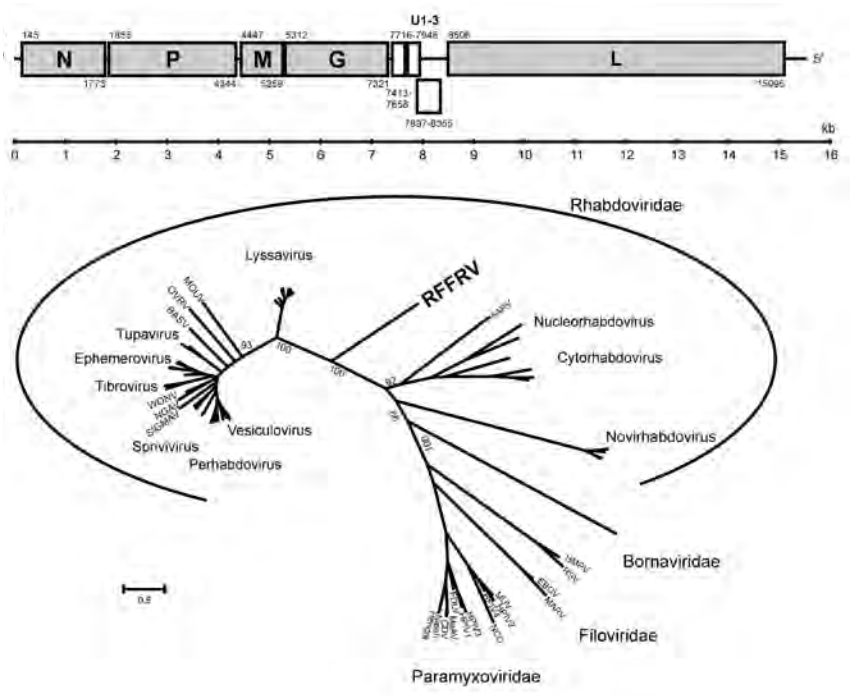

Figure. Genome organization and phylogenetic analysis of RFFRV. A) Genome organization of RFFRV. Indicated are the locations of the major ORFs (including the positions of the first and last nucleotide) and 3 theoretical minor ORFs between the G and L genes. B) Phylogenetic maximum-likelihood tree using the WAG+F+I+G model and 100 bootstrap replicates in MEGA5 (http://www.megasoftware.net) of the deduced amino acid sequence of the L genes of various viruses of the order Mononegavirales. G, glycoprotein; L, RNA-dependent RNA polymerase; M, matrix; N, nucleoprotein; ORF, open reading frame; P, phosphoprotein; RFFRV, RFFRV, red fox fecal rhabdovirus. Only bootstrap values in the close proximity of the branch of the RFFRV are indicated. Scale bar indicates nucleotide substitutions per site. Viruses and GenBank accession numbers are shown in the expanded figure legend online (http://wwwnc.cdc.gov/EID/article/20/12/14-0236-F1.htm).

Acknowledgments

We thank all researchers and institutions for their invaluable help during sampling and for providing the specimens used in this study, especially Patricia Lizarraga, Laura Elorza, Ricardo Gutierrez, and Luis Javier Chueca.

This work was funded by the European Community's Seventh Framework Program (FP7/2007–2013) under the project "European Management Platform for Emerging and Re-emerging Infectious Disease Entities" European Community grant agreement no. 223498; the Virgo Consortium; and the Niedersachsen-Research Network on Neuroinfectiology of the Ministry of Science and Culture of Lower Saxony, Germany. In addition, this research was funded partially by the Basque Government through the research group on "Systematics, Biogeography and Population Dynamics" (ref. IT317-10; GIC10/76).

A.R.-G. holds a postdoctoral fellowship awarded by the Department of Education, Universities and Research of the Basque Government (ref. DKR-2012-64) and was awarded a short-visit research grant from the ConGenOmics Research networking program of the European Science Foundation to visit the Department of Viroscience, Erasmus Medical Centre and develop the current research project.

Rogier Bodewes,[1] Aritz Ruiz-Gonzalez,[1] Anita C. Schürch, Albert D.M.E. Osterhaus, and Saskia L. Smits

Author affiliations: Erasmus Medical Centre, Rotterdam, the Netherlands (R. Bodewes, A.C. Schürch, A.D.M.E. Osterhaus, S.L. Smits); University of the Basque Country, Vitoria-Gasteiz, Spain (A. Ruiz-Gonzalez); National Institute for Environmental Protection and Research, Ozzano dell'Emilia, Italy (A. Ruiz-Gonzalez); and Viroclinics Biosciences, Rotterdam (A.D.M.E. Osterhaus, S.L. Smits)

DOI: http://dx.doi.org/10.3201/eid2012.140236

References

1. International Committee on Taxonomy of Viruses. Virus taxonomy: 2013 release [cited 2014 Feb 9]. http://www.ictvonline.org/virusTaxonomy.asp
2. Matha IS, Salunke SR. Immunogenicity of purified Vero cell rabies vaccine used in the treatment of fox-bite victims in India. Clin Infect Dis. 2005;40:611–3. http://dx.doi.org/10.1086/427700
3. Bodewes R, Ruiz-Gonzalez A, Schapendonk CM, van den Brand JM, Osterhaus AD, Smits SL. Viral metagenomic analysis of feces of wild small carnivores. Virol J. 2014;11:89. http://dx.doi.org/10.1186/1743-422X-11-89
4. Palacios G, Forrester NL, Savji N, Travassos da Rosa AP, Guzman H, Detoy K, et al. Characterization of Farmington virus, a novel virus from birds that is distantly related to members of the family *Rhabdoviridae*. Virol J. 2013;10:219. http://dx.doi.org/10.1186/1743-422X-10-219
5. Albertini AA, Ruigrok RW, Blondel D. Rabies virus transcription and replication. Adv Virus Res. 2011;79:1–22. http://dx.doi.org/10.1016/B978-0-12-387040-7.00001-9
6. Coll JM. The glycoprotein G of rhabdoviruses. Arch Virol. 1995;140:827–51. http://dx.doi.org/10.1007/BF01314961
7. Käll L. Krogh A, Sonnhammer EL. A combined transmembrane topology and signal peptide prediction method. J Mol Biol. 2004;338:1027–36. http://dx.doi.org/10.1016/j.jmb.2004.03.016
8. Gubala AJ, Proll DF, Barnard RT, Cowled CJ, Crameri SG, Hyatt AD, et al. Genomic characterisation of Wongabel virus reveals novel genes within the *Rhabdoviridae*. Virology. 2008;376:13–23. http://dx.doi.org/10.1016/j.virol.2008.03.004
9. McWilliam SM, Kongsuwan K, Cowley JA, Byrne KA, Walker PJ. Genome organization and transcription strategy in the complex GNS-L intergenic region of bovine ephemeral fever rhabdovirus. J Gen Virol. 1997;78:1309–17.

[1]These authors contributed equally to this article.

Address for correspondence: Rogier Bodewes, Erasmus Medical Centre, Department of Viroscience Dr. Molewaterplein 50, 3015GE Rotterdam, the Netherlands; email: r.bodewes@erasmusmc.nl

Ngari Virus in Goats during Rift Valley Fever Outbreak, Mauritania, 2010

To the Editor: Ngari virus (NRIV) is a single-stranded RNA virus belonging to the family *Bunyaviridae*, genus *Orthobunyavirus*. The genome comprises 3 segments, the small (S), medium (M), and large (L) segments, which encode the nucleocapsid (N) protein, the 2 glycoproteins Gn and Gc, and the RNA-dependent RNA-polymerase, respectively. Sequence analysis showed that NRIV is a reassortant between Bunyamwera virus (BUNV) and Batai virus (BATV), both from the genus *Orthobunyavirus*. S and L segments derived from BUNV, and the M segment derived from BATV (*1*,*2*). NRIV is more virulent than BUNV and BATV and is associated with hemorrhagic fever. NRIV was first isolated from *Aedes simpsoni* mosquitoes in 1979 and from humans in 1993, both in Senegal (*3*). During 1997 and 1998, humans were affected with hemorrhagic fever diseases in Kenya and Somalia that were caused by Rift Valley fever virus (RVFV) and by NRIV (*2*,*4*).

In 2010, during an ongoing RVFV outbreak in Mauritania, we collected 163 serum samples (62 from camels, 8 from cattle, and 93 from small ruminants) (*5*). RVFV RNA was isolated from serum samples as described previously (*5*). Further molecular testing of the samples was conducted by a SYBRGreen–based real-time reverse transcription PCR (RT-PCR) adapted from a conventional RT-PCR and based on generic primers (bun_group_forw 5′-CTGCTAACACCAGCAGTACTTTTGAC-3′ and bun_group_rev 5′-TGGAGGGTAAGACCATCGTCAGGAACTG-3′) that target a 250-nt sequence of the S segment of Bunyamwera serogroup members (*6*). Real-time RT-PCR was performed in a CFX 96 real-time PCR system (Bio-Rad, Hercules, CA, USA) by using 5 μL RNA with a QuantiTect SYBR Green RT-PCR Kit (QIAGEN, Hilden Germany) in a final volume of 25 μL. Cycling conditions included RT at 50°C for 30 min and 95°C for 15 min, followed by amplification with 44 cycles of 95°C for 15 s, 55°C for 25 s, 72°C for 30 s, and 77°C for 5 s. A melting curve analysis was then performed starting with 95°C for 60 s, and a temperature gradient was conducted from 68°C to 94°C in increments of 0.2°C.

Of the 163 serum samples tested, 2 samples from goats resulted in a positive signal with cycle thresholds of 23 (sample 51) and 28 (sample 65), respectively. Both samples showed similar melting peaks at ≈78.2°C and shared the identical partial nucleotide sequence of the S segment. The sequence belongs to the Bunyamwera serogroup, but the short partial sequence was not sufficient for accurate virus determination and identification. For this reason, both serum samples were used to inoculate cell monolayers of Vero E6 cells that were assayed for virus replication. Only sample 51 displayed a cytopathic effect after 72 h and was further analyzed. We isolated the viral RNA from cell culture with TRIzol reagent

(Invitrogen, Carlsbad, CA, USA) and used it to prepare a sequencing library according to a recently published protocol (*7*) but using Illumina adaptors (Illumina, San Diego, CA, USA). We sequenced the resulting library using the Illumina MiSeq instrument with v2 chemistry.

We recovered full-length genome sequences of the S, M, and L segments of the virus and deposited them in GenBank (accession nos. KJ716848–716850). Phylogenetic analysis of complete genome sequences indicated that the virus belongs to the Ngari virus group and showed high homology to previous NRIV isolates in all 3 segments (Figure). As for all previous NRIV strains, the new isolate was highly similar to BUNV regarding the S and the L segment (Figure, panels A, C); the M segment was highly similar to BATV (Figure, panel B).

This evidence supports the extension of the range of NRIV infection to goats (complete sequences already had been derived from a human and from mosquitoes [*8*]) and demonstrates the occurrence of NRIV during the 2010 RVFV outbreak in Mauritania. We are aware of only 1 additional report of NRIV-infected sheep (in 1988), also in Mauritania, although no further characterization or isolation has been conducted (*9*). Both NRIV-positive samples were negative for RVFV RNA but positive for RVFV-specific IgG. In addition, sample 51 contained IgM against RVFV (*5*), indicating possible co-infection of RVFV and NRIV. Because both ELISAs rely on detection of antibodies against RVFV N protein, which is highly divergent to the deduced NRIV N sequence, cross-reactivity is highly unlikely but needs to be substantiated. Both samples originated from the Adrar region, which was the center of an unusual RVFV outbreak in Mauritania in 2010 (*10*).

The possible clinical importance to livestock and the circulation of NRIV among mosquitoes, livestock, and humans needs to be clarified. No further information about clinical signs of sampled animals or reports of human NRIV cases is available. Because infection with both RVFV and NRIV induces hemorrhagic fever, affected humans also should be tested for NRIV infection. Further development of specific molecular and serologic diagnostic tools for NRIV should be pursued to obtain more information about NRIV distribution in

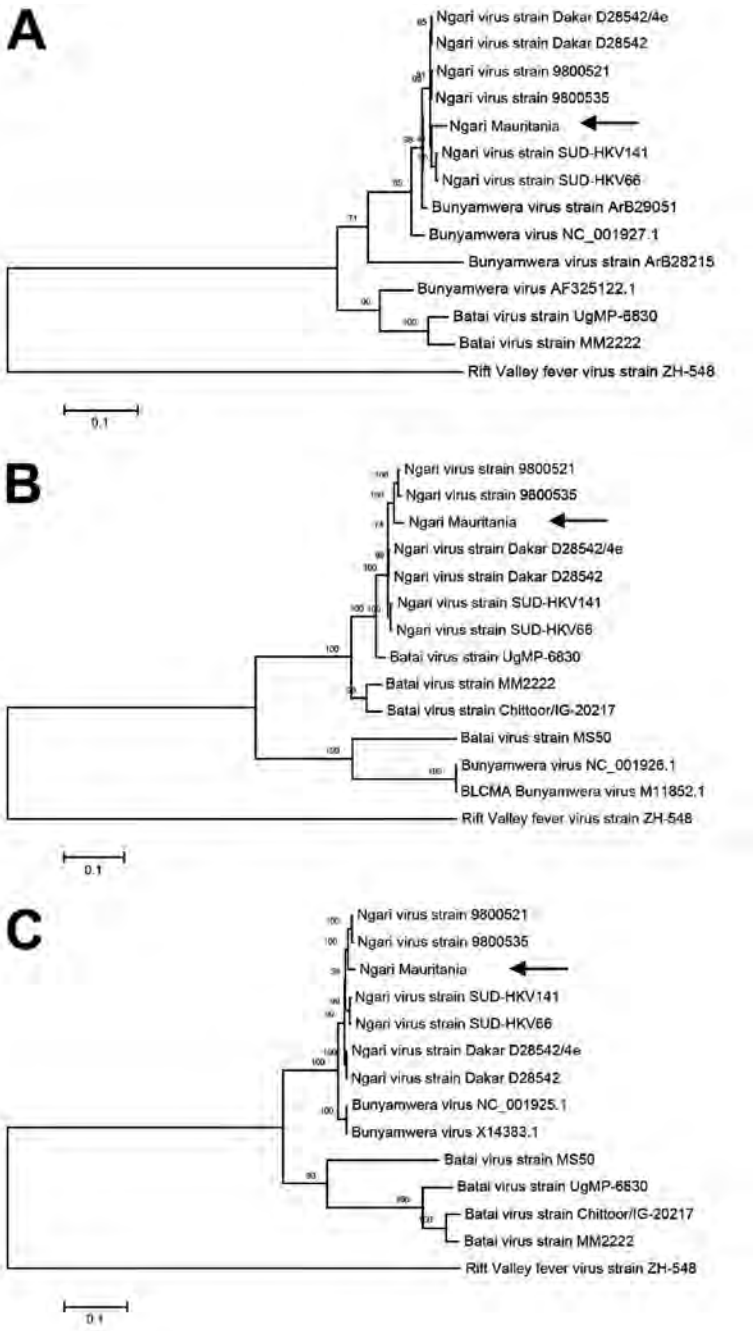

Figure. Phylogenetic tree of Ngari virus–derived A) small (975 bp), B) medium (4,507 bp), and C) large (6,887) segment sequences of Bunyamwera and Batai viruses compared with isolate obtained from a goat in Mauritania in 2010 (arrows). The tree was constructed on the basis of the nucleotide sequences of the 3 complete segments by using the neighbor-joining method (1,000 bootstrap replications). The tree was rooted to the sequence of Rift Valley fever virus strain ZH-548. Scale bars indicate substitutions per nucleotide position.

humans and livestock in Mauritania and other African countries.

Martin Eiden, Ariel Vina-Rodriguez, Bezeid O. El Mamy, Katia Isselmou, Ute Ziegler, Dirk Höper, Susanne Jäckel, Anne Balkema-Buschmann, Hermann Unger, Baba Doumbia, and Martin H. Groschup

Author affiliations: Friedrich-Loeffler-Institut, Greifswald-Insel Riems, Germany (M. Eiden, A. Vina-Rodriguez, U. Ziegler, D. Höper, S. Jäckel, A. Balkema-Buschmann, M.H. Groschup); Centre National de l'Elevage et de Recherches Vétérinaires, Nouakchott, Mauritania (B.O. El Mamy, K. Isselmou, B. Doumbia); Joint FAO/IAEA Division of Nuclear Techniques in Food and Agriculture, Vienna, Austria (H. Unger); and Ministère du Développement Rural, Nouakchott (B. Doumbia)

DOI: http://dx.doi.org/10.3201/eid2012.140787

References

1. Gerrard SR, Li L, Barrett AD, Nichol ST. Ngari virus is a Bunyamwera virus reassortant that can be associated with large outbreaks of hemorrhagic fever in Africa. J Virol. 2004;78:8922–6. http://dx.doi.org/10.1128/JVI.78.16.8922-8926.2004
2. Briese T, Bird B, Kapoor V, Nichol ST, Lipkin WI. Batai and Ngari viruses: M segment reassortment and association with severe febrile disease outbreaks in East Africa. J Virol. 2006;80:5627–30. http://dx.doi.org/10.1128/JVI.02448-05
3. Zeller HG, Diallo M, Angel G, Traoré-Lamizana M, Thonnon J, Digoutte JP, et al. Ngari virus (Bunyaviridae: Bunyavirus). First isolation from humans in Senegal, new mosquito vectors, its epidemiology [in French]. Bull Soc Pathol Exot. 1996;89:12–6.
4. Bowen MD, Trappier SG, Sanchez AJ, Meyer RF, Goldsmith CS, Zaki SR, et al. RVF Task Force. A reassortant bunyavirus isolated from acute hemorrhagic fever cases in Kenya and Somalia. Virology. 2001;291:185–90. http://dx.doi.org/10.1006/viro.2001.1201
5. Jäckel S, Eiden M, El Mamy BO, Isselmou K, Vina-Rodriguez A, Doumbia B, et al. Molecular and serological studies on the Rift Valley fever outbreak in Mauritania in 2010. Transbound Emerg Dis. 2013;60(Suppl 2):31–9. http://dx.doi.org/10.1111/tbed.12142
6. Lambert AJ, Lanciotti RS. Consensus amplification and novel multiplex sequencing method for S segment species identification of 47 viruses of the *Orthobunyavirus*, *Phlebovirus*, and *Nairovirus* genera of the family *Bunyaviridae*. J Clin Microbiol. 2009;47:2398–404. http://dx.doi.org/10.1128/JCM.00182-09
7. Steglich C, Grund C, Ramp K, Breithaupt A, Höper D, Keil G, et al. Chimeric Newcastle disease virus protects chickens against avian influenza in the presence of maternally derived NDV immunity. PLoS ONE. 2013;8:e72530. http://dx.doi.org/10.1371/journal.pone.0072530
8. Groseth A, Weisend C, Ebihara H. Complete genome sequencing of mosquito and human isolates of Ngari virus. J Virol. 2012;86:13846–7. http://dx.doi.org/10.1128/JVI.02644-12
9. Gonzalez JP. Activities du laboratoire d'ecology viral. Rapp sur la fonct tech de l'Institut Pasteur de Dakar. 1988;89:100–18.
10. El Mamy AB, Baba MO, Barry Y, Isselmou K, Dia ML, El Kory MO, et al. Unexpected Rift Valley fever outbreak, northern Mauritania. Emerg Infect Dis. 2011;17:1894–6. http://dx.doi.org/10.3201/eid1710.110397

Address for correspondence: Martin H. Groschup, Friedrich-Loeffler-Institut, Südufer 10, 17493 Greifswald-Insel Riems, Germany; email: martin.groschup@fli.bund.de

Peste des Petits Ruminants Virus, Eastern Asia

To the Editor: Peste des petits ruminants virus (PPRV) is reported globally with increasing frequency. Recently, PPRV has been detected in areas where it is considered endemic and in neighboring areas where it previously has not been reported. The reporting of "first cases" in regions where PPRV has been considered endemic is of little surprise and perhaps represents increased interest both in agricultural practices and diagnostic capacity (*1*–*3*). Increased development of the small ruminant health sector, expanding small ruminant populations, increased trade movement, and rinderpest eradication might all have affected PPRV detection (*4*). The latter theory is of great interest because rinderpest eradication may have affected the epidemiology of PPRV through complete removal of cross-protective rinderpest infection of small ruminants and cessation of small ruminant vaccination with the rinderpest vaccine to prevent PPRV infection. Indeed, the potential effect of rinderpest eradication on PPRV epidemiology should not be understated because it might have profoundly affected PPRV emergence by enabling free transmission and spread of the virus, perhaps overcoming the genetic and geographic bottlenecks created by rinderpest circulation and/or the use of rinderpest vaccines. In addition, rinderpest eradication has highlighted the possibility that PPRV could be eradicated by using comparable systems and tools (*5*).

Historically, PPRV has been identified across much of the developing world; genetic analyses has grouped viruses into 4 lineages that were originally thought to be phylogeographically restricted (*6*). However, in recent years, lineages of PPRV have apparently emerged in new areas. This has been most convincingly demonstrated with the detection of lineage IV virus—a lineage thought restricted to the Indian subcontinent and the Middle East—across northern and central Africa (online Technical Appendix Figure, http://wwwnc.cdc.gov/EID/article/20/12/14-0907-Techapp1.pdf) (*7*,*8*). However, reporting of PPRV in areas where it has not been previously detected is perhaps of greater interest. This is increasingly the case across southern and eastern Asia where virologic and serologic evidence of circulating PPRV has been reported (*6*)

During 2014, PPRV caused extensive agricultural losses across

China. Although regions within China had previously reported relatively small outbreaks, during December 2013–June 2014, the virus appears to have greatly extended its distribution. In 2007, PPRV was detected for the first time in the Ngari region of southwestern Tibet (*9*). This emergence was thought to have arisen through the circulation of mild forms of PPRV infection and the unfamiliarity of agricultural workers and professionals (e.g., veterinarians, farmers, livestock owners) with the disease and the inability to differentiate between mild forms of PPRV infections and other diseases of small ruminants. PPRV returned in 2008 and 2010 and was controlled by using stamping-out procedures, animal movement control, and increased screening of herds. The disease was controlled without the use of vaccines in 2008; vaccination was used in 2010 (*10*).

Three years passed without reports of PPRV infections in Tibet or elsewhere in China before the virus was detected in Xinjiang, China's largest administrative division, in December 2013. Xinjiang, an area of 1.6 million km^2, borders Afghanistan, India, Kazakhstan, Kyrgyzstan, Mongolia, Pakistan, Russia, and Tajikistan, several of which have reported PPRV infection. Within 2 months, PPRV had caused 3 outbreaks with rates of illness (and death) of 17% (2%), 58% (11%), and 79% (19%), respectively. Measures to contain these outbreaks were implemented as in 2007; however, during April and May 2014, the number of PPRV outbreaks increased sharply across much of China, including in Anhui, Guizhou, Guangxi, Hubei, Hunan, Shanxi, Xinjiang, Yunnan, and Zhejiang Provinces (Figure). The origin of these outbreaks remains undefined; however, the ability of the virus to circulate causing mild clinical disease and its presence in numerous bordering countries suggest several possibilities regarding the source of disease, including spread from the original China outbreaks. Similarly the threat of further spread from China to neighboring countries cannot be ignored.

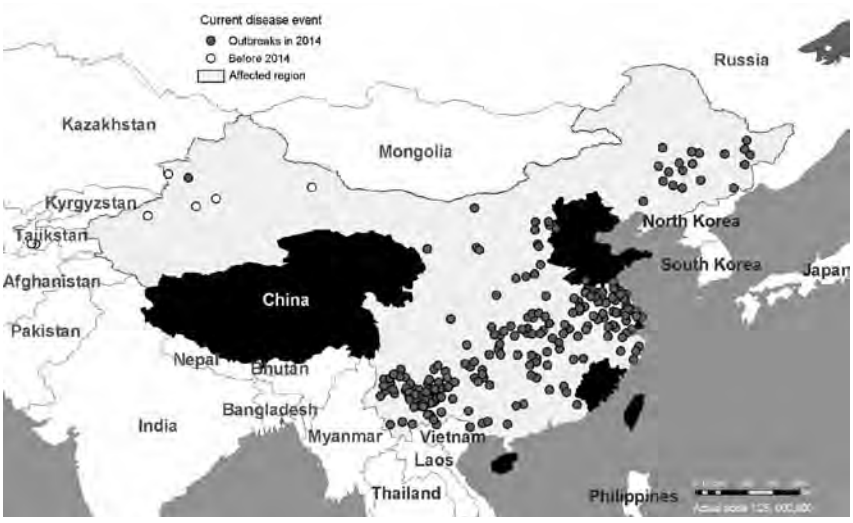

Figure. Outbreaks of peste des petits ruminants virus across China during December 2013–May 2014. Data are from ProMed alerts during the period described (*10*).

Once the current situation has been resolved, full genetic analysis of the viruses causing the outbreaks should be conducted because it might indicate the direction of spread. A further area of interest is the application and choice of control measures. Although predicting the spread of a viral pathogen is impossible, especially across the vast distances involved in the current reports, the experiences in China might influence future responses to incursions of PPRV into areas where PPRV previously has not been documented. The current lack of disease in areas where vaccination was reported in 2010 could explain the continued absence of disease from such areas while other regions are significantly affected (*10*). Effective vaccines against PPRV have been available for decades and will now, as both reactive and preventive tools, aid in controlling and preventing onward transmission of this viral pathogen. Once the situation in China is under control, where this emerging infection of small ruminants will appear next remains to be seen.

Acknowledgments

We thank Helen Roberts for generating the Figure.

A.C.B. and S.P. are funded in part by a Biotechnology and Biological Sciences Research Council Combating Infectious Diseases of Livestock for International Development grant BB/H009485/1.

Ashley C. Banyard, Zhiliang Wang, and Satya Parida

Author affiliations: Animal and Plant Health Agency, Weybridge, UK (A.C. Banyard); Ministry of Agriculture of the People's Republic of China, Qingdao, China (Z. Wang); and The Pirbright Institute, Pirbright, UK (S. Parida)

DOI: http://dx.doi.org/10.3201/eid2012.140907

References

1. Cosseddu GM, Pinoni C, Polci A, Sebhatu T, Lelli R, Monaco F. Characterization of peste des petits ruminants virus, Eritrea, 2002–2011. Emerg Infect Dis. 2013;19:160–1. http://dx.doi.org/10.3201/eid1901.121072
2. El Arbi AS, El Mamy AB, Salami H, Isselmou E, Kwiatek O, Libeau G, et al. Peste des petits ruminants virus, Mauritania. Emerg Infect Dis. 2014;20:333–6. http://dx.doi.org/10.3201/eid2002.131345
3. Munir M, Zohari S, Suluku R, Leblanc N, Kanu S, Sankoh FA, et al. Genetic

characterization of peste des petits ruminants virus, Sierra Leone. Emerg Infect Dis. 2012;18:193–5. http://dx.doi.org/10.3201/eid1801.111304
4. Libeau G, Diallo A, Parida S. Evolutionary genetics underlying the spread of peste des petits ruminants virus. Anim Front. 2014;4:14–20. http://dx.doi.org/10.2527/af.2014-0003
5. Baron MD, Parida S, Oura CA. Peste des petits ruminants: a suitable candidate for eradication? Vet Rec. 2011;169:16–21. http://dx.doi.org/10.1136/vr.d3947
6. Banyard AC, Parida S, Batten C, Oura C, Kwiatek O, Libeau G. Global distribution of peste des petits ruminants virus and prospects for improved diagnosis and control. J Gen Virol. 2010;91:2885–97. http://dx.doi.org/10.1099/vir.0.025841-0
7. De Nardi M, Lamin Saleh SM, Batten C, Oura C, Di Nardo A, Rossi D. First evidence of peste des petits ruminants (PPR) virus circulation in Algeria (Sahrawi territories): outbreak investigation and virus lineage identification. Transbound Emerg Dis. 2012;59:214–22. http://dx.doi.org/10.1111/j.1865-1682.2011.01260.x
8. Kwiatek O, Ali YH, Saeed IK, Khalafalla AI, Mohamed OI, Obeida AA, et al. Asian lineage of peste des petits ruminants virus, Africa. Emerg Infect Dis. 2011;17:1223–31. http://dx.doi.org/10.3201/eid1707.101216
9. Wang Z, Bao J, Wu X, Liu Y, Li L, Liu C, et al. Peste des petits ruminants virus in Tibet, China. Emerg Infect Dis. 2009;15:299–301. http://dx.doi.org/10.3201/eid1502.080817
10. ProMedMail. Peste des petits ruminants—China (11): Sheep, goat, spread, OIE, request for information. ProMed 2014 May 5. http://www.promedmail.org, archive no. 20140511.2465094.

Address for correspondence: Ashley C. Banyard, Wildlife Zoonoses and Vector Borne Disease Research Group, APHA, Weybridge, New Haw, Surrey KT15 3NB, UK; email: ashley.banyard@apha.gsi.gov.uk

Possible *Exiguobacterium sibiricum* Skin Infection in Human

To the Editor: The genus *Exiguobacterium* was first described in 1983 by Collins et al., who characterized the species *E. aurantiacum* (*1*). Since then, 9 new species have been added: *E. acetylicum, E. antarcticum, E. undae, E. oxidotolerans, E. aestuarii, E. marinum, E. mexicanum, E. artemiae,* and *E. sibiricum* (*2*,*3*). The genus *Exiguobacterium* belongs to the group of coryneform bacteria, which encompasses aerobically growing, non–spore-forming, irregularly shaped, gram-positive rods (*2*). *Exiguobacterium* spp. have been isolated from a wide range of habitats, including cold and hot environments (*3*). Although strains of *Exiguobacterium* spp. have been isolated from human clinical specimens (e.g., skin, wounds, and cerebrospinal fluid), the clinical significance of these bacteria is poorly understood (*4*). We present a case of cutaneous infection possibly caused by *E. sibiricum.*

In January 2014, a previously healthy 66-year-old farmer was admitted to the Health Center of Molina de Aragón (Guadalajara, Spain) with a 7-day history of an ulcer on the dorsal surface of the second finger on his right hand with a painful black eschar surrounded by edema, greenish exudate, erythema, and a broken blister. The lesion had progressively increased in size. The patient was a hunter who had handled the skin of a deer and a wild boar 4 days before. He had no history of trauma or receipt of antimicrobial drugs. At admission, he was afebrile with no systemic symptoms. Cutaneous anthrax was suspected on the basis of the clinical appearance of the lesion and the patient's contact with animals. An exudate sample was obtained for culture, and treatment with oral ciprofloxacin (500 mg/12 hour) was initiated. The Gram-stained sample showed leukocytes without organisms. Culture was performed according to standard practice.

Colonies observed after 24 hours of incubation on blood agar in pure culture were gray but turned orange after 48 hours. The colonies appeared mucoid and were nonhemolytic. Gram staining revealed wide, short, non–spore-forming, gram-positive rods. The isolate was motile, catalase positive, oxidase negative, and it fermented glucose and lactose. Reactions for indole, urea, and bile esculin were negative. The strain did not grow on McConkey agar and was facultatively anaerobic. The strain was initially identified as *Bacillus* spp. and was sent to the National Reference Laboratory of Majadahonda (Madrid, Spain) for species identification. There, the isolate was identified as *E. sibiricum* by means of 16S rRNA sequence analysis according to a previously reported method (*5*). The fragment of 16S RNA gene obtained from this isolate was 1,413 bp, and similarity with GenBank sequences was 99.6% (GenBank accession nos. CP00122, GQ869573, and others).

After the organism was identified, we found that it was able to grow on blood agar at 4°C after 6 days of incubation. Antimicrobial drug susceptibility testing was performed by using the Etest method (AB Biodisk, Solna, Sweden) on Mueller-Hinton agar plates incubated at 37°C for 24 hours. The isolate was susceptible to penicillin (MIC 0.023 mg/L), cefotaxime (0.5 mg/L), imipenem (0.047 mg/L), levofloxacin (0.19 mg/L), vancomycin (0.5 mg/L), clindamycin (0.125 mg/L), erythromycin (0.047 mg/L), gentamicin (0.094 mg/L), doxycycline (0.032 mg/L), linezolid (0.5 mg/L), and daptomycin (0.5 mg/L). The patient's clinical outcome was good, and the lesion resolved after 10 days of continuous ciprofloxacin therapy.

This patient's cutaneous infection and the morphologic appearance of the lesion resembled cutaneous anthrax.

Initially, the Gram-stained appearance and culture were compatible with those of *Bacillus* species other than *B. anthracis*. In this sense, cutaneous infections caused by *Bacillus* species other than *B. anthracis* have been reported and are clinically similar to cutaneous anthrax (*6*). Isolation of coryneform bacteria from the ulcer may represent colonization rather than true infection, and the absence of the organism on the initial Gram-stained slides may support contamination. However, the evidence points to *E. sibiricum* as a pathogen and not a contaminant because it was the only organism isolated, and Gram staining of the exudate revealed leukocytes. In addition, the patient had not previously received any antimicrobial drug that could change the result of the culture. Moreover, the isolate was susceptible to ciprofloxacin, and clinical response to this drug was good. However, we cannot absolutely rule out another organism as the cause of the infection or co-infection with some uncultured bacterium.

Identification of *Exiguobacterium* spp. based on conventional methods is difficult and should be confirmed with molecular assays. Bacteria in this genus can be misidentified as *Oerskovia xanthineolytica* when the API Coryne kit (bioMérieux, Marcy l'Étoile, France) is used (*7*); 16S rRNA gene sequencing seems to be useful for identification of *E. sibiricum* (*8*). Consequently, the frequency of this infection can be underdiagnosed. In patients with lesions suspected of being cutaneous anthrax, *E. sibiricum* should be considered as a potential cause and should be differentiated from *B. anthracis* (Table) (*9*,*10*).

This case of human infection was most likely caused by *E. sibiricum*. Identification of this organism is difficult, and it can be confused with *Bacillus* spp. *E. sibiricum* should be considered as a possible cause of lesions suspected of being cutaneous anthrax.

Table. Microbiological and clinical characteristics of *Exiguobacterium sibiricum* and *Bacillus anthracis**

Characteristic	*E. sibiricum*	*B. anthracis*
Colony on blood agar	Mucoid and orange	Gray-white to white
Spore production	–	+ (central)
Motility	+	–
Hemolysis on blood agar	–	–
Penicillin susceptibility	+	+
Catalase production	+	+
Indole production	–	–
Growth at 4°C	+	–
Anaerobic growth	+	+
Cutaneous infection	Ulcer, black eschar, blister	Eschar, malignant pustule
Other infections	None reported	Intestinal anthrax, pulmonary anthrax, meningitis

*+, present; –, absent.

Daniel Tena, Nora Mariela Martínez, Josefa Casanova, Juan Luis García, Elena Román, María José Medina, and Juan Antonio Sáez-Nieto

Author affiliations: Hospital Universitario de Guadalajara, Guadalajara, Spain (D. Tena, N.M. Martínez); Centro de Salud de Molina de Aragón, Guadalajara (J. Casanova, J.L. García); Servicios Periféricos de Salud y Bienestar Social, Guadalajara (E. Román); and Centro Nacional de Microbiología, Madrid, Spain (M.J. Medina, J.A. Sáez-Nieto)

DOI: http://dx.doi.org/10.3201/eid2012.140493

References

1. Collins MD, Lund BM, Farrow JAE, Schleifer KH. Chemotaxonomic study of an alkalophilic bacterium, *Exiguobacterium aurantiacum* gen. nov. J Gen Microbiol. 1983;129:2037–42.
2. Farrow JAE, Wallbanks S, Collins MD. Phylogenetic interrelationships of round–spore-forming bacilli containing cell walls based on lysine and the non–spore-forming genera *Caryophanon, Exiguobacterium, Kurthia,* and *Planococcus.* Int J Syst Bacteriol. 1994;44:74–82.
3. Vishnivetskaya TA, Kathariou S, Tiedje JM. The *Exiguobacterium* genus: biodiversity and biogeography. Extremophiles. 2009;13:541–55. http://dx.doi.org/10.1007/s00792-009-0243-5
4. Hollis DG, Weaver RE. Gram-positive organisms: a guide to identification. Special Bacteriology Section. Atlanta Centers for Disease Control; 1981.
5. Drancourt M, Bollet C, Carliotz A, Martelin R, Gayralt JP, Raoult D. 16S ribosomal DNA sequence analysis of a large collection of environmental and clinical identified bacterial isolates. J Clin Microbiol. 2000;38:3623–30.
6. Tena D, Martínez-Torres JA, Pérez-Pomata MT, Sáez-Nieto JA, Rubio V, Bisquert J. Cutaneous infection due to *Bacillus pumilus*: report of 3 cases. Clin Infect Dis. 2007;44:e40–2. http://dx.doi.org/10.1086/511077
7. Kenny F, Xu J, Millar BC, McClurg RB, Moore JE. Potential misidentification of a new *Exiguobacterium* sp. as *Oerskovia xanthineolytica* isolated from blood culture. Br J Biomed Sci. 2006;63:86.
8. Murayama M, Kakinuma Y, Maeda Y, Rao JR, Matsuda M, Xu J, et al. Molecular identification of airborne bacteria associated with aerial spraying of bovine slurry waste employing 16S rRNA gene PCR and gene sequencing techniques. Ecotoxicol Environ Saf. 2010;73:443–7. http://dx.doi.org/10.1016/j.ecoenv.2009.10.003
9. Rodrigues DF, Ivanova N, He Z, Huebner M, Zhou J, Tiedje JM. Architecture of thermal adaptation in an *Exiguobacterium sibiricum* strain isolated from 3 million year old permafrost: a genome and transcriptome approach. BMC Genomics. 2008;9:547–64. http://dx.doi.org/10.1186/1471-2164-9-547
10. Logan NA, Popovic T, Hoffmaster A. *Bacillus* and other aerobic endospore-forming bacteria. In: Murray PR, Baron EJ, Jorgensen JH, Landry ML, Pfaller MA, editors. Manual of clinical microbiology. 9th ed. Washington (DC): ASM Press;2007. p. 455–73.

Address for correspondence: Daniel Tena, Sección de Microbiología, Hospital Universitario de Guadalajara, C/, Donantes de sangre s/n, 19002 Guadalajara. Spain; email: danielt@sescam.jccm.es

Hepacivirus Infection in Domestic Horses, Brazil, 2011–2013

To the Editor: An estimated ≈150 million persons (3% of the world population) are chronically infected with hepatitis C virus (HCV). This virus is the prototype of the genus *Hepacivirus* and a major cause of liver cirrhosis and hepatocellular carcinoma around the world. Every year, 3–4 million persons become infected with HCV, and ≈350,000 die of this infection (*1*).

Development of an HCV vaccine has been hampered by the difficulty of in vitro cultivation of the agent and by lack of animal models for studies of viral functions and host immune reactions (*1*,*2*). The only effective experimental model that can be infected with HCV and in which the course of infection is similar to that in humans is the chimpanzee.

Since the discovery of HCV-like virus in dogs with respiratory disease and nonspecific gastrointestinal disorder in the United States in 2011, tentatively named canine hepacivirus (*2*), new hepaciviruses have been detected in insectivorous bats (*3*), Old World monkeys (*4*), wild rodents (*5*,*6*), and domestic horses (*6*–*8*). These animals could potentially serve as HCV models, but the accuracy of HCV tissue tropism, pathology, and immunology in natural hosts needs to be demonstrated.

No official nomenclature for these recently described hepaciviruses has been defined by the International Committee of Viral Taxonomy. In this article, we refer to the viruses detected in horses as conventional nonprimate hepaciviruses (NPHVs). The aim of this study was to verify NPHV infection in horses from 8 locations in the eastern Brazilian Amazon.

During January 2011–November 2013, serum samples were collected from 300 equids in 7 cities and 1 district of the State of Pará, Brazil (online Technical Appendix, http://wwwnc.cdc.gov/EID/article/20/12/14-0603-Techapp1.pdf). Samples came from 265 horses (*Equus caballus*), 30 mules (*Equus mulus*), and 5 donkeys (*Equus asinus*). All procedures for obtaining and using the samples were approved by the Ethics Committee on the Use of Animals in Research from the Evandro Chagas Institute (protocol code 0023/2012 CEUA/IEC/CENP/SVS/MS).

Viral RNA was extracted from serum samples by using the TRIzol LS Reagent (Invitrogen, Carlsbad, CA, USA), and a target sequence in the nonstructural 3 protein (NS3) region of the NPHV genome was amplified from the cDNA by using a previously reported nested PCR protocol (*8*). Second-round product reactions of ≈380 bp were considered positive.

We used the BigDye Terminator version 3.1 Cycle Sequencing Kit and an ABI 3500 Genetic Analyzer (both from Applied Biosystems, Foster City, CA, USA) for sequencing. To obtain consensus sequences, we used BioEdit software, version 7.0.5.3 (http://www.mbio.ncsu.edu/BioEdit/BioEdit.html). To phylogenetically analyze the virus sequences based on an NS3 partial nucleotide sequence of 294 bp, we used the maximum-likelihood method with the Kimura 2-parameter model in MEGA version 5.1 (http://www.megasoftware.net) (bootstrap, 1,000 replicates). The nucleotide distance was calculated by using PAUP version 4.0 software (http://paup.csit.fsu.edu/). The sequences obtained in this study have been assigned GenBank accession nos. KJ469442–KJ469466.

Of the 300 serum samples, 25 (8.3%) were positive for NPHV by nested reverse transcription PCR; these results were confirmed by nucleotide sequencing. This prevalence of NPHV infection among horses in Brazil is higher than that reported for other countries (*6*–*8*).

The prevalence among competition horses (19.1%) was remarkably higher than that among farm (6.3%) and cart horses (6.2%). Many possibilities for the higher prevalence in the first group, such as exposure to nonsterile needles shared by a large number of animals, must be considered; however, further studies are needed to investigate this hypothesis.

No mules or donkeys tested in this study were infected by NPHV. A similar finding for another study has been reported (*8*), which might suggest that these species are not natural hosts for NPHV.

Until now, it has been impossible to associate *Hepacivirus* infection in horses with clinical hepatic disease (*7*,*8*). All infected horses for which information was available were healthy at the time of sampling. Our finding of high NPHV prevalence among horses is consistent with findings of previous studies in which NPHV-mediated disease was not found, suggesting that the course of infection is chronic and largely asymptomatic, similar to that of HCV infection in humans.

The sequences reported in this study shared close genetic relationships with previously reported NPHV sequences from dogs and horses (Figure) (*2*,*6*–*8*). The nucleotide distances of the sequences ranged from 0 to 19.9%.

Many of these new isolates were grouped according to geographic origin, except for 2 sequences that grouped distantly from other isolates from Neotropical regions. One isolate (KJ469449), from a Quarter horse, was closely related to NPHV detected in horses in the United States (*7*); similarity was ≈94%. The other sequence from a Neotropical region (KJ469466), from a Marajoara horse, grouped closer to the NPHV from horses in Germany (*6*); similarity was as high as 95%.

NPHV, one of the viruses most closely genetically related to HCV, is present in the Neotropics and was identified in the eastern Brazilian Amazon. The infection seems to be enzootic in the studied horse population and to be geographically dispersed in northeastern Pará State.

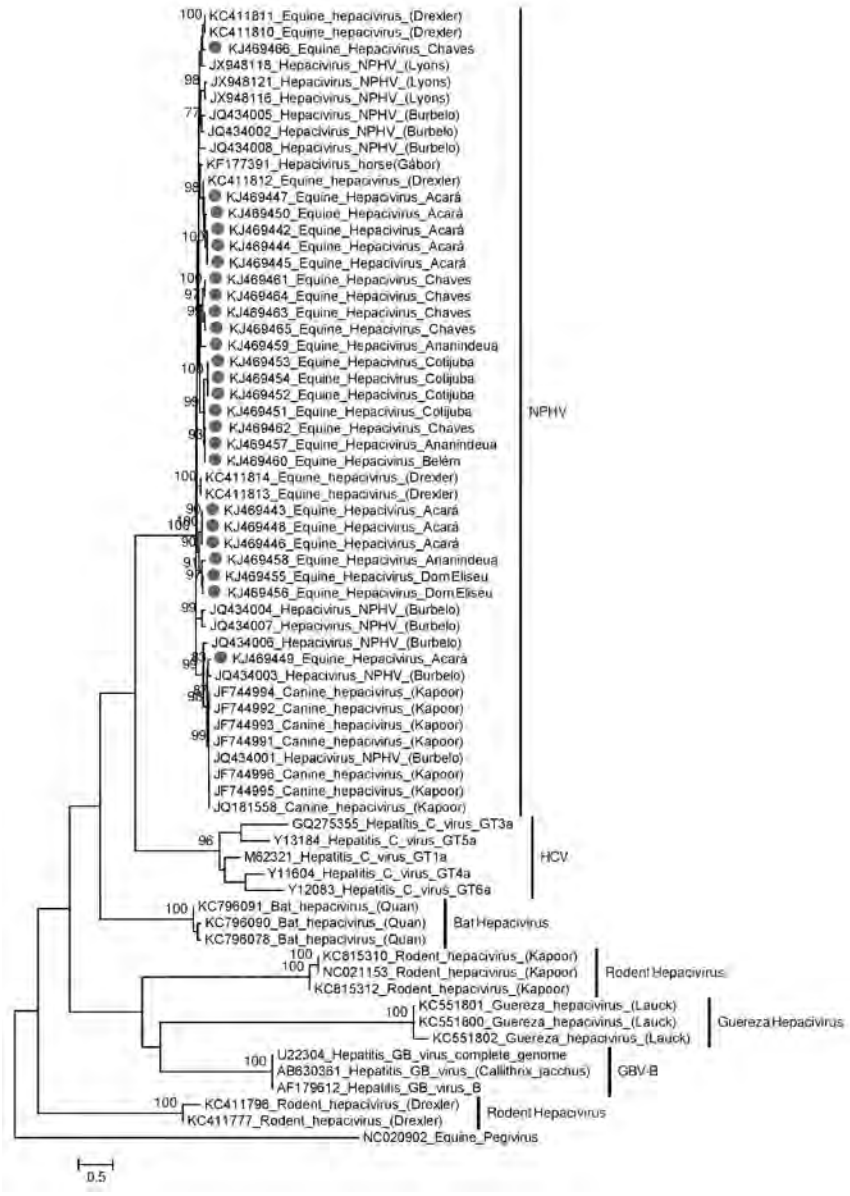

Figure. Maximum-likelihood phylogenetic tree of the partial nucleotide sequences of the nonstructural protein 3 region (294 bp) of *Hepacivirus*. The retrieved sequences from GenBank are indicated by the accession number followed by the species from which each was isolated. The 25 sequences obtained from 300 equids in 7 cities and 1 district of the State of Pará, Brazil, during January 2011–November 2013, are indicated with a dot and are identified by their GenBank accession numbers followed by their community of origin. Bootstrap values (1,000 replicates) >70% are listed at the nodes. One sequence of equine *Pegivirus* was used as an outgroup. GBV-B, GB virus B; HCV, hepatitis C virus; NPHV, nonprimate hepaciviruses. Scale bar indicates nucleotide substitutions per site.

Bernard Salame Gemaque, Alex Junior Souza de Souza, Manoel do Carmo Pereira Soares, Andreza Pinheiro Malheiros, Andrea Lima Silva, Max Moreira Alves, Michele Soares Gomes-Gouvêa, João Renato Rebello Pinho, Heriberto Ferreira de Figueiredo, Djacy Barbosa Ribeiro, Jonan Souza da Silva, Leopoldo Augusto Moraes, Ana Silvia Sardinha Ribeiro, and Washington Luiz Assunção Pereira

Author affiliations: Universidade Federal Rural da Amazônia, Belém, Brazil (B.S. Gemaque, H.F. de Figueiredo, D.B. Ribeiro, J.S. da Silva, A.S.S. Ribeiro, W.L.A. Pereira); Instituto Evandro Chagas, Belém (B.S. Gemaque, A.J.S. de Souza, M.C.P. Soares, A.P. Malheiros, A.L. Silva, M.M. Alves); Universidade de São Paulo, São Paulo, Brazil (A.J.S. de Souza, M.S. Gomes-Gouvêa, J.R.R. Pinho); and Universidade Federal do Pará, Belém (L.A. Moraes)

Acknowledgments

We thank Elton Everton, Antonio Soares, Fabricio Resende, André Chagas, Pedro Freitas, Andre Meneses, the Coordenação de Aperfeiçoamento de Pessoal de Nível Superior, the members of the Laboratório de Patologia Animal, and Projeto Carroceiro for help with obtaining the samples.

This study was undertaken with financial support of the Instituto Evandro Chagas/Secretaria de Vigilância em Saúde/Ministério da Saúde.

DOI: http://dx.doi.org/10.3201/eid2012.140603

References

1. World Health Organization. Hepatitis C. Fact sheet no. 164. 2013. Updated April 2014 [cited 2013 Dec 5]. http://www.who.int/mediacentre/factshe ets/fs164/en/
2. Kapoor A, Simmonds P, Gerold G, Qaisar N, Jain K, Henriquez JA, et al. Characterization of a canine homolog of hepatitis C virus. Proc Natl Acad Sci U S A. 2011;108:11608–13. http://dx.doi.org/10.1073/pnas.1101794108
3. Quan PL, Firth C, Conte JM, Williams SH, Zambrana-Torrelio CM, Anthony SJ, et al. Bats are a major natural reservoir for hepaciviruses and pegiviruses. Proc Natl Acad Sci U S A. 2013;110:8194–9. http://dx.doi.org/10.1073/pnas.1303037110
4. Lauck M, Sibley SD, Lara J, Purdy MA, Khudyakov Y, Hyeroba D, et al. A novel hepacivirus with an unusually long and intrinsically disordered NS5A protein in a wild Old World primate.

J Virol. 2013;87:8971–81. http://dx.doi.org/10.1128/JVI.00888-13
5. Kapoor A, Simmonds P, Scheel TK, Hjelle B, Cullen JM, Burbelo PD, et al. Identification of rodent homologs of hepatitis C virus and pegiviruses. MBio, 2013;4: e00216-1 [cited 2013 Dec 5]. . http://www.ncbi.nlm.nih.gov/pubmed/23572554 http://dx.doi.org/10.1128/mBio.00216-13
6. Drexler JF, Corman VM, Müller MA, Lukashev AN, Gmyl A, Coutard B, et al. Evidence for novel hepaciviruses in rodents. PLoS Pathog. 2013;9:e1003438. http://dx.doi.org/10.1371/journal.ppat.1003438
7. Burbelo PD, Dubovi EJ, Simmonds P, Medina JL, Henriquez JA, Mishra N, et al. Serology-enabled discovery of genetically diverse hepaciviruses in a new host. J Virol. 2012;86:6171–8. http://dx.doi.org/10.1128/JVI.00250-12
8. Lyons S, Kapoor A, Sharp C, Schneider BS, Wolfe ND, Culshaw G, et al. Nonprimate hepaciviruses in domestic horses, United Kingdom. Emerg Infect Dis. 2012;18:1976–82. http://dx.doi.org/10.3201/eid1812.120498

Address for correspondence: Alex de Souza, Instituto Evandro Chagas, Seção de Hepatologia, Av. Almirante Barroso, 492 Belém, Pará 66093-020, Brazil; email: souzajralex@gmail.com

Hepatitis E Virus Genotype 4 in Yak, Northwestern China

To the Editor: Hepatitis E virus (HEV; family *Hepeviridae*, genus *Hepevirus*) is a positive-stranded RNA virus with a genome of ≈7.2 kb that contains 3 open reading frames (*1*,*2*). On the basis of sequence analysis, mammalian HEVs are classified into 4 recognized genotypes (*3*,*4*). HEV genotypes 1 and 2 are restricted to humans and are often associated with large outbreaks and epidemics in developing countries, especially in Africa and Asia. Genotypes 3 and 4 are zoonotic and have been detected in humans, pigs, and other animal species (*1*,*3*–*6*).

Yaks (*Bos grunniens*) live on the cold highland (altitude >3,000 m, average annual temperature <0°C) surrounding the Qinghai-Tibet Plateau, which includes Qinghai and Gansu Provinces in northwest China. Domestic yaks are usually slaughtered for meat at 3 years of age. Infectious pathogens in yaks have been reported only recently (*7*,*8*). On the basis of the high prevalence of HEV in human and pigs in China and close human–yak contact in the Tibet region (*4*,*5*), we sought to determine if HEV infects yaks.

During March–September 2013, we collected 167 fecal samples from yaks <3 years of age; 92 were from Qinghai Province (56 <1 year of age) and 75 from Gansu Province (48 <1 year of age). Soon after sampling, 10% (wt/vol) fecal suspensions were prepared by using sterile phosphate-buffered saline (0.01 mmol/L phosphate, pH 7.2–7.4; 0.15 mmol/L NaCl, 0.1% diethyl pyrocarbonate). After centrifugation, supernatants were separated, and total RNAs were extracted by using TRIzol reagent (Invitrogen, Carlsbad, CA, USA). RNAs were used as templates to amplify full-length cDNA by reverse transcription PCR (RT-PCR; SuperScript III Synthesis Kit, Invitrogen), according to the manufacturer's instructions. A positive control sample (GenBank accession no. JU119961) and negative control (water) were included.

Briefly, 10 pairs of primers were designed based on HEV genotype 4 (GenBank accession nos. JU119961, JQ740781, AB291965, and AB602440) (online Technical Appendix Table 1, http://wwwnc.cdc.gov/EID/article/20/12/13-1599-Techapp1.pdf) to obtain the HEV genome consisting of all the 3 open reading frames. RT-PCR was then performed in a 25-μL volume containing 2-μL templates and 0.1 μmol/L of each primer; cycles were 94°C for 2 min, followed by 38 cycles of 94°C for 30 s, 59°C for 30 s, and 72°C for 1 min, with a final extension step of 10 min at 72°C. RT-PCR–amplified DNA fragments of the expected sizes were sequenced in a 310 Genetic Analyzer/Sanger Sequencer (Invitrogen). The complete genome sequences were assembled on the basis of 10 amplified sequences. Phylogenetic analysis was performed for the complete genome sequences of the detected sequences compared with all other mammalian HEV sequences available in GenBank.

We found that 3 (3.26%) of the 92 samples were positive for the HEV genotype 4 genome sequence; all samples were from yaks <1 year of age from Qinghai Province (online Technical Appendix Table 2). Sequence analysis revealed 100% identity of the full-length genomes of the 3 HEV sequences (7,234 bp; sequence submitted to GenBank as CHN-QH-YAK, accession no. KF736234). Phylogenetic analysis demonstrated that all 19 mammalian HEVs grouped into 4 clades corresponding to the 4 HEV genotypes. The sequence we identified belonged to genotype 4 and was most closely related to China/Xinjiang/swine (GenBank accession no. JU119961; 99.14% identity) and to China/Nanjing/human (GenBank accession no. JQ740781; 93.84% identity) (Figure).

We found HEV genotype 4 infection in yaks, but prevalence was low (3.26%), and only young yaks in Qinghai Province were affected. In comparison, studies have shown that swine are an established reservoir of HEV worldwide (*3*,*5*,*9*) and that 20%–100% of pigs are infected with HEV (*3*,*4*,*9*,*10*). Our findings suggest that yak is an emerging but imperfect host for this virus. The HEV genome sequence derived from infected yak shared 99.14% identity with the

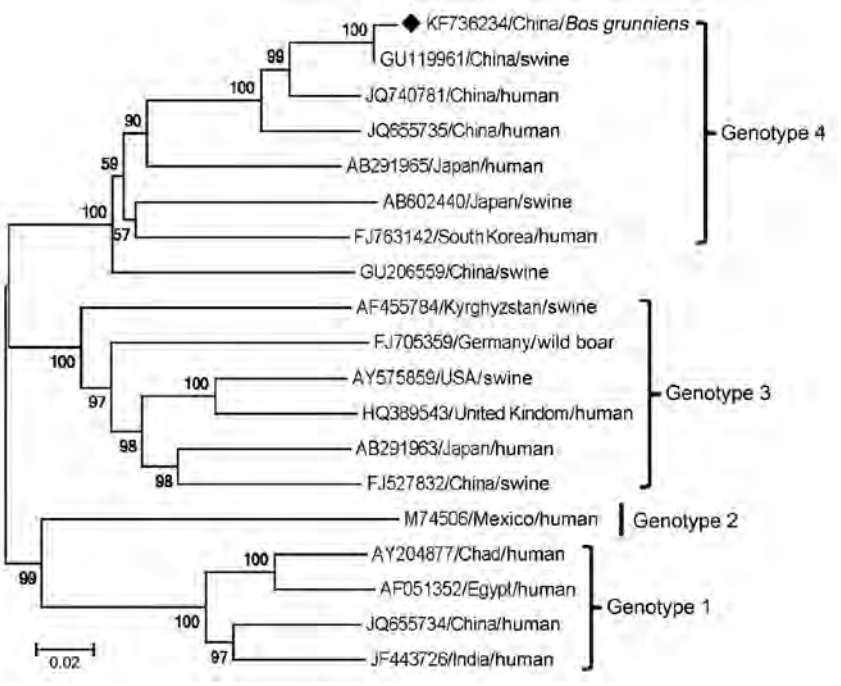

Figure. Phylogenetic analysis of hepatitis E virus (HEV) based on the complete genome sequences of HEVs using the neighbor-joining method with MEGA 4.0 software (http://www.megasoftware.net). Black diamond indicates the newly identified yak HEV sequence from Qinghai, China (GenBank accession no. KF736234). Another 18 sequences were collected from GenBank, including 7 sequences of genotype 4 (GU119961, JQ740781, JQ655735, AB291965, AB602440, FJ763141, GU206559), 6 of genotype 3 (AF455784, FJ705359, AY575859, HQ389543, AB291963, FJ527832), 1 of genotype 2 (M74596), and 4 of genotype 1 (AY204877, AF051352, JQ655734, JF443726). Bootstrap values of >50% are indicated for the corresponding nodes based on a bootstrapping with 1,000 replicates. GenBank accession numbers and geographic and animal species origin are shown. Scale bar indicates nucleotide substitutions per site.

China/Xinjiang/swine isolate, suggesting the Qinghai isolate evolved and was transmitted from the Xinjiang swine isolate. Like the swine isolate, this yak isolate probably possesses the potential to infect humans. Because persons in the Tibet region eat undercooked yak milk and meat, yaks may become an emerging reservoir of HEV genotype 4.

In addition, the high sequence identity (93.84%–99.14%) among isolates from China, including China/Qinghai/yak, China/Xinjiang/swine, China/Nanjing/human, and China/Beijing/human, demonstrates a complicated, transregional and cross-species transmission cycle for HEV genotype 4 in China. We cannot determine why yaks in Qinghai Province were affected and those in Gansu Province were not, but a neighboring pig farm may have served as a source for HEV transmission. More research is needed to determine the prevalence of HEV genotype 4 in various human and animal populations with concomitant virus isolation and phylogenetic analysis.

Acknowledgment

We thank China Animal Health and Epidemiology Center for their valuable assistance in sample collection.

This work was supported by a grant from the National Natural Science Foundation of China No. 31260616 and the Fuxi Foundation of Exceptional Talent at Gansu Agricultural University.

Fang Xu,[1] Yangyang Pan,[1] Abdul Rasheed Baloch, Lili Tian, Meng Wang, Wang Na, Lingqiang Ding, and Qiaoying Zeng

Author affiliations: Gansu Agricultural University, Lanzhou, China (F. Xu, Y. Pan, W. Na, Q. Zeng); Northwest A&F University, Yangling, China (A.R. Baloch, M. Wang); China Animal Health and Epidemiology Center, Qingdao, China (L. Tian); and Sichuan Agricultural University, Yaan, China (L. Ding)

DOI: http://dx.doi.org/10.3201/eid2012.131599

References

1. Abravanel F, Lhomme S, Dubois M, Peron JM, Alric L, Kamar N, et al. Hepatitis E virus. Med Mal Infect. 2013;43:263–70. http://dx.doi.org/10.1016/j.medmal.2013.03.005
2. Berto A, Mesquita JR, Hakze-van der Honing R, Nascimento MS, van der Poel WH. Detection and characterization of hepatitis E virus in domestic pigs of different ages in Portugal. Zoonoses Public Health. 2012;59:477–81. http://dx.doi.org/10.1111/j.1863-2378.2012.01488.x
3. Pavio N, Meng X-J, Renou C. Zoonotic hepatitis E: animal reservoirs and emerging risks. Vet Res. 2010;41:46. http://dx.doi.org/10.1051/vetres/2010018
4. Song YJ, Park WJ, Park BJ, Lee JB, Park SY, Song CS, et al. Hepatitis E virus infections in humans and animals. Clin Exp Vaccine Res. 2014;3:29–36. http://dx.doi.org/10.7774/cevr.2014.3.1.29
5. Meng XJ. Hepatitis E virus: animal reservoirs and zoonotic risk. Vet Microbiol. 2010;140:256–65. http://dx.doi.org/10.1016/j.vetmic.2009.03.017
6. Panda SK, Thakral D, Rehman S. Hepatitis E virus. Rev Med Virol. 2007;17:151–80. http://dx.doi.org/10.1002/rmv.522
7. Bai X, Zhao A, Lan R, Xin Y, Xie H, Meng Q, et al. Shiga toxin–producing *Escherichia coli* in yaks (*Bos grunniens*) from the Qinghai-Tibetan Plateau, China. PLoS ONE. 2013;8:e65537. http://dx.doi.org/10.1371/journal.pone.0065537
8. Chen Q, Gong X, Zheng F, Cao X, Li Z, Zhou J. Seroprevalence of *Chlamydophila abortus* infection in yaks (*Bos grunniens*) in Qinghai, China. Trop Anim Health Prod. 2014;46:503–7. http://dx.doi.org/10.1007/s11250-013-0519-8
9. Zhu YM, Dong SJ, Si FS, Yu RS, Li Z, Yu XM, et al. Swine and human

[1]These authors contributed equally to this article.

hepatitis E virus (HEV) infection in China. J Clin Virol. 2011;52:155–7. http://dx.doi.org/10.1016/j.jcv.2011.06.023

10. Feagins AR, Opriessnig T, Huang YW, Halbur PG, Meng XJ. Cross-species infection of specific-pathogen-free pigs by a genotype 4 strain of human hepatitis E virus. J Med Virol. 2008;80:1379–86. http://dx.doi.org/10.1002/jmv.21223

Address for correspondence: Qiaoying Zeng, The College of Veterinary Medicine, Gansu Agricultural University, Lanzhou, China; email: zengqy@gsau.edu.cn

Peste des Petits Ruminants Virus, Tunisia, 2012–2013

To the Editor: Peste des petits ruminants (PPR) is a viral disease of sheep and goats caused by peste des petits ruminants virus (PPRV), a negative-sense, single-stranded RNA virus of the genus *Morbillivirus*. Illness and death can be high (>90%) when PPR occurs in populations of immunologically naive sheep and goats (*1*). Mortality rates are ≈10%–40% in disease-endemic areas (*2*). Because of its economic effects and ability to spread rapidly, PPR has been included among reportable diseases by the World Organization for Animal Health.

In the past 20 years, PPR has shown rapid spread throughout large areas of Africa and Asia (*2*). A unique serotype of PPRV circulates and is classified into 4 genetically distinct lineages (*3*). The geographic distribution of lineages I and II is restricted mainly to western and central Africa and that of lineage III to eastern Africa. Lineage IV is more widely distributed throughout eastern Africa (*4*,*5*), the Near and Middle East, and large areas of Asia (*3*).

In 2008, PPR occurred in Morocco, and 257 cases were reported in goats and sheep over a 6-month period (*3*). In 2011, PPR was officially reported in Algeria (*3*). Genetic analysis showed that PPRV strains isolated in Morocco and Algeria belonged to lineage IV (*4*–*6*). Although PPR has been reported in Tunisia since 2011 (*7*), no data are available on the molecular characterization of PPRV circulating in this country.

During September 2012–January 2013, clinical signs compatible with PPR in ovine and caprine flocks were reported to the Tunisian veterinary service. Ocular, nasal, oral, and rectal swab specimens were obtained from animals showing clinical signs of this disease. Swab specimens were sent to the Institute de la Recherche Vétérinaire de Tunisie in Tunis for laboratory confirmation. Total RNA from swab samples was extracted by using the NucleoSpin RNA Virus Kit (Macherey-Nagel, Düren, Germany) according to the manufacturer's instructions. The presence of the PPR viral RNA was determined in samples by using a specific reverse transcription PCR reported by Polci et al. (*8*). Laboratory tests confirmed circulation of PPRV in farms near Kairouan and Sidi Bouzid.

Aliquots of RNA samples were shipped to the Istituto Zooprofilattico Sperimentale dell'Abruzzo e del Molise in Teramo, Italy, for genetic characterization. RNA was amplified by using the reverse transcription PCR reported by Couacy-Hymann et al. (*9*). Amplicons from virus- positive samples were purified by using the QIAquick PCR Purification Kit (QIAGEN, Valencia, CA, USA) and used for direct sequencing. Sequencing reactions were performed by using the Big Dye Terminator Kit (Applied Biosystems, Foster City, CA, USA), and nucleotide sequences were determined by using the ABI PRISM 3100 DNA sequencer (Applied Biosystems). Amplification and sequencing were repeated twice to avoid introduction of artificial substitutions. Raw sequence data were assembled by using Contig Express (Vector NTI suite 9.1; Invitrogen, Carlsbad, CA, USA), and a 351-nt fragment of the nucleoprotein coding sequence was obtained after deletion of primer sequences.

Two sequences were obtained, 1 from the Kairouan outbreak and 1 from the Sidi Bouzid outbreak. The 2 sequences generated in this study were submitted to GenBank (accession nos. KM068121 and KM068122). Sequences showed nearly complete identity at nucleotide and amino acid levels; there was 1 nucleotide substitution. The BLAST (http://www.ncbi.nlm.nih.gov) was used to detect homologous regions in sequence databases. Sequences were aligned by using ClustalW (http://www.genome.jp/tools/clustalw/) and MEGA version 6 (*10*). Phylogenetic analysis was performed with a 255-nt sequence of the PPRV nucleoprotein gene by using the neighbor-joining method with bootstrap support (1,000 replicates) in MEGA version 6 (*10*) and reference strains representing the 4 lineages of PPRV that have been isolated in different years or countries (Figure).

Our results indicate that lineage IV of PPRV is present in Tunisia. PPRV isolates from the outbreaks in Sidi Bouzid in 2012 and Kairouan in 2013 are closely related to viruses responsible for PPR outbreaks in Morocco in 2008 (*4*) and Algeria in 2010 (*6*). These isolates are closely related to strains from Saudi Arabia, which were detected in Eritrea in 2005 (*5*) and in Sudan in 2008 (*4*). These data suggest that a unique PPRV strain is circulating across this area of the Maghreb. PPRV circulation is maintained probably by the abundant trade in ruminants between Tunisia and neighboring countries. This information highlights the need for a regional approach to control PPR in northern Africa.

The Istituto Zooprofilattico Sperimentale dell'Abruzzo e del Molise G. Caporale is supported by the Italian Ministry of Health.

Soufien Sghaier,[1] Gian Mario Cosseddu,[1] Sonia Ben Hassen, Salah Hammami, Héni Haj Ammar, Antonio Petrini, and Federica Monaco

Author affiliations: Istituto Zooprofilattico Sperimentale dell'Abruzzo e del Molise G. Caporale, Teramo, Italy (G.M. Cosseddu, A. Petrini, F. Monaco); Institut de la Recherche Vétérinaire de Tunisie, Tunis, Tunisia (S. Sghaier, S. Ben Hassen); Ecole Nationale de Médecine Vétérinaire de Sidi Thabet, Sidi Thabet, Tunisia (S. Hammami); and Ministère de l'Agriculture, Tunis (H. Haj Ammar)

DOI: http://dx.doi.org/10.3201/eid2012.141116

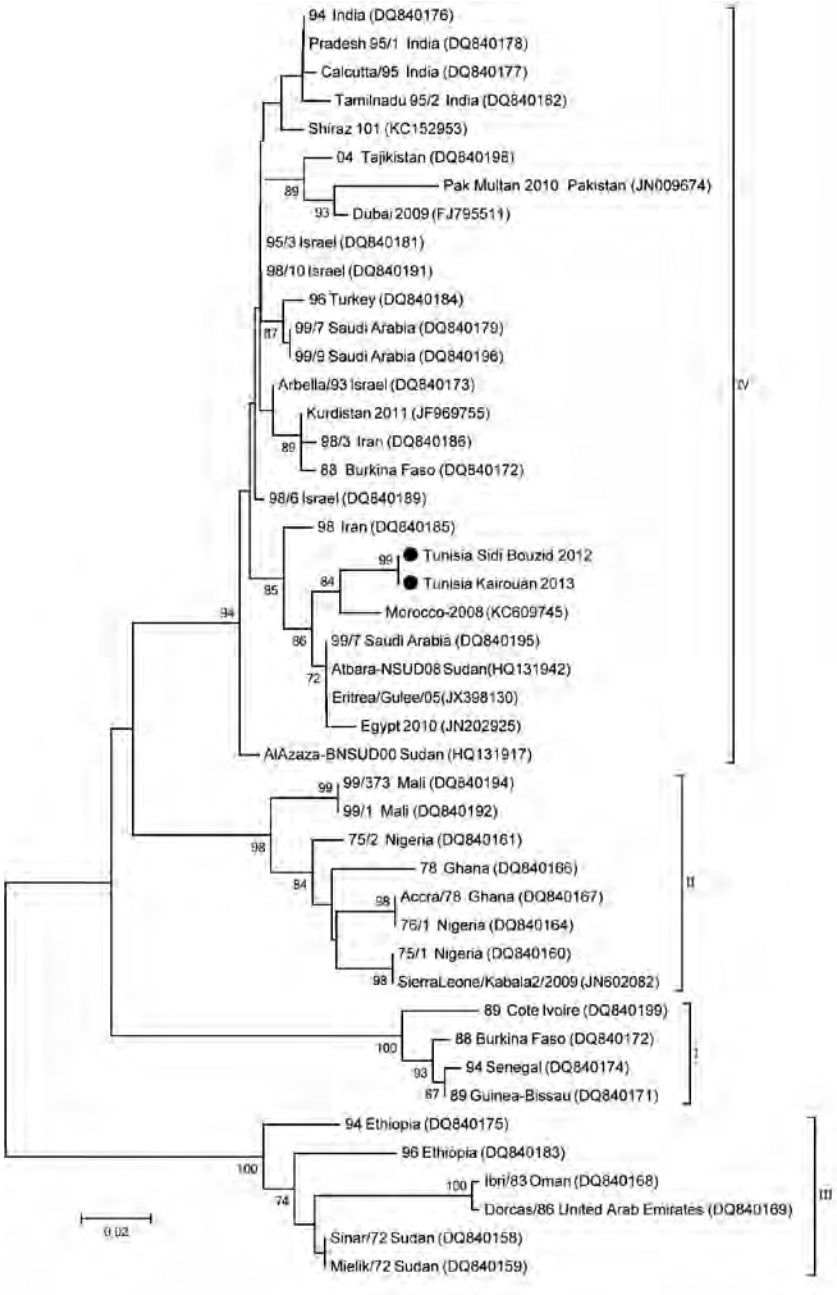

Figure. Phylogenetic tree showing genetic relationships among peste des petits ruminants virus (PPRV) isolates. The tree was constructed on the basis of a 255-nt fragment of nucleoprotein gene of PPRV. Sequences obtained in this study are indicated by black circles. Lineages are indicated on the right. Viruses were identified by using the nomenclature of PPRV isolates (GenBank accession numbers are indicated in parentheses). Analysis was performed by using MEGA 6 software (*10*) and neighbor-joining (maximum composite likelihood) methods. Bootstrap support values >70 are shown (1,000 replicates). Scale bar indicates nucleotide substitutions per site.

References

1. Albina E, Kwiatek O, Minet C, Lancelot R, Servan de Almeida R, Libeau G. Peste des petits ruminants, the next eradicated animal disease? Vet Microbiol. 2013;165:38–44. http://dx.doi.org/10.1016/j.vetmic.2012.12.013
2. Baron MD, Parida S, Oura CA. Peste des petits ruminants: a suitable candidate for eradication? Vet Rec. 2011;169:16–21. http://dx.doi.org/10.1136/vr.d3947
3. Munir M, Zohari S, Berg M. Molecular biology and pathogenesis of peste des petits ruminants virus. New York: Springer; 2013.
4. Kwiatek O, Ali YH, Saeed IK, Khalafalla AI, Mohamed OI, Obeida AA, et al. Asian lineage of peste des petits ruminants virus, Africa. Emerg Infect Dis. 2011;17:1223–31. http://dx.doi.org/10.3201/eid1707.101216
5. Cosseddu GM, Pinoni C, Polci A, Sebhatu T, Lelli R, Monaco F. Characterization of peste des petits ruminants virus, Eritrea, 2002–2011. Emerg Infect Dis. 2013;19:160–1. http://dx.doi.org/10.3201/eid1901.121072
6. De Nardi M, Lamin Saleh SM, Batten C, Oura C, Di Nardo A, Rossi D. First evidence of peste des petits ruminants (PPR) virus circulation in Algeria (Sahrawi territories): outbreak investigation and virus lineage identification. Transbound Emerg Dis. 2012;59:214–22. http://dx.doi.org/10.1111/j.1865-1682.2011.01260.x
7. Office International des Epizooties (OIE). WAHID Interface, 2011. Event summary: peste des petits ruminants, Tunisia [cited 2014 Jun 21]. http://www.oie.int/wahis_2/public/wahid.php/Reviewreport/Review/viewsummary?fupser=&dothis=&reportid=10579
8. Polci A, Cosseddu GM, Ancora M, Pinoni C, El Harrak M, Sebhatu TT, et al.

[1]These authors contributed equally to this article.

Development and preliminary evaluation of a new real-time RT-PCR assay for detection of peste des petits ruminants virus genome. Transbound Emerg Dis. 2013. Jul 19. [Epub ahead of print]. http://dx.doi.org/10.1111/tbed.12117

9. Couacy-Hymann E, Roger F, Hurard C, Guillou JP, Libeau G, Diallo A. Rapid and sensitive detection of peste des petits ruminants virus by a polymerase chain reaction assay. J Virol Methods. 2002;100:17–25. http://dx.doi.org/10.1016/S0166-0934(01)00386-X

10. Tamura K, Stecher G, Peterson D, Filipski A, Kumar S. MEGA6: molecular evolutionary genetics analysis version 6.0. Mol Biol Evol. 2013;30:2725–9. http://dx.doi.org/10.1093/molbev/mst197

Address for correspondence: Gian Mario Cosseddu, Istituto Zooprofilattico Sperimentale dell'Abruzzo e del Molise G. Caporale, Campo Boario, 64100 Teramo, Italy; email: g.cosseddu@izs.it

Correction: Vol. 20, No. 1

In the article Foodborne Trematodiasis and *Opisthorchis felineus* Acquired in Italy (H. F. Wunderink et al.), author Wouter Rozemeijer's name was spelled incorrectly. The article has been corrected online (http://wwwnc.cdc.gov/eid/article/20/1/13-0476_article).

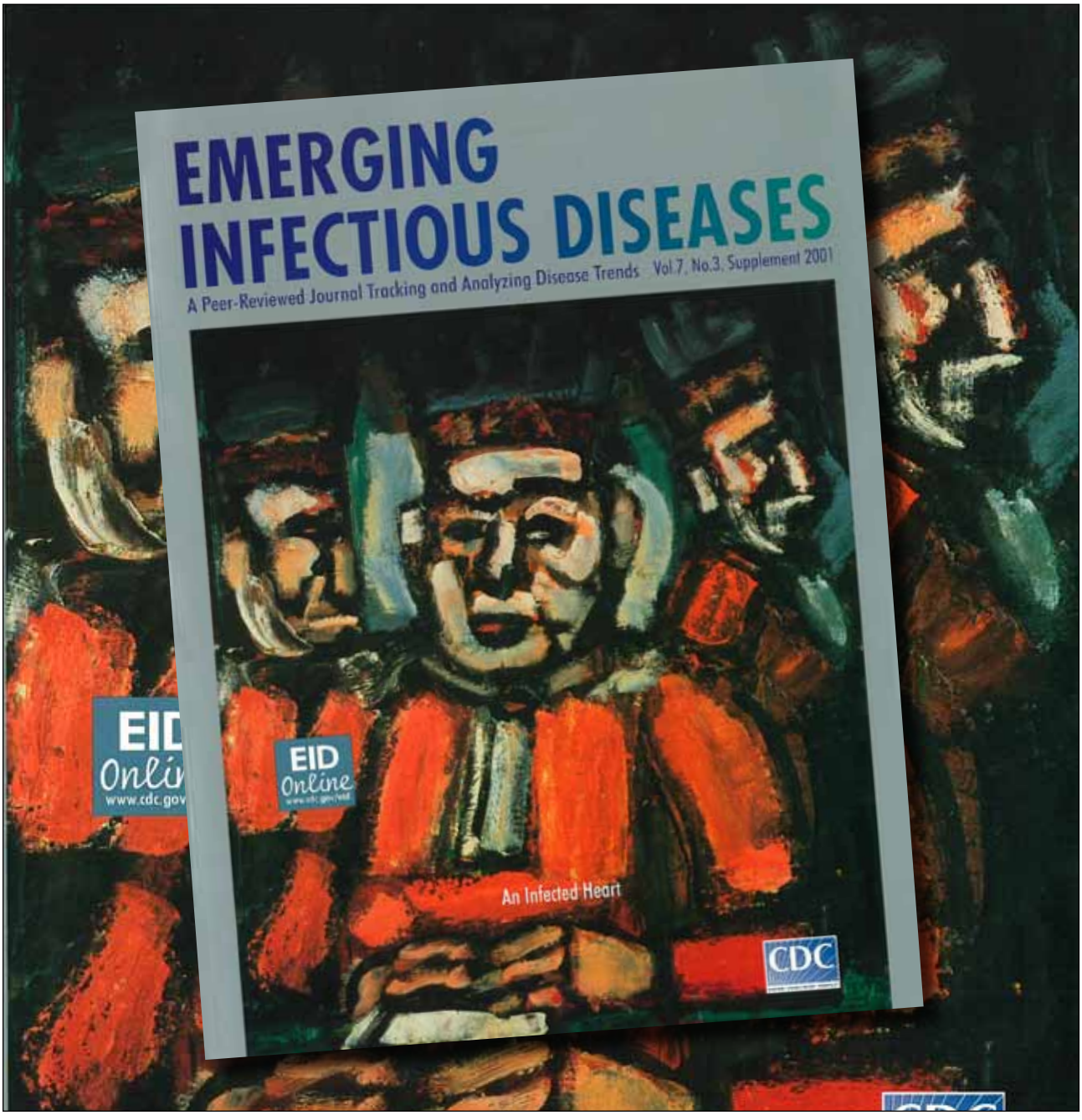

Fred Tomaselli *Starling* (detail), 2010. Photo collage, acrylic, and resin on wood panel 80 x 80 in. (203.2 x 203.2 cm) ©The artist/ Courtesy James Cohan Gallery, New York/Shanghai

Variation Is the Exploration of Possibilities

Byron Breedlove

Born in 1956, American artist Fred Tomaselli grew up in Orange, California, and in 1982, he graduated from California State University, Fullerton, with a degree in painting and drawing. In the early 1980s, Tomaselli became established in the "Downtown L.A." art, music, and drug countercultures. Since 1985, he has lived and worked in Brooklyn, New York.

Author affiliation: Centers for Disease Control and Prevention, Atlanta, Georgia, USA

DOI: http://dx.doi.org/10.3201/eid2012.AC2012

He is best known for his visually stunning hybrid creations—part painting and part mosaic—and for his series of collages based on front-page articles from *The New York Times*. His works have been exhibited widely throughout the world and are in collections at many prominent museums.

Tomaselli collects and incorporates unusual materials into his works, including pharmaceutical and street drugs and myriad images of plants, birds, and body parts cut from catalogs and magazines, suspending them in layers of clear epoxy resin. If bugs, leaves, and other debris become trapped in the sticky resin, Tomaselli keeps them.

He acknowledges the influence of Eastern and Western decorative traditions such as quilts, tapestries, and mosaics, art forms that feature details and repetition. Tomaselli considers his approach to art as a way of reorganizing and reframing information. He once explained to an interviewer, "When I combine these little chunks of information, it's not unlike the way nature stacks up genes to build everything from viruses to humans. I tend to see each small bit like an individual cell, a piece of binary code, or a strand of DNA that accumulates, accrues, and grows into my images."

Tomaselli wants viewers to lose themselves in his art, even to the point of experiencing the sort of confusion and exaltation attributed to Stendhal syndrome. He describes his art as being "about artificial immersive environments, about escapism," themes spawned by his upbringing in suburban California, where amusement parks, shopping malls, and recreational drugs were pervasive.

The artist created this month's dazzling cover image, *Starling*, for an exhibit at the Brooklyn Museum. The starling's head juts from the bottom left amidst searing fluid-like ribbons of red, blue, and yellow. Various insects, perhaps food the bird has eaten, comprise its neck and stomach. This stylized starling may be launching into one of its species' complex soliloquies or devouring figs from the trees growing in the artist's yard. Radiant, precise pulsing kaleidoscopic patterns float across the top third of the painting. The bird's head provides a reference point, but exploring the array of swirling colors, exploding shapes, dots, and specks proves irresistible. The juxtaposition of colorful microscopic and celestial images contrasted against a black background recurs in much of Tomaselli's art.

Starlings were first introduced into the United States in 1890 when Eugene Schieffelin released 60 of them in New York City's Central Park, not far from the Brooklyn Museum that now houses Tomaselli's *Starling*. Schieffelin, who belonged to the American Acclimatization Society, wanted to introduce each species of bird mentioned in the Shakespeare's works into the United States. (Shakespeare mentioned a starling in *Henry IV*, Part 1, Act 1, Scene 3, wherein Hotspur seeks revenge on King Henry, who refuses to pay the ransom for Hotspur's brother-in-law Mortimer: "Nay / I'll have a starling shall be taught to speak / Nothing but 'Mortimer,' and give him/ To keep his anger still in motion.")

An estimated 200 million of these iridescent interlopers, recognized by their purple and green chests and throats and their rasping, screeching songs, are entrenched across the United States (invasive starlings are also found in Canada, South Africa, New Zealand, and Australia). A *New York Times* article written a century after their importation notes that the starling "has distinguished itself as one of the costliest and most noxious birds on our continent." Starlings roost in massive colonies, displace native species of birds, pose problems for air travel, damage crops and fruit trees, and help spread diseases, offsetting any benefits they add by eating insects.

Starlings and other bird species could potentially harbor harmful agents, including those that cause influenza, histoplasmosis, cryptococcosis, and West Nile encephalitis in humans. When present in massive numbers or under the right circumstances, such wild bird populations may be more than a nuisance and possibly pose health threats. Some pathogens hosted by bird species are capable of reorganizing and reframing their genetic information. In his recently published book *Spillover: Animal Infections and the Next Human Pandemic*, David Quammen used the phrase "variation is the exploration of possibilities" when discussing mutations in viruses—which also sounds like Tomaselli's approach to creating his multifaceted collages.

Acknowledgment

I thank Louise E. Shaw for making me aware of the artwork of Fred Tomaselli and for helping obtain permission to use *Starling*.

Bibliography

1. Ayers R. A conversation with artist Fred Tomaselli [cited 2014 Sept 15] http://www.huffingtonpost.com/robert-ayers/i-think-its-hilarious-rob_b_786621.html
2. Boon ACM, Sandbulte MR, Seiler P, Webby RJ, Songserm T, Guan Y, et al. Role of terrestrial wild birds in ecology of influenza A virus (H5N1). Emerg Infect Dis. 2007;13:1720–4 http://wwwnc.cdc.gov/eid/article/13/11/07-0114. http://dx.doi.org/10.3201/eid1311.070114
3. Gaukler SM, Linz GM, Sherwood JS, Dyer NW, Bleier WJ, Wannemuehler YM, et al. *Escherichia coli, Salmonella,* and *Mycobacterium avium* subsp. *paratuberculosis* in wild European starlings at a Kansas cattle feedlot. Avian Dis. 2009;53:544–51. http://dx.doi.org/10.1637/8920-050809-Reg.1
4. Lescaze Z. Fred Tomaselli is off drugs [cited 2014 Sept 15]. http://observer.com/2014/05/fred-tomaselli-is-off-drugs/
5. Linz G, Homan H, Gaukler S, Penry L, Bleier W. European starlings: a review of an invasive species with far-reaching impacts. Managing vertebrate invasive species. Proceedings of an international symposium; Fort Collins, Colorado; 2007 Aug 7–9 [cited 2014 Sept 16]. http://www.aphis.usda.gov/wildlife_damage/nwrc/symposia/invasive_symposium/nwrc_TOC_index.shtml
6. Mirsky S. Shakespeare to blame for introduction of European starlings to U.S. [cited 2014 Sept 16]. http://www.scientificamerican.com/article/call-of-the-reviled/?page=1
7. Quammen D. Spillover: animal infections and the next human pandemic. New York: W.W. Norton & Company; 2013.
8. Shields F. Artists in conversation: Fred Tomaselli [cited 2014 Sept 23]. http://bombmagazine.org/article/3625/

Address for correspondence: Byron Breedlove, EID Journal, Centers for Disease Control and Prevention, 1600 Clifton Rd NE, Mailstop E41, Atlanta, GA 30329-4027, USA; email: wbb1@cdc.gov

EMERGING INFECTIOUS DISEASES

Upcoming Issue

Pneumonic Plague Outbreak, Northern Madagascar, 2011

Health Care Response to CCHF in US Soldier and Nosocomial Transmission to Health Care Providers, Germany, 2009

Tularemia in Children, Turkey

Protocol for Metagenomic Virus Discovery in Infectious Disease Settings

Epidemiology and Ecology of Tularemia in Sweden, 1984–2012

Melioidosis in Gabon, 2012–2013

Molecular Epidemiology and Genetic Diversity of *Orientia tsutsugamushi* from Patients with Scrub Typhus, India

Clinical Course and Long-Term Outcome of Hantavirus-Associated Nephropathia Epidemica, Germany

WU Polyomavirus in Respiratory Epithelial Cells from Lung Transplant Patient with Job Syndrome

Treponema pallidum PCR for Detection of Primary Syphilis Ulcers

Detection of Zika Virus in Urine

Oseltamivir-Resistant Influenza A(H1N1)pdm09 Viruses, United States, 2013–14

Foot-and-Mouth Disease Virus Serotype SAT 3 in Long-Horned Ankole Calf, Uganda

Avian Influenza (H7N9) Virus Infection in Chinese Tourist in Malaysia, 2014

Continuing Effect of Serogroup A Meningococcal Polysaccharide Conjugate Vaccine, Chad

Increased Outbreaks Associated with Nonpasteurized Milk, United States, 2007–2012

Prevalence of Antibodies to *Borrelia burgdorferi* sensu lato among Adults, Germany, 2008–2011

Characterization of a Multidrug-Resistant, Novel *Bacteroides* Genomospecies

Hospital-Associated Transmission of *Brucella melitensis* outside the Laboratory

Complete list of articles in the January issue at http://www.cdc.gov/eid/upcoming.htm

Upcoming Infectious Disease Activities

2015

February 23–25, 2015
CROI
Conference on Retroviruses and Opportunistic Infections
Seattle, WA, USA
http://www.croi2014.org/

April 20– 23, 2015
EIS
Epidemic Intelligence Service Conference
http://www.cdc.gov/eis/conference.html

May 30–June 2, 2015
American Society for Microbiology General Meeting
New Orleans, LA, USA
http://gm.asm.org/

August 2015 (Rescheduled)
ICEID
International Conference on Emerging Infectious Diseases
Atlanta, GA, USA

2016

March 2–5, 2016
ISID
17th International Congress on Infectious Diseases
Hyderabad, India

Announcements

To submit an announcement, send an email message to EIDEditor (eideditor@cdc.gov). Include the date of the event, the location, the sponsoring organization(s), and a website that readers may visit or a telephone number or email address that readers may contact for more information.

Announcements may be posted on the journal Web page only, depending on the event date.

EMERGING INFECTIOUS DISEASES
A Peer-Reviewed Journal Tracking and Analyzing Disease Trends

Emerging Infectious Diseases thanks the following reviewers for their support through thoughtful, thorough, and timely reviews in 2014. We apologize for any inadvertent omissions.

Tande Aaron
Abu Abdul-Quader
Joseph Abrams
Sazaly AbuBakar
Rodolfo Acuna-Soto
Bishwa Adhikari
Toïdi Adékambi
Rakesh Aggarwal
Patricia V. Aguilar
Adriano Aguzzi
Shama Desai Ahuja
Munirul Alam
Cesar G. Albariño
Ryan J. Albert
Antonio Alcami
Heather Alexander
Kathleen A. Alexander
Michael Alifrangis
Julio Álvarez
Paulo C. Alves
Irina V. Alymova
Ananda Amarasinghe
Alongkorn Amonsin
Abhijeet Anand
Katherine L. Anders
Alicia D. Anderson
Larry Anderson
Laurent Andreoletti
Fred Angulo
Filippo Ansaldi
Denise Antona
Markus Antwerpen
Anucha Apisarnthanarak
Charles Smith Apperson
Maiken Cavling Arendrup
Paul Mathew Arguin
Mary Ari
Frederic Ariey
Nimalan Arinaminpathy
Nichole Arrigo
Stephanie Ascough
David Ashkin
Alex Asidi
Robert L. Atmar
Cecile Aubron
Tatjana Avsic
Fatih Mustafa Awad-El-Kariem
Taj Azarian
Andrew S. Azman
Eduardo Azziz-Baumgartner
Germán Añez
Romaine Basmaci
Richard Bendall
Shawn Babiuk
P. Bryon Backenson
John Baddley
Stephen Baker
Susan C. Baker
Madhu Smita Bal
Michael Ballesteros
Sharon Balter
Sapna Bamrah
Krisztian Banyai
Ashley C. Banyard
Alan Barbour
John R. Barnes
Ian Barr
Roberto Barrera
M. Bailor Barrie
Alfred Sidney Barritt
Pennan M. Barry
Albert Barskey
Aldert Bart
Kalpana Baruah
Sridhar Basavaraju
Alison Jane Basile
Roger Bate
Mara Battilani
Michael Benjamin Batz
Elsa Baumeister
Daniel G. Bausch
Iacopo Baussano
Roger Baxter
Sally Baylis
Daniel Beachler
Bernard Beall
Ben Beard
David Beasley
Mark Edward Beatty
Barry J. Beaty
Emily S. Beeler
Casey Barton Behravesh
Ermias Belay
Beth P. Bell
David M. Bell
Michael Bell
Jessica A. Belser
Graham John Belsham
M. Eric Benbow
Irene Benech
Maria Benko
Nicholas Bennett
Stephen R. Benoit
Kimberley S.M. Benschop
Mikael Berg
Ruth L. Berkelman
Allison Bermingham
Kathryn Bernard
Kyle T. Bernstein
Robert Bernstein
Gwladys Bertin
Zulfiqar Ahmed Bhutta
Giske Biesbroek
Matthew Biggerstaff
Zeno Bisoffi
Paritosh Kumar Biswas
Adam Bjork
Steven Black
Carina Blackmore
Stuart Blacksell
Anna Blackstock
Carol D. Blair
Lucas Scott Blanton
Karen C. Bloch
Sharon Bloom
Lucille Blumberg
Seth Blumberg
Andrea K. Boggild
Stephane Bonacorsi
E.P. Bonnet
Remy Bonnin
Robert A. Bonomo
Marc J.M. Bonten
Matthias Borchert
Andrew Borman
Ray Borrow
Stacey Bosch
Gregory Bossart
Katharine Bossart
Icaro Boszczowski
Emmanuel Bottieau
German Bou
Olivier Bouchaud
Henri-Jean Boulouis
Jérôme Bouquet
Donald Hugh Bouyer
Anna Bowen
Michael D. Bowen
Richard A. Bowen
Dwight Bowman
Walter Boyce
Philip Brachman
Kristy K. Bradley
Robert Bradsher
Marieta Braks
Mary E. Brandt
Aaron Brault
Byron Breedlove
Carolyn Bridges
Thomas Briese
Margo A. Brinton
Benjamin Bristow
Seth C. Britch
Christopher Broder
I. Brook
Philippe Brouqui
Betty Ann Brown
Clive Brown
Corrie Brown
Kevin Brown
Paul W. Brown
Barbara A. Brown-Elliott
Juliet E. Bryant
Anthony Bryceson
Kate Buchacz
Udo Buchholz
Michael Buchmeier
Christopher B. Buck
Christine Budke
James W. Buehler
Dora Buonfrate
Peter Burbelo

Jacqueline Burkholder
Andreas Burkovski
Felicity Burt
Michael P. Busch
Jay Butler
Bilal Butt
Jae-Won Byun
Lorenzo Cáceres
Victor Caceres
Michael Caffrey
David P. Calfee
Charles H. Calisher
Douglas Call
Ilana L.B.C. Camargo
Emmanuelle Cambau
Christine Campese
Rafael Cantón
Jun Cao
Wuchun Cao
Yongchang Cao
Lorenza Capucci
Carol J. Cardona
Yehuda Carmeli
Luis Roman Carrasco
Kris K. Carter
Pamela K. Cassiday
Mariana Castanheira
Elizabeth Castañeda
Simon Cauchemez
Dominique Caugant
Luciano Pamplona de Góes Cavalcanti
Joseph Cavanaugh
Bernard Cazelles
Peter Cegielski
D. Ceroni
Chanhee Chae
Joon-seok Chae
Rana Chakraborty
Eng-Soon Chan
Meera A. Chand
Michelle Chang
Shan-Chwen Chang
David Andrew Chapman
Louisa Elaine Chapman
Macarthur Charles
Rémi N. Charrel
Margo Chase-Topping
Honglin Chen
Li-Mei Chen
Weijun Chen
Zhuo (Adam) Chen
Allen C. Cheng
James D. Cherry
Daniel Stephen Chertow
Chuen-Sheue Chiang
Francisco Chiaravalloti-Neto
Sekai Chideya
Jamie Childs
Sadegh Chinikar
Amit Chitnis
John Chitty
Charles Yen Chiu
B.B. Chomel
Anuradha Chowdhary
Gerardo Chowell
George Christopher
Daniel K.W. Chu
May C. Chu
Paul R. Cieslak
Gustavo Cilla
Sandro Cinti
Marco Ciotti
C. Graham Clark
Michael L. Clawson
Angela Ahlquist Cleveland
Eleanor Click
Murray Cohen
Nicole J. Cohen
Amanda C. Cohn
Matthew E. Coldiron
Stewart Cole
Melissa G. Collier
Peter Collignon
Barry G. Combs
James A. Comer
Richard Compans
Diana L. Connor
John Connor
J. Lyle Conrad
Franz J. Conraths
Paul Converse
Walt Cook
Geoffrey Coombs
Celia Cordon
Martin Cormican
Margaret Cortese
Michel Cot
Pierre Coursaget
Ben Cowling
Christina Coyle
Philip Edward Coyne
John Andrew Crump
Pascal Crépey
Marie Rene Culhane
Nigel A. Cunliffe
Bart J. Currie
Sandra Currie
Sally J. Cutler
Cristina Da Silva Carias
Ron Dagan
Charles Daley
Janet Daly
Patrick James Danaher
David Dance
Nicholas Daniels
Richard Norman Danila
M. Carolina Danovaro-Holliday
Gautam Dantas
Gregory A. Dasch
Alexandre Dasilva
Anand Date
Virginia M. Dato
Irja Davidkin
Charles T. Davis
Jeffrey Paul Davis
Todd Davis
William G. Davis
Bernard Davoust
Fred de Boer
Kris De Clercq
Cillian F. De Gascun
Xavier de Lamballerie
Gonzalo de Prat-Gay
Henry J. C. de Vries
Aruni De Zoysa
James DeCaprio
Kevin Michael DeCock
Deborah Dean
Jacqueline Deen
Aldo Dekker
Francis Delpeyroux
Eric Delwart
Alicia Demirjian
Amanda Dempsey
David Dennis
Dan Denoon
Xavier Deparis
Gordana Derado
Kathryn Deriemer
Malini Desilva
Ulrich Desselberger
Gregor Devine
Gregory Deye
Angela Di Cesare
Adama Diallo
Fredi Alexander Diaz-Quijano
Binh A. Diep
Katharina Dittmar
Linda K. Dixon
Gaston Djomand
Gerhard Dobler
Mehmet Doganay
Yohei Doi
Thomas Doker
Sheila Dollard
Fernanda C. Domingues
Ruben O. Donis
Gé A. Donker
Flavia B. dos Santos
John Douglas
Douglas Dover
Walter R. Dowdle
Michael Drebot
Steven J. Drews
Jan Felix Drexler
Jan Drobeniuc
Christian Drosten
J. Stephen Dumler
Keith Eastwood
Gregory Ebel
Hideki Ebihara
Miriam Eddyani
Sophie Edouard
Paul H. Edelstein
John Edwards
Kathryn Edwards
Paul V. Effler
Androulla Efstratiou
Joseph Egger
Bernhard Ehlers
Martin Eiden
Rebecca J. Eisen
Edward M. Eitzen
Hashem El-Serag
Elamin H. Elbasha
Brett Richard Ellis
Esther Ellis
Kirt Emery
Jorgen Engberg
David M. Engelthaler
Fred Enright
Moshe Ephros
Jonathan H. Epstein
Dean D. Erdman
Marina Eremeeva
Charles D. Ericsson
Ananias A. Escalante
Vanessa Escuret
Mathew Dioh Esona
Fernando Esperon
Miranda Angelica Espinosa
Sandra Essbauer
Pedro J. Esteves
Magnus Evander
Jessica Fairley
Shufang Fan
Eileen C. Farnon
C. Paddy Farrington
Herman Favoreel
Alicia Feagins
H.M. Feder
Katherine Feldman
Heinz Feldmann
Mariet C.W. Feltkamp
Li Feng
Stefan Fernandez
Marcelo Ferreira
Patricia Ferrieri

Gerhard Feurle
Elisabeth Fichet-Calvet
Amy P. Fiebelkorn
Richard Fielding
Barry Fields
Patricia I. Fields
Stacy R. Finkbeiner
Marc A. Fischer
Scott Fitzgerald
Brendan Flannery
Luciana Flannery
Jaroslav Flegr
Jason P. Folster
Kevin Fonseca
Arnaud Fontanet
Anthony Fooks
Mary Foote
Joseph Forrester
Ron A.M. Fouchier
Pierre-Edouard Fournier
James G. Fox
LeAnne M. Fox
Brian D. Foy
Anne Marie France
Stephen C. Francesconi
Donald P. Francis
Leticia Franco
Alexander Franz
John Fraser
Rachel Friedman
Alexander W. Friedrich
Matthew Frieman
Hans-Peter Fuehrer
Paula Fujiwara
M. Fulde
Charles Fulhorst
Isaac Chun-Hai Fung
Gülsah Gabriel
Kenneth L. Gage
Joanna Gaines
John Galgiani
Gale Galland
Renee Galloway
Manoj Gambhir
Neel R. Gandhi
Sumanth Gandra
George Fu Gao
Robert Garcea
Julian E.Garcia-Rejon
Michael A. Gardam
Roberto C. Garza
Paul Gastanaduy
Joel C. Gaydos
Jay E. Gee
Helen Gelband
Gregory G. Gensheimer
Kathleen Gensheimer
Jon Gentsch
Dylan George
Sue Gerber
Peter Gerner-Smidt
Anne G. Gershon
Smita Ghosh
Giovanni M. Giammanco
Kirsten V. Gilardi
Rodica Gilca
John Gimnig
Christian Giske
Daniel Glikman
Cyrille Goarant
Mark Goettel
Edward Goldstein
Susan Goldstein
Katja Verena Goller
Beatriz Gomez
Satish Gopal
Marga Goris
Nicole Gottdenker
Yuval Gottlieb
Marcelo Gottschalk
Ernest Andrew Gould
Frédérique Gouriet
Joelle Gouy de Bellocq
Elena A. Govorkova
John Douglas Grabenstein
Yonatan Grad
Stephen Roger Graves
Gregory C. Gray
Kim Y. Green
Frederic Grenouillet
David E. Griffith
Hajo Grundmann
Yi Guan
Jeannette Guarner
Jonathan Benjamin Gubbay
Duane Gubler
Marta A. Guerra
Richard L. Guerrant
Ricardo E. Guertler
Alice Guh
Jean-Luc Guérin
Miklós Gyuranecz
Bart Haagmans
Walter Haas
Meredith Hackel
John Hackett
C.A. Hage
Stefan Hagmann
Rana Hajjeh
Patrick G. Halbur
Aron J. Hall
Scott B. Halstead
Davidson Howes Hamer
Alan William Hampson
George Han
Xiang Y. Han
Bill Hanage
Jon Michael Hanifin
Stephan Harbarth
John Harding
Susan Hariri
James Michael Harris
Ruth Harvey
Karyn A. Havas
Arie H. Havelaar
Harry W. Haverkos
Fiona Havers
Frederick G. Hayden
Lia Marian Haynes
Katrina Hedberg
Wiebke Hellenbrand
David K. Henderson
Katherine Hendricks
Tom Hennessy
Ronnie Henry
Steven Henry
Jean-Michel Heraud
Liv Hesstvedt
Graham J. Hickling
Vincent Hill
Julia K. Hilliard
Alison F. Hinckley
Alan R. Hinman
Joe Hinnebusch
Rogier Hintzen
Wolfgang Hladik
Robert Michael Hoekstra
Thomas Hoenen
Mike Holbrook
Scott Holmberg
Edward C. Holmes
Kathryn V. Holmes
Nadine M. Holmes
Kathryn E. Holt
Lori Holtz
Timothy Holtz
Mary Hondalus
Peter Horby
C. Robert Horsburgh
Hans-Peter Horz
Paul Hoskisson
Duane Hospenthal
Eric Houpt
Joppe W.R. Hovius
John Hoxmeier
Yana Emmy Hoy-Schulz
Daniela F. Hozbor
Po-Ren Hsueh
Angela Song-En Huang
Yaowei Huang
James Hughes
Kristina G. Hultén
Kimberly B. Hummel
Elizabeth Hunsperger
A.C. Hurt
David Hutton
Mark Huycke
Jessica Hwang
Rachel Idowu
Kashef Ijaz
Allison Imrie
Pewpan M. Intapan
Shahed Iqbal
Miren Iturriza-Gómara
Danielle A. Iuliano
Masaaki Iwaki
Jacques Izopet
Mary Anne Jackson
Paul J. Jackson
Jan Jacobs
George Jacoby
Seema Jain
Denise Jamieson
J. Michael Janda
Naveed Zafar Janjua
Ana Maria Jansen
Petrus Jansen van Vuren
Helen Jenkins
Kwang Cheol Jeong
Michael A. Jhung
Baoming Jiang
Ling Jin
Gary Johanning
Anders Johansson
Michael A. Johansson
Reimar Johne
Barbara J.B. Johnson
Barbara W. Johnson
James R. Johnson
Judith Ann Johnson
Yvette Joyce Johnson
Bryony Anne Jones
Jeremy F. Jones
Timothy Jones
Lisa Jones-Engel
Marcel Jonges
Colleen Beth Jonsson
Jonathan James Juliano
Barbara C. Kahl
Adriana E. Kajon
Manish Kakkar
Alexander Jennings Kallen
Nassim Kamar
Mary L. Kamb
Saleem Kamili
Amit Kapoor
William Karesh
Erik A. Karlsson
Stephanie Karst
Shannon Kasperbauer
Cecilia Kato
Mark A. Katz

Carol A. Kauffman
Hiroki Kawabata
Yoshihiro Kawaoka
Ghazi Kayali
Colleen Kelly
Daryl J. Kelly
Tara Anne Kelly
Russell Kempker
Alain Kenfak-Foguena
Yoav Keynan
Gil Kersh
Jay S. Keystone
Hiroshi Kida
James Kile
Mary L. Killian
Lindsay Kim
Peter Daniel Kirkland
Carl D. Kirkwood
Todd Kitten
Anne Kjemtrup
Curtis Klages
Terry A. Klein
Ben Klekamp
Jan A.J.W. Kluytmans
Stephen Knabel
Jenny Knapp
Barbara Knust
Maja Kodani
Cristian Koepfli
Claudia Kohl
Katrin Kohl
Gotaro Kojima
Denis Kolbasov
Amy Kolwaite
Nicholas Komar
Kenneth K. Komatsu
Qinzhong Kong
Lisa M. Koonin
Marion P.G. Koopmans
Eran Kopel
Ram Koppaka
Stephen Korsman
Michael Kosoy
Frederick T. Koster
Barbara Kowalcyk
Lidija Cvetko Krajinovic
Laura Kramer
Peter James Krause
Robert Krause
Aimie Kreimer
Katharina Kreppel
Elmar Krieger
Karen A. Krogfelt
Thomas G. Ksiazek
Matthew J. Kuehnert
Kiersten J. Kugeler
Edward J. Kuijper
Fumiaki Kura
Preeta K. Kutty
Ekaterina Kurbatova
Patrick Kwan
Zaharoula Kyriakopoulou
Regina C. LaRocque
Alain B. Labrique
Marcelo B. Labruna
Marcus Lacerda
Justin Lack
Angie Lackenby
Shamez Ladhani
Theresa Lamagni
Amy J. Lambert
Patrick J. Lammie
Christoph Lange
Adam J. Langer
Simone Lanini
K. Laoprasopwattana
Sophie Larrieu
Lars Olof Larsson
Estrella Lasry
Susanna K.P. Lau
James LeDuc
Sylvie Lecollinet
Phillip Lederer
Edith R. Lederman
Chang-Won Lee
Changhee Lee
Vernon J. Lee
Youn-Jeong Lee
James Leggett
David Leiby
Herwig Leirs
Jeffrey Lennox
Agnes Lepoutre
Paul Levett
Michael L. Levin
Myron M. Levine
Nicola S. Lewis
Sheri H. Lewis
Taru Lienemann
Poh Lian Lim
Yusen Eason Lin
John A. Linder
David Lindsay
Kenneth J. Linthicum
W. Ian Lipkin
Michael Libman
Tom Lipscomb
Marc Lipsitch
Galina Yu Lipskaya
Susan E. Little
Cara Litvin
Anastasia P. Litvintseva
Ming-Tsan Liu
Pei Liu
Xiufan Liu
Josep M. Llibre
Robert Lochhead
Shawn R. Lockhart
Mark Loeb
Christopher H. Logue
Kavita S. Lole
David R. Lonsway
Benjamin A. Lopman
Nicola Low
Stephen Luby
Naomi Lucchi
Alexander N. Lukashev
Joan Lunney
Sun Lunquan
Francisco Luquero
Michael Lynch
Ruth Lynfield
Marshall Lyon
Young S. Lyoo
Max Maurin
Oriol Mitja
David Mabey
N. James MacLachlan
Calman A. MacLennan
Tracey MacNamara
Jessica R. MacNeil
Kevin R. Macaluso
Catherine Macken
Ryan A. Maddox
Fabrizio Maggi
Brian W.J. Mahy
Martin C.J. Maiden
Matthias Maiwald
Balaji Manicassamy
Nina Marano
Francine Marciano-Cabral
Anthony Marfin
Mona Marin
Axel A. B. Marinović
Wanda Markotter
Tom Marrie
Glenn Andrew Marsh
Laurent Marsollier
Douglas Marthaler
Santiago Mas-Coma
Carl Jeffries Mason
Henry Masur
Robert Massung
Barun Mathema
Jelle Matthijnssens
Simonetta Mattiucci
Ana Mattos-Guaraldi Luiza
Larissa May
Brad J. McCall
John McCauley
Andrea McCollum
Malcolm McCrae
Jon McCullers
L. Clifford McDonald
Marian McDonald
Linda McDougal
Jeffrey McFarland
Lesley McGee
Peter McIntyre
Kelly T. McKee
Pamela McKenzie
Robert McLean
Rita McManamon
Laura McMullan
Ruth McNerney
Geraldine M. McQuillan
Jennifer H. McQuiston
John McQuiston
Jodie McVernon
Oleg Mediannikov
Patrik Medstrand
Jacques F. Meis
Eyal Meltzer
Martin I. Meltzer
Humberto R. Mendoza
X.J. Meng
Sarah Meno
Anna Meredith
Mark Messonnier
Herrmann Meyer
Sarah A. Meyer
Craig Meyers
Benedict Michael
Gabriel John Milinovich
Bess Miller
Elizabeth Miller
Jeffrey Miller
S. Millership
Mathieu Million
Alexander James Millman
James N. Mills
Philip David Minor
Anna Minta
Chad Mire
Rajal Mody
Igor Mokrousov
Claudia Molins
Abelardo C. Moncayo
Stephan S. Monroe
Joel M. Montgomery
Susan P. Montgomery
Frits R. Mooi
Ronald L. Moolenaar
Patrick Moonan
Chester Moore
Andrew Moorehead
Gina Mootrey
John S. Moran
David Morens
Pedro L. Moro
J. Glenn Morris
Dale Morse

Stephen S. Morse
Muhammad G. Morshed
Kathleen S. Moser
Eric Mossel
Anthony Mounts
Hercules Moura
Richard W. Moyer
Atis Muehlenbachs
Nicolas J. Mueller
Olli Muerman
Michael R. Mulvey
U.G. Munderloh
Vincent Munster
Manoj V. Murhekar
Frederick A. Murphy
Kristy O. Murray
Darwin Murrell
Carmen Muñoz-Almagro
Jorge Muñoz-Jordán
L. Silvia Munoz-Price
Khin Saw Myint
Francis Mégraud
Thomas Müller
Petra Müllner
Graeme Robert Nimmo
Thierry Naas
Irving Nachamkin
Yoshiro Nagao
Minoru Nakao
Allyn Kiyo Nakashima
Mitsuo Narita
Roger S. Nasci
Sheila Nathan
Thomas R. Navin
Shiri Navon-Venezia
Scott Naysmith
Linda Neff
Peter Nejsum
Christina Nelson
Kenrad Nelson
Martha Nelson
Noele Nelson
Paul N. Newton
Terry Fei Fan Ng
Ann Nguyen
Stuart T. Nichol
William L. Nicholson
Loredana Nicoletti
Matthias Niedrig
Stefan Niemann
Andreas Nitsche
Allan Nix
John Nkengasong
Carl Erik Nord
Helen Norder
Patrice Nordmann
Ryan T. Novak
Norbert Nowotny
Andrew Noymer
Marcio R. T. Nunes
Thomas Nutman
Daniel O'Brien
Annette O'Connor
Steve Oberste
Chris Ockenhouse
Norio Ohashi
Juan P. Olano
Francisco Olea-Popelka
Kevin J. Olival
Rosely M. Z. Oliveira
Sonja J. Olsen
Donald Robert Olson
Ken E. Olson
Tanja Opriessnig
Walter A. Orenstein
Ynes Ortega
Lynda Osadebe
Nikolaus Osterrieder
Stephen Ostroff
José A. Oteo
Luiz Shozo Ozaki
Christopher D. Paddock
Paula Julieta Padula
Pawin Padungtod
Slobodan Paessler
Kristen Page
Nicola Page
Gustavo Palacios
Peter Palese
Mitchell Palmer
Xiaoli L. Pang
Mary Pantin-Jackwood
Anna Papa
John R. Papp
Peter G. Pappas
Daniel Paris
Benjamin J. Park
Wan Beom Park
Philippe Parola
Colin Parrish
Christopher M. Parry
Michele Parsons
Ajanta Patel
Anita Patel
Jean Patel
Manisha Patel
Mary Evans Patrick
John Patton
Ryne Paulose
Andrew T. Pavia
Boris I. Pavlin
Daniel C. Payne
Michael Pearce
Adriana Peci
Joseph S. Malik Peiris
Olli A.T. Peltoniemi
Maurice Pensaert
Pasi Penttinen
Eli Perencevich
Sabine Pereyre
Vanessa Perez
David Perlin
Stanley Perlman
Jean-Marie Peron
Leonard Peruski
Joseph F. Perz
Ted Pestorius
Thomas A. Peterman
Timothy R. Peters
Jeannine M. Petersen
Lyle Petersen
Trevor N. Petney
Melinda M. Pettigrew
Eric Pevzner
Marisa Peyre
Christophe N. Peyrefitte
Günter M. Pfaff
Michael Pfaller
Martin Pfeffer
Tung Phan
Renaud Piarroux
Mathieu Picardeau
María Inés Picollo
Stephane Picot
Satish Pillai
Allan Pillay
Paola Pilo
Benjamin A. Pinsky
Adriano Pinter
Amelia Pinto
Nelson Pinto
James Pipas
Antonio Piralla
John Pitman
Johann D. Pitout
Tyrone Pitt
Jean-Christopher Plantier
Matthias Pletz
Mateusz Plucinski
Gerd Pluschke
Laurent Poirel
Philip M. Polgreen
Marjorie Pollack
Leo Poon
Kyle Popovich
Françoise Portaels
Frank Post
Tonia Poteat
Morris Potter
Christine Pourcel
Spyros Pournaras
Ann M. Powers
S.J. Pravinkumar
Wolfgang Preiser
Joseph Prescott
Rebecca Prevots
Patricia Priest
Simon Lawrence Priestnall
Anna K. Psaroulaki
Michael A. Purdy
Krista Queen
Le Mai Quynh
Ingrid Brigitte Rabe
Peter MacGarr Rabinowitz
Vincent Racaniello
Elliot Raizes
Sreekumari Rajeev
T. Ramamurthy
Kunal Rambhia
M. Ramirez
Didier Raoult
Vera Aleksandrovna Rar
Sonja Ann Rasmussen
Elizabeth Rea
Mark Reacher
Terri Rebmann
Ashok Kumar Reddy
Henry Redel
Carrie Reed
Nicholas Reich
William Reisen
David A. Relman
Chantal Reusken
Randall Rockne Reves
Mary G. Reynolds
Josiah Rich
Allen L. Richards
Gene Richardson
Juergen A. Richt
Joachim Richter
Sandra S. Richter
Rebeca Rico-Hesse
Julia Ridpath
Yasuko Rikihisa
George Franklin Risi
Caterina Rizzo
Jill Carolyne Roberts
Rebecca Roberts
Sally Roberts
Tamalee Roberts
Lucy Robertson
Ashley Robinson
Dan Rock
Luis L. Rodriguez
Peter L. Roeder
Michael Roehrl
Jean Marc Rolain
Dionne Bezerra Rolim
Pierre E. Rollin
Buathong Rome
Jose Romero
Thomas Romig

Lijun Rong
M.M. Ronn
Ronald Rosenberg
Philip Rosenthal
Paul Rota
Carol Rubin
Karen M. Rudolph
James Rudrik
Charles Rupprecht
Theresa M. Russell
Edward T. Ryan
Helio S. Sader
Jeroen Saeij
Daniel R. Salomon
Anthony Sanchez
Guillermo Sanchez
Pedro Sanchez-Cordon
Juhani Sand
M.J. Satlin
M. Sato
Harry Michael Savage
Nicholas J. Savill
Souleymane Sawadogo
Charles Schable
Troels Scheel
Flemming Scheutz
Oliver Schildgen
Neil W. Schluger
Connie Schmaljohn
George Schmidt
Jonas Schmidt-Chanasit
Lawrence B. Schonberger
Gunther Schonrich
Tony Schountz
Martin Schriefer
Joanne Schulte
Constance Schultsz
Myron G. Schultz
Stacey L. Schultz-Cherry
Tom G. Schwan
Eli Schwartz
Ira Schwartz
Herbert P. Schweizer
David Scollard
Aaron E. Scott
Phillip Scott
Robert Douglas Scott
Carlos Seas
Barbara Seaworth
Isaac See
Julie Segre
Lynne Sehulster
James J. Sejvar
Tsutomu Sekizaki
Salaam Semaan
Parham Sendi
Piseth Seng
Mary Serdula
Jose Augusto Serpa
Donald Seto
Daniel J. Sexton
Yael Shachor-Meyouhas
Sean V. Shadomy
Shira Chani Shafir
Kajari Shah
Sural Shah
Sadia Shakoor
Wayne Shandera
Andi L. Shane
Umid M. Sharapov
Tyler M. Sharp
Jana Shaw
Michael Shaw
Beth Shaz
Elizabeth Sheridan
Alexander M. Shestopalov
Wun-Ju Shieh
Beletshachew Shiferaw
Miriam Shiferaw
Tom Shimabukuro
Hiroyuki Shimizu
Nahoko Shindo
Sinhg Shivakumar
Carol Hopkins Sibley
Lynne Sigler
Ellen Silbergeld
Amanda Mae Simanek
Peter Simmonds
Raj Kumar Singh
James Singleton
Tarja Sironen
Paiboon Sithithaworn
Maria Sjölund-Karlsson
Anders Sjöstedt
Michael A. Skinner
Mary P.E. Slack
Pamela L.C. Small
Matthew R. Smallman-Raynor
Caroline Smith DeWaal
Anthony Marius Smith
Bryan L. Smith
Gavin Smith
Kimothy Smith
Kirk Smith
Kristine Smith
Rachel Mann Smith
Tara C. Smith
Eveline Snelders
David Snydman
Cristina Socolovschi
Olusegun Soge
Christophe Sola
Gerard Sonder
Gail L. Sondermeyer
Stephanie Sonnberg
Sunil Sood
Frank J. Sorvillo
Erica Spackman
Anne Catherine Spaulding
Stanley Spinola
Kirsten St. George
Judy St. Leger
Kirby Stafford
Danielle Stanek
Gerold Stanek
J. Erin Staples
Klaus Stark
William M. Stauffer
A. Steens
Robert Steffen
Sandra Steiner
Ivo Steinmetz
Lori Stevens
Roger W. Stich
O. Colin Stine
Robyn Stoddard
Justin Stoler
Susan Stramer
Steffanie A. Strathdee
Raymond Strikas
Franc Strle
Nancy Strockbine
Ute Stroeher
James Eric Strong
Michael J. Studdert
John R. Su
Kanta Subbarao
Derek J. Sullivan
Nancy Sullivan
Patrick S. Sullivan
Sheena G. Sullivan
Rebecca H. Sunenshine
Leonardo Susta
Roland Sutter
Deanna Sutton
Tohru Suzuki
Larry Svenson
Robert Swanepoel
David Swayne
William Switzer
Jose-Manuel Sánchez-Vizcaino
Maria Söderlund-Venermo
Hiroshi Takahasi
Eugenia Tognotti
Enrico Tortoli
H. Tachibana
Daisuke Takamatsu
Emi Takashita
Ben Tall
Eldin Talundzic
Mario Tamburri
Azaibi Tamin
Kathrine Tan
Julian Wei-Tze Tang
Caroline Tapparel
Arnaud Tarantola
Cheryl Lea Tarr
Phillip Irwin Tarr
Jacqueline Tate
Andrew James Tatem
Jeffery Karl Taubenberger
Robert V. Tauxe
Christopher Taylor
Steve M. Taylor
William Pendrich Taylor
Richard S. Tedder
Sam Telford
Glenn Telling
Chong-Gee Teo
Karen Terio
Robert B. Tesh
Eyasu Habtu Teshale
Gaëtan Texier
Wilhelm Alexander Tham
Etienne Thiry
H. Lucy Thomas
Gavin Thompson
George Thompson
Reimar Thomsen
Sharmi Thor
Michael Tibbetts
Tejpratap Tiwari
Kelvin Kai-Wang To
Rafal Tokarz
Herbert Tomaso
Stephen Mark Tompkins
Steven Y. Tong
Suxiang Tong
Stephen Toovey
Mia Torchetti
Paul Torgerson
Montserrat Torremorell
Sherry Towers
David Trees
William E. Trick
Ralph A. Tripp
Susan Trock
Krzysztof Trzciński
Raymond Tsang
Jean I. Tsao
Hiroshi Tsunemitsu
Terrence Tumpey
Paul Turner
Gregory J. Tyrrell
V. Udhayakumar
Marcela Uhart
Anne-Catrin Uhlemann
Thomas Uldrick
Elizabeth R. Unger
Steve Unwin

Timothy M. Uyeki
Gabriele Vaccari
Antti Vaheri
Gustavo Valbuena
Chris A. Van Beneden
Marie F. Van Bressem
H. Rogier van Doorn
Neeltje van Doremalen
Maria D. Van Kerkhove
Esther van Kleef
Annelies van Rie
J.N. Van Tham
Pieter-Paul A. M. van Thiel
Arie Van der Ende
Frank van der Meer
Wim H. M. van der Poel
Sabine van der Sanden
Tjip van der Werf
Ktelijn Vandemaele
Edouard Vannier
Olli Vapalahti
Jay Kumar Varma
Shawn Vasoo
Muriel Vayssier-Taussat
Marietjie Venter
Paul Verweij
Didrik Frimann Vestrheim
Cecile G. Viboud
Stalin Victor
Dhanasekaran Vijaykrishna
Holenarasipur R. Vikram
Amy Vincent
Joseph M. Vinetz
Jan Vinjé
Abinash Virk
Katherina Vizcaychipi
Anne von Gottberg
Bettie Voordouw
Duc J. Vugia
Julio A. Vázquez
Supaporn Wacharapluesadee
David M. Wagner
Kenneth Waldrup
David H. Walker
Hongquan Wan
Xiu-Feng Wan
David Wang
Hua Wang
Lin-Fa Wang
Qiu-Hong Wang
Shih-Min Wang
Xin Wang
John W. Ward
Mary Warrell
Steve Wassilak
Tokiko Watanabe
Stephen Waterman
Ray Waters
John Watson
Scott C. Weaver
Bryant James Webber
Richard J. Webby
J. Todd Weber
Robert G. Webster
Scott Weese
Gary Weil
Daniel Weinberger
Robert A. Weinstein
Will Weldon
Nancy Wengenack
Bruce G. Weniger
Ulrich Wernery
Jim Werngren
Joseph L. Wheat
Jean Whichard
Sara Whitehead
Chris A. Whitehouse
Brian Wickes
Marc-Alain Widdowson
Martin Wiedmann
Joost Wiersinga
Mark H. Wilcox
Annelies Wilder-Smith
Jason Wilken
John Williams
John K. Williams
Maya Williams
G. David Williamson
Nick Wilson
Carla A. Winston
Kevin L. Winthrop
James Winton
Thorsten Wolff
Frank Wong
Patrick C.Y. Woo
Gary Wormser
Henry Wu
Ho-Sheng Wu
Joseph T. Wu
Nan-ping Wu
William H. Wunner
Fujie Xu
Pablo Yagupsky
Seiji P. Yamamoto
Chunfu Yang
Jiyong Yang
Ruifu Yang
H. Yen
W. Katherine Yih
Tzeng Yih-Ling
Renata Yokota
Zabulon Yoti
Mary Younan
Victor L. Yu
Xuejie Yu
Kwok-Yung Yuen
Thomas MacKay Yuill
Jean Ralph Zahar
Sherif Zaki
Roland Zell
Galina Zemtsova
Dominik Zenner
George G. Zhanel
Jianqiang Zhang
Xuming Zhang
Yan Zhang
Lun Zhao-Rong
Duping Zheng
Haijian Zhou
Hong Zhou
Hua Chen Zhu
Emily Zielinski-Gutierrez
Matteo Zignol
Jakob Zinsstag
Jennifer Zipprich
Jane Zucker

Thank you EID Reviewers

We only maintain high standards because of your support. EID's Impact Factor of 7.327 ranked it 3rd of 70 infectious disease journals. The Google Scholar h-Index data rank EID 1st of the top 20 publications in Epidemiology and 7th among the top 20 publications in Communicable Diseases. The electronic table of contents goes to more than 80,000 subscribers each month.

All articles published in the Emerging Infectious Diseases journal are peer-reviewed by volunteers from around the globe, enabling us to bring you high-quality content about new and emerging infectious diseases and trends world-wide. In addition to these pages, a list of reviewers is posted at

http://wwwnc.cdc.gov/eid/page/reviewers

Please report any errors to eideditor@cdc.gov.

CDC Health Information for International Travel 2014

The Yellow Book

CENTERS FOR DISEASE CONTROL AND PREVENTION,

20%
DISCOUNT WITH
PROMO CODE
32130

Clearly written and featuring full-color illustrations, the book provides easy-to-read disease risk maps, travel vaccine recommendations, information on where to find health care during travel, advice for those traveling with infants and children, a comprehensive catalog of travel-related diseases, detailed country-specific information, and itineraries for several popular tourist destinations.

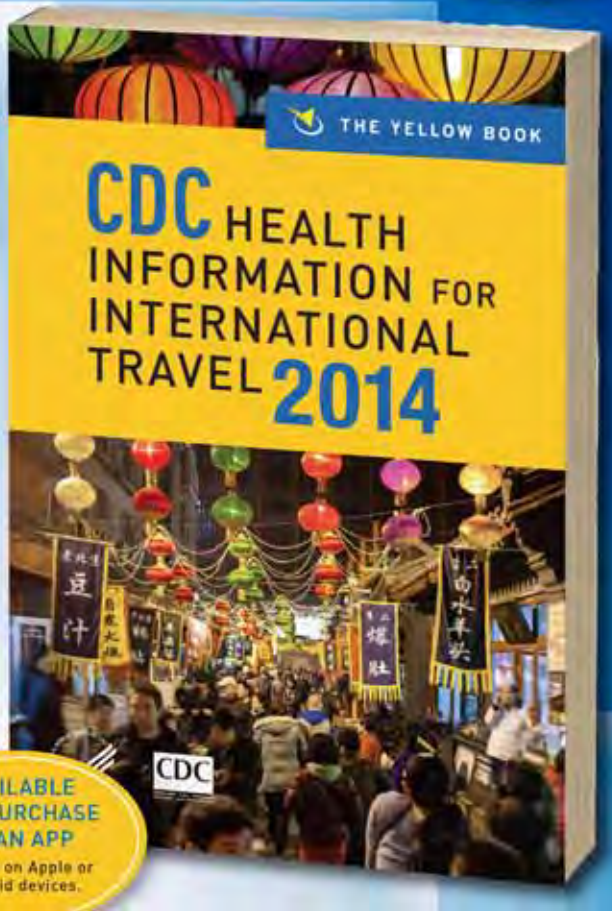

AVAILABLE FOR PURCHASE AS AN APP
For use on Apple or Android devices.

Apr 2013 | 688 pp.
ISBN: 9780199948499
Paperback ~~$47.50~~ **$38.00**

FOUR *easy* WAYS TO ORDER

Phone: 800.451.7556 | Fax: 919.677.1303 | Web: www.oup.com/us
Mail: Oxford University Press Order Dept., 2001 Evans Road Cary, NC, 27513

OXFORD
UNIVERSITY PRESS

Earning CME Credit

To obtain credit, you should first read the journal article. After reading the article, you should be able to answer the following, related, multiple-choice questions. To complete the questions (with a minimum 75% passing score) and earn continuing medical education (CME) credit, please go to http://www.medscape.org/journal/eid. Credit cannot be obtained for tests completed on paper, although you may use the worksheet below to keep a record of your answers. You must be a registered user on Medscape.org. If you are not registered on Medscape.org, please click on the "Register" link on the right hand side of the website to register. Only one answer is correct for each question. Once you successfully answer all post-test questions you will be able to view and/or print your certificate. For questions regarding the content of this activity, contact the accredited provider, CME@medscape.net. For technical assistance, contact CME@webmd.net. American Medical Association's Physician's Recognition Award (AMA PRA) credits are accepted in the US as evidence of participation in CME activities. For further information on this award, please refer to http://www.ama-assn.org/ama/pub/about-ama/awards/ama-physicians-recognition-award.page. The AMA has determined that physicians not licensed in the US who participate in this CME activity are eligible for AMA PRA Category 1 Credits™. Through agreements that the AMA has made with agencies in some countries, AMA PRA credit may be acceptable as evidence of participation in CME activities. If you are not licensed in the US, please complete the questions online, print the certificate and present it to your national medical association for review.

Article Title

Bacterial Pathogens Associated with Hidradenitis Suppurativa, France

CME Questions

1. You are seeing a 40-year-old woman with a 3-year history of mild hidradenitis suppurativa (HS). She wants to know more about her condition. What can you tell her?

A. The overall prevalence of HS may be as high as 2%
B. The principal mechanism responsible for HS is a deficit in cellular immunity
C. There appears to be no genetic component to HS
D. Only staphylococcus species have been isolated previously from HS lesions

2. According to the results of the current study by Guet-Revillet and colleagues, which of the following types of bacteria is most likely to be isolated from an HS lesion taken from this patient?

A. *Staphylococcus lugdunensis*
B. Coagulase-negative staphylococci
C. *S. aureus*
D. *Streptococcus pyogenes*

3. The patient presents 1 year later with more severe HS. Which of the following organisms is most likely to be found on culture from lesions vs normal skin?

A. Actinomycetes
B. Corynebacteria
C. Enterobacteriaceae
D. *Propionibacterium* spp.

4. Which of the following statements regarding metagenomic testing in the current study is most accurate?

A. There was poor correlation between metagenomic testing and culture results
B. There was good correlation between metagenomic testing and culture results
C. No bacterial orders were consistently identified
D. Metagenomic testing was helpful to differentiate between organisms in Hurley stage II and III disease

Activity Evaluation

1. The activity supported the learning objectives.				
Strongly Disagree				Strongly Agree
1	2	3	4	5
2. The material was organized clearly for learning to occur.				
Strongly Disagree				Strongly Agree
1	2	3	4	5
3. The content learned from this activity will impact my practice.				
Strongly Disagree				Strongly Agree
1	2	3	4	5
4. The activity was presented objectively and free of commercial bias.				
Strongly Disagree				Strongly Agree
1	2	3	4	5

Earning CME Credit

To obtain credit, you should first read the journal article. After reading the article, you should be able to answer the following, related, multiple-choice questions. To complete the questions (with a minimum 75% passing score) and earn continuing medical education (CME) credit, please go to http://www.medscape.org/journal/eid. Credit cannot be obtained for tests completed on paper, although you may use the worksheet below to keep a record of your answers. You must be a registered user on Medscape.org. If you are not registered on Medscape.org, please click on the "Register" link on the right hand side of the website to register. Only one answer is correct for each question. Once you successfully answer all post-test questions you will be able to view and/or print your certificate. For questions regarding the content of this activity, contact the accredited provider, CME@medscape.net. For technical assistance, contact CME@webmd.net. American Medical Association's Physician's Recognition Award (AMA PRA) credits are accepted in the US as evidence of participation in CME activities. For further information on this award, please refer to http://www.ama-assn.org/ama/pub/about-ama/awards/ama-physicians-recognition-award.page. The AMA has determined that physicians not licensed in the US who participate in this CME activity are eligible for AMA PRA Category 1 Credits™. Through agreements that the AMA has made with agencies in some countries, AMA PRA credit may be acceptable as evidence of participation in CME activities. If you are not licensed in the US, please complete the questions online, print the certificate and present it to your national medical association for review.

Article Title

Seroconversion for Infectious Pathogens among UK Military Personnel Deployed to Afghanistan, 2008–2011

CME Questions

1. You are consulting for the Department of Defence regarding infectious diseases anticipated in military personnel returning from Afghanistan. According to the biosurveillance study by Newman and colleagues, which of the following statements about seroconversion of UK military personnel deployed to Afghanistan between 2008 and 2011 against various vector-borne and zoonotic diseases is correct?

A. The highest seroconversion rate during deployment was against hantavirus
B. Seroconversion rate against sandfly fever virus was 3.1%
C. Seroconversion rate against Crimean-Congo hemorrhagic fever virus was 2.7%
D. Seroconversion against *Coxiella* was not reported

2. According to the biosurveillance study by Newman and colleagues, which of the following statements about asymptomatic and symptomatic cases of seroconversion among UK military personnel deployed to Afghanistan is correct?

A. Most seroconversions were associated with high-grade fever
B. Only 30% of patients with seroconversion against hantavirus were symptomatic
C. More than one-third of all volunteers reported experiencing "flu-like" symptoms while on operations in the Helmand province
D. An estimated 64.7% of Q-fever seroconversions were asymptomatic

3. According to the biosurveillance study by Newman and colleagues, which of the following statements about clinical and public health implications of the findings would most likely be correct?

A. Continued surveillance is no longer needed
B. Human or animal (for the zoonotic pathogens) reservoirs in the local populations of the Helmand region for these diseases are unlikely
C. Rapid, field-capable, point-of-care diagnostics are needed in regions, or situations, where full laboratory diagnostic facilities are not practical or available
D. Change in military operations or environmental factors is unlikely to affect incidence

Activity Evaluation

1. The activity supported the learning objectives.				
Strongly Disagree				Strongly Agree
1	2	3	4	5
2. The material was organized clearly for learning to occur.				
Strongly Disagree				Strongly Agree
1	2	3	4	5
3. The content learned from this activity will impact my practice.				
Strongly Disagree				Strongly Agree
1	2	3	4	5
4. The activity was presented objectively and free of commercial bias.				
Strongly Disagree				Strongly Agree
1	2	3	4	5

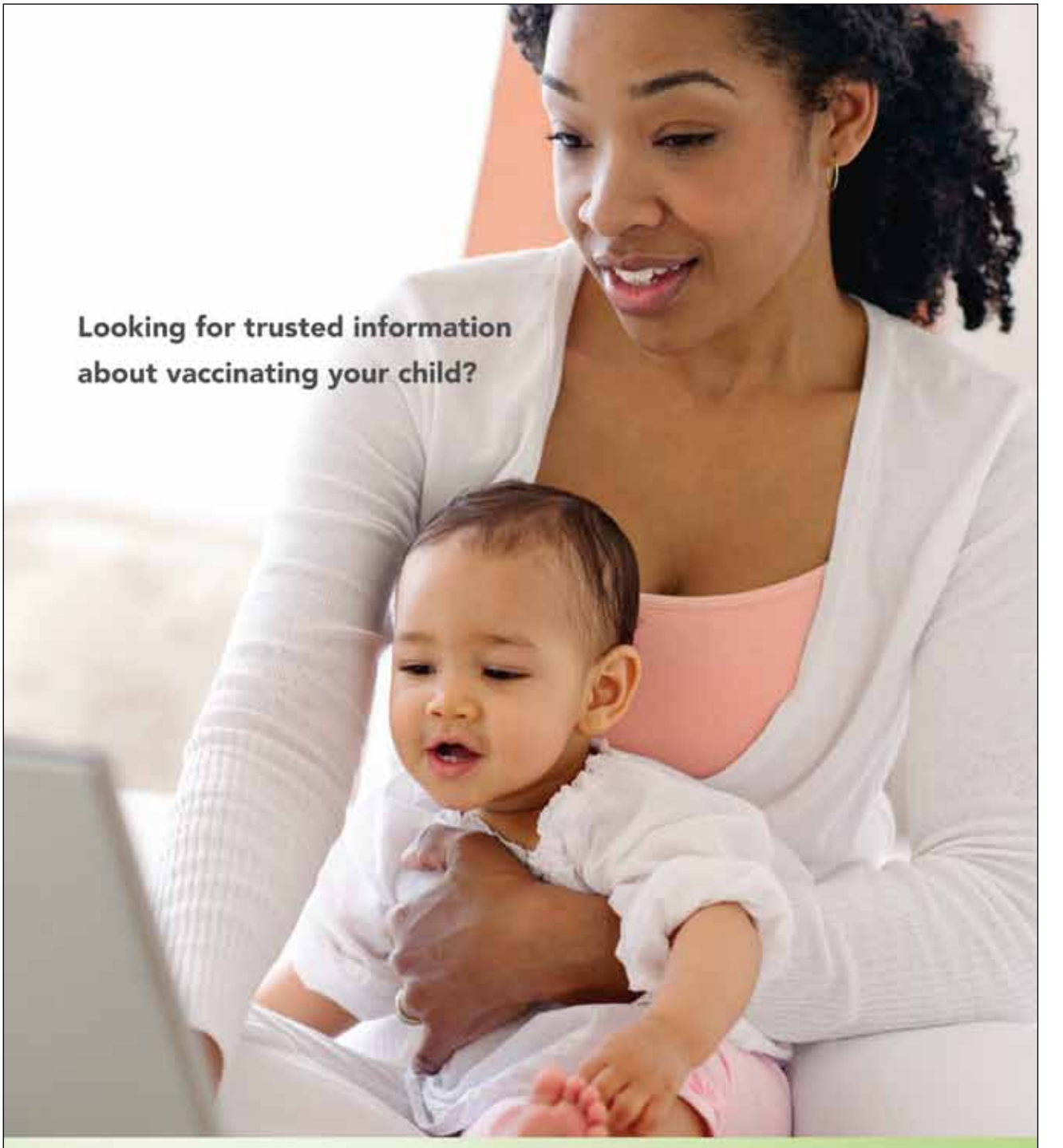

Visit www.cdc.gov/vaccines/parents. Learn about the vaccines your baby needs from a reliable source. The CDC's website explains the 14 diseases vaccines prevent, CDC's recommended schedule, possible side effects, how to comfort your baby during vaccine visits and more. Talk to your child's doctor, and visit our website to get the facts about vaccines.

U.S. Department of Health and Human Services
Centers for Disease Control and Prevention

Immunization. Power to Protect.

Emerging Infectious Diseases is a peer-reviewed journal established expressly to promote the recognition of new and reemerging infectious diseases around the world and improve the understanding of factors involved in disease emergence, prevention, and elimination.

The journal is intended for professionals in infectious diseases and related sciences. We welcome contributions from infectious disease specialists in academia, industry, clinical practice, and public health, as well as from specialists in economics, social sciences, and other disciplines. Manuscripts in all categories should explain the contents in public health terms. For information on manuscript categories and suitability of proposed articles, see below and visit http://wwwnc.cdc.gov/eid/pages/author-resource-center.htm.

Summary of Authors' Instructions

Author's Instructions. For a complete list of EID's manuscript guidelines, see the author resource page: http://wwwnc.cdc.gov/eid/page/author-resource-center.

Manuscript Submission. To submit a manuscript, access Manuscript Central from the Emerging Infectious Diseases web page (www.cdc.gov/eid). Include a cover letter indicating the proposed category of the article (e.g., Research, Dispatch), verifying the word and reference counts, and confirming that the final manuscript has been seen and approved by all authors. Complete provided Authors Checklist.

Manuscript Preparation. For word processing, use MS Word. Set the document to show continuous line numbers. List the following information in this order: title page, article summary line, keywords, abstract, text, acknowledgments, biographical sketch, references, tables, and figure legends. Appendix materials and figures should be in separate files.

Title Page. Give complete information about each author (i.e., full name, graduate degree(s), affiliation, and the name of the institution in which the work was done). Clearly identify the corresponding author and provide that author's mailing address (include phone number, fax number, and email address). Include separate word counts for abstract and text.

Keywords. Use terms as listed in the National Library of Medicine Medical Subject Headings index (www.ncbi.nlm.nih.gov/mesh).

Text. Double-space everything, including the title page, abstract, references, tables, and figure legends. Indent paragraphs; leave no extra space between paragraphs. After a period, leave only one space before beginning the next sentence. Use 12-point Times New Roman font and format with ragged right margins (left align). Italicize (rather than underline) scientific names when needed.

Biographical Sketch. Include a short biographical sketch of the first author—both authors if only two. Include affiliations and the author's primary research interests.

References. Follow Uniform Requirements (www.icmje.org/index.html). Do not use endnotes for references. Place reference numbers in parentheses, not superscripts. Number citations in order of appearance (including in text, figures, and tables). Cite personal communications, unpublished data, and manuscripts in preparation or submitted for publication in parentheses in text. Consult List of Journals Indexed in Index Medicus for accepted journal abbreviations; if a journal is not listed, spell out the journal title. List the first six authors followed by "et al." Do not cite references in the abstract.

Tables. Provide tables within the manuscript file, not as separate files. Use the MS Word table tool, no columns, tabs, spaces, or other programs. Footnote any use of boldface. Tables should be no wider than 17 cm. Condense or divide larger tables. Extensive tables may be made available online only.

Figures. Submit editable figures as separate files (e.g., Microsoft Excel, PowerPoint). Photographs should be submitted as high-resolution (600 dpi) .tif or .jpeg files. Do not embed figures in the manuscript file. Use Arial 10 pt. or 12 pt. font for lettering so that figures, symbols, lettering, and numbering can remain legible when reduced to print size. Place figure keys within the figure. Figure legends should be placed at the end of the manuscript file.

Videos. Submit as AVI, MOV, MPG, MPEG, or WMV. Videos should not exceed 5 minutes and should include an audio description and complete captioning. If audio is not available, provide a description of the action in the video as a separate Word file. Published or copyrighted material (e.g., music) is discouraged and must be accompanied by written release. If video is part of a manuscript, files must be uploaded with manuscript submission. When uploading, choose "Video" file. Include a brief video legend in the manuscript file.

Types of Articles

Perspectives. Articles should not exceed 3,500 words and 40 references. Use of subheadings in the main body of the text is recommended. Photographs and illustrations are encouraged. Provide a short abstract (150 words), 1-sentence summary, and biographical sketch. Articles should provide insightful analysis and commentary about new and reemerging infectious diseases and related issues. Perspectives may address factors known to influence the emergence of diseases, including microbial adaptation and change, human demographics and behavior, technology and industry, economic development and land use, international travel and commerce, and the breakdown of public health measures.

Synopses. Articles should not exceed 3,500 words and 40 references. Use of subheadings in the main body of the text is recommended. Photographs and illustrations are encouraged. Provide a short abstract (150 words), 1-sentence summary, and biographical sketch. This section comprises concise reviews of infectious diseases or closely related topics. Preference is given to reviews of new and emerging diseases; however, timely updates of other diseases or topics are also welcome.

Research. Articles should not exceed 3,500 words and 40 references. Use of subheadings in the main body of the text is recommended. Photographs and illustrations are encouraged. Provide a short abstract (150 words), 1-sentence summary, and biographical sketch. Report laboratory and epidemiologic results within a public health perspective. Explain the value of the research in public health terms and place the findings in a larger perspective (i.e., "Here is what we found, and here is what the findings mean").

Policy and Historical Reviews. Articles should not exceed 3,500 words and 40 references. Use of subheadings in the main body of the text is recommended. Photographs and illustrations are encouraged. Provide a short abstract (150 words), 1-sentence summary, and biographical sketch. Articles in this section include public health policy or historical reports that are based on research and analysis of emerging disease issues.

Dispatches. Articles should be no more than 1,200 words and need not be divided into sections. If subheadings are used, they should be general, e.g., "The Study" and "Conclusions." Provide a brief abstract (50 words); references (not to exceed 15); figures or illustrations (not to exceed 2); tables (not to exceed 2); and biographical sketch. Dispatches are updates on infectious disease trends and research that include descriptions of new methods for detecting, characterizing, or subtyping new or reemerging pathogens. Developments in antimicrobial drugs, vaccines, or infectious disease prevention or elimination programs are appropriate. Case reports are also welcome.

Another Dimension. Thoughtful essays, short stories, or poems on philosophical issues related to science, medical practice, and human health. Topics may include science and the human condition, the unanticipated side of epidemic investigations, or how people perceive and cope with infection and illness. This section is intended to evoke compassion for human suffering and to expand the science reader's literary scope. Manuscripts are selected for publication as much for their content (the experiences they describe) as for their literary merit. Include biographical sketch.

Letters. Letters commenting on recent articles as well as letters reporting cases, outbreaks, or original research, are welcome. Letters commenting on articles should contain no more than 300 words and 5 references; they are more likely to be published if submitted within 4 weeks of the original article's publication. Letters reporting cases, outbreaks, or original research should contain no more than 800 words and 10 references. They may have 1 figure or table and should not be divided into sections. No biographical sketch is needed.

Commentaries. Thoughtful discussions (500–1,000 words) of current topics. Commentaries may contain references (not to exceed 15) but no abstract, figures, or tables. Include biographical sketch.

Books, Other Media. Reviews (250–500 words) of new books or other media on emerging disease issues are welcome. Title, author(s), publisher, number of pages, and other pertinent details should be included.

Conference Summaries. Summaries of emerging infectious disease conference activities (500–1,000 words) are published online only. They should be submitted no later than 6 months after the conference and focus on content rather than process. Provide illustrations, references, and links to full reports of conference activities.

Online Reports. Reports on consensus group meetings, workshops, and other activities in which suggestions for diagnostic, treatment, or reporting methods related to infectious disease topics are formulated may be published online only. These should not exceed 3,500 words and should be authored by the group. We do not publish official guidelines or policy recommendations.

Photo Quiz. The photo quiz (1,200 words) highlights a person who made notable contributions to public health and medicine. Provide a photo of the subject, a brief clue to the person's identity, and five possible answers, followed by an essay describing the person's life and his or her significance to public health, science, and infectious disease.

Etymologia. Etymologia (100 words, 5 references). We welcome thoroughly researched derivations of emerging disease terms. Historical and other context could be included.

Announcements. We welcome brief announcements of timely events of interest to our readers. Announcements may be posted online only, depending on the event date. Email to eideditor@cdc.gov.